EMERGING INFECTIOUS DISEASES®

CDC
Centers for Disease Control and Prevention

Bacterial Infections

October 2020

Yi Taek-gyun (c. 1808–1883), *Books and Scholars' Accouterments* (late 1800s). Ten-panel folding screen; ink and color on silk, Overall size: 77 3/4 in x 155 1/2 in/197.5 cm x 395 cm; painting size: 54 13/16 in x 130 1/4 in/139.3 cm x 330.8 cm. Open access image from Cleveland Museum of Art, Cleveland, Ohio, USA; Leonard C. Hanna, Jr. Fund.

EMERGING INFECTIOUS DISEASES®

Emerging Infectious Diseases is published monthly by the Centers for Disease Control and Prevention, 1600 Clifton Rd NE, Mailstop H16-2, Atlanta, GA 30329-4027, USA. Telephone 404-639-1960; email, eideditor@cdc.gov

EMERGING INFECTIOUS DISEASES®

Bacterial Infections **October 2020**

On the Cover

***Books and Scholars' Accouterments*, late 1800s. Yi Taek-gyun (Korean, 1808-after 1883).** Ten-panel folding screen; ink and color on silk; overall: 197.5 x 395 cm (77 3/4 x 155 1/2 in.); painting only: 139.3 x 330.8 cm (54 13/16 x 130 1/4 in.). The Cleveland Museum of Art, Leonard C. Hanna, Jr. Fund 2011.37

About the Cover p. 2537

Synopses

EMERGING INFECTIOUS DISEASES®
October 2020

Research

Dispatches

Another Dimension

Research Letters

EMERGING INFECTIOUS DISEASES®
October 2020

Comment Letters

Books and Media

About the Cover

Etymologia

Online Reports

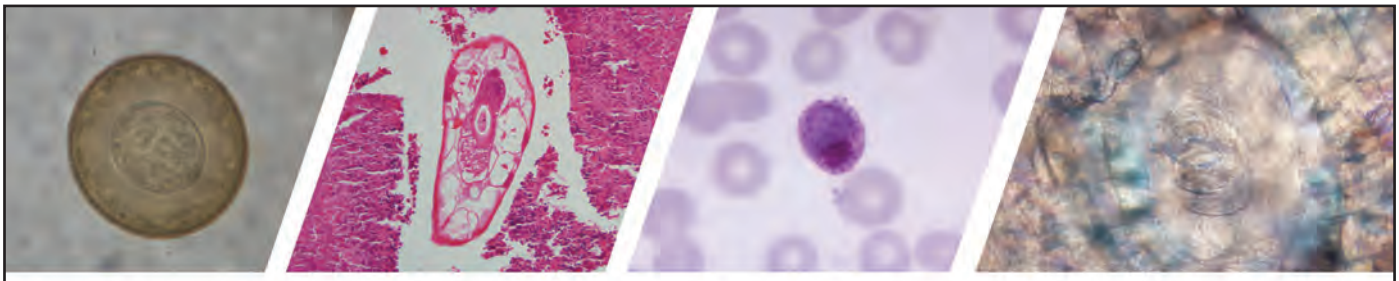

DPDx

Diagnostic Assistance and Training in Laboratory Identification of Parasites

A free service of CDC available to laboratorians, pathologists, and other health professionals in the United States and abroad

- Diagnosis from photographs of worms, histological sections, fecal, blood, and other specimen types
- Expert diagnostic review
- Formal diagnostic laboratory report
- Submission of samples via secure file share

Visit the DPDx website for information on laboratory diagnosis, geographic distribution, clinical features, parasite life cycles, and training via Monthly Case Studies of parasitic diseases.

www.cdc.gov/dpdx
dpdx@cdc.gov

CS272346-DE

U.S. Department of Health and Human Services
Centers for Disease Control and Prevention

Healthcare-Associated Legionnaires' Disease, Europe, 2008-2017

Julien Beauté, Diamantis Plachouras, Sven Sandin, Johan Giesecke, Pär Sparén

Medscape EDUCATION ACTIVITY

In support ofs improving patient care, this activity has been planned and implemented by Medscape, LLC and Emerging Infectious Diseases. Medscape, LLC is jointly accredited by the Accreditation Council for Continuing Medical Education (ACCME), the Accreditation Council for Pharmacy Education (ACPE), and the American Nurses Credentialing Center (ANCC), to provide continuing education for the healthcare team.

Medscape, LLC designates this Journal-based CME activity for a maximum of 1.00 ***AMA PRA Category 1 Credit(s)™***. Physicians should claim only the credit commensurate with the extent of their participation in the activity.

Successful completion of this CME activity, which includes participation in the evaluation component, enables the participant to earn up to 1.0 MOC points in the American Board of Internal Medicine's (ABIM) Maintenance of Certification (MOC) program. Participants will earn MOC points equivalent to the amount of CME credits claimed for the activity. It is the CME activity provider's responsibility to submit participant completion information to ACCME for the purpose of granting ABIM MOC credit.

All other clinicians completing this activity will be issued a certificate of participation. To participate in this journal CME activity: (1) review the learning objectives and author disclosures; (2) study the education content; (3) take the post-test with a 75% minimum passing score and complete the evaluation at http://www.medscape.org/journal/eid; and (4) view/print certificate. For CME questions, see page 2540.

Release date: September 17, 2020; Expiration date: September 17, 2021

Learning Objectives

Upon completion of this activity, participants will be able to:

- Compare different sources of LD in the European Union
- Analyze temporal trends in LD in the European Union
- Assess demographic variables among patients with LD
- Evaluate the microbiology and prognosis of healthcare-associated LD

CME Editor

Deanna Altomara, BA, Copyeditor, Emerging Infectious Diseases. *Disclosure: Deanna Altomara, BA, has disclosed no relevant financial relationships.*

CME Author

Charles P. Vega, MD, Health Sciences Clinical Professor of Family Medicine, University of California, Irvine School of Medicine, Irvine, California. *Disclosure: Charles P. Vega, MD, has disclosed the following relevant financial relationships: served as an advisor or consultant for Johnson & Johnson Pharmaceutical Research & Development, LLC; GlaxoSmithKline; served as a speaker or a member of a speakers bureau for Genentech; GlaxoSmithKline.*

Authors

Disclosures: ***Julien Beauté, PhD; Diamantis Plachouras, PhD; Sven Sandin, PhD; Johan Giesecke, PhD;*** *and* ***Pär Sparén, PhD,*** *have disclosed no relevant financial relationships.*

Healthcare-associated Legionnaires' disease (HCA LD) can cause nosocomial outbreaks with high death rates. We compared community-acquired LD cases with HCA LD cases in Europe during 2008-2017 using data from The European Surveillance System. A total of 29 countries reported 40,411 community-acquired and 4,315 HCA LD cases. Of the HCA LD cases, 2,937 (68.1%) were hospital-acquired and 1,378 (31.9%) were linked to other healthcare facilities. The odds of having HCA LD were higher for women, children and persons <20 years of age, and persons ≥60 years of age. Out of the cases caused by *Legionella pneumophila* with a known serotype, community-acquired LD was more likely to be caused by *L. pneumophila* serogroup 1 (92.3%) than was HCA LD (85.1%). HCA LD patients were more likely to die. HCA LD is associated with specific patient demographics, causative strains, and outcomes. Healthcare facilities should consider these characteristics when designing HCA LD prevention strategies.

Author affiliations: European Centre for Disease Prevention and Control, Stockholm, Sweden (J. Beauté, D. Plachouras); Karolinska Institutet, Stockholm (J. Beauté, S. Sandin, J. Giesecke, P. Sparén); Icahn School of Medicine at Mount Sinai, New York, New York, USA (S. Sandin); Seaver Autism Center for Research and Treatment at Mount Sinai, New York (S. Sandin)

DOI: https://doi.org/10.3201/eid2610.181889

Legionnaires' disease (LD) is a severe pneumonia caused by *Legionella*, a genus of gram-negative bacteria found in aquatic environments and human-made water systems (*1*). LD is a notifiable condition in all 30 European Union (EU) and European Economic Area (EEA) countries, where ≈70% of reported cases are community-acquired, ≈20% are travel-associated, and ≈10% are healthcare-associated (HCA) (*2*). In 2015, HCA LD accounted for 20% of all cases in the United States reported to the Centers for Disease Control and Prevention (*3*). The overall EU–EEA LD notification rate increased during 2011–2017 for unknown reasons (*2*,*4*).

Public health professionals should not overlook HCA LD; although it is relatively uncommon, it is associated with nosocomial outbreaks, underdiagnosis, and a high death rate of ≈30% (*5*–*7*). During 2006–2017, nearly 25% of identified outbreaks in the United States and several countries in Europe occurred in hospital or healthcare settings (*6*). During 2005–2009 in the United Kingdom and 2008–2010 in Spain, ≈3%–4% of HCA pneumonia cases were caused by *Legionella* (*8*,*9*). Hospital patients and residents of long-term care facilities are more likely to have LD risk factors, such as older age, chronic conditions, history of organ transplantation, or immunodeficiency (*7*). As such, hospital patients and residents of long-term care facilities might be more susceptible to *Legionella* (*10*).

Inhalation and aspiration are major modes of HCA LD transmission (*11*); potable water is a common source of infection (*7*). Because *Legionella* can colonize hospital water systems, possible sources of nosocomial infection include bathing, steam-heated towels, humidifiers, decorative fountains, and some medical devices (*12*,*13*). In children, HCA LD has been reported in association with heated birthing pools (*14*). HCA LD can be prevented by reducing the colonization of *Legionella* in hospitals (*15*). We describe the epidemiology of HCA LD in Europe using EU surveillance data to determine its differences from community–acquired LD in terms of seasonality, demographics, causative pathogens, and outcomes.

Methods

LD Data

The European Legionnaires' disease Surveillance Network, which comprises Iceland, Norway, and all 28 EU member states, including the United Kingdom, operates under the European Centre for Disease Prevention and Control (Stockholm, Sweden). Each state annually reports its LD cases to The European Surveillance System database hosted by the European Centre for Disease Prevention and Control. Countries report their LD cases with variables such as patient age, patient sex, date of disease onset, probable setting of infection (e.g., travel-associated), whether the case-patient is part of a cluster, laboratory method used for diagnosis, causative pathogen, and clinical outcome. LD patients who travelled (abroad or domestically) 2–10 days before disease onset are considered to have travel-associated LD. Many EU–EEA countries define HCA LD on the basis of whether the patient was in a hospital or healthcare facility ≤10 days before disease onset (*16*–*18*). Community-acquired LD is a diagnosis of exclusion (i.e., non-HCA, non–travel-associated). We defined a locally acquired case as any case not associated with travel.

Our analysis included all locally acquired cases reported during 2008–2017 that met the 2012 EU–EEA case definition of confirmed and probable cases of LD (*19*). We excluded travel-associated cases because they encompass heterogeneous exposures. We reclassified LD cases reported before 2012 according to the 2012 EU–EEA case definition. We defined hospital-acquired cases as those reported from a hospital, whereas HCA LD cases comprised hospital-acquired cases and cases reported from other healthcare facilities (e.g., nursing homes). We made this distinction for 2 main reasons. First, hospital patients, independent of age, might be immunocompromised and therefore more susceptible to LD. Second, the duration of *Legionella* exposure might be shorter for patients admitted to the hospital for acute care than for residents of long-term care facilities.

Statistical Analyses

We compared the characteristics of HCA LD patients and community-acquired LD patients. We sorted patients into 8 groups by age at diagnosis (*2*). We compared their characteristics by using the χ^2 test with a 2-sided p value of <0.05. In addition, we used logistic regression to analyze the odds of acquiring HCA or community-acquired LD, the odds of death, and the confounding effects of age and sex.

In a subanalysis of culture-confirmed cases (i.e., cases ascertained by isolation of *Legionella* spp. from respiratory secretions or any normally sterile site), we compared the causative pathogens of HCA LD patients with community-acquired LD patients. We grouped *Legionella* isolates by species and monoclonal subtypes; we further classified monoclonal subtypes by the virulence-associated epitope recognized by monoclonal antibody (mAb) 3/1 of the Dresden Panel

(*10*). We further explored the factors associated with outcome in a subset analysis of culture-confirmed cases with information about the causative strain. We used Stata 14 (StataCorp LLC, https://www.stata.com) for all statistical analyses.

Results

During 2008-2017, a total of 30 countries in Europe reported 64,409 LD cases. We excluded 446 (0.7%) of these case-patients because a laboratory method for diagnosis was not reported. We further excluded 6,788 (10.5%) LD patients, including all case-patients from Sweden, because setting of infection was not reported. These exclusions resulted in a preliminary analysis dataset of 57,175 LD patients. Of these, LD for 40,411 (70.7%) were reported as community-acquired, 11,512 (20.1%) as travel-associated, 4,315 (7.5%) as HCA, and 937 (1.6%) as associated with other settings. We then excluded travel-associated cases and those associated with other settings, resulting in our analysis dataset of 44,726 LD patients reported by 29 countries, of whom 40,411 (90.4%) had community-acquired LD and 4,315 (9.6%) had HCA LD (Table 1).

The annual number of locally acquired LD cases fluctuated from 3,357 cases in 2011 to 6,074 in 2017 (Figure 1). During 2011-2017, diagnoses of community-acquired LD and HCA LD increased. The average proportion of HCA LD among all LD cases was 10.7%, fluctuating between 9.3% in 2010 and 12.7% in 2009.

The highest proportions of HCA LD cases occurred in countries that reported <200 locally acquired cases. In Cyprus, Estonia, Hungary, Iceland, Luxembourg, and Poland, this proportion was >25%. Of the countries that reported ≥200 cases, the highest proportions of HCA LD occurred in Belgium (23.5%), France (15.5%), and Denmark (14.4%). Latvia and Norway did not report any HCA LD cases. Of the 4,315 HCA LD cases, 2,937 (68.1%) were hospital-acquired and 1,378 (31.9%) were linked to other healthcare facilities. Confirmation was slightly higher for community-acquired cases than for HCA LD (94.8% vs. 94.1%; $p<0.05$). France and Italy reported 2,763 (64.0%) HCA LD cases.

Demographic Data

Of the 4,310 HCA LD patients for whom sex was known, 2,499 (58.0%) were male, resulting in a male:female ratio of 1.4:1. However, the proportion of HCA LD was higher for female LD patients than

Table 1. Locally acquired cases of Legionnaires' disease, European Union–European Economic Area, 2008–2017

Country	Community-acquired cases, no. (%)	Healthcare-associated cases, no. (%)	Total, no. (%)
Austria	841 (2.1)	63 (1.5)	904 (2.0)
Belgium	234 (0.6)	72 (1.7)	306 (0.7)
Bulgaria	9 (<0.1)	1 (<0.1)	10 (<0.1)
Croatia*	124 (0.3)	6 (0.1)	130 (0.3)
Cyprus	0	9 (0.2)	9 (<0.1)
Czech Republic	505 (1.2)	44 (1.0)	549 (1.2)
Denmark	813 (2.0)	137 (3.2)	950 (2.1)
Estonia	33 (0.1)	20 (0.5)	53 (0.1)
Finland	27 (0.1)	4 (0.1)	31 (0.1)
France	8,564 (21.2)	1,571 (36.4)	10,135 (22.7)
Germany	3,197 (7.9)	290 (6.7)	3,487 (7.8)
Greece	182 (0.5)	28 (0.6)	210 (0.5)
Hungary	48 (0.1)	101 (2.3)	149 (0.3)
Iceland	9 (<0.1)	4 (0.1)	13 (<0.1)
Ireland	44 (0.1)	5 (0.1)	49 (0.1)
Italy	11,307 (28.0)	1,192 (27.6)	12,499 (27.9)
Latvia	231 (0.6)	0	231 (0.5)
Lithuania	18 (<0.1)	6 (0.1)	24 (0.1)
Luxembourg	1 (<0.1)	2 (<0.1)	3 (<0.1)
Malta	18 (<0.1)	1 (<0.1)	19 (<0.1)
Netherlands	2,129 (5.3)	58 (1.3)	2,187 (4.9)
Norway	117 (0.3)	0	117 (0.3)
Poland	24 (0.1)	19 (0.4)	43 (0.1)
Portugal	1,096 (2.7)	62 (1.4)	1,158 (2.6)
Romania	8 (<0.1)	1 (<0.1)	9 (<0.1)
Slovakia	52 (0.1)	9 (0.2)	61 (0.1)
Slovenia	653 (1.6)	1 (<0.1)	654 (1.5)
Spain	8,352 (20.7)	501 (11.6)	8,853 (19.8)
United Kingdom	1,775 (4.4)	108 (2.5)	1,883 (4.2)
Total	40,411 (100.0)	4,315 (100.0)	44,726 (100.0)

*Croatia started reporting Legionnaires' disease in 2013.

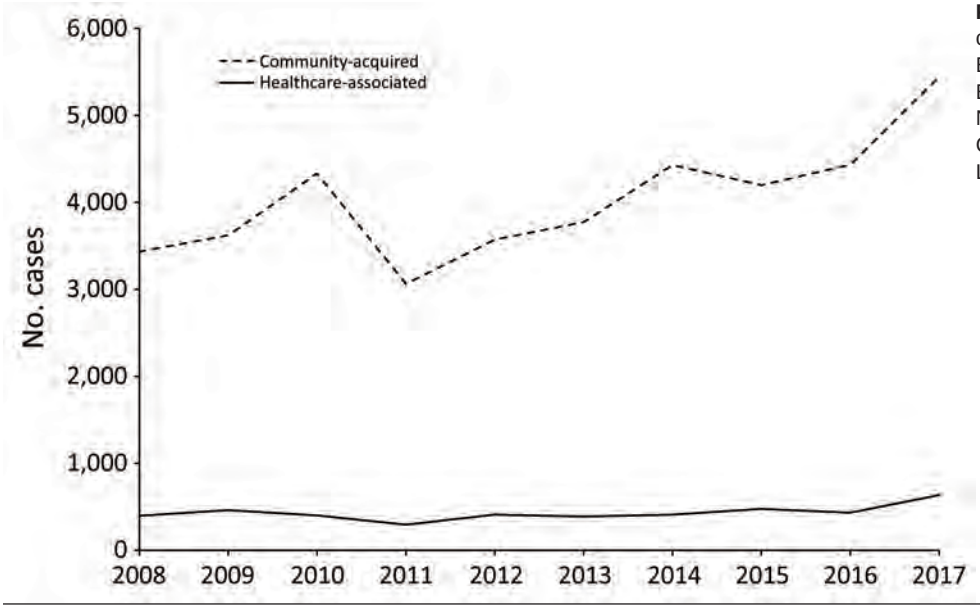

Figure 1. Locally acquired cases of Legionnaires' disease, European Union–European Economic Area, 2008–2017. Not included are data from Croatia, which started reporting Legionnaires' disease in 2013.

for male LD patients (14.2% vs. 7.8%; p<0.01). The male:female ratio was lower (0.9:1) for both younger (<20 years of age) and older (≥80 years of age) patients; the ratio peaked at 2.2:1 for patients 40–49 years of age. Of the 4,313 HCA LD patients for whom age was known, 2,650 (61.4%) were ≥70 years of age. The proportion of HCA LD patients ≥70 years of age was higher for patients linked to other healthcare facilities than for those linked to hospitals (80.0% vs. 52.8%; p<0.01). After adjustment for age, year, and reporting country, women were more likely than men to have acquired their infection in a healthcare facility (odds ratio [OR] 1.60, 95% CI 1.49–1.71) (Table 2). Patients <20 years of age of were twice as likely as patients 50–59 years of age to have HCA LD (OR 2.04, 95% CI 1.25–3.33). The risk for an HCA LD

Table 2. Main characteristics of locally acquired cases of Legionnaires' disease with adjusted predictors of healthcare-associated Legionnaires' disease, European Union–European Economic Area, 2008–2017*

Characteristic	Community-acquired cases, no. (%)	Healthcare-associated cases, no. (%)	Univariate logistic regression, OR (95% CI)	Multivariable logistic regression, OR (95% CI)†
Total	40,411 (100.0)	4,315 (100.0)		
Sex				
M	29,411 (73.0)	2,499 (58.0)	Referent	Referent
F	10,899 (27.0)	1,811 (42.0)	1.96 (1.83–2.09)	1.60 (1.49–1.71)
Unknown	101	5	Not included	Not included
Age at diagnosis, y				
<20	167 (0.4)	32 (0.7)	3.55 (2.41–5.24)	2.04 (1.25–3.33)
20–29	645 (1.6)	33 (0.8)	0.95 (0.66–1.36)	0.84 (0.57–1.23)
30–39	2,099 (5.2)	85 (2.0)	0.75 (0.59–0.95)	0.68 (0.53–0.87)
40–49	5,603 (13.9)	244 (5.7)	0.81 (0.69–0.94)	0.83 (0.71–0.98)
50–59	9,233 (22.9)	498 (11.5)	Referent	Referent
60–69	8,858 (21.9)	771 (17.9)	1.61 (1.44–1.81)	1.65 (1.46–1.86)
70–79	7,626 (18.9)	1,042 (24.2)	2.53 (2.27–2.83)	2.57 (2.29–2.88)
≥80	6,127 (15.2)	1,608 (37.3)	4.87 (4.38–5.41)	4.58 (4.11–5.12)
Unknown	53	2	Not included	Not included
Cluster status			Not tested	Not tested
Sporadic	27,609 (94.0)	2,325 (89.4)	Not tested	Not tested
Clustered	1,764 (6.0)	275 (10.6)	Not tested	Not tested
Unknown	11,038	1,715	Not tested	Not tested
Culture confirmation			Not tested	Not tested
Yes	4,200 (10.4)	684 (15.9)	Not tested	Not tested
No	36,211 (89.6)	3,631 (84.1)	Not tested	Not tested
Outcome			Not tested	Not tested
Alive	26,630 (91.4)	2,301 (71.2)	Not tested	Not tested
Dead	2,518 (8.6)	930 (28.8)	Not tested	Not tested
Unknown	11,263	1,084	Not tested	Not tested

*OR, odds ratio.
†Adjusted for year and reporting country.

diagnosis increased with age for patients ≥60 years of age, peaking for patients ≥80 years of age (OR 4.58, 95% CI 4.11–5.12).

Seasonality

The monthly distribution of onset peaked in August and September for both community-acquired and HCA LD (Figure 2). The proportion of community-acquired LD cases that developed during June–November was greater than that of HCA LD (66.9% vs. 55.8%; p<0.01).

Laboratory Test Results

During 2008–2017, The European Surveillance System recorded 48,197 laboratory test results for the 44,726 LD patients included in this analysis. LD diagnosis by urinary antigen test (UAT) was more common for community-acquired than HCA LD cases (88.7% vs. 84.3%; p<0.01). On the other hand, culture confirmation of LD was more common for HCA LD than community-acquired cases (15.9% vs. 10.4%; p<0.01) (Table 2). Of the 4,884 culture-confirmed cases, 2,205 (45.1%) were also ascertained by UAT.

Among HCA LD cases, the proportion of culture-confirmed cases was higher for hospital-acquired cases than cases linked to other healthcare settings (18.8% vs. 9.7%; p<0.01). PCR diagnosis was more likely for HCA LD than for community-acquired LD (6.8% vs. 5.0%; p<0.01). For both community-acquired and HCA LD, the proportion of cases ascertained on the basis of a single high titer of a specific serum antibody was similar (≈2.5%). The proportion of cases diagnosed by a 4-fold rise in titer or by direct immunofluorescence assay also was similar for both groups (<1% for both tests).

Pathogens

Of the 4,859 culture-confirmed cases reported with a known causative pathogen species, 4,739 (97.5%) were caused by *Legionella pneumophila*. This proportion was similar for community-acquired and HCA LD cases (97.4% vs. 98.1%; p = 0.31) (Table 3). Of the 4,533 laboratory-confirmed cases of *L. pneumophila* reported with a known serogroup, 4,137 (91.3%) were caused by *L. pneumophila* serogroup 1. This proportion was higher for community-acquired cases than HCA LD cases (92.3% vs. 85.1%; p<0.01). Following *L. pneumophila* serogroup 1 (537/684 culture-confirmed HCA LD), the most common serogroups associated with culture-confirmed HCA LD were *L. pneumophila* serogroups 3 (33 cases), 6 (15 cases), and 5 (11 cases). Of the 107 community-acquired cases with culture confirmation of other *Legionella* species, 48 (44.9%) were caused by *L. longbeachae*. The European Surveillance System did not record any HCA cases of *L. longbeachae*.

Of the 856 culture-confirmed cases caused by *L. pneumophila* serogroup 1 for which isolates were subtyped using mAbs, 679 (79.3%) tested positive for mAb 3/1 (Table 4). This proportion was higher for community-acquired than HCA LD (83.6% vs. 43.3%; p<0.01).

Outcomes

Of the 32,379 case-patients with known outcomes, 3,448 (10.6%) died (Table 5). The proportion of patients who died was higher for those with HCA than

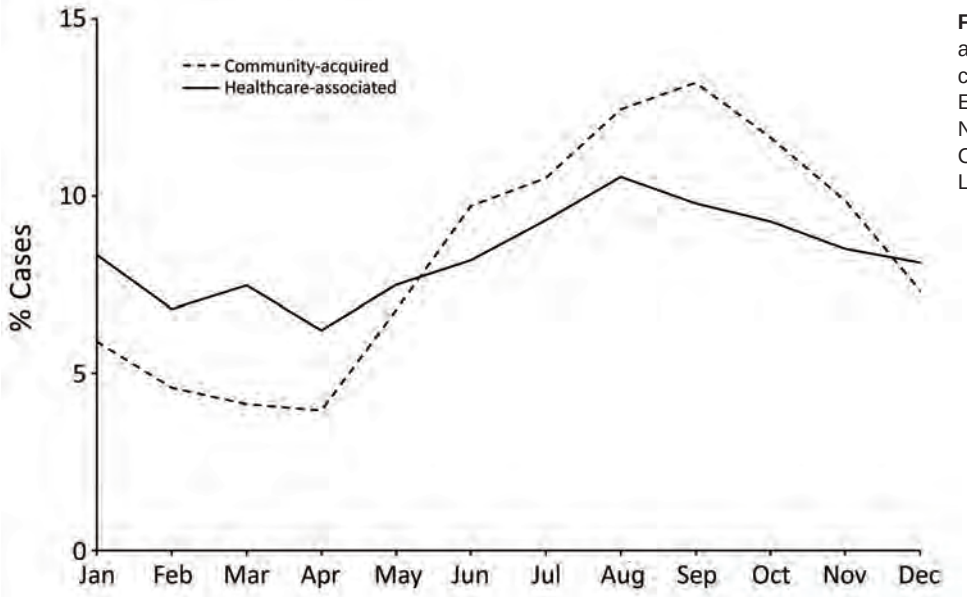

Figure 2. Timing of onset of locally acquired Legionnaires' disease cases, European Union–European Economic Area, 2008–2017. Not included are data from Croatia, which started reporting Legionnaires' disease in 2013.

Table 3. Causative pathogen of culture-confirmed, locally-acquired cases of Legionnaires' disease, European Union–European Economic Area, 2008–2017

Species, serogroup	Community-acquired cases, no. (%)	Healthcare-associated cases, no. (%)
Legionella pneumophila		
1	3,600 (85.7)	537 (78.5)
2	22 (0.5)	3 (0.4)
3	126 (3.0)	33 (4.8)
4	15 (0.4)	7 (1.0)
5	15 (0.4)	11 (1.6)
6	52 (1.2)	15 (2.2)
7	11 (0.3)	0
8	12 (0.3)	2 (0.3)
9	3 (0.1)	0
10	16 (0.4)	8 (1.2)
11	0	0
12	1 (0.0)	2 (0.3)
13	1 (0.0)	
14	1 (0.0)	1 (0.1)
15	6 (0.1)	
Mixed	6 (0.1)	4 (0.6)
Non–serogroup 1*	15 (0.4)	8 (1.2)
Unknown	169 (4.0)	37 (5.4)
Subtotal *L. pneumophila* all serogroups	4,071 (96.9)	668 (97.7)
L. anisa	4 (0.1)	2 (0.3)
L. bozemanii	15 (0.4)	2 (0.3)
L. cincinnatiensis	1 (0.0)	0
L. dumoffii	4 (0.1)	2 (0.3)
L. feeleii	1 (0.0)	0
L. longbeachae	48 (1.1)	0
L. macechernii	2 (0.0)	0
L. micdadei	10 (0.2)	2 (0.3)
L. sainthelensi	1 (0.0)	0
L. wadsworthii	0	1 (0.1)
Legionella other species	21 (0.5)	4 (0.6)
Subtotal *L.* all other species	107 (2.5)	13 (1.9)
Legionella species unknown	22 (0.5)	3 (0.4)
Total	4,200 (100.0)	684 (100.0)

*Non–serogroup 1 refers to samples that do not belong to serogroup 1, but that do not have an identified serogroup.

community-acquired LD (28.8% vs. 8.6%; p<0.01). This proportion was similar for patients with hospital-acquired LD and LD linked to other healthcare facilities (29.2% vs. 28.1%; p = 0.52). After adjustment for age, sex, year, and reporting country, the death rate was higher for HCA than community-acquired LD (OR 3.02, 95% CI 2.75–3.32). The death rate was higher for hospital-acquired LD than for LD linked to other healthcare facilities (OR 3.50, 95% CI 3.14–3.91) (Table 5). After we restricted our analysis to the 4,121 culture-confirmed cases for which information was available about causative species and serogroups, the death rate for HCA LD remained higher than for community-acquired LD (OR 2.60, 95% CI 2.11–3.22). Patients infected by *L. pneumophila* non-serogroup 1 had a higher risk for death than those infected by *L. pneumophila* serogroup 1 (OR 2.17, 95% CI 1.61–2.92). Infection with other species was not associated with a higher death rate. Of the 690 culture-confirmed cases caused by *L. pneumophila* serogroup 1 for which information about monoclonal subtype was available, patients with HCA LD still had a higher death rate than those with community-acquired LD (OR 1.93, 95% CI 1.04–3.58); cases caused by mAb 3/1–negative strains were 4 times more likely to be fatal than those caused by mAb 3/1–positive strains (OR 4.20, 95% CI 2.32–7.61).

Clusters

Of the 31,973 LD patients with known cluster status, 2,039 (6.4%) were part of a cluster. This proportion was higher for HCA LD patients than community-acquired LD patients (10.6% vs. 6.0%; p<0.01).

Discussion

In this surveillance sample from 29 EU–EEA countries, ≈10% of locally acquired LD cases were HCA. This analysis included >4,300 HCA LD cases reported during a 10-year period, providing a valuable overview of HCA LD epidemiology in Europe. A few countries accounted for most cases, a phenomenon that might limit the generalizability of the results (*2*,*20*). Although some countries might have more stringent preventive measures for hospitals, the characteristics of HCA LD patients themselves are unlikely to differ substantially across

Table 4. Monoclonal subtype for *L. pneumophila* serogroup 1 isolates, European Union–European Economic Area, 2008–2017

Monoclonal subtype	Community-acquired cases, no. (%)	Healthcare-associated cases, no. (%)
Monoclonal antibody 3/1–positive*		
Allentown	4 (0.5)	1 (1.1)
Allentown/France	198 (25.8)	8 (8.9)
Benidorm	105 (13.7)	9 (10.0)
France	1 (0.1)	0
Knoxville	197 (25.7)	5 (5.6)
Philadelphia	135 (17.6)	16 (17.8)
Subtotal	640 (83.6)	39 (43.3)
Monoclonal antibody 3/1–negative		
Bellingham	38 (5.0)	11 (12.2)
Camperdown	4 (0.5)	0
Heysham	0	1 (1.1)
OLDA	26 (3.4)	15 (16.7)
Oxford	3 (0.4)	1 (1.1)
Oxford/OLDA	55 (7.2)	23 (25.6)
Subtotal	126 (16.4)	51 (56.7)
Total	766 (100.0)	90 (100.0)

*Monoclonal types are grouped by the presence (or lack) of the virulence-associated epitope recognized by the monoclonal antibody 3/1 (Dresden Panel) (*10*).

countries. In addition, we adjusted for the reporting countries in our statistical analyses. Most of the countries with a proportion of HCA LD >25% were also countries with low LD notification rates (<0.5 cases/100,000 population) during 2011–2015 (*2*). This finding suggests that these countries are better able to diagnose and report HCA than community-acquired LD cases. Some of these countries have reported challenges in ascertaining LD, including lack of clinical awareness, lack of testing, and lack of on-site diagnostic tests (*2*).

In Europe, HCA LD disproportionately affects older persons; 61.4% of case-patients are ≥70 years of age. However, HCA LD should not be overlooked in children. LD patients <20 years of age are twice as likely to have HCA LD than patients 50–59 years of age. Although the risk for HCA LD remains higher for men and boys than for women and girls (male:female ratio of 1.4:1), LD in female patients is 60% more likely to be HCA than it is in male patients. Some risk factors for community-acquired LD might be associated with sex. For example, activities that women might be less likely to engage in, such as home plumbing or working in transportation or construction, could be risk factors for LD (*21*,*22*).

The incidence of HCA LD varied less by season than it did for community-acquired LD, probably because healthcare facilities are less exposed to external environmental conditions. *Legionella*

Table 5. Characteristics of locally acquired cases of Legionnaires' disease and adjusted predictors of death, European Union–European Economic Area, 2008–2017*

Characteristic	Survival, no. (%)	Death, no. (%)	Univariate logistic regression, OR (95% CI)	Multivariable logistic regression, OR (95% CI)†
Total	28,931 (100.0)	3,448 (100.0)		
Sex				
M	20,653 (71.6)	2,318 (67.4)	0.82 (0.76–0.89)	1.11 (1.02–1.21)
F	8,197 (28.4)	1,119 (32.6)	Referent	Referent
Unknown	81	11	Not included	Not included
Age at diagnosis, y				
<20	156 (0.5)	13 (0.4)	1.39 (0.78–2.47)	0.87 (0.44–1.72)
20–29	517 (1.8)	12 (0.3)	0.39 (0.22–0.69)	0.38 (0.21–0.68)
30–39	1,581 (5.5)	63 (1.8)	0.66 (0.51–0.87)	0.68 (0.52–0.89)
40–49	4,097 (14.2)	177 (5.1)	0.72 (0.60–0.86)	0.71 (0.59–0.86)
50–59	6,706 (23.2)	402 (11.7)	Referent	Referent
60–69	6,264 (21.7)	613 (17.8)	1.63 (1.43–1.86)	1.55 (1.35–1.76)
70–79	5,282 (18.3)	872 (25.3)	2.75 (2.43–3.12)	2.53 (2.23–2.87)
≥80	4,305 (14.9)	1,292 (37.5)	5.01 (4.45–5.64)	4.36 (3.85–4.93)
Unknown	23	4	Not included	Not included
Setting of infection				
Community	26,630 (92.0)	2,518 (73.0)	Referent	Referent
Hospital	1,534 (5.3)	631 (18.3)	4.35 (3.93–4.81)	3.50 (3.14–3.91)
Other healthcare facility	767 (2.7)	299 (8.7)	4.12 (3.59–4.74)	2.26 (1.94–2.63)

*OR, odds ratio.
†Adjusted for year and reporting country.

spp. often colonize hospital water systems (*23*). These water systems might offer year-round favorable conditions for *Legionella*, which multiplies at 25°C–42°C (*24*).

Legionella spp. causing HCA LD differ from those commonly observed in community-acquired LD. Although *L. pneumophila* caused most infections regardless of the setting, we observed a lower proportion of *L. pneumophila* serogroup 1 in HCA LD cases. This discrepancy may be of concern because UAT, the dominant laboratory method used to ascertain LD, has a poor sensitivity to non–*L. pneumophila* serogroup 1 strains (*25*). In our study, ≈45% of culture-confirmed cases were also ascertained by UAT. Because we could not determine whether the culture sequentially followed the UAT or whether the tests were performed independently, we might have overestimated the cases caused by *L. pneumophila* serogroup 1. Of the cases caused by *L. pneumophila* serogroup 1, mAb 3/1–negative strains were more common in HCA LD patients, whereas mAb 3/1–positive strains were more common in community-acquired LD patients. These results confirm earlier reports that mAb 3/1–negative strains were more frequent in hospital-acquired infections (*10*). The association of HCA LD with less virulent strains probably reflects patient demographic variables; immunocompromised patients might be more highly concentrated in healthcare facilities than in the general community. Although non–*L. pneumophila* species caused only a few cases, the proportion of cases caused by those species (except for *L. longbeachae*, which only causes community-acquired LD and is frequently associated with exposure to composts and potting soils [*26*]) was higher in patients with HCA than community-acquired LD. Patients with non–*L. pneumophila* infections might be more likely to be immunocompromised (*27*).

Nearly 30% of HCA LD patients in this analysis died. The risk for death was 2–3 times higher for HCA LD than for community-acquired LD. Some strains such as MAb 3/1–negative strains were also associated with a higher risk for death, probably because these strains of LD tend to infect more severely ill patients.

The HCA LD diagnosis might mask 2 different populations: younger but more severely ill patients who acquired infection in the hospital and older but less severely ill patients who acquired infection from other healthcare facilities. Hospital-acquired LD might be more likely to affect immunocompromised patients with underlying conditions. The large proportion of non–hospital-acquired LD in patients ≥70 years of age suggests that many might be residents of long-term care facilities. In these facilities, caretakers might have difficulty obtaining sputum samples or might not suspect LD. Furthermore, microbiology laboratory capacity might be limited (*28*), as suggested by the low proportion of culture-confirmed cases in these settings.

There is no European standard for defining HCA LD. Epidemiologists in charge of national LD surveillance report LD cases with the probable setting of infection. These reports might misclassify LD patients who were infected in the community but admitted to the hospital during the incubation period (as reported in a patient with a possible incubation of >20 days [*29*]). Because the LD attack rate is very low, this situation is highly unlikely. In addition, epidemiologists classifying these cases might follow some definition (either national or not publicly available) for HCA LD, most likely on the basis of time between date of symptom onset and date of admission to hospital. Assuming equal rates of infection for both community-acquired and HCA LD, a study estimated that a cutoff of 6 days would identify HCA LD with a predictive value of ≥77% (*30*).

In conclusion, HCA LD cases are responsible for a large proportion of LD diagnoses in Europe and differ from community-acquired cases in many aspects, including demographic characteristics, causative pathogens, and outcome. Given the severity of the disease, officials must identify cases and control outbreaks as quickly as possible. An agreed-on case definition for HCA LD might streamline the surveillance process.

Acknowledgments

We thank our colleagues in the European Legionnaires' disease Surveillance Network who provided the data. We thank Daniela Schmid, Günther Wewalka, Olivier Denis, Stéphanie Jacquinet, Denis Piérard, Sophie Quoilin, Iskra Tomova, Despo Pieridou, Ioanna Gregoriou, Maria Koliou, Vladimir Drašar, Irena Martinková, Charlotte Kjelsø, Søren Anker Uldum, Irina Dontsenko, Rita Peetso, Sari Jaakola, Jaana Kusnetsov, Outi Lyytikäinen, Silja Mentula, Christine Campese, Sophie Jarraud, Bonita Brodhun, Christian Lück, Anastasia Flountzi, Elisavet Mouratidou, Ágnes Fehér, Thorolfur Gudnason, Guðrún Sigmundsdóttir, Julie Arnott, Joan O'Donnell, Tara Mitchell, Maria Grazia Caporali, Maria Luisa Ricci, Maria Cristina Rota, Antra Bormane, Jelena Galajeva, Oksana Savicka, Migle Janulaitiene, Simona Zukauskaite-Sarapajeviene, Paul Reichert, Jackie Maistre Melillo, Tanya Melillo Fenech, Graziella Zahra, Petra Brandsema, Manon Haverkate, Dominique Caugant, Heidi Lange, Michal Czerwinski,

Katarzyna Piekarska, Teresa Fernandes, Maria Teresa Marques, Marina Ramos, Daniela Badescu, Gratiana Chicin, Odette Popovici, Danka Šimonyiová, Margita Špaleková, Maja Sočan, Darja Kese, Rosa Cano-Portero, Carmen Pelaz Antolin, Margareta Löfdahl, Gavin Dabrera, Ross Cameron, Tim Harrison, Jim McMenamin, Falguni Naik, Nick Phin, Kevin Pollock, and Emmanuel Robesyn for providing data and reading the draft manuscript.

About the Author

Dr. Beauté is a medical epidemiologist in the Surveillance and Response Support Unit at the European Centre for Disease Prevention and Control. His research interests include the surveillance of infectious diseases, especially in specific settings, such as travel and healthcare.

References

1. Fields BS, Benson RF, Besser RE. *Legionella* and Legionnaires' disease: 25 years of investigation. Clin Microbiol Rev. 2002;15:506–26. https://doi.org/10.1128/CMR.15.3.506-526.2002
2. Beauté J; The European Legionnaires' Disease Surveillance Network. Legionnaires' disease in Europe, 2011 to 2015. Euro Surveill. 2017;22. https://doi.org/10.2807/1560-7917.ES.2017.22.27.30566
3. Soda EA, Barskey AE, Shah PP, Schrag S, Whitney CG, Arduino MJ, et al. Vital signs: health care-associated Legionnaires' disease surveillance data from 20 states and a large metropolitan area - United States, 2015. MMWR Morb Mortal Wkly Rep. 2017;66:584–9. https://doi.org/10.15585/mmwr.mm6622e1
4. European Centre for Disease Prevention and Control. Annual epidemiological report for 2017—Legionnaires' disease. Stockholm: The Centre; 2019.
5. European Centre for Disease Prevention and Control. Legionnaires' disease in Europe, 2015. ECDC surveillance report. Stockholm: The Centre; 2017.
6. Hamilton KA, Prussin AJ II, Ahmed W, Haas CN. Outbreaks of Legionnaires' disease and Pontiac fever 2006-2017. Curr Environ Health Rep. 2018;5:263–71. https://doi.org/10.1007/s40572-018-0201-4
7. Sabria M, Yu VL. Hospital-acquired legionellosis: solutions for a preventable infection. Lancet Infect Dis. 2002;2:368–73. https://doi.org/10.1016/S1473-3099(02)00291-8
8. Chalmers JD, Taylor JK, Singanayagam A, Fleming GB, Akram AR, Mandal P, et al. Epidemiology, antibiotic therapy, and clinical outcomes in health care-associated pneumonia: a UK cohort study. Clin Infect Dis. 2011;53:107–13. https://doi.org/10.1093/cid/cir274
9. Polverino E, Torres A, Menendez R, Cillóniz C, Valles JM, Capelastegui A, et al.; HCAP Study investigators. Microbial aetiology of healthcare associated pneumonia in Spain: a prospective, multicentre, case-control study. Thorax. 2013;68:1007–14. https://doi.org/10.1136/thoraxjnl-2013-203828
10. Helbig JH, Bernander S, Castellani Pastoris M, Etienne J, Gaia V, Lauwers S, et al. Pan-European study on culture-proven Legionnaires' disease: distribution of *Legionella pneumophila* serogroups and monoclonal subgroups. Eur J Clin Microbiol Infect Dis. 2002;21:710–6. https://doi.org/10.1007/s10096-002-0820-3
11. Blatt SP, Parkinson MD, Pace E, Hoffman P, Dolan D, Lauderdale P, et al. Nosocomial Legionnaires' disease: aspiration as a primary mode of disease acquisition. Am J Med. 1993;95:16–22. https://doi.org/10.1016/0002-9343(93)90227-G
12. Decker BK, Palmore TN. The role of water in healthcare-associated infections. Curr Opin Infect Dis. 2013;26:345–51. https://doi.org/10.1097/QCO.0b013e3283630adf
13. Stephens JH, Shaw DD, Koehler AP. *Legionella pneumophila*: probable transmission from a contaminated respiratory device. Commun Dis Intell Q Rep. 2015;39:E201–3.
14. Collins SL, Afshar B, Walker JT, Aird H, Naik F, Parry-Ford F, et al. Heated birthing pools as a source of Legionnaires' disease. Epidemiol Infect. 2016;144:796–802. https://doi.org/10.1017/S0950268815001983
15. Almeida D, Cristovam E, Caldeira D, Ferreira JJ, Marques T. Are there effective interventions to prevent hospital-acquired Legionnaires' disease or to reduce environmental reservoirs of *Legionella* in hospitals? A systematic review. Am J Infect Control. 2016;44:e183–8. https://doi.org/10.1016/j.ajic.2016.06.018
16. Santé Publique France. Legionellosis notification form [updated 2017 Feb 6] [cited 2020 Jul 16]. https://demarches administratives.fr/formulaires/cerfa-12202-02-maladie-a-declaration-obligatoire-legionellose
17. Istituto Superiore di Sanità. Linee guida per la prevenzione ed il controllo della legionellosi. 2015 May 13 [cited 2020 Jul 16]. http://old.iss.it/binary/iss4/cont/C_17_pubblicazioni_2362.pdf
18. Public Health England. Legionnaires' disease: case definitions. [updated 2017 Feb 6] [cited 2020 Jul 16]. https://www.gov.uk/government/publications/legionnaires-disease-clinical-case-definitions
19. European Commission. Commission Implementing Decision 2012/506/EU of 8 August 2012 amending Decision 2002/253/EC laying down case definitions for reporting communicable diseases to the community network under decision no 2119/98/EC of the European Parliament and of the Council [cited 2020 Jul 16]. https://op.europa.eu/en/publication-detail/-/publication/10ed460f-0711-11e2-8e28-01aa75ed71a1/language-en
20. Beauté J, Zucs P, de Jong B; European Legionnaires' Disease Surveillance Network. Legionnaires' disease in Europe, 2009–2010. Euro Surveill. 2013;18:20417. https://doi.org/10.2807/ese.18.10.20417-en
21. Farnham A, Alleyne L, Cimini D, Balter S. Legionnaires' disease incidence and risk factors, New York, New York, USA, 2002–2011. Emerg Infect Dis. 2014;20:1795–802. https://doi.org/10.3201/eid2011.131872
22. Straus WL, Plouffe JF, File TM Jr, Lipman HB, Hackman BH, Salstrom SJ, et al. Risk factors for domestic acquisition of Legionnaires disease. Ohio Legionnaires Disease Group. Arch Intern Med. 1996;156:1685–92. https://doi.org/10.1001/archinte.1996.00440140115011
23. Goetz AM, Stout JE, Jacobs SL, Fisher MA, Ponzer RE, Drenning S, et al. Nosocomial Legionnaires' disease discovered in community hospitals following cultures of the water system: seek and ye shall find. Am J Infect Control. 1998;26:8–11. https://doi.org/10.1016/S0196-6553(98)70054-9
24. Katz SM, Hammel JM. The effect of drying, heat, and pH on the survival *of Legionella pneumophila*. Ann Clin Lab Sci. 1987;17:150–6.
25. Phin N, Parry-Ford F, Harrison T, Stagg HR, Zhang N, Kumar K, et al. Epidemiology and clinical management of Legionnaires' disease. Lancet Infect Dis. 2014;14:1011–21. https://doi.org/10.1016/S1473-3099(14)70713-3

26. Currie SL, Beattie TK. Compost and *Legionella longbeachae*: an emerging infection? Perspect Public Health. 2015;135:309–15. https://doi.org/10.1177/1757913915611162
27. Muder RR, Yu VL. Infection due to *Legionella* species other than *L. pneumophila*. Clin Infect Dis. 2002;35:990–8. https://doi.org/10.1086/342884
28. Seenivasan MH, Yu VL, Muder RR. Legionnaires' disease in long-term care facilities: overview and proposed solutions. J Am Geriatr Soc. 2005;53:875–80. https://doi.org/10.1111/j.1532-5415.2005.53270.x
29. Bargellini A, Marchesi I, Marchegiano P, Richeldi L, Cagarelli R, Ferranti G, et al. A culture-proven case of community-acquired *Legionella* pneumonia apparently classified as nosocomial: diagnostic and public health implications. Case Rep Med. 2013;2013:303712. https://doi.org/ 10.1155/2013/303712
30. Lessler J, Brookmeyer R, Perl TM. An evaluation of classification rules based on date of symptom onset to identify health-care associated infections. Am J Epidemiol. 2007;166:1220–9. https://doi.org/10.1093/aje/kwm188

Address for correspondence: Julien Beauté, European Centre for Disease Prevention and Control (ECDC), Gustav III:s boulevard 40, 169 73 Solna, Sweden; email: julien.beaute@ecdc.europa.eu

Lessons Learned from a Decade of Investigations of Shiga Toxin–Producing *Escherichia coli* Outbreaks Linked to Leafy Greens, United States and Canada

Katherine E. Marshall, April Hexemer, Sharon L. Seelman, Marianne K. Fatica, Tyann Blessington, Maha Hajmeer, Hannah Kisselburgh, Robin Atkinson, Kristin Hill, Davendra Sharma, Michael Needham, Vi Peralta, Jeffrey Higa, Karen Blickenstaff, Ian T. Williams, Michael A. Jhung, Matthew Wise, Laura Gieraltowski

Medscape EDUCATION ACTIVITY

In support of improving patient care, this activity has been planned and implemented by Medscape, LLC and Emerging Infectious Diseases. Medscape, LLC is jointly accredited by the Accreditation Council for Continuing Medical Education (ACCME), the Accreditation Council for Pharmacy Education (ACPE), and the American Nurses Credentialing Center (ANCC), to provide continuing education for the healthcare team. Medscape, LLC designates this Journal-based CME activity for a maximum of 1.00 ***AMA PRA Category 1 Credit(s)™***. Physicians should claim only the credit commensurate with the extent of their participation in the activity.

Successful completion of this CME activity, which includes participation in the evaluation component, enables the participant to earn up to 1.0 MOC points in the American Board of Internal Medicine's (ABIM) Maintenance of Certification (MOC) program. Participants will earn MOC points equivalent to the amount of CME credits claimed for the activity. It is the CME activity provider's responsibility to submit participant completion information to ACCME for the purpose of granting ABIM MOC credit.

All other clinicians completing this activity will be issued a certificate of participation. To participate in this journal CME activity: (1) review the learning objectives and author disclosures; (2) study the education content; (3) take the post-test with a 75% minimum passing score and complete the evaluation at http://www.medscape.org/journal/eid; and (4) view/print certificate. For CME questions, see page 2541.

Release date: September 16, 2020; Expiration date: September 16, 2021

Learning Objectives

Upon completion of this activity, participants will be able to:

- Describe epidemiologic findings of STEC outbreaks linked to leafy greens, according to epidemiologic, laboratory, and traceback data from US and Canadian STEC O157 and non-STEC O157 outbreaks linked to leafy greens during 2009 to 2018
- Determine barriers to solving outbreaks linked to leafy greens, according to epidemiologic, laboratory, and traceback data from US and Canadian STEC O157 and non-STEC O157 outbreaks linked to leafy greens during 2009 to 2018
- Identify research and public policy needs to prevent future STEC outbreaks linked to leafy greens, according to epidemiologic, laboratory, and traceback data from US and Canadian STEC O157 and non-STEC O157 outbreaks linked to leafy greens during 2009 to 2018

CME Editor

Deborah Wenger, MBA, Copyeditor, Emerging Infectious Diseases. *Disclosure: Deborah Wenger, MBA, has disclosed no relevant financial relationships.*

CME Author

Laurie Barclay, MD, freelance writer and reviewer, Medscape, LLC. *Disclosure: Laurie Barclay, MD, has disclosed no relevant financial relationships.*

Authors

Disclosures: ***Katherine E. Marshall, MPH; April Hexemer, MSc; Sharon L. Seelman, MS, MBA; Marianne K. Fatica, PhD; Tyann Blessington, PhD, MS, MPH; Maha Hajmeer, PhD; Hannah Kisselburgh, RN, MP; Robin Atkinson, BSc; Kristin Hill, MSc; Davendra Sharma, MSc; Michael Needham, MPH; Vi Peralta, MPH; Jeffrey Higa, MPH; Karen Blickenstaff, MS; Ian T. Williams, PhD, MS; Michael A. Jhung, MD, MPH; Matthew Wise, MPH, PhD;*** *and* ***Laura Gieraltowski, PhD, MPH,*** *have disclosed no relevant financial relationships.*

Author affiliations: Centers for Disease Control and Prevention, Atlanta, Georgia, USA (K.E. Marshall, H. Kisselburgh, I.T. Williams, M.A. Jhung, M. Wise, L. Gieraltowski); Public Health Agency of Canada, Ottawa, Ontario, Canada (A. Hexemer), Food and Drug Administration, College Park, Maryland, USA (S.L. Seelman, M.K. Fatica, T. Blessington, K. Blickenstaff), California Department of Public Health, Sacramento, California, USA (M. Hajmeer, M. Needham); California Department of Public Health, Richmond, California, USA (V. Peralta), California Department of Public Health, Los Angeles, California, USA (J. Higa); Canada Food Inspection Agency, Ottawa (R. Atkinson, K. Hill, D. Sharma).

DOI: https://doi.org/10.3201/eid2610.191418

Shiga toxin–producing *Escherichia coli* (STEC) cause substantial and costly illnesses. Leafy greens are the second most common source of foodborne STEC O157 outbreaks. We examined STEC outbreaks linked to leafy greens during 2009–2018 in the United States and Canada. We identified 40 outbreaks, 1,212 illnesses, 77 cases of hemolytic uremic syndrome, and 8 deaths. More outbreaks were linked to romaine lettuce (54%) than to any other type of leafy green. More outbreaks occurred in the fall (45%) and spring (28%) than in other seasons. Barriers in epidemiologic and traceback investigations complicated identification of the ultimate outbreak source. Research on the seasonality of leafy green outbreaks and vulnerability to STEC contamination and bacterial survival dynamics by leafy green type are warranted. Improvements in traceability of leafy greens are also needed. Federal and state health partners, researchers, the leafy green industry, and retailers can work together on interventions to reduce STEC contamination.

Shiga toxin–producing *Escherichia coli* (STEC) cause an estimated 265,000 illnesses (*1*) and cost $280 million (*2*) annually in the United States. STEC infection can occur through exposure to contaminated food, water, or the environment or contact with infected animals or humans. STEC are broadly categorized by serogroup: STEC O157 and non-O157 STECs (all other serogroups). Infection with STEC O157, although less common than those caused by non-O157 STECs, can be severe. Persons infected with STEC O157 are more likely to be hospitalized and develop hemolytic uremic syndrome (HUS) more frequently than those infected with non-O157 STECs (*3*).

In the United States, STEC O157 outbreaks were first linked to contaminated leafy greens in 1995 and non-O157 STEC outbreaks in 2010 (*4*–*6*). In Canada, STEC O157 outbreaks have been linked to leafy greens since 2012 (Public Health Agency of Canada [PHAC], unpub. data). Leafy greens are the second most common source of foodborne STEC O157 outbreaks in both countries, after ground beef (*4*,*5*) (A. Hexemer, unpub. data). Many animals can be STEC hosts, but ruminants, primarily cattle, are considered the major reservoir (*7*–*10*). STEC shed from cattle and wild animals can directly contaminate leafy greens or indirectly contaminate them through irrigation water, runoff, or dust containing feces (*8*,*11*–*13*).

Most US-produced leafy greens (98%) are grown in California and Arizona (*14*). Leafy greens consumed in the United States are grown principally in the desert regions of California, Arizona, and Mexico in the winter months (November–March), and in the central coastal regions of California in the spring, summer, and fall months (April–October) (*15*). Most leafy greens consumed in Canada are imported from the United States (D. Burgoyne, Canadian Food Inspection Agency, pers. comm., 2019 May 31).

We reviewed epidemiologic, laboratory, and traceback data from STEC O157 and non–O157 outbreaks in the United States and Canada linked to leafy greens during 2009–2018. We summarize epidemiologic findings, describe barriers to solving outbreaks, and identify research needs to prevent future leafy green outbreaks.

Methods

We collected data on STEC O157 and non–O157 outbreaks that were linked to leafy greens during 2009–2018 from the following sources: Centers for Disease Control and Prevention (CDC) Foodborne Disease Outbreak Surveillance System (FDOSS; 2009–2017 only); internal CDC and PHAC databases used to manage multistate outbreak investigations; and PulseNet, the national molecular subtyping network for foodborne disease surveillance (*16*). We defined an outbreak as ≥2 similar illnesses in persons with a common exposure. Outbreaks for which STEC was listed as the single causative pathogen, with ≥2 culture-confirmed cases of infection, and for which leafy greens were listed as a suspected or confirmed source, were included in this report. HUS was identified by physician diagnosis.

Local, state or provincial, and federal health officials assessed 3 types of evidence (epidemiologic, traceback, and microbiologic) to determine outbreak sources during an investigation. For epidemiologic evidence, health officials interviewed ill persons to gather detailed information on foods they ate, determine whether any foods were reported more frequently than expected (compared with the FoodNet population survey [*17*]), and determine whether persons ate food from the same point of sale (e.g., grocery stores, restaurants) or event (collectively defined as a subcluster). For traceback evidence, officials collected and evaluated records documenting the movement of foods to and from all points in a distribution chain (e.g., receipts, grocery store shopper cards, restaurant rewards numbers, invoices, bills of lading) to determine whether there was a common point of contamination from at least two distinct points of sale. The Canada Food Inspection Agency (CFIA) conducted traceback to points of importation, based on methodology employed in Canada (*18*). For microbiologic evidence, officials sampled foods

and environments of restaurants, production facilities, or growing areas suspected to be the source of outbreaks and conducted microbiologic testing for the outbreak strain. Food sources were classified as suspected or confirmed outbreak vehicles based on the evidence collected during the investigation. For outbreaks linked to a single event or meal, only 1 type of evidence (epidemiologic, traceback, or microbiologic) was needed to be considered confirmed. For multistate outbreaks, or outbreaks during which ill persons reported exposures in multiple venues, vehicles were classified as suspected if only 1 type of evidence was identified and confirmed if ≥2 types of evidence were identified.

Outbreaks that occurred in both the United States and in Canada were counted as a single outbreak if they occurred at the same time and had the same outbreak strain. Outbreaks were classified by the state or province where ill persons were exposed to leafy greens.

We calculated the outbreak duration as the number of days between the first and last illness onset dates. We defined the outbreak investigation lag as the number of days between the first illness onset date and the date the coordinating agency began its investigation. We compared median outbreak size by vehicle status using the Kruskal-Wallis test and leafy green type by vehicle status using the Fisher exact test. We defined seasonality using the date of first illness onset for each outbreak and divided the year into 4 periods: spring (March–May), summer (June–August), fall (September–November), and winter (December–February). Outbreak vehicles were categorized as leafy greens according to the Interagency Food Safety Analytics Collaboration categorization schema (*19*). Outbreak strains were characterized using 2-enzyme pulsed-field gel electrophoresis.

CDC, FDA, PHAC, US state and local, and Canadian provincial health departments described outbreaks via press releases, Internet, Facebook, and Twitter posts to inform the public of measures they could take to protect themselves. Data on outbreak announcements were collected from CDC, FDA, and PHAC. Additional announcements may have been posted by state or provincial and local health departments but were not captured in this report.

Results

Epidemiology

We identified 40 outbreaks of STEC infections during 2009–2018 with leafy greens as a confirmed (18 outbreaks) or suspected (22 outbreaks) source (Appendix Table, https://wwwnc.cdc.gov/EID/article/26/10/19-1418-App1.pdf). One additional STEC outbreak linked to leafy greens was excluded from analysis because it was caused by an ill food handler. Each year, 1–9 outbreaks occurred (Figure 1). Thirty-one outbreaks occurred in the United States only (22 multistate, 9 single state), 4 in Canada only (all multiprovince), and 5 in both Canada and the United States (4 multistate and multiprovince, 1 single state and multiprovince). These 40 outbreak investigations included 1,212 reported illnesses (1,146 laboratory-confirmed), 420 hospitalizations, 77 cases of HUS, and 8 deaths (Table 1). Ill persons ranged in age from <1 to 95 years (median 26); 63% were female. Outbreaks ranged from 3 to 248 (median 16) laboratory-confirmed illnesses; outbreaks with leafy greens as a confirmed source were larger than those with a suspected source (median 31 illnesses vs. 10 illnesses; $p = 0.006$).

Romaine lettuce was identified more often than any other type of leafy green as the outbreak source. Among the 29 (73%) STEC outbreaks with information on a specific leafy green type, 24 implicated a single type: 13 (54%) romaine, 4 (17%) spinach, 4 (17%) iceberg, and 1 (4%) each of cabbage, green leaf, and kale. (In 2015, the US investigation identified romaine lettuce as the outbreak source, and the Canadian investigation was not able to determine a specific type of leafy green. In 2017, the Canadian investigation linked an outbreak of STEC O157 to romaine lettuce, and the US investigation did not result in enough epidemiologic evidence to implicate a specific type of leafy greens. For the purposes of this article, the leafy green type was classified as unknown for these outbreaks.) Among the 24 outbreaks linked to a single lettuce type, 11 were confirmed, and romaine was more likely to be confirmed than any other leafy green type (10/13 vs. 1/11; $p = 0.002$). Five outbreaks were linked to multiple leafy green types: 3 romaine and iceberg, 1 butter and radicchio, and 1 spinach and spring mix (Table 2).

More STEC outbreaks linked to leafy greens began during the fall (18, 45%) than spring (11, 28%), summer (7, 18%), or winter (4, 10%) (Figures 2, 3). More outbreaks began in October (9 outbreaks, 23%) and April (8 outbreaks, 20%) than any other month. The median outbreak duration was 21 days (range 1–162 days). The median investigation lag was 22 days.

Environmental and Laboratory Testing

STEC O157 was the most common cause of leafy green STEC outbreaks. Among the 40 STEC

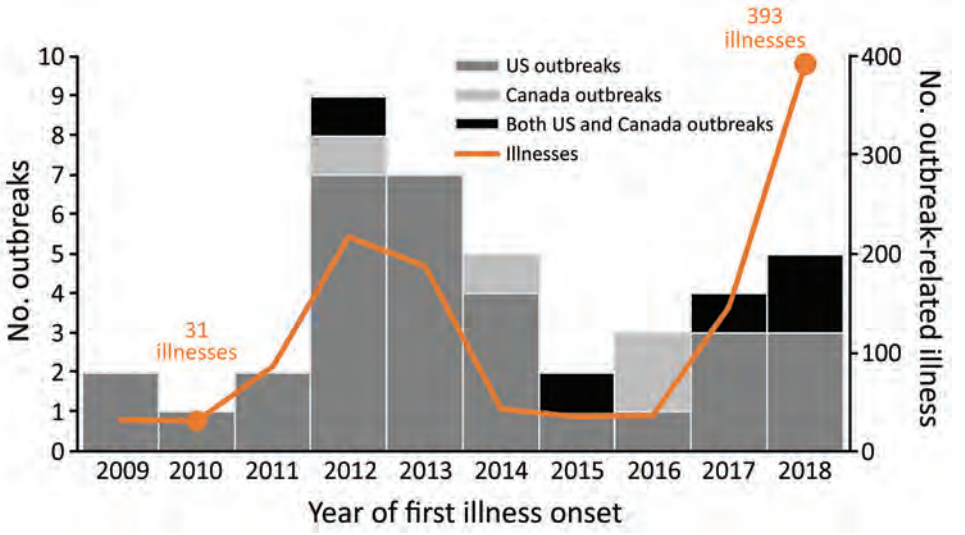

Figure 1. Number of Shiga toxin–producing *Escherichia coli* outbreaks (n = 40) linked to leafy greens in the United States, Canada, or both countries, and all outbreak-related illnesses (n = 1,212), by year of first illness onset, 2009–2018.

outbreaks, 32 (80%) were caused by STEC O157; 3 by (8%) STEC O145; 2 (5%) by STEC O26; 1 (3%) each by serogroups STEC O111 and STEC O126; and 1 by both STEC O26 and STEC O157 (Appendix Table).

Of investigations with information, investigators found the outbreak strain in leafy greens in 2 outbreaks, and in the environment where greens were processed or grown in 4 outbreaks (Appendix Table). In 1 investigation, the outbreak strain was isolated from irrigation canal water samples collected upstream and downstream from a cattle concentrated animal feeding operation (CAFO) and in the area of several romaine farms identified during traceback (*20*). In a second investigation, the outbreak strain was isolated from sediment from a water reservoir on a romaine farm identified through traceback (*21*). In 2 other outbreak investigations, isolates collected during a separate project assessing STEC prevalence in California Central Coast watersheds were uploaded to PulseNet and matched the outbreak strains (*22*).

Traceback

In the United States, traceback was conducted by FDA (15 outbreaks) and the California Department of Public Health (CDPH; 11 outbreaks). Some traceback investigations overlapped with multiple agencies investigating the same incident. Each traceback included 2–23 points of sale (median 4); 1–9 ill persons were associated with each point of sale. Points of sale were distributed across 1–12 states (median 2). When both FDA and CDPH conducted traceback for a multistate outbreak, FDA data were used to calculate the median. For some outbreaks, US and Canadian information was combined to determine a common source; data from Canada were removed from the US summary for these results.

CFIA conducted traceback for 7 of 9 outbreaks. For these 7 outbreaks, leafy greens were traced back from 2–30 points of service, 1–11 distributors/processors, multiple brands, and ≤21 suppliers. Two examples that highlight the complexity of traceback include an outbreak in 2012 linked to iceberg and

Table 1. STEC outbreaks linked to contaminated leafy greens in the United States and Canada, 2009–2018*

Characteristic	US	Canada	Binational	All STEC
Outbreaks	31	4	5	40
Vehicle status				
Confirmed	14	1	3	18
Suspected	17	3	2	22
Serogroup				
STEC O157	24	4	4	32
Non-O157 STEC	7	0	0	7
Both	0	0	1	1
Total cases	677	65	470	1,212
Confirmed primary cases	621	65	460	1,146
Hospitalizations	203	26	191	420
Cases of HUS	35	4	38	77
Deaths	1	0	7	8

*HUS, hemolytic uremic syndrome; STEC, Shiga toxin–producing *Escherichia coli*.

Table 2. STEC outbreaks linked to leafy greens by type of leafy green implicated, United States and Canada, 2009–2018*

Leafy green type	Outbreaks with information for type of leafy green†	Outbreaks with single known type of leafy green implicated	Outbreak-related illnesses attributed to outbreak with single type of implicated leafy green
Romaine	16 (40)	13 (54)	617 (84)
Iceberg	7 (18)	4 (17)	54 (7)
Spinach	5 (13)	4 (17)	32 (4)
Cabbage	1 (3)	1 (4)	16 (2)
Kale	1 (3)	1 (4)	7 (1)
Green leaf	1 (3)	1 (4)	5 (0.7)
Butter lettuce	1 (3)	NA	NA
Radicchio	1 (3)	NA	NA
Spring mix	1 (3)	NA	NA
Unknown	11 (28)‡	NA	NA
Total	40	24	731

*Values are no. (%) except as indicated. NA, not applicable; STEC, Shiga toxin–producing *Escherichia coli*.
†More than 1 type of leafy green may have been reported for a given outbreak.
‡This includes two outbreaks that occurred in both the US and Canada. In 2015, the US investigation identified romaine lettuce as the outbreak source, and the Canadian investigation was not able to determine a specific type of leafy green. In 2017, the Canadian investigation linked an outbreak of STEC O157 to romaine lettuce, and the US investigation did not result in enough epidemiologic evidence to implicate a specific type of leafy green. For the purposes of this study, the leafy green type for these outbreaks was classified as unknown. For 1 outbreak, multiple leafy green types, including kale, spinach, and romaine, were reported and traced back but the leafy green type remained unknown.

romaine mix imported to Canada from the United States, which was mixed and packaged in 21 product combinations comprising 18 lots. A second outbreak in 2015 was not linked to a specific leafy green type, but multiple greens (kale, spinach, and romaine) were reported and traced back; investigators identified 53 potentially implicated products from 11 distributors. Most leafy greens were imported to Canada from the United States.

Public Messaging and Product Action

Five (12.5%) of 40 outbreaks resulted in a food recall (Appendix Table). Recalled items included bagged shredded romaine, bagged spinach and spring mix, shredded iceberg and romaine, and ready-to-eat salads and sandwich wraps containing romaine. In a fall 2018 outbreak linked to romaine lettuce, potentially contaminated romaine lettuce was not recalled because it was no longer available for sale. However, the implicated firm voluntarily recalled other leafy greens and vegetables that came into contact with agricultural water from a reservoir with sediment that yielded the outbreak strain.

Nine (23%) leafy green STEC outbreaks were publicly announced by federal agencies, usually when there was an action that consumers could take to prevent illness (https://www.cdc.gov/foodsafety/outbreaks/investigating-outbreaks/communication/index.html). These actions included not eating recalled leafy greens (4 outbreaks) or not eating leafy greens grown in a specific region or county (2 outbreaks). Three outbreak postings did not advise consumers to take action around any specific leafy greens but informed the public of the investigation. Leafy greens were usually out of the supply chain (and therefore unavailable to consumers) by the time the investigation identified them as the outbreak source, minimizing the ongoing risk to the public and reducing the need for immediate public notification.

Discussion

Over the past decade, multiple STEC outbreaks linked to leafy greens occurred in the United States and Canada, causing illness that was widespread and often severe. Most STEC outbreaks linked to leafy greens were caused by STEC O157, even though non-O157 STEC cause more sporadic US illnesses and are more frequently isolated from cattle (*10*); reasons for this discrepancy are unclear.

Despite year-round US leafy green production, 73% of STEC outbreaks linked to leafy greens began during the spring or fall. This seasonality was noted in a previous study of STEC O157 outbreaks (*5*); however, reasons for this seasonal pattern are unclear. Seasonal differences in consumption and production are one possible explanation. However, US data from 2007 (CDC FoodNet, unpub. data) and Canadian data from 2014–2015 (*23*) indicate that leafy green consumption changed little by month and did not show increases during the spring and fall. Data for leafy greens produced in 2009 showed some variation in domestic shipment volume by month but did not show an apparent increase in shipments in the spring and fall (*14*). Notably, the peak outbreak months in our report (October and April) coincided with the period when growers have historically used the short-term California Central Valley growing region to fill the gap in leafy green production between the California Central Coast and the desert regions of California, Arizona, and Mexico (*24*). We could not further assess any potential link between outbreak timing and harvest location because the movement of growing and harvesting

operations varies by year and company, and there was a limited number of outbreaks during 2009–2018 for which growing locations were identified. Additional data on growing and harvesting practices, intrinsic factors of leafy greens that might make them susceptible to contamination, and the effect of climate or specific weather events during the growing seasons are needed to further assess seasonality of outbreaks.

Environmental assessments rarely occurred during investigations of leafy green outbreaks.

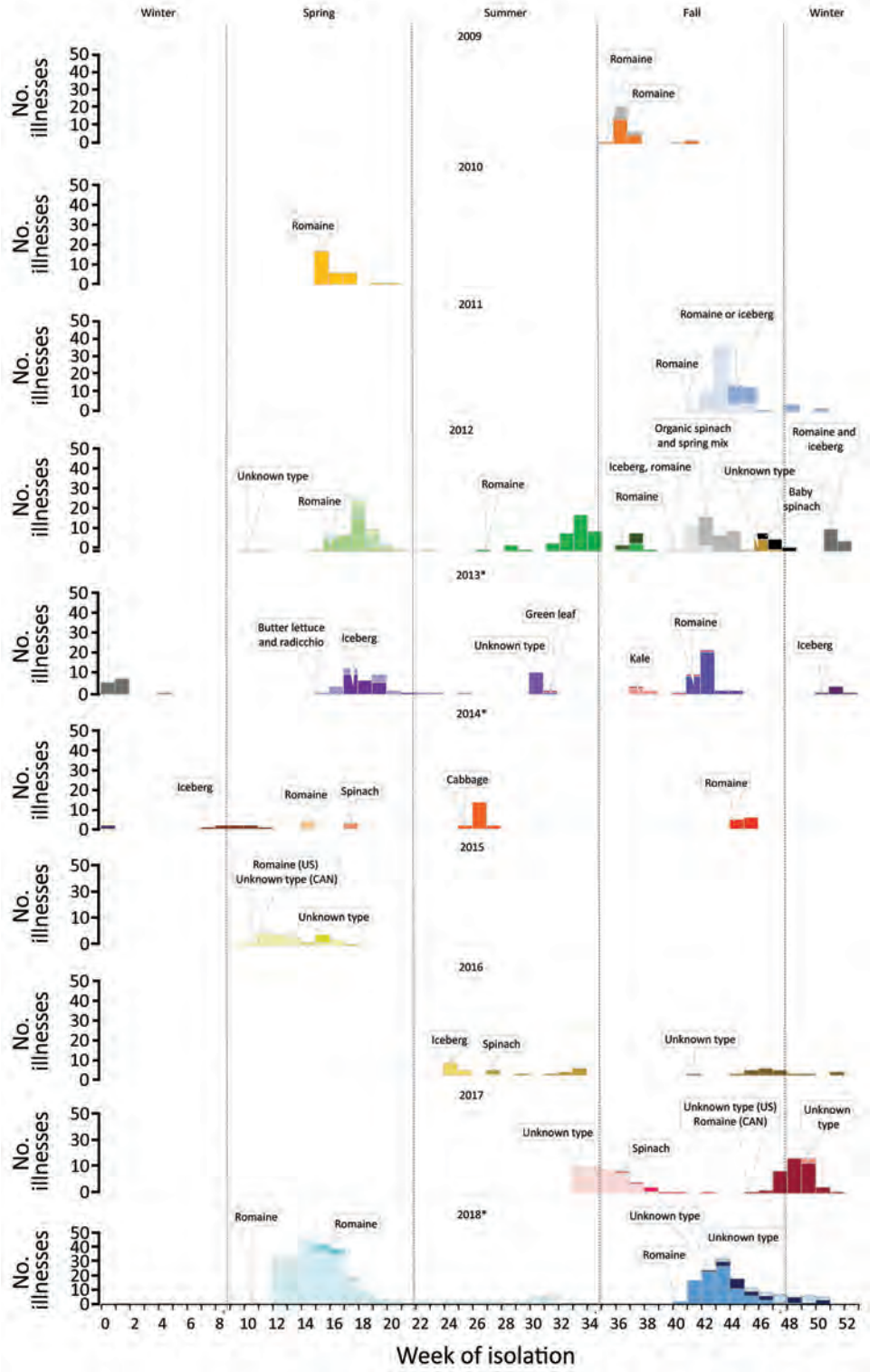

Figure 2. Outbreak-related Shiga toxin–producing *Escherichia coli* illnesses (n = 1,124) linked to leafy greens, by isolation date, outbreak, and vehicle, United States and Canada, 2009–2018. Data on isolation date were available for 1,124 (98%) of 1,146 laboratory-confirmed illnesses. Illness onset date was not systematically collected for each case. Each color represents a different outbreak. *During these years, each season started 1 week earlier.

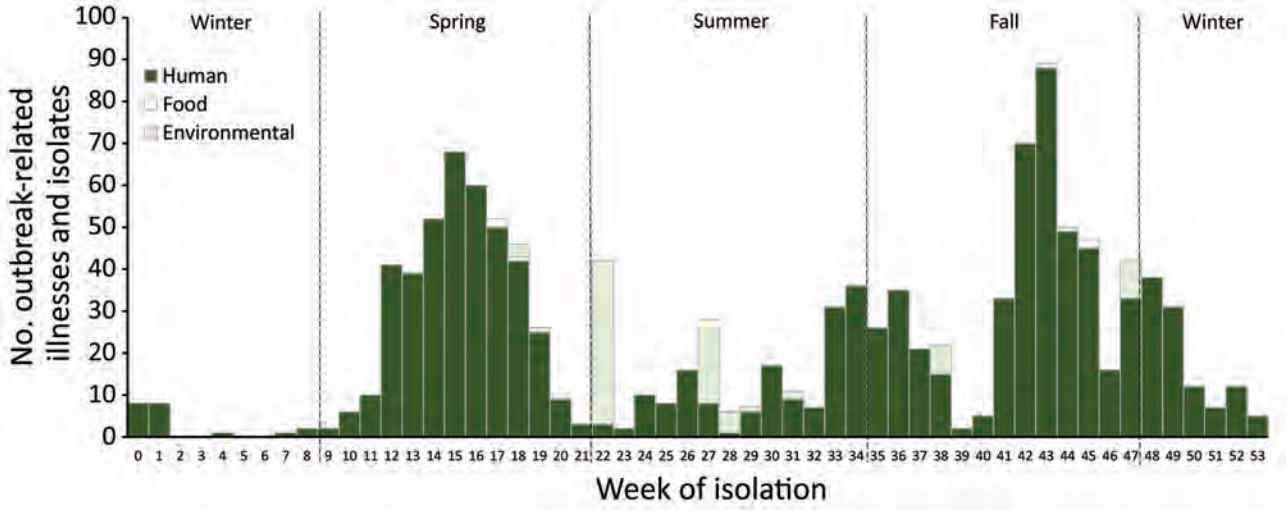

Figure 3. Outbreak-related Shiga toxin–producing *Escherichia coli* laboratory-confirmed illnesses (n = 1,124 illnesses for which information was available) and food (n = 8; spinach, romaine) and environmental isolates (n = 86; soil, water, sediment, scat) linked to leafy greens, by week of isolation, United States and Canada, 2009–2018.

Environmental assessments can occur only after epidemiologic and traceback investigations identify where implicated product is grown, processed, or distributed. Although they are resource intensive, these assessments can provide valuable insight into outbreak causes and identify possible areas to target for prevention efforts. Environmental assessments conducted during multiple leafy green investigations have suggested a possible link between product contamination and STEC contamination of nearby soil or water caused by cattle or wild pigs (*25*,*26*), dairy farms (*27*), or CAFOs (*28*). These findings build on 2 studies conducted in leafy green growing regions in California; one identified a higher prevalence of STEC O157 in a watershed near cattle (*29*), and another detected STEC O157 in beef cattle feces, mostly during dates in the spring and fall when leafy greens are typically grown, although the number of samples that yielded STEC O157 was small (*13*). Furthermore, some leafy green growing regions are home to large numbers of cattle: the Central Valley growing region (encompassing Fresno, Tulare, and Kings Counties) had >1.8 million head of cattle in 2016–2017, comprising nearly one third of all cattle in California (*30*). Conducting additional environmental assessments to better understand the relationship between cattle and leafy green growing locations, water, and the occurrence and timing of outbreaks may be beneficial.

More STEC outbreaks were linked to romaine than to any other type of leafy green, similar to an analysis of leafy greens–related incidents linked to California (*31*). More iceberg was harvested and available for purchase than romaine each year during 2009–2017, although romaine harvest and availability increased over time (*32*,*33*). The share of category dollars spent on iceberg and romaine was the same during 2012, higher for iceberg in 2013–2014, and higher for romaine in 2016–2017 (*34*). Together, these data suggest that even though romaine increased in popularity, it is unlikely that this alone explains why more STEC outbreaks in the past decade were linked to romaine than to any other leafy green. Because standard investigation questionnaires include questions about multiple leafy green types, such as spinach, iceberg, kale, and romaine (*35*), investigational bias toward romaine is unlikely. Romaine may have some characteristics that may make it more vulnerable to STEC contamination, including its shape and physiology (romaine is tall with loosely clumped leaves, open at the top; iceberg is smaller with compact leaves). Additional studies comparing the likelihood of STEC contamination and bacterial survival dynamics by leafy green type are warranted.

More than half of STEC outbreak investigations identified leafy greens as a suspected, rather than confirmed, source. Several characteristics of leafy green outbreaks make them inherently difficult to solve, and therefore challenging to implement timely interventions to reduce illness. The short shelf life of leafy greens (12–16 days) (*36*), the lag in identifying outbreaks (22 days), and the short duration of most outbreaks (21 days) all limit opportunities for investigators to interview ill persons in a timely fashion. This limitation can hamper hypothesis generation and limit opportunities to test leafy greens for contamination. Finally, because leafy greens, especially

iceberg and romaine, are commonly consumed in the United States (*17*) and Canada (*23*), it can be difficult to show that they were eaten more often than expected by ill persons who are part of outbreaks. Establishing an epidemiologic link between cases and contaminated leafy greens often requires other corroborating pieces of evidence (e.g., brand or variety) to implicate a specific leafy green type. To help solve outbreaks, investigators have used successful strategies such as subcluster and purchase record analyses (*37*–*39*).

Traceback investigations for leafy green outbreaks are complex. First, product information from packaging is rarely available when an investigation begins. Therefore, ill persons are asked to remember crucial information needed to identify and trace leafy greens (e.g., purchase location and date, type/brand) instead of simply referring to an open package. Second, associating leafy greens at a point of sale location with a particular distribution lot can be challenging. Even though lot information may be available on the packaging for prepackaged leafy greens, points of sale may not record and track it after the packages are received. Investigators rely solely on records collected at each point in the distribution chain to determine the lots and source of a product, but they often lack the data elements needed to link lots of incoming shipments of products with lots of outgoing shipments. Finally, commingling of leafy greens from different farms throughout the distribution chain further complicates efforts to identify a single lot or source.

Complete, detailed records of transactions at each point along the fork-to-farm continuum are critical to accurately and quickly trace leafy greens during an outbreak investigation. Several strategies could increase the likelihood of success. Industry could assist by maintaining records that are consistently available, accurate, and complete. Retailers that sell leafy greens could consider developing systems to track lot and source information for leafy greens after they are received. Retailers may also wish to require producers be able to trace leafy greens and components of packaged mixes back to the farms from which they were harvested.

Several policies and recommendations were put into place before and after the study to improve the safety of leafy greens and prevent future outbreaks. In 2011, the US FDA Food Safety Modernization Act (FSMA) was signed into law (*40*). Under that law, in 2016, the Final Rule for Produce Safety went into effect, which established science-based minimum standards for the safe growing, harvesting, packing, and holding of US produce, including leafy greens. The first major compliance date for produce other than sprouts was in January 2018 (*41*). Routine regulatory inspections were set to begin in spring 2019, and compliance with agricultural water requirements were extended to become effective in 2022 (*42*). In 2007, the California and Arizona leafy greens industries each formed their own leafy greens products handler marketing agreement and enacted food safety recommendations (*43*) after a large 2006 STEC O157 outbreak linked to spinach (*25*). In response to the 2 large 2018 outbreaks, in 2019, California and Arizona Leafy Greens Products Handler Marketing Agreement modified their recommendations for leafy green growers, including increasing buffer zones between CAFOs and leafy green fields; requiring environmental assessments after severe weather events; requiring that all lot data be identified for products entering the marketplace; limiting or prohibiting the use of surface water for overhead irrigation of leafy greens before harvest; and requiring farmers to categorize sources of water, consider how it is applied to leafy greens, and test and sanitize it if needed (*44*–*47*). Future analyses should be conducted to assess the effect of these policies, recommendations, and any other implemented changes.

STEC outbreaks linked to leafy greens have continued to occur over the past decade. The combination of challenges investigators face during epidemiologic and traceback investigations of leafy greens make timely communication of actionable advice for consumers difficult. Despite challenges, results from leafy green outbreak investigations have led to changes in industry recommendations. However, knowledge gaps remain, including the drivers of the seasonality of leafy green outbreaks, and knowledge of why outbreaks are disproportionately linked to romaine lettuce. Investigators should work with federal and state health partners, the research community, the leafy green industry, and retailers to fill these knowledge gaps and collect additional information. Additional efforts should include identifying data points that would improve traceability of leafy greens during outbreaks. Collectively, these efforts can help inform prevention strategies to avoid or mitigate future outbreaks and lead to further changes in the way food is grown and processed, which could make leafy greens safer for the public to consume.

Acknowledgments

We thank Mackenzie Tewell, Arizona Department of Health Services; Philippe Belanger, Public Health Agency of Canada; state, provincial, and local health departments; and the FDA Human and Animal Food Divisions.

About the Author

Ms. Marshall is an epidemiologist and deputy lead of the Prevention and Evaluation Activity in the Outbreak Response and Prevention Branch, Division of Foodborne, Waterborne and Environmental Diseases, Centers for Disease Control and Prevention, Atlanta, GA, USA. Her research interests are food safety, prevention of enteric diseases and outbreaks of *Salmonella*, Shiga toxin-producing *Escherichia coli*, and *Listeria monocytogenes* infections.

References

1. Scallan E, Hoekstra RM, Angulo FJ, Tauxe RV, Widdowson MA, Roy SL, et al. Foodborne illness acquired in the United States—major pathogens. Emerg Infect Dis. 2011;17:7–15. https://doi.org/10.3201/eid1701.P11101
2. Hoffmann S, Batz MB, Morris JG Jr. Annual cost of illness and quality-adjusted life year losses in the United States due to 14 foodborne pathogens. J Food Prot. 2012;75:1292–302. https://doi.org/10.4315/0362-028X.JFP-11-417
3. Gould LH, Demma L, Jones TF, Hurd S, Vugia DJ, Smith K, et al. Hemolytic uremic syndrome and death in persons with *Escherichia coli* O157:H7 infection, foodborne diseases active surveillance network sites, 2000–2006. Clin Infect Dis. 2009;49:1480–5. https://doi.org/10.1086/644621
4. Rangel JM, Sparling PH, Crowe C, Griffin PM, Swerdlow DL. Epidemiology of *Escherichia coli* O157:H7 outbreaks, United States, 1982–2002. Emerg Infect Dis. 2005;11:603–9. https://doi.org/10.3201/eid1104.040739
5. Heiman KE, Mody RK, Johnson SD, Griffin PM, Gould LH. *Escherichia coli* O157 outbreaks in the United States, 2003–2012. Emerg Infect Dis. 2015;21:1293–301. https://doi.org/10.3201/eid2108.141364
6. Ackers M-L, Mahon BE, Leahy E, Goode B, Damrow T, Hayes PS, et al. An outbreak of *Escherichia coli* O157:H7 infections associated with leaf lettuce consumption. J Infect Dis. 1998;177:1588–93. https://doi.org/10.1086/515323
7. Borczyk AA, Karmali MA, Lior H, Duncan LMC. Bovine reservoir for verotoxin-producing *Escherichia coli* O157:H7. Lancet. 1987;329:98. https://doi.org/10.1016/s0140-6736(87)91928-3
8. Persad AK, Lejeune JT. Animal reservoirs of Shiga toxin-producing *Escherichia coli*. Microbiol Spectr. 2015;2:EHEC-0027-2014. https://doi.org/ 0.1128/microbiolspec.EHEC-0027-2014
9. Gyles C. Shiga toxin-producing *Escherichia coli*: an overview. J Anim Sci. 2007;85(suppl_13):E45–62. https://doi.org/10.2527/jas.2006-508
10. Montenegro MA, Bülte M, Trumpf T, Aleksić S, Reuter G, Bulling E, et al. Detection and characterization of fecal verotoxin-producing *Escherichia coli* from healthy cattle. J Clin Microbiol. 1990;28:1417–21. https://doi.org/10.1128/JCM.28.6.1417-1421.1990
11. Yanamala S, Miller M, Loneragan G, Gragg S, Brashears M. Potential for microbial contamination of spinach through feedyard air/dust growing in close proximity to cattle feedyard operations. J Food Saf. 2011;31:525–9. https://doi.org/10.1111/j.1745-4565.2011.00330.x
12. Berry ED, Wells JE, Bono JL, Woodbury BL, Kalchayanand N, Norman KN, et al. Effect of proximity to a cattle feedlot on *Escherichia coli* O157:H7 contamination of leafy greens and evaluation of the potential for airborne transmission. Appl Environ Microbiol. 2015;81:1101–10. https://doi.org/10.1128/AEM.02998-14
13. Benjamin L, Jay-Russell MT, Atwill ER, Cooley M, Carychao D, Larsen R, et al. Risk factors for *Escherichia coli* O157 on beef cattle ranches located near a major produce production region. Epidemiol Infect. 2015;143:81–93. https://doi.org/10.1017/S0950268814000521
14. United States Department of Agriculture. U.S. lettuce statistics, tables 1, 2, 39, 40; 2011 [cited 2019 Jan 23]. https://usda.library.cornell.edu/concern/publications/cc08hf60z
15. Jay-Russell MT, Hake AF, Bengson Y, Thiptara A, Nguyen T. Prevalence and characterization of *Escherichia coli* and *Salmonella* strains isolated from stray dog and coyote feces in a major leafy greens production region at the United States–Mexico border. PLoS One. 2014;9:e113433. https://doi.org/10.1371/journal.pone.0113433
16. Swaminathan B, Barrett TJ, Hunter SB, Tauxe RV, Force CPT; CDC PulseNet Task Force. PulseNet: the molecular subtyping network for foodborne bacterial disease surveillance, United States. Emerg Infect Dis. 2001;7:382–9. https://doi.org/10.3201/eid0703.017303
17. Centers for Disease Control and Prevention. Foodborne Active Surveillance Network (FoodNet) population survey atlas of exposures, 2006–2007 [cited 2019 May 1]. https://www.cdc.gov/foodnet/surveys/population.html
18. Health Canada, Public Health Agency of Canada, Canadian Food Inspection Agency. Weight of evidence: factors to consider for appropriate and timely action in a foodborne illness outbreak investigation; 2011 [cited 2019 May 1]. https://www.canada.ca/content/dam/hc-sc/migration/hc-sc/fn-an/alt_formats/pdf/pubs/securit/2011-food-illness-outbreak-eclosion-malad-ailments-eng.pdf
19. Richardson LC, Bazaco MC, Parker CC, Dewey-Mattia D, Golden N, Jones K, et al. An updated scheme for categorizing foods implicated in foodborne disease outbreaks: a tri-agency collaboration. Foodborne Pathog Dis. 2017;14:701–10. https://doi.org/10.1089/fpd.2017.2324
20. Bottichio L, Keaton A, Thomas D, Fulton T, Tiffany A, Frick A, et al. Shiga toxin–producing *Escherichia coli* infections associated with romaine lettuce—United States, 2018. Clin Infect Dis. 2019;ciz1182. https://doi.org/10.1093/cid/ciz1182
21. Centers for Disease Control and Prevention. Food safety alert: outbreak of *E. coli* infections linked to romaine lettuce; 2019 [cited 2019 Jan 23]. https://www.cdc.gov/ecoli/2018/o157h7-11-18/index.html
22. Cooley MB, Quiñones B, Oryang D, Mandrell RE, Gorski L. Prevalence of shiga toxin producing *Escherichia coli*, *Salmonella enterica*, and *Listeria monocytogenes* at public access watershed sites in a California central coast agricultural region. Front Cell Infect Microbiol. 2014;4:30. https://doi.org/10.3389/fcimb.2014.00030
23. Public Health Agency of Canada. Foodbook report 2014–2015. November 2015 [cited 2019 May 31]. https://www.canada.ca/en/public-health/services/publications/food-nutrition/foodbook-report.html
24. Smith RCM, Daugovish O, Koike S, Natwick E, Smith H, Subbarao K, et al. Leaf lettuce production in California: University of California Agricultural and Natural Resources Vegetable Research and Information Center 2011 [cited 2019 Oct 1]. https://anrcatalog.ucanr.edu/pdf/7216.pdf
25. Sharapov UM, Wendel AM, Davis JP, Keene WE, Farrar J, Sodha S, et al. Multistate outbreak of *Escherichia coli* O157:H7 infections associated with consumption of fresh spinach: United States, 2006. J Food Prot. 2016;79:2024–30. https://doi.org/10.4315/0362-028X.JFP-15-556
26. Jay MT, Cooley M, Carychao D, Wiscomb GW, Sweitzer RA, Crawford-Miksza L, et al. *Escherichia coli* O157: H7 in feral

swine near spinach fields and cattle, central California coast. Emerg Infect Dis. 2007;13:1908–11. https://doi.org/10.3201/eid1312.070763
27. Gelting RJ, Baloch M. A systems analysis of irrigation water quality in environmental assessments related to foodborne outbreaks. Aquat Procedia. 2013;2:130–7. https://doi.org/10.1016/j.aqpro.2013.07.011
28. US Food and Drug Administration. Environmental assessment of factors potentially contributing to the contamination of romaine lettuce implicated in a multi-state outbreak of *E. coli* O157:H7. 2018 [cited 2019 May 24]. https://www.fda.gov/food/outbreaks-foodborne-illness/environmental-assessment-factors-potentially-contributing-contamination-romaine-lettuce-implicated
29. Cooley M, Carychao D, Crawford-Miksza L, Jay MT, Myers C, Rose C, et al. Incidence and tracking of *Escherichia coli* O157:H7 in a major produce production region in California. PLoS One. 2007;2:e1159. https://doi.org/10.1371/journal.pone.0001159
30. California Department of Food and Agriculture. California agricultural statistics review, 2016–2017 [cited 2019 Oct 1]. https://www.nass.usda.gov/Statistics_by_State/California/Publications/Annual_Statistical_Reviews/2017/2016cas-all.pdf2016-2017
31. Turner K, Moua CN, Hajmeer M, Barnes A, Needham M. Overview of leafy greens–related food safety incidents with a California link: 1996 to 2016. J Food Prot. 2019;82:405–14. https://doi.org/10.4315/0362-028X.JFP-18-316
32. United States Department of Agriculture Economic Research Service. Vegetables and pulses yearbook tables 2018. US per capita availability of selected, commerically produced, fresh and processing vegetables and dry pulse crops, 1970–2017 [cited 2019 May 1]. https://www.ers.usda.gov/data-products/vegetables-and-pulses-data/vegetables-and-pulses-yearbook-tables
33. National Agricultural Statistics Service. Vegetables, lettuce; 2018 [cited 2018 Jan 24]. https://www.nass.usda.gov/Statistics_by_Subject/index.php?sector=CROPS
34. Nielsen Perishables Group. Consumer perishables databook, 2012–2017. New York: McFadden Grocery Headquarters; 2012–2017.
35. Centers for Disease Control and Prevention. Foodborne disease outbreak investigation and surveillance tools; 2017 [cited 2019 May 1]. https://www.cdc.gov/foodsafety/outbreaks/surveillance-reporting/investigation-toolkit.html
36. Food and Drug Administration. Program information manual retail food protection: recommendations for the temperature control of cut leafy greens during storage and display in retail food establishments. 2010 [cited 2019 April 24]. https://www.fda.gov/food/retail-food-industry-regulatory-assistance-training/program-information-manual-retail-food-protection-recommendations-temperature-control-cut-leafy
37. Angelo KM, Chu A, Anand M, Nguyen T-A, Bottichio L, Wise M, et al. Outbreak of *Salmonella* Newport infections linked to cucumbers—United States, 2014. MMWR Morb Mortal Wkly Rep. 2015;64:144–7.
38. Gieraltowski L, Julian E, Pringle J, Macdonald K, Quilliam D, Marsden-Haug N, et al. Nationwide outbreak of *Salmonella* Montevideo infections associated with contaminated imported black and red pepper: warehouse membership cards provide critical clues to identify the source. Epidemiol Infect. 2013;141:1244–52. https://doi.org/ 10.1017/S0950268812001859
39. Miller BD, Rigdon CE, Robinson TJ, Hedberg C, Smith KE. Use of global trade item numbers in the investigation of a *Salmonella* Newport outbreak associated with blueberries in Minnesota, 2010. J Food Prot. 2013;76:762–9. https://doi.org/10.4315/0362-028X.JFP-12-407
40. Food and Drug Administration. FDA Food Safety Modernization Act (FSMA). 2013 [cited 2013 Oct 2]. https://www.fda.gov/food/guidance-regulation-food-and-dietary-supplements/food-safety-modernization-act-fsma
41. Standards for the growing, harvesting, packing, and holding of produce for human consumption, 80 FR 74353; 2015 [cited 2019 May 1]. https://www.govinfo.gov/app/details/FR-2015-11-27/2015-28159
42. US Food and Drug Administration. Proposed extension of agricultural water compliance dates, 21 CFR 112; 2017 [cited 2019 Jan 17]. https://www.federalregister.gov/documents/2017/09/13/2017-19434/standards-for-the-growing-harvesting-packing-and-holding-of-produce-for-human-consumption-extension
43. California Leafy Greens Marketing Agreement. California leafy green products handler marketing agreement. 2018 [cited 2018 Aug 27]. http://www.caleafygreens.ca.gov/about-us
44. California Leafy Greens Marketing Agreement. Technical committees recommend metrics changes; 2018 [cited 2018 Dec 7]. http://www.caleafygreens.ca.gov/2018/08/committees-metrics-changes
45. California Leafy Greens Marketing Agreement. New, more stringent food safety practices adopted to prevent outbreaks; 2019 [cited 2019 Apr 24]. https://lgma.ca.gov/2019/04/new-practices-prevent-outbreaks
46. Arizona Leafy Greens Marketing Agreement. Arizona LGMA updates food safety practices for the upcoming growing season; 2018 [cited 2018 Dec 7]. https://www.arizonaleafygreens.org/single-post/2018/09/18/Arizona-LGMA-updates-food-safety-practices-for-the-upcoming-growing-season
47. Arizona Leafy Greens Marketing Committee. Commodity specific food safety guidelines for the production and harvest of lettuce and leafy greens; 2019 [cited 2019 Aug 29]. https://www.arizonaleafygreens.org/guidelines2019

Address for correspondence: Katherine E. Marshall, Centers for Disease Control and Prevention, 1600 Clifton Rd NE, Mailstop H24-10, Atlanta, GA 30329-4027, USA; email: uwj0@cdc.gov

Operating Protocols of a Community Treatment Center for Isolation of Patients with Coronavirus Disease, South Korea

EunKyo Kang,[1] Sun Young Lee,[1] Hyemin Jung, Min Sun Kim, Belong Cho, Yon Su Kim

Most persons with confirmed coronavirus disease (COVID-19) have no or mild symptoms. During the COVID-19 pandemic, communities need efficient methods to monitor asymptomatic patients to reduce transmission. We describe the structure and operating protocols of a community treatment center (CTC) run by Seoul National University Hospital (SNUH) in South Korea. SNUH converted an existing facility into a CTC to isolate patients who had confirmed COVID-19 but mild or no symptoms. Patients reported self-measured vital signs and symptoms twice a day by using a smartphone application. Medical staff in a remote monitoring center at SNUH reviewed patient vital signs and provided video consultation to patients twice daily. The CTC required few medical staff to perform medical tests, monitor patients, and respond to emergencies. During March 5–26, 2020, we admitted and treated 113 patients at this center. CTCs could be an alternative to hospital admission for isolating patients and preventing community transmission.

Since the first suspected case was reported in December 2019 (*1*,*2*), the number of coronavirus disease (COVID-19) cases has risen steeply worldwide (*3*,*4*). In South Korea, COVID-19 outbreaks occurred at religious facilities and the number of cases increased drastically, especially in Daegu City and the North Gyeongsang Province, and the number of patients with asymptomatic or mild symptoms increased exponentially (*5*,*6*). In the early stages of the COVID-19 epidemic, all patients with diagnosed COVID-19 were hospitalized in negative-pressure isolation units to treat the disease and prevent the spread of infection. However, because the infection spread rapidly, the number of patients exceeded the number of available negative-pressure isolation beds. Because of limited medical resources and the COVID-19 epidemic curve, concerns grew that new facilities would be needed to isolate and care for patients in South Korea.

The National Health Insurance System (NHIS) of South Korea offers complete access to healthcare for the entire population (*13*). South Korea's medical utilization rate is the highest, 16.6 outpatient visits per capita per year, among Organization for Economic Cooperation and Development (OECD) countries (*14*). Citizens of South Korea have high access to medical services. Before the COVID-19 pandemic, no one in the country anticipated a situation in which hospital admission would be denied. South Korea has 2.6 times more hospital beds than other OECD countries, 12.3/1,000 population. However, the country only has 1,027 negative-pressure isolation beds, and these are not distributed across all regions. When the COVID-19 pandemic reached South Korea, the number of available negative-pressure isolation beds decreased, and patients could not be admitted to the hospital because of the shortage of medical facilities, especially in regions where outbreaks mainly occurred.

When an imbalance between the demand and supply of medical resources exists, adequate triage of patients is critical for allocating limited resources to patients who can benefit the most (*7*). In a large-scale study from China, Wu et al. (*8*) suggested that ≈80% of COVID-19 symptomatic patients were reported to have mild upper respiratory infection without hypoxia, and only 20% of infected patients needed medical services. Until March 25, 2020, the crude mortality rate in South Korea was 1.4%, and estimates suggested the severity of COVID-19 in the country would not be high (*9*). However, considering asymptomatic carrier transmission (*10*), the high reproductive number (R_0 = 2.2) (*11*), and the possibility

Author affiliation: Seoul National University Hospital, Seoul, South Korea

DOI: https://doi.org/10.3201/eid2610.201460

[1]These first authors contributed equally to this article.

of sudden deterioration (*12*), even patients with mild or no symptoms should be isolated and monitored.

On March 2, 2020, the government of South Korea started operating community treatment centers (CTCs) to provide quarantine, regular examination, and monitoring for asymptomatic and mildly symptomatic patients with laboratory-confirmed COVID-19. By March 25, a total of 17 CTCs were serving patients with mild symptoms nationwide. The CTC is designed to monitor and isolate patients with mild conditions during emerging infectious disease outbreaks. We describe the structure and operating protocols of a CTC operated by Seoul National University Hospital (SNUH) during the COVID-19 pandemic.

Materials and Methods

Study Setting in the SNUH-CTC

SNUH is a teaching hospital with 1,700 beds. The Mungyeong Human Resource Development (HRD) Center, 153 km from SNUH, is a 7-story, 100-room facility with accommodations that is normally used for training SNUH staff. SNUH converted Mungyeong HRD to a CTC in cooperation with the government's CTC operating policy and established a monitoring center inside SNUH. SNUH-CTC began operating on March 5, 2020 as the third CTC in the country.

Admission and Discharge Criteria

Screening Criteria for Patients for CTC

The Korea Centers for Disease Control and Prevention (KCDC) classified the severity of COVID-19 into very severe, severe, mild, and asymptomatic (*15*) (Appendix Table 1, https://wwwnc.cdc.gov/EID/article/26/10/20-1460-App1.pdf). Mild COVID-19 is defined as alert and meeting ≥1 of the following conditions: <50 years old, ≥1 underlying conditions, and temperature <38°C with antipyretic drugs. Asymptomatic is defined as a patient who is alert, <50 years old, has no underlying disease, is a nonsmoker, and has a temperature of <37.5°C without antipyretic drugs. Patients classified as severe or very severe were admitted to hospitals; CTCs only accepted patients classified as having mild or asymptomatic COVID-19.

Patients with mild COVID-19 met ≥1 of the following criteria for CTC admission: they did not necessarily require hospitalization; they only required monitoring; they were unable to properly self-isolate (for instance, they had no suitable place to live or lived with persons in a high-risk group); or, as determined by local government, they needed to be admitted to a CTC. Medical staff assessed patients and excluded persons at high-risk for deterioration from CTCs and recommended hospitalization.

Criteria for Discharge from the CTC

KCDC has 2 criteria for releasing patients from quarantine. Symptomatic patients can be discharged if symptoms disappear and they have negative results on 2 reverse-transcription PCR (RT-PCR) tests ≥24 hours apart. KCDC recommended PCR amplification of the viral E gene as a screening test and amplification of the RdRp region of the open reading frame 1b gene as a confirmatory test. RT-PCR is considered positive only when all the genes are detected, based on the opinions of experts who detected weak and nonspecific amplification in the clinical specimens of patients who received negative results. Asymptomatic patients can be discharged if they have 2 negative RT-PCR tests ≥24 hours apart within 7 days of diagnosis.

We conducted our study in accordance with the World Health Association's Declaration of Helsinki (https://www.wma.net). The study was approved by the institutional review board of SNUH (IRB no. H-2003-163-1112).

Results

Overall Structure

SNUH-CTC consisted of 2 centers: the patient center in Mungyeong HRD, where patients were admitted, and the monitoring center in Seoul at SNUH, where medical staff provided video consultation services (Figure 1). In the patient center, personnel from the Ministry of Health and Welfare, local government, hospitals, military, police, and fire agencies stayed and provided various services necessary for the operation of the CTC (Appendix Table 2).

Patient Center

We divided the Mungyeong HRD Center into a clean area, in which medical and operating staff worked, and a contaminated area, where patients lived. Each area had a designated entrance separate from the other. We designated an area between the clean and contaminated areas as a gray zone in which personnel could remove personal protective gear or perform other required activities, such as collecting patient samples or removing waste (Figure 2).

Mungyeong HRD Center had internet service and SNUH installed an additional network to access the hospital's electronic medical record (EMR) system. Supplies for conducting RT-PCR tests, such as

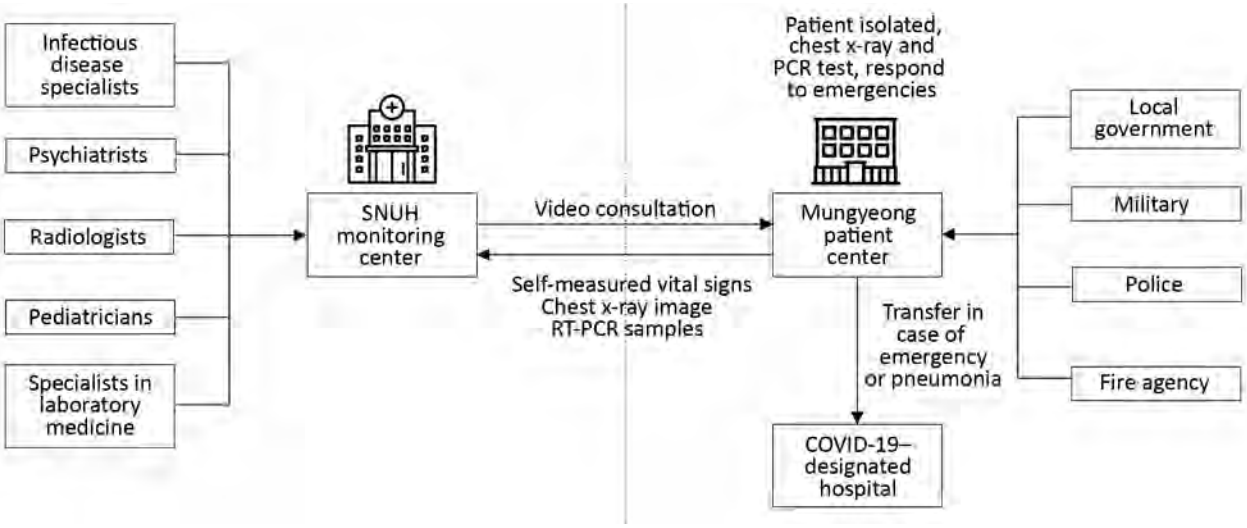

Figure 1. Overall structure of the SNUH community treatment center (SNUH-CTC) for isolating mildly symptomatic or asymptomatic patients with coronavirus disease, South Korea. SNUH-CTC was divided into a monitoring center at SNUH in Seoul and a patient center 153 km away in Mungyeong. Boxes indicate various agencies and organizations the provided staff to help run SNUH-CTC and support operations. Arrows indicate direction of information, services, or patient transport. RT-PCR, reverse transcription PCR; SNUH, Seoul National University Hospital.

swabs and a refrigerator, and a mobile radiography bus were placed next to the building. According to the national guidelines for COVID-19, physicians collected RT-PCR samples on a 2-day cycle for negative cases and on a 3- or 7-day cycle for positive cases and sent the samples to SNUH to be tested.

To detect pneumonia early, patients with abnormal findings on chest imaging had daily chest radiographs until normalization; patients without abnormal findings had chest radiographs every 3 days. Radiographs were read by a radiologist in SNUH through the picture archiving and communication system. RT-PCR and radiographic results could be checked in the Mungyeong HRD and the SNUH monitoring center through the EMR system. Essential medicines, such as antipyretic drugs and cough medicines, were stored in the Mungyeong HRD and provided by a physician's prescription.

A physician or nurse was always on duty in the Mungyeong HRD patient center to respond to emergencies. The physicians came from many specialties, including emergency medicine, family medicine, and general surgery, to address various patient conditions and emergencies. During the day, 2 physicians and 2 nurses were on duty; at night 1 physician and 2 nurses were on duty. During each shift, 1 physician acted as the medical director, and 1 nurse acted as an infection manager. All staff, including medical staff, were checked twice a day for fever and respiratory symptoms, such as cough, sputum, stuffy nose, sore throat, chest discomfort, and dyspnea. When staff reported symptoms, the medical director checked the staff member and provided a RT-PCR test if necessary.

Each room of the Mungyeong HRD patient center was equipped with an automatic blood pressure monitor, digital thermometer, and pulse oximeter so that patients could check vital signs independently. Meals were provided three times a day, and laundry was done by patients in their rooms. Most patients were not permitted to have visitors, but children could be visited by parents or guardians.

Monitoring Center

The monitoring center at SNUH was equipped with computers and monitors, smartphone devices, webcams, headsets for video consultation, and 2 large dashboard monitors to check the patients' vital signs and symptoms. Patients admitted to the CTC checked their blood pressure, body temperature, pulse, respiratory rate, and oxygen saturation at 9 AM and 4:30 PM each day. Patients reported their symptoms, including respiratory symptoms, twice a day through a questionnaire sent through a smartphone application, and the nurse on duty monitored the responses and vital signs. The nurse provided video consultations twice a day from 9 AM–12 PM and 5–8 PM. If the nurse decided that video consultation with a doctor was necessary, the doctor provided additional consultation. The doctor regularly monitored patients' vital signs and symptoms once a day and conducted regular video consultations once every 2 days. On average, nurses and doctors provided video consultations

for ≈5 minutes per patient per consult and monitored patients' symptoms and vital signs for ≈3 minutes per patient monitoring session (Appendix Table 3).

Radiologists at SNUH read and provided results for patients' chest radiographs. When patients had abnormal radiography findings or the patient's symptoms worsened, the physician at Mungyeong HRD Center consulted with an infectious disease specialist at SNUH.

Patients in the CTC underwent a comprehensive psychiatric assessment once a week to evaluate for depressive mood, anxiety, risk for suicide, and posttraumatic stress. The questionnaire included a standard depression module, a generalized anxiety disorder assessment, suicidality screening, a posttraumatic stress disorder checklist, and somatic symptom assessment. For high-risk groups, psychiatrists conducted a separate in-depth psychological consultation by using the video consultation system.

The video consultation model for patients in isolation with diagnosed COVID-19 integrated an interprofessional clinical team to provide patient-centered care. By reducing direct face-to-face consultations

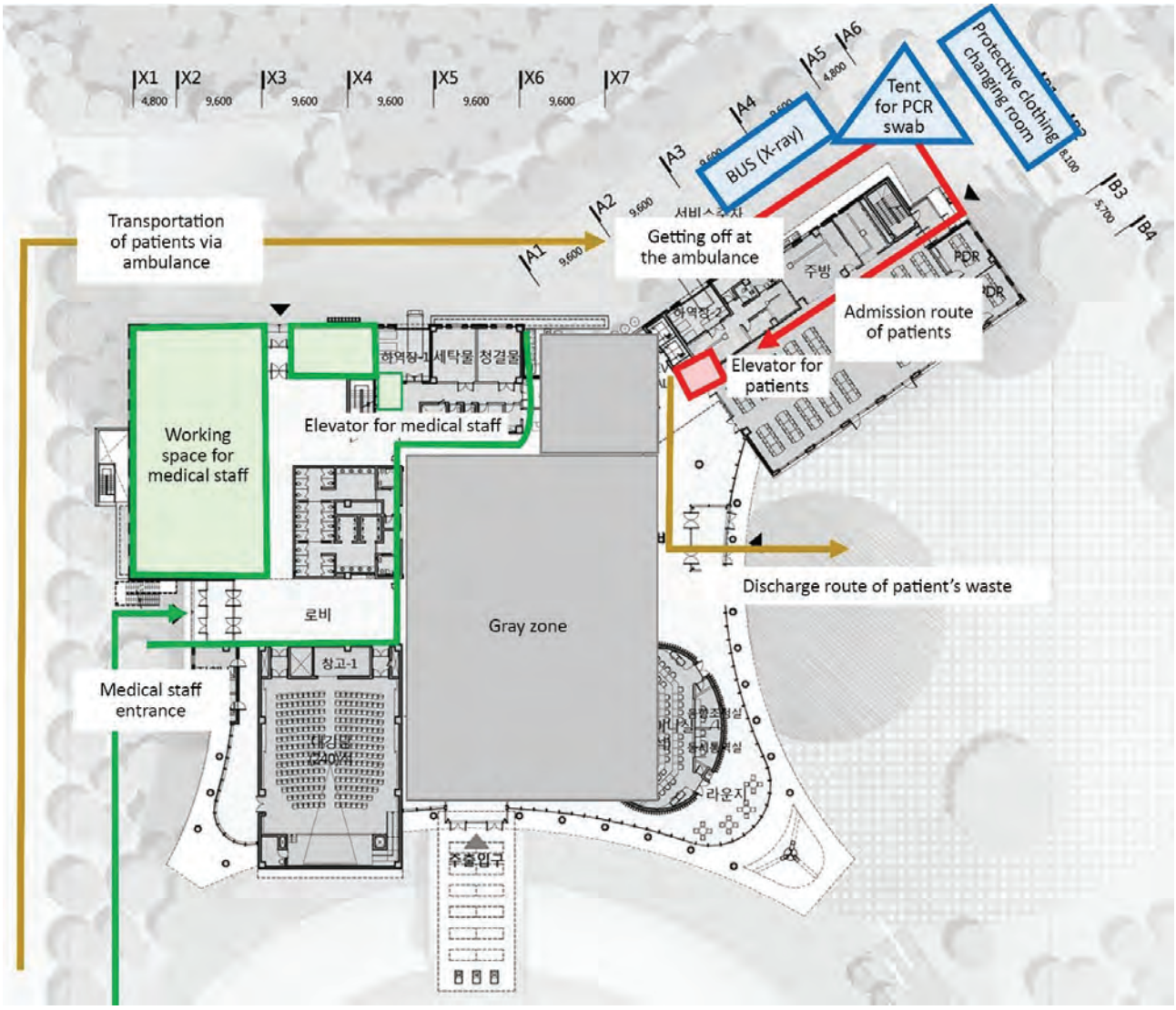

Figure 2. Diagram of the patient center of Seoul National University Hospital community treatment center (SNUH-CTC) located in the Mungyeong Human Resource Development (HRD) Center, Mungyeong, South Korea. CTCs were set up to isolate and monitor mildly symptomatic or asymptomatic patients with coronavirus disease. Green indicates the clean areas in which staff worked. Red indicates contaminated areas in which patients stayed. Gray zone indicates areas in which staff performed other activities, such as collecting patient's samples or removing waste. Yellow indicates routes for patient admission and removal of patient waste. Blue indicates external services kept outside of the building.

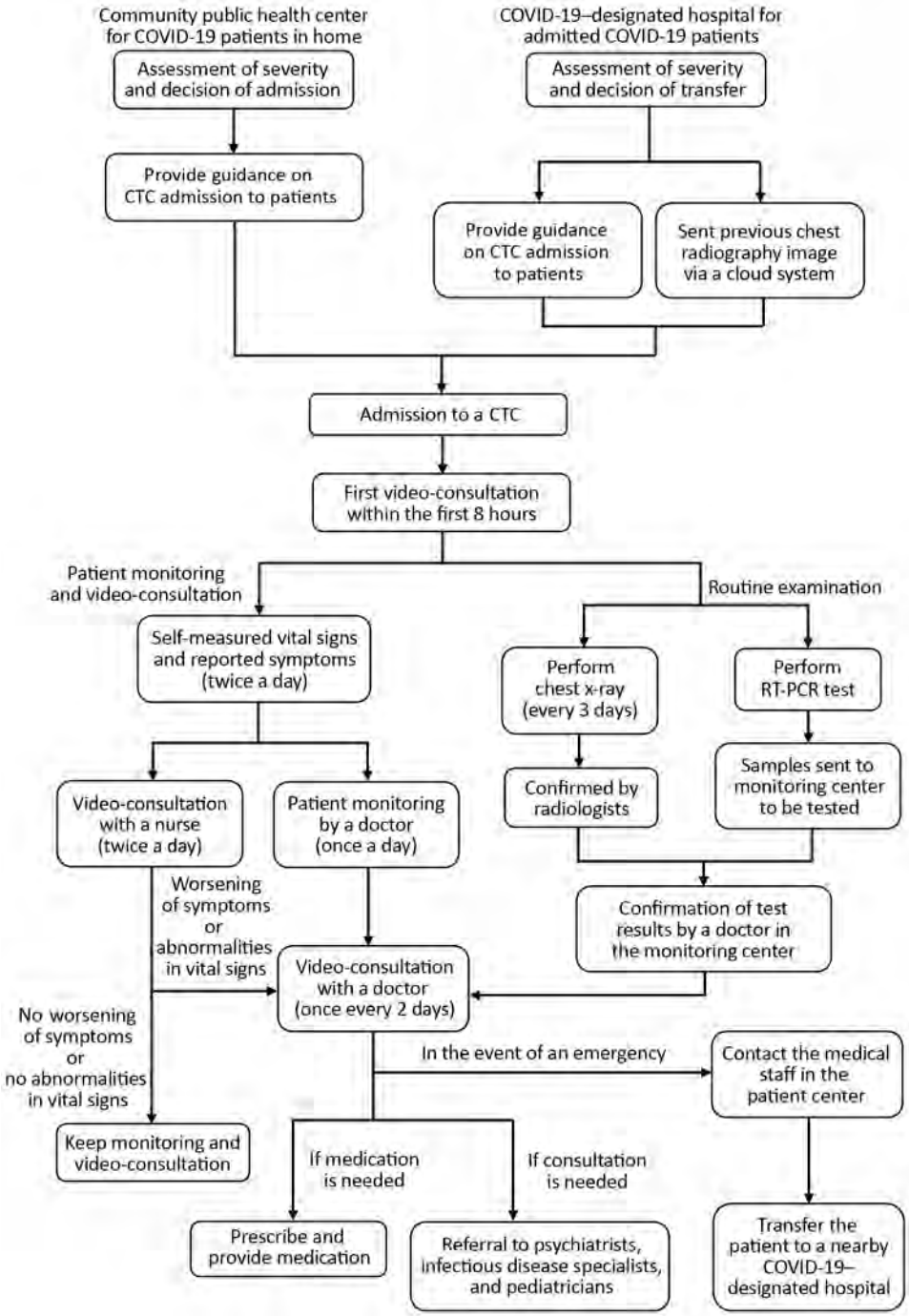

Figure 3. Flow chart of protocols for admission and management of mildly symptomatic or asymptomatic patients with coronavirus disease admitted to the Seoul National University Hospital community treatment center (SNUH-CTC) for isolation and monitoring, South Korea. COVID-19, coronavirus disease; CTC, community treatment center; RT-PCR, reverse transcription PCR.

with infectious patients, we helped ensure the safety of medical staff. Video consultation was essential for providing patient care and helped integrate services, including monitoring vital signs and patient symptoms; providing consultation with nurses, physicians, infectious disease specialists, and radiologists; and in-depth psychological consultation by a psychiatrist, when needed.

Preparation for Emergencies

The CTC established an emergency referral system with nearby medical institutions to respond to emergencies or increased symptoms. In an emergency, medical staff on duty in the CTC donned protective gear to visit the patient's room. The patient center was equipped with an emergency cart normally used in the hospital, a portable oxygen tank, and a stretcher

with a negative-pressure air tent for transferring patients to the ambulance area, if needed.

Patients requiring hospitalization were transferred to a hospital with a negative-pressure isolation unit that KCDC designated for treating COVID-19 patients. Criteria for transport to a hospital included abnormal vital signs measured every day for ≥3 days or evidence of pneumonia on chest radiographs. Patients were transferred by ambulance from the nearest ambulance station. If an emergency occurred, such as abrupt respiratory failure, the patient was first transferred to the nearest emergency department for treatment and stabilization before being transferred to a hospital bed (Figure 3).

Characteristics of Patients in the SNUH-CTC

In total, 113 patients were admitted to the SNUH-CTC during March 5–26, 2020. Among patients, 59 (52.2%) were female and, 54 (47.8%) were male, the average age was 30.4 years (range 9–65 years), and 7 (6.2%) had underlying conditions, 4 of whom had hypertension.The average number of days of illness before admission to the CTC was 5.1 days. Among patients admitted with symptoms, 31 (27.4%) had cough, and 1 (0.9%) had fever. Four (3.5%) patients developed fever within 3 days after admission. Twelve (10.6%) patients had abnormalities in chest radiographs performed on the day of admission, but most were nonspecific haziness or opacity; only 1 patient appeared to have pneumonia (Table 1).

Outcomes of Patients in the SNUH-CTC

During March 5–26, the SNUH-CTC admitted 113 patients; 103 were admitted directly from home, and 10 were transferred from the hospital during the recovery period. During the 3 weeks studied, 49 patients recovered and were discharged, and 2 patients were transferred to a COVID-19–designated facility for hospitalization (Table 2). The average length of stay in the CTC was 15.7 days (interquartile range [IQR] 5–21 days), and the average interval from diagnosis to discharge was 19.5 days (IQR 10–27 days). One patient was transferred to a hospital after persistent pneumonia on chest radiographs for 3 days, and another patient was transferred for close monitoring because dyspnea developed and the patient needed oxygen at 1 L/min. In both cases, the medical staff staying in the CTC evaluated the patients in their rooms and decided to transfer them after detecting the deterioration on consultation. Both patients were safely admitted to the hospital.

Discussion

South Korea established CTCs for isolation and monitoring of patients with no or mild symptoms of COVID-19 during a pandemic in which the demand for medical resources have exceeded the supply. SNUH converted an existing accommodation facility into a medical facility and provided video consultation via a smartphone to minimize staff contact with infectious patients. The hospital operated the CTC and provided medical services and public officials from the Ministry of Health and Welfare, local government, military, police, and the fire agency supported the operation by providing food delivery and patient transfer. During the 3-week operation, 113 asymptomatic and mildly symptomatic patients were admitted to SNUH-CTC for monitoring and care.

As COVID-19 spreads worldwide, the shortage of medical resources has become a serious problem in many countries (*16*,*17*). The lack of medical resources, such as hospital beds, intensive care units, and ventilators, can hinder the ability to treat patients

Table 1. Characteristics of 113 patients with mild or asymptomatic coronavirus disease admitted to the Seoul National University Hospital community treatment center for isolation and monitoring, South Korea

Characteristics	Value
Sex	
M	54 (47.8)
F	59 (52.2)
Age, y (mean ± SD)	30.4 ± 12.9
Average length of illness, d (mean ± SD)	5.1 ± 3.5
Fever	
At admission	1 (0.9)
≤3 d	4 (3.5)
≤2 weeks	15 (13.3)
Never	98 (86.7)
Symptoms at admission	
Cough	31 (27.4)
Sputum	25 (22.1)
Rhinorrhea	18 (15.9)
Chest discomfort	8 (7.1)
Sore throat	7 (6.2)
Dyspnea	5 (4.4)
Underlying conditions	
Hypertension	4 (3.5)
Diabetes	1 (0.9)
Asthma	1 (0.9)
Chronic bronchitis	1 (0.9)
None	106 (93.8)
Vital signs, mean (SD)	
Systolic blood pressure, mm Hg	113.6 (11.8)
Diastolic blood pressure, mm Hg	75.9 (9.2)
Respiratory rate, times/min	16.6 (5.4)
Heart rate, bpm	82.6 (11.5)
Body temperature, °C	36.3 (0.6)
Oxygen saturation, %	96.1 (4.5)
Chest radiograph†	
Abnormal	12 (10.6)
Within normal limits	101 (89.4)

*Values are no. (%) except as indicated.
†At admission to the community treatment center.

Table 2. Admission and discharge of patients in the Seoul National University Hospital community treatment center, South Korea

Category	No. (%)	Mean days (interquartile range)		
		Quarantine time before admission	Length of stay	From diagnosis to discharge
Admission				
From home	103 (91.2)	5.8 (3–5)		
From hospital	10 (8.8)	11.6 (6–16.8)		
Discharge method				
Recovered	49 (43.4)		15.7 (5–21)	19.5 (10–27)
Transferred	2 (1.8)			
Not discharged	62 (54.8)			

adequately (*18*,*19*). In addition, during the pandemic crisis, a shortage of quarantine facilities, in this case hospitals, could increase the transmission of infectious diseases (*20*). When the demand for medical resources is greater than the supply, proper patient triage and resource allocation are crucial. During this pandemic, hospitals might not have sufficient medical equipment, such as ventilators and extracorporeal membrane oxygenation, for all patients. To maximize resources and save the most patients, hospitals with sufficient medical equipment can provide medical services for critically ill patients. However, carefully monitoring the disease progress, even for mild conditions, can assist in documenting clinical course of emerging infectious diseases. In addition, appropriate isolation of patients who test positive for COVID-19 can prevent further spread of disease (*20*).

South Korea has many acute care beds and high medical accessibility with the NHIS (*21*). Despite an 80% ratio of asymptomatic and mildly symptomatic patients in the early stages of the epidemic, all COVID-19 patients in South Korea were admitted to negative-pressure isolation rooms according to the principle of first come, first served (*8*). As the pandemic rapidly progressed, hospital beds became scarce (*22*), and >2,000 patients waited at home for hospital admission, including patients in high-risk groups, such as persons ≥65 years of age and those with underlying conditions (*23*). Before CTCs were opened in South Korea, at least 2 patients died at home waiting for hospital admission and the need for medical facilities and redistribution of medical resources increased (*22*,*24*). Some patients hospitalized in the early stages of the endemic did not need active treatment but were required to be isolated and monitored. However, infected patients who were already hospitalized could not be discharged because of the possibility of sudden deterioration and difficulties in the control and monitoring during self-isolation at home (*20*).

A new quarantine model is needed to ensure beds in fully equipped hospitals for severe disease cases and the capacity to monitor and isolate asymptomatic and mildly symptomatic patients. For the current COVID-19 pandemic, South Korea implemented CTCs as an intermediate model between self-isolation at home and hospital isolation. The core aim of CTCs is to isolate patients in single rooms with bathrooms and provide care with telemedicine. Because the CTC model can be adapted as surge capacity in various types of facilities, such as resorts and hotels, CTCs could quickly secure a quarantine bed in a pandemic crisis. We found that CTCs can be an alternative to fully functioning hospitals and home isolation. CTCs enabled the country to preserve hospital resources for the sickest patients and isolate patients from the community to prevent further transmission. In addition, CTCs provided an opportunity for physicians to observe COVID-19 disease progression and triage patients who deteriorate to higher care, instead of leaving patients at home.

We found that allowing patients to independently measure their vital signs and providing telemedicine consultations had several advantages. First, reduced contact between healthcare workers and patients minimized the risk for infection for healthcare workers. During the pandemic, the infection or quarantine of healthcare workers will exacerbate the problem of already scarce medical resources (*16*). Second, because telemedicine is possible regardless of distance, CTCs would enable regions with sufficient resources to support regions with insufficient resources. In our model, the CTC and the monitoring centers were >100 km apart. The SNUH-CTC used a video consultation model instead of conventional telephone interviews because we could observe additional visual signs or diagnostic clues through video conferences (*25*,*26*). By using self-measurement equipment and advanced telecommunication technology, including smartphones, we were able to maximize these services.

South Korea opened its first CTC on March 2; by March 26, a total of 3,292 patients were admitted to 17 CTCs, representing 35.6% of the 9,241 cumulative confirmed COVID-19 cases in the country. During those 24 days, no deaths or instances of respiratory failure were reported in the 17 CTCs operated. The

CTC model offers safe monitoring and isolation for asymptomatic or mildly symptomatic patients with diagnosed COVID-19 during the pandemic. During shortages of medical resources, appropriate triage of patients and allocation of resources are needed so that critically ill patients receive the highest level of care and patients with less severe infection can be safely monitored and treated. The CTC model also could be useful during natural disasters in which the demand for medical care overwhelms the supply.

We note a few limitations of CTCs. First, because a CTC is not a hospital, appropriate response to emergencies, such as respiratory failure, might be difficult. During our CTC operations, we chose to transfer patients to surrounding COVID-19–designated hospitals for emergency treatment; future planning should include hospitals with emergency services within a short distance of the CTC. Second, because we were not able to observe patients in real time, we might not have detected a sudden emergency. To protect patient privacy, we did not install a closed-circuit television in patient rooms, but we trained the patients to contact the medical staff immediately if they had a medical emergency. However, other countermeasures, such as patient alarm bells in each room, might be needed. Third, the CTC also is a quarantine facility; patient discomfort and depression might increase during long-term admission. To try to assure patients' mental health, we provided various psychiatric interventions; in addition to other medical services, mental health should be built into further isolation and quarantine models. Fourth, our CTC did not have a negative-pressure isolation function as an infectious disease facility.

In conclusion, to safely isolate and monitor the asymptomatic and mildly symptomatic patients with COVID-19, South Korea developed the CTC model as an intermediate between hospitalization and self-isolation at home. By classifying patients according to the disease severity and underlying conditions, asymptomatic and mildly symptomatic patients can be safely monitored and treated at CTCs.

Acknowledgments

We sincerely thank all SNUH staff, soldiers, firefighters, police officers, civil servants, volunteers, and supporters who helped open and operate the SNUH community treatment center.

About the Author

Dr. Lee is a clinical assistant professor of Public Healthcare Center, Seoul National University Hospital. Her research interests are emergency medical system and health policies. Dr. Kang is a clinical assistant professor of Public Healthcare Center and Department of Family Medicine, Seoul National University Hospital. Her research interests are chronic disease management, palliative care, self-management of patients, and health policies.

References

1. Chen N, Zhou M, Dong X, Qu J, Gong F, Han Y, et al. Epidemiological and clinical characteristics of 99 cases of 2019 novel coronavirus pneumonia in Wuhan, China: a descriptive study. Lancet. 2020;395:507–13. https://doi.org/10.1016/S0140-6736(20)30211-7
2. Huang C, Wang Y, Li X, Ren L, Zhao J, Hu Y, et al. Clinical features of patients infected with 2019 novel coronavirus in Wuhan, China. Lancet. 2020;395:497–506. https://doi.org/10.1016/S0140-6736(20)30183-5
3. Kinross P, Suetens C, Gomes Dias J, Alexakis L, Wijermans A, Colzani E, et al.; ECDC Public Health Emergency Team. Rapidly increasing cumulative incidence of coronavirus disease (COVID-19) in the European Union/European Economic Area and the United Kingdom, 1 January to 15 March 2020. Euro Surveill. 2020;25:2000285. https://doi.org/10.2807/1560-7917.ES.2020.25.11.2000285
4. Lai CC, Wang CY, Wang YH, Hsueh SC, Ko WC, Hsueh PR. Global epidemiology of coronavirus disease 2019 (COVID-19): disease incidence, daily cumulative index, mortality, and their association with country healthcare resources and economic status. Int J Antimicrob Agents. 2020;55:105946. https://doi.org/10.1016/j.ijantimicag.2020.105946
5. Won J, Lee S, Park M, Kim TY, Park MG, Choi BY, et al. Development of a laboratory-safe and low-cost detection protocol for SARS-CoV-2 of the coronavirus disease 2019 (COVID-19). Exp Neurobiol. 2020;29:107–119. https://doi.org/10.5607/en20009
6. Kwon KT, Ko J-H, Shin H, Sung M, Kim JY. Drive-through screening center for COVID-19: a safe and efficient screening system against massive community outbreak. J Korean Med Sci. 2020;35:e123. https://doi.org/10.3346/jkms.2020.35.e123
7. Institute of Medicine. Crisis standards of care: a toolkit for indicators and triggers. Washington (DC): The National Academies Press; 2013. https://doi.org/10.17226/18338
8. Wu Z, McGoogan JM. Characteristics of and important lessons from the coronavirus disease 2019 (COVID-19) outbreak in China: summary of a report of 72,314 cases from the Chinese Center for Disease Control and Prevention. JAMA. 2020 Feb 24 [Epub ahead of print]. https://doi.org/10.1001/jama.2020.2648
9. Korea Center for Disease Control and Prevention. The updates on COVID-19 in Korea as of 25 March. 2020 Mar 25. [cited 2020 April 10] https://www.cdc.go.kr/board/board.es?mid=a30402000000&bid=0030
10. Bai Y, Yao L, Wei T, Tian F, Jin D-Y, Chen L, et al. Presumed asymptomatic carrier transmission of COVID-19. JAMA. 2020;323:1406–7. PubMed https://doi.org/10.1001/jama.2020.2565
11. Li Q, Guan X, Wu P, Wang X, Zhou L, Tong Y, et al. Early transmission dynamics in Wuhan, China, of novel coronavirus–infected pneumonia. N Engl J Med. 2020;382:1199–207. https://doi.org/10.1056/NEJMoa2001316

12. Goh KJ, Choong MC, Cheong EH, Kalimuddin S, Duu Wen S, Phua GC, et al. Rapid progression to acute respiratory distress syndrome: review of current understanding of critical illness from COVID-19 infection. Ann Acad Med Singapore. 2020;49:108–18.
13. Jeong H-S. Korea's National Health Insurance—lessons from the past three decades. Health Aff (Millwood). 2011;30:136–44. https://doi.org/10.1377/hlthaff.2008.0816
14. Organization for Economic Cooperation and Development. OECD Health Statistics 2019 [cited 2020 Apr 10]. https://www.oecd.org/health/health-data.htm
15. Korea Centers for Disease Control and Prevention. COVID-19 response guidelines 8th edition [in Korean] [cited 2020 Apr 10]. http://www.cdc.go.kr/board.es?mid=a20507020000&bid=0019&act=view&list_no=366558
16. Emanuel EJ, Persad G, Upshur R, Thome B, Parker M, Glickman A, et al. Fair allocation of scarce medical resources in the time of Covid-19. N Engl J Med. 2020;382:2049–55. https://doi.org/10.1056/NEJMsb2005114
17. Truog RD, Mitchell C, Daley GQ. The toughest triage—allocating ventilators in a pandemic. N Engl J Med. 2020 Mar 23 [Epub ahead of print]. PubMed https://doi.org/10.1056/NEJMp2005689
18. Ji Y, Ma Z, Peppelenbosch MP, Pan Q. Potential association between COVID-19 mortality and health-care resource availability. Lancet Glob Health. 2020;8:e480. https://doi.org/10.1016/S2214-109X(20)30068-1
19. Grasselli G, Pesenti A, Cecconi M. Critical care utilization for the COVID-19 outbreak in Lombardy, Italy: early experience and forecast during an emergency response. JAMA. 2020 Mar 13 [Epub ahead of print]. https://doi.org/10.1001/jama.2020.4031
20. Hellewell J, Abbott S, Gimma A, Bosse NI, Jarvis CI, Russell TW, et al.; Centre for the Mathematical Modelling of Infectious Diseases COVID-19 Working Group. Feasibility of controlling COVID-19 outbreaks by isolation of cases and contacts. Lancet Glob Health. 2020;8:e488–96. https://doi.org/10.1016/S2214-109X(20)30074-7
21. Lee SY, Khang YH, Lim HK. Impact of the 2015 Middle East Respiratory Syndrome Outbreak on Emergency Care Utilization and Mortality in South Korea. Yonsei Med J. 2019;60:796–803. https://doi.org/10.3349/ymj.2019.60.8.796
22. Tanne JH, Hayasaki E, Zastrow M, Pulla P, Smith P, Rada AG. Covid-19: how doctors and healthcare systems are tackling coronavirus worldwide. BMJ. 2020;368:m1090. https://doi.org/10.1136/bmj.m1090
23. Guan WJ, Ni ZY, Hu Y, Liang WH, Ou CQ, He JX, et al. Clinical characteristics of coronavirus disease 2019 in China. NEJM. 2020;382:1708–20. PubMed https://doi.org/10.1056/NEJMoa2002032
24. Korean Society of Infectious Diseases; Korean Society of Pediatric Infectious Diseases; Korean Society of Epidemiology; Korean Society for Antimicrobial Therapy; Korean Society for Healthcare-associated Infection Control and Prevention; Korea Centers for Disease Control and Prevention. Report on the epidemiological features of coronavirus disease 2019 (COVID-19) outbreak in the Republic of Korea from January 19 to March 2, 2020. J Korean Med Sci. 2020;35:e112. https://doi.org/10.3346/jkms.2020.35.e112
25. Donaghy E, Atherton H, Hammersley V, McNeilly H, Bikker A, Robbins L, et al. Acceptability, benefits, and challenges of video consulting: a qualitative study in primary care. Br J Gen Pract. 2019;69:e586–94. https://doi.org/ 10.3399/bjgp19X704141
26. Greenhalgh T, Koh GCH, Car J. Covid-19: a remote assessment in primary care. BMJ. 2020;368:m1182. https://doi.org/10.1136/bmj.m1182

Address for correspondence: Yon Su Kim; Department of Internal Medicine, Seoul National University College of Medicine and Hospital, 101 Daehak-Ro, Jongno-Gu, Seoul, 03080, South Korea; email: yonsukim@snu.ac.kr

Community Treatment Centers for Isolation of Asymptomatic and Mildly Symptomatic Patients with Coronavirus Disease, South Korea

Won Suk Choi,[1] Hyoung Seop Kim,[1] Bongyoung Kim,[2] Soomin Nam, Jang Wook Sohn[2]

As a part of measures to decrease spikes in coronavirus disease (COVID-19) cases and deaths outside of hospitals, the government of South Korea introduced a plan for community treatment centers (CTCs) to isolate and monitor patients with mild COVID-19 symptoms. We assessed outcomes of 568 patients admitted to 3 CTCs near Daegu. More (64.6%) women than men (35.4%) were admitted, and the mean age of patients was 36.0 years (SD ±15.0 years). Among all patients, 75.7% remained asymptomatic while at the CTCs. The mean time patients remained at CTCs was 19.6 days (SD ±5.8 days) from the day of diagnosis until our study ended on March 23, 2020. Because they offer appropriate clinical triaging and daily monitoring for patients, CTCs are a safe alternative to medical institutions for asymptomatic or mildly symptomatic patients with COVID-19.

Since initial reports of coronavirus disease (COVID-19) from Wuhan, China, 267,013 confirmed COVID-19 cases have been reported from 184 countries, as of March 22, 2020 (*1*). In South Korea, severe acute respiratory syndrome coronavirus 2 (SARS-CoV-2), which causes COVID-19, was detected in a person from China who entered the country from Wuhan on January 19, 2020 (*2*). After an outbreak was identified among a religious group in Daegu and the neighboring regions on February 18, 2020, the cumulative number of cases in South Korea increased dramatically (*3*). Because of the sharp increase in cases in this region, it was impossible to accommodate all patients in hospitals. The shortage of hospital beds left >2,000 persons with confirmed COVID-19 waiting many days at home for a hospital admission. Unfortunately, several persons died at home while waiting or during transportation to the hospital. As a part of measures to decrease spikes in COVID-19 caseloads in and deaths outside of hospitals, the government of South Korea converted private dormitories and state-run institutions into community-based isolation facilities for patients with laboratory-confirmed COVID-19, but mild or no symptoms. These community treatment centers (CTCs) enabled the efficient use of medical institutions and compensated for the shortcomings of self-isolation. South Korea opened its first CTC on March 2, 2020, and by March 19, 2020, 16 CTCs with a total of 3,818 beds were distributed across the country. We describe the operating processes of 3 CTCs near Daegu, South Korea, and analyze the clinical characteristics and disease progression in admitted patients.

Author affiliations: Korea University, Seoul, South Korea (W.S. Choi, J.W. Sohn); National Health Insurance Ilsan Hospital, Goyang, South Korea (H.S. Kim, S. Nam); Hanyang University, Seoul (B. Kim)

DOI: https://doi.org/10.3201/eid2610.201539

Materials and Methods

Participating Community Treatment Centers

The 3 CTCs that participated in this study each had a capacity to house 136–235 patients (Figure 1). All patients were from Daegu, where a large outbreak occurred, and tested positive for SARS-CoV-2 by real-time reverse transcription PCR (rRT-PCR) assays of upper respiratory tract (nasal and pharyngeal) or lower respiratory tract (sputum) specimens. Patients admitted to CTCs were classified as having mild or asymptomatic COVID-19 by epidemiologic investigators in Daegu. According to Korea Centers for Disease Control and Prevention (KCDC) guidelines (*4*), asymptomatic patients were alert, <50 years of age, nonsmokers who had no concurrent conditions and body temperature <37.5°C without antipyretic drugs.

[1]These first authors contributed equally to this article.

[2]These authors contributed equally to this article.

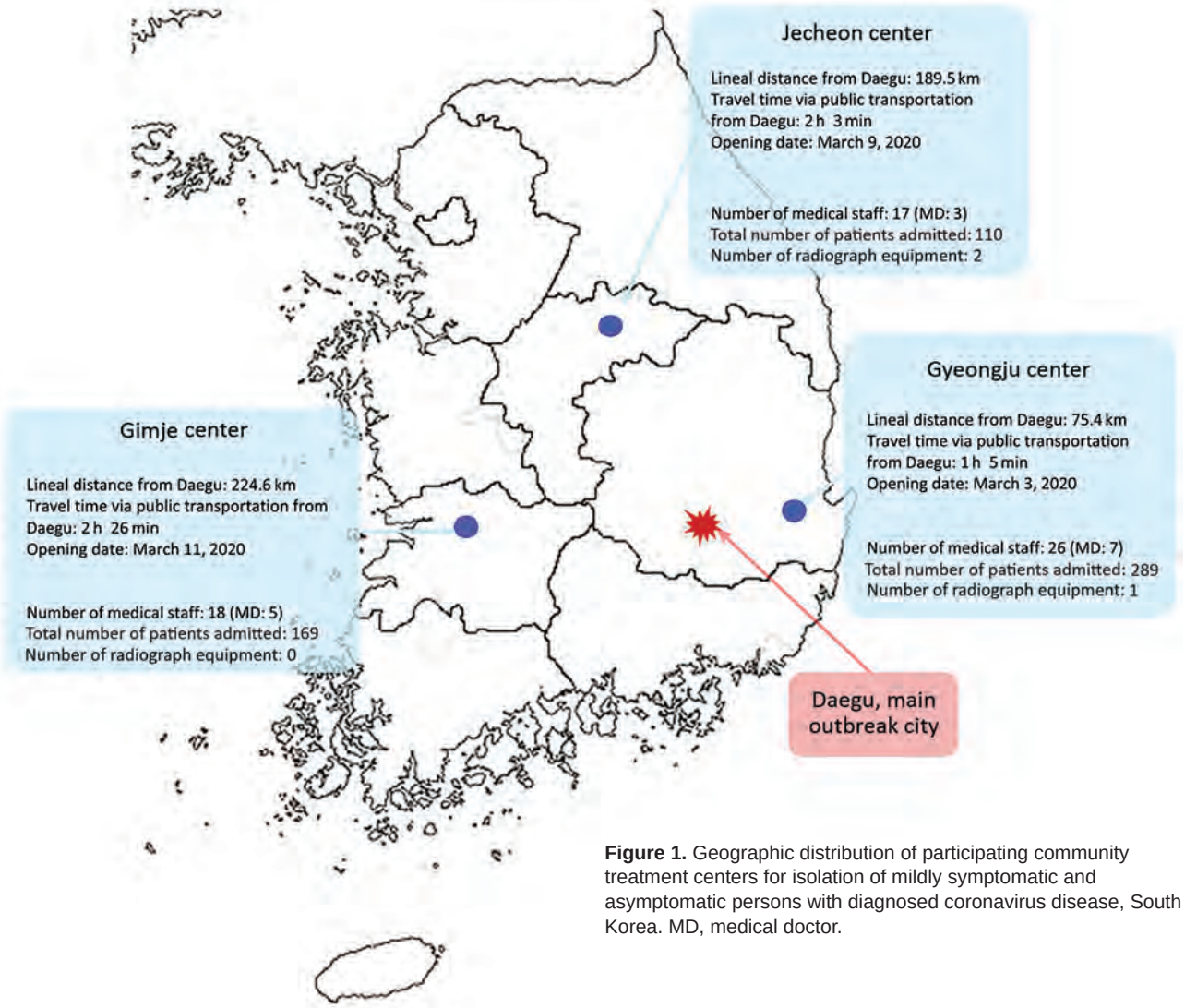

Figure 1. Geographic distribution of participating community treatment centers for isolation of mildly symptomatic and asymptomatic persons with diagnosed coronavirus disease, South Korea. MD, medical doctor.

Patients with mild disease were alert and met ≥1 of the following criteria: age <50 years, no concurrent conditions, and body temperature <38°C with antipyretics (*4*). Patients were admitted to CTCs because they could not self-isolate at home for medical or nonmedical reasons, including impaired performance of daily activities and unfeasibility of home isolation. Children were admitted and most were in infected family groups who were housed together in the centers. Patients with laboratory-confirmed COVID-19 who met at ≥1 of the following criteria were considered severe cases and were hospitalized immediately for treatment: ≥65 years of age; ≥1 underlying condition, such as diabetes, chronic kidney disease, chronic liver disease, chronic pulmonary disease, chronic cardiovascular disease, hematologic malignancy, undergoing chemotherapy, or use of immunosuppressants; required oxygen therapy; or needed special care, including persons who were severely obese, pregnant, or required renal dialysis (*4*).

Candidates for CTC admission arrived at the centers from their homes by designated buses offered by the Daegu local government. The buildings in all CTCs were divided into clean and contaminated zones. The clean zone was the working and living space designated for staff and the contaminated zone was the isolation space designated for patients. When entering the contaminated zone all staff were required to wear personal protective equipment, including N95 respirators, gloves, goggles, and hooded coveralls.

The 3 CTCs opened on different days; Gyeongju on March 3, Jecheon on March 9, and Gimje on March 11. Each CTC was paired with a large hospital that coordinated and established operations and dispatched medical staff, including 1 physician and 1 nurse per CTC, and other necessary staff. The Gyeongju CTC

had 1 radiograph unit and the Jecheon CTC had 2 radiograph units; Gimje CTC did not have an radiograph unit (Table 1). In addition to the medical professionals from private hospitals, the Gimje and Gyeongju CTCs included army physicians, public health physicians, and volunteer nurses, recruited for system operations. The Jecheon CTC was operated solely by medical professionals dispatched from a public hospital. Medical professionals stationed at each CTC monitored patients' conditions, collected patient specimens for rRT-PCR, and were on hand for emergencies requiring hospital transfer.

Apart from healthcare professionals, Daegu local government, in cooperation with the central government, primarily managed CTCs and provided administrative support, including providing medical equipment and meals. In addition, personnel from the military, police, and fire departments were stationed at the CTCs to provide operational services, including food delivery, access control, and patient transfer in emergencies. Each CTC required 64–72 personnel per day to maintain operations.

Discharge Criteria

Discharge decisions were based on rRT-PCR assays of nasopharyngeal or sputum specimens to detect SARS-CoV-2 (*5*). Green Cross Laboratories (https://www.gclabs.co.kr) performed rRT-PCR for all 3 CTCs by using Allplex 2019-nCoV assays (Seegene Medical Foundation, https://www.seegenetech.com). KCDC set discharge guidelines, which required negative results for 2 serial rRT-PCR tests performed ≥24 hours apart (*6*).

Monitoring and Testing Processes

During isolation in the CTCs, patients had their temperatures and respiratory symptoms checked ≥2 times each day, either by medical staff or by using self-monitoring equipment. Medical staff determined whether chest radiography or measurement of oxygen saturation were needed at admission, worsening of symptoms, or discharge. Each CTC had medications for symptomatic treatment, such as antipyretics and antitussives, which were prescribed by the medical staff. Each center had a portable oxygen tank if needed.

For patients with no fever, pulmonary symptoms, or use of antipyretics, an rRT-PCR test was performed ≥7 days from the day of diagnosis. Subsequent rRT-PCR tests were performed ≥24 hours later if the initial result was negative or in 2–7 days if the initial result was positive or inconclusive. Patients who developed symptoms such as dyspnea, chest pain, or chest tightness or had abnormal findings suggesting pneumonia on chest radiographs were transferred to a hospital. Patients were discharged when they met the rRT-PCR testing requirements provided by KCDC (Figure 2).

Data Collection

We used CTC records to collect data on patients from the day of admission to March 22, 2020. Basic medical information was collected by CTC staff through a web-based questionnaire or a telephone interview at the time of admission. Patients were asked the date of symptom onset, the date of COVID-19 diagnosis, whether they had underlying

Table 1. Characteristics of 3 community treatment centers, South Korea

Characteristics	Gimje	Gyeongju	Jecheon
Patient capacity	210	235	136
Opening date	2020 Mar 11	2020 Mar 3	2020 Mar 9
Matching hospital	Hanyang University Seoul Hospital	Korea University Medical Center	National Health Insurance Service Ilsan Hospital
No. medical staff			
Doctors, public sector*	4	6	3
Doctors, private sector	1	1	0
Registered nurses	7	9	6
Assistant nurses	6	9	2
Other†	0	1	6
No. staff from other sectors			
Local government	10	10	8
Central government, including the Ministry of Health and Welfare	3	3	2
Facilities management	6	6	16
Disinfection	10	9	11
Military	10	8	4
Police	6	8	6
Fire	1	1	1
No. radiography units	0	1	2

*Includes public health doctors, army doctors, and doctors from a public hospital.
†Includes radiologic technicians, physical therapists, occupational therapists.

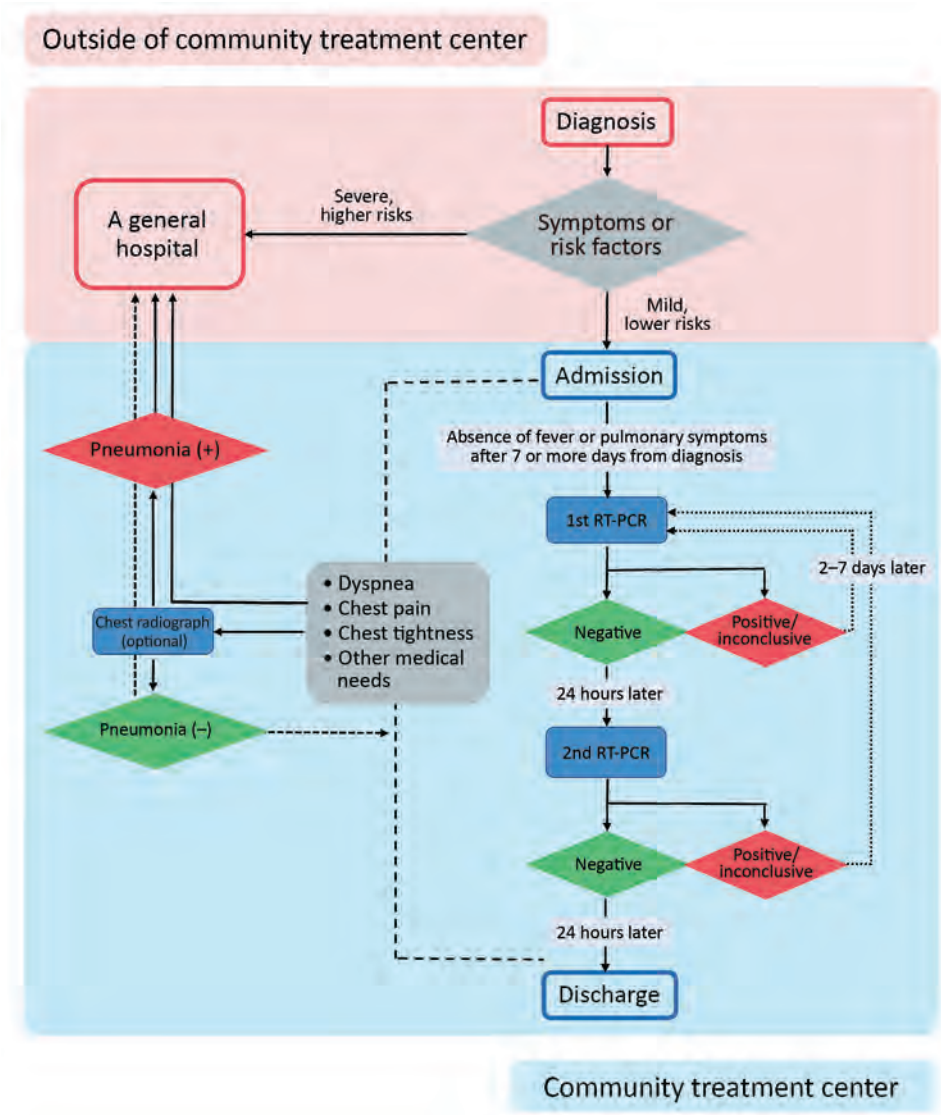

Figure 2. Flowchart demonstrating assessment before admission to community treatment centers, real-time reverse transcription PCR testing, and discharge process for mildly symptomatic and asymptomatic patients with diagnosed coronavirus disease, South Korea. RT-PCR, reverse transcription PCR.

conditions, and whether they had symptoms associated with COVID-19 (Appendix, https://wwwnc.cdc.gov/EID/article/26/10/20-1539-App1.pdf). A questionnaire for daily health self-monitoring was distributed 2 times a day and asked for self-monitored temperatures, whether patients had symptoms associated with COVID-19, and whether they had other healthcare-related questions (Appendix). The Gimje and Jecheon CTCs used text messaging to distribute links to questionnaires that were refined by using a Google survey platform (https://www.google.com). The Gyeongju CTC used a personal health record-based real-time monitoring system (Softnet, https://www.softnet.co.kr) and provided instructions to the patients at admission; staff called patients who did not complete the questionnaire on time.

Statistical Analysis

To analyze clinical characteristics of patients with persistent detection of SARS-CoV-2 by rRT-PCR for ≥28 days, we excluded patients who met the following criteria from the analysis: patients staying at the center on the 28th day from the day of initial diagnosis; and patients with no rRT-PCR test results or only 1 negative rRT-PCR test result performed after the 28th day from the day of initial diagnosis. We conducted all statistical analyses by using SPSS Statistics 24.0 for Windows (IBM Corp., https://www.ibm.com). We analyzed categorical variables by using the χ^2 test or Fisher exact test, as appropriate. We analyzed continuous variables by using independent *t* tests and considered 2-tailed $p<0.05$ statistically significant.

The study protocol was approved by the Institutional Review Board (IRB) of Korea University Ansan

Hospital, Seoul (IRB no. 2020AS0083). The requirement for written informed consent from patients was waived due to the nature of the study and unfeasibility related to the same.

Results

Clinical Characteristics of Patients

By March 23, 2020, a total of 568 patients had been admitted to the 3 CTCs: Gimje admitted 169 (29.7%), Gyeongju admitted 289 (50.9%), and Jecheon admitted 110 (19.4%). At the end of the study period, 356 (62.7%) patients remained in the centers, 200 (35.2%) had returned home and into society, and 12 (2.1%) were transferred to hospitals for further treatment (Table 2).

More women (64.6%) were admitted than men (35.4%), and the mean age of patients was 36.0 years (SD ±15.0 years). A small proportion (6.3%) of patients had >1 chronic disease requiring medication, such as diabetes and hypertension. Many (75.7%) remained asymptomatic over the course of the disease, but 138 (24.3%) reported symptoms associated with COVID-19. The most common symptoms were cough (11.6%) and nasal congestion (9.8%).

The mean number of rRT-PCR tests performed for each patient was 2.83 (SD ±1.17), and 33.3% (189/568) of patients were released from isolation at the 2nd follow-up test. Of the patients remaining in the CTCs, 12.4% (47/379) were released after the 3rd follow-up test and 14.5% (48/332) after the 4th. Among the first

Table 2. Clinical characteristics of 568 patients with no or mild symptoms of coronavirus disease isolated 3 in community treatment centers, South Korea*

Characteristics	Total, n = 568	Gimje, n = 169	Gyeongju, n = 289	Jecheon, n = 110
Current statistics				
In isolation in community treatment center	356 (62.7)	131 (77.5)	147 (50.9)	78 (70.9)
Discharged with recovery	200 (35.2)	33 (19.5)	137 (47.4)	30 (27.3)
Transferred to a hospital	12 (2.1)	5 (3.0)	5 (1.7)	2 (1.8)
Sex				
F	367 (64.6)	101 (59.8)	185 (64.0)2	81 (73.6)
M	201 (35.4)	68 (40.2)	104 (36.0)	29 (26.4)
Age, mean ±SD	36.0 ± 15.0	33.4 ± 14.6	37.8 ± 14.5	35.0 ± 16.2
Underlying conditions†	36 (6.3)	3 (1.8)	26 (9.0)	7 (6.4)
COVID-19 symptoms over the course of disease‡				
N	430 (75.7)	115 (68.0)	238 (82.4)	77 (70.0)
Y	138 (24.3)	54 (32.0)	51 (17.6)	33 (30.0)
rRT-PCR tests per patient, mean ±SD	2.83 ± 1.17	2.82 ± 1.04	2.73 ± 1.26	3.11 ± 1.09
rRT-PCR tests needed before discharge criteria met, % patients§				
2	33.3 (189/568)	23.7 (40/169)	43.3 (125/289)	21.8 (24/110)
3	12.4 (47/379)	17.8 (23/129)	11.6 (19/164)	5.8 (5/86)
4	14.5 (48/332)	7.5 (8/106)	19.3 (28/145)	14.8 (12/81)
rRT-PCR results				
Follow-up 1	N = 558	N = 166	N = 284	N = 108
Negative	307 (55.0)	65 (39.2)	188 (66.2)	54 (50.0)
Positive	143 (25.6)	56 (33.7)	58 (20.4)	29 (26.9)
Inconclusive	108 (19.4)	45 (27.1)	38 (13.4)	25 (23.1)
Follow-up 2	N = 539	N = 164	N = 267	N = 108
Negative	295 (54.7)	85 (51.8)	172 (64.4)	38 (35.2)
Positive	119 (22.1)	32 (19.5)	50 (18.7)	37 (34.3)
Inconclusive	125 (23.2)	47 (28.7)	45 (16.9)	33 (30.5)
Follow-up 3	N = 292	N = 96	N = 123	N = 73
Negative	14 (49.0)	42 (43.8)	72 (58.5)	29 (39.7)
Positive	53 (18.1)	20 (20.8)	16 (13.0)	17 (23.3)
Inconclusive	96 (32.9)	34 (35.4)	35 (28.5)	27 (37.0)
Follow-up 4	N = 152	N = 33	N = 74	N = 45
Negative	81 (53.3)	20 (60.6)	39 (52.7)	22 (48.9)
Positive	202 (13.2)	1 (3.0)	12 (16.2)	7 (15.5)
Inconclusive	51 (33.5)	12 (36.4)	23 (31.1)	16 (35.6)
Days in isolation, mean ±SD¶				
All patients, 2020 Mar 23	19.6 ± 5.8	17.9 ± 5.2	21.3 ± 5.9	17.9 ± 5.5
Patients currently admitted	22.2 ± 5.0	19.1 ± 5.0	25.9 ± 3.4	20.7 ± 2.6
Patients discharged with recovery	15.6 ± 4.0	14.5 ± 3.7	16.7 ± 3.6	11.6 ± 3.5
Patients transferred to a hospital	9.6 ± 5.2	11.0 ± 3.7	11.4 ± 4.4	1.5 ± 2.1

*As of March 23, 2020. Values are no. (%) except where otherwise indicated. CTC, community treatment center; rRT-PCR, real-time reverse transcription PCR.
†Includes any chronic disease requiring medication, such as diabetes or hypertension.
‡Includes fever, dyspnea, cough, sputum, nasal congestion, decreased sense of smell or taste, sore throat, or diarrhea.
§Two negative results >24 h apart are required before patient discharge.
¶Includes the period of self-isolation at home before being admitted at the center.

follow-up rRT-PCR tests, which marked the beginning of the discharge process, 55.0% were negative, 25.6% positive, and 19.4% inconclusive. The proportion of positive results showed a decreasing trend, but inconclusive results showed an increasing trend (Table 2).

The mean number of days patients remained at the CTCs from the date of initial diagnosis until discharge or the end of the study period on March 23, 2020, was 19.6 (SD ±5.8). For discharged patients, the mean number of days between diagnosis and discharge was 15.6 (SD ±4.0). The mean number of days between COVID-19 diagnosis and transfer of a patient to the hospital was 9.6 (SD ±5.2).

Clinical Characteristics of Patients with Persistent Viral Detection >28 days

A total of 19 patients had positive or inconclusive rRT-PCR results ≥28 days after initial diagnosis. Among them, 78.9% were female, 22.1% were male, the mean age was 38.4 years (SD ±13.6 years), 5.3% had underlying conditions, and 15.8% had COVID-19 symptoms. No statistically significant differences in overall clinical characteristics were noted between patients with persistent detection of virus ≥28 days and others. Additional rRT-PCR tests (mean 4.05, SD ±1.08) were performed for patients with persistent viral detection compared with those who were discharged <28 days after diagnosis (mean 2.76, SD ±1.10; p<0.001) (Table 3).

Clinical Characteristics of Patients Transferred to Hospitals

A total of 12 patients were transferred to hospitals; 5 each from Gimje and Gyeongju and 2 from Jecheon. The median age of patients transferred to a hospital was 43.5 years (interquartile range [IQR] 34.25–60.25 years), and 58.3% were women. Three (25.0%) patients had underlying conditions, including schizophrenia, hypertension, and diabetes. Eight (66.7%) patients were transferred with symptoms suggesting aggravated COVID-19; 2 were transferred with medical issues not associated with COVID-19; 2 were transferred for special care, including a 2-year-old who was too young to be taken care of at a CTC and a pregnant woman. One patient was transferred for personal reasons. The median number of days from admission to hospital transfer was 2.5 days (IQR 2.0–6.75 days) (Table 4).

Discussion

Our experience illustrates that CTC operations can be a safe alternative to conventional medical institutions. South Korea introduced CTCs to cope with the rapidly growing number of patients with COVID-19 who required isolation and monitoring but did not necessarily need to be hospitalized for treatment. Patients admitted to CTCs maintained a stable clinical course, but the time to discharge was long.

Isolation facilities for mild cases were vital to helping overcome COVID-19 outbreaks in the country, particularly because >80% of cases were not severe and did not require special therapies, such as oxygen supplementation or parenteral fluid infusion (*7*). Introducing CTCs effectively ensured that hospital beds were available for patients with moderate or severe disease. In Daegu, during the first phase of the outbreak, some patients likely died due to the unavailability of hospital beds (*8*), and increasing admissions could have led to the collapse of the healthcare system. Because of several timely countermeasures, including the rapid establishment of CTCs, the mortality rate for COVID-19 in South Korea remained lower (2.4%) than in other countries, including the United States, 6.0%; Japan, 4.3%; China, 5.6%; Iran, 6.0%; and Italy, 14.1% (*9*). In addition, CTCs helped curb virus transmission in the population. Although violation of the self-isolation orders in South Korea is punishable by law, some cases of nonadherence have been witnessed (*10*).

Table 3. Characteristics of 337 asymptomatic or mildly symptomatic patients with prolonged detection of severe acute respiratory syndrome coronavirus 2 admitted to community treatment centers for isolation, South Korea*

Center	Positive rRT-PCR >28 d, no. (%)	Release from isolation ≤28 d, no. (%)	p value
Gimje	1 (5.3)	83 (26.1)	0.077
Gyeongju	16 (84.2)	189 (59.4)	ND
Jecheon	2 (1.1)	46 (14.5)	ND
Sex			
F	15 (78.9)	202 (63.5)	0.173
M	4 (21.1)	116 (36.5)	Referent
Mean age, y, ±SD	38.4 ± 13.6	36.5 ± 15.4	0.595
Presence of underlying conditions†	1 (5.3)	27 (8.5)	1.000
Presence of signs and symptoms‡	3 (15.8)	63 (19.8)	1.000
No. rRT-PCR tests, mean ±SD	4.05 ± 1.08	2.76 ± 1.10	<0.001

*ND, not done; rRT-PCR, real-time reverse transcription PCR.
†Includes any chronic underlying condition requiring medication, such as diabetes or hypertension.
‡Includes fever, dyspnea, cough, sputum, nasal congestion, decreased sense of smell or taste, sore throat, or diarrhea.

Table 4. Clinical characteristics of 12 patients with coronavirus disease transferred from community treatment centers to a hospital, South Korea*

Age, y/sex	Center	Underlying conditions	Reason for transfer	Symptoms and signs suggesting pneumonia at transfer: Fever, temperature ≥37.5°C	Desaturation, SpO_2 <95	Abnormal findings on chest radiograph	No. days from admission to transfer
56/F	Gimje	No	Dyspnea	No	No	NA	1
42/F	Gimje	No	Cough, chest tightness	No	No	NA	2
42/M	Gimje	No	Purulent otorrhea	No	No	NA	3
45/M	Gimje	No	Dyspnea	No	No	NA	6
38/F	Gimje		Personal issue†	No	No	NA	10
27/M	Gyeongju	Schizophrenia	Aggravation of schizophrenia	No	No	NA	14
65/F	Gyeongju	Hypertension	Fever	Yes	No	Yes	2
58/M	Gyeongju	Diabetes mellitus, hypertension	Dyspnea	No	Yes	NA	2
2/F	Gyeongju	No	Need for special care‡	No	No	NA	2
33/F	Gyeongju	No	Need for special care§	No	No	NA	7
61/F	Jecheon	No	Dyspnea	No	No	Yes	3
65/M	Jecheon	No	Dyspnea, pleuritic pain	No	No	Yes	1

*NA, not applicable.
†Patient's child admitted to hospital with confirmed coronavirus disease during her admission; she asked to transfer to the hospital where her child was admitted.
‡Patient too young to be in the center without parents.
§Patient 9 weeks pregnant at admission.

The KCDC patient classification system for COVID-19 severity was essential for operating the CTCs. As part of city- and province-level patient management teams, epidemiologic investigators classified all confirmed cases by severity and ensured patients with severe symptoms were hospitalized and that other patients received appropriate treatment options (*6*). For patients without severe disease, epidemiologic investigators decided whether to send them to a hospital or a CTC on the basis of hospital bed capacity. Because hospital beds were unavailable in the middle of the outbreak, some patients admitted to CTCs did not meet the criteria of mild disease precisely. In our study, 42 patients were not classified accurately and should have been hospitalized instead of admitted to CTCs. Of them, 6 patients experienced intensified symptoms and were transferred to hospitals (data not shown). Such misclassification can be attributed to the urgent situation in Daegu and the surrounding areas and the unfamiliarity with the novel patient classification system. Fortunately, misclassifications decreased over time.

Most patients with COVID-19 admitted to CTCs were asymptomatic or had only mild symptoms over the course of the disease. Patients who were discharged from the hospitals but still had positive viral detection could be admitted to CTCs, but we did not have any patients of this demographic in our study.

Of note, ≈90% of patients were asymptomatic at the time of admission (data not shown). Extensive and aggressive testing was performed on close contacts of SARS-CoV-2 infected patients in Daegu, especially among members of a specific religious group in which a large outbreak occurred, which possibly contributed to the exceptionally high proportion of asymptomatic cases. Another finding of note was that 5.6% (19/337) of patients had positive or inconclusive rRT-PCR test results, even ≥28 days after diagnosis, which could indicate that viral shedding continues longer than assumed. A study of 56 patients with mild to moderate COVID-19 symptoms indicated that the median duration of viral shedding was 24 days, and the longest was 42 days (*11*). Data from another study of 137 patients showed that the median duration of viral detection was 12 days, and the maximum was 45 days (*12*). However, viral RNA detection does not imply infectivity. According to a report from the US Centers for Disease Control and Prevention, when viral RNA in upper respiratory samples was continuously detected in a patient following clinical recovery, the RNA concentration was generally below the level at which replication-competent virus can be isolated reliably (*13*).

Our study has several limitations. First, data on patients, especially those who were still in the CTCs at the end of the study, did not reflect the complete clinical course, and we were not able to evaluate the time between the diagnosis and discharge for all patients. Of note, observation of the entire clinical course of patients was not possible because some CTCs closed and patients were transferred to other centers as the outbreak was stabilized; for instance, Jecheon closed on April 3,

Gimje on April 7, and Gyeongju on April 14. Operation of all CTCs that opened for the outbreak in Daegu and surrounding areas ended on April 30, 2020. Because the COVID-19 pandemic continues, we decided to present the data collected up to March 23 to provide information on CTCs and the clinical characteristics of patients with mild disease. Second, because of the evolving emergency, protocols for patient care varied slightly among centers and a standardized protocol still does not exist. A standardized protocol for patient care that includes the discharge process and transfer criteria should be developed in preparation for a potential second wave of the pandemic. Finally, data collection for clinical symptoms and other medical conditions was dependent on web- or application-based questionnaires and the information obtained might be exaggerated or underestimated. To compensate for this, direct communication or telecommunication was used in extraordinary situations and for those who failed to respond to questionnaires; the response rate was >80% in each center.

In conclusion, 75.7% of patients admitted to CTCs in South Korea were asymptomatic, and most maintained a stable clinical course until discharge. Appropriate clinical triaging and CTC operations that include daily patient monitoring are a safe alternative to medical institutions for asymptomatic and mildly symptomatic patients diagnosed with COVID-19 during a pandemic.

Acknowledgments

We thank Jingyeong Yoo, Sehwan An, JeonWook Kwon, MunYoung Chang, and DoHyeon Yun for their collaboration in data collection and Editage (https://www.editage.co.kr) for English language editing.

All authors were stationed at CTCs, participated in the operations at each facility, and facilitated treatment for mild COVID-19 cases. W.S.C. and J.W.S. were stationed at the Gyeongju CTC; H.S.K. and S.N. were stationed at the Jecheon CTC; and B.K. was stationed at the Gimje CTC.

About the Author

Dr. Choi is a professor of infectious diseases at Korea University, Seoul. His research interests include influenza viruses and vaccine-preventable diseases.

References

1. World Health Organization (WHO). Novel coronavirus (COVID-19) situation report—62. Geneva: The Organization; 2020 Mar 22 [cited 2020 May 15]. https://www.who.int/docs/default-source/coronaviruse/situation-reports/20200322-sitrep-62-covid-19.pdf?sfvrsn=755c76cd_2
2. Kim JY, Choe PG, Oh Y, Oh KJ, Kim J, Park SJ, et al. The first case of 2019 novel coronavirus pneumonia imported into Korea from Wuhan, China: implication for infection prevention and control measures. J Korean Med Sci. 2020;35:e61. https://doi.org/10.3346/jkms.2020.35.e61
3. Korean Society of Infectious Diseases. Korean Society of Pediatric Infectious Diseases; Korean Society of Epidemiology; Korean Society for Antimicrobial Therapy; Korean Society for Healthcare-associated Infection Control and Prevention; Korea Centers for Disease Control and Prevention. Report on the epidemiological features of coronavirus disease 2019 (COVID-19) outbreak in the Republic of Korea from January 19 to March 2, 2020. J Korean Med Sci. 2020;35:e112. https://doi.org/10.3346/jkms.2020.35.e112
4. Center Accident Investigation Headquarters in South Korea. Guideline for countermeasures for COVID-19 2020 Version 8–1, 10 [in Korean] [cited 2020 May 15]. https://www.cdc.go.kr/board/board.es?mid=a20507020000&bid=0019&act=view&list_no=367279&tag=&nPage=1#
5. Corman VM, Landt O, Kaiser M, Molenkamp R, Meijer A, Chu DKW, et al. Detection of 2019 novel coronavirus (2019-nCoV) by real-time RT-PCR. Euro Surveill. 2020;25:2000045. https://doi.org/10.2807/1560-7917.ES.2020.25.3.2000045
6. Korea Centers for Disease Control and Prevention. COVID-19 patient treatment & management. 2020 Apr 3 [cited 2020 Mar 25]. http://ncov.mohw.go.kr/en/baroView.do?brdId=11&brdGubun=112&dataGubun=&ncvContSeq=&contSeq=&board_id=
7. Guan WJ, Ni ZY, Hu Y, Liang WH, Ou CQ, He JX, et al. Clinical characteristics of coronavirus disease 2019 in China. N Engl J Med. 2020;382:1708–20. https://doi.org/10.1056/NEJMoa2002032
8. Hyun-ju O. Daegu battles shortage of hospital beds, medical personnel. The Korea Herald; 2020 Feb 27 [cited 2020 May 15]. http://www.koreaherald.com/view.php?ud=20200227000789
9. Korea Centers for Disease Control and Prevention. Global locations with COVID-19. 2020 [cited 2020 Mar 25]. http://ncov.mohw.go.kr/en/bdBoardList.do?brdId=16&brdGubun=163&dataGubun=&ncvContSeq=&contSeq=&board_id=&gubun=
10. Shin H. South Korea warns of deportation, jail for quarantine violators. Reuters. 2020 Mar 26 [cited 2020 May 15]. https://in.reuters.com/article/health-coronavirus-south-korea/south-korea-warns-of-deportation-jail-for-quarantine-violators-idINKBN21D14G
11. Xiao AT, Tong YX, Zhang S. Profile of RT-PCR for SARS-CoV-2: a preliminary study from 56 COVID-19 patients. Clin Infect Dis. 2020 Apr 19 [Epub ahead of print]. https://doi.org/10.1093/cid/ciaa460
12. Lin A, He ZB, Zhang S, Zhang JG, Zhang X, Yan WH. Early risk factors for the duration of SARS-CoV-2 viral positivity in COVID-19 patients. Clin Infec Dis. 2020 Apr 27 [Epub ahead of print]. https://doi/10.1093/cid/ciaa490
13. US Centers for Disease Control and Prevention. Symptom-based strategy to discontinue isolation for persons with COVID-19: decision memo; updated 2020 May 3 [cited 2020 May 15]. https://www.cdc.gov/coronavirus/2019-ncov/community/strategy-discontinue-isolation.html

Addresses for correspondence: Bongyoung Kim, Department of Internal Medicine, Hanyang University College of Medicine, 222-1, Wangsimni-ro, Seongdong-gu, Seoul 04763, South Korea; email: sobakas@hanyang.ac.kr

Clinical Course of Asymptomatic and Mildly Symptomatic Patients with Coronavirus Disease Admitted to Community Treatment Centers, South Korea

Yong-Hoon Lee,[1] Chae Moon Hong,[1] Dae Hyun Kim, Taek Hoo Lee, Jaetae Lee

We evaluated the clinical course of asymptomatic and mildly symptomatic patients with laboratory-confirmed coronavirus disease (COVID-19) admitted to community treatment centers (CTCs) for isolation in South Korea. Of 632 patients, 75 (11.9%) had symptoms at admission, 186 (29.4%) were asymptomatic at admission but developed symptoms during their stay, and 371 (58.7%) remained asymptomatic during their entire clinical course. Nineteen (3.0%) patients were transferred to hospitals, but 94.3% (573/613) of the remaining patients were discharged from CTCs upon virologic remission. The mean virologic remission period was 20.1 days (SD ± 7.7 days). Nearly 20% of patients remained in the CTCs for 4 weeks after diagnosis. The virologic remission period was longer in symptomatic patients than in asymptomatic patients. In mildly symptomatic patients, the mean duration from symptom onset to virologic remission was 11.7 days (SD ± 8.2 days). These data could help in planning for isolation centers and formulating self-isolation guidelines.

Coronavirus disease (COVID-19) is an infectious disease caused by a novel coronavirus, now called severe acute respiratory syndrome coronavirus 2 (SARS-CoV-2). COVID-19 has been spreading rapidly in many countries worldwide since the pandemic began in Wuhan, the capital of Hubei Province in China, in December 2019 (*1*,*2*). In South Korea, a confirmed case of COVID-19 was reported on January 20, 2020, and the number of confirmed cases has increased markedly since late February, especially in the Daegu and Gyeongsangbuk-do regions (*3*). Mass infection at a religious institution in Daegu City was the main cause of the surge in COVID-19 cases, which affected almost two thirds of the patients diagnosed in Daegu. To prevent further spread in the community, all members of this group were screened for SARS-CoV-2, regardless of whether they had symptoms. Real-time reverse transcription PCR (rRT-PCR) analysis of the nasopharyngeal swab samples from 10,459 persons showed 4,259 (40.7%) were positive for SARS-CoV-2 (*4*).

The exponential increase in COVID-19 cases in this area was so severe that local and government medical institutions were not able to handle the surge. Thus, many symptomatic patients, including some with advanced respiratory insufficiency, had to wait at home for hospitalization because no beds were available (*3*,*5*). In addition, hospital overload because of crowding with patients diagnosed with COVID-19 prevented adequate allocation of medical resources for patients with higher mortality risk because of age and presence of underlying conditions. To promote efficient allocation of advanced medical resources to severe COVID-19 patients, on March 2, 2020, South Korea implemented community treatment centers (CTCs), novel institutions to accommodate and monitor asymptomatic to mildly symptomatic case-patients who do not require hospital admission (*6*).

The clinical spectrum of COVID-19 could range from asymptomatic to severe pneumonia with respiratory failure and even death (*7*–*9*). Several studies have been published on the clinical characteristics or outcomes of COVID-19, but most analyzed data from hospitalized patients (*10*–*12*). To date, details of

Author affiliations: Kyungpook National University Hospital, Daegu, South Korea (Y.H. Lee, C.M. Hong, T.H. Lee, J. Lee); Kyungpook National University, Daegu (Y.H. Lee, T.H. Lee, J. Lee); Keimyung University Dongsan Medical Center, Daegu (D.H. Kim)

DOI: https://doi.org/10.3201/eid2610.201620

[1]These first authors contributed equally to this article.

the natural course of COVID-19 in patients with no or mild symptoms in out-of-hospital settings has not been well documented. We describe the demographic and clinical characteristics of patients at 2 CTCs in Daegu, South Korea, and factors associated with treatment outcomes in such patients.

Materials and Methods

Study Design and Patient Classification

All patients included in the study tested positive for SARS-CoV-2 by rRT-PCR analysis of oral or nasal swab samples (*13*). After diagnosis, patients were isolated at home, and volunteer doctors interviewed patients through telephone calls ≥2 times a day. The volunteer doctors also performed risk assessment and patient classifications. Staff from the Department of Health and Welfare of Daegu Metropolitan City determined when and where patients would be admitted.

In South Korea, the COVID-19 risk assessment evolved gradually. During our study period, the Korea Centers for Disease Control and Prevention (KCDC) defined high-risk patients as persons ≥65 years of age, those with oxygen saturation <90% on room air, or those with chronic underlying diseases (*14*). KCDC guidelines also classified COVID-19 cases as asymptomatic, mild, severe, or very severe (*14*).

We used KCDC guidelines to classify patients. Asymptomatic patients were defined as persons <50 years of age with no underlying conditions who were nonsmokers and had a body temperature of <37.5°C without taking antipyretic drugs. Mildly symptomatic patients were defined as persons <50 years of age with ≥1 underlying condition and a temperature of <38°C with antipyretic drugs. Severe patients were defined as persons who were alert but had dyspnea or temperature ≥38°C despite taking antipyretic drugs. Very severe patients were persons who had decreased alertness.

After assessment by staff from the Department of Health and Welfare of Daegu Metropolitan City, severe, very severe, and high-risk patients were admitted to hospitals. Only asymptomatic or mildly symptomatic patients were admitted to CTCs. Because of the rapid surge of patients and hospital overload, however, some high-risk asymptomatic and mildly symptomatic patients were transferred to our CTCs.

Our study included patients treated at 2 CTCs during March 2–31, 2020. We collected data until April 12. We retrospectively collected data from electronic medical records (EMR) on patients' age and sex; underlying conditions; clinical, laboratory, and radiographic findings; treatment; and outcomes. We defined respiratory symptoms as dyspnea, cough, sputum, rhinorrhea, or sore throat and gastrointestinal symptoms as diarrhea, dyspepsia, or constipation. The institutional review board of Kyungpook National University Hospital (KNUH) approved this study design and informed consent was waived (IRB no. 2020–04–038).

CTCs

The 2 CTCs were existing facilities temporarily converted for patient isolation in Daegu. CTC1 was the Daegu National Education Training Institute, which had 160 rooms. CTC2 was a student dormitory of Kyungpook National University that had 480 rooms. Both CTCs were affiliated with KNUH in Daegu. During our study, the maximum number of patients per day was 150 at CTC1 and 383 at CTC2. Each patient had a separate room, except for families with young children, who stayed together. Patients were asked to remain inside their rooms during their entire admission to prevent spreading the infection.

CTC1 was open during March 2–April 30, 2020. CTC2 was open during March 8–28, 2020. Patients were transferred to CTC1 when CTC2 closed. KNUH dispatched doctors, nurses, medical technicians, and portable radiograph machines to each center and installed EMR and picture archiving and communication systems, from which authorized medical staff in KNUH could access data. Medical staff in CTCs and KNUH actively communicated with each other for patients' care.

Patients were assessed by doctors and nurses through telephone 2 times every day. Body temperature and respiratory symptoms were routinely assessed by self-monitoring and reporting. If patients complained of symptoms, medical staff went to the patient's room and examined them. Chest radiography and oxygen saturation measurement were performed at physicians' discretion. Conservative treatment, such as antipyretics, was provided for mild symptoms, but patients who needed advanced medical care were transferred to the hospital.

Laboratory Procedures

Physicians at the CTCs obtained nasopharyngeal and oropharyngeal swab specimens from patients for rRT-PCR testing. Specimens were sent to KNUH, and rRT-PCR analysis was performed for detecting SARS-CoV-2 by using Allpex 2019-nCoV Assay (Seegene Medical Foundation, https://www.seegenetech.com). A medical laboratory specialist interpreted results as negative, positive, or inconclusive.

Patients were assessed 5–7 days after admission to a CTC; if the rRT-PCR result was negative for SARS-CoV-2, another test was performed after 24 hours. If initial rRT-PCR result was positive, the next test was performed 3–5 days later. If the result was inconclusive, the next test was performed 2 days later. Patients were considered to be in virologic remission when 2 serial nasopharyngeal samples tested negative ≥24 h apart.

Statistical Analysis

We noted continuous and categorical variables as mean ± SD and no. (%). We defined the virologic remission period as the number of days from diagnosis to virologic remission. We performed a log-rank test to evaluate each factor related to hospitalization and virologic remission, such as age, sex, underlying conditions, and symptoms. We excluded patients transferred to the hospital from our analysis of virologic remission because their data were unavailable after transferred to hospital. We generated Kaplan-Meier curves for visualization of cumulative virologic remission rate of asymptomatic and mildly symptomatic patients. We analyzed data by using R version 3.6.3 software (https://www.r-project.org), and we considered $p<0.05$ statistically significant.

Results

Patient Characteristics

Among 640 patients treated at 2 CTCs, we excluded 8 from our analysis, 7 because we did not have enough data, and 1 because the patient was transferred from the hospital and discharged soon after symptom improvement. We analyzed data on 632 patients, 272 from CTC1 and 360 from CTC2. Among patients included, 430 (68.0%) were female and 202 (32.0%) male; the mean age was 40.6 years (SD ± 17.3 years), and 112 (17.7%) patients had ≥1 underlying condition. After COVID-19 diagnosis, patients were self-isolated at home an average of 7.8 days (SD ± 3.8 days) before admission to a CTC.

Among 632 patients, only 31 (4.9%) were symptomatic at diagnosis; 44 (7.0%) were asymptomatic at diagnosis but developed symptoms by the time they were admitted to the CTC. Among patients who were asymptomatic at the time of admission, 186 (29.4%) developed symptoms during CTC admission and 371 (58.7%) remained asymptomatic. During their illnesses, 187 patients (29.6%) had respiratory symptoms: 87 (13.8%) had cough, 78 (12.3%) had sputum, 45 (7.1%) had rhinorrhea, 45 (7.1%) had sore throat, and 10 (1.6%) had dyspnea. Fifty-four (8.5%) patients had gastrointestinal symptoms, such as abdominal pain or diarrhea; 30 (4.7%) patients had headache, 24 (3.8%) had fever, and 37 (5.9%) had other symptoms (Table 1).

Nineteen patients (3.0%) were transferred to the hospital (Table 2). Statistically significant correlations with transfer to hospital included age >50 years ($p = 0.005$), having ≥1 underlying condition ($p<0.0001$), and developing symptoms during the course of illness ($p<0.0001$). Among the 19 patients transferred to the hospital, 14 (73.7%) had respiratory symptoms, 2 (10.5%) had gastrointestinal symptoms, 2 (10.5%) reported headache, 5 (26.3%) had fever, and 5 (26.3%) had other symptoms or conditions, such as severe anxiety and pregnancy.

Virologic Remission

After excluding patients transferred to the hospital, 578/613 (94.3%) had virologic remission and were discharged from CTCs. A total of 2,522 rRT-PCR tests were performed (range 2–14/patient); 1,425 (56.6%) were negative, 733 (29.1%) were inconclusive, and 364 (14.5%) were positive. The virologic remission period was 20.1 days (SD ± 7.7 days; range 7–45 days). Among 613 patients, 2 (0.3%) had virologic remission within 1 week, 157 (25.6%) within 2 weeks, 362 (59.1%) within 3 weeks, 489 (79.8%) within 4 weeks, and 550 (89.7%) within 5 weeks. Sixty-seven (10.9%) patients were symptomatic when they entered the CTC, 175 (28.5%) were asymptomatic at the time of admission but develop symptoms during isolation, and 371 (60.5%) remained asymptomatic (Figure 1). The virologic remission period was 19.0 days (SD ± 7.4 days; range 7–43 days) for patients who were symptomatic at the time of entrance to the CTC, 23.1 days (SD ± 7.7 days; range 8–45 days) for those who were asymptomatic at CTC admission but developed symptoms during isolation, and 19.1 days (SD ± 7.5 days; range 7–45 days) for asymptomatic patients.

Among 613 patients, 242 (39.5%) developed symptoms during their illness. The mean number of days from symptom onset to virologic remission for patients who developed symptoms was 11.7 days (SD ± 8.2 days; range 2–41 days). Among 242 patients, 90 (37.2%) had virologic remission ≤1 week after symptom onset, 149 (61.6%) ≤2 weeks, 188 (77.7%) ≤3 weeks, 207 (85.5%) ≤4 weeks, and 219 (90.5%) during week 5 or longer (Figure 2).

Symptomatic patients had a longer remission period, 21.8 days (SD ± 7.6 days), than asymptomatic patients 19.1 days (SD ± 7.5 days; $p<0.0001$) (Figure 3). Respiratory symptoms had statistically significant correlation to the virologic remission period

(p<0.0001). However, we noted no statistically significant differences in virologic remission period related to gastrointestinal symptoms (p = 0.07), headache (p = 0.1), fever (p = 0.1), and other symptoms (p = 0.4). We also saw no statistically significant differences in the remission period according to sex (p = 0.1), age (p = 0.5), or underlying conditions (p = 0.7).

Discussion

We investigated the clinical characteristics and outcomes COVID-19 cases in asymptomatic and mildly symptomatic patients admitted for isolation and monitoring in 2 CTCs in South Korea. The mean duration from diagnosis to virologic remission was 20.1 days. For patients with mild symptoms, the virologic remission period was much longer than for asymptomatic patients (Figure 3).

The average age of the patients was ≈40 years; 68% were female and 32% were male. Demographic characteristics are linked to the population of religious institution in Daegu when CTCs were introduced, which seems to have had a demographic effect on our study population. Most (58.7%) patients remained asymptomatic during admission. Among patients with symptoms, cough and sputum were common, but fever, the most commonly observed symptom in studies involving hospitalized patients with COVID-19 (*9*,*10*), was less common in our patients, likely because of the CTC admission criteria. According to KCDC guidelines, patients with high fever or dyspnea were excluded from CTC admission because that might have required advanced medical treatment not available in CTCs (*14*).

A recent study that analyzed the viral dynamics of 76 hospitalized patients reported that severe COVID-19 cases tended to have viral loads ≈60 times higher than mild cases, with a longer viral shedding period (*15*). Although data on the relationship between clinical course and viral load in asymptomatic to mildly symptomatic patients with COVID-19 are lacking in our patients, the time from symptom onset to discharge was ≈12 days, which is ≈10 days shorter than the data from a study of hospitalized patients with COVID-19 (*8*). In terms of the natural course of COVID-19, this difference in recovery period suggests that the higher the disease severity and viral load, the longer it takes for virologic remission. Similarly, in our study, patients with symptomatic manifestation had a greater delay in the virologic remission period compared with asymptomatic patients. In particular,

Table 1. Characteristics of 632 patients with diagnosed coronavirus disease admitted to community treatment centers for isolation, South Korea*

Characteristics	Total	Hospitalized, n = 19	p value	Released or in remission, n = 578	p value
Sex					
M	202 (32.0)	6 (31.6)	0.9	187 (32.4)	0.1
F	430 (68.0)	13 (68.4)	Referent	391 (67.6)	Referent
Age, y					
Mean ± SD	40.6 ± 17.3		0.005†		0.5†
<20	44 (7.0)	2 (10.5)		38 (6.6)	
20–29	204 (32.3)	1 (5.3)		194 (33.6)	
30–39	74 (11.7)	0		70 (12.1)	
40–49	76 (12.0)	3 (15.8)		69 (11.9)	
50–59	118 (18.7)	5 (26.3)		105 (18.2)	
≥60	116 (18.4)	8 (42.1)		102 (17.6)	
Underlying conditions					
None	520 (82.3)	10 (52.6)	Referent	482 (83.4)	Referent
≥1 condition	112 (17.7)	9 (47.4)	<0.0001	96 (16.6)	0.7
Hypertension	55 (8.7)	4 (21.1)	0.05	47 (8.1)	0.9
Diabetes	12 (1.9)	0	0.5	10 (1.7)	0.6
Dyslipidemia	22 (3.5)	1 (5.3)	0.6	20 (3.5)	0.3
Respiratory disease	16 (2.5)	0	0.5	16 (2.8)	0.3
Heart disease	5 (0.8)	1 (5.3)	0.006	4 (0.7)	0.2
Other	43 (6.8)	7 (36.8)	<0.0001	35 (6.1)	0.8
Symptoms					
None	371 (58.7)	0	Referent	359 (62.1)	Referent
Any symptom	261 (41.3)	19 (100.0)	<0.0001	219 (37.9)	<0.0001
Respiratory	187 (29.6)	14 (73.7)	0.0001	155 (26.8)	<0.0001
Gastrointestinal	54 (8.5)	2 (10.5)	0.9	47 (8.1)	0.07
Headache	30 (4.7)	2 (10.5)	0.2	26 (4.5)	1.0
Fever	24 (3.8)	5 (26.3)	<0.0001	16 (2.8)	0.1
Other	37 (5.9)	5 (26.3)	0.0001	29 (5.0)	0.4

*Values are no. (%) patients except as indicated. p values calculated by using log-rank test.
†Age ≥50 y.

Table 2. Characteristics of 19 patients with coronavirus disease transferred from isolation in community treatment centers to hospitals, South Korea*

Age, y/sex	No. days from diagnosis to CTC admission	No. days in CTC	Underlying conditions	Reason for transfer
13/F	7	3	None	Severe anxiety
12/F	8	4	Allergic rhinitis	Severe anxiety
53/F	2	2	None	Severe cough, abnormality on chest radiograph, oxygen saturation 94%
42/F	5	18	None	Severe cough and sputum
64/F	3	3	None	Severe headache and chest discomfort
53/F	3	3	None	Severe cough, sputum, GGOs on chest radiograph
59/F	2	5	Claustrophobia	Severe cough, sputum, poor oral intake
70/F	8	22	Hypertension	Persistent fever (38.5°C) after medication
86/F	5	9	Hypertension	Old age, abnormality on chest radiograph
23/F	6	14	Pregnancy	Pregnancy
69/M	6	3	Dyslipidemia, arrhythmia, Parkinson's disease	Dyspnea, underlying conditions
67/F	3	3	Cerebral aneurysm, postoperative state	Dyspnea, abnormality on chest radiograph
51/M	4	2	Hypertension, hepatitis B, hepatocellular carcinoma, post-operative state	Oxygen saturation 82%
66/M	3	15	None	Severe anxiety
57/M	4	3	None	Oxygen saturation 88%, tachycardia
47/F	11	3	None	Dyspnea
49/F	4	7	Meniere's disease, claustrophobia	Severe anxiety
60/M	11	23	None	Dyspnea
80/M	5	22	Hypertension	Old age, abnormality on chest radiograph

*CTC, community treatment center; GGOs, ground glass opacities.

patients who were asymptomatic at admission to a CTC but symptomatic during follow up tended to have a longer virologic remission period, suggesting this patient subgroup might have peaked in disease severity or viral load during CTC admission. Therefore, even patients who are asymptomatic at the time of CTC admission should be followed closely to determine if they experience symptoms and then carefully managed during admission.

We had limited resources to perform rRT-PCR and could not perform daily testing for all obtained oral and nasal swabs samples. However, we did perform 2,522 rRT-PCR tests for early discharge from the center. In addition to the detection of SARS-CoV-2 in samples from the respiratory tract, viral RNA detection in stool samples and the possibility of active replication in the gastrointestinal tract have been suggested (*16*), but these tests were not clinically feasible in our facilities. A recent study reported virologic analysis of 9 cases of COVID-19 after the first week of symptoms but found no live virus isolates despite ongoing high concentrations of viral RNA (*16*).

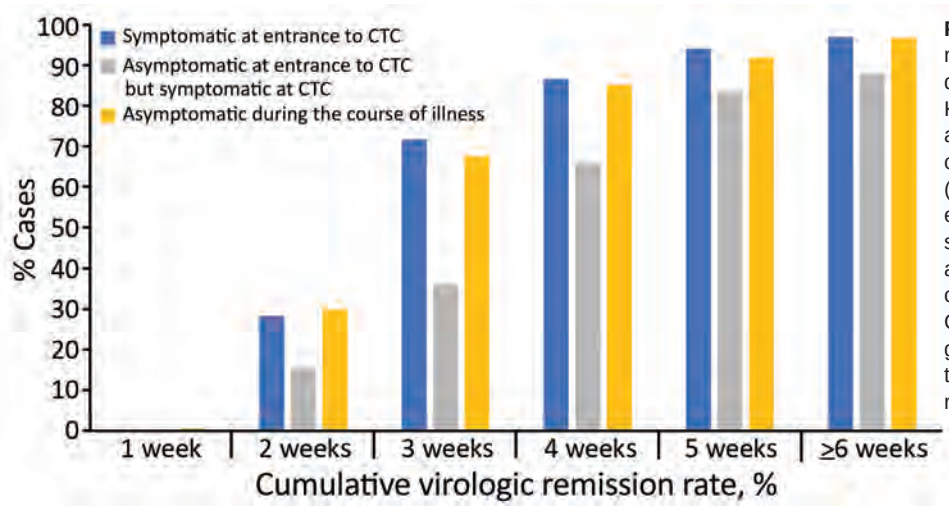

Figure 1. Cumulative virologic remission rate for coronavirus disease in patients in South Korea who were symptomatic at the time of entrance to a community treatment center (CTC), asymptomatic at the time of entrance to the CTC but developed symptoms during CTC admission, and asymptomatic during the course of illness after diagnosis. Cumulative remission rates of each group were calculated according to the time from diagnosis to virologic remission.

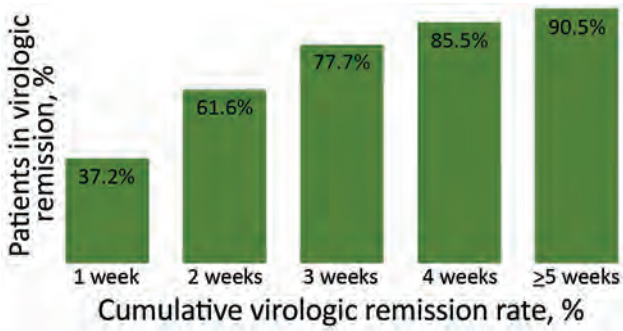

Figure 2. Cumulative virologic remission rate for coronavirus disease in mildly symptomatic patients in South Korea after symptom onset. Cumulative virologic remission rate of mildly symptomatic patients was calculated according to the time of the symptom onset to virologic remission.

Therefore, further studies are needed to verify the relationship between viral RNA detected by rRT-PCR and infectivity of SARS-CoV-2.

Patient isolation is essential for preventing the spread of COVID-19. For practical operation of CTCs, we need to estimate the stay of the patients. Our results show that 59.1% of patients showed virologic remission at 3 weeks after diagnosis. In addition, ≈20% of the patients remained in CTC for ≥28 days after diagnosis. Combined with the fact that symptomatic patients took longer to discharge than asymptomatic cases, these data might be helpful for planning the establishment of isolation centers and formulation of self-isolation guidelines.

Nineteen (3.0%) patients at CTCs were transferred to hospitals, similar to recently reported data from another CTC in South Korea (*6*). The patients who were transferred were generally ≥50 years of age with underlying conditions, and the main reasons were worsening respiratory symptoms or abnormalities on chest radiographs. Although a CTC is not strictly a medical institution, we deployed a mobile radiology facility to our centers to help screen patients with pneumonia. In addition to symptoms caused by SARS-CoV-2 infection, 4 patients were transferred because of severe anxiety; 2 were adolescents and reported severe anxiety during isolation and separation from families. A previous report also had a case of hospital transfer due to serious psychiatric problems, including suicidal ideation (*6*). Therefore, successful CTC operation requires an established system capable of early detection of psychological symptoms and consultation with a psychiatrist.

Recent studies reported that age ≥65 years and presence of underlying conditions are the factors most related to outcomes for patients with COVID-19 (*11*,*12*). However, the time from diagnosis to remission in our study did not differ by age group. In asymptomatic or mildly symptomatic patients, as in our study population, the effect of age or underlying disease in terms of viral clearance might be minimal and further research is needed. However, in terms of hospitalization after clinical deterioration, older persons and those with underlying conditions tended to be more vulnerable and should be carefully monitored.

Our study has several limitations. First, CTCs did not have the capacity for the meticulous medical record keeping found in a hospital, and laboratory

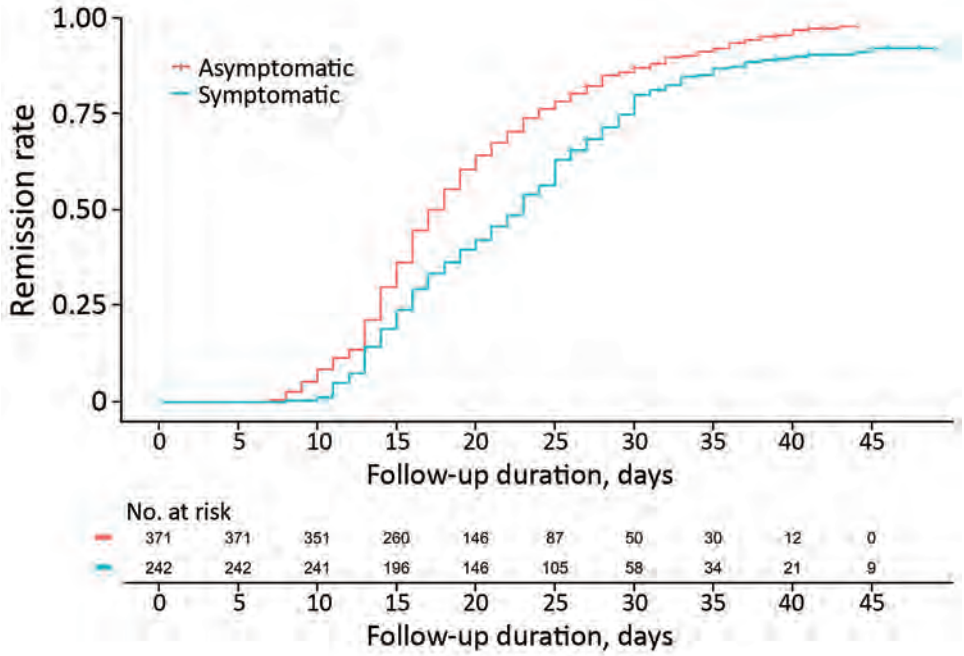

Figure 3. Virologic remission of coronavirus disease patients in South Korea according to symptoms. We noted a significant difference in virologic remission period between the asymptomatic and mildly symptomatic patients (p<0.0001).

tests other than rRT-PCR for SARS-CoV-2 were not available. Second, we do not have data on reinfection or reactivation after discharge. Last, because timing of SARS-CoV-2 infection before diagnostic testing is unclear, the actual time interval from the date of the infection to virologic remission could be longer than we report in our study.

In conclusion, our results demonstrate the natural course of COVID-19 in a large population of asymptomatic and mildly symptomatic patients. These data might be helpful for planning isolation centers and formulating self-isolation guidelines for the public.

Acknowledgments

We thank the city of Daegu, Kyungpook National University, Kyungpook National University Hospital, Daegu National Education Training Institute, Daegu Medical Association, and Daegu Center for Infectious Disease Control and Prevention for assistance in fighting COVID-19. We would like to thank Editage (https://www.editage.co.kr) for English language editing.

This work was supported by the research grants from Daegu Medical Association COVID-19 scientific committee and the Korea Health Technology R&D Project, Ministry of Health & Welfare, South Korea (grant no. HI16C1501).

About the Author

Dr. Lee is an assistant professor in the division of Pulmonary and Critical Care Medicine, Department of Internal Medicine, School of Medicine, Kyungpook National University, and Kyungpook National University Hospital. Dr. Hong is clinical assistant professor in Kyungpook National University Hospital.

References

1. World Health Organization. Coronavirus disease 2019 (COVID-19) situation report—77. Geneva: The Organization; 2020 Apr 6 [cited 2020 Apr 6]. https://www.who.int/docs/default-source/coronaviruse/situation-reports/20200406-sitrep-77-covid-19.pdf
2. Zhu N, Zhang D, Wang W, Li X, Yang B, Song J, et al.; China Novel Coronavirus Investigating and Research Team. A novel coronavirus from patients with pneumonia in China, 2019. N Engl J Med. 2020;382:727–33. https://doi.org/10.1056/NEJMoa2001017
3. Korean Society of Infectious Diseases; Korean Society of Pediatric Infectious Diseases; Korean Society of Epidemiology; Korean Society for Antimicrobial Therapy; Korean Society for Healthcare-associated Infection Control and Prevention; Korea Centers for Disease Control and Prevention. Report on the epidemiological features of coronavirus disease 2019 (COVID-19) outbreak in the Republic of Korea from January 19 to March 2, 2020. J Korean Med Sci. 2020;35:e112. https://doi.org/10.3346/jkms.2020.35.e112
4. Daegu Metropolitan City. Daily briefing of COVID-19 in Daegu City, 2020 April 12 [in Korean]. [cited 2020 Apr 12]. http://www.daegu.go.kr/dgcontent/index.do?menu_id=00936590&menu_link=/icms/bbs/selectBoardArticle.do&bbsId=BBS_02098
5. Korea Centers for Disease Control and Prevention. The updates of COVID-19 in the Republic of Korea as of 2 March. [cited 2020 Apr 6]. https://www.cdc.go.kr/board/board.es?mid=a20501000000&bid=0015
6. Park PG, Kim CH, Heo Y, Kim TS, Park CW, Kim CH. Out-of-hospital cohort treatment of coronavirus disease 2019 patients with mild symptoms in Korea: an experience from a single community treatment center. J Korean Med Sci. 2020;35:e140. https://doi.org/10.3346/jkms.2020.35.e140
7. Chen N, Zhou M, Dong X, Qu J, Gong F, Han Y, et al. Epidemiological and clinical characteristics of 99 cases of 2019 novel coronavirus pneumonia in Wuhan, China: a descriptive study. Lancet. 2020;395:507–13. https://doi.org/10.1016/S0140-6736(20)30211-7
8. Huang C, Wang Y, Li X, Ren L, Zhao J, Hu Y, et al. Clinical features of patients infected with 2019 novel coronavirus in Wuhan, China. Lancet. 2020;395:497–506. https://doi.org/10.1016/S0140-6736(20)30183-5
9. Wang D, Hu B, Hu C, Zhu F, Liu X, Zhang J, et al. Clinical characteristics of 138 hospitalized patients with 2019 novel coronavirus-infected pneumonia in Wuhan, China. JAMA. 2020;323:1061–9. https://doi.org/10.1001/jama.2020.1585
10. Guan WJ, Ni ZY, Hu Y, Liang WH, Ou CQ, He JX, et al.; China Medical Treatment Expert Group for Covid-19. Clinical characteristics of coronavirus disease 2019 in China. N Engl J Med. 2020;382:1708–20. https://doi.org/10.1056/NEJMoa2002032
11. Yang X, Yu Y, Xu J, Shu H, Xia J, Liu H, et al. Clinical course and outcomes of critically ill patients with SARS-CoV-2 pneumonia in Wuhan, China: a single-centered, retrospective, observational study. Lancet Respir Med. 2020;8:475–81. https://doi.org/10.1016/S2213-2600(20)30079-5
12. Zhou F, Yu T, Du R, Fan G, Liu Y, Liu Z, et al. Clinical course and risk factors for mortality of adult inpatients with COVID-19 in Wuhan, China: a retrospective cohort study. Lancet. 2020;395:1054–62. https://doi.org/10.1016/S0140-6736(20)30566-3
13. World Health Organization. Laboratory testing for coronavirus disease 2019 (COVID-19) in suspected human cases: interim guidance, 2 March 2020. Geneva: The Organization [cited 2020 Apr 6] https://www.who.int/publications-detail/laboratory-testing-for-2019-novel-coronavirus-in-suspected-human-cases-20200117
14. Korea Centers for Disease Control and Prevention. Guidelines for management of COVID-19 [in Korean] [cited 2020 Apr 6]. https://www.cdc.go.kr/board/board.es?mid=a20507020000&bid=0019
15. Liu Y, Yan LM, Wan L, Xiang TX, Le A, Liu JM, et al. Viral dynamics in mild and severe cases of COVID-19. Lancet Infect Dis. 2020 Mar 19 [Epub ahead of print]. https://doi.org/10.1016/S1473-3099(20)30232-2
16. Wölfel R, Corman VM, Guggemos W, Seilmaier M, Zange S, Müller MA, et al. Virological assessment of hospitalized patients with COVID-2019. Nature. 2020 Apr 1 [Epub ahead of print]. https://doi.org/10.1038/s41586-020-2196-x

Address for Correspondence: Jaetae Lee, School of Medicine, Kyungpook National University, 130 Dongdeok-ro, Jung Gu, Daegu 41944, South Korea; email: jaetae@knu.ac.kr

Nationwide External Quality Assessment of SARS-CoV-2 Molecular Testing, South Korea

Heungsup Sung,[1] Myung-Guk Han, Cheon-Kwon Yoo, Sang-Won Lee, Yoon-Seok Chung, Jae-Sun Park, Mi-Na Kim, Hyukmin Lee, Ki Ho Hong, Moon-Woo Seong, Kyunghoon Lee, Sail Chun, Wee Gyo Lee, Gye-Cheol Kwon, Won-Ki Min[1]

External quality assessment (EQA) is essential for ensuring reliable test results, especially when laboratories are using assays authorized for emergency use for newly emerging pathogens. We developed an EQA panel to assess the quality of real-time reverse transcription PCR assays being used in South Korea to detect severe acute respiratory syndrome coronavirus 2 (SARS-CoV-2). With the participation of 23 public health organization laboratories and 95 nongovernmental laboratories involved in SARS-CoV-2 testing, we conducted qualitative and semiquantitative performance assessments by using pooled respiratory samples containing different viral loads of SARS-CoV-2 or human coronavirus OC43. A total of 110 (93.2%) laboratories reported correct results for all qualitative tests; 29 (24.6%) laboratories had ≥1 outliers according to cycle threshold values. Our EQA panel identified the potential weaknesses of currently available commercial reagent kits. The methodology we used can provide practical experience for those planning to conduct evaluations for testing of SARS-CoV-2 and other emerging pathogens in the future.

The current outbreak of coronavirus disease (COVID-19), caused by severe acute respiratory syndrome coronavirus 2 (SARS-CoV-2), continues to spread. As of June 27, 2020, the pandemic had affected 214 countries, resulting in 9,653,048 recorded cases and 491,128 deaths (*1*,*2*). Early detection of SARS-CoV-2 and immediate isolation of infected patients from the susceptible population is important for preventing the spread of infection (*3*). Real-time reverse transcription PCR (rRT-PCR) is currently the most reliable method for diagnosing COVID-19 (*4*).

Since March 2, 2020, the number of newly reported cases in South Korea appears to be declining; the mean number of daily new confirmed cases decreased to 40 by the end of June (*5*). Intensive SARS-CoV-2 testing helped to contain the spread of the disease in South Korea. Since March 1, South Korea (population ≈51 million) has performed ≈20,000 tests per day by using rRT-PCR. The outstanding achievements of the public health response were attributable to the rapid expansion of diagnostic testing capabilities resulting from the collaboration between the public and private sectors. In June 2016, South Korea enacted emergency use authorization (EUA) legislation with the aim of supplying commercial kits to meet the demands of nongovernmental clinical laboratories and to guarantee quality assurance through mandatory technical training regarding standardized laboratory guidelines and external quality assessment (EQA) (*6*).

As of March 31, after successfully completing a proficiency testing panel consisting of 7-plasmid DNA specimens, a total of 95 nongovernmental clinical laboratories were conducting SARS-CoV-2 tests by using 5 different EUA kits (*6*). However, the nucleic acid extraction methods, rRT-PCR reagents, and thermocyclers used differed among laboratories. EQAs using pooled respiratory samples spiked with inactivated cultured SARS-CoV-2 had indicated the possible effects of these variations on assay performance, thereby allowing

Author affiliations: University of Ulsan College of Medicine and Asan Medical Center, Seoul, South Korea (H. Sung, M.-N. Kim, S. Chun, W.K. Min); Korea Centers for Disease Control and Prevention, Chungcheongbuk-do, South Korea (M.-G. Han, C.-K. Yoo, S.-W. Lee, Y.-S. Chung, J.-S. Park); Yonsei University College of Medicine, Seoul (H. Lee); Seoul Medical Center, Seoul (K.-H. Hong); Seoul National University College of Medicine, Seoul (M.-W. Seong, K. Lee); Ajou University School of Medicine, Suwon, South Korea (W.G. Lee); Chungnam National University School of Medicine, Daejeon, South Korea (G.-C. Kwon)

DOI: https://doi.org/10.3201/eid2610.202551

[1]These authors contributed equally to this article.

the participating laboratories to assess the quality and identify the possible weaknesses and strengths of the currently used diagnostic methods (*7*,*8*). Therefore, we developed an EQA panel to assess the quality of SARS-CoV-2 rRT-PCR assays in South Korea.

Methods

Participants

Because participation in the nationwide EQA requested by the Korea Centers for Disease Control (KCDC) was mandatory for the 118 laboratories conducting SARS-CoV-2 tests, these laboratories were included in the our study by default. Because the study was a survey and an EQA that did not include personal identifiers or patient data, the requirement for institutional review board approval was waived (waiver no. AMC IRB 2020-0547). The upper and lower respiratory tract samples from SARS-CoV-2–negative patients were also included in the study.

Specimen Preparation

To construct the SARS-CoV-2 proficiency test panel, Vero cells (ATCC CCL-81, American Type Culture Collection, https://www.atcc.org) were inoculated with the SARS-CoV-2 KNIH001 strain (from KCDC) and cultured at 37°C at 5% CO_2 for 5 days (*9*). Infection was confirmed by assessing the cytopathic effects and by rRT-PCR assays using primers and probe sets described previously by Corman et al. (*10*). The titer was 1.0×10^6 PFU/mL, and the cycle threshold (C_t) value of the SARS-CoV-2 *E* gene was ≈16. The virus was inactivated at 70°C for 1 hour. No infectious virus was detected on testing for residual infectivity after heat treatment by inoculation in cell culture. Dilution matrices were established by using pooled nasopharyngeal aspirates, to represent upper respiratory tract samples, and pooled sputum or bronchoalveolar lavage fluids, to represent lower respiratory tract samples. All pooled samples were negative for common respiratory viruses and SARS-CoV-2. Liquillizer (MetaSystems, https://metasystems-international.com) was added to the pooled lower respiratory tract samples for dilution to achieve a final concentration of 10%.

The proficiency test panel included 4 each of upper and lower respiratory tract samples containing serial 10-fold dilutions of SARS-CoV-2–positive cell culture supernatant ($1{:}2 \times 10^2$-$1{:}2 \times 10^5$), 1 human coronavirus OC43 (HCoV-OC43)–positive/SARS-CoV-2–negative upper respiratory tract sample, and 1 negative lower respiratory tract sample. The samples were immediately frozen at -70°C after aliquoting. Although participants were informed that the materials were nonbiohazardous, we recommended that they be handled according to general basic requirements regarding human specimens.

Validation and Dispatch of Panel Tests and Collection of EQA Results

To validate stability and homogeneity, EQA panel samples were assayed by 3 extraction systems, 4 EUA reagents, and 2 thermocyclers. For assessing homogeneity, 3 panels were selected at random and assayed in triplicates, generating 9 test results; for stability, samples were maintained at -70°C for 1 day, 3 days, and 7 days. Three panels from each storage condition were then selected at random and assayed 3 times. EQA samples were shipped on dry ice with temperature monitoring by Green Cross Labcell (http://www.gclabcell.co.kr). Delivery to all laboratories, including those on Jeju Island, was completed within 10 hours. The Korean Association of External Quality Assessment Service (KEQAS) was responsible for the transport of the EQA material, collection of the EQA results, and evaluation of results. All EQA data, including those of test sample volumes, extraction reagents and instruments, and elution volumes, were submitted through the KEQAS program web site (http://eqas.keqas.org).

Evaluating the EQA Results and Statistical Analysis

For qualitative evaluations, only samples with an ≥80% agreement rate compared with the expected results were evaluated (*11*). All EUA kits included the manufacturer's instructions for threshold settings or use of an exclusive interpretation–viewer program from the manufacturer. For evaluations of semiquantitative data, the mean, median, and interquartile ranges of the C_t values were converted to box-and-whisker plots. Outliers were defined when determined by a double-sided Grubbs test, when a negative result for positive sample was given, or when any C_t value in negative samples was reported. The outlier frequencies were compared by using the χ^2 test. The likelihood ratios for different tests were calculated from a 2 × k table. For homogeneity and stability tests, the mean value and percentage coefficient of variation (%CV) of the 9 results from triplicated assays of 3 samples were analyzed, and assumption of homogeneity of variance was tested by using Levine's test of equality of variances. Homogeneity and stability were satisfactory when the %CV was <5 and p value was ≥0.05. MedCalc Statistical Software version 19.2.1 (MedCalc Software Ltd, https://www.medcalc.org) was used for all statistical analyses.

Results

Participating Laboratories

Twenty-three public laboratories conducting COVID-19 tests, including 18 regional Institutes of Health and Environment, 4 National Quarantine Stations, and 1 Armed Force Medical Science Research Institute, participated, along with 95 nongovernmental clinical laboratories. Sixty-six (55.9%) laboratories were located in the Seoul, Incheon, and Gyeonggi metropolitan areas, in which 49.6% of the total population of South Korea resides.

SARS-CoV-2 Testing Protocols

Protocols for SARS-CoV-2 rRT-PCR varied among the 118 participating laboratories (Figure 1). Ninety-five nongovernmental clinical laboratories were allowed to use only 1 of the 5 EUA rRT-PCR reagents. Five regional Institutes of Health and Environment used laboratory-developed tests using the primers and probes described by Corman et al. (*10*) and AgPath-ID 1-step RT-PCR reagents (ThermoFisher Scientific, https://www.thermofisher.com). A large variance in extraction steps, reagents, instruments, sample volumes, and elution volumes (i.e., sample volume equivalent RNA input) was observed (Figures 1, 2). For SARS-CoV-2 detection, 67 laboratories (56.8%) used the PowerChek 2019-nCoV Kit (Kogene Biotech, http://www.kogene.co.kr), which was the first EUA SARS-CoV-2 assay cleared by KCDC and the Korea Food and Drug Administration, and 38 laboratories (32.2%) used the Allplex 2019-nCoV Kit (Seegene, http://www.seegene.com).

Qualitative rRT-PCR Results

Because the lower respiratory tract sample with the highest dilution (nCoV-2041) showed 78.8% (93/118) agreement compared with the expected results, lower respiratory tract sample results were excluded from the final analysis. A total of 110 laboratories (93.2%) reported correct results for all qualitative tests.

Among the 38 laboratories using the Allplex 2019-nCoV Kit (Seegene), 8 (21.1%) laboratories had ≥1 incorrect results, in which all incorrect results were reported from lower respiratory tract samples (nCoV-20–41, -42, -43, or -45) (Appendix Table 1, https://wwwnc.cdc.gov/EID/article/26/10/20-2551-App1.pdf). Eighty laboratories using the other EUA kits or WHO primers and probes provided correct results for all evaluable results. The likelihood ratio of unacceptable results from the Allplex 2019-nCoV Kit compared with the other kits was 0.273 (95% CI 0.201-0.370). Other kits 95% CIs of likelihood ratios included 1.000. Extraction reagent kits used by laboratories that reported incorrect results were STARMag DNA/RNA Extraction Kit (Seegene) and NucliSENS easyMAG

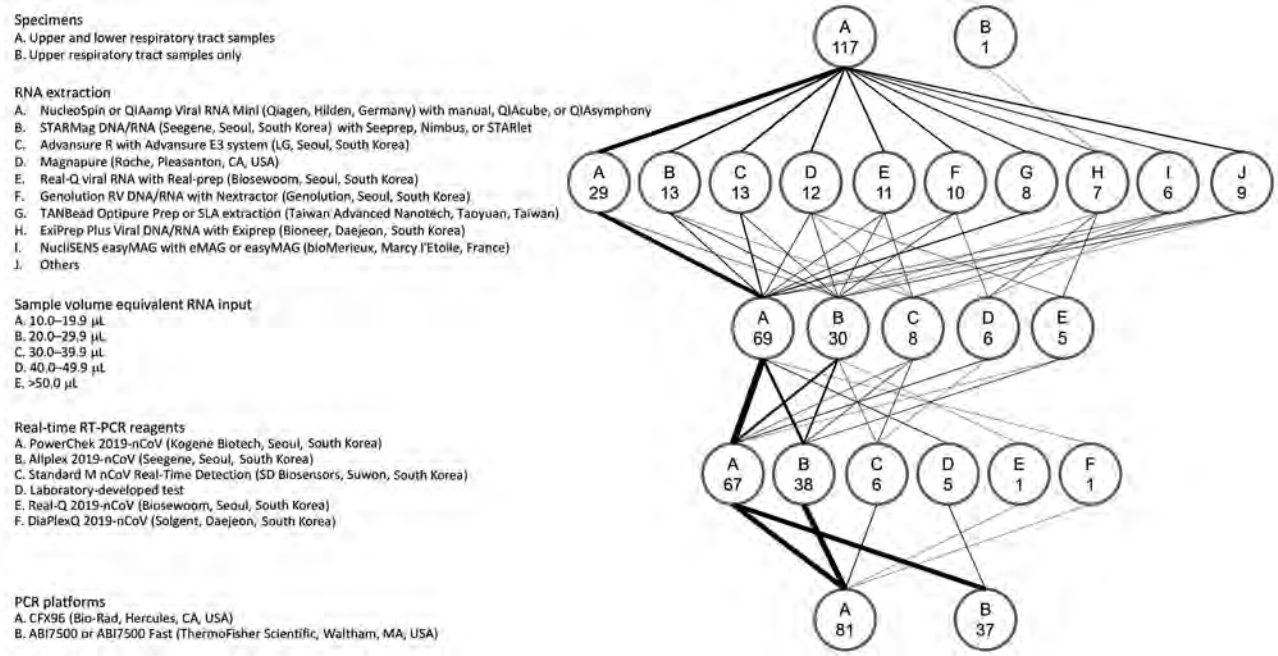

Figure 1. Protocols used for real-time RT-PCR in 118 laboratories participating in an external quality assessment of severe acute respiratory syndrome coronavirus 2 testing, South Korea, March 23–27, 2020. The flow diagram shows the variations in specimens tested, RNA extraction platforms, PCR reagents and amplification platforms, and sample volume equivalent RNA input used in the PCR reaction. The weight of the lines reflects the number of laboratories using a particular step. Numbers in the circles indicate number of laboratories. RT-PCR, reverse transcription PCR.

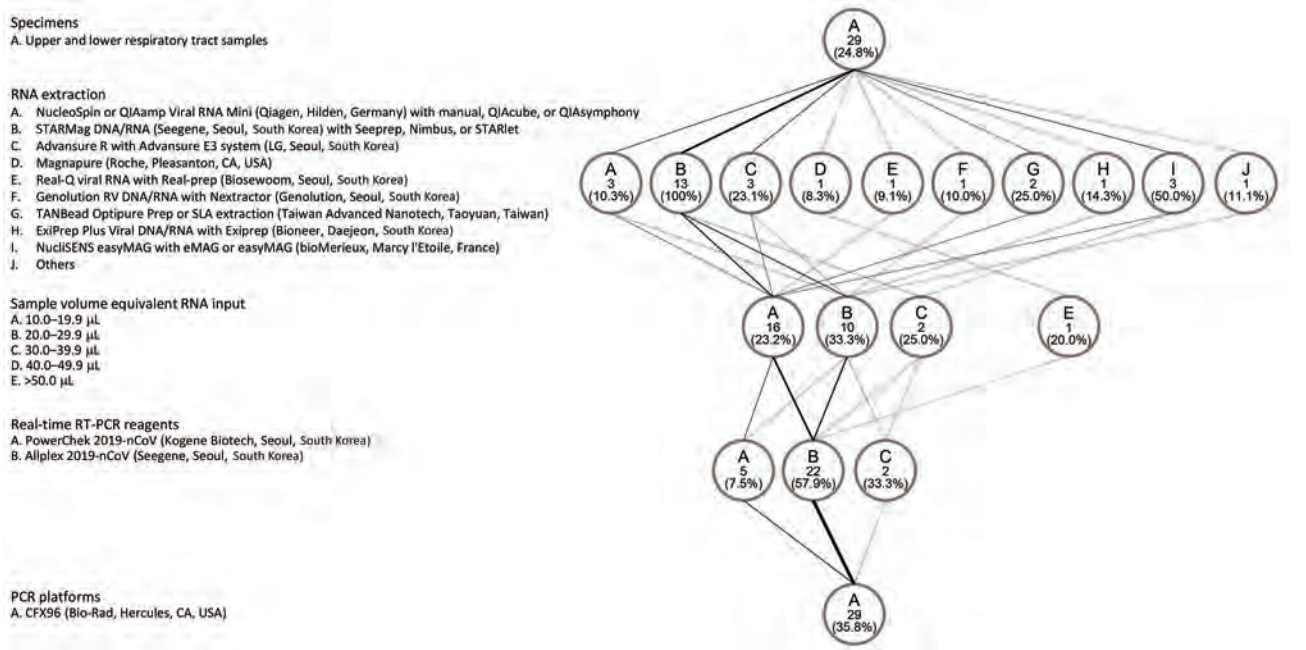

Figure 2. Protocols used for laboratories that reported ≥1 outliers in results of real-time RT-PCR tests for severe acute respiratory syndrome coronavirus 2, South Korea, March 23–27, 2020. The flow diagram shows the variations in specimens tested, RNA extraction platforms, PCR reagents and amplification platforms, and sample volume equivalent RNA input used in the PCR reaction. The weight of the lines reflects the number of laboratories using a particular step. Numbers in the circles indicate number of laboratories. RT-PCR, reverse transcription PCR.

Extraction Kit (bioMérieux, https://www.biomerieux.com) used by 3 laboratories. The other 2 laboratories used Advansure R Extraction Kit (LG Chem, https://www.lgchem.com) or Exiprep Plus Viral DNA/RNA Extraction Kit (Bioneer, https://eng.bioneer.com).

Semiquantitative Results by C_t value

The C_t values of the SARS-CoV-2 *RdRp* gene for each EUA assay, except for the DiaPlexQ 2019-nCoV kit (Solgent, http://www.solgent.com), which detects the *ORF1a* and *N* genes, and expected C_t value for each sample for PowerChek 2019-nCoV and Allplex 2019-nCoV are shown in Table 1. *E* gene and *RdRp* gene C_t values from 67 laboratories using the PowerChek 2019-nCoV reagents and *E* gene, *RdRp* gene, and *N* gene C_t values from 38 laboratories using the Allplex 2019-nCoV reagents are shown in Figure 3.

For extraction kits, all 13 laboratories using the STARMag DNA/RNA extraction kit had ≥1 outlier

Table 1. Test results for severe acute respiratory syndrome coronavirus 2 *RdRp* gene obtained from the proficiency test provider (expected value), Asan Medical Center, Seoul, and from participating laboratories according to the reagent used, South Korea, March 23–27, 2020*

		PowerChek		Allplex				
Sample no.	Dilution	Expected value	Participating laboratories, N = 67	Expected value	Participating laboratories, N = 38†	Standard M, N = 6	Laboratory-developed test, N = 5	Real-Q, N = 1
41	1:2 × 10^5	33.60	33.64 ± 1.73	34.37	34.64 ± 2.23‡	30.38 (29.44–35.46)§	34.32 (32.57–34.62)	38.27
42	1:2 × 10^2	24.62	24.16 ± 1.68	25.67	26.29 ± 2.34	21.28 (19.98–27.54)	25.94 (23.28–28.07)	24.06
43	1:2 × 10^4	30.73	30.60 ± 1.45	31.34	32.05 ± 2.43¶	27.49 (26.79–33.39)	31.66 (30.01–32.83)	30.54
45	1:2 × 10^3	27.69	27.71 ± 1.66	28.73	29.40 ± 2.51#	24.67 (23.51–31·21)	28.12 (26.77–29.05)	27.31
46	1:2 × 10^3	24.82	25.61 ± 0.76	26.12	26.07 ± 1.11	22.18 (21.50–23.46)	27.78 (25.74–28.49)	26.61
48	1:2 × 10^2	21.27	22.06 ± 0.85	22.49	22.41 ± 1.06	19.06 (17.20–19.86)	24.07 (22.04–25.02)	22.96
49	1:2 × 10^5	32.14	32.57 ± 0.96	32.55	32.35 ± 1.13	29.36 (27.49–30.02)	34.39 (32.18–35.42)	33.36
50	1:2 × 10^4	28.58	29.19 ± 0.83	29.45	29.32 ± 1.10	25.82 (24.20–27.01)	31.29 (29.38–32.40)	29.21

*Cycle threshold values are shown. Mean ± SD is shown for the results obtained by using the PowerChek 2019-nCoV and Allplex 2019-nCoV kits. Median and range are shown for the results obtained by using the Standard M nCoV-Detection and laboratory-developed tests.
†For nCoV-20–41–45, the number of laboratories was 37.
‡Calculated after exclusion of negative results from 9 laboratories.
§Calculated after exclusion of negative results from 1 laboratory.
¶Calculated after exclusion of negative results from 3 laboratories.
#Calculated after exclusion of negative results from 1 laboratory.

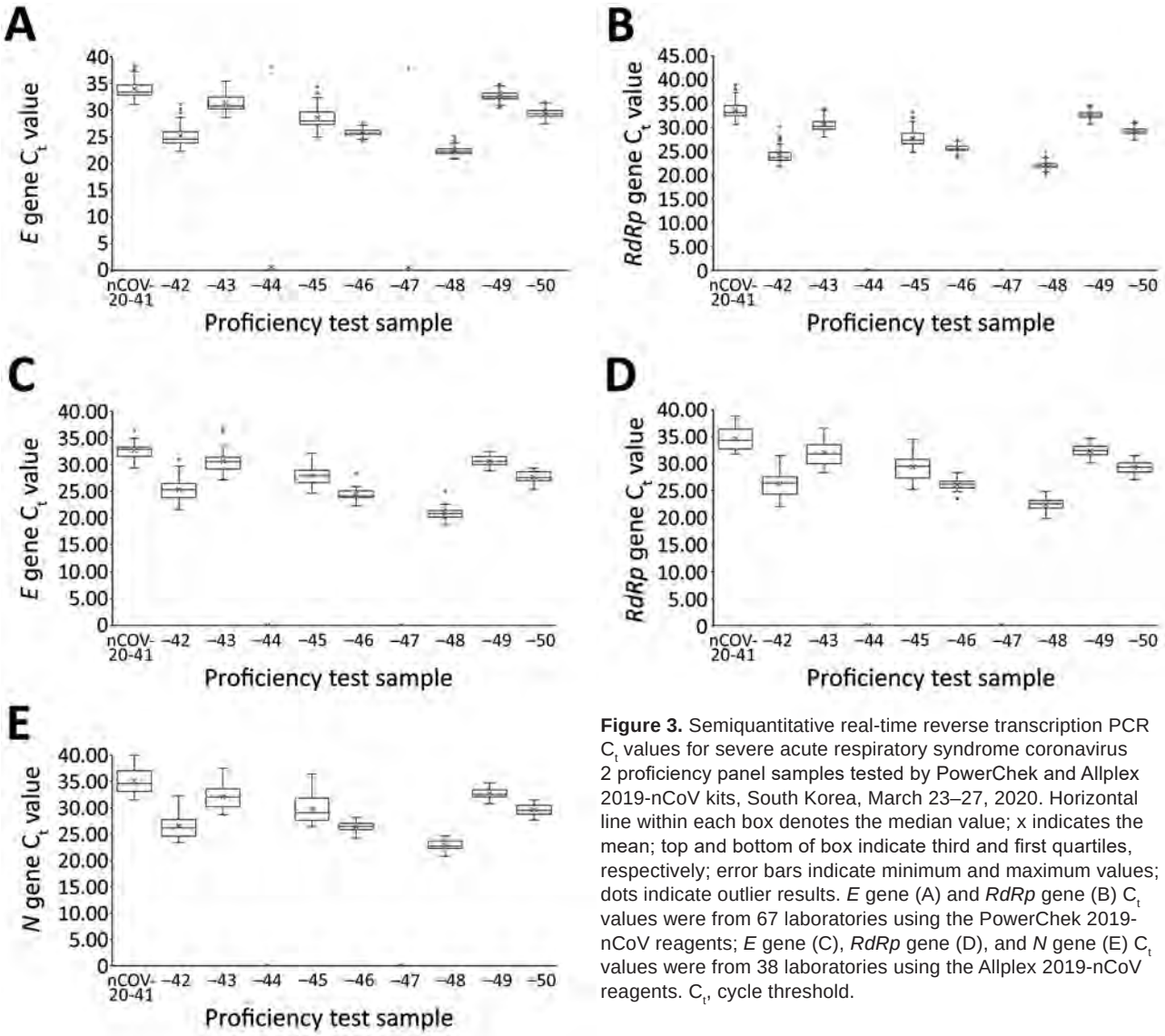

Figure 3. Semiquantitative real-time reverse transcription PCR C_t values for severe acute respiratory syndrome coronavirus 2 proficiency panel samples tested by PowerChek and Allplex 2019-nCoV kits, South Korea, March 23–27, 2020. Horizontal line within each box denotes the median value; x indicates the mean; top and bottom of box indicate third and first quartiles, respectively; error bars indicate minimum and maximum values; dots indicate outlier results. *E* gene (A) and *RdRp* gene (B) C_t values were from 67 laboratories using the PowerChek 2019-nCoV reagents; *E* gene (C), *RdRp* gene (D), and *N* gene (E) C_t values were from 38 laboratories using the Allplex 2019-nCoV reagents. C_t, cycle threshold.

results (Figure 2). The likelihood ratio of outliers from the STARMag DNA/RNA kit compared with the other kits was 0.000 (95% CI 0.000-0.205). Other extraction kits 95% CIs of likelihood ratios included 1.000.

Among the laboratories using the PowerCheck 2019-nCoV kit, five (0.7%, 5/670) outliers occurred in the *E* gene C_t values at 5 (7.5%) laboratories. Three (0.4%, 3/670) outliers occurred in the *RdRp* gene C_t values from 2 (3.0%) laboratories (Appendix Table 2).

Among the laboratories using the Allplex 2019-nCoV kit, 37 (9.9%) outliers occurred in *E* gene results, 13 (3.5%) in *RdRp* gene results, and 5 (1.3%) in *N* gene results (Appendix Table 2). The frequency of total outliers for the Allplex 2019-nCoV kit was significantly higher than those for the PowerChek 2019-nCoV kit (4.9% vs. 0.6%; p<0.0001). Except for 2 outliers for the *E* gene, all other outliers were negative results for lower respiratory samples that should have been positive. Among the laboratories using the Standard M nCoV Real-Time Detection kit (SD Biosensor, http://www.sdbiosensor.com), 2 laboratories (33.3%) that used the STARMag extraction kit reported negative results for the nCoV-20–41 sample.

Variation by Extraction Method and rRT-PCR Reagent of EQA samples

For the Standard M nCoV Real-Time Detection kit, the *E* gene C_t value was lower, by ≈2.8, than that of the Allplex nCoV-2019 kit and lower, by ≈3.9, than that of the PowerChek nCoV-2019 kit. For the Real-Q viral RNA extraction kit, the *E* gene C_t value was lower, by ≈1.4, than that of the NucliSENS easyMAG

extraction kit. For the STARMag DNA/RNA extraction kit, 1 negative result occurred for the nCoV-20–41 *E* gene. However, the results were positive for the *RdRp* and *N* genes using the Allplex nCoV-2019 kit.

Homogeneity and Stability of EQA Samples

For homogeneity tests, the mean C_t value and %CV of each target gene using the NucliSENS easyMAG kit for extraction and the Allplex nCoV-2019 kit for amplification are shown in Table 2. All the C_t values were within acceptable ranges, with %CVs <5. For stability tests, C_t values obtained for the SARS-CoV-2 EQA panel were also within acceptable ranges, with %CVs <5 (data not shown).

Discussion

The most important element for reducing the transmission of SARS-CoV-2 is the early detection of SARS-CoV-2 in patients. Shortening the time to diagnosis could substantially reduce the risk for transmission of SARS-CoV-2 (*12*). Performing diagnostic tests for newly emerging pathogens, such as SARS-CoV-2, exclusively in governmental and public laboratories substantially increases the delay resulting from logistics and analytical processes. As a result, diagnosis and isolation of patients, contact tracing, and even treatment of symptomatic patients can be delayed. Thus, rapid extension of diagnostic testing for emerging pathogens to nongovernmental clinical laboratories has many advantages, such as shorter turnaround times (*13*). To ensure reliable test results, EQA is a fundamental element, especially when using EUA diagnostic kits for newly emerging pathogens (*8*,*14*). The EQA we describe is unique because of its nationwide scale and because it included public and nongovernmental clinical laboratories conducting SARS-CoV-2 testing. This EQA was well-timed to support the laboratory responses to minimize the ongoing outbreak. All public and nongovernmental laboratories conducting SARS-CoV-2 molecular diagnostics reported their results in this nationwide EQA assessment in South Korea. The performance of the participants was good; overall accuracy was 100% for upper respiratory tract samples and 93.2% for lower respiratory tract samples.

On the basis of the laboratory results, the nCoV-20–41 sample was omitted from qualitative analysis. Initially, cultured SARS-CoV-2 were heat-inactivated at 65°C for 30 minutes (*15*). However, the second passage of cell cultures with inactivated viruses showed equivocal cytopathic effects, and therefore, the cultured viruses were further heat-inactivated at 70°C for 1 hour. The relatively high temperature and prolonged heat inactivation might have caused viral capsid denaturation and release of RNA. Viral RNA in the lower respiratory samples are vulnerable to degradation by RNase because of the lack of preservatives, in contrast to that observed in the universal transport medium used for upper respiratory tract samples. C_t values of the lower respiratory tract samples might have been higher than those of the upper respiratory tract samples, despite aliquoting the same amount of virus. Including replicate samples using the same matrix for assessing test consistency is preferred.

Among 118 public and nongovernment clinical laboratories, 8 (6.8%) laboratories using the Allplex 2019-nCoV kit reported ≥1 incorrect results for lower respiratory tract samples in the qualitative assessment. Whether this finding was attributable to the matrix effects of the proficiency test samples or the decreased sensitivity of the Allplex 2019-nCoV kit is unclear. Because the Liquillizer mucolytic agent was added to the inactivated virus-spiked lower respiratory tract samples, it could have adversely affected the extraction or the amplification procedures, although no interference with molecular methods has been observed by the manufacturer (*16*). Laboratories that had incorrect results on their qualitative tests were asked to take corrective actions by reevaluating

Table 2. Severe acute respiratory syndrome coronavirus 2 external quality assessment panel homogeneity tests of triplicate test results of 3 samples using the NucliSENS easyMAG extraction and Allplex nCoV-2019 kits performed at the Asan Medical Center, Seoul, South Korea, as a proficiency test provider, March 23, 2020*

	E gene		*RdRp* gene		*N* gene	
Sample no.	Mean C_t	%CV	Mean C_t	%CV	Mean C_t	%CV
41	33.82	4.5	34.37	1.6	34.38	0.5
42	25.15	1.4	25.67	1.8	26.67	0.5
43	30.33	1.5	31.34	1.5	31.55	0.7
44	ND	ND	ND	ND	ND	ND
45	27.52	2.2	28.73	0.3	29.05	0.7
46	24.47	0.7	26.12	0.3	27.05	0.2
47	ND	ND	ND	ND	ND	ND
48	20.68	2.5	22.49	0.6	23.49	0.3
49	31.07	0.8	32.55	0.6	33.32	0.9
50	27.89	0.9	29.45	0.2	30.35	0.6

*C_t, cycle threshold; EQA, external quality assessment; %CV, percentage coefficient of variation; ND, not detected.

their nucleic acid extraction protocols and internal quality control processes according to the laboratory guidelines (*4*,*17*) and implementing the routine use of a commercial reference material. A follow-up EQA consisting of 5 samples was conducted a month later, and clinical laboratories participated in a follow-up EQA showed all acceptable results.

For the assessment of semiquantitative data, only 0.6% outlier results were obtained by 67 laboratories using the PowerChek 2019-nCoV kit. In contrast, 4.9% outlier results were reported from 38 laboratories using the Allplex nCoV 2019-nCoV kit. For the PowerChek 2019-nCoV kit, which uses 2 PCR tubes, 2 separate tubes for both the *E* and *RdRp* genes are necessary per sample, and the volume of RNA is 5 µL per reaction tube (*4*,*17*). For the Allplex 2019-nCoV kit, the internal control is directly added into the sample, and the volume of RNA is 8 µL. The target genes are the *E*, *RdRp*, and *N* genes. The manufacturers' reported limit of detection for the *E* gene is 28.5 copies/reaction for the PowerChek 2019-nCoV kit and 100 copies/reaction for the Allplex 2019-nCoV kit. Whether the lower limit of detection and decreased multiplexing (each gene and an internal control per tube for the PowerChek 2019-nCoV kit vs. 3 target genes and an internal control per tube for the Allplex 2019-nCoV kit) affected the performance of the 2 reagents or whether matrix effects occurred during use of the Allplex 2019-nCoV kit requires further investigation.

The first step in nucleic acid amplification tests requires extraction and purification of nucleic acids from the target organism (*18*). All 13 laboratories using the STARMag DNA/RNA extraction kit reported ≥1 outliers. During the preevaluation of the extraction systems and EUA rRT-PCR assays that were performed in the central laboratory before dispatch, a combination of STARMag DNA/RNA extraction and Allplex 2019-nCoV kits showed a negative result for the *E* gene in the nCoV-20–41 specimen, which had the lowest viral load. Specimen viscosity and higher rates of PCR inhibition account for sputum being the most difficult specimen type to analyze in the laboratory (*19*). Although the manufacturer of the STARMag DNA/RNA extraction kit claims that sputum and bronchoalveolar lavage are suitable types of specimens, laboratories should verify these claims and assess the performance of nucleic acid amplification tests when using this reagent for extracting RNA from lower respiratory tract samples. The laboratories given incorrect qualitative results were requested to compare their nucleic acid extraction system with the QIAamp Viral RNA Mini kit (QIAGEN, https://www.qiagen.com) (*17*).

All EQA samples were adequately homogeneous and stable on storage at -70°C. Because the complete process of this EQA, from proficiency test panel preparation, panel freezing, and logistics to completion of testing and result reporting, was finished within a week, the assessment was conducted in 7 days. The reliability of the virus panels used in the EQA was found to be stable.

Our study has some limitations. First is the small number of negative SARS-CoV-2 samples to evaluate cross-contamination, including only 2 negative samples. More negative samples placed adjacent to the highest SARS-CoV-2 sample should be included in future EQA for the evaluation of cross-contamination. Second, the potential matrix effect of the additives to the lower respiratory tract samples was not evaluated properly. Thus, for the laboratories using the Allplex 2019-nCoV kit, the performance of the reagent when using lower respiratory tract samples might not have been assessed adequately. Because variations occurred in the tested specimen types, RNA extraction platforms, PCR reagents and amplification platforms, and the amount of RNA used in the PCR reaction, many potential variables could have affected the results. Third is the small volume of EQA samples. A sufficient amount of sample for certification of multiplex technicians is recommended for certain EQA exercises; however, EQA samples were enough for ≈4 test runs when using a QIAamp Viral RNA Mini kit. Fourth, the EQA panel had limitations regarding test consistency evaluation; measured values varied between sample types because of a potential matrix effect, despite having the same viral loads from both upper and lower respiratory samples. An international EQA that includes replicate samples for consistency evaluation is ongoing, and the laboratories conducting SARS-CoV-2 testing are highly encouraged to participate in that program.

In conclusion, this report summarizes the nationwide EQA of SARS-CoV-2 molecular testing carried out by public and nongovernmental laboratories. The observation that 6.8% of laboratories reported false-negative results shows room for improvement. Laboratories with deficiencies were requested to take additional corrective actions and then participated in a follow-up EQA. This study indicates that EQAs should be performed for all laboratories involved in COVID-19 diagnostic testing on a regular basis for evaluation of potential weaknesses in SARS-CoV-2 molecular testing procedures. This action will help to increase the quality of results. The EQA methodology used in this study will also help other countries to evaluate their own assays for SARS-CoV-2 testing.

Acknowledgments

We are especially grateful to John Jeongseok Yang for English proofreading and feedback.

This work was supported by the Korea Centers for Disease Control and Prevention (grant no. 4837-301) and the Bio and Medical Technology Development Program of the National Research Foundation of Korea grant funded by the South Korea government (grant no. NRF-2016M3A9B6918716).

The opinions expressed by authors contributing to this journal do not necessarily reflect the opinions of the Korea Centers for Disease Control and Prevention or the institutions with which the authors are affiliated.

About the Author

Dr. Sung is a laboratory director and professor at the Department of Laboratory Medicine, University of Ulsan College of Medicine and Asan Medical Center. His research interests include clinical microbiology and infectious diseases.

References

1. World Health Organization. Coronavirus disease 2019 (COVID-19) situation report–159 [cited 2020 Jun 28]. https://www.who.int/emergencies/diseases/novel-coronavirus-2019/situation-reports
2. Centers for Disease Control and Prevention. Coronavirus disease 2019 (COVID-19). World map [cited 2020 Jun 28]. https://www.cdc.gov/coronavirus/2019-ncov/global-covid-19/world-map.html
3. Hanson KE, Caliendo AM, Arias CA, Janet A, Englund JA, Lee MJ, et al. Infectious Diseases Society of America guidelines on the diagnosis of COVID-19 [cited 2020 May 6]. https://www.idsociety.org/practice-guideline/covid-19-guideline-diagnostics
4. Hong KH, Lee SW, Kim TS, Huh HJ, Lee J, Kim SY, et al. Guidelines for laboratory diagnosis of coronavirus disease 2019 (COVID-19) in Korea. Ann Lab Med. 2020;40:351–60. https://doi.org/10.3343/alm.2020.40.5.351
5. Korea Centers for Disease Control and Prevention. COVID-19 [cited 2020 Jun 28]. http://ncov.mohw.go.kr
6. Sung H, Yoo CK, Han MG, Lee SW, Lee H, Chun S, et al. Preparedness and rapid implementation of external quality assessment helped quickly increase COVID-19 testing capacity in the Republic of Korea. Clin Chem. 2020;66:979–81. https://doi.org/10.1093/clinchem/hvaa097
7. Pas SD, Patel P, Reusken C, Domingo C, Corman VM, Drosten C, et al. First international external quality assessment of molecular diagnostics for MERS-CoV. J Clin Virol. 2015;69:81–5. https://doi.org/10.1016/j.jcv.2015.05.022
8. Binnicker MJ. Emergence of a novel coronavirus disease (COVID-19) and the importance of diagnostic testing: why partnership between clinical laboratories, public health agencies, and industry is essential to control the outbreak. Clin Chem. 2020;66:664–6. https://doi.org/10.1093/clinchem/hvaa071
9. Kim JM, Chung YS, Jo HJ, Lee NJ, Kim MS, Woo SH, et al. Identification of coronavirus isolated from a patient in Korea with COVID-19. Osong Public Health Res Perspect. 2020;11:3–7. https://doi.org/10.24171/j.phrp.2020.11.1.02
10. Corman VM, Landt O, Kaiser M, Molenkamp R, Meijer A, Chu DKW, et al. Detection of 2019 novel coronavirus (2019-nCoV) by real-time RT-PCR. Euro Surveill. 2020;25:2000045. https://doi.org/10.2807/1560-7917.ES.2020.25.3.2000045
11. College of American Pathologists. Proficiency testing manual [cited 2020 Jun 28]. https://documents.cap.org/documents/2019-ProficiencyTesting-Manual_FINAL.pdf
12. Rong XM, Yang L, Chu HD, Fan M. Effect of delay in diagnosis on transmission of COVID-19. Math Biosci Eng. 2020;17:2725–40. https://doi.org/10.3934/mbe.2020149
13. Chang J, Lee HY, Seong MW, Kim MN, Sung H. External quality assessment of molecular diagnostics for Zika virus and Middle East respiratory syndrome coronavirus in Korea. Southeast Asian J Trop Med Public Health. 2019;50:840–7.
14. Leclercq I, Batéjat C, Burguière AM, Manuguerra JC. Heat inactivation of the Middle East respiratory syndrome coronavirus. Influenza Other Respir Viruses. 2014;8:585–6. https://doi.org/10.1111/irv.12261
15. Madej RM. Proficiency testing and external quality assessment for molecular microbiology. In: Persing DH, Tenover FC, Hayden RT, Ieven M, Miller MB, Nolte FS, et al., editors. Molecular microbiology: diagnostic principles and practice. 3rd ed. Washington (DC): ASM Press; 2016. p. 754–65.
16. Fisher Scientific. MetaSystems Liquillizer Mucolytic Agent [cited 2020 May 1]. https://www.fishersci.com/shop/products/liquillzr-mucolytc-agent-250ml/22200371
17. Sung H, Roh KH, Hong KH, Seong MW, Ryoo N, Kim HS, et al. COVID-19 molecular testing in Korea: practical essentials and answers from the experts based on experience of emergency use authorization assays. Ann Lab Med. 2020;40:439–47.
18. Charlton CL, Babady E, Ginocchio CC, Hatchette TF, Jerris RC, Li Y, et al. Practical guidance for clinical microbiology laboratories: viruses causing acute respiratory tract infections. Clin Microbiol Rev. 2018;32:e00042–18. https://doi.org/10.1128/CMR.00042-18
19. Sung H, Yong D, Ki CS, Kim JS, Seong MW, Lee H, et al. Comparative evaluation of three homogenization methods for isolating Middle East respiratory syndrome coronavirus nucleic acids from sputum samples for real-time reverse transcription PCR. Ann Lab Med. 2016;36:457–62. https://doi.org/10.3343/alm.2016.36.5.457

Address for correspondence: Won-Ki Min or Heungsup Sung, Department of Laboratory Medicine, University of Ulsan College of Medicine and Asan Medical Center, 88 Olympic-ro 43-gil, Songpa-gu, Seoul 05505, South Korea; email: wkmin@amc.seoul.kr or sung@amc.seoul.kr

Impact of Social Distancing Measures on Coronavirus Disease Healthcare Demand, Central Texas, USA

Xutong Wang,[1] Remy F. Pasco,[1] Zhanwei Du,[1] Michaela Petty, Spencer J. Fox, Alison P. Galvani, Michael Pignone, S. Claiborne Johnston, Lauren Ancel Meyers

Social distancing orders have been enacted worldwide to slow the coronavirus disease (COVID-19) pandemic, reduce strain on healthcare systems, and prevent deaths. To estimate the impact of the timing and intensity of such measures, we built a mathematical model of COVID-19 transmission that incorporates age-stratified risks and contact patterns and projects numbers of hospitalizations, patients in intensive care units, ventilator needs, and deaths within US cities. Focusing on the Austin metropolitan area of Texas, we found that immediate and extensive social distancing measures were required to ensure that COVID-19 cases did not exceed local hospital capacity by early May 2020. School closures alone hardly changed the epidemic curve. A 2-week delay in implementation was projected to accelerate the timing of peak healthcare needs by 4 weeks and cause a bed shortage in intensive care units. This analysis informed the Stay Home-Work Safe order enacted by Austin on March 24, 2020.

Severe acute respiratory syndrome coronavirus 2 (SARS-CoV-2) appeared in Wuhan, China, during December 2019, and coronavirus disease (COVID-19) caused by this virus was declared a pandemic on March 11, 2020, by the World Health Organization (*1*). As of June 24, a total of 193 countries, areas, or territories had reported 9,129,146 confirmed COVID-19 cases and 473,797 deaths. Substantial outbreaks have occurred in India, Russia, Brazil, and the United States; the United States has the highest cumulative confirmed number of cases and deaths (*2*).

The United States reported its first imported SARS-CoV-2 case from Wuhan on January 20, in Washington (*3*), 6 days ahead of California (*4*) and 40 days ahead of New York, New York (*5*); the first locally infected cases were reported on February 28 (*6*). As of June 24, all 50 states had reported confirmed cases, 48 had reported community spread, and cumulative confirmed COVID-19 cases were 2,336,615 and deaths were 121,117 (*7*). Surges in COVID-19 hospitalizations have compromised local healthcare systems in New York (*8*) and Seattle (*9*).

Beginning in March 2020, states and cities implemented extensive social distancing measures to contain the spread of SARS-CoV-2, including school closures, limits on mass gatherings, shelter-in-place orders, travel restrictions, and bans on nonessential commercial activities. By early April, 45 states had issued a statewide shelter-in-place order or ≥1 city-level stay-at-home order, affecting >316 million persons. As of June 25, all measures have expired or relaxed (*10*). The timing of the orders varied; California was the first state to enact strict orders on March 19 and South Carolina the last on April 7 (*10*). These measures dramatically slowed the pace of the pandemic during April and May, but confirmed COVID-19 cases and hospitalizations have been increasing since early June, particularly in Arizona, Florida, Texas, and California (*11*).

As COVID-19 emerged into a global threat, we took a national pandemic influenza model that was built through a pandemic preparedness contract with the Centers for Disease Control and Prevention (CDC;

Author affiliations: The University of Texas at Austin, Austin, Texas, USA (X. Wang, R.F Pasco, Z. Du, M. Petty, S.J. Fox, L. Ancel Meyers); Yale University School of Public Health, New Haven, Connecticut, USA (A.P. Galvani); The University of Texas at Austin Dell Medical School, Austin (M. Pignone, S. Claiborne Johnston); Santa Fe Institute, Santa Fe, New Mexico, USA (L. Ancel Meyers)

DOI: https://doi.org/10.3201/eid2510.201702

[1]These authors contributed equally to this article.

Atlanta, GA, USA) and adapted it to model the spread and control of COVID-19 within and between 217 US cities. We used this model to project the potential effects of school closures coupled with social distancing, in terms of reducing cases, deaths, hospitalizations, intensive care unit (ICU) visits, and ventilator needs, on local, regional, and national scales. We have focused our analysis on Austin, which is the capital of Texas and the fastest growing city in the United States, as a representation of major US metropolitan areas. The scenarios and inputs (e.g., epidemiologic parameters) were determined in consultation with CDC and the Regional Healthcare System Executive Council of the Austin–Travis County Emergency Operations Command.

Methods

We focused on the Austin–Round Rock Statistical Metropolitan Area, which had a population of 2.17 million persons in 2018, but the qualitative findings and impact of social distancing will apply to cities throughout the United States. We analyzed a compartmental model that incorporates age-specific high risk proportions and contact rates to measure the effects of 2 key interventions, school closures and social distancing measures, which reduce nonhousehold contacts by a specified percentage. We estimated the effects of these measures on cases, hospitalizations, ICU visits, ventilator needs, and deaths.

We built a stochastic age- and risk-structured susceptible-exposed-asymptomatic-symptomatic-hospitalized-recovered (SEAYHR) model of SARS-CoV-2 transmission (Appendix Figure 1, https://wwwnc.cdc.gov/EID/article/26/10/20-1702-App1.pdf). Persons were separated into 5 age groups, <1–4, 5–17, 18–49, 50–64, and ≥65 years of age, on the basis of population data for the 5-county Austin–Round Rock Metropolitan Area from the 2017 American Community Survey (*12*). Each age group was divided into a low-risk and high-risk group on the basis of prevalence of chronic conditions estimated for the Austin population (Appendix Figure 2) (*13*–*16*). We also estimated the proportion of pregnant women in each age group as a special risk class (*17*). All persons were assumed to be susceptible to the disease. Infected persons were modeled to enter a latent period in which they were symptom-free and not yet infectious (*18*) and then progressed to either a symptomatic or asymptomatic compartment, both infectious. Asymptomatic persons were assumed to have the same infectious period as symptomatic persons but lower infectiousness. The rates at which symptomatic case-patients were moved to a hospitalized compartment and died depended on age and risk group. Recovered persons were considered fully immune. Deaths were assumed to occur after hospitalization. We provide a detailed description of the methods used (Appendix).

All model parameters (Appendix Tables 1–3) were based on published estimates from COVID-19 studies, as well as input from CDC and Austin. We assumed a basic reproduction number (R_0) of 2.2 (*19*) and considered 2 different doubling times, 7.2 days (low growth rate) (*19*–*21*) and 4 days (high growth rate) (*22*–*24*). We provide a sensitivity analysis for an R_0 of 3.5 (Appendix). Age-specific contact rates were estimated by using contact matrices published by Prem et al. and are adjusted to model school closures and various levels of social distancing (*25*). Transmission rates were estimated by fitting simulations to a given R_0 and epidemic doubling time. The latent period (i.e., noninfectious beginning of the incubation period) was sampled from a triangular distribution from 1.9 days to 3.9 days and a mean of 2.9 days (*26*,*27*), and the infectious period was sampled from a triangular distribution from 5.3 days to 7.3 days and a mean of 6.3 days (*27*). We assumed that 43% of infections are asymptomatic and that asymptomatic cases are two thirds as infectious as symptomatic cases (*28*,*29*). Following planning scenarios of CDC, we assumed that the infection hospitalization rate and infection fatality rate was 10 times higher in high-risk than low-risk persons within each age group.

Simulations began with 5 imported symptomatic cases in the 18–49-year-old age group on March 1, 2020, and were updated at 2.4-hour intervals. For each combination of epidemic scenarios (low/high growth rate) and intervention strategies (school closure policy with different levels of social distancing), we ran 100 stochastic simulations and reported the medians and 95% prediction intervals (ranges) at weekly intervals.

School Closure Policies

As part of a CDC modeling network, we initially modeled a large number of school closure policies, with variable implementation time and duration. To simulate school closures, we decreased the daily age-specific contact rates by the estimated number of contacts that occur within schools (*25*,*30*). The school-specific contact numbers encompass all interactions among students and teachers occurring at all educational levels, from elementary schools through colleges and universities. In our model, school closures reduced daily contacts by 15% for persons <1–4 years of age, 26% for persons 5–17 years of age, 9% for persons 18–49 of age, 9% for persons 50–64 of age, and 2% for

persons ≥64 years of age. We reported only 2 of these strategies to demonstrate the effects of implementation time: closure immediately after the first confirmed case (March 14) and delayed closure 2 months after the first confirmed case (May 14). In both cases, we assumed that schools remain closed through the end of the summer vacation (August 18, 2020), which corresponds to a 23-week duration for the early closure and a 14-week duration for the late closure. The early closure scenario roughly corresponded to Austin announcing the first 2 confirmed cases on March 13 and major school districts closing the next day. In our simulations, the median cumulative number of symptomatic COVID-19 cases by March 14th was 38 (interquartile range [IQR] 27–53) and 14 (IQR 9–19), assuming a 4-day and 7-day doubling period, respectively; by May 14, median cumulative symptomatic cases increased to 530,426 (IQR 114,151–783,667) and 3,206 (IQR 561–7,611), respectively.

Social Distancing Measures

In addition to school closures, we considered the effect of various levels of social distancing that decreased nonhousehold contacts by 25%, 50%, 75%, and 90% overall. These levels were chosen to correspond to increasingly more severe levels of restriction on social interaction from limiting large crowds to near-total restriction on out-of-home movement except for healthcare and basic necessities.

Age-stratified contact rates (*25*) were derived from the POLYMOD diary-based study in Europe (*30*) and separated in contacts occurring at home, at school, at work and elsewhere. We used the national US age distribution (*31*) to aggregate these estimates from 17 to the 5 age groups of our model (Appendix Tables 4–7). We combined these matrices to model 4 different types of days: normal school days (all contacts); normal weekends and short weekday holidays (all but school and work contacts; adults are assumed to work during the long summer break); weekdays during school closures/social distancing; and weekend or weekday holiday during school closure/social distancing. To model school closures with social distancing, we included all household contacts plus a specified proportion of contacts outside the home. On weekdays, this proportion included a proportion of contacts occurring at work and elsewhere; on weekends and holidays (excluding summer vacation), it included just contacts occurring elsewhere. Days were assigned to 1 of these 4 contact models on the basis of the 2019–2020 and 2020–2021 school calendars from the Austin Independent School District, which was the largest public school district in the metropolitan area, serving ≈22.7% of the Austin Round Rock Statistical Metropolitan Area population.

Healthcare Demands

We assumed that hospitalized cases were admitted on average 5.9 days (L. Tindale et al., unpub. data, https://doi.org/10.1101/2020.03.03.20029983) after symptom onset, with the infection hospitalization rate depending on the age and risk group (Appendix Table 1). Hospitalized case-patients who recovered were considered discharged an average of 11 days after admission; deaths occurred an average of 7.82 days after admission. We estimated the number ICU beds and ventilators needed to care for COVID-19 case-patients each day on the basis of age-specific rates provided by the CDC (Appendix Table 3) and assuming that the average duration of ICU care and ventilation support are 8 days and 5 days, respectively. There is some uncertainty regarding how these estimates might change when healthcare facilities reach or exceed capacity because of a lack of available postdischarge care and inefficiency in the healthcare system caused by worker illness. Thus, we also tested an alternative scenario with longer duration of hospital stay, ICU care, and ventilation (Appendix). We did not consider potential excess deaths resulting from lack of access to adequate healthcare during pandemic surges.

Results

Our analyses focus on 2 key levers of intervention: the speed of implementation and the extent of social distancing. We considered 2 scenarios for the epidemic growth rate of COVID-19 and project 5 outcomes: cases, hospitalizations, ICU care, ventilator needs, and deaths.

Regardless of epidemic growth rate, school closures alone had little effect on the burden of the epidemic. These closures would flatten the curve slightly if enacted immediately after the detection of the first case (Figure 1). High levels of social distancing, when coupled with school closures, substantially delayed and dampened the epidemic peak. The impact of the measures depended on early implementation. Under both the slower and faster epidemic growth scenarios (i.e., 7-day and 4-day doubling times), immediate measures beginning on March 14 were much more effective than 2-month delayed measures at slowing transmission throughout the spring and summer of 2020 (Figure 1). Given that recent estimates for the doubling time in US cities are short, ranging from 2.4 to 3 days (*24*,*32*), this finding suggests that proactive measures were justified, because delayed measures

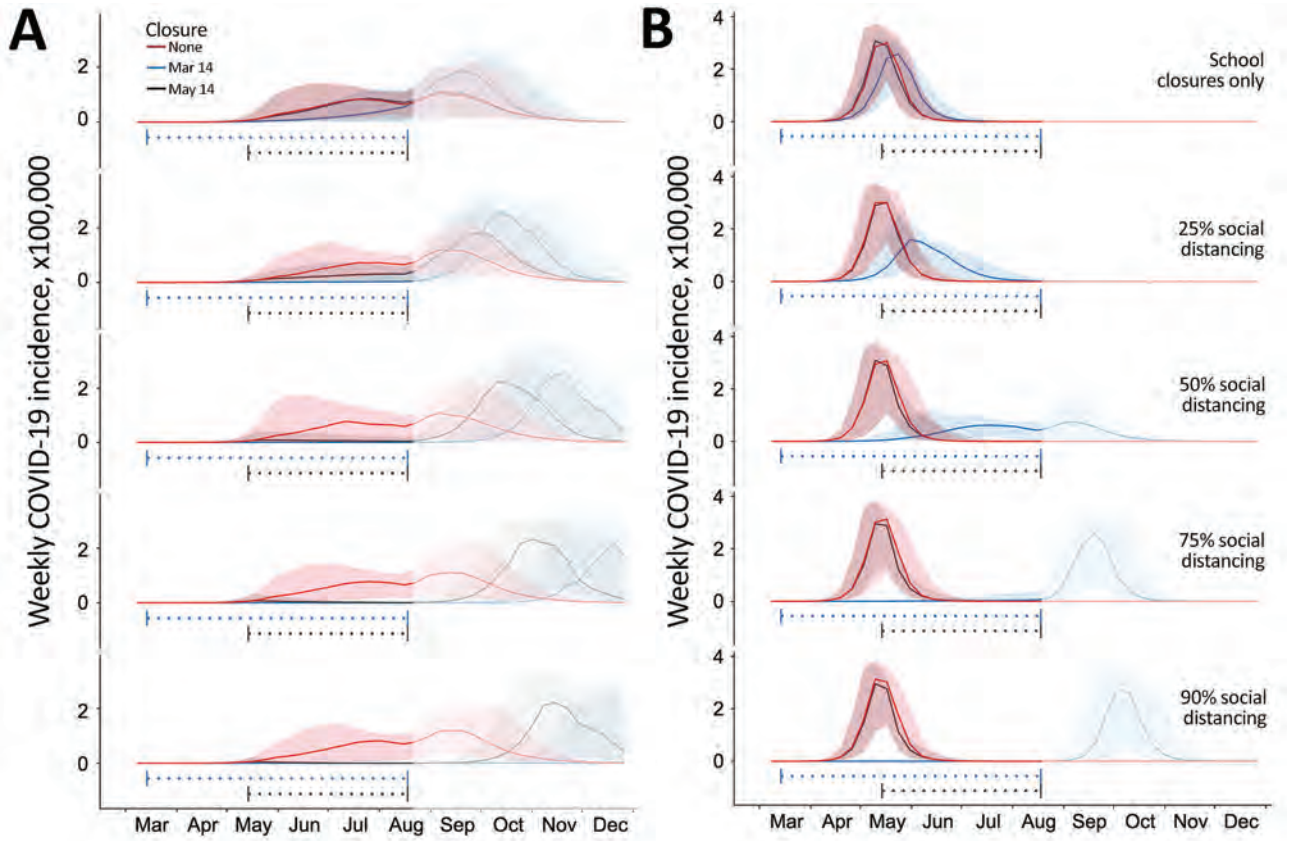

Figure 1. Projected weekly incident of COVID-19 cases in Austin–Round Rock Metropolitan Statistical Area, Texas, USA. Graphs show simulation results for different levels of social distancing and implementation times, assuming an epidemic doubling time of A) 7.2 days (*18–20,22*) or B) 4 days (*22–24*). Each graph displays 3 projections: a baseline assuming no social distancing (red), social distancing implemented March 14–Aug 17, 2020 (blue), and social distancing implemented May 14–Aug 17, 2020 (black). From top to bottom, the graphs in each column correspond to increasingly stringent social distancing measures: school closures plus social distancing that reduces nonhousehold contacts by 0%, 25%, 50%, 75%, or 90%. Solid lines indicate medians of 100 stochastic simulations; shading indicates inner 95% ranges of values. The horizontal dotted lines beneath the curves indicate intervention periods. The faded mid-August to December time range indicates long-range uncertainty regarding COVID-19 transmission dynamics and intervention policies. COVID-19, coronavirus disease.

would have been almost entirely ineffective. If the reproduction is higher than we assumed, then more vigilant social distancing would be required to slow spread (Appendix). Although the immediate school closure on March 14 had little impact on the initial wave, the August opening of schools would be expected to amplify a fall wave if the population is not yet close to herd immunity.

To assess the impact of social distancing measures on mitigating healthcare surge in the Austin–Round Rock Statistical Metropolitan Area, we considered the more plausible 4-day doubling time scenario (Table 1; Figure 2). Social distancing measures that reduced nonhousehold contacts by <50% were projected to delay but not prevent a healthcare crisis. Only the 75% and 90% contact reduction scenarios were projected to reduce hospitalizations, ICU care, and ventilator needs below the estimated capacity for the metropolitan area (Table 2). If 50% social distancing were implemented on March 28 instead of March 14 (i.e., a 2-week delay), we would expect COVID-19 ICU requirements to exceed local capacity by the end of June instead of only reaching capacity by the end of July (i.e., a 4-week acceleration) (Appendix). Under scenarios that predict overwhelming healthcare surges, we likely underestimate deaths because we do not account for excess deaths for persons with COVID-19 or other medical conditions, such as cancer or cardiovascular disease, who might not receive timely or safe care.

Under the naive scenario that school closures and social distancing measures are lifted entirely on the first day of the 2020–2021 academic year (August 18) (*33*), the pace and extent of COVID-19 transmission in the fall would depend on how many persons were infected (and thereby immunized)

Table 1. Estimated cumulative COVID-19 cases, healthcare requirements, and deaths, Austin–Round Rock metropolitan statistical area, Texas, USA, March 1–August 17, 2020*

Outcome	No measures	School closure	School closure and 50% social distancing	School closure and 75% social distancing	School closure and 90% social distancing
Cases	1,139,633 (1,092,754–1,173,408)	1,098,755 (1,016,794–1,143,147)	596,304 (215,897–854,094)	34,232 (2,871–244,959)	2,013 (642–11,358)
Hospitalizations	79,120 (75,373–82,608)	76,698 (70,091–80,602)	36,534 (11,474–57,912)	1,889 (159–13,512)	125 (32–660)
ICU	13,312 (12,673–13,890)	12,897 (11,786–13,540)	6141 (1,929–9,736)	318 (27–2,273)	21 (5–111)
Ventilators	6,274 (5,973–6,545)	6,077 (5,554–6,377)	2,893 (909–4,587)	150 (13–1,071)	10 (3–53)
Deaths	9,646 (9,031–10,206)	9,324 (8,481–9,954)	3,698 (995–6,751)	176 (13–1,315)	13 (1–70)

*Values are medians (95% prediction intervals) across 100 stochastic simulations based on parameters in Table 1. COVID-19, coronavirus disease; ICU, intensive care unit.

during the spring and summer (Figure 1). As cumulative incidence approaches the herd immunity threshold of roughly 55% of the population, the effective reproduction number (R_t) decreases. Once this 55% threshold is surpassed, the reproduction number decreases below 1, and the virus would be unable to spread widely, even if social distancing measures are lifted. Assuming the faster 4-day epidemic doubling time (Figure 1, panel B), a minimum of 50% social distancing is necessary to suppress transmission over the summer. Under 75% or 90% social distancing, the lifting of measures on August 18 would be expected to produce epidemic peaks in the middle or end of September, respectively. Assuming the slower 7-day doubling time (Figure 1, panel A), even delayed social distancing would be expected to forestall the start of the epidemic from spring to fall. The higher fall peaks that were produced under the most extreme social distancing, assuming a 7-day doubling time, stem from baseline contact patterns (in the absence of social distancing): a COVID-19 epidemic that begins in the spring would be naturally dampened by the 3-month summer vacation period when children are out of school, whereas a fall start would be amplified by the start of the academic year.

Discussion

As COVID-19 emerged as a global threat in early 2020, we rapidly adapted a pandemic influenza model that was under development as part of an effort coordinated by CDC to build a strategic national modeling resource for pandemic planning and response. The analyses provided in this report originated in time-sensitive requests from CDC, Austin, and the state of Texas to evaluate the potential impact of school closures and social distancing on the emergence and spread of COVID-19 in US cities. Our projections indicate that, without extensive social distancing measures, the emerging outbreak would quickly surpass healthcare capacity in the region. However, with extensive social distancing, the number of cases, hospitalizations, and deaths could be substantially reduced throughout the summer of 2020. Although these analyses are specific to the Austin–Round Rock metropolitan area, we expect that the impacts of the mitigation strategies will be qualitatively similar for cities throughout the United States.

Our epidemiologic projections and conclusions regarding the urgent need for extensive social distancing are consistent with a recent analysis by Imperial College London (*34*). However, we assume that a lower percentage of hospitalized patients receive critical care (15%–20% vs. 30%) and consequently project a lower peak ICU demand. In sensitivity analyses with more extreme assumptions about critical care requirements, the projected peak demand increases accordingly (Appendix). The local focus of our model, which incorporates city-specific data regarding demographics, high-risk conditions, contact patterns, and healthcare resource availability, enables us to project near-term healthcare demands and provide actionable insights for local healthcare and governmental decision-makers.

We conducted these analyses to inform decision making in a rapidly evolving environment with substantial uncertainty. On March 6, 2020, Austin declared a local state of disaster and cancelled the South by Southwest Conference and Festival, which was expected to draw 417,400 visitors from around the world and bring $355.9 million to the local economy (*35*). Evidence of community transmission appeared within days of the first confirmed COVID-19 case in Austin on March 13. Shortly after, the University of Texas at Austin, one of the largest public universities with >50,000 students, and the largest public school district in Austin announced school closures (*36*,*37*). On March 24, Austin issued a Stay Home-Work Safe order to eliminate all nonessential business and travels (*38*). Leaders of Austin requested the healthcare analyses (Figure 2) in the days leading up to the

order of March 24 and requested that we release a preliminary report to educate the public (*39*).

Social distancing measures, including school closures, restrictions on travel, mass gatherings and commercial activities, and more extensive shelter-in-place advisories, aim to decrease disease transmission within a population by preventing contacts between persons. Our analyses project the effect of such measures on the transmission dynamics of COVID-19 but do not consider the economic, social and psychological costs of social distancing measures, including the socioeconomic disparities in burden and illness and death resulting from reductions in health and mental healthcare services (*40*,*41*).

There is an urgent need to project the relative effects of different levels of social distancing in light of their potential societal costs, including school closures, partial work and travel restrictions and cocooning of the high risk, so that restrictions can be strategically lifted without compromising public health. In particular, school closures are often deployed earlier than more extensive social distancing measures. However, such closures can be costly, particularly for low-income families who might rely on lunch programs and be unable to afford childcare (*42*,*43*), and our analysis suggests that they might only slightly reduce the pace of transmission and peak hospital surge. However, the role of children in community transmission of COVID-19 remains uncertain; thus, school closures are prudent at this time. Children represent a low proportion of confirmed cases worldwide (*44*,*45*), perhaps reflecting that COVID-19 is less severe in children than adults (*46*). If we learn that the prevalence or infectiousness of COVID-19 is low in children, then opening schools may be a reasonable first step toward resuming normalcy.

Although our model incorporates considerable detail regarding the natural history of COVID-19, age- and location-specific contact patterns, and the demographic and risk composition of the Austin–Round Rock Statistical Metropolitan Area, it does

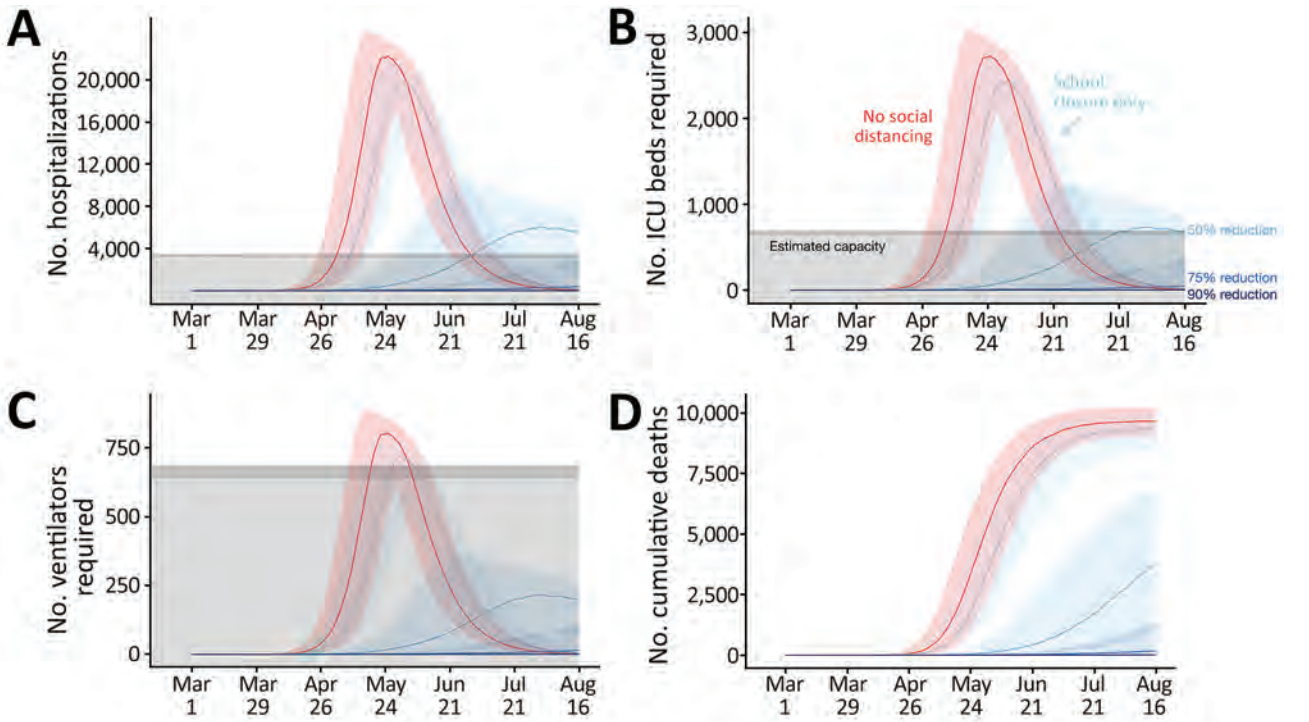

Figure 2. Projected COVID-19 healthcare demand and cumulative deaths in Austin–Round Rock Metropolitan Statistical Area, Texas, USA. Graphs show simulation results across multiple levels of social distancing, assuming a basic reproductive number of 2.2 with a 4-day epidemic doubling time. Extensive social distancing is expected to substantially reduce the burden of COVID-19 A) hospitalizations, B) patients requiring ICU care, C) patients requiring mechanical ventilation, and D) cumulative deaths. Red lines indicate projected COVID-19 transmission assuming no interventions under the parameters given in Table A1. Blue lines indicate increasing levels of social distancing interventions, from light to dark: school closures plus social distancing interventions that reduce nonhousehold contacts by either 0%, 50%, 75%, or 90%. Lines and shading indicate medians and inner 95% ranges of values across 100 stochastic simulations. Gray shaded region indicates estimated surge capacity for COVID-19 patients in the Austin-Round Rock Metropolitan Statistical Area as of March 28, 2020, which is calculated on the basis of 80% of the total 4,299 hospital beds, 90% of the total 755 ICU beds, and 755 mechanical ventilators. COVID-19, coronavirus disease; ICU, intensive care unit.

Table 2. Estimated peak COVID-19 cases and healthcare demands, Austin–Round Rock metropolitan statistical area, Texas, USA, March 1–August 17, 2020*

Outcome	No measures	School closure	School closure and 50% social distancing	School closure and 75% social distancing	School closure and 90% social distancing
Cases	272,978 (228,088–327,181)	237,428 (176,910–281,441)	64,779 (33,837–110,968)	4,643 (267–35,148)	163 (42–1,279)
New cases daily	54,106 (47,301–62,646)	43,535 (33,691–50,105)	10,573 (6,297–16,768)	851 (57–5,436)	32 (10–212)
Hospitalizations	23,073 (20,961–24,695)	20,671 (17,193–22,473)	6,804 (3,088–10,271)	402 (31–2,963)	18 (5–105)
ICU	2,831 (2,575–3,033)	2,532 (2,107–2,759)	833 (377–1,254)	50 (4–362)	2 (1–13)
Ventilators	835 (760–895)	746 (621–814)	245 (111–369)	15 (1–107)	1 (0–4)

*Values are medians (95% prediction intervals) across 100 stochastic simulations based on parameters in Table 1. COVID-19, coronavirus disease; ICU, intensive care unit.

not explicitly capture neighborhood, household, or other community structure that can serve to amplify or impede transmission (*47–49*). In addition, we ignored the possible importation of COVID-19 cases from other cities, under the assumption that the additional cases would have a negligible impact, particularly during the period of exponential growth. Although large numbers of introductions could undermine mitigation efforts that radically suppress transmission, we conjecture that such efforts would include travel restrictions, contact tracing and other measures to contain emerging clusters. Our model also does not evaluate other potentially effective interventions, such as increased levels of selective testing and isolation.

These analyses rely on recently published estimates for transmission rate and severity of COVID-19, as well as best estimates from expert opinions from CDC and Dell Medical School. There is still much we do not understand about the transmission dynamics of SARS-CoV-2, including its R_0, the infectiousness of asymptomatic case-patients (*28*), and the extent to which infections confer future immunity (*50*), all of which are key to anticipating future pandemic waves. As of June 2020, it is likely most US cities remain far from herd immunity. Even in New York, New York, which experienced a substantially larger first wave than other cities, serologic surveys suggest that only 22.7% of the population has been exposed (E.S. Rosenberg et al., unpub. data, https://doi.org/10.1101/2020.05.25.20113050). However, summer surges in transmission in some cities might infect large numbers of persons by the beginning of the fall semester. In that case, resolving these key uncertainties will be critical to projecting the full impact of school openings. Our understanding of COVID-19 is evolving so rapidly that we expect there might be consensus around different estimates for key transmission and severity parameters by the time this work is published. Thus, we emphasize the qualitative but not quantitative results of the analysis.

Given the rapid spread of COVID-19, early and extensive social distancing are both viable and necessary for preventing catastrophic hospital surges. Despite this study's uncertainties in key parameters and the focus on a single city, the expansion and containment of COVID-19 in cities worldwide suggest that these insights are widely applicable. This framework can be updated as situational awareness of COVID-19 improves to provide a quantitative sounding board as public health agencies evaluate strategies for mitigating risks while sustaining economic activity in the United States.

Acknowledgments

We thank Matthew Biggerstaff, Michael Johannson, the FluCode network at CDC, Steven Adler, and the White House Coronavirus Task Force for providing critical discussions and parameter guidance

About the Author

Ms. Wang is a PhD candidate at the University of Texas at Austin. Her primary research interest is mathematical and statistical modeling of infectious disease dynamics.

References

1. The Washington Post. WHO declares a pandemic of coronavirus disease COVID-19, 2020 Mar 11 [cited 2020 Mar 25]. https://www.washingtonpost.com/health/2020/03/11/who-declares-pandemic-coronavirus-disease-covid-19
2. World Health Organization. Novel coronavirus (2019-nCoV) situation reports [cited 2020 Mar 30]. https://www.who.int/emergencies/diseases/novel-coronavirus-2019/situation-reports
3. Holshue ML, DeBolt C, Lindquist S, Lofy KH, Wiesman J, Bruce H, et al.; Washington State 2019-nCoV Case Investigation Team. First case of 2019 novel coronavirus in the United States. N Engl J Med. 2020;382:929–36. https://doi.org/10.1056/NEJMoa2001191
4. Wheeler I. Orange County coronavirus patient released, in good condition, health officials say. Orange County Register. Orange County Register. 2020 Feb 4 [cited 2020 Mar 26]. https://www.ocregister.com/risk-of-catching-coronavirus-in-so-cal-is-low-health-officials-say

5. Goldstein J, McKinley J. Second case of coronavirus in N.Y. sets off search for others exposed. The New York Times. 2020 Mar 3 [cited 2020 Mar 26]. https://www.nytimes.com/2020/03/03/nyregion/coronavirus-new-york-state.html
6. Centers for Disease Control and Prevention. Coronavirus 2019; 2020 [cited 2020 Mar 25]. https://www.cdc.gov/media/releases/2020/t0228-COVID-19-update.html
7. Centers for Disease Control and Prevention. Coronavirus disease 2019 (COVID-19) in the US; 2020 [cited 2020 Mar 25]. https://www.cdc.gov/coronavirus/2019-ncov/cases-updates/cases-in-us.html
8. Koenig D. NYC hospitals struggle with coronavirus surge. WebMD. 2020 [cited 2020 Mar 28]. https://www.webmd.com/lung/news/20200326/nyc-hospitals-struggle-with-coronavirus-surge
9. Bush E, Gilbert D. Short-staffed and undersupplied: coronavirus crisis strains Seattle area's capacity to deliver care. The Seattle Times. 2020 Mar 12 [cited 2020 Mar 28]. https://www.seattletimes.com/seattle-news/health/short-staffed-and-undersupplied-coronavirus-crisis-strains-seattle-areas-capacity-to-deliver-care
10. Mervosh S, Lu D, Swales V. See which states and cities have told residents to stay at home. The New York Times, 2020 Mar 24 [cited 2020 Mar 28]. https://www.nytimes.com/interactive/2020/us/coronavirus-stay-at-home-order.html
11. Adeline S, Jin CH, Hurt A, Wilburn T, Wood D, Talbot R. Tracking the pandemic: are coronavirus cases rising or falling in your state? NPR. 2020 Jun 25 [cited 2020 Jun 25]. https://www.npr.org/sections/health-shots/2020/03/16/816707182/map-tracking-the-spread-of-the-coronavirus-in-the-u-s
12. US Census Bureau. American Community Survey (ACS) [cited 2019 Nov 19]. https://www.census.gov/programs-surveys/acs
13. Centers for Disease Control and Prevention. 500 cities project: Local data for better health; 2019 [cited 2020 Mar 19]. https://www.cdc.gov/500cities/index.htm
14. Centers for Disease Control and Prevention. HIV surveillance report, 2016. 2017 Nov [cited 2020 Jul 8]. https://www.cdc.gov/hiv/library/reports/hiv-surveillance.html
15. Morgan OW, Bramley A, Fowlkes A, Freedman DS, Taylor TH, Gargiullo P, et al. Morbid obesity as a risk factor for hospitalization and death due to 2009 pandemic influenza A(H1N1) disease. [Internet]. PLoS One. 2010;5:e9694. https://doi.org/10.1371/journal.pone.0009694
16. Sturm R, Hattori A. Morbid obesity rates continue to rise rapidly in the United States. Int J Obes. 2013;37:889–91. https://doi.org/10.1038/ijo.2012.159
17. Centers for Disease Control and Prevention. Estimating the number of pregnant women in a geographic area. Division of Reproductive Health [cited 2020 Jul 8]. https://www.cdc.gov/reproductivehealth/emergency/pdfs/PregnacyEstimatoBrochure508.pdf
18. Du Z, Xu X, Wu Y, Wang L, Cowling BJ, Meyers LA. Serial interval of COVID-19 among publicly reported confirmed cases. Emerg Infect Dis. 2020;26:1341–3. https://doi.org/10.3201/eid2606.200357
19. Li Q, Guan X, Wu P, Wang X, Zhou L, Tong Y, et al. Early transmission dynamics in Wuhan, China, of novel coronavirus-infected pneumonia. N Engl J Med. 2020;382:1199–207. https://doi.org/10.1056/NEJMoa2001316
20. Wu JT, Leung K, Leung GM. Nowcasting and forecasting the potential domestic and international spread of the 2019-nCoV outbreak originating in Wuhan, China: a modelling study. Lancet. 2020;395:689–97. https://doi.org/10.1016/S0140-6736(20)30260-9
21. Du Z, Wang L, Cauchemez S, Xu X, Wang X, Cowling BJ, et al. Risk for transportation of coronavirus disease from Wuhan to other cities in China. Emerg Infect Dis. 2020;26:1049–52. https://doi.org/10.3201/eid2605.200146
22. Kraemer MU, Yang C-H, Gutierrez B, Wu C-H, Klein B, Pigott DM, et al.; Open COVID-19 Data Working Group. The effect of human mobility and control measures on the COVID-19 epidemic in China. Science. 2020;368:493–7. https://doi.org/10.1126/science.abb4218
23. Muniz-Rodriguez K, Chowell G, Cheung C-H, Jia D, Lai P-Y, Lee Y, et al. Doubling time of the COVID-19 epidemic by province, China. Emerg Infect Dis. 2020;26: August; Epub ahead of print. https://doi.org/10.3201/eid2608.200219
24. Roser M, Ritchie H, Ortiz-Ospina E. Coronavirus disease (COVID-19): statistics and research. Our world in data, 2020 [cited 2020 Jul 8]. https://ourworldindata.org/coronavirus?fbclid=IwAR2qRdLFRmugoD0w_r13O4HAOHrL1hiHfduyB2XvtXNjtQ5GGW6Dg9EsIZA
25. Prem K, Cook AR, Jit M. Projecting social contact matrices in 152 countries using contact surveys and demographic data. PLOS Comput Biol. 2017;13:e1005697. https://doi.org/10.1371/journal.pcbi.1005697
26. Zhang J, Litvinova M, Wang W, Wang Y, Deng X, Chen X, et al. Evolving epidemiology and transmission dynamics of coronavirus disease 2019 outside Hubei province, China: a descriptive and modelling study. Lancet Infect Dis. 2020;20:793–802. https://doi.org/10.1016/S1473-3099(20)30230-9
27. He X, Lau EH, Wu P, Deng X, Wang J, Hao X, et al. Temporal dynamics in viral shedding and transmissibility of COVID-19. Nat Med. 2020;26:672–5. https://doi.org/10.1038/s41591-020-0869-5
28. He D, Zhao S, Lin Q, Zhuang Z, Cao P, Wang MH, et al. The relative transmissibility of asymptomatic COVID-19 infections among close contacts. Int J Infect Dis. 2020;94: 145–7. https://doi.org/10.1016/j.ijid.2020.04.034
29. Gudbjartsson DF, Helgason A, Jonsson H, Magnusson OT, Melsted P, Norddahl GL, et al. Spread of SARS-CoV-2 in the Icelandic population. N Engl J Med. 2020;382:2302–15. https://doi.org/10.1056/NEJMoa2006100
30. Mossong J, Hens N, Jit M, Beutels P, Auranen K, Mikolajczyk R, et al. Social contacts and mixing patterns relevant to the spread of infectious diseases. PLoS Med. 2008;5:e74. https://doi.org/10.1371/journal.pmed.0050074
31. United Nations. Record view: population by age, sex and urban/rural residence [cited 2020 Mar 22]. http://data.un.org/Data.aspx?d=POP&f=tableCode%3a22
32. Siegel E. Why "exponential growth" is so scary for the COVID-19 coronavirus. Forbes Magazine, 2020 Mar 17 [cited 2020 Mar 30]. https://www.forbes.com/sites/startswithabang/2020/03/17/why-exponential-growth-is-so-scary-for-the-covid-19-coronavirus
33. Austin Independent School District. Calendar of events, 2020 [cited 2020 Mar 26]. https://www.austinisd.org/calendar
34. Ferguson NM, Laydon D, Nedjati-Gilani G, Imai N, Ainslie K, Baguelin M, et al. Impact of non-pharmaceutical interventions (NPIs) to reduce COVID-19 mortality and healthcare demand, 2020. Imperial College London. 2020 [cited 2020 Jul 8]. https://sciencebusiness.net/sites/default/files/inline-files/Imperial-College-COVID19-NPI-modelling-16-03-2020.pdf
35. SXSW. Facts, figures & quotes. SXSW Conference & Festivals [cited 2020 Mar 25]. https://www.sxsw.com/facts-figures-quotes

36. Austin Independent School District. Important message. 2020 Mar 13 [cited 2020 Mar 26]. https://www.austinisd.org/announcements/2020/03/13/important-message-mensaje-importante
37. The University of Texas at Austin. COVID-19 updates. Guidance related to the coronavirus disease, 2020 [cited 2020 Mar 26]. https://coronavirus.utexas.edu/all-campus-communications-covid-19
38. City of Austin, Texas. Coronavirus disease. 2019 (COVID-19) [cited 2020 Mar 25]. http://www.austintexas.gov/COVID19
39. University of Texas News. A new Texas COVID-19 pandemic toolkit shows the importance of social distancing. 2020 Mar 26 [cited 2020 Mar 28]. https://news.utexas.edu/2020/03/26/a-new-texas-covid-19-pandemic-toolkit-shows-the-importance-of-social-distancing
40. Chen Q, Liang M, Li Y, Guo J, Fei D, Wang L, et al. Mental health care for medical staff in China during the COVID-19 outbreak. Lancet Psychiatry. 2020;7:e15–6. https://doi.org/10.1016/S2215-0366(20)30078-X
41. Maharaj S, Kleczkowski A. Controlling epidemic spread by social distancing: do it well or not at all. BMC Public Health. 2012;12:679. https://doi.org/10.1186/1471-2458-12-679
42. Lempel H, Epstein JM, Hammond RA. Economic cost and health care workforce effects of school closures in the U.S. PLoS Curr. 2009;1:RRN1051. https://doi.org/10.1371/currents.RRN1051
43. Araz OM, Damien P, Paltiel DA, Burke S, van de Geijn B, Galvani A, et al. Simulating school closure policies for cost effective pandemic decision making. BMC Public Health. 2012;12:449. https://doi.org/10.1186/1471-2458-12-449
44. Guan W-J, Ni Z-Y, Hu Y, Liang W-H, Ou C-Q, He J-X, et al.; China Medical Treatment Expert Group for Covid-19. Clinical characteristics of coronavirus disease 2019 in China. N Engl J Med. 2020;382:1708–20. https://doi.org/10.1056/NEJMoa2002032
45. Verity R, Okell LC, Dorigatti I, Winskill P, Whittaker C, Imai N, et al. Estimates of the severity of coronavirus disease 2019: a model-based analysis. Lancet Infect Dis. 2020;20:669–77. https://doi.org/10.1016/S1473-3099(20)30243-7
46. Liu W, Zhang Q, Chen J, Xiang R, Song H, Shu S, et al. Detection of COVID-19 in children in early January 2020 in Wuhan, China. N Engl J Med. 2020;382:1370–1. https://doi.org/10.1056/NEJMc2003717
47. Hoen AG, Hladish TJ, Eggo RM, Lenczner M, Brownstein JS, Meyers LA. Epidemic wave dynamics attributable to urban community structure: a theoretical characterization of disease transmission in a large network. J Med Internet Res. 2015;17:e169. https://doi.org/10.2196/jmir.3720
48. Meyers LA, Pourbohloul B, Newman ME, Skowronski DM, Brunham RC. Network theory and SARS: predicting outbreak diversity. J Theor Biol. 2005;232:71–81. https://doi.org/10.1016/j.jtbi.2004.07.026
49. Volz EM, Miller JC, Galvani A, Ancel Meyers L. Effects of heterogeneous and clustered contact patterns on infectious disease dynamics. PLOS Comput Biol. 2011;7:e1002042. https://doi.org/10.1371/journal.pcbi.1002042
50. Long Q-X, Tang X-J, Shi Q-L, Li Q, Deng H-J, Yuan J, et al. Clinical and immunological assessment of asymptomatic SARS-CoV-2 infections. Nat Med. 2020;Jun 18 {Epub ahead of print].. https://doi.org/10.1038/s41591-020-0965-6

Address for correspondence: Lauren Ancel Meyers, Department of Integrative Biology, The University of Texas at Austin, 1 University Station C0990, Austin, TX 78712, USA; email: laurenmeyers@austin.utexas.edu

Multicenter Prevalence Study Comparing Molecular and Toxin Assays for *Clostridioides difficile* Surveillance, Switzerland

Andreas F. Widmer, Reno Frei, Ed J. Kuijper, Mark H. Wilcox, Ruth Schindler, Violeta Spaniol, Daniel Goldenberger, Adrian Egli, Sarah Tschudin-Sutter

Public health authorities in the United States and Europe recommend surveillance for *Clostridioides difficile* infections among hospitalized patients, but differing diagnostic algorithms can hamper comparisons between institutions and countries. We compared surveillance based on detection of *C. difficile* by PCR or enzyme immunoassay (EIA) in a nationwide *C. difficile* prevalence study in Switzerland. We included all routinely collected stool samples from hospitalized patients with diarrhea in 76 hospitals in Switzerland on 2 days, 1 in winter and 1 in summer, in 2015. EIA *C. difficile* detection rates were 6.4 cases/10,000 patient bed-days in winter and 5.7 cases/10,000 patient bed-days in summer. PCR detection rates were 11.4 cases/10,000 patient bed-days in winter and 7.1 cases/10,000 patient bed-days in summer. We found PCR used alone increased reported *C. difficile* prevalence rates by ≤80% compared with a 2-stage EIA-based algorithm.

Since its identification as a cause of antibiotic-associated pseudomembraneous colitis in 1978 (*1*), *Clostridioides difficile* has emerged as a major healthcare-associated pathogen worldwide. In the United States, *C. difficile* infection (CDI) rates doubled during 1996–2003 (*2*), and rates of CDI were reported to be 76.9 cases/10,000 discharges in 2005 (*3*). In a more recent national point-prevalence study including US healthcare facility in-patients, 13/1,000 patients were found to be either infected or colonized (*4*), a higher rate than had been previously estimated. In a national point-prevalence study of nosocomial infections in the United States, *C. difficile* was the most common causative pathogen overall (*5*). The increase largely has been attributed to the emergence of the hypervirulent strain, PCR ribotype 027 (RT027), which was identified as causative strain in 82% of cases during CDI outbreaks in Quebec, Canada, during 2001–2003 and accounted for 31% of all cases of healthcare-associated infections in the United States in 2011 (*6*–*9*). In Europe, CDI incidence varies across hospitals and countries with a weighted mean of 4.1 cases/10,000 patient-days per hospital in 2008 (*10*). The most recent study on CDI prevalence in Europe suggests an increase in the number of cases, reporting a mean of 7.0 cases/10,000 patient-bed days and ranging among countries from 0.7 to 28.7 cases/10,000 patient-bed days (*11*). The most common ribotype identified was RT027, which was detected in 4 countries: Germany, Hungary, Poland, and Romania (*11*).

To estimate and compare the burden of CDI across the United States, the US Centers for Disease Control and Prevention (CDC) began population-based CDI surveillance in 10 locations in 2011 (*12*). The European Centre for Disease Prevention and Control (ECDC) began coordinating CDI surveillance in acute care hospitals in Europe in 2016 (*13*). Both authorities provide case definitions based on different diagnostic approaches, including detection of *C. difficile* toxin A and B by enzyme immunoassay (EIA) or detection of toxin-producing *C. difficile* organisms by PCR. However, the use of different diagnostic algorithms to detect *C. difficile* might hamper comparisons between institutions and countries. Therefore, in a nationwide *C. difficile* multicenter prevalence study in Switzerland, we systematically compared surveillance measures based on detection of *C. difficile* in stool by either PCR as a stand-alone

Author affiliations: University Hospital Basel, Basel, Switzerland (A.F. Widmer, R. Frei, R. Schindler, V. Spaniol, D. Goldenberger, A. Egli, S. Tschudin-Sutter); Leiden University Medical Center, Leiden, the Netherlands (E.J. Kuijper); Leeds Institute of Biomedical and Clinical Sciences, University of Leeds, and Leeds Teaching Hospitals, Leeds, UK (M.H. Wilcox)

DOI: https://doi.org/10.3201/eid2610.190804

test or by a 2-stage algorithm consisting of an EIA to detect glutamate dehydrogenase (GDH) and toxins A and B.

Methods

Study Design

We performed a nationwide multicenter prevalence study of toxigenic *C. difficile* detected in stool samples routinely collected from hospitalized patients with diarrhea. Our study followed the design of a previous point-prevalence study for maximal comparibility between our results and data from Europe (*11*). University Hospital Basel, a tertiary care center in Switzerland, coordinated the study. All hospitals participating in Swissnoso (https://www.swissnoso.ch), a national infection prevention network, were asked to participate. The Swissnoso network consists of 85 acute care hospitals that account for a total of 26,341 beds.

The Ethics Committee Northwest and Central Switzerland (Ethikkommission Nordwest-und Zentralschweiz) issued a declaration of no objection for this study. We adhered to STROBE guidelines for reporting on observational studies (*14*).

Sample Collection

All stool samples collected from inpatients >1 year of age with diarrhea that were submitted to the microbiology laboratory on 2 specified sampling days, 1 in winter and 1 in summer, in 2015 were eligble for inclusion. Only 1 sample per patient was included. In addition, stool samples that tested positive for toxigenic *C. difficile* ≤1 week prior to each study day also were collected from all institutions to obtain a more detailed estimate of ribotype distribution in Switzerland.

We collected the following institutional data for all hospitals and their affiliated microbiology laboratories: contact information; detailed information

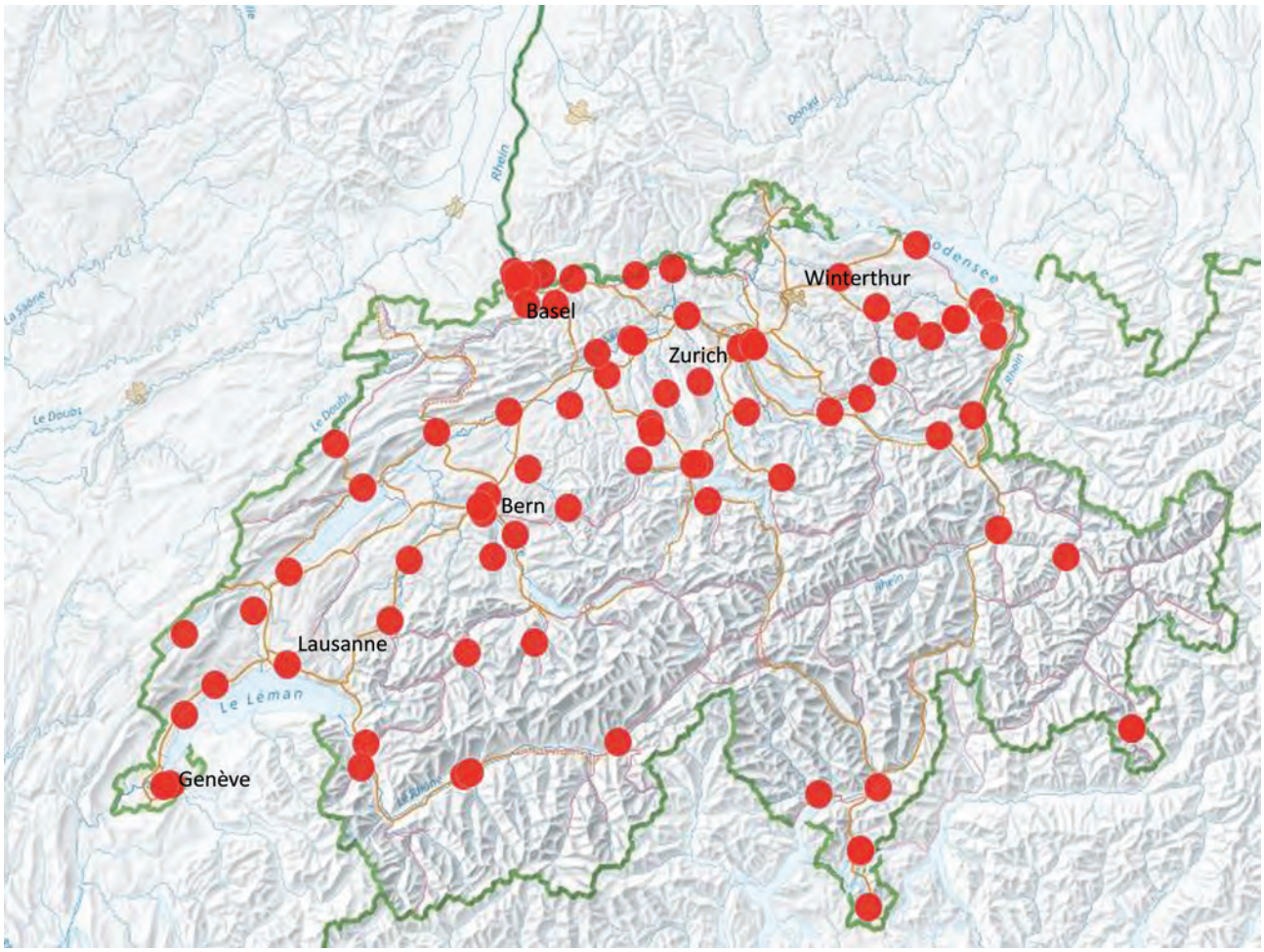

Figure 1. Distribution of centers participating in a prevalence study comparing molecular and toxin assays for nationwide surveillance of *Clostridioides difficile*, Switzerland. Red circles represent location of participating centers.

regarding laboratory diagnostics in place; and detailed information on the total number of admissions, number of beds, and number of patients hospitalized on the 2 days of the study. We also collected information on the total number of diagnosed CDI cases at each institution during the study year. For each eligible stool sample, we collected the following data: date of sample collection, age and gender of patient, ward location and clinical specialty, institution, whether a *C. difficile* test was ordered by the treating physician, and result of the *C. difficile* test if testing was performed at the local laboratory.

Procedures

We tested all stool samples at the Division of Clinical Microbiology of the University Hospital Basel by using a 2-stage algorithm consisting of EIA and PCR. We performed EIA to detect GDH and toxins A and B by using C. DIFF QUIK CHEK COMPLETE (Techlab, https://www.techlab.com), following the manufacturer's instructions. We then performed PCR to detect the toxin B gene by using the RealStar PCR Kit (Altona Diagnostics, https://www.altona-diagnostics.com). For detected *C. difficile*, we performed strain typing by using high-resolution capillary gel-based PCR ribotyping according to the method previously described by Stubbs et al. (*15*).

Outcomes

We calculated reported and measured rates of detected toxigenic *C. difficile* per 10,000 patient bed-days across participating institutions. We compared differences in testing algorithms for detection of toxigenic *C. difficile* across institutions in Switzerland and performance characteristics of diagnostic algorithms. We considered the proportion of missed toxigenic *C. difficile* cases and ribotype distributions as additional outcomes. We further assessed the proportion of laboratories using optimized *C. difficile* diagnostic tests, which we defined as using an algorithm recommended by the European Society of Clinical Microbiology and Infectious Diseases (*16*).

Statistical Analyses

We separately calculated rates for each diagnostic algorithm performed in the coordinating center laboratory. In addition, we separately calculated rates for dedicated children's hospitals. We defined missed *C. difficile* cases as those in which tests were negative at the participating hospital's laboratory but positive at our institution. We used descriptive statistics to report ribotypes and differences in diagnostic algorithms across all participating institutions. All analyses were perfomed in Stata version 15.1 (StataCorp,https://www.stata.com).

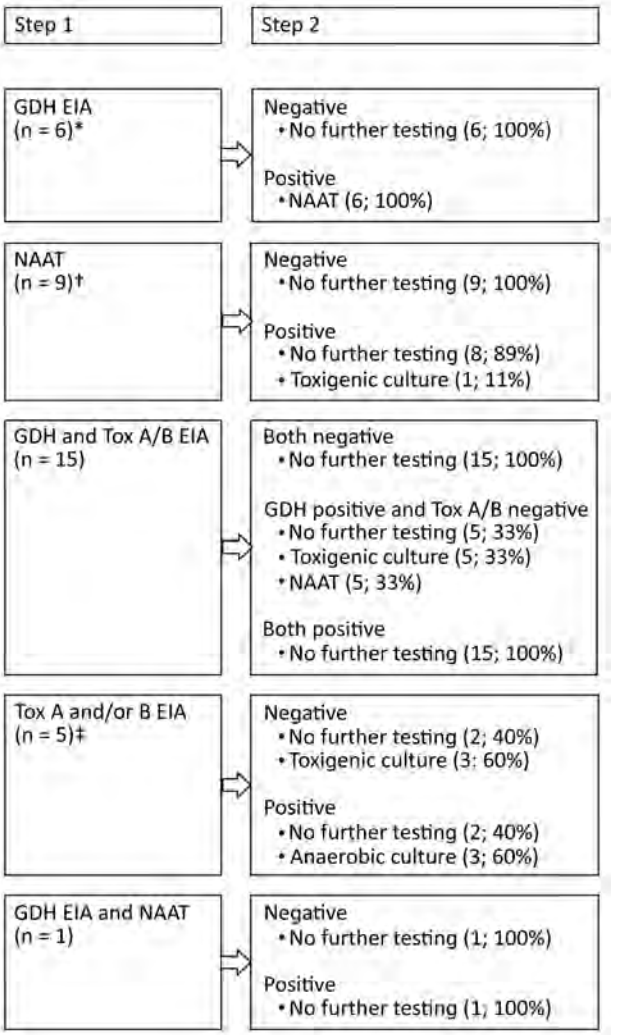

Figure 2. Testing algorithms at the 36 laboratories participating in a prevalence study comparing molecular and toxin assays for nationwide surveillance of *Clostridioides difficile*, Switzerland. EIA, enzyme immunoassay; GDH, glutamate dehydrogenase; NAAT, nucleic acid amplification test; Tox, toxin. *Seven samples taken during the summer sampling period. †Ten samples taken during the summer sampling period. ‡Three samples taken during the summer sampling period.

Results

Participating institutions included 76/85 (89.4%) institutions belonging to the Swissnoso network. Among participating institutions, 5 were academic teaching hospitals, 3 were dedicated children's hospitals, and 36 were affiliated microbiology laboratories. Participating institutions were distributed across all geographic regions of Switzerland (Figure 1).

Participating institutions reported collecting a fecal sample for microbiological workup in ≈65% (SD ±25%) of all patients with hospital-onset diarrhea. Among participating institutions, 15/76 (19.7%) did not begin CDI treatment before fecal sample collection. Among institutions that intitiated treatment before collecting fecal samples, 23/76 (30.3%) began treatment in <2% of patients, 12/76 (15.8%) began treatment in 3%–5% of patients, 8/76 (10.5%) began treatment in 6%–10% of patients, and 1 (1.3%) began treatment in 11%–20% of patients. The other 17 (22%) institutions were not able to provide an estimate of these data.

Overall, 354 stool samples were submitted to the coordinating center, of which 338 were eligible for study inclusion; 16 samples were excluded because they were not liquid, their submitted data were incomplete, or they were duplicate samples from 1 patient. Among 338 samples included, 250 were collected as part of the point-prevalence study. We excluded 8 of these because the samples were collected from patients <1 year of age. In all, we included 242 samples in the point-prevalence study.

Diagnostic Algorithms

Among the 36 participating laboratories, 1 routinely tested all diarrheal stool samples for toxigenic *C. difficile* and 35 tested only if a specific test was requested. Optimized diagnostic tests for detection of toxigenic *C. difficile* were used by 58% (21/36) of laboratories in the winter sampling period and by 61% (22/36) in the summer sampling period. Among laboratories not following the recommendations of the European Society of Clinical Microbiology and Infectious Diseases (*16*), 9 in the winter sampling period and 10 in the summer sampling period used a nucleic acid amplification test (NAAT) alone, and 5 in the winter sampling period and 3 in the summer sampling period used EIAs for A and B toxins either as a standalone test or as an initial screening test. Only 1 laboratory reported having established PCR ribotyping methodologies (Figure 2).

Point-Prevalence Analyses

We collected demographic characteristics of patients whose stool samples tested positive by our testing algorithms (Table 1). *C. difficile* tests were required and performed for 68% (165/242) of stool samples; 6% (27/165) were reported as positive by the affiliated microbiology laboratory.

At the coordinating center, we detected *C. difficile* in 9% (21/242) of samples by EIA for GDH and A and B toxins and in 12% (30/242) of samples by PCR alone. Among all 27 samples reported as positive by the participating centers, we confirmed 18 (67%) by EIA and 24 (89%) by PCR. Among 138 samples reported as negative by the participating centers, 1 (1%) sample tested positive by EIA and 3 (2%) tested positive by PCR at the coordinating center. Among 77 samples not tested for *C. difficile* at the participating centers, we detected *C. difficile* in 2 (3%) by EIA and in 3 (4%) by PCR. Among 21 stool samples that tested positive by EIA at the coordinating center, a *C. difficile* test was not requested in 2 (10%) cases. Among 30 samples that tested positive by PCR at the coordinating center, a *C. difficile* test was not requested in 3 cases (10%; Table 2).

Measured detection and testing rates of toxigenic *C. difficile* were higher than the reported rates across all participating institutions (Table 3). Depending on the diagnostic algorithm applied, the largest difference in prevalence across all institutions was measured during the winter sampling period, which had a prevalence of 6.4 cases/10,000 patient bed-days by EIA and 11.4 cases/10,000 patient bed-days by PCR alone. Thus, across all institutions, rates of toxigenic

Table 1. Demographic data for 242 patients whose stool samples were included in the study of detection of *Clostridioides difficile* via PCR and enzyme immunoassay for glutamate dehydrogenase and A and B toxins, Switzerland*

		Method of *Clostridioides difficile* detection	
Demographics	All patients	EIA for GDH and A and B toxins, n = 21	PCR, n = 30
Median age, y (IQR)	63 (44–80)	79 (59–86)	78 (55–85)
Sex			
M	104 (43.0)	6 (28.6)	10 (33.3)
F	131 (54.1)	15 (71.4)	20 (66.7)
Not reported	7 (2.9)	0	0
Clinical specialty			
Medical	127 (52.5)	11 (52.4)	11 (36.7)
Surgery	43 (17.8)	3 (14.3)	6 (20.0)
Obstetrics, gynocology	3 (1.2)	0	0
Pediatrics	21 (8.7)	1 (4.8)	3 (10.0)
Other	28 (11.6)	5 (23.8)	7 (23.3)
Not reported	20 (8.3)	1 (4.8)	3 (10.0)
Intensive care	40 (16.5)	5 (23.8)	5 (16.7)

*Values are reported as no. (%) except where indicated. EIA, enzyme immunoassay; GDH, glutamate dehydrogenase; IQR, Interquartile range.

Table 2. Underdiagnosis and misdiagnosis of *Clostridioides difficile* infection at participating hospitals, Switzerland*

Method of detection	No. samples submitted	No. samples tested	Undiagnosed, no. (% of all positive samples)	False-positive, no. (%)	False-negative, no. (%)
EIA for GDH and A and B toxins	242	165	2 (9.5)	9 (5.5)	1 (0.6)
PCR	242	165	3 (10)	3 (1.8)	3 (1.8)

*EIA, enzyme immunoassay; GDH, glutamate dehydrogenase.

C. difficile detection by PCR alone were ≤80% higher than detection rates by EIA for GDH and A and B toxins. In addition, detection rates by PCR alone were ≤100% higher in dedicated children's hospitals (Table 3).

Ribotype Distribution

We cultured and ribotyped 107 toxigenic *C. difficile* strains, 29 from the 2 point-prevalence days and 78 collected ≤1 week before each prevalence day. We identified a large diversity of *C. difficile* ribotypes, 23 (22%) had not been referenced before. The ribotypes most commonly identified included RT014 (12/107; 11%), presumably hypervirulent RT078 (9/107; 8%), RT001 (7/107; 7%), and RT002 (7/107; 7%) (Figure 3).

Discussion

In this nationwide multicenter study, we found that PCR as a stand-alone test increased reported *C. difficile* prevalence rates ≤80% compared with a 2-stage EIA-based algorithm. At first glance, this finding was not surprising given the higher sensitivity of EIA (*16*). However, the fact that our results and conclusions are based on a nationwide cohort representing all geographic regions of Switzerland adds to the study's credibility. In addition, our results strengthen the advice of the European Society of Clinical Microbiology and Infectious Diseases study group for *C. difficile* against use of a single commercial test for diagnosing CDI because of the low positive predictive values when CDI prevalence is low, 46% at a CDI prevalence of 5% (*16*). However, CDC and ECDC protocols for CDI surveillance define a case of CDI as the combination of diarrheal stool and a positive PCR (*12*,*13*). In addition, the clinical practice guidelines for CDI in adults and children published by the Infectious Diseases Society of America and Society for Healthcare Epidemiology of America recommend testing by different approaches, such as multistep algorithms or NAAT, depending on the degree of clinical suspicion (*17*). Based on a systematic review and meta-analysis, the American Society of Microbiology also recommends different approaches, including NAAT-only testing, and algorithms that include GDH and NAAT or GDH, toxins, and NAAT (*18*). Although these recommendations stand to reason for detection of CDI in individual patients, our results challenge their utility for meaningful comparisons in surveillance studies and suggest that uniform definitions should be provided.

On both point-prevalence days, we noted a higher nationwide rate of toxigenic *C. difficile* than previously reported in incidence studies performed at different institutions in Switzerland (*19*–*21*). Our findings suggest that CDI rates have increased during the last decade in Switzerland, a finding that is in line with reports from other countries in Europe (*11*). Using the same diagnostic algorithm, diagnostic test, and a similar study design to the multicenter point-prevalence study of CDI in hospitalized patients with diarrhea in Europe, the nationwide mean prevalence rates are comparable in Switzerland (mean 6.1 cases/10,000 patient bed-days) and Europe (7.0 cases/10,000 patient bed-days) (*11*). Because we only included liquid stools in our study, our mean prevalence rate of 9.3 cases/10,000 patient bed-days measured by PCR fulfills the ECDC case definition and further shows that CDI is increasing substantially nationwide.

We found a lower proportion of missed detection of toxigenic *C. difficile* in Switzerland (9.5%), driven by the absence of clinical suspicion, compared with Europe (23%), which equates to 1 missed case of *C. difficile* per day among the included institutions in Switzerland. False-negative testing accounted for 1

Table 3. Reported and measured detection and testing rates of toxigenic *Clostridioides difficile*, Switzerland, 2015*

Institutions and testing methods	Reported rate/10,000 patient bed-days	Measured rate/10,000 patient bed-days, winter (range)	Measured rate/10,000 patient bed-days, summer (range)	Mean measured rate/10,000 patient bed-days (range)	Testing rate/10,000 patient bed-days (range)
All institutions	3.8 (0–11)				67.5 (0–3,202)
EIA		6.4 (0–387)	5.7 (0–475)	6.1 (0–475)	
NAAT		11.4 (0–387)	7.1 (0–475)	9.3 (0–475)	
Children's hospitals	1.1 (0.4–1.1)				22.5 (7.0–46.7)
EIA		33.7 (0–73)	0	16.9 (0–73)	
NAAT		67.3 (0–99)	0	33.6 (0–99)	

EIA, enzyme immuno assay; GDH, glutamate dehydrogenase; NAAT, nucleic acid amplification tests.

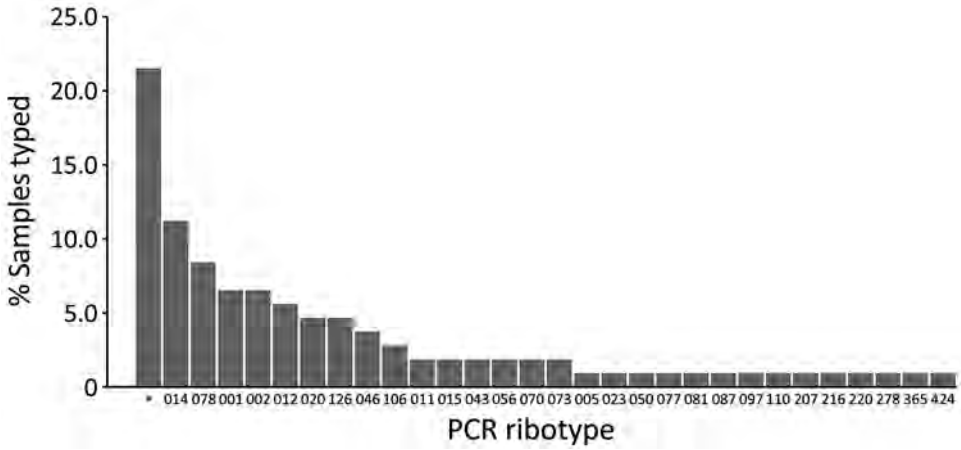

Figure 3. Distribution of PCR ribotypes among 107 samples collected in a prevalence study comparing molecular and toxin assays for nationwide surveillance of *Clostridioides difficile*, Switzerland. *Unknown ribotype.

additional missed diagnosis during both point-prevalence days, which extrapolates to ≈550 missed cases of *C. difficile* per year among hospitals across the nation.

We detected a variety of different RTs during our study period, 21% of which had not been referenced before. Of note, we did not recover hypervirulent RT027, but RT078 was the third most common strain circulating in Switzerland during our study. In contrast, a point-prevalence study in Europe identified RT027 as the most commonly circulating strain during its study period but did not detect RT078. RT078 has been associated with similarly severe disease manifestations as RT027, but RT078 has been reported to affect younger patients and to be linked more commonly with community-associated disease in the Netherlands (22). RT078 has been isolated from piglets with diarrhea, possibly suggesting ongoing transmission by introduction to the food chain because isolates from humans and pigs were found to be highly genetically related (22). A component of RT078 infections also was reported in Northern Ireland, which has a large pig population and ≈1:1 ratio of cattle to humans (23). In Switzerland, RT078 has been isolated previously from 6 wastewater treatment plants, suggesting its dissemination in the community (24). Except for both hypervirulent RT027 and RT078, we identified other similarities in RT distribution between Switzerland and the rest of Europe; RT014, RT001, RT002, and RT020 were among the 10 most commonly identified ribotypes in both settings.

Our study has some limitations, most of which are intrinsic to point-prevalence studies. First, our study only reflects frequency of toxigenic *C. difficile* detected on 2 days in 2015; therefore, we cannot draw solid conclusions regarding incidence. We expanded the timeframe for assessing the distribution of ribotypes circulating in Switzerland by an additional week for each prevalence day, but this still represents a limited collection of the true incidence. Second, we cannot rule out introduction of bias to testing policies at the participating hospitals, which might have increased testing on the 2 point-prevalence days. However, we did not provide any promotional information regarding our study, so alterations in daily clinical practice among treating physicians is unlikely on these 2 days. Third, we only included liquid stool samples for analyses, but we did not consider any other preanalytical factors, such as the use of laxatives, for testing eligibility. Finally, we applied surveillance definitions recommended by CDC and ECDC rather than defintions used for the clinical diagnosis of CDI in individual patients, such as detection of *C. difficile* in the context of symptoms related to CDI. Therefore, we cannot rule out detection of toxigenic *C. difficile* from colonization rather than infection in some cases.

In conclusion, this nationwide multicenter study reveals that PCR as a stand-alone test results in an increase of *C. difficile* prevalence rates of ≤80% compared with a 2-stage EIA-based algorithm. Our findings underscore the need for consistent testing algorithms for meaningful interinstitutional and nationwide comparisons. Our results also challenge the utility of the current CDC and ECDC case definitions and highlight the need for uniform recommendations on diagnostic approaches.

Acknowledgments

We acknowledge and thank the ESCMID (European Society of Clinical Microbiology and Infectious Diseases). Study group for *C. difficile* (ESGCD) for professional support. We also thank all participating centers and laboratories (Appendix, https://wwwnc/cdc.gov/EID/article/26/10/19-0804-App1.pdf).

Astellas Pharmaceuticals Europe provided financial support for this study. The funder did not influence the study design and did not contribute to data collection,

data analysis, data interpretation, or writing of the report. Astellas Pharma Europe reviewed the report for factual accuracy before submission, in line with the terms of the funding agreement. The corresponding author had full access to all data in the study and had final responsibility for the decision to submit for publication. Alere provided C. DIFF QUIK CHEK COMPLETE test kits for conducting EIAs to detect GDH and toxins A and B.

The authors declare the following possible conflicts of interest: A.W. is a member of the Astellas and Merck Sharp & Dohme Corp. advisory boards for *C. difficile* and reports grants from the Swiss National Science Foundation. S.T.-S. is a member of the Astellas and Merck Sharp & Dohme Corp. advisory boards for *C. difficile* and reports grants from the Swiss National Science Foundation (grant nos. NRP72 and 407240_167060), the Gottfried und Julia Bangerter-Rhyner Stiftung, and the Fund for the Promotion of Teaching and Research of the Voluntary Academic Society, Basel.

About the Author

Dr. Widmer is head of the infection control program at University Hospital Basel, University of Basel, Switzerland. His research interests include all aspects of *Clostridioides difficile* and the epidemiology and prevention of hospital-acquired infections.

References

1. Bartlett JG, Moon N, Chang TW, Taylor N, Onderdonk AB. Role of *Clostridium difficile* in antibiotic-associated pseudomembranous colitis. Gastroenterology. 1978;75:778–82. https://doi.org/10.1016/0016-5085(78)90457-2
2. McDonald LC, Owings M, Jernigan DB. *Clostridium difficile* infection in patients discharged from US short-stay hospitals, 1996–2003. Emerg Infect Dis. 2006;12:409–15. https://doi.org/10.3201/eid1203.051064
3. Elixhauser A, Jhung M. *Clostridium difficile*-associated disease in U.S. hospitals, 1993–2005: statistical brief #50; Healthcare Cost and Utilization Project (HCUP). Rockville (MD, USA): Agency for Healthcare Research and Quality; 2008 [cited 2019 May 26]. https://www.hcup-us.ahrq.gov/reports/statbriefs/sb50.jsp
4. Jarvis WR, Schlosser J, Jarvis AA, Chinn RY. National point prevalence of *Clostridium difficile* in US health care facility inpatients, 2008. Am J Infect Control. 2009;37:263–70. https://doi.org/10.1016/j.ajic.2009.01.001
5. Magill SS, Edwards JR, Bamberg W, Beldavs ZG, Dumyati G, Kainer MA, et al.; Emerging Infections Program Healthcare-Associated Infections and Antimicrobial Use Prevalence Survey Team. Multistate point-prevalence survey of health care–associated infections. N Engl J Med. 2014;370:1198–208. https://doi.org/10.1056/NEJMoa1306801
6. Pépin J, Saheb N, Coulombe MA, Alary ME, Corriveau MP, Authier S, et al. Emergence of fluoroquinolones as the predominant risk factor for *Clostridium difficile*-associated diarrhea: a cohort study during an epidemic in Quebec. Clin Infect Dis. 2005;41:1254–60. https://doi.org/10.1086/496986
7. Loo VG, Poirier L, Miller MA, Oughton M, Libman MD, Michaud S, et al. A predominantly clonal multi-institutional outbreak of *Clostridium difficile*-associated diarrhea with high morbidity and mortality. N Engl J Med. 2005;353:2442–9. https://doi.org/10.1056/NEJMoa051639
8. O'Donoghue C, Kyne L. Update on *Clostridium difficile* infection. Curr Opin Gastroenterol. 2011;27:38–47. https://doi.org/10.1097/MOG.0b013e3283411634
9. Lessa FC, Mu Y, Bamberg WM, Beldavs ZG, Dumyati GK, Dunn JR, et al. Burden of *Clostridium difficile* infection in the United States. N Engl J Med. 2015;372:825–34. https://doi.org/10.1056/NEJMoa1408913
10. Bauer MP, Notermans DW, van Benthem BH, Brazier JS, Wilcox MH, Rupnik M, et al.; ECDIS Study Group. *Clostridium difficile* infection in Europe: a hospital-based survey. Lancet. 2011;377:63–73. https://doi.org/10.1016/S0140-6736(10)61266-4
11. Davies KA, Longshaw CM, Davis GL, Bouza E, Barbut F, Barna Z, et al. Underdiagnosis of *Clostridium difficile* across Europe: the European, multicentre, prospective, biannual, point-prevalence study of Clostridium difficile infection in hospitalised patients with diarrhoea (EUCLID). Lancet Infect Dis. 2014;14:1208–19. https://doi.org/10.1016/S1473-3099(14)70991-0
12. US Centers for Disease Control and Prevention. *Clostridioides difficile* infection (CDI) tracking. [cited 2019 May 26]. https://www.cdc.gov/hai/eip/cdiff-tracking
13. European Centre for Disease Prevention and Control. Surveillance and disease data for *Clostridium difficile* infections. [cited 2019 May 26]. https://ecdc.europa.eu/en/clostridium-difficile-infections/surveillance-and-disease-data
14. von Elm E, Altman DG, Egger M, Pocock SJ, Gøtzsche PC, Vandenbroucke JP; STROBE Initiative. The Strengthening the Reporting of Observational Studies in Epidemiology (STROBE) statement: guidelines for reporting observational studies. Lancet. 2007;370:1453–7. https://doi.org/10.1016/S0140-6736(07)61602-X
15. Stubbs SL, Brazier JS, O'Neill GL, Duerden BI. PCR targeted to the 16S-23S rRNA gene intergenic spacer region of *Clostridium difficile* and construction of a library consisting of 116 different PCR ribotypes. J Clin Microbiol. 1999;37:461–3. https://doi.org/10.1128/JCM.37.2.461-463.1999
16. Crobach MJ, Planche T, Eckert C, Barbut F, Terveer EM, Dekkers OM, et al. European Society of Clinical Microbiology and Infectious Diseases: update of the diagnostic guidance document for *Clostridium difficile* infection. Clin Microbiol Infect. 2016;22(Suppl 4):S63–81. https://doi.org/10.1016/j.cmi.2016.03.010
17. McDonald LC, Gerding DN, Johnson S, Bakken JS, Carroll KC, Coffin SE, et al. Clinical practice guidelines for *Clostridium difficile* infection in adults and children: 2017 update by the Infectious Diseases Society of America (IDSA) and Society for Healthcare Epidemiology of America (SHEA). Clin Infect Dis. 2018;66:987–94. https://doi.org/ 10.1093/cid/ciy149
18. Kraft CS, Parrott JS, Cornish NE, Rubinstein ML, Weissfeld AS, McNult P, et al. A laboratory medicine best practices systematic review and meta-analysis of nucleic acid amplification tests (NAATs) and algorithms including NAATs for the diagnosis of *Clostridioides* (*Clostridium*) *difficile* in adults. Clin Microbiol Rev. 2019;32:e00032–18. https://doi.org/10.1128/CMR.00032-18
19. Fenner L, Frei R, Gregory M, Dangel M, Stranden A, Widmer AF. Epidemiology of *Clostridium difficile*-associated disease at University Hospital Basel including molecular characterisation of the isolates 2006–2007. Eur J Clin

Microbiol Infect Dis. 2008;27:1201–7. https://doi.org/10.1007/s10096-008-0564-9
20. Vernaz N, Sax H, Pittet D, Bonnabry P, Schrenzel J, Harbarth S. Temporal effects of antibiotic use and hand rub consumption on the incidence of MRSA and *Clostridium difficile*. J Antimicrob Chemother. 2008;62:601–7. https://doi.org/10.1093/jac/dkn199
21. Kohler P, Bregenzer-Witteck A, Rafeiner P, Schlegel M. Presumably hospital-transmitted *Clostridium difficile* infections based on epidemiological linkage. Swiss Med Wkly. 2013; 143:w13824. https://doi.org/10.4414/smw.2013.13824
22. Goorhuis A, Bakker D, Corver J, Debast SB, Harmanus C, Notermans DW, et al. Emergence of *Clostridium difficile* infection due to a new hypervirulent strain, polymerase chain reaction ribotype 078. Clin Infect Dis. 2008;47:1162–70. https://doi.org/10.1086/592257
23. Patterson L, Wilcox MH, Fawley WN, Verlander NQ, Geoghegan L, Patel BC, et al. Morbidity and mortality associated with *Clostridium difficile* ribotype 078: a case–case study. J Hosp Infect. 2012;82:125–8. https://doi.org/10.1016/j.jhin.2012.07.011
24. Romano V, Pasquale V, Krovacek K, Mauri F, Demarta A, Dumontet S. Toxigenic *Clostridium difficile* PCR ribotypes from wastewater treatment plants in southern Switzerland. Appl Environ Microbiol. 2012;78:6643–6. https://doi.org/10.1128/AEM.01379-12

Address for correspondence: Sarah Tschudin-Sutter, MD, MSc; Division of Infectious Diseases and Hospital Epidemiology, University Hospital Basel, Petersgraben 4, CH-4031 Basel, Switzerland; email: sarah.tschudin@usb.ch

Effectiveness of 23-Valent Pneumococcal Polysaccharide Vaccine against Invasive Pneumococcal Disease in Adults, Japan, 2013–2017

Reiko Shimbashi, Motoi Suzuki, Bin Chang, Hiroshi Watanabe, Yoshinari Tanabe, Koji Kuronuma, Kengo Oshima, Takaya Maruyama, Hiroaki Takeda, Kei Kasahara, Jiro Fujita, Junichiro Nishi, Tetsuya Kubota, Keiko Tanaka-Taya, Tamano Matsui, Tomimasa Sunagawa, Kazunori Oishi, Adult IPD Study Group

The decline in the proportion of pneumococcal conjugate vaccine (PCV)–covered serotypes among adult invasive pneumococcal disease (IPD) patients might change the overall effectiveness of the 23-valent pneumococcal polysaccharide vaccine (PPSV23) because its effectiveness differs according to serotype. Using the indirect cohort method, we calculated the effectiveness of PPSV23 against IPD among adults in Japan to assess the impact of the national pediatric PCV program. Clinical and epidemiologic information and pneumococcal isolates were collected from IPD patients ≥20 years of age through enhanced IPD surveillance during April 2013–December 2017. Adjusted effectiveness against PPSV23-serotype IPD was 42.2%. Despite a substantial decline in the proportion of 13-valent PCV serotypes during the study period (45% to 31%), the change in effectiveness for PPSV23-serotype IPD was limited (47.1% to 39.3%) and only marginal in the elderly population (39.9% to 39.4%). The pediatric PCV program had limited impact on PPSV23 effectiveness against IPD in adults.

Streptococcus pneumoniae is a major cause of illness and death among adults (*1*). Pneumonia is the most common form of pneumococcal disease in adults, whereas invasive pneumococcal disease (IPD), including meningitis and bacteremia, has severe clinical manifestations with a high case-fatality ratio (*2*). Because incidence of adult IPD is high among older adults, it is a public health concern, particularly in countries with aging populations, such as Japan (*3*,*4*).

Two types of pneumococcal vaccines are currently available for adults: the 23-valent pneumococcal polysaccharide vaccine (PPSV23) and the 13-valent pneumococcal conjugate vaccine (PCV13). According to a systematic review, the effectiveness of PPSV23 against IPD among adults ≥50 years of age was 54% (*5*). The CAPITA trial showed that the efficacy of PCV13 against IPD among adults ≥65 years of age was 75% (*6*). Since 2014, both PPSV23 and PCV13 have been recommended for older persons in the United States (*7*), whereas only PPSV23 is recommended in other high-income countries.

Discussions over adult pneumococcal vaccination programs are complicated because of differences in vaccine effectiveness (VE) by serotype and age group. Previous studies have suggested that VE of PPSV23 differs by serotype (*8*,*9*), so overall VE might vary on the basis of the distribution of serotypes among the vaccinated population. In many countries, the proportion of PCV-covered serotypes among adult IPD patients has been decreasing since the introduction of pediatric PCVs (*10*–*13*); this

Author affiliations: National Institute of Infectious Diseases, Tokyo, Japan (R. Shimbashi, M. Suzuki, B. Chang, K. Tanaka-Taya, T. Matsui, T. Sunagawa, K. Oishi); Tohoku University Graduate School of Medicine, Miyagi, Japan (R. Shimbashi, M. Suzuki, K. Oshima); Kurume University School of Medicine, Fukuoka, Japan (H. Watanabe); Niigata Prefectural Shibata Hospital, Niigata, Japan (Y. Tanabe); Sapporo Medical University School of Medicine, Hokkaido, Japan (K. Kuronuma); National Hospital Organization Mie National Hospital, Mie, Japan (T. Maruyama); Yamagata Saisei Hospital, Yamagata, Japan (H. Takeda); Nara Medical University, Nara, Japan (K. Kasahara); Graduate School of Medicine, University of the Ryukyus, Okinawa, Japan (J. Fujita); Kagoshima University Graduate School of Medical and Dental Sciences, Kagoshima, Japan (J. Nishi); Kochi Medical School, Kochi University, Kochi, Japan (T. Kubota); Toyama Institute of Health, Toyama, Japan (K. Oishi)

DOI: https://doi.org/10.3201/eid2610.191531

decline might have changed the effectiveness of PPSV23 against PPSV23-serotype IPD. However, the effect of pediatric PCV programs on VE of PPSV23 among adults has not been fully established. In addition, a few studies have suggested that VE is lower among older adults, but evidence is limited (*9*,*14*).

In Japan, PCV7 was licensed in November 2010, included in the routine immunization program for children in April 2013, and replaced by PCV13 in October 2013; PPSV23 was included in the routine immunization program for adults ≥65 years of age in 2014. We conducted this study to investigate whether VE of PPSV23 against IPD among adults ≥20 years of age was affected by the pediatric PCV program. We assessed the change in the proportion of PCV-covered serotypes among adult IPD patients across the study period and that in overall VE. We also explored the differences in VE according to age group and other population characteristics.

Methods

Study Population

Under the revised Infectious Disease Control Law, national IPD surveillance was implemented in Japan in 2013. Since then, physicians have been required to report all IPD patients and their basic information to the nearest local public health centers. To collect more detailed clinical and epidemiologic information and *S. pneumoniae* isolates from adult IPD patients, in April 2013 the Adult IPD Study Group initiated enhanced surveillance covering 10 of the 47 prefectures of Japan (*15*). Details of the study design and methods have been described elsewhere (*15*,*16*). In brief, all IPD patients ≥15 years of age who had been identified in the local health centers were recruited for enhanced surveillance, and their clinical and epidemiologic information, including PPSV23 vaccination history, was collected by research collaborators by using a standardized case form. *S. pneumoniae* isolates and clinical specimens were collected from hospital laboratories or prefectural public health institutes and transferred to the National Institute of Infectious Diseases for further testing. A patient was defined as having IPD if the culture was positive for *S. pneumoniae* or if *S. pneumoniae*–specific DNA (*lytA* gene) was detected by PCR assay in samples collected from normally sterile sites, such as blood and cerebrospinal fluid. To investigate the effectiveness of PPSV23 among adults, we excluded IPD patients ≥15–19 years in this study. IPD patients ≥20 years of age who had been enrolled in the study during April 2013–December 2017 and whose clinical and epidemiologic information and microbiologic testing results were available were included in the analyses.

Microbiological Testing

S. pneumoniae isolates were serotyped by using the capsule Quellung reaction with rabbit antisera (Statens Serum Institute, https://en.ssi.dk) after culturing overnight. Clinical specimens were serotyped by using the multiplex serotyping PCR assay as described previously (*15*,*17*). Because the Quellung reaction could not distinguish between serotypes 11A and 11E, these serotypes were grouped into serogroup 11A/E and considered to be the PPSV23 serotype. Isolates that did not react with any antiserum were classified as nontypeable. One isolate per patient was included in our analysis.

Pneumococcal Vaccination Policy in Japan

In Japan, PPSV23 was included in the national immunization program in October 2014 for all persons ≥65 years of age and those 60–65 years of age with underlying diseases, such as heart disease, kidney disease, respiratory disease, and immunocompromised condition attributable to HIV infection. The cost of vaccination is partly subsidized by the local government. A national catch-up campaign targeting persons ≥65 years of age also was launched in 2014. For persons 2–59 years of age with high-risk conditions (e.g., a history of splenectomy), the cost of vaccination is covered by health insurance. According to an estimate by Japan's Ministry of Health, Labor, and Welfare, 33%–38% of persons ≥65 years of age were vaccinated with PPSV23 during 2014–2017 (*18*). In our study, PPSV23 vaccination status was obtained from medical records and confirmed by patients or their guardians. Patients were considered vaccinated only if they had received ≥1 dose of PPSV23 in the 5 years before the hospital visit.

PCV7 was approved for the voluntary vaccination of children in February 2010, included in the routine immunization program for children in April 2013, and replaced with PCV13 in November 2013. The coverage rate of the third dose of PCV13 among children was 98% in 2017 (*18*). PCV13 was approved for adults ≥65 years of age in June 2014, but its coverage rate among this age group remains very low (<1%). In our study, only 4 of 1,121 patients reported having been vaccinated with PCV13.

Procedures

VE of PPSV23 against IPD was calculated by using an indirect cohort method (Broome's method). The indirect cohort method is a case-control design and has been used to estimate VE of pneumococcal vaccines by

using pneumococcal disease surveillance data (*9*,*19*). In our study, a case was defined as illness in a patient with IPD caused by a PPSV23 serotype (PPSV23-serotype IPD), including serotypes 1, 2, 3, 4, 5, 6B, 7F, 8, 9N, 9V, 10A, 11A, 12F, 14, 15B, 17F, 18C, 19A, 19F, 20, 22F, 23F, and 33F; a control was defined as a patient with IPD caused by a non-PPSV23 serotypes. For the serotype-specific VE estimates, a case was defined as illness in patients with IPD caused by a specific serotype, and a control was defined as a patient with IPD caused by a non-PPSV23 serotype. We compared the odds of PPSV23 vaccination history in cases and controls and calculated VE as (1 – odds ratio) × 100%.

The patients were classified into 4 age groups: 20–39, 40–64, 65–79, and 80 years of age. Patients were considered to have immunocompromised conditions if they had any of the following conditions: a history of splenectomy, transplantation, asplenia or hyposplenia, HIV infection, malignancy, autoimmune disease, and complement deficiency (*20*,*21*). The patients' body mass index (BMI) values were grouped as low (<18.5 kg/m^2), normal (18.5–24.9 kg/m^2), and high (≥25 kg/m^2). Clinical manifestations in IPD patients were classified as pneumonia, meningitis, bacteremia, and other conditions according to the physicians' report. Because the IPD incidence is higher in the autumn and winter seasons compared with other seasons (*22*), we defined a high season (epidemiologic weeks 1–22 and 49–52) and a low season (epidemiologic weeks 23–48). To assess the effect of the pediatric PCV program, we divided the study period into 2 phases according to the year of diagnosis: the first phase (2013–2015) and the second phase (2016–2017).

Statistical Analyses

The characteristics of cases and controls were compared by using the χ^2 test or Fisher exact test, as appropriate. We used logistic regression models to estimate VE. Because sex, age, study site, year of diagnosis, season, BMI group, presence of an underlying condition, and smoking status were deemed to be potential confounders on the basis of prior knowledge (*9*), all factors were included in the final multiple logistic regression models. CIs were adjusted for clustering at the local health center level by using robust SEs.

We estimated VE of IPD for PPSV23 serotypes, PCV13 serotypes excluding 6A (PCV13 non–6A serotype), including serotypes 1, 3, 4, 5, 6B, 7F, 9V, 14, 18C, 19A, 19F, and 23F, and PPSV23 serotypes excluding PCV13 serotypes (PPSV23 non–PCV13 serotypes). The serotype-specific VE was estimated for each serotype if its number of isolates was >30. To explore the potential effect of cross-immunity produced by PPSV23 on serogroup 6, VE of IPD for serotypes 6A, 6B, 6C, and 6D was calculated excluding these serotypes from the controls. VE was stratified by the 2 study phases (2013–2015 and 2016–2017). We also conducted stratified analyses to investigate the potential effect of modifications by sex, age group (persons <65 years of age and those ≥65 years of age), the presence of underlying conditions, BMI group, and clinical manifestations. The stratum-specific estimates of VE were compared by using a Wald test (test for interaction).

PPSV23 vaccination history was not documented for 23% of our patients. This group was coded as no record and included in our primary analyses. In a sensitivity analysis, this group was considered to have missing data, and multiple imputations were performed. All analyses were performed by using Stata version 15 (StataCorp, https://www.stata.com).

Ethics

This study was approved by the Ethics Committee of the National Institute of Infectious Diseases (approval no. 707) and conducted according to the principles expressed in the Declaration of Helsinki. The requirement for obtaining informed consent from all participants was waived because the data do not contain any patient identifiers, and samples were taken as part of standard patient care.

Results

During the study period (April 2013–December 2017), a total of 1,824 IPD patients ≥20 years of age were identified through the national IPD surveillance program in the study prefectures (*24*). Among them, 1,138 patients were enrolled in the study (Appendix Figure, https://wwwnc.cdc.gov/EID/article/26/10/19-1531-App1.pdf). *S. pneumoniae* isolates or clinical specimens were not available for 15 patients, and clinical and epidemiologic data were not available for an additional 2 patients. After excluding these patients, 1,121 patients were eligible for our analyses. *S. pneumoniae* was identified in 1,117 patients (99.6%), and *S. pneumoniae*–specific DNA was detected in 4 patients (0.4%).

The characteristics of the 1,121 IPD patients are summarized in Table 1. A total of 679 (61%) patients were men, and the median age was 70 years (range 22–103 years). Among all IPD patients, 746 (66.5%) were classified as having PPSV23-serotype IPD and 375 (33.5%) were classified as having non–PPSV23-serotype IPD. PPSV23-serotype IPD patients less frequently had immunocompromised conditions and more frequently had pneumonia compared with non–PPSV23-serotype IPD patients; otherwise, characteristics were similar between the 2 groups.

Table 1. Characteristics of 1,121 invasive pneumococcal disease patients with and without PPSV23 serotype, Japan, 2013–2017*

Characteristic	Total	PPSV23 serotype, n = 746	Non-PPSV23 serotype, n = 375	p value
Sex				
M	679 (61)	443 (59)	236 (63)	0.251
F	442 (39)	303 (41)	139 (37)	
Age group, y				
20–39	55 (5)	34 (5)	21 (6)	0.437
40–64	309 (28)	211 (28)	98 (26)	
65–79	427 (38)	291 (39)	136 (36)	
≥80	330 (29)	210 (28)	120 (32	
Study site, prefecture				
Hokkaido	138 (12)	85 (11)	53 (14)	0.612
Miyagi	133 (12)	92 (12)	41 (11)	
Yamagata	95 (8)	69 (9)	26 (7)	
Niigata	211 (19)	144 (19)	67 (18)	
Mie	113 (10)	78 (10)	35 (9)	
Nara	80 (7)	51 (7)	29 (8)	
Kochi	38 (3)	27 (4)	11 (3)	
Fukuoka	222 (20)	146 (20)	76 (20)	
Kagoshima	45 (4)	28 (4)	17 (5)	
Okinawa	46 (4)	26 (3)	20 (5)	
Year				
2013	45 (4)	33 (4)	12 (3)	0.602
2014	201 (18)	134 (18)	67 (18)	
2015	213 (19)	146 (20)	67 (18)	
2016	286 (26)	180 (24)	106 (28)	
2017	363 (32)	243 (33)	120 (32)	
Unknown	13 (1)	10 (1)	3 (1)	
Season†				
High season	722 (64)	492 (66)	230 (61)	0.152
Low season	385 (34)	243 (33)	142 (38)	
Unknown	14 (1)	11 (1)	3 (1)	
BMI group, kg/m^2				
<18.5	257 (23)	171 (23)	86 (23)	0.895
18.5–24.9	526 (47)	346 (46)	180 (48)	
≥25	167 (15)	111 (15)	56 (15)	
Unknown	171 (15)	118 (16)	53 (14)	
Underlying conditions				
Immunocompromised conditions	314 (28)	175 (23)	139 (37)	<0.001
Other conditions	479 (43)	324 (43)	155 (41)	
Without underlying conditions	256 (23)	198 (27)	58 (15)	
Unknown	72 (6)	49 (7)	23 (6)	
Smoking history				
Yes	390 (35)	265 (36)	125 (33)	0.709
No	559 (50)	370 (50)	189 (50)	
Unknown	172 (15)	111 (15)	61 (16)	
Alcohol intake				
Yes	184 (16)	121 (16)	63 (17)	0.439
No	750 (67)	493 (66)	257 (69)	
Unknown	187 (17)	132 (18)	55 (15)	
Clinical manifestations				
Pneumonia	665 (59)	480 (64)	185 (49)	<0.001
Meningitis	169 (15)	94 (13)	75 (20)	
Bacteremia	188 (17)	104 (14)	84 (22)	
Other‡	98 (9)	68 (9)	30 (8)	
Unknown	1 (0)	0 (0)	1 (0)	
Fatal outcome				
Yes	204 (18)	137 (18)	67 (18)	0.838
No	917 (82)	609 (82)	308 (82)	
PPSV23 vaccination within 5 y				
Yes	103 (9)	58 (8)	45 (12)	<0.001
No	765 (68)	539 (72)	226 (60)	
Unknown	253 (23)	149 (20)	104 (28)	

*Values are no. (%) unless indicated. BMI, body mass index; EW, epidemiologic week; PPSV23, 23-valent pneumococcal polysaccharide vaccine.
†High season indicates the period from EW 1 to EW 22 and from EW 49 to EW 52, whereas low season indicates the period from EW 23 to EW 48.
‡Includes arthritis, endocarditis, sinusitis, otitis media, vertebritis, cholecystitis, aortic aneurysm, and pleurisy.

After we controlled for confounders, VE against PPSV23-serotype IPD was 42.2% (95% CI 13.4 to 61.4) (Table 2). VE against PCV13 non–6A-serotype IPD was 35.3% (95% CI –8.4% to 61.5%) and that against PPSV23 non–PCV13-serotype IPD was 44.5% (95% CI 9.6% to 65.9%). Sensitivity analyses showed similar VE estimates (Appendix Table 1). A high level of effectiveness was observed for serotypes 19A (70.3% [95% CI 13.3% to 89.8%]), 12F (70.8% [95% CI 1.0% to 91.4%]), and 10A (73.6% [95% CI 5.9% to 92.6%]). Low-to-moderate effectiveness was observed for serotypes 3 (34.1% [95% CI –34.4% to 67.7%]), 22F (22.7% [95% CI –88.8% to 68.4%]), 11A/E (20.7% [95% CI –145.4% to 74.4%]), and 7F (22.4% [95% CI –176.8% to 78.2%]); however, their CIs were wide because of the limited sample size.

The trend in the proportion of vaccine-covered serotypes among adult IPD patients during the study period is shown in the Figure. The proportion of PCV13 serotypes was 45% in the first phase of the study (2013–2015) and 31% in the second phase (2016–2017). When we stratified the patients by age group, the decline was 24% (41% in the first phase and 17% in the second phase) among patients 20–64 years of age and 10% (47% in the first phase and 37% in the second phase) among those ≥65 years of age.

VE against PPSV23-serotype IPD among persons ≥20 years of age in the first phase was 47.1% (95% CI –4.7% to 73.3%) and in the second phase was 39.3% (95% CI –2.9% to 64.2%) (p = 0.953 by test for interaction) (Table 3). When we focused on persons ≥65 years of age, VE point estimates in the 2 phases showed almost identical values (39.9% in the first phase and 39.4% in the second; p = 0.809). For persons 20–64 years of age, VE point estimates showed a decreasing trend (77.1%in the first phase and 41.0% in the second; p = 0.124); however, the CIs were wide.

Our subgroup analyses showed that VE against PPSV23-serotype IPD was 59.0% (95% CI 17.9% to 79.6%) among persons 20–64 years of age and 39.2% (95% CI 2.0% to 62.2%) among those ≥65 years of age, but this difference was not statistically significant level (p = 0.17 by test for interaction) (Table 4). When we stratified the age group further, VE was 44.6% (95% CI –14.5% to 73.2%) among persons 65–79 years of age and 31.3% (95% CI –47.7% to 68.1%) among those ≥80 years of age. Higher VE was observed in persons with a normal BMI (70.6% [95% CI 47.7% to 83.5%]) than in those with a low BMI (7.4% [95% CI –108.1% to 58.8%]) or a high BMI (–136.5% [95% CI –826.6% to 39.6%]). VE did not differ by patients' underlying diseases. Among persons ≥65 years of age, VE for IPD with pneumonia was 52.8% (95% CI 16.5% to 73.3%) and for IPD without pneumonia was 9.8% (95% CI –134.4% to 65.3%) (Appendix Table 2). Among persons 20–64 years of age, VE for IPD with pneumonia was 23.0% (95% CI –272.2% to 84.1%) and for IPD without pneumonia was 88.8% (95% CI –12.0% to 98.9%).

Discussion

VE of PPSV23 against PPSV23-serotype IPD was 42.2% among adults ≥20 years of age in Japan. VE against PCV13 non–6A-serotype IPD and that against PPSV23 non–PCV13-serotype IPD were almost comparable. Despite an observed reduction in the proportion of PCV13 serotypes among adult IPD patients during the study period, the change in VE against PPSV23-serotype IPD was limited among adults ≥20 years of age and only marginal among those ≥65 years of age.

Large declines in the incidence of adult pneumococcal disease caused by PCV serotypes have been reported in many countries because of the indirect effect of pediatric PCVs (*10*,*25*–*27*). A pooled analysis of 10 countries in Europe demonstrated that during 2009–2015, incidence of PCV7-serotype IPD among adults ≥65 years of age declined by 77% and incidence of PCV13 non–PCV7-serotype IPD among the same age group declined 38% (*26*). The indirect effect of pediatric PCVs is particularly important when making adult pneumococcal vaccination policies because it might affect

Table 2. Overall and serotype-specific effectiveness of PPSV23 against invasive pneumococcal disease in adults ≥20 years of age, Japan, 2013–2017*

Serotype	No. cases	No. controls	Crude VE, % (95% CI)	Adjusted VE,† % (95% CI)
PPSV23 serotype	746	375	46.0 (17.8 to 64.5)	42.2 (13.4 to 61.4)
PCV13, non–6A serotype	392	375	40.6 (3.8 to 63.3)	35.3 (–8.4 to 61.5)
PPSV23, non–PCV13 serotype	354	375	51.7 (18.7 to 71.3)	44.5 (9.6 to 65.9)
Serotype 3	152	375	43.1 (–11.9 to 71.1)	34.1 (–34.4 to 67.7)
Serotype 19A	111	375	72.7 (29.1 to 89.5)	70.3 (13.3 to 89.8)
Serotype 12F	99	375	80.2 (34.4 to 94.0)	70.8 (1.0 to 91.4)
Serotype 22F	83	375	34.1 (–47.1 to 70.5)	22.7 (–88.8 to 68.4)
Serotype 10A	80	375	75.7 (19.2 to 92.7)	73.6 (5.9 to 92.6)
Serotype 11A/E	41	375	30.7 (–106.7 to 76.8)	20.7 (–145.4 to 74.4)
Serotype 7F	30	375	31.5 (–138.6 to 80.3)	22.4 (–176.8 to 78.2)

*BMI, body mass index; PCV13, 13-valent pneumococcal conjugate vaccine; PPSV23, 23-valent pneumococcal polysaccharide vaccine; VE, vaccine effectiveness.
†Adjusted for sex, age, prefecture, year, season, BMI group, underlying conditions, and smoking history with clustering by public health center.

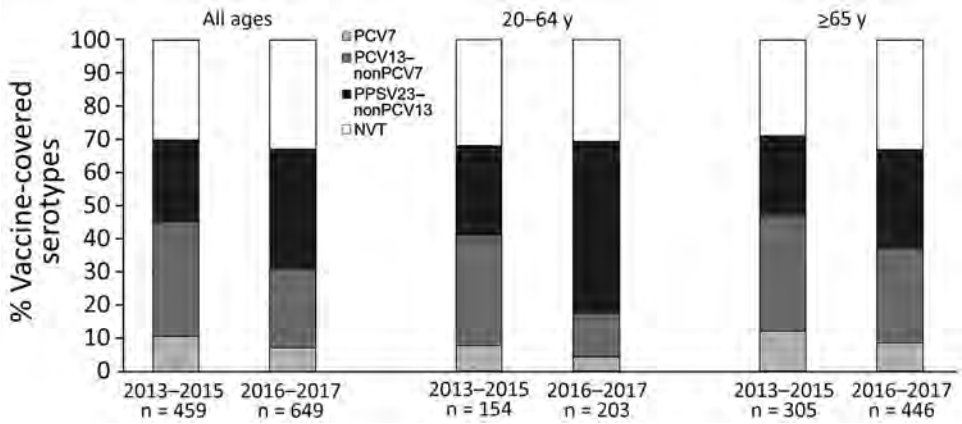

Figure. Percentage of vaccine-covered serotypes among pneumococcal isolates from 1,108 invasive pneumococcal disease patients ≥20 years of age, stratified by year and age group, Japan, 2013–2017. NVT, non–vaccine type; PCV7, 7-valent pneumococcal conjugate vaccine; PCV13, 13-valent pneumococcal conjugate vaccine; PPSV23, 23-valent pneumococcal polysaccharide vaccine.

the effectiveness and population impact of adult vaccines. In our study, the proportion of PCV13 serotypes among adult IPD patients decreased from 45% to 31%, whereas the proportion of PPSV23 non–PCV13 serotypes increased from 25% to 36%. Because the effectiveness of pneumococcal vaccines is known to differ by serotype, this change in the serotype distribution might have changed overall PPSV23 effectiveness. However, in our study, VE values against PCV13 non–6A-serotype IPD (35.3% [95% CI –8.4% to 61.5%]) and PPSV23 non–PCV13-serotype IPD (44.5% [95% CI 9.6% to 65.9%]) did not differ substantially. Consequently, the change in VE point estimates among adults ≥20 years of age was limited during the study period (47.1% in the first phase and 39.3% in the second), and no change was observed among those ≥65 years of age (39.9% in the first phase and 39.4% in the second). Our findings suggest that VE of PPSV23 among adults in Japan is moderate and remained constant during the 4-year study period under the impact of pediatric PCV13.

In the current study, VE values against IPD varied by serotype; high VE was observed against serotypes 19A, 12F, and 10A, and low-to-moderate VE was observed against serotypes 3, 22F, 11A/E, and 7F. Serotype 3 was the leading serotype observed in our patients, as has been the case in other countries (*28*). Studies have shown that the efficacy of pneumococcal vaccines against serotype 3 is limited (*28*). The observed low-to-moderate VE in our study (34.1% [95% CI -34.4% to 67.7%]) was consistent with previous studies (*8*,*9*,*29*). Recently, we reported the emergence of serotype 12F among adult IPD patients in Japan (*16*), and that serotype was the third leading serotype (9%) identified in our patients. Increases in incidence of serotype 12F have been observed in other countries after the introduction of pediatric PCVs (*30*,*31*). Studies have suggested that this serotype is associated with outbreaks and a high invasiveness potential (*32*–*34*). The high VE against serotype 12F (70.8% [95% CI 1.0% to 91.4%]) observed in our study suggests that PPSV23 vaccination is an effective measure to reduce its impact.

When we stratified the patients by age group, VE was 59% (95% CI 17.9% to 79.6%) for persons 20–64 years of age and 39.2% (95% CI 2% to 62.2%) for those ≥65 years of age; however, this difference was not statistically significant (p = 0.17 by test for interaction). A declining trend in PPSV23 effectiveness with age has been reported previously (*9*,*14*). A study conducted in Spain showed that VE against IPD was 54.2% in adults 60–69 years of age, 54.1% in adults 70–79 years of age, and 25.5% in adults ≥80 years of age (*9*). These observations might be explained by the decline in pneumococcal polysaccharide immunity with increasing age (*35*). We found that VE was lower among persons with a low or high BMI than among those with a normal BMI (p = 0.005 by test for interaction). Malnutrition, including undernutrition and overnutrition, is known to be associated with immune

Table 3. Effectiveness of PPSV23 against invasive pneumococcal disease in adults >20 years of age, by age group and study period, Japan, 2013–2017*

	Adjusted VE,† % (95% CI)		
Age group, y	2013–2015	2016–2017	p value by test for interaction
Overall	47.1 (–4.7 to 73.3)	39.3 (–2.9 to 64.2)	0.953
20–64	77.1 (–110.4 to 97.5)	41.0 (–128.8 to 84.8)	0.124
≥65	39.9 (–28.4 to 71.9)	39.4 (–6.1 to 65.3)	0.809

*BMI, body mass index; PPSV23, 23-valent pneumococcal polysaccharide vaccine; VE, vaccine effectiveness.
†Adjusted for sex, age, prefecture, year, season, BMI group, underlying conditions, and smoking history with clustering by public health center.

Table 4. Stratified analyses of the effectiveness of PPSV23 against invasive pneumococcal disease in adults ≥20 years of age, Japan, 2013–2017*

Characteristic	No. cases	No. controls	Crude VE, % (95% CI)	Adjusted VE,† % (95% CI)	p value
Sex					
M	443	236	41.5 (2.0 to 65.0)	38.7 (−5.1 to 64.3)	0.917
F	303	139	52.7 (2.5 to 77.1)	48.5 (5.3 to 72.0)	
Age group, y					
20–64	245	119	72.5 (13.6 to 91.3)	59.0 (17.9 to 79.6)	0.170
≥65	501	256	41.7 (7.2 to 63.3)	39.2 (2.0 to 62.2)	
Clinical manifestations					
Pneumonia	480	185	55.8 (26.2 to 73.5)	50.6 (16.0 to 70.9)	0.284
Meningitis	94	75	46.9 (−76.6 to 84.1)	35.6 (−100.0 to 79.2)	
Bacteremia	104	84	41.8 (−78.2 to 81.0)	34.7 (−72.1 to 75.2)	
Other‡	68	30	NA	NA	
BMI group, kg/m^2					
<18.5	171	86	11.3 (−109.4 to 62.4)	7.4 (−108.1 to 58.8)	0.005
18.5–24.9	346	180	73.2 (50.8 to 85.4)	70.6 (47.7 to 83.5)	
≥25	111	56	−133.3 (−765.0 to 37.1)	−136.5 (−826.6 to 39.6)	
Underlying conditions					
Immunocompromised	175	139	41.0 (−22.0 to 71.4)	41.2 (−27.6 to 72.9)	0.971
Other condition	324	155	48.5 (7.2 to 71.4)	48.2 (6.0 to 71.5)	
No underlying condition	198	58	48.8 (−113.3 to 87.7)	51.5 (−116.0 to 89.1)	

*BMI, body mass index; NA, not available; PPSV23, 23-valent pneumococcal polysaccharide vaccine; VE, vaccine effectiveness.
†Adjusted for sex, age, prefecture, year, season, BMI group, underlying conditions, and smoking history with clustering by public health center.
‡Includes arthritis, endocarditis, sinusitis, otitis media, vertebritis, cholecystitis, aortic aneurysm, and pleurisy.

defects (*36*) and poor vaccine-induced immune responses (*37*). On the other hand, VE did not differ between persons with and without underlying conditions. A similar finding was observed in a previous study conducted in Japan; the effectiveness of PPSV23 against pneumococcal pneumonia among adults ≥65 years of age did not differ by their underlying condition status (*29*). These observations might be at least partially explained by the low prevalence of HIV infection in adults in Japan. Only 1 patient was recorded as being HIV-positive in our study.

VE for bacteremic pneumococcal pneumonia among persons ≥65 years of age was 52.8% (95% CI 16.5% to 73.3%), whereas among persons 20–64 years of age it was 23.0% (95% CI −272.2% to 84.1%) (p = 0.064 by test for interaction). Because pneumonia is the most common manifestation of pneumococcal disease among the elderly population (*15*), this finding might support the current PPSV23 recommendations. On the other hand, although the CI was wide, the VE point estimate for non–pneumonia-associated IPD, such as meningitis and occult bacteremia (i.e., bacteremia without an identifiable focus of infection), was high in the younger age group. The potential difference in PPSV23 effectiveness according to population characteristics and clinical manifestations is particularly important when creating efficient vaccination policies. Further studies are needed to understand the mechanisms underlying our observations.

In Japan, PPSV23 was introduced into the adult immunization program in 2014, but its vaccination coverage rate was only ≈30% in 2017. Recently, the Ministry of Health, Labor, and Welfare decided to extend the duration of the catch-up campaign for persons ≥65 years of age until 2023. The continued moderate PPSV23 effectiveness under the impact of the pediatric PCV13 program we observed provides supporting evidence for the current adult pneumococcal vaccination policy. However, making decisions regarding the adult PPSV23 program is still challenging for several reasons, such as its low level of efficacy in the older age group (*8*,*9*) and limited evidence supporting repeated vaccinations (*38*,*39*). Continuous monitoring of the serotype distribution and VE among adults is warranted. On the other hand, high VE among younger adults, particularly for meningitis and occult bacteremia, might facilitate a discussion regarding the potential expansion of the target age group.

Our study has limitations. First, 37.6% of the patients identified in the local health centers were not included in our study. The inclusion rate was especially low at the beginning of the study period; however, the baseline characteristics of the patients did not differ between the enrolled and nonenrolled patients (Appendix Table 3). The effect of selection bias on our VE estimates must have been minimal. Second, vaccination history was not documented in 23% of our patients. Our sensitivity analyses showed almost identical estimates, so we do not believe this shortcoming affects our observations. Third, we used the indirect cohort method, which is equivalent to the test-negative design, to estimate the PPSV23 effectiveness. Although this design is less susceptible to bias associated with confounding by healthcare-seeking behavior, as in the

nature of observational study design, the bias is unlikely to be eliminated (*40*,*41*). However, our VE estimates are comparable with previous estimates resulting from other study designs (*5*), so the effect of bias is probably minimal. Finally, only a history of PPSV23 vaccination within 5 years was available. Patients who had received the latest PPSV23 >5 years before diagnosis were classified as unvaccinated. If VE lasted >5 years, our VE estimates might have underestimated actual VEs. Also, our study could not assess the waning of effectiveness over the 5 years.

In conclusion, the effectiveness of PPSV23 against IPD is moderate among adults ≥20 years of age in Japan. Although the proportion of PCV13 serotypes among adult IPD patients has been substantially decreasing because of the indirect effect of the pediatric PCV program, the change in PPSV23 effectiveness was limited.

Acknowledgments

We sincerely thank the staff of the local public health centers who collected bacterial isolates and case report forms from the hospitals and the staff of the public health institutes and laboratories who worked for the Adult IPD Study Group (http://www.nih.go.jp/niid/ja/ibi.html).

This work was supported by MHLW HA Program Grant Number JPMH20HA1005.

About the Author

Dr. Shimbashi is a researcher on the field of vaccination at the National Institute of Infectious Diseases in Japan. Her primary research interests are vaccine effectiveness, vaccine adverse events, and vaccine communication strategies.

References

1. Peto L, Nadjm B, Horby P, Ngan TT, van Doorn R, Van Kinh N, et al. The bacterial aetiology of adult community-acquired pneumonia in Asia: a systematic review. Trans R Soc Trop Med Hyg. 2014;108:326–37. https://doi.org/10.1093/trstmh/tru058
2. Houseman C, Chapman KE, Manley P, Gorton R, Wilson D, Hughes GJ. Decreasing case fatality rate following invasive pneumococcal disease, North East England, 2006–2016. Epidemiol Infect. 2019;147:e175. https://doi.org/10.1017/S0950268819000657
3. Drijkoningen JJ, Rohde GG. Pneumococcal infection in adults: burden of disease. Clin Microbiol Infect. 2014;20 (Suppl 5):45–51. https://doi.org/10.1111/1469-0691.12461
4. Morimoto K, Suzuki M, Ishifuji T, Yaegashi M, Asoh N, Hamashige N, et al.; Adult Pneumonia Study Group-Japan (APSG-J). The burden and etiology of community-onset pneumonia in the aging Japanese population: a multicenter prospective study. PLoS One. 2015;10:e0122247. https://doi.org/10.1371/journal.pone.0122247
5. Kraicer-Melamed H, O'Donnell S, Quach C. The effectiveness of pneumococcal polysaccharide vaccine 23 (PPV23) in the general population of 50 years of age and older: A systematic review and meta-analysis. Vaccine. 2016;34:1540–50. https://doi.org/10.1016/j.vaccine.2016.02.024
6. Bonten MJ, Huijts SM, Bolkenbaas M, Webber C, Patterson S, Gault S, et al. Polysaccharide conjugate vaccine against pneumococcal pneumonia in adults. N Engl J Med. 2015;372:1114–25. https://doi.org/10.1056/NEJMoa1408544
7. Tomczyk S, Bennett NM, Stoecker C, Gierke R, Moore MR, Whitney CG, et al.; Centers for Disease Control and Prevention (CDC). Use of 13-valent pneumococcal conjugate vaccine and 23-valent pneumococcal polysaccharide vaccine among adults aged ≥65 years: recommendations of the Advisory Committee on Immunization Practices (ACIP). MMWR Morb Mortal Wkly Rep. 2014;63:822–5.
8. Andrews NJ, Waight PA, George RC, Slack MP, Miller E. Impact and effectiveness of 23-valent pneumococcal polysaccharide vaccine against invasive pneumococcal disease in the elderly in England and Wales. Vaccine. 2012;30:6802–8. https://doi.org/10.1016/j.vaccine.2012.09.019
9. Gutierrez Rodriguez MA, Ordobas Gavin MA, Garcia-Comas L, Sanz Moreno JC, Cordoba Deorador E, Lasheras Carbajo MD, et al. Effectiveness of 23-valent pneumococcal polysaccharide vaccine in adults aged 60 years and over in the Region of Madrid, Spain, 2008–2011. Euro Surveill. 2014;19:20922. https://doi.org/10.2807/1560-7917.ES2014.19.40.20922
10. Djennad A, Ramsay ME, Pebody R, Fry NK, Sheppard C, Ladhani SN, et al. Effectiveness of 23-valent polysaccharide pneumococcal vaccine and changes in invasive pneumococcal disease incidence from 2000 to 2017 in those aged 65 and over in England and Wales. EClinicalMedicine. 2019;6:42–50. https://doi.org/10.1016/j.eclinm.2018.12.007
11. Ubukata K, Takata M, Morozumi M, Chiba N, Wajima T, Hanada S, et al.; Invasive Pneumococcal Diseases Surveillance Study Group. Effects of pneumococcal conjugate vaccine on genotypic penicillin resistance and serotype changes, Japan, 2010–2017. Emerg Infect Dis. 2018;24:2010–20. https://doi.org/10.3201/eid2411.180326
12. Naucler P, Galanis I, Morfeldt E, Darenberg J, Örtqvist Å, Henriques-Normark B. Comparison of the impact of pneumococcal conjugate vaccine 10 or pneumococcal conjugate vaccine 13 on invasive pneumococcal disease in equivalent populations. Clin Infect Dis. 2017;65:1780–9. https://doi.org/10.1093/cid/cix685
13. Càmara J, Marimón JM, Cercenado E, Larrosa N, Quesada MD, Fontanals D, et al. Decrease of invasive pneumococcal disease (IPD) in adults after introduction of pneumococcal 13-valent conjugate vaccine in Spain. PLoS One. 2017;12:e0175224. https://doi.org/10.1371/journal.pone.0175224
14. Singleton RJ, Butler JC, Bulkow LR, Hurlburt D, O'Brien KL, Doan W, et al. Invasive pneumococcal disease epidemiology and effectiveness of 23-valent pneumococcal polysaccharide vaccine in Alaska native adults. Vaccine. 2007;25:2288–95. https://doi.org/10.1016/j.vaccine.2006.11.065
15. Fukusumi M, Chang B, Tanabe Y, Oshima K, Maruyama T, Watanabe H, et al.; Adult IPD Study Group. Invasive pneumococcal disease among adults in Japan, April 2013 to March 2015: disease characteristics and serotype distribution. BMC Infect Dis. 2017;17:2. https://doi.org/10.1186/s12879-016-2113-y
16. Shimbashi R, Chang B, Tanabe Y, Takeda H, Watanabe H, Kubota T, et al.; Adult IPD Study Group. Epidemiological and clinical features of invasive pneumococcal disease caused by serotype 12F in adults, Japan. PLoS One. 2019;14:e0212418. https://doi.org/10.1371/journal.pone.0212418

17. da Gloria Carvalho M, Pimenta FC, Jackson D, Roundtree A, Ahmad Y, Millar EV, et al. Revisiting pneumococcal carriage by use of broth enrichment and PCR techniques for enhanced detection of carriage and serotypes. J Clin Microbiol. 2010;48:1611–8. https://doi.org/10.1128/JCM.02243-09
18. Ministry of Health, Labor, and Welfare. The vaccine coverage in routine immunization program in Japan from 1995 to 2017 [cited 2019 Aug 10]. https://www.mhlw.go.jp/topics/bcg/other/5.html
19. Broome CV, Facklam RR, Fraser DW. Pneumococcal disease after pneumococcal vaccination: an alternative method to estimate the efficacy of pneumococcal vaccine. N Engl J Med. 1980;303:549–52. https://doi.org/10.1056/NEJM198009043031003
20. Dominguez A, Salleras L, Fedson DS, Izquierdo C, Ruiz L, Ciruela P, et al. Effectiveness of pneumococcal vaccination for elderly people in Catalonia, Spain: a case-control study. Clin Infect Dis. 2005;40:1250–7. https://doi.org/10.1086/429236
21. Jackson LA, Neuzil KM, Yu O, Benson P, Barlow WE, Adams AL, et al.; Vaccine Safety Datalink. Effectiveness of pneumococcal polysaccharide vaccine in older adults. N Engl J Med. 2003;348:1747–55. https://doi.org/10.1056/NEJMoa022678
22. Weinberger DM, Grant LR, Steiner CA, Weatherholtz R, Santosham M, Viboud C, et al. Seasonal drivers of pneumococcal disease incidence: impact of bacterial carriage and viral activity. Clin Infect Dis. 2014;58:188–94. https://doi.org/10.1093/cid/cit721
23. Kim HW, Lee S, Kim KH. Serotype 6B from a pneumococcal polysaccharide vaccine induces cross-functional antibody responses in adults to serotypes 6A, 6C, and 6D. Medicine (Baltimore). 2016;95:e4854. https://doi.org/10.1097/MD.0000000000004854
24. Infectious Disease Surveillance Center, National Institute of Infectious Diseases. The number of weekly reports of the notifiable diseases [cited 2019 Aug 10]. https://www.niid.go.jp/niid/ja/idwr.html
25. Mackenzie GA, Hill PC, Jeffries DJ, Hossain I, Uchendu U, Ameh D, et al. Effect of the introduction of pneumococcal conjugate vaccination on invasive pneumococcal disease in The Gambia: a population-based surveillance study. Lancet Infect Dis. 2016;16:703–11. https://doi.org/10.1016/S1473-3099(16)00054-2
26. Hanquet G, Krizova P, Valentiner-Branth P, Ladhani SN, Nuorti JP, Lepoutre A, et al.; SpIDnet/I-MOVE+ Pneumo Group. Effect of childhood pneumococcal conjugate vaccination on invasive disease in older adults of 10 European countries: implications for adult vaccination. Thorax. 2019;74:473–82. https://doi.org/10.1136/thoraxjnl-2018-211767
27. Moore MR, Link-Gelles R, Schaffner W, Lynfield R, Lexau C, Bennett NM, et al. Effect of use of 13-valent pneumococcal conjugate vaccine in children on invasive pneumococcal disease in children and adults in the USA: analysis of multisite, population-based surveillance. Lancet Infect Dis. 2015;15:301–9. https://doi.org/10.1016/S1473-3099(14)71081-3
28. Linley E, Bell A, Gritzfeld JF, Borrow R. Should pneumococcal serotype 3 be included in serotype-specific immunoassays? Vaccines (Basel). 2019;7:E4. https://doi.org/10.3390/vaccines7010004
29. Suzuki M, Dhoubhadel BG, Ishifuji T, Yasunami M, Yaegashi M, Asoh N, et al.; Adult Pneumonia Study Group-Japan (APSG-J). Serotype-specific effectiveness of 23-valent pneumococcal polysaccharide vaccine against pneumococcal pneumonia in adults aged 65 years or older: a multicentre, prospective, test-negative design study. Lancet Infect Dis. 2017;17:313–21. https://doi.org/10.1016/S1473-3099(17)30049-X
30. Slotved HC, Dalby T, Hoffmann S. The effect of pneumococcal conjugate vaccines on the incidence of invasive pneumococcal disease caused by ten non-vaccine serotypes in Denmark. Vaccine. 2016;34:769–74. https://doi.org/10.1016/j.vaccine.2015.12.056
31. Rokney A, Ben-Shimol S, Korenman Z, Porat N, Gorodnitzky Z, Givon-Lavi N, et al. Emergence of *Streptococcus pneumoniae* serotype 12F after sequential introduction of 7- and 13-valent vaccines, Israel. Emerg Infect Dis. 2018;24:453–61. https://doi.org/10.3201/eid2403.170769
32. Hoge CW, Reichler MR, Dominguez EA, Bremer JC, Mastro TD, Hendricks KA, et al. An epidemic of pneumococcal disease in an overcrowded, inadequately ventilated jail. N Engl J Med. 1994;331:643–8. https://doi.org/ 10.1056/NEJM199409083311004
33. Sandgren A, Sjostrom K, Olsson-Liljequist B, Christensson B, Samuelsson A, Kronvall G, et al. Effect of clonal and serotype-specific properties on the invasive capacity of *Streptococcus pneumoniae*. J Infect Dis. 2004;189:785–96. https://doi.org/10.1086/381686
34. Schillberg E, Isaac M, Deng X, Peirano G, Wylie JL, Van Caeseele P, et al. Outbreak of invasive *Streptococcus pneumoniae* serotype 12F among a marginalized inner-city population in Winnipeg, Canada, 2009-2011. Clin Infect Dis. 2014;59:651–7. https://doi.org/10.1093/cid/ciu366
35. Adler H, Ferreira DM, Gordon SB, Rylance J. Pneumococcal capsular polysaccharide immunity in the elderly. Clin Vaccine Immunol. 2017;24:e00004–00017. https://doi.org/10.1128/CVI.00004-17
36. Bourke CD, Berkley JA, Prendergast AJ. Immune dysfunction as a cause and consequence of malnutrition. Trends Immunol. 2016;37:386–98. https://doi.org/10.1016/j.it.2016.04.003
37. Painter SD, Ovsyannikova IG, Poland GA. The weight of obesity on the human immune response to vaccination. Vaccine. 2015;33:4422–9. https://doi.org/10.1016/j.vaccine.2015.06.101
38. Kawakami K, Kishino H, Kanazu S, Takahashi K, Iino T, Sawata M, et al. Time interval of revaccination with 23-valent pneumococcal polysaccharide vaccine more than 5 years does not affect the immunogenicity and safety in the Japanese elderly. Hum Vaccin Immunother. 2018;14:1931–8. https://doi.org/10.1080/21645515.2018.1456611
39. Clutterbuck EA, Lazarus R, Yu LM, Bowman J, Bateman EA, Diggle L, et al. Pneumococcal conjugate and plain polysaccharide vaccines have divergent effects on antigen-specific B cells. J Infect Dis. 2012;205:1408–16. https://doi.org/10.1093/infdis/jis212
40. Sullivan SG, Tchetgen Tchetgen EJ, Cowling BJ. Theoretical basis of the test-negative study design for assessment of influenza vaccine effectiveness. Am J Epidemiol. 2016;184:345–53. https://doi.org/10.1093/aje/kww064
41. Omori R, Cowling BJ, Nishiura H. How is vaccine effectiveness scaled by the transmission dynamics of interacting pathogen strains with cross-protective immunity? PLoS One. 2012;7:e50751. https://doi.org/10.1371/journal.pone.0050751

Address for correspondence: Motoi Suzuki, Infectious Disease Surveillance Center, National Institute of Infectious Diseases, 1-23-1 Toyama, Shinjuku, Tokyo 162-8640, Japan; email: mosuzuki@niid.go.jp

Sequential Acquisition of Human Papillomavirus Infection at Genital and Anal Sites, Liuzhou, China

Feixue Wei,[1] Yingying Su,[1] Xuelian Cui, Xiaojuan Yu, Yafei Li, Qiaoqiao Song, Kai Yin, Shoujie Huang, Mingqiang Li, Jun Zhang, Ting Wu, Ningshao Xia

Little is known about the risk for acquiring a concordant human papillomavirus (HPV) infection in a genital (or anal) site after an anal (or genital) HPV infection. We collected 3 sets of anogenital specimens at 6-month intervals from 2,309 men and 2,378 women in Liuzhou, China, and tested these specimens for HPV. The risk for sequential anal HPV infection in participants with a previous genital HPV infection was higher than for participants without an infection (hazard ratio [HR] 4.4, 95% CI 3.4–5.8 for women and HR 2.6, 95% CI 1.4–4.6 for men). For sequential genital HPV infection, women with a previous anal infection had a higher risk (HR 1.9, 95% CI 1.2–3.1), but no major difference was found for men (HR 0.7, 95% CI 0.2–1.9). Our study indicates that autoinoculation might play a major role in anogenital HPV transmission, in addition to direct sexual intercourse, especially for anal infection in women.

Oncogenic human papillomavirus (HPV) infection can cause cancers at the anogenital site (*1*–*3*). Globally, HPV-attributable anogenital cancers include ≈570,000 cervical, 8,500 vulvar, 12,000 vaginal, 13,000 penile, and 35,000 anal cases (*4*,*5*). Although HPV spreads mainly through sexual contact, a study conducted among men who have sex with women (MSW) estimated an anal HPV infection prevalence of 12.2% (*6*). Another cohort study in Hawaii, USA, observed that women with no receptive anal sex still had anal HPV infections (*7*). These facts imply that other modes of transmission, independent of penile–anal penetration, are possible for acquiring anal HPV infections. Recently, Lin et al. (*8*) conducted a collaborative pooled analysis in paired cervical and anal samples and found a strong association between the presence of high-risk HPV (HR-HPV) at these 2 sites at the type-specific level, suggesting having the same source of infection either from the same sexual partner, autoinoculation within different anogenital sites, or both.

Two studies have assessed the risk for sequential HPV infection with a concordant genotype of an anatomic site, followed by infection at another site, and showed that autoinoculation might be a way to transmit HPV infection. One study focused on women in Hawaii and observed that the hazard ratios (HRs) for cervical-to-anal HPV infection was 20.5 (95% CI 16.3–25.7) and the HR for anal-to-cervical HPV infection was 8.33 (95% CI 6.36–12.20) (*9*). The other study focused on MSW in the United States, Brazil, and Mexico (HIM study) and reported that the HR of infection with any of the 9-valent vaccine–related types from the genital-to-anal site was 2.80 (95% CI 1.32–5.99) (*10*). However, both studies were conducted in relatively sexually active persons (e.g., 45.2% of women in Hawaii had >7 lifetime sexual partners [*7*] and 42.4% of MSW in the HIM study had >9 lifetime sexual partners [*10*)]). Whether the autoinoculation risk between genital and anal sites is similarly high in persons with relatively conservative sexual attitudes remains unknown. Furthermore, the contribution of autoinoculation for HPV infection at different anogenital sites of different sexes remains to be deeply explored.

In this study, we enrolled men and women from the general population in Liuzhou, China, of which 56% of the participants had only 1 lifetime sexual partner (*11*). The purpose of this study was to assess the risk for sequential type-specific and grouped HPV infection of genital and anal sites.

Author affiliations: Xiamen University School of Public Health, Xiamen, China (F. Wei, Y. Su, X. Yu, Y. Li, Q. Song, S. Huang, J. Zhang, T. Wu, N. Xia); Liuzhou Center for Disease Control and Prevention, Liuzhou, China (X. Cui, K. Yin, M. Li)

DOI: https://doi.org/10.3201/eid2610.191646

[1]These authors contributed equally to this article.

Methods

Study Population

During May 2014–July 2016, we conducted an observational cohort study to evaluate the natural history of genital and anal HPV infections among the general population in Liuzhou, China (*12*). Men and women who were 18–55 years of age, sexually active before enrollment, had never had an HPV vaccination, and had no plan to relocate in the next year were recruited by posters, flyers, and television advertisements. Women who were pregnant were excluded from the study (*13*). Written informed consent was obtained from each participant, and the protocol was approved by the Ethics Committee of the Liuzhou Center for Disease Control and Prevention.

Genital and Anal HPV DNA Samples

At the enrollment visit, each participant was individually interviewed by a trained interviewer by using a questionnaire to collect baseline information on characteristics and hygienic and sexual behaviors. For women, 2 iCleanhcy-flocked swabs (Huachenyang Corporation, https://www.hcymedical.com) were independently used to collect exfoliated vaginal and vulvar samples. For men, a combined specimen from the penis, glans penis, coronary sulcus, and prepuce (if available) was collected by using a prewetted swab. For both sexes, a prewetted swab was used to sweep 360° around the perianal area and was then inserted ≈1.5–2.0 cm into the anal canal and rotated 360° to obtain exfoliated cells (*11*,*14*). Anogenital samples were obtained by using the same methods twice more, 6 and 12 months after enrollment.

The HPV DNA of each specimen was extracted and amplified by using the GP5+/6+ primer system. HPV genotyping was performed by using MeltPro (Zeesan Biotech Co., http://www.zeesandx.com) to test 16 different types, including 13 HR-HPV types (HPV-16, -18, -31, -33, -35, -39, -45, -51, -52, -56, -58, -59, and -68) and 3 low-risk types (HPV-6, -11, and -66). For all samples, we also tested for glyceraldehyde-3-phosphate dehydrogenase to assess the adequacy of the samples. Only glyceraldehyde-3-phosphate dehydrogenase–positive or HPV DNA–positive samples were deemed effective samples. We combined the results of vaginal and vulvar samples to represent the status of female genital HPV infection, and positive results for either vaginal or vulvar samples were defined as genital positive.

Statistical Analysis

We selected participants in the following 4 sets to analyze the risk for sequential genital or anal HPV infections in persons with or without a previous same-type HPV infection at the other site (Figure 1): 1) set A, genital HPV positive and anal negative at the previous visit and having ≥1 effective follow-up visit for the anal site; 2) set B, both genital and anal HPV negative at the previous visit and having ≥1 effective follow-up visit for the anal site; 3) set C, anal HPV positive and genital HPV negative at the previous visit and having ≥1 effective follow-up visit for the genital site; 4) set D, both anal and genital HPV negative at the previous visit and having ≥1 effective follow-up visit for the genital site. For each type-specific and grouped HPV type, different participants were included in the 4 sets. Persons who were in any of these sets were finally included in the analytic set of this study. Baseline characteristics of men and women included and not included in the analytic set were compared by using χ^2 tests.

Incidence rates and 95% CIs for sequential anal HPV infection were assessed by analyzing data from set A and set B. We then calculated HRs and 95% CIs for HPV types by comparing the incidence rates between those with previous genital infections (set A) and those without previous genital infections (set B) by using Cox regression models. Similarly, we also examined the risk for sequential HPV infection in the genital site among participants with or without previous anal infection by using data for set C and set D. Incidence rates and HRs of grouped HPV (HPV-6/11; HPV-16/18; 9V-HPV: 9-valent vaccine-related HPV types, -6, -11, -16, -18, -31, -33, -45, -52, and -58; HR-HPV; and any HPV) infection were also assessed. The analysis unit for grouped infection was based on the individual, but we also performed a sensitivity analysis based on the infection. Considering that some participants might experience ≥1 infection during the study, a robust sandwich estimator, Wei-Lin-Weissfeld Cox regression, that adjusted for within-subject correlations, was used to analyze the HRs of grouped HPV infection. HRs and 95% CIs of sequential infection were also evaluated after excluding the influence of factors of demographics, health behavior, and sexual behavior.

The Kaplan-Meier method was used to calculate the cumulative probability of any HPV infection at the genital (or anal) site with or without a previous infection of the same genotype at the anal (or genital) site by sex. Comparison of the differences in the cumulative incidence between groups was performed by using the log-rank test. All analyses were performed by using SAS version 9.4 (SAS Institute, https://www.sas.com), and a p value <0.05 was considered statistically significant.

Results

Characteristics of Cohorts

Among 2,309 men and 2,378 women enrolled in the observational cohort, 1,489 (64.5%) men and 2,022 (85.0%) women who supplied effective genital and anal samples at the previous visit and having ≥1 effective anal or genital sample at follow-up visits were included in the analytic set (Appendix Table 1, https://wwwnc.cdc.gov/EID/article/26/10/19-1646-App1.pdf). These men were followed-up for a median of 12.5 (range 5.2–19.0) months; the women were followed-up for a median of 12.4 (range 5.1–20.1) months. The median age of the men was 40 (interquartile range 31–47) years, and the median age of the women was 39 (interquartile range 30–47) years. Compared with men, women had lower education levels, more conservative sexual behavior, and more hygienic practices. The remaining 820 men and 356 women, who were younger, more sexually active, and more likely to have unfixed sexual partners, were not included in the analytic set (Appendix Table 1).

Incidence Rates of Sequential Anal HPV Infections among Participants with or without Previous Genital Infection by Sex

Incidence rates of anal infection were 8.8 (95% CI 5.2–14.8)/1,000 person-months for any HPV in men with previous genital infection and 3.8 (95% CI 2.9–4.9)/1,000 person-months for men without previous genital infection; the HR was 2.6 (95% CI 1.4–4.6) for previously genital-positive men versus genital-negative men (Table 1, https://wwwnc.cdc.gov/EID/article/26/10/19-1646-T1.htm). For women, the risk for acquiring an anal infection of any HPV type was also higher in women with a preceding concordant genital HPV infection than in women without a preceding genital infection (HR 4.4, 95% CI 3.4–5.8). Similarly, increased incidence rates of sequential genital-to-anal infections were also reported for most of the other grouped HPV types in both sexes. After excluding the influence of demographics, health behaviors, and sexual behavior factors, persons with genital HPV infections at previous visits still had a higher risk for acquiring an anal infection in the follow-up visit; HRs ranged from 2.4 to 2.7 for men and from 4.1 to 4.5 for women (Appendix Table 2).

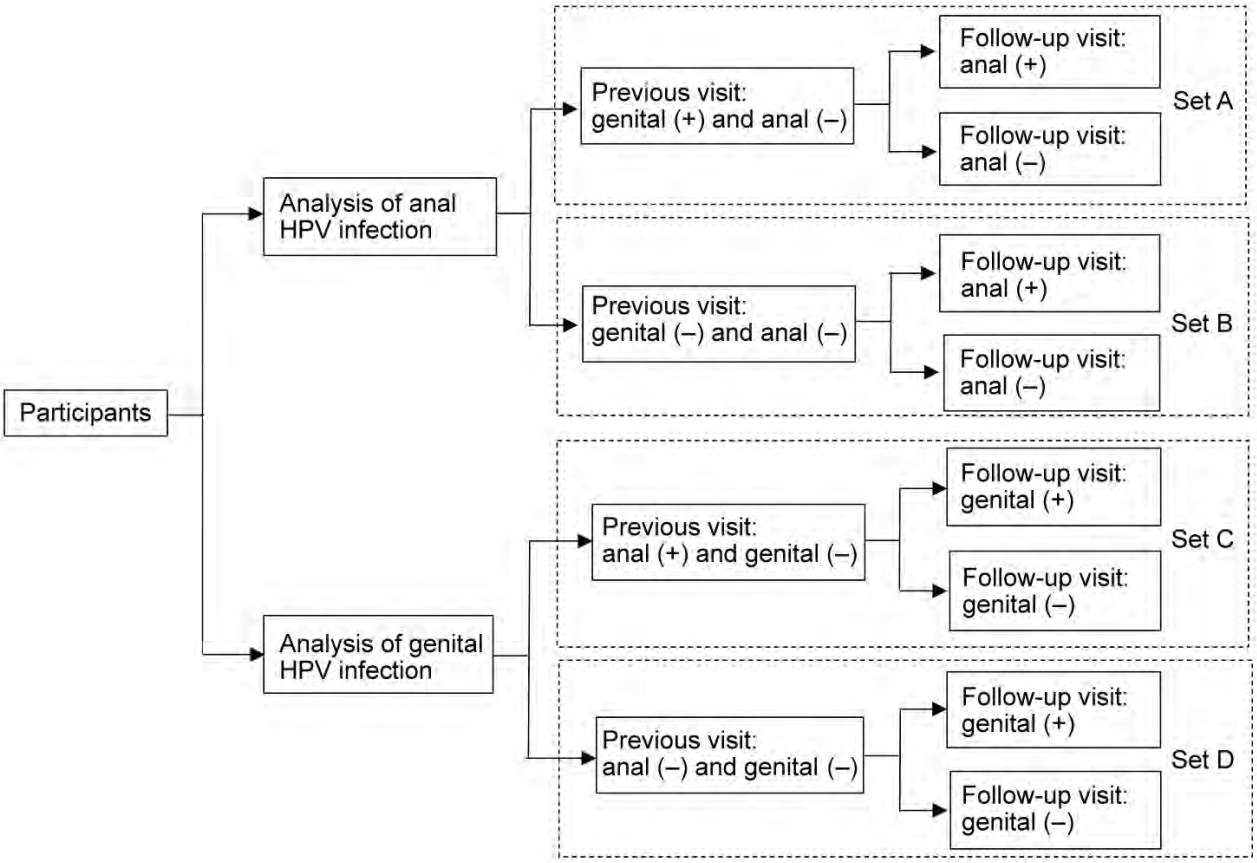

Figure 1. Study sets for assessment of risk for sequential genital and anal HPV infection after infection of the other site among men and women, Liuzhou, China. HPV, human papillomavirus.

When the analytic unit was based on infection, the risks of sequential genital-to-anal grouped HPV infection in both sexes were still statistically significant (all p<0.05) and had higher HRs (Appendix Table 3). For example, for any HPV infection, the HR of genital-to-anal HPV infection was 33.6 (95% CI 18.5–61.0) for men and 55.8 (95% CI 42.9–72.7) for women. In the type-specific HPV analysis, patients of both sexes who had previous genital HPV infection had higher incidence rates of subsequent anal HPV infection. Compared with men, women with previous genital infection had a higher risk of acquiring an anal infection (p = 0.0013) (Figure 2, panel A). A sex difference was also found in anal incidence among participants without previous genital infection for any HPV type (p = 0.0224) (Figure 2, panel E).

Incidence Rates of Sequential Genital HPV Infections among Participants with or without Previous Anal Infection by Sex

The risk for sequential genital infection with any HPV in women who had an anal HPV infection at previous visits was 1.9 times (95% CI 1.2–3.1) higher than that for women who had no anal HPV infection (Table 2, https://wwwnc.cdc.gov/EID/article/26/10/19-1646-T2.htm). The HRs of anal-to-genital HPV infection remained significantly different when we excluded the effect of demographics, health behaviors, and sexual behaviors (all p<0.05) (Appendix Table 4).

In addition, the risk for genital HR-HPV, 9V-HPV, and HPV 6/11 infections in women also increased after anal HPV infection with a concordant type. For men, sex differences were only found in anal-to-genital sequential infections of types 16/18 and 6/11. However, the results based on the infection analysis showed that the risk for acquiring all grouped HPV infections in a genital site was higher in both sexes among participants with previous infections in the anal site versus those without previous infections (Appendix Table 5). For each HPV type analysis, previous anal HPV infection was strongly associated with the sequential genital concordance type of HPV infection, particularly for types 11, 16, and 31 in men and types 6, 33, 39, 51, 52, 56, 58, and 66 in women (Table 2). We found no sex difference in the cumulative probability of sequential genital infections either in previously infected or uninfected persons (Figure 2, panels B, F).

Differences in Sequential Genital and Anal Infections among Participants with or without Previous HPV Infection at Anal or Genital Sites

Among participants without previous HPV infection at the other site, incidence rates for genital HPV infection were higher than those for anal HPV infection in men and women (both p<0.0001) (Figure 2, panels G, H). However, for participants with previous HPV infection at the other site, participants were more likely to acquire an anal infection than a genital infection, although the difference was not significant (p = 0.0758 for women and p = 0.6027 for men) (Figure 2, panels C, D).

Discussion

In both sexes, we observed a dramatically increased risk for acquiring sequential HPV infection at the anal site among participants who were genitally positive for concordant HPV types in previous visits compared with persons who had genitally negative results. In a similar fashion, an increased risk for sequential acquisition of a genital HPV infection was also observed in both sexes with a previous concordant anal HPV infection compared with those without previous anal infection, although no significant difference was found for any HPV and HR-HPV types in men on the basis of individual calculation. However, for type-specific HPV, men with a previous anal infection had a higher risk for acquiring a genital infection. Furthermore, if we calculated HRs on the basis of infection instead of person, we found that men with previous anal HPV infection had higher risk for sequentially acquiring genital infection for any HPV types than those without previous anal infection (HR 8.8, 95% CI 3.1–24.8). For genital-to-anal and anal-to-genital infections, women had higher risk than men, which might be caused by differences between female mucosal epithelium and male keratinized epithelium and the sex differences in the anatomy of genitalia.

In both sexes, if no previous HPV infection was present in the other site, the incidence of HPV infection was higher at the genital site than at the anal site. It is easy to interpret this phenomenon as reflecting the finding that genital intercourse is always the major sexual behavior in women and heterosexual men (*15–18*). However, if previous HPV infection existed at the other site, the incidence of concordant HPV infection increased dramatically in the anus and became even higher than that at the genital site, although a significant difference was not reached. These data implied that, for anal HPV infection, genital-to-anal transmission might play a greater role than direct intercourse for women and also make a relatively major contribution for men. This conclusion is concordant with a previous study in which a history of anal sex was not significantly associated with sequential acquisition of an incident anal infection after a concordant HPV infection of the cervix (*9*).

In the same cohort in Liuzhou, we observed a longer persistence of any HPV type in both genital and anal sites in women compared with men (*12,19*). This observation is concordant with the data in the analysis we describe in this article, showing that the HRs of incident infection by any type of HPV seems higher in women who were positive for the same HPV type at the other site versus women who

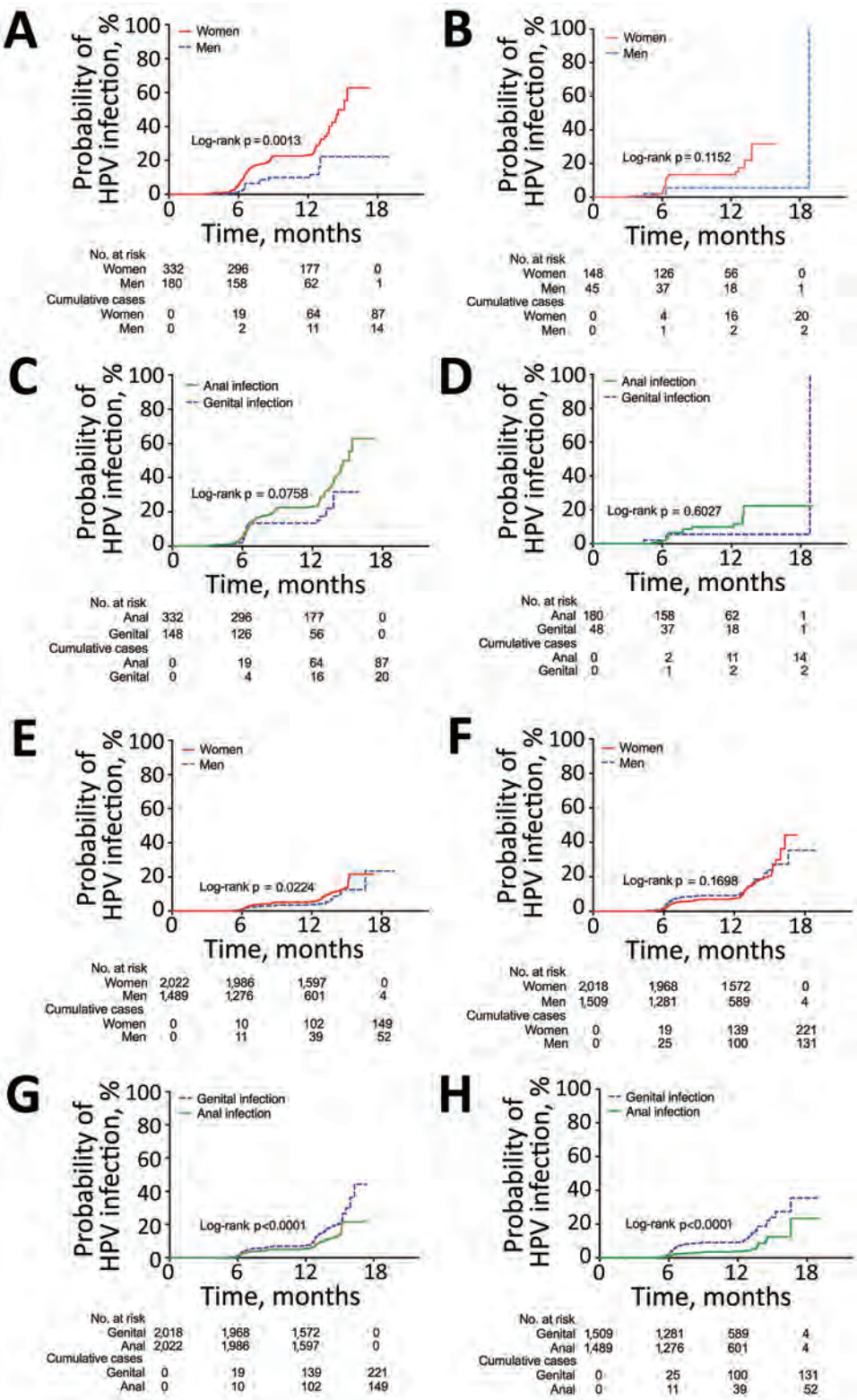

Figure 2. Kaplan-Meier estimates of the cumulative probability of sequential anogenital HPV infections, by sex and by site, Liuzhou, China. A) Anal HPV infection in participants with previous genital infection, by sex; B) genital HPV infection in participants with previous anal infection, by sex; C) genital or anal HPV infection in women with previous anal or genital infection, by site; D) genital or anal HPV infection in men with previous anal or genital infection, by site; E) anal HPV infection in participants without previous genital infection, by sex; F) genital HPV infection in participants without previous anal infection, by sex; G) genital or anal HPV infection in women without previous anal or genital infection, by site; H) genital or anal HPV infection in men without previous anal or genital infection, by site. HPV, human papillomavirus.

were negative compared with men. In addition, HR-HPV infection at the genital site was more difficult to clear than the anal infection in both sexes (*12*), which could partially explain the relatively high HRs in genital-to-anal infection compared with anal-to-genital infection in men and women.

Similar phenomena were observed in the only 2 previous studies that focused on sequential HPV acquisition between anal and genital sites (*9*,*10*). Goodman et al. reported a high risk for cervical-to-anal HPV infection and anal-to-cervical HPV infection with respective HRs of 14.2 (95% CI 9.86–20.5) and 7.08 (95% CI 3.94–12.7) for HR-HPV types in women in Hawaii (*9*). The other study focused on sequential HPV infection among anogenital sites in MSW from the HIM study and found that the HR of genital-to-anal infection with 9V-HPV was 2.61 (95% CI 1.20–6.00) and of anal-to-genital infection with 9V-HPV was 1.18 (95% CI 0.64–2.01) (*10*).

Given that 99.7% of participants in our study were heterosexual, along with the results of the 2 studies just described (*9*,*10*), we can well understand the observations that heterosexual men and women not engaging in anal sex also have positive HPV samples at the anal site (*6*,*7*,*13*). These infections might be acquired by other methods, such as autoinoculation and partner-assisted inoculation (including use of a sex toy or digital sex). This suggestion was reported in previous studies, which showed that digital sex (performed by self or sexual partners) can cause transmission events between the genital site and anal site in both sexes (*20*,*21*).

A nonsexual habit might also result in autoinoculation. Simpson et al. (*22*) studied the associations among different wiping habits after urination/defecation and anal HPV infection or related conditions. Results showed that front-to-back wiping after urination or defecation were both related to an increased prevalence of anal HR-HPV, abnormal anal cytology, and histologically proven neoplasia. More studies should be conducted to clarify the association between types of nonsexual behaviors and anal–genital HPV infection.

The strengths of our study are the large sample size and the use of the same methods to collect and test anogenital samples from males and females, which make it possible to directly compare sex differences in sequential infection among different sites. Despite these strengths, there are still limitations. Information regarding anal sex among participants was not collected, which made it impossible to analyze the relationship between sexual behavior at anal site and anal HPV infection. As is the case for other studies focused on sequential analysis of HPV infection at different sites (*9*,*10*), there is no way to know the previous HPV status of the transmitted site before baseline visit. Therefore, it is possible that the sequential HPV infection was a latent infection rather than a transmission event from the transmission site.

In conclusion, men and women with previous HPV infection at the genital or anal site had a higher risk for sequentially acquiring a concordant HPV infection at the other site. For anogenital HPV infection, autoinoculation of HPV might play a major role, in addition to that of sexual intercourse, especially for anal HPV infection in women. Therefore, there is no need to focus on anal sexual intercourse and its associated stigma when discussing anal cancer and its prevention.

This study was supported by grants from the National Science and Technology Major Project (grant no. 2015ZX09101034 to N.X.), the National Natural Science Foundation of China (grant nos. 81673240 to T.W. and 81601805 to Y.S.), and the Scientific Research Foundation of State Key Laboratory of Molecular Vaccinology and Molecular Diagnostics (grant no. 2018ZY001 to N.X.).

About the Author

Ms. Wei is a PhD student in National Institute of Diagnostics and Vaccine Development in Infectious Diseases, School of Public Health, Xiamen University, Xiamen, Fujian, China. Her primary research interests are the epidemiology of HPV infections and HPV-related diseases.

References

1. Herrero R, González P, Markowitz LE. Present status of human papillomavirus vaccine development and implementation. Lancet Oncol. 2015;16:e206–16. https://doi.org/10.1016/S1470-2045(14)70481-4
2. Parkin DM, Bray F. The burden of HPV-related cancers. Vaccine. 2006;24 (Suppl 3:S3):11–25.
3. Franco EL, de Sanjosé S, Broker TR, Stanley MA, Chevarie-Davis M, Isidean SD, et al. Human papillomavirus and cancer prevention: gaps in knowledge and prospects for research, policy, and advocacy. Vaccine. 2012;30(Suppl 5):F175–82. https://doi.org/10.1016/j.vaccine.2012.06.092
4. Bray F, Ferlay J, Soerjomataram I, Siegel RL, Torre LA, Jemal A. Global cancer statistics 2018: GLOBOCAN estimates of incidence and mortality worldwide for 36 cancers in 185 countries. CA Cancer J Clin. 2018;68:394–424. https://doi.org/10.3322/caac.21492
5. de Sanjosé S, Diaz M, Castellsagué X, Clifford G, Bruni L, Muñoz N, et al. Worldwide prevalence and genotype distribution of cervical human papillomavirus DNA in women with normal cytology: a meta-analysis. Lancet Infect Dis. 2007;7:453–9. https://doi.org/10.1016/ S1473-3099(07)70158-5
6. Nyitray AG, Carvalho da Silva RJ, Baggio ML, Lu B, Smith D, Abrahamsen M, et al. Age-specific prevalence

of and risk factors for anal human papillomavirus (HPV) among men who have sex with women and men who have sex with men: the HPV in men (HIM) study. J Infect Dis. 2011;203:49–57. https://doi.org/10.1093/infdis/jiq021
7. Hernandez BY, McDuffie K, Zhu X, Wilkens LR, Killeen J, Kessel B, et al. Anal human papillomavirus infection in women and its relationship with cervical infection. Cancer Epidemiol Biomarkers Prev. 2005;14:2550–6. https://doi.org/10.1158/1055-9965.EPI-05-0460
8. Lin C, Slama J, Gonzalez P, Goodman MT, Xia N, Kreimer AR, et al. Cervical determinants of anal HPV infection and high-grade anal lesions in women: a collaborative pooled analysis. Lancet Infect Dis. 2019;19:880–91. https://doi.org/10.1016/S1473-3099(19)30164-1
9. Goodman MT, Shvetsov YB, McDuffie K, Wilkens LR, Zhu X, Thompson PJ, et al. Sequential acquisition of human papillomavirus (HPV) infection of the anus and cervix: the Hawaii HPV cohort study. J Infect Dis. 2010;201:1331–9. https://doi.org/10.1086/651620
10. Pamnani SJ, Nyitray AG, Abrahamsen M, Rollison DE, Villa LL, Lazcano-Ponce E, et al. Sequential acquisition of anal human papillomavirus (HPV) infection following genital infection among men who have sex with women: the HPV infection in men (HIM) study. J Infect Dis. 2016;214:1180–7. https://doi.org/10.1093/infdis/jiw334
11. Wei F, Yin K, Wu X, Lan J, Huang S, Sheng W, et al. Human papillomavirus prevalence and associated factors in women and men in south China: a population-based study. Emerg Microbes Infect. 2016;5:e119. https://doi.org/10.1038/emi.2016.118
12. Wei F, Guo M, Huang S, Li M, Cui X, Su Y, et al. Sex differences in the incidence and clearance of anogenital human papillomavirus infection in Liuzhou, China: an observational cohort study. Clin Infect Dis. 2020;70:82–9. https://doi.org/10.1093/cid/ciz168
13. Wei F, Li M, Wu X, Yin K, Lan J, Sheng W, et al. The prevalence and concordance of human papillomavirus infection in different anogenital sites among men and women in Liuzhou, China: a population-based study. Int J Cancer. 2018;142:1244–51. https://doi.org/10.1002/ijc.31128
14. Wei F, Sheng W, Wu X, Yin K, Lan J, Huang Y, et al. Incidence of anogenital warts in Liuzhou, south China: a comparison of data from a prospective study and from the national surveillance system. Emerg Microbes Infect. 2017;6:e113. https://doi.org/10.1038/emi.2017.100
15. Burchell AN, Winer RL, de Sanjose S, Franco EL. Epidemiology and transmission dynamics of genital HPV infection. Vaccine. 2006;24 (Suppl 3:S3):52–61.
16. Carter JR, Ding Z, Rose BR. HPV infection and cervical disease: a review. Aust N Z J Obstet Gynaecol. 2011;51:103–8. https://doi.org/10.1111/j.1479-828X.2010.01269.x
17. Stanley M. Pathology and epidemiology of HPV infection in females. Gynecol Oncol. 2010;117(Suppl):S5–10. https://doi.org/10.1016/j.ygyno.2010.01.024
18. Gravitt PE. The known unknowns of HPV natural history. J Clin Invest. 2011;121:4593–9. https://doi.org/10.1172/JCI57149
19. Wei F, Su Y, Yao X, Cui X, Bian L, Yin K, et al. Sex differences in the incidence and clearance of anal human papillomavirus infection among heterosexual men and women in Liuzhou, China: an observational cohort study. Int J Cancer. 2019;145:807–16. https://doi.org/10.1002/ijc.32255
20. Partridge JM, Hughes JP, Feng Q, Winer RL, Weaver BA, Xi LF, et al. Genital human papillomavirus infection in men: incidence and risk factors in a cohort of university students. J Infect Dis. 2007;196:1128–36. https://doi.org/10.1086/521192
21. Sonnex C, Strauss S, Gray JJ. Detection of human papillomavirus DNA on the fingers of patients with genital warts. Sex Transm Infect. 1999;75:317–9. https://doi.org/10.1136/sti.75.5.317
22. Simpson S Jr, Blomfield P, Cornall A, Tabrizi SN, Blizzard L, Turner R. Front-to-back and dabbing wiping behaviour post-toilet associated with anal neoplasia and HR-HPV carriage in women with previous HPV-mediated gynaecological neoplasia. Cancer Epidemiol. 2016;42:124–32. https://doi.org/10.1016/j.canep.2016.04.001

Address for correspondence: Ting Wu, School of Public Health, Xiamen University, Xiamen 361102, Fujian, China; email: wuting@xmu.edu.cn

Association between Shiga Toxin–Producing *Escherichia coli* O157:H7 *stx* Gene Subtype and Disease Severity, England, 2009–2019

Lisa Byrne, Natalie Adams, Claire Jenkins

Signs and symptoms of Shiga toxin–producing *Escherichia coli* (STEC) serogroup O157:H7 infection range from mild gastrointestinal to bloody diarrhea and hemolytic uremic syndrome (HUS). We assessed the association between Shiga toxin gene (*stx*) subtype and disease severity for ≈3,000 patients with STEC O157:H7 in England during 2009–2019. Odds of bloody diarrhea, HUS, or both, were significantly higher for patients infected with STEC O157:H7 possessing *stx2a* only or *stx2a* combined with other *stx* subtypes. Odds of severe signs/symptoms were significantly higher for isolates encoding *stx2a* only and belonging to sublineage Ic and lineage I/II than for those encoding *stx2a* only and belonging to sublineage IIb, indicating that *stx2a* is not the only driver causing HUS. Strains of STEC O157:H7 that had *stx1a* were also significantly more associated with severe disease than strains with *stx2c* only. This finding confounds public health risk assessment algorithms based on detection of *stx2* as a predictor of severe disease.

In England, infection with Shiga toxin–producing *Escherichia coli* (STEC) serogroup O157:H7 is relatively rare; ≈650 cases are reported each year (*1*). However, STEC O157:H7 is a pathogen of public health concern because of its potential to cause severe disease. In England, almost two thirds of case-patients reportedly experience bloody diarrhea and 5%–14% of infections progress to the severe condition of hemolytic uremic syndrome (HUS) (*2*–*6*).

Predictors of whether HUS will develop after STEC infection include pathogen and host factors. Most at risk for development of HUS after STEC infection are children; HUS is the leading cause of renal failure in children in developed countries, including the United Kingdom and the United States (*7*). Some studies have demonstrated that female sex is also associated with HUS (*2*,*8*–*10*).

Author affiliation: Public Health England, London, UK

DOI: https://doi.org/10.3201/eid2610.200319

The STEC pathotype is defined by the presence of the genes encoding Shiga toxin (Stx) type 1, type 2, or both, which are located on bacteriophage incorporated into the bacterial genome (*11*). Stx1 and Stx2 can be further divided into subtypes Stx1a-1d and Stx2a-2g. Previous studies have demonstrated an association between Stx subtype and disease severity; strains producing Stx2, particularly the Stx2a subtype, are more associated with severe disease and HUS (*12*–*16*). These findings have led to the development and implementation of differential case management and public health management of cases based on Stx profile–derived STEC pathotypes in England and elsewhere (*17*–*19*).

The STEC O157:H7 population has previously been delineated into 3 main lineages (I, I/II, and II) (*20*) and 7 sublineages (Ia, Ib, Ic, IIa, IIb, IIc, and I/II). When STEC O157:H7 emerged in England in the 1980s, the dominant lineage was I/II. Phylogenetic analyses in which hierarchical single-linkage clustering performed on pairwise single-nucleotide polymorphism (SNP) difference between strains was used revealed that almost all isolates belonging to lineage I/II fell within a 250 single-linkage SNP cluster, or clade. During the 1990s, sublineage I/II was replaced by a 250 single-linkage SNP clade within sublineage Ic (*20*,*21*). More recently, a decline in sublineage Ic and a concurrent increase in sublineage IIb have been observed (*14*,*22*). The emergence of each clade appears to coincide with the acquisition of phage encoding the *stx2a* gene, which, if causing more severe disease, increases the likelihood that those cases will be detected (*20*).

The evidence base for the differential public health management of STEC cases based on pathotype has been assimilated from relatively small studies, which prompted a review of the data in England. We therefore explored the association between Stx

subtype, particularly the role of Stx2a, and disease severity in England for ≈3,000 cases of STEC O157:H7 reported in the 11-year period 2009–2019.

Materials and Methods

Data, Setting, and Source

For this study, we used an observational study design. In January 2009, Public Health England (PHE) implemented the National Enhanced Surveillance System for STEC (NESSS) in England. In brief, it captures standardized epidemiologic and microbiological data for all cases of STEC reported in England through an Enhanced Surveillance Questionnaire (ESQ). For each case, these data are reconciled with microbiological data in NESSS (*3*).

We included data on all STEC O157:H7 cases in England reported from January 1, 2009, through December 31, 2019, for which the patient submitted an ESQ and whose isolates had undergone whole-genome sequencing. For each case-patient, we extracted and coded as binary variables the following: clinical data on reported signs/symptoms (nonbloody diarrhea, bloody diarrhea, vomiting, nausea, abdominal pain, and fever); whether the patient was asymptomatic, hospitalized, or died; and whether HUS developed. We coded the responses as negative when clinical symptoms were blank on the ESQ and case-patients were not recorded as being asymptomatic. We also extracted age and sex of case-patients and categorized them as children (≤16 years of age) or adults, according to a priori knowledge that children are most at risk for STEC infection and for disease progression to HUS. The outcome of interest was disease severity. Case-patients were coded as having severe disease if bloody diarrhea, HUS, or death were reported. Asymptomatic persons and case-patients with nonbloody diarrhea were considered to have mild disease. We linked data derived from whole-genome sequencing, including Stx subtype and lineage, to each case.

Laboratory Methods

In England, all fecal specimens from patients with hospital-acquired and community-acquired cases of gastrointestinal disease submitted to local hospital laboratories are tested for *E. coli* O157:H7. All isolates are submitted to the PHE Gastrointestinal Bacteria Reference Unit for confirmation. Since July 2015, all isolates have been sequenced for routine surveillance (National Center for Biotechnology Information Short Read Archive Bioproject no. PRJNA248042). Therefore, we included in this study all isolates received since July 2015 from case-patients with completed ESQs. In addition, we included isolates of STEC O157:H7 submitted to the Gastrointestinal Bacteria Reference Unit from January 2009 through June 2015 and sequenced as part of previous studies from case-patients with ESQs (*20*). The process for whole-genome sequencing has been described in detail (*14*).

Statistical Analyses

We used Stata 13.1 (StataCorp, https://www.stata.com) for our analyses. We described cases with respect to clinically mild and severe disease by patient age, sex, and Stx subtype. We used logistic regression to investigate the relationship between Stx subtype and disease severity, adjusting for age and sex. For each variable, we calculated odds ratios (ORs) for case-patients reporting severe disease compared with those reporting mild disease. We chose the Stx2c subtype as the baseline for Stx subtype because this subtype is associated with less severe disease. To further explore the phylogenetic relationships within Stx2a isolates, we used logistic regression to investigate the relationship between Stx2a sublineages and disease severity, adjusting for age and sex. For each variable, we calculated ORs for case-patients reporting severe disease compared with those reporting mild disease.

Results

Descriptive

NESSS clinical data were available for 3,241 STEC O157:H7 case-patients with genomic strain data in England during 2009–2019. Of those, 2,891 (89.2%) reported diarrheal symptoms, including 1,862 (57.5 %) who had experienced bloody diarrhea. HUS reportedly developed in 86 (2.6 %) case-patients. Thus, 1,889 (58.3%) case-patients in the dataset were categorized as having severe disease, although this proportion varied by Stx subtype (Table 1). Case-patients categorized as having mild disease accounted for 41.7 % of the dataset and included 110 asymptomatic persons. Over half (56.8 %) of case-patients in the dataset were female and 36.5 % were children ≤16 years of age. Severe disease was more frequently reported among female than male patients, although this difference was not significant (59.7 % vs. 56.4 %; $p = 0.09$), and among adults than among children (62.7% vs. 50.5 %; $p \leq 0.01$).

Genomic typing data were available for isolates from 3,225 (99.5%) cases. Most (81.4%) isolates belonged to 5 specific clades within 5 sublineages: 1c (n = 789), IIa (n = 438), IIc (n = 932), I/II (n = 133), and IIb (n = 336). Infections with isolates in sublineage

Table 1. Disease severity of 3,241 clinical cases of Shiga toxin–producing *Escherichia coli* O157:H7 Stx subtype infection, by patient age, sex, and isolate Stx subtype, England, 2009–2019*

Variable	All cases, no. (%)	Mild illness, no. (%)†	Severe illness, no. (%)‡	HUS, no. (%)
All O157s	3,241	1,352 (41.7)	1,889 (58.3)	86 (2.7)
Age group				
Child	1,185 (36.5)	586 (49.5)	599 (50.5)	66 (5.6)
Adult	2,056 (63.5)	766 (37.3)	1,290 (62.7)	20 (1.0)
Sex				
F	1,841 (56.8)	742 (40.3)	1,099 (59.7)	54 (2.9)
M	1,400 (43.2)	610 (43.6)	790 (56.4)	32 (2.3)
Stx subtype				
stx2c stx1a	903 (28)	286 (31.7)	617 (68.3)	0
stx2c	675 (20.9)	535 (79.3)	140 (20.7)	2 (0.3)
stx2a	686 (21.3)	254 (37)	432 (63)	27 (3.9)
stx2a stx2c	829 (25.7)	240 (29)	589 (71)	50 (6.0)
stx1a	32 (1)	13 (40.6)	19 (59.4)	0
stx2a stx1a	51 (1.6)	9 (17.6)	42 (82.4)	0
stx2a stx2c stx1a	49 (1.5)	9 (18.4)	40 (81.6)	0
No Stx subtype§	16 (0.5)	6 (0.4)	10 (0.5)	0

*HUS, hemolytic uremic syndrome.
†Asymptomatic or nonbloody diarrhea.
‡Bloody diarrhea, HUS, or death.
§Isolates underwent whole-genome sequencing, but Stx subtype was not available.

IIa were mostly attributed to a large outbreak associated with imported salad leaves in 2016 (*23*); the other 4 sublineages were associated with domestic acquisition of infection within the United Kingdom (Table 2) (*24*).

The dataset contained data for 86 case-patients with HUS, of which 32 were male and 54 were female. Most (66) HUS case-patients were children; infection progressed to HUS for 5.9% (66/1,119) of children, compared with 0.98% (20/2,039) of adults (Table 1).

Table 2. Disease severity of 3,225 clinical cases of Shiga toxin–producing *Escherichia coli* O157:H7 Stx subtype infection, by isolate Stx subtype and sublineage, England, 2009–2019

Lineage, stx profile	All cases, no. (%)	Mild illness, no. (%)*	Severe illness, no. (%)†
Ic			
stx2c stx1a	2 (0.3)	0	2 (100)
stx2c	15 (1.9)	9 (60)	6 (40)
stx2a	309 (39.2)	97 (31.4)	212 (68.6)
stx2a stx2c	455 (57,7)	129 (28.4)	326 (71.6)
stx1a	1 (0.1)	0	1 (100)
stx2a stx1a	7 (0.9)	0	7 (100)
stx2a stx2c stx1a	0	0	0
I/II			
stx2c stx1a	0	0	0
stx2c	1 (0.8)	0	1 (100)
stx2a	82 (61.7)	9 (11)	73 (89)
stx2a stx2c	50 (37.6)	14 (28)	36 (72)
stx1a	0	0	0
stx2a stx1a	0	0	0
stx2a stx2c stx1a	0	0	0
IIb			
stx2c stx1a	5 (1.5)	2 (40)	3 (60)
stx2c	60 (17)	47 (78.3)	13 (21.7)
stx2a	257 (76.5)	134 (52.1)	123 (47.9)
stx2a stx2c	14 (4.2)	4 (28.6)	10 (71.4)
stx1a	0	0	0
stx2a stx1a	0	0	0
stx2a stx2c stx1a	0	0	0
Other			
stx2c stx1a	896 (7.8)	284 (41.9)	612 (58.1)
stx2c	599 (67.4)	479 (80.1)	120 (19.9)
stx2a	38 (3.4)	14 (21.1)	24 (78.9)
stx2a stx2c	310 (14.9)	93 (37.8)	217 (62.2)
stx1a	31 (1.6)	13 (66.7)	18 (33.3)
stx2a stx1a	44 (4.5)	9 (20)	35 (80)
stx2a stx2c stx1a	49 (0.4)	9 (0)	40 (0)

*Asymptomatic or nonbloody diarrhea.
†Bloody diarrhea, hemolytic uremic syndrome, or death.

Severity by Subtype and Multiplicative Nature

The strains of STEC O157:H7 in this dataset had genes encoding Stx1a, Stx2a, or Stx2c, or combinations of those 3 subtypes (Table 1). Of those strains that harbored 1 *stx* subtype, those that had *stx1a* or *stx2a* were significantly more associated with severity than those that had *stx2c* (Tables 1–3). Comparisons of the *stx* subtype profiles exhibited by STEC O157:H7 indicated that strains with >1 *stx* subtype gene are associated with higher odds of severe disease than those with 1 *stx* subtype gene (Table 3). When *stx2c*, for which disease severity was lowest, was coupled with *stx1a*, the odds of severity increased (OR 7.89, 95% CI 6.23–9.97) to that comparable to strains possessing *stx2a* only (OR 7.04, 95% CI 5.51–9.00). The highest odds of severe disease were among case-patients infected with strains harboring *stx2a* and *stx1a* (OR 19.45, 95% CI 9.20–41.16).

The most common *stx* profile in isolates from HUS case-patients was *stx2a/stx2c* (n = 50), followed by *stx2a* (n = 27) (Table 1). Only 2 HUS case-patients were infected with strains that did not have *stx2a* (both *stx2c* only). Five sublineages were represented among isolates from HUS case-patients: sublineage Ic (n = 54), sublineage IIa (n = 12), sublineage IIc (n = 6), lineage I/II (n = 12), and sublineage IIb (n = 2).

Subtype Stx2a is associated with 3 sublineages common in the United Kingdom: Ic, IIb, and I/II (Table 2). To explore the relationship between sublineage, clade, and severe disease, we conducted analysis by clade for Stx2a and Stx2a/2c. We found no significant difference in the odds of severity and clade for isolates encoding both Stx2a and Stx2c (Table 4). For isolates encoding Stx2a only, odds of severe symptoms were significantly higher for patients infected with isolates belonging to sublineage Ic and sublineage I/II than sublineage IIb (Table 4). Furthermore, isolates from only 2 HUS case-patients in the study belonged to sublineage IIb, despite the presence of Stx2a.

Discussion

This large study of enhanced microbiological and epidemiologic data captured detailed clinical outcomes linked to molecular typing and phylogenetic analysis for adults and children infected with STEC O157:H7 in England. STEC O157:H7 is a rare but potentially very serious infection and particularly in children and elderly persons is likely to result in their interaction with healthcare services. Frontline laboratories have long had diagnostics in place and routinely screen all fecal specimens for STEC O157:H7. Therefore, NESSS captures data for a high proportion of STEC O157:H7 cases in England and is probably representative of STEC cases nationally.

Although our dataset is comprehensive, the potential for an inherent surveillance bias toward detecting more severe disease exists. Conversely, STEC HUS is underascertained in NESSS (PHE in-house data) because of challenges with the diagnosis of this condition. Moreover, for the most part, patient's symptoms are self-reported; therefore, misclassification bias is possible, although because of the temporality of data collection, we consider bias to be low.

In our study, although HUS developed in more children ≤16 years of age, risk for severe disease seems to be lower than for those >16 years of age. It is possible that children are more likely to be taken for healthcare visits regardless of illness severity; therefore, our surveillance system is more likely to pick up milder cases of STEC infection in children than in adults.

Previous studies have documented the association between the presence of Stx2a and the development of HUS; thus, monitoring the presence and

Table 3. Univariate and multivariable regression analysis of disease severity for 3,225 patients with Shiga toxin–producing *Escherichia coli* O157:H7 infection, by isolate Stx subtype and patient age and sex, England, 2009–2019

	Univariate	Multivariable*	
Category	OR (95% CI)	OR (95% CI)	p value
Stx subtype			
stx2c stx1a	8.24 (6.53–10.40)	7.89 (6.23–9.97)	<0.001
stx2c	Referent 1.00	Referent	
stx2a	6.5 (5.10–8.28)	7.04 (5.51–9.00)	<0.001
stx2a stx2c	9.38 (7.38–11.91)	10.12 (7.94–12.90)	<0.001
stx1a	5.58 (2.69–11.58)	5.44 (2.61–11.36)	<0.001
stx2a stx1a	17.83 (8.48–37.51)	19.45 (9.20–41.16)	<0.001
stx2a stx2c stx1a	16.98 (8.05–35.83)	17.38 (8.20–36.86)	<0.001
Age group			
Adult	Referent 1.00	Referent	
Child	0.61 (0.3–0.70)	0.56 (0.48–0.66)	<0.001
Sex			
M	Referent 1.00	Referent	
F	1.14 (0.99–1.31)	1.09 (0.93–1.27)	0.286

*Adjusted for all other covariates in the model.

Table 4. Univariate and multivariable regression analysis of disease severity of Shiga toxin–producing *Escherichia coli* O157:H7 infection by sublineage, England, 2009–2019

Category	Univariate OR (95% CI)	Multivariable* OR (95% CI)	Multivariable* p value
Stx2a only strains, n = 648			
Sublineage			
IIb	Referent		
Ic	2.46 (1.75–3.46)	2.60 (1.83–3.677)	<0.001
I/II	9.09 (4.37–18.93)	8.91 (4.26–18.63)	<0.001
Age group			
Adult	Referent	Referent	
Child	0.65 (0.44–0.97)	0.62 (0.40–0.95)	0.03
Sex			
M	Referent	Referent	
F	1.10 (0.74–1.63)	1.16 (0.76–1.78)	0.50
Stx2a/2c strains, n = 505			
Sublineage			
Ic	Referent		
I/II	1.03 (0.54–1.98)	0.998 (0.521–1.91)	0.997
Age group			
Adult	Referent		
Child	0.77 (0.52–1.13)	0.79 (0.535–1.167)	0.237
Sex			
M	Referent		
F	1.3 (0.88–1.91)	1.267 (0.859–1.87)	0.232

*Adjusted for all other covariates in the model.

emergence of strains harboring this Stx subtype in the STEC population is needed (*12*–*17*,*19*). Most of these studies included STEC from a wide variety of different serotypes, exhibiting a variety of Stx subtypes and relatively small datasets. In contrast, we analyzed a large dataset, focusing on a single serotype characterized by limited number of Stx subtype combinations. Doing so enabled us to make direct comparisons between specific Stx profiles without the confounding influence of the wide variety of virulence factors expressed by different STEC serotypes.

Our analysis revealed that the acquisition of *stx1a* by STEC O157:H7 also increases the association with severity. This association is significant in strains of STEC O157:H7 *stx2c* that acquire *stx1a*; the odds of severe disease from strains harboring *stx1a/stx2c* are comparable to the odds of severe disease from strains that have *stx2a* when compared with *stx2c* only. This finding supports previous findings that serogroups other than STEC O157 harboring *stx1a* only have been isolated from patients reporting severe and prolonged gastrointestinal symptoms (e.g., STEC O117) (*25*). Cases of bloody diarrhea and HUS caused by STEC *stx1*-only strains do occur, albeit at a lower frequency than cases caused by STEC harboring *stx2* (*26*). However, the fact that *stx1a*-only isolates were not detected in our HUS cohort may support using presence of *stx2a* as a predictor of the highest likelihood of HUS development.

Analysis of the sublineages associated with HUS highlighted the rarity of sublineage IIb, despite increasing numbers of cases detected in the United Kingdom belonging to lineage IIb carrying *stx2a* (*14*). This finding correlates with the analysis showing that despite the presence of *stx2a*, isolates belonging to sublineage IIb are significantly less likely to be associated with severity than isolates belonging to sublineage 1c and I/II. These results indicate that the presence of *stx2a* is not the only driver behind HUS and that other factors are at play. These factors may include the *stx*-bacteriophage backbone, the *stx*-bacteriophage insertion site (*24*), copy number of the *stx2a* subtype gene, mutations in the *stx2a* subtype gene, or other gene mutations or deletions that may be involved in the expression of the toxin in vivo. A previous study (*27*) found that phylogenetic lineage seems to be predictive of HUS risk among those ≥10 years of age only and that lineage does not seem to explain HUS progression among children <10 years of age. They also observed that different lineages were observed at varying frequencies across age groups, suggestive of differences in exposure and acquisition of STEC.

This large study, which explored the association between STEC O157:H7 Stx subtype and disease severity in England over an 11-year period, provides further evidence that STEC O157:H7 exhibiting *stx* profiles that included *stx2a* only or in combination with other *stx* subtypes were more likely to be isolated from patients reporting bloody diarrhea, HUS, or both. However, we also observed that strains of STEC O157:H7 that had *stx1a* and *stx2a* only, or in combination with other *stx* subtypes, were significantly more associated with severe disease outcomes

than those strains of STEC O157:H7 that had *stx2c* only. This finding confounds the clinical and public health risk assessment algorithms in many counties, including the United Kingdom, that are based on using detection of *stx2* as a predictor of severe gastrointestinal disease.

Acknowledgments

We thank Saira Butt, Bhavita Vishram, Nalini Purohit, and Mike Harte for their contributions to NESSS in England and all public health practitioners who report to the system. We also thank all the laboratory staff in the Gastrointestinal Bacteria Reference Unit, especially Michael Wright, Amy Gentle, Neil Perry, and Dawn Hedges.

About the Author

Dr. Byrne is the lead epidemiologist for STEC at the National Infection Service, PHE, London, UK. Her research interests include public health surveillance of STEC and HUS and the investigation of outbreaks of foodborne gastrointestinal disease.

References

1. Public Health England. Shiga toxin-producing Escherichia coli (STEC) data: 2017 [cited 2019 Jan 31]. https://assets.publishing.service.gov.uk/government/uploads/system/uploads/attachment_data/file/774291/STEC_O157_report.pdf
2. Launders N, Byrne L, Jenkins C, Harker K, Charlett A, Adak GK. Disease severity of Shiga toxin-producing *E. coli* O157 and factors influencing the development of typical haemolytic uraemic syndrome: a retrospective cohort study, 2009-2012. BMJ Open. 2016;6:e009933. https://doi.org/10.1136/bmjopen-2015-009933
3. Byrne L, Jenkins C, Launders N, Elson R, Adak GK. The epidemiology, microbiology and clinical impact of Shiga toxin-producing *Escherichia coli* in England, 2009–2012. Epidemiol Infect. 2015;143:3475–87. https://doi.org/10.1017/S0950268815000746
4. Dundas S, Todd WT, Stewart AI, Murdoch PS, Chaudhuri AK, Hutchinson SJ. The central Scotland *Escherichia coli* O157:H7 outbreak: risk factors for the hemolytic uremic syndrome and death among hospitalized patients. Clin Infect Dis. 2001;33:923–31. https://doi.org/10.1086/322598
5. Gould LH, Demma L, Jones TF, Hurd S, Vugia DJ, Smith K, et al. Hemolytic uremic syndrome and death in persons with *Escherichia coli* O157:H7 infection, foodborne diseases active surveillance network sites, 2000-2006. Clin Infect Dis. 2009;49:1480–5. https://doi.org/10.1086/644621
6. Wong CS, Mooney JC, Brandt JR, Staples AO, Jelacic S, Boster DR, et al. Risk factors for the hemolytic uremic syndrome in children infected with *Escherichia coli* O157:H7: a multivariable analysis. Clin Infect Dis. 2012;55:33–41. https://doi.org/10.1093/cid/cis299
7. Lynn RM, O'Brien SJ, Taylor CM, Adak GK, Chart H, Cheasty T, et al. Childhood hemolytic uremic syndrome, United Kingdom and Ireland. Emerg Infect Dis. 2005;11:590–6. https://doi.org/10.3201/eid1104.040833
8. Honda T. Factors influencing the development of hemolytic uremic syndrome caused by enterohemorrhagic *Escherichia coli* infection: from a questionnaire survey to in vitro experiment. Pediatr Int. 1999;41:209–12. https://doi.org/10.1046/j.1442-200X.1999.4121042.x
9. Byrne L, Vanstone GL, Perry NT, Launders N, Adak GK, Godbole G, et al. Epidemiology and microbiology of Shiga toxin-producing *Escherichia coli* other than serogroup O157 in England, 2009-2013. J Med Microbiol. 2014;63:1181–8. PubMed https://doi.org/10.1099/jmm.0.075895-0
10. Smith KE, Wilker PR, Reiter PL, Hedican EB, Bender JB, Hedberg CW. Antibiotic treatment of *Escherichia coli* O157 infection and the risk of hemolytic uremic syndrome, Minnesota. Pediatr Infect Dis J. 2012;31:37–41. https://doi.org/10.1097/INF.0b013e31823096a8
11. Croxen MA, Law RJ, Scholz R, Keeney KM, Wlodarska M, Finlay BB. Recent advances in understanding enteric pathogenic *Escherichia coli*. Clin Microbiol Rev. 2013;26:822–80. https://doi.org/10.1128/CMR.00022-13
12. Ethelberg S, Olsen KE, Scheutz F, Jensen C, Schiellerup P, Engberg J, et al. Virulence factors for hemolytic uremic syndrome, Denmark. Emerg Infect Dis. 2004;10:842–7. https://doi.org/10.3201/eid1005.030576
13. Persson S, Olsen KE, Ethelberg S, Scheutz F. Subtyping method for *Escherichia coli* Shiga toxin (verocytotoxin) 2 variants and correlations to clinical manifestations. J Clin Microbiol. 2007;45:2020–4. https://doi.org/10.1128/JCM.02591-06
14. Byrne L, Dallman TJ, Adams N, Mikhail AFW, McCarthy N, Jenkins C. Highly pathogenic clone of Shiga toxin-producing *Escherichia coli* O157:H7, England and Wales. Emerg Infect Dis. 2018;24:2303–8. https://doi.org/10.3201/eid2412.180409
15. Brandal LT, Wester AL, Lange H, Løbersli I, Lindstedt BA, Vold L, et al. Shiga toxin-producing *Escherichia coli* infections in Norway, 1992-2012: characterization of isolates and identification of risk factors for haemolytic uremic syndrome. BMC Infect Dis. 2015;15:324. https://doi.org/10.1186/s12879-015-1017-6
16. Naseer U, Løbersli I, Hindrum M, Bruvik T, Brandal LT. Virulence factors of Shiga toxin-producing *Escherichia coli* and the risk of developing haemolytic uraemic syndrome in Norway, 1992-2013. Eur J Clin Microbiol Infect Dis. 2017;36:1613–20. https://doi.org/10.1007/s10096-017-2974-z
17. Veneti L, Lange H, Brandal L, Danis K, Vold L. Mapping of control measures to prevent secondary transmission of STEC infections in Europe during 2016 and revision of the national guidelines in Norway. Epidemiol Infect. 2019;147:e267. https://doi.org/10.1017/S0950268819001614
18. Public Health England. Shiga toxin-producing *Escherichia coli*: public health management [cited 2019 Jan 31]. https://www.gov.uk/government/publications/shiga-toxin-producing-escherichia-coli-public-health-management
19. Werber D, Scheutz F. The importance of integrating genetic strain information for managing cases of Shiga toxin-producing *E. coli* infection. Epidemiol Infect. 2019;147:e264. PubMed https://doi.org/10.1017/S0950268819001602
20. Dallman TJ, Ashton PM, Byrne L, Perry NT, Petrovska L, Ellis R, et al. Applying phylogenomics to understand the emergence of Shiga-toxin-producing *Escherichia coli* O157:H7 strains causing severe human disease in the UK. Microb Genom. 2015;1:e000029. https://doi.org/10.1099/mgen.0.000029
21. Adams NL, Byrne L, Smith GA, Elson R, Harris JP, Salmon R, et al. Shiga toxin–producing *Escherichia coli* O157, England and Wales, 1983–2012. Emerg Infect Dis. 2016;22:590–7. https://doi.org/10.3201/eid2204.151485

22. Mikhail AFW, Jenkins C, Dallman TJ, Inns T, Douglas A, Martín AIC, et al. An outbreak of Shiga toxin-producing *Escherichia coli* O157:H7 associated with contaminated salad leaves: epidemiological, genomic and food trace back investigations. Epidemiol Infect. 2018;146:187–96. https://doi.org/10.1017/S0950268817002874
23. Gobin M, Hawker J, Cleary P, Inns T, Gardiner D, Mikhail A, et al. National outbreak of Shiga toxin-producing *Escherichia coli* O157:H7 linked to mixed salad leaves, United Kingdom, 2016. Euro Surveill. 2018;23. PubMed https://doi.org/10.2807/1560-7917.ES.2018.23.18.17-00197
24. Yara DA, Greig DR, Gally DL, Dallman TJ, Jenkins C. Comparison of Shiga toxin-encoding bacteriophages in highly pathogenic strains of Shiga toxin-producing *Escherichia coli* O157:H7 in the UK. Microb Genom. 2020;6:e000334. https://doi.org/10.1099/mgen.0.000334
25. Dallman T, Cross L, Bishop C, Perry N, Olesen B, Grant KA, et al. Whole genome sequencing of an unusual serotype of Shiga toxin-producing *Escherichia coli*. Emerg Infect Dis. 2013;19:1302–4. PubMed https://doi.org/10.3201/eid1908.130016
26. EFSA BIOHAZ Panel, Koutsoumanis K, Allend A, Alvarez-Ordóñez A, Bover-Cid S, Chemaly M, et al. Pathogenicity assessment of Shiga toxin-producing *Escherichia coli* (STEC) and the public health risk posed by contamination of food with STEC. EFSA Journal. 2020;18:5697.
27. Tarr GAM, Shringi S, Oltean HN, Mayer J, Rabinowitz P, Wakefield J, et al. Importance of case age in the purported association between phylogenetics and hemolytic uremic syndrome in Escherichia coli O157:H7 infections. Epidemiol Infect. 2018;146:1550–5. PubMed https://doi.org/10.1017/S0950268818001632

Address for correspondence: Lisa Byrne, Public Health England, Gastrointestinal Infections, 61 Colindale Ave, London NW9 5EQ, UK; email: lisa.byrne@phe.gov.uk; and Claire Jenkins, Public Health England, Gastrointestinal Bacteria Reference Unit, 61 Colindale Ave, London NW9 5EQ, UK; email: claire.jenkins1@phe.gov.uk

Rapid, Sensitive, Full-Genome Sequencing of Severe Acute Respiratory Syndrome Coronavirus 2

Clinton R. Paden,[1] Ying Tao,[1] Krista Queen, Jing Zhang, Yan Li, Anna Uehara, Suxiang Tong

We describe validated protocols for generating high-quality, full-length severe acute respiratory syndrome coronavirus 2 genomes from primary samples. One protocol uses multiplex reverse transcription PCR, followed by MinION or MiSeq sequencing; the other uses singleplex, nested reverse transcription PCR and Sanger sequencing. These protocols enable sensitive virus sequencing in different laboratory environments.

In December 2019, severe acute respiratory syndrome coronavirus 2 (SARS-CoV-2), the etiologic agent of coronavirus disease 2019 (COVID-19), emerged in Wuhan, China. Since then, it has rapidly spread worldwide (*1*–*3*), causing 7,039,918 confirmed cases, including 404,396 deaths, in 188 countries or regions as of June 9, 2020 (*4*). Because SARS-CoV-2 has shown the capacity to spread rapidly and lead to a range of manifestations in infected persons, from asymptomatic infection to mild, severe, or fatal disease, it is essential to identify genetic variants to track spread and understand any changes in transmissibility, tropism, and pathogenesis.

We describe the design and use of 2 PCR-based methods for sequencing SARS-CoV-2 clinical specimens. The first is a multiplex PCR panel, followed by sequencing on either the Oxford Nanopore MinION apparatus (https://nanoporetech.com) or an Illumina MiSeq apparatus (https://www.illumina.com). When coupled with MinION sequencing, our protocol can be implemented outside a traditional laboratory and can be completed in a single workday, similar to previous mobile genomic surveillance of Ebola and Zika virus outbreaks (*5*,*6*). In addition, we provide a complementary singleplex, nested PCR strategy, which improves sensitivity for samples with lower viral load and is compatible with Sanger sequencing.

Author affiliations: Centers for Disease Control and Prevention, Atlanta, Georgia, USA (C. Paden, Y. Tao, K. Queen, J. Zhang, Y. Li, A. Uehara, S. Tong); IHRC, Atlanta (J. Zhang); Oak Ridge Institute for Science and Education, Oak Ridge, Tennessee, USA (A. Uehara)

DOI: https://doi.org/10.3201/eid2610.20.1800

The Study

On January 10, 2020, the first SARS-CoV-2 genome sequence was released online (*7*). That day, we designed 2 complementary panels of primers to amplify the virus genome for sequencing.

For the first panel, we used the PRIMAL primer design tool (*5*) to design multiplex PCRs to amplify the genome by using only a few PCRs (Appendix, https://wwwnc.cdc.gov/EID/article/26/10/20-1800-App1.pdf). The final design consists of 6 pools of primers optimized for sensitivity and assay flexibility. The amplicons average 550 bp with 100-bp overlaps to enable sequencing on either the Oxford MinION or Illumina MiSeq.

For the second panel, we designed sets of primers to generate nested, tiling amplicons across the SARS-CoV-2 genome (Appendix) for enhanced sensitivity in samples with lower viral loads. Each amplicon is 322–1,030 bp with an average overlap of 80 bp. These amplicons are designed to be amplified and sequenced individually on Sanger instruments but might also be pooled for sequencing on next-generation sequencing platforms.

To determine the sensitivity of each sequencing strategy, we generated a set of 6 ten-fold serial dilutions of a SARS-CoV-2 isolate (J. Harcourt, unpub. data, https://doi.org/10.1101/2020.03.02.972935). Virus RNA was diluted into a constant background of A549 human cell line total nucleic acid (RNaseP cycle threshold [C_t] 29). We quantitated each dilution by using the Centers for Disease Control and Prevention SARS-CoV-2 real-time reverse transcription PCR for the nucleocapsid 2 gene (*8*). The 6

[1]These authors contributed equally to this article.

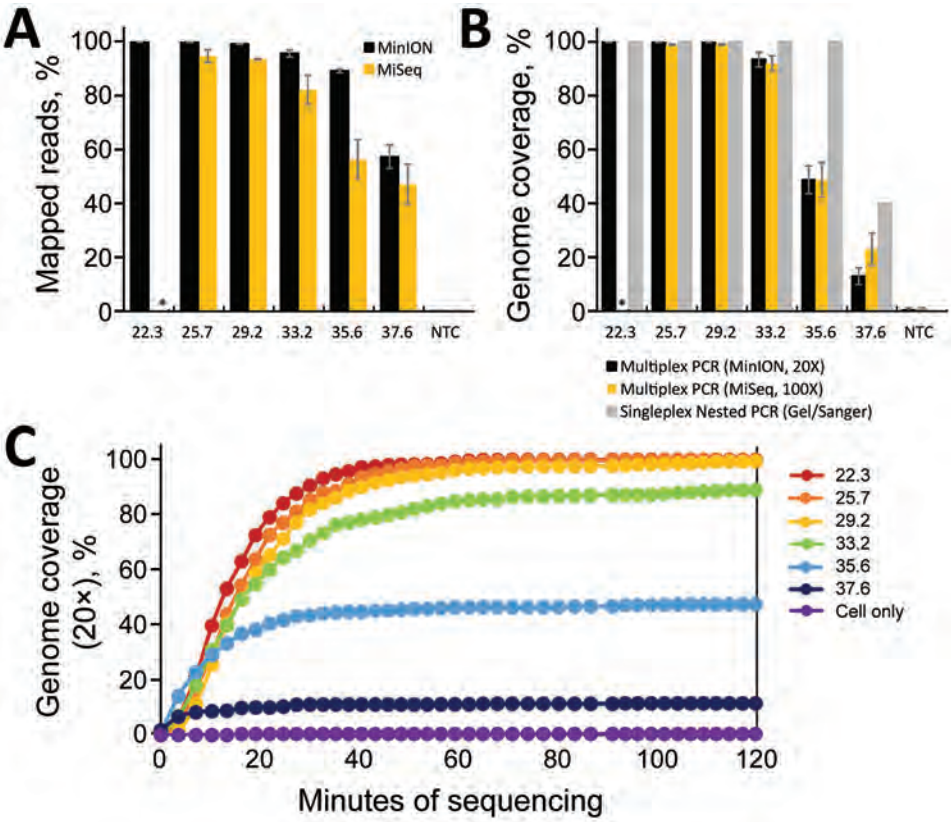

Figure 1. Limits of detection for sequencing severe acute respiratory syndrome coronavirus 2. Triplicate serial dilutions of virus isolate A12 (J. Harcourt, unpub. data, https://doi.org/10.1101/2020.03.02.972935) were amplified by using the singleplex or multiplex primer set. Multiplex amplicons were barcoded, library-prepped, and sequenced on an Oxford MinION apparatus (https://nanoporetech.com) or an Illumina MiSeq apparatus (https://www.illumina.com). A) Percentage of reads that map to the virus genome for each sample. B) Percentage of virus genome that is covered at >20× depth by the multiplex amplicons on the MinION (black) or >100× depth on the MiSeq (orange), or covered by the nested, singleplex amplicons (gray) (measured by presence or absence on a gel). C) Real-time analysis of MinION sequencing data. Each data point represents the average 20× genome coverage of three replicates. NTC, nontemplate controls (human cell nucleic acid carried through the PCR and library preparation). Asterisk (*) indicates that samples were not analyzed at that dilution.

dilutions spanned C_t values from 22 to 37, corresponding to ≈2×10^0 to 1.8×10^5 copies. We amplified triplicate samples at each dilution by using the multiplex PCR pools. Next, we pooled, barcoded, and made libraries from amplicons of each sample by using the ligation-based kit and PCR barcode expansion kit (Appendix). MinION sequencing was performed on an R9.4.1 or R10.3 flow cell (Oxford) until we obtained >1–2 million raw reads. From those reads, 50%–60% of them could be demultiplexed. In

Table 1. Genome consensus accuracy for sequencing severe acute respiratory syndrome coronavirus 2*

Virus titer (cycle threshold)	% Coverage, 20×†	Indels	Indel bases	Single-nucleotide polymorphisms	% Identity†
22.3	99.659	0	0	0	100
	99.722	0	0	0	100
	99.635	0	0	0	100
25.7	99.635	0	0	0	100
	99.615	0	0	0	100
	99.642	0	0	0	100
29.2	99.508	0	0	0	100
	99.635	0	0	0	100
	99.615	0	0	0	100
33.2	93.024	1	1	0	100
	93.603	2	35	0	100
	87.894	0	0	0	100
35.6	41.653	1	1	0	100
	51.266	0	0	1	99.993
	50.821	1	15	2	99.987
37.6	14.634	0	0	1	99.977
	9.317	0	0	0	100
	12.363	0	0	0	100

*Because the 5′ and 3′ ends are primer sequences, 100% coverage is not possible.
†Percentage of covered bases identical to reference sequence, excludes indels and low-coverage bases.

addition, we sequenced these amplicons by using the Illumina MiSeq for comparison (Appendix).

For MinION sequencing, the reads were basecalled and analyzed by using an in-house read mapping pipeline (Appendix). For samples with C_t ≤29, we obtained >99% SARS-CoV-2 reads and >99% genome coverage at 20× depth, decreasing to an average of 93% genome coverage at C_t 33.2 and 48% at C_t 35 (Figure 1, panels A, B). Furthermore, we were able to obtain full genomes at >20× reading depth within the first 40–60 min of sequencing (Figure 1, panel C).

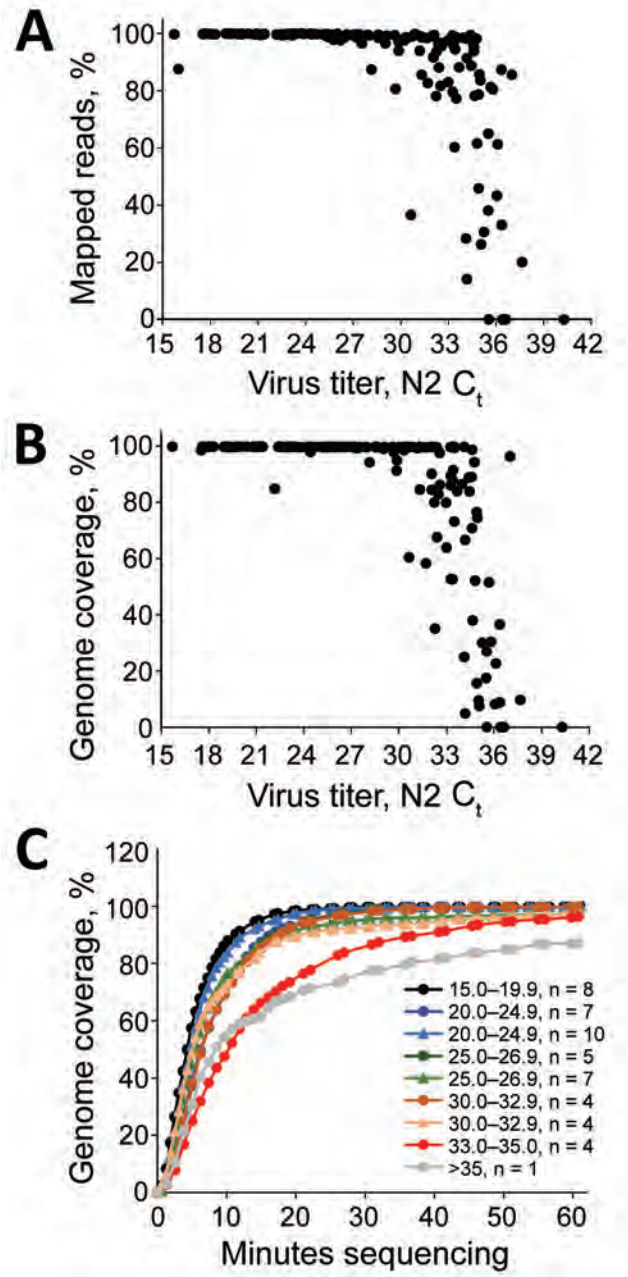

Figure 2. Sequencing of severe acute respiratory syndrome coronavirus 2 clinical samples. A, B) Percentage mapped (A) and percentage genome coverage (B) for 167 clinical severe acute respiratory syndrome coronavirus 2 samples amplified by using a multiplex PCR strategy and sequenced on the MinION apparatus (https://nanoporetech.com). C) Time-lapse of 20× genome coverage obtained for clinical specimens at the indicated cycle threshold values. Data points indicate average coverage over time for various samples and grouped by run and the indicated C_t values. C_t, cycle threshold; N2, nucleoprotein 2.

Consensus accuracy, including single-nucleotide polymorphisms and indels, is critical for determining coronavirus lineage and transmission networks. For high-consensus–level accuracy, we filtered reads based on length, mapped them to the reference sequence (GenBank accession no. RefSeq NC_045512), trimmed primers based on position, and called variants with Medaka (https://github.com) (Appendix). Each Medaka variant was filtered by coverage depth (>20×) and by the Medaka model-derived variant quality (>30). We used the variant quality score as a heuristic to filter remaining noise from the Medaka variants compared with Sanger-derived sequences. After these steps, the data approaches 100% consensus accuracy (Table 1). Identical results were found by using the R9.4.1 pore through samples with C_t values through 33.2. The larger deletions in some of the samples with C_t values >33.2 (Table 1) do not appear to be sequencing errors because they are also detected as minor populations within higher-titer samples.

In the MiSeq data, we observed a similar trend in percent genome coverage at 100× depth, and a slightly lower percentage mapped reads compared with Nanopore data (Figure 1, panels A, B). Increased read depth using the MiSeq potentially enables increased sample throughput. However, the number of available unique dual indices limits actual throughput.

For the nested, singleplex PCR panel, we amplified the same serial dilutions with each nested primer set (Appendix). The endpoint dilution for full-genome coverage is a C_t ≈35 (Figure 1, panel B). At the C_t 37 dilution, we observed major amplicon dropout; at this dilution, there are <10 copies of the genome on average/reaction.

These protocols enabled rapid sequencing of initial clinical cases of infection with SARS-CoV-2 in the United States. For these cases, we amplified the virus genome by using the singleplex PCR and sequenced the amplicons by using the MinION and Sanger instruments to validate MinION consensus accuracy. The MinION produced full-length genomes in <20 min of sequencing, and Sanger data was available the following day.

We used the multiplex PCR strategy for subsequent SARS-CoV-2 clinical cases (n = 167) with C_t values ranging from 15.7 to 40 (mean 28.8, median

Table 2. Comparison of input, time, and cost requirements for sequencing 1 or 96 specimens of severe acute respiratory syndrome coronavirus 2

		1 sample		96 samples	
Method	Input, μL*	Turnaround time	Approximate cost/sample†	Turnaround time	Approximate cost/sample†
Multiplex/MinION	10	6–8 h	$528.70	8–10 h	$35.88
Multiplex/MiSeq	10	30–68 h‡	$1,443.29	30–68 h‡	$57.87
Singleplex/Sanger	190	16–18 h	$354.40	17–19 d	$354.40

*Assumes a process with 200 μL of resuspended respiratory specimen (from a total of 2 mL), extracted, and eluted into 100 μL. See Appendix (https://wwwnc.cdc.gov/EID/article/26/10/20-1800-App1.pdf) for details.
†Includes specific enzyme and reagent costs; excludes common laboratory supplies and labor costs.
‡Varies according to the sequencing kit used.

29.1). In cases with a C_t <30, we observed an average of 99.02% specific reads and 99.2% genome coverage at >20× depth (Figure 2, panels A, B). Between C_t 30 and 33, genome coverage varied by sample, and decreased dramatically at higher C_t values, analogous to the isolate validation data. For these samples, we multiplexed 20–40 barcoded samples/flowcell. Enough data are obtained with 60 min of MinION sequencing for most samples, although for higher titer samples, 10–20 min of sequencing is sufficient (Figure 2, panel C).

Up-to-date primer sequences, protocols, and analysis scripts are available on GitHub (https://github.com/CDCgov/SARS-CoV-2_Sequencing/tree/master/protocols/CDC-Comprehensive). Data from this study is deposited in the National Center for Biotechnology Information Sequence Read Archive (BioProjects PRJNA622817 and PRJNA610248).

Conclusions

Full-genome sequencing is a critical tool in understanding emerging viruses. Initial sequencing of SARS-CoV-2 showed limited genetic variation (*9,10*). However, some signature variants have been useful for describing the introduction and transmission dynamics of the virus (*11*; T. Bedford et al., unpub. data, https://doi.org/10.1101/2020.04.02.20051417; X. Deng et al., unpub. data, https://doi.org/10.1101/2020.03.27.20044925; M. Worobey et al., unpub. data, https://doi.org/10.1101/2020.05.21.109322).

We provide 2 validated PCR target-enrichment strategies that can be used with MinION, MiSeq, and Sanger platforms for sequencing SARS-CoV-2 clinical specimens. These strategies ensure that most laboratories have access to ≥1 strategies.

The multiplex PCR strategy is effective at generating full genome sequences up to C_t 33. The singleplex, nested PCR is effective up to C_t 35, varying based on sample quality. The turnaround time for the multiplex PCR MinION protocol is ≈8 hours from nucleic acid to consensus sequence and that for Sanger sequencing is ≈14 18 hours (Table 2). The multiplex PCR protocols offer an efficient, cost-effective, scalable system, and add little time and complexity as sample numbers increase (Table 2). Results from this study suggest multiplex PCR might be used effectively for routine sequencing, complemented by singleplex, nested PCR for low-titer virus samples and confirmation sequencing.

Acknowledgments

We thank the Respiratory Viruses Branch, Division of Viral Disease, National Center for Immunization and Respiratory Diseases, Centers for Disease Control and Prevention, for helping in organizing samples used in this study.

About the Author

Dr. Paden is a virologist and bioinformatician in the Division of Viral Diseases, National Center for Immunization and Respiratory Diseases, Centers for Disease Control and Prevention, Atlanta, GA. His primary research interest is identifying and characterizing novel and emerging pathogens.

References

1. Holshue ML, DeBolt C, Lindquist S, Lofy KH, Wiesman J, Bruce H, et al.; Washington State 2019-nCoV Case Investigation Team. First case of 2019 novel coronavirus in the United States. N Engl J Med. 2020;382:929–36. https://doi.org/10.1056/NEJMoa2001191
2. Patel A, Jernigan DB, Abdirizak F, Abedi G, Aggarwal S, Albina D, et al.; 2019-nCoV CDC Response Team. Initial public health response and interim clinical guidance for the 2019 novel coronavirus outbreak—United States, December 31, 2019–February 4, 2020. MMWR Morb Mortal Wkly Rep. 2020;69:140–6. https://doi.org/10.15585/mmwr.mm6905e1
3. Wang C, Horby PW, Hayden FG, Gao GF. A novel coronavirus outbreak of global health concern. Lancet. 2020; 395:470–3. https://doi.org/10.1016/S0140-6736(20)30185-9
4. World Health Organization. Coronavirus disease 2019 (COVID-19) situation report 141 [cited 2020 Jun 9]. https://www.who.int/emergencies/diseases/novel-coronavirus-2019/situation-reports
5. Quick J, Grubaugh ND, Pullan ST, Claro IM, Smith AD, Gangavarapu K, et al. Multiplex PCR method for MinION and Illumina sequencing of Zika and other virus genomes directly from clinical samples. Nat Protoc. 2017;12:1261–76. https://doi.org/10.1038/nprot.2017.066

6. Quick J, Loman NJ, Duraffour S, Simpson JT, Severi E, Cowley L, et al. Real-time, portable genome sequencing for Ebola surveillance. Nature. 2016;530:228–32. https://doi.org/10.1038/nature16996
7. Holmes EC, Novel YZ. 2019 coronavirus genome, 2020 [cited 2020 Apr 5]. http://virological.org/t/novel-2019-coronavirus-genome/319
8. COVID-19 Investigation Team. Clinical and virologic characteristics of the first 12 patients with coronavirus disease 2019 (COVID-19) in the United States. Nat Med. 2020;26:861–8. https://doi.org/10.1038/s41591-020-0877-5
9. Andersen K. Clock and TMRCA based on 27 genomes, 2020 [cited 2020 Jan 25]. http://virological.org/t/clock-and-tmrca-based-on-27-genomes/347
10. Lu R, Zhao X, Li J, Niu P, Yang B, Wu H, et al. Genomic characterisation and epidemiology of 2019 novel coronavirus: implications for virus origins and receptor binding. Lancet. 2020;395:565–74. https://doi.org/10.1016/S0140-6736(20)30251-8
11. Andersen KG, Rambaut A, Lipkin WI, Holmes EC, Garry RF. The proximal origin of SARS-CoV-2. Nat Med. 2020;26:450–2. https://doi.org/10.1038/s41591-020-0820-9

Address for correspondence: Suxiang Tong, Centers for Disease Control and Prevention, 1600 Clifton Rd NE, Mailstop H18-6, Atlanta, GA 30329-4027, USA; email: sot1@cdc.gov

Effect of Nonpharmaceutical Interventions on Transmission of Severe Acute Respiratory Syndrome Coronavirus 2, South Korea, 2020

Sukhyun Ryu, Seikh Taslim Ali, Cheolsun Jang, Baekjin Kim, Benjamin J. Cowling

We analyzed transmission of coronavirus disease outside of the Daegu-Gyeongsangbuk provincial region in South Korea. We estimated that nonpharmaceutical measures reduced transmissibility by a maximum of 33% without resorting to a strict lockdown strategy. To optimize epidemic control, continuous efforts to monitor the transmissibility are needed.

Infection with severe acute respiratory syndrome coronavirus 2 (SARS-CoV-2) was identified in South Korea on January 20, 2020 (*1*). By April 21, 2020, a total of 10,683 cases of coronavirus disease (COVID-19) in South Korea had been confirmed and 237 persons had died (*2*) (Figure 1, panel A). A large number of COVID-19 cases and deaths resulted from superspreading events in the Daegu-Gyeongsangbuk provincial region of South Korea (Figure 1, panel B). On February 23, 2020, during the early phase of the outbreak as the number of COVID-19 cases increased, public health authorities in South Korea raised the infectious disease alert to its highest level (*3*). Subsequently, enhanced screening and testing in the community (operation of drive-through screening centers and designation of private hospitals where COVID-19 screening testing was available) were implemented (*4*,*5*).

On April 19, 2020, public health authorities in South Korea started to relax social distancing measures, which had been implemented on March 21, 2020; as of April 21, 2020, the COVID-19 epidemic in South Korea had been contained. Recent studies have examined how public health interventions can contain COVID-19 outbreaks (*6*,*7*). However, in the absence of information on public health measures against transmission of SARS-CoV-2 in South Korea, we estimated the transmissibility of SARS-CoV-2 and evaluated the effects of the public health measures implemented outside the Daegu-Gyeongsangbuk provincial region in South Korea.

Author affiliations: Konyang University College of Medicine, Daejeon, South Korea (S. Ryu, C. Jang, B. Kim); The University of Hong Kong, Hong Kong, China (S.T. Ali, B.J. Cowling)

DOI: https://doi.org/10.3201/eid2610.201886

The Study

We collected data published by local public health authorities in South Korea, including the city or provincial departments of public health. The data comprised date of exposure; date of illness onset; and the source of infection, including contact history and demographic characteristics (e.g., patient birth year and sex). We extracted these line list data of cases by using an electronic data-extraction form. We divided the study into 2 periods, before and after the declaration of highest public alert: period 1 (January 20–February 23, 2020) and period 2 (February 24–April 21, 2020). We restricted our analysis to all other regions in South Korea that excluded Daegu-Gyeongsangbuk provincial region, where there were superspreading events and the data have not been made publicly available (*8*). Over the entire 3-month study period (January 20–April 21, 2020), data were collected for 2,023 cases, which accounted for 98% of the 2,066 reported cases from the South Korea Ministry of Health and Welfare.

The median case-patient age was 42 (range 1–102) years, and 820 (41%) case-patients were male (Table). We analyzed the statistical differences in patient age and sex between periods 1 and 2 by using the χ^2 test but did not identify any significant differences. The proportion of cases imported from Daegu-Gyeongsangbuk provincial regions was 31% in period 1 and

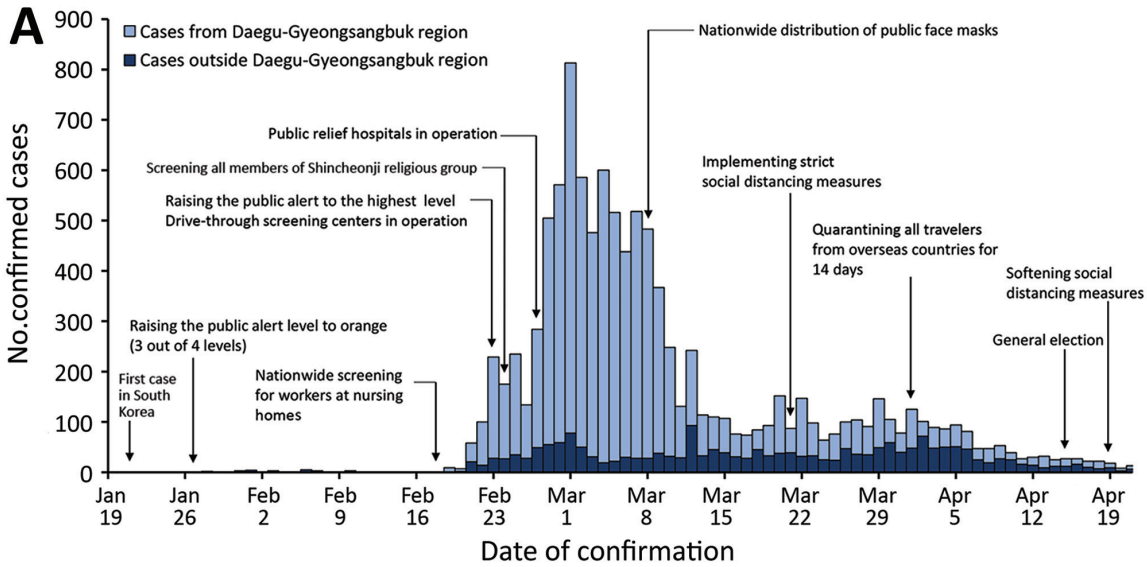

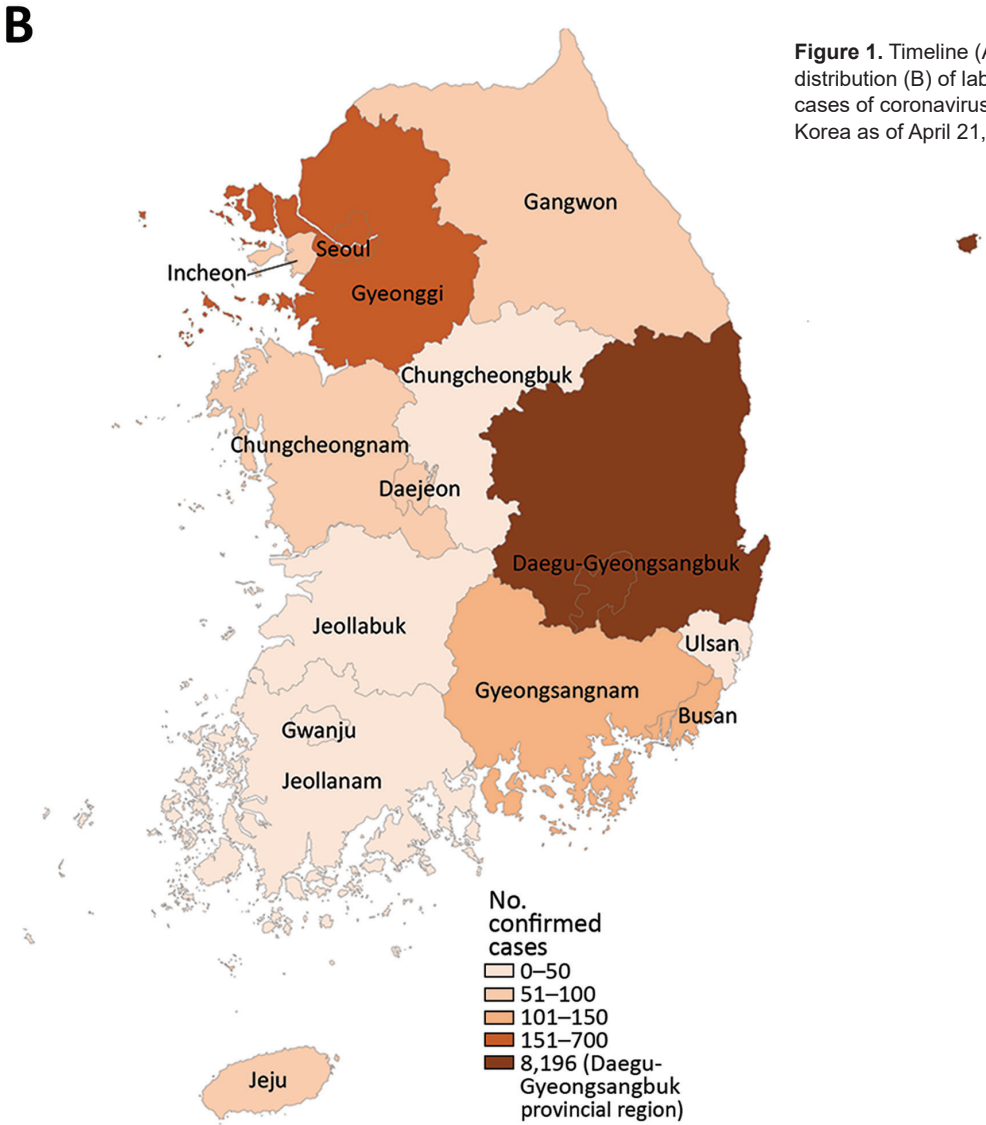

Figure 1. Timeline (A) and geographic distribution (B) of laboratory-confirmed cases of coronavirus disease in South Korea as of April 21, 2020.

Table. Demographic characteristics of 2,023 persons with confirmed cases of coronavirus disease, from publicly available data on April 21, 2020, South Korea, outside of Daegu-Gyeongsangbuk provincial region*

Characteristic	All, no. (%)	Period 1, no. (%)†	Period 2, no. (%)‡
Age group, y			
0–19	123 (6)	11 (5)	112 (6)
20–39	715 (35)	104 (50)	611 (34)
40–59	619 (31)	50 (24)	569 (31)
60–79	295 (15)	37 (18)	258 (14)
≥80y	50 (3)	6 (3)	44 (2)
Unknown	221 (11)	0	221(12)
Sex			
M	820 (41)	107 (56)	713 (39)
F	953 (47)	100 (43)	853 (47)
Unknown	250 (12)	1 (1)	249 (14)
Type of transmission§			
Local	892 (44)	116 (55)	776 (43)
Imported from Daegu-Gyeongsangbuk	155 (8)	65 (31)	90 (5)
Imported from abroad	552 (27)	16 (8)	536 (30)
Cases occurring in large clusters	424 (21)	11 (5)	413 (23)

*Assignment to period was based on date of symptom onset. If cases were asymptomatic or date of symptom onset date was not reported, we used the date of case confirmation.
†Jan 20–Feb 23, 2020; n = 208.
‡Feb 24–Apr 21, 2020; n = 1,815.
§Source of infection is provided for all cases; if not identified, we considered the case to have occurred by local transmission.

decreased to 5% in period 2. However, during the same periods, the proportion of cases imported from abroad and cases occurring in large clusters increased from 8% to 30% and from 5% to 23%.

We analyzed the time interval between illness onset and laboratory confirmation for 818 symptomatic case-patients. We estimated the mean time interval from symptom onset to confirmation of COVID-19 during periods 1 and 2 by fitting 3 parametric distributions (Weibull, gamma, and log-normal) and based our selection of best fit on the Akaike information criterion (*9*). We found the log-normal distribution to be the best fit for this time interval, with a mean of 4.6 (95% CI 0.0–12.4) for period 1 and a substantial reduction to 3.4 (0.0–9.0) for period 2 (Appendix, https://wwwnc.cdc.gov/EID/article/26/10/20-1886-App1.pdf).

To estimate the incubation period, we analyzed data from 181 case-patients for whom precise contact history with other confirmed case-patients was known. The incubation period was estimated by fitting 3 parametric distributions and best fitted by the log-normal distribution; the overall estimated median incubation period was 4.7 (95% CI 0.1–15.6) days (Appendix). We identified 44 clusters of infection and 79 case-patients who had had clear exposure to only 1 index case-patient among these clusters (Appendix). Overall, serial intervals were negative for 8 of the 79 transmission pairs. We estimated the serial interval distribution by fitting a normal distribution to all 79 observations (*10*). We estimated a mean (± SD) serial interval to be 3.9 (± 4.2) days (Appendix).

In mid-February 2020, the number of cases rapidly increased; the largest proportion of cases was among persons who had been infected in Daegu-Gyeongsangbuk provincial region and traveled to other regions of South Korea (Figure 2, panel A). To investigate the effectiveness of nonpharmaceutical interventions implemented in South Korea (Appendix), we estimated the instantaneous effective reproduction number (R_t), a real-time measure of transmission intensity, from daily onset of cases and our estimated serial interval distribution by using the EpiEstim package in R (*11*,*12*). R_t is defined as the mean number of secondary infections per primary case with illness onset at time *t*; R_t<1 indicates that the epidemic is under control.

We present the daily estimates of R_t from February 16, 2020, because the stable estimate of R_t was not available due to the low number of confirmed cases (Figure 2, panel B). At the end of period 1, on February 21, mean R_t peaked at 2.53 (95% credible interval [CrI] 1.90–3.25) and then started to decline faster to <1 by February 29. R_t further declined and remained at <1 during the rest of period 2, indicating the potential effect of nonpharmaceutical interventions implemented over time (Figure 2, panel B). Specifically, mean R_t was 2.03 (CrI 1.89–2.17) before the 1-week period when the declared public alert was at the highest level and reduced to 1.37 (CrI 1.27–1.47) in the following 1-week period, corresponding to a 32.59% (95% CI 23.78%–41.41%) reduction in transmissibility. Similarly, along with the high public alert, the implementation of strict social distancing measures on March 12, 2020, was

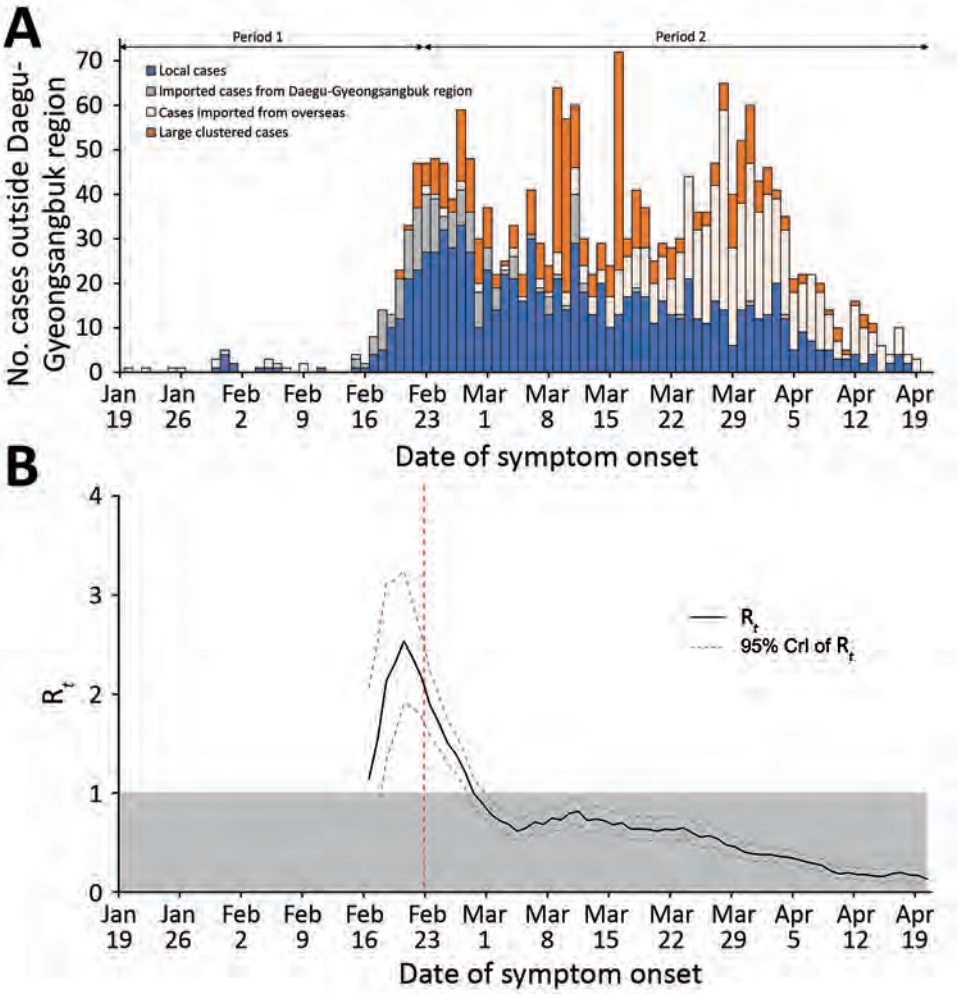

Figure 2. Incidence and estimated daily effective reproductive number (R_t) of coronavirus disease in regions outside of Daegu-Gyeongsanbuk provincial region, South Korea, as of April 21, 2020. A) The epidemic curve shows the daily number of patients with confirmed cases and symptom onset. For case-patients who did not report any symptoms on the date of case confirmation (n = 1,205 cases; 60% of total), the date of confirmation was plotted instead. B) Daily estimated R_t and 95% CrI of R_t; shading indicates the area below the epidemic threshold of R_t = 1. The vertical dashed line indicates the start of the highest public alert on February 23, 2020. CrI, credible interval.

associated with an R_t reduction of an additional 9.75% (95% CI 7.23%–12.29%).

Conclusions

Combined nonpharmaceutical interventions, including enhanced screening and quarantining of persons with suspected and confirmed cases and social distancing measures, were implemented over time. Our results suggest that those interventions, without a lockdown, reduced the transmissibility of SARS-CoV-2 in regions outside of the Daegu-Gyeongsangbuk provincial region, in South Korea.

Our study has some limitations. First, in our analysis of the changes of transmissibility of SARS-CoV-2, we did not include the large clustered cases reported as superspreading events because in these large clusters, the reporting date may not be a good proxy for the date of infection and would overestimate R_t (*13*). Second, it is uncertain how many cases were still undetected. This proportion may potentially mislead the actual time trends of number of infections in the population. Third, we based our estimation of time delay on self-reported data, which are not free from reporting (recall) bias. Fourth, government-generated data, including dates of symptom onset, were not available; therefore, we retrieved online case reports, which could have resulted in some inaccuracies in the information used in our analyses. However, the daily numbers of confirmed cases from the collected line list we used was similar to the numbers in the official daily reports (Appendix).

Our findings suggest that the nonpharmaceutical interventions implemented in South Korea during the COVID-19 outbreak effectively reduced virus transmissibility and suppressed local spread. However, the population of South Korea is still susceptible to further outbreaks or epidemic waves. Because social distancing measures will be relaxed while opportunities for importation of infections from abroad continue, ongoing monitoring of the effective reproductive number can provide relevant information to help policymakers control a potential second wave of COVID-19.

Acknowledgments

We appreciate the South Korea public health authorities' response to COVID-19.

About the Author

Dr. Ryu is an assistant professor of preventive medicine at Konyang University, Daejeon, South Korea. His research interests include infectious disease epidemiology with a focus on public health interventions.

References

1. Ryu S, Chun BC; Korean Society of Epidemiology 2019-nCoV Task Force Team. An interim review of the epidemiological characteristics of 2019 novel coronavirus. Epidemiol Health. 2020;42:e2020006. https://doi.org/10.4178/epih.e2020006
2. Korea Centers for Disease Control and Prevention. The updates of COVID-19 in Republic of Korea. 2020 [cited 2020 Apr 28]. https://www.cdc.go.kr/board/board.es?mid=a30402000000&bid=0030
3. Kim I, Lee J, Lee J, Shin E, Chu C, Lee SK. KCDC risk assessments on the initial phase of the COVID-19 0utbreak in Korea. Osong Public Health Res Perspect. 2020;11:67–73. https://doi.org/10.24171/j.phrp.2020.11.2.02
4. Kwon KT, Ko JH, Shin H, Sung M, Kim JY. Drive-through screening center for COVID-19: a safe and efficient screening system against massive community outbreak. J Korean Med Sci. 2020;35:e123. https://doi.org/10.3346/jkms.2020.35.e123
5. Korean Ministry of Health and Welfare. List of public relief hospitals [in Korean] [cited 2020 May 15]. https://www.mohw.go.kr/react/popup_200128.html
6. Zhang J, Litvinova M, Wang W, Wang Y, Deng X, Chen X, et al. Evolving epidemiology and transmission dynamics of coronavirus disease 2019 outside Hubei Province, China: a descriptive and modelling study. Lancet Infect Dis. 2020;S1473-3099(20)30230-9. https://doi.org/10.1016/S1473-3099(20)30230-9
7. Cowling BJ, Ali ST, Ng TWY, Tsang TK, Li JCM, Fong MW, et al. Impact assessment of non-pharmaceutical interventions against coronavirus disease 2019 and influenza in Hong Kong: an observational study. Lancet Public Health. 2020;5:e279–88. https://doi.org/10.1016/S2468-2667(20)30090-6
8. COVID-19 National Emergency Response Center, Epidemiology & Case Management Team, Korea Centers for Disease Control & Prevention; COVID-19 National Emergency Response Center, Epidemiology and Case Management Team, Korea Centers for Disease Control and Prevention. Coronavirus disease-19: the first 7,755 cases in the Republic of Korea. Osong Public Health Res Perspect. 2020;11:85–90. https://doi.org/10.24171/j.phrp.2020.11.2.05
9. Akaike H. Information theory and an extension of the maximum likelihood principle. In: Parzen E, Tanabe K, Kitagawa G, editors. Selected papers of Hirotugu Akaike. New York, NY: Springer New York; 1998. p. 199–213.
10. Du Z, Xu X, Wu Y, Wang L, Cowling BJ, Meyers LA. Serial interval of COVID-19 among publicly reported confirmed cases. Emerg Infect Dis. 2020;26:1341–3. https://doi.org/10.3201/eid2606.200357
11. Cori A, Ferguson NM, Fraser C, Cauchemez S. A new framework and software to estimate time-varying reproduction numbers during epidemics. Am J Epidemiol. 2013;178:1505–12. https://doi.org/10.1093/aje/kwt133
12. Thompson RN, Stockwin JE, van Gaalen RD, Polonsky JA, Kamvar ZN, Demarsh PA, et al. Improved inference of time-varying reproduction numbers during infectious disease outbreaks. Epidemics. 2019;29:100356. https://doi.org/10.1016/j.epidem.2019.100356
13. Leung K, Wu JT, Liu D, Leung GM. First-wave COVID-19 transmissibility and severity in China outside Hubei after control measures, and second-wave scenario planning: a modelling impact assessment. Lancet. 2020;395:1382–93. https://doi.org/10.1016/S0140-6736(20)30746-7

Address for correspondence: Sukhyun Ryu, Department of Preventive Medicine, Konyang University College of Medicine, R707, Myungok-Euihak Gwan, 158, Gwanjeodong-ro, Seogu, Daejeon, South Korea; email: gentryu@onehealth.or.kr

Main Routes of Entry and Genomic Diversity of SARS-CoV-2, Uganda

Daniel Lule Bugembe,[1] John Kayiwa,[1] My V.T. Phan,[1] Phionah Tushabe, Stephen Balinandi, Beatrice Dhaala, Jonas Lexow, Henry Mwebesa, Jane Aceng, Henry Kyobe, Deogratius Ssemwanga, Julius Lutwama, Pontiano Kaleebu, Matthew Cotten

We established rapid local viral sequencing to document the genomic diversity of severe acute respiratory syndrome coronavirus 2 entering Uganda. Virus lineages closely followed the travel origins of infected persons. Our sequence data provide an important baseline for tracking any further transmission of the virus throughout the country and region.

Severe acute respiratory syndrome coronavirus 2 (SARS-CoV-2) (*1*,*2*), the cause of coronavirus disease (COVID-19), has been spreading globally since it was first reported in Wuhan, China, on December 30, 2019 (*3*,*4*), infecting >10 million persons and causing massive disruption of daily lives and substantial economic consequences (*5*). Given the expanding pandemic and the absence of effective vaccines and antiviral drugs, the best strategy to control the spread of SARS-CoV-2 might be testing, contact tracing, and quarantining. Early implementation of diagnostic testing enables contact tracing and quarantining to reduce transmission in the community and can protect limited healthcare resources.

The importation of SARS-CoV-2 into Africa was inevitable given the volume of air travel and movement of tourists, traders, and workers between countries. We document COVID-19 outbreak preparedness and response in Uganda, a landlocked country in East Africa with entry by international flight or overland from bordering countries. The experience in Uganda provides a unique opportunity to follow virus transmission when early strong interventions are applied. We describe the importation of COVID-19 into Uganda and SARS-CoV-2 genomic data acquired from local sequencing efforts.

Author affiliations: UK Medical Research Council–Uganda Virus Research Institute and London School of Hygiene and Tropical Medicine Uganda Research Unit, Entebbe, Uganda (D. Lule Bugembe, B. Dhaala, J. Lexow, D. Ssemwanga, P. Kaleebu, M. Cotten); Uganda Virus Research Institute, Entebbe (J. Kiyawa, P. Tushabe, S. Balinandi, D. Ssemwanga, J. Lutwama, P. Kaleebu); Erasmus Medical Center, Rotterdam, the Netherlands (M.V.T. Phan); Uganda Ministry of Health, Kampala, Uganda (H. Mwebesa, J. Aceng, H. Kyobe); UK Medical Research Council–University of Glasgow Centre for Virus Research, Glasgow, Scotland, UK (M. Cotten)

DOI: https://doi.org/10.3201/eid2610.202575

The Study

Africa's first case COVID-19 was recorded in Egypt on February 14, 2020 (*6*), and as of June 30, a total of 52 countries in Africa had reported cases. In anticipation of COVID-19 entry into Africa, the Uganda Virus Research Institute (UVRI) established SARS-CoV-2 diagnostics capacity in early February. The screening of all international arrivals and quarantine of suspected case-patients began March 19. The first COVID-19 case was detected in a returning traveler on March 21. Immediately after this first case was identified, a ban on international passenger flights was implemented on March 22, followed by a ban on local travel and public gatherings on March 27. After public health officials recognized that international truck drivers arriving with cargo from neighboring countries (primarily Kenya and Tanzania) posed a risk for virus importation, testing of truck drivers was initiated on April 13 at main border entry points (Figure 1) (https://www.health.go.ug/category/events-and-updates/page/4), and as of May 18, entry into Uganda required a negative SARS-CoV-2 test. A timeline shows various measures of public health preparedness and response, including testing activity, the total number of cases in Uganda, cases among truck drivers, and important intervention dates (Appendix Figure 1, https://wwwnc.cdc.gov/EID/article/26/10/20-2575-App1.pdf).

As of June 30, public health officials in Uganda had detected >1,500 cases in the country or at points

[1]These first authors contributed equally to this article.

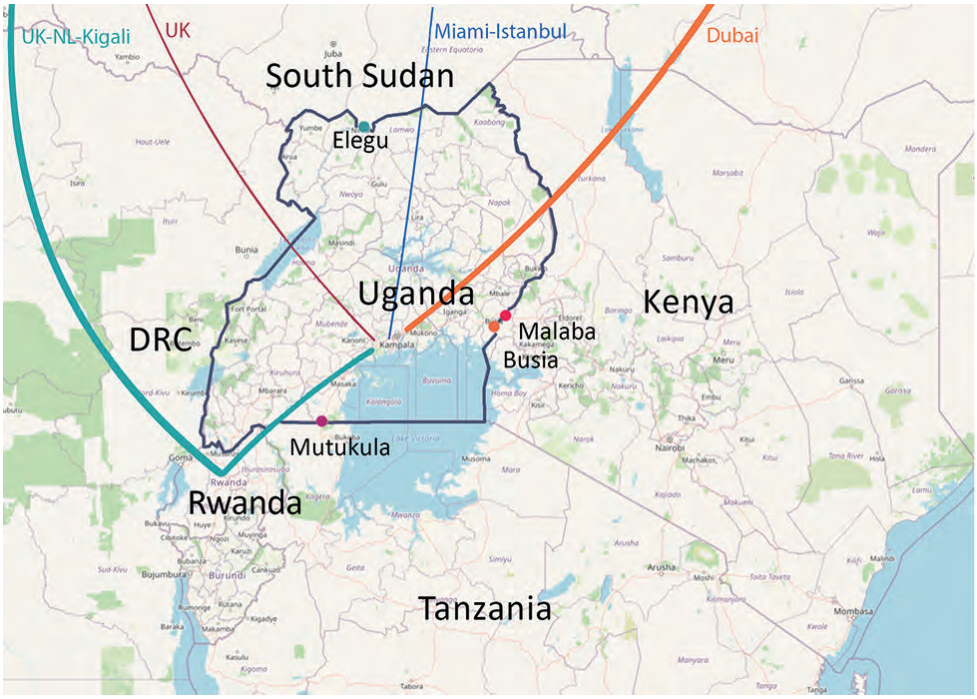

Figure 1. International flight routes of imported cases (colored lines) and the 4 main points of land entry into Uganda from Kenya, Tanzania, and South Sudan (colored dots).

of entry and had conducted >150,000 diagnostics tests. Approximately 2,000 tests per day have been performed at UVRI, which is designated as a Center of Excellence for Evaluation of COVID-19 Diagnostics by the Africa Centres for Disease Control and Prevention, by using real-time reverse transcription PCR assays on respiratory swabs samples from suspected case-patients (*7*). To facilitate virus tracing, we established local sequencing capacity to determine full viral genome sequences from confirmed COVID-19 case-patients.

We report 20 SARS-CoV-2 genomic sequences from Uganda, obtained from 14 persons arriving from regions with circulating SARS-CoV-2 and 6 truck drivers screened at Uganda points-of-entry (Table; Figure 1). This study was approved by the UVRI

Table. Summary characteristics of SARS-CoV-2 genomes obtained from 20 persons entering Uganda*

Genome	GISAID ID†	Sample date	C_t	Patient age, y	Patient travel history	Lineage‡
hCoV-19/Uganda/UG001/2020	EPI_ISL_451183	2020 Mar 23	19	48	Miami to Istanbul	A
hCoV-19/Uganda/UG002/2020	EPI_ISL_451184	2020 Mar 26	19	43	Dubai	A
hCoV-19/Uganda/UG003/2020	EPI_ISL_451185	2020 Mar 27	22	10	UK	B.1.1
hCoV-19/Uganda/UG004/2020	EPI_ISL_451186	2020 Mar 27	18	25	UK to NL to Rwanda	B.1.1.1
hCoV-19/Uganda/UG005/2020	EPI_ISL_451187	2020 Mar 27	18	26	UK to NL to Rwanda	B
hCoV-19/Uganda/UG006/2020	EPI_ISL_451188	2020 Mar 30	23	27	UK to NL to Rwanda	B
hCoV-19/Uganda/UG007/2020	EPI_ISL_451189	2020 Mar 30	21	8	UK to NL to Rwanda	B.1.1.1
hCoV-19/Uganda/UG008/2020	EPI_ISL_451190	2020 Mar 30	22	7	UK to NL to Rwanda	B.1.1.1
hCoV-19/Uganda/UG009/2020	EPI_ISL_451191	2020 Mar 30	20	9	UK to NL to Rwanda	B.1.1.1
hCoV-19/Uganda/UG010/2020	EPI_ISL_451192	2020 Mar 30	22	27	UK to NL to Rwanda	B.1.1.1
hCoV-19/Uganda/UG011/2020	EPI_ISL_451193	2020 Mar 30	21	29	Contact	B.4
hCoV-19/Uganda/UG012/2020	EPI_ISL_451194	2020 Mar 22	24	37	Dubai	A
hCoV-19/Uganda/UG013/2020	EPI_ISL_451195	2020 Mar 22	23	35	Dubai	B
hCoV-19/Uganda/UG014/2020	EPI_ISL_451196	2020 Mar 25	27	31	Dubai	B.1.1.1
hCoV-19/Uganda/UG015/2020	EPI_ISL_451197	2020 Apr 27	16	27	Kenya, by truck	B.1
hCoV-19/Uganda/UG016/2020	EPI_ISL_451198	2020 Apr 27	19	52	Kenya, by truck	B.1
hCoV-19/Uganda/UG017/2020	EPI_ISL_451199	2020 Apr 20	22	42	Tanzania, by truck	A
hCoV-19/Uganda/UG018/2020	EPI_ISL_451200	2020 May 1	28	22	Tanzania, by truck	B.1
hCoV-19/Uganda/UG019/2020	EPI_ISL_451201	2020 Apr 30	29	39	Kenya, by truck	B.1
hCoV-19/Uganda/UG020/2020	EPI_ISL_451202	2020 May 1	25	47	Kenya, by truck	B.1

*C_t, cycle threshold (based on diagnostic real-time reverse transcription PCR; NL, the Netherlands; SARS-CoV-2, severe acute respiratory syndrome coronavirus 2; UK, United Kingdom.
†Virus genomes sequences available from GISAID (https://www.gisaid.org).
‡SARS-CoV-2 lineages determined by using CoV-GLUE (*13*).

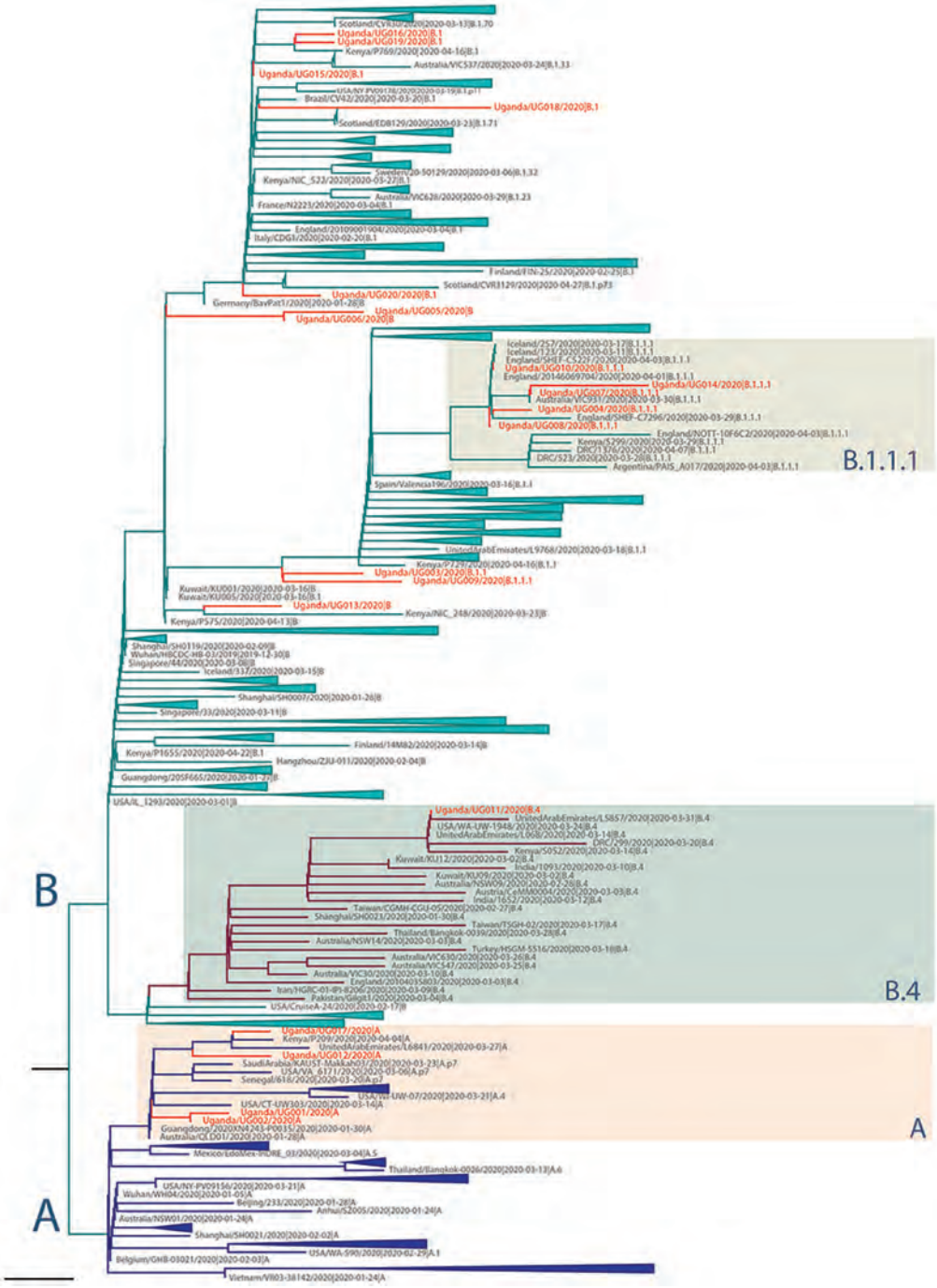

Figure 2. Maximum-likelihood phylogenetic tree of severe acute respiratory syndrome coronavirus 2 (SARS-CoV-2) genomes in Uganda. The full SARS-CoV-2 genomes used for phylogenetic lineage nomenclature (A. Rambaut et al., unpub. data, https://doi.org/10.1101/2020.04.17.046086) as defined on May 19, 2020, were retrieved from GISAID (http://www.gisaid.org) (*8*). Identical sequences were removed, and a total of 395 global representative sequences from each phylogenetic lineage type were selected for further phylogenetic analyses. The reported Uganda sequences, combined with the global SARS-CoV-2 sequences, were aligned by using MAFFT (*9*) and untranslated regions at 5′ and 3′ were trimmed. Maximum-likelihood phylogenetic tree was constructed in RAxML (*10*), under the general time-reversible plus gamma distribution model as best-fitted substitution model determined by IQ-TREE (*11*) and run for 100 pseudo-replicates. The resulting tree was visualized in Figtree (*12*) and rooted at the point of splitting lineage A and B. Scale bar indicates 6×10^{-5} nucleotide substitutions per site. The branch length is drawn to the scale of nucleotide substitutions per site. The Uganda genomes are indicated in red. The 2 major lineages of SARS-CoV-2 (A and B) are indicated to the left of the tree; the main groups of the Uganda genomes (A, B1.1.1, B4) are indicated by colored boxes to the right of the tree.

Research and Ethics Committee (approval no. 00001354, study reference no. GC/127/20/04/771).

We compared the 20 SARS-CoV-2 genomes detected in Uganda with genomes detected globally. The Uganda genomes belonged to phylogenetic lineages A, B, B.1, B.1.1, B.1.1.1, and B.4, among which lineage B.1 has the largest number of sequences that have spread to >20 countries in Europe, the Americas, Asia, and Australia (https://github.com/hCoV-2019/lineages). Genome UG001 (from a traveler arriving from the United States), genomes UG002 and UG012 (from travelers arriving from Dubai), and genome UG017 (from a truck driver from Tanzania) fall within SARS-CoV-2 lineage A (A. Rambaut et al., unpub. data, https://doi.org/10.1101/2020.04.17.046086), with the nearest known genomes occurring in Asia, Australia, Kenya, and the United States (Figure 2). Genome UG011 was from a contact of a Uganda case-patient and is most related to USA/WA-UW-1948 and UnitedArabEmirates/L068 strains within lineage B.4 (Figure 2). Genomes UG004, UG007, UG008, and UG010 were detected in a group of travelers returning from the United Kingdom; these genomes fall within lineage B.1.1.1, which included other United Kingdom–derived genomes (Figure 2). Also in this lineage is genome UG014, detected in a traveler returning from Dubai. Additional sequences from a traveling group (UG005 and UG006) were assigned to lineage B, whereas UG003 (assigned to lineage B.1.1) and UG009 (assigned to lineage B.1.1.1) were closely related to the lineage B.1.1.1, containing genomes from the traveling group in whom genomes UG004, UG007, UG008, and UG010 were detected. Genome UG013 (from a traveler returning from Dubai) belonged to lineage B and was closely related to strains from Asia and Kenya. SARS-CoV-2 genomes identified from returning travelers from Dubai belonged to different lineages (UG002 and UG012 of lineage A, UG013 of lineage B, and UG014 of lineage B.1.1.1), suggesting these travelers contracted the virus from multiple sources despite sharing similar travel routes.

In addition to air traffic, another means of SARS-CoV-2 entry into Uganda is with drivers of cargo trucks entering the country through 4 main entry points from Kenya, Tanzania, and South Sudan (Figure 1). All 4 genomes from truck drivers from Kenya belonged to lineage B.1, whereas genomes from truck drivers from Tanzania belonged to lineage A and B.1 (Table). The truck driver viral genomes did not cluster closely with any current local Uganda genomes, suggesting that these truck drivers contracted the virus outside Uganda, although the sample size is too small for firm conclusions. Careful monitoring and additional sequence data from truck driver and community cases will enable an estimate of the amount of transmission that might occur between truck drivers and the general population of Uganda.

An indication of the current SARS-CoV-2 genomic sequence diversity (Appendix Figure 2) is the single nucleotide changes from the original Wuhan-1 strain (GenBank accession no. NC_045512). The Uganda strains differ at 5–20 positions across the ≈30 kb genome, including a small number of changes in the spike protein–coding region, which is a main target for vaccines. The spike protein showed 1 polymorphism with the lineage A viruses (including 4 Uganda virus sequences), encoding D614, whereas all other clades encoded G614 in the spike protein.

Conclusions

We describe the initial SARS-CoV-2 genomes imported into Uganda. We observed 6 lineages among 20 genomes, which were imported through returning air travelers and truck drivers entering Uganda. We shared all sequences with the public health community by depositing in the GISAID public database (https://www.gisaid.org, accession nos. EPI_ISL_451183–202) (*8*).

Since the governmental ban on international flights was implemented in the last week of March, no further imported COVID-19 cases from international air travelers into Uganda have been reported, underscoring the effectiveness of these policy measures. However, the increasing detection of SARS-CoV-2 in apparently healthy truck drivers is concerning. The quantity of viral RNA levels in some truck driver samples is high (cycle threshold values 16–19), yet these persons were still capable of driving a truck, indicating mild symptoms. This combination of high viral levels and sufficient health to continue normal activities could lead to further spread of the virus within the community without effective quarantine measures. The current efforts to increase community testing and truck drivers contact tracing and quarantine are essential to identify new cases and prevent further spread of the virus in Uganda.

Acknowledgments

We thank all global SARS-CoV-2 sequencing groups for their open and rapid sharing of sequence data and GISAID for providing an effective platform for making these data available. We are grateful to the Oxford Nanopore Technologies and the ARTIC Network for their extensive support with protocols and analysis software. We thank Ana Da Silva Filipe, David Robertson, Richard Orton, and Damien Tully for their support in setting up the MinION

sequencing. We acknowledge the contributions of the Uganda Ministry of Health and its COVID-19 Scientific Advisory Committee, the National COVID-19 Task Force, and the staff of the Emerging and Remerging Infections Department of the Uganda Virus Research Institute, and the US Centers for Disease Control and Prevention.

M.V.T.P. was supported by a Marie Sklodowska-Curie Individual Fellowship, funded by European Union's Horizon 2020 research and innovation program (grant agreement no. 799417). The SARS-CoV-2 diagnostic and sequencing award is jointly funded by the UK Medical Research Council (MRC) and the UK Department for International Development (DFID) under the MRC–DFID Concordat agreement (grant agreement no. NC_PC_19060) and is also part of the European and Developing Countries Clinical Trials Partnership 2 program supported by the European Union. The diagnostics also were supported by the World Health Organization, the US Centers for Disease Control and Prevention, and the Jack Ma Foundation, among others. The Uganda Medical Informatics Centre high performance computer was supported by UK MRC (grant no. MC_EX_MR/L016273/1) to P.K. The study is also supported by a Wellcome Epidemic Preparedness–Coronavirus grant, jointly funded by the Wellcome Trust and UK DFID (grant agreement no. 220977/Z/20/Z) awarded to M.C.

About the Author

Mr. Lule Bugembe is a scientist at the UK Medical Research Council–Uganda Virus Research Institute and London School of Hygiene and Tropical Medicine Uganda Research Unit in Entebbe. His primary research interests include the use of bioinformatics and computational analysis of human host and pathogen genetic data to predict infectious disease trends and help with their control.

References

1. Edward C. Holmes, Yong-Zhen Zhang EC. Initial genome release of novel coronavirus [cited 2020 May 7]. http://virological.org/t/initial-genome-release-of-novel-coronavirus/319
2. Zhu N, Zhang D, Wang W, Li X, Yang B, Song J, et al.; China Novel Coronavirus Investigating and Research Team. A novel coronavirus from patients with pneumonia in China, 2019. N Engl J Med. 2020;382:727–33. https://doi.org/10.1056/NEJMoa2001017
3. Li Q, Guan X, Wu P, Wang X, Zhou L, Tong Y, et al. Early transmission dynamics in Wuhan, China, of novel coronavirus–infected pneumonia. N Engl J Med. 2020;382:1199–207.
4. Yang X, Yu Y, Xu J, Shu H, Xia J, Liu H, et al. Clinical course and outcomes of critically ill patients with SARS-CoV-2 pneumonia in Wuhan, China: a single-centered, retrospective, observational study. Lancet Respir Med. 2020;8:475–81. https://doi.org/10.1016/S2213-2600(20)30079-5
5. Johns Hopkins University Center for Systems Science and Engineering. COVID-19 dashboard. 2020 [cited 2020 May 7]. https://www.arcgis.com/apps/opsdashboard/index.html#/bda7594740fd40299423467b48e9ecf6
6. World Health Organization. COVID-19 cases top 10,000 in Africa. 2020 [cited 2020 May 7]. https://www.afro.who.int/news/covid-19-cases-top-10-000-africa
7. Corman VM, Landt O, Kaiser M, Molenkamp R, Meijer A, Chu DK, et al. Detection of 2019 novel coronavirus (2019-nCoV) by real-time RT-PCR. Euro Surveill. 2020;25:25. https://doi.org/10.2807/1560-7917.ES.2020.25.3.2000045
8. Shu Y, McCauley J. GISAID: global initiative on sharing all influenza data—from vision to reality. Euro Surveill. 2017;22:30494. https://doi.org/10.2807/1560-7917.ES.2017.22.13.30494
9. Katoh K, Standley DM. MAFFT multiple sequence alignment software version 7: improvements in performance and usability. Mol Biol Evol. 2013;30:772–80. https://doi.org/10.1093/molbev/mst010
10. Stamatakis A. RAxML version 8: a tool for phylogenetic analysis and post-analysis of large phylogenies. Bioinformatics. 2014;30:1312–3. https://doi.org/10.1093/bioinformatics/btu033
11. Nguyen L-T, Schmidt HA, von Haeseler A, Minh BQ. IQ-TREE: a fast and effective stochastic algorithm for estimating maximum-likelihood phylogenies. Mol Biol Evol. 2015;32:268–74. https://doi.org/10.1093/molbev/msu300
12. Rambaut A. FigTree. 2019 [cited 2020 May 7]. http://tree.bio.ed.ac.uk/software/figtree
13. Josh B. Singer, Gifford R, Cotten M, Robertson DL. CoV-GLUE project. 2020 [cited 2020 May 7]. http://cov-glue.cvr.gla.ac.uk

Address for correspondence: Matthew Cotten, UK Medical Research Council–Uganda Virus Research Institute and London School of Hygiene and Tropical Medicine Uganda Research Unit, Nakiwogo Rd 51–59, PO Box 49, Entebbe, Uganda; email: matthew.cotten@lshtm.ac.uk

High Proportion of Asymptomatic SARS-CoV-2 Infections in 9 Long-Term Care Facilities, Pasadena, California, USA, April 2020

Matt Feaster, Ying-Ying Goh

Our analysis of coronavirus disease prevalence in 9 long-term care facilities demonstrated a high proportion (40.7%) of asymptomatic infections among residents and staff members. Infection control measures in congregate settings should include mass testing–based strategies in concert with symptom screening for greater effectiveness in preventing the spread of severe acute respiratory syndrome coronavirus 2.

Severe acute respiratory syndrome coronavirus 2 (SARS-CoV-2) is a novel human coronavirus that causes coronavirus disease (COVID-19). The disease was detected in the United States on January 20, 2020, and had caused >1.7 million cases and >100,000 deaths as of June 1, 2020 (*1*,*2*). As the pandemic continues, data consistently show that older adults, particularly those with ≥1 underlying medical conditions, experience higher hospitalization rates and increased vulnerability to in-hospital death (*3*,*4*).

Long-term care facilities (LTCFs) in the United States, including skilled nursing facilities (SNFs) and assisted living facilities (ALFs), are populated by older adults and adults needing residential care for underlying medical conditions who are at increased risk of more severe COVID-19–associated illness (*4*,*5*). ALF residents generally require a limited amount of care, such as help getting dressed or assistance with medications, whereas SNF residents have acute or chronic health conditions, or both, that require 24-hour onsite medical care and often rehabilitative care and therapy.

The city of Pasadena, California, USA, is an independent local public health jurisdiction that has a disproportionately high representation of older adults compared with other southern California local public health jurisdictions. More than 12.0% of Pasadena's population is >70 years of age, compared with 9.1% in Los Angeles County (*6*), and Pasadena has >1,253 licensed SNF beds, which is 2.4 times the rate (per 100,000 residents) of SNF beds as in the Los Angeles County public health jurisdiction (*7*). The Pasadena Public Health Department (PPHD) recognized that this large population of medically fragile adults was at high risk for illness and death from COVID-19 as it spread through California, especially after early reports of nursing facility outbreaks in late February (*8*).

Extensive COVID-19–specific outreach and education efforts with skilled nursing facilities by PPHD staff began in late January 2020. In the second week of March, the PPHD received a report of laboratory-confirmed COVID-19 in a Pasadena resident (not facility-associated); a report of COVID-19 in a LTCF employee was received on March 31. By mid-April, the PPHD had opened investigations for facilities with >1 confirmed COVID-19 case in 14 of 15 SNFs in the city jurisdiction and 3 of 26 ALFs. By the end of April, 19 facilities in Pasadena had completed mandatory facilitywide screenings for SARS-CoV-2 to aid in the investigation and control of COVID-19 transmission.

The Study

Facilitywide testing of staff and residents was completed in all facilities by the end of April, with thousands of test results available by early May. This analysis was restricted to facilities with ≥3 linked cases. Facilities excluded from the analysis had singular cases, non–epidemiology-linked cases, or no reported COVID-19 cases at the time of the initial mass testing. Of the 19 facilities, 9 (8 SNFs and 1 ALF) had evidence

Author affiliation: City of Pasadena Public Health Department, Pasadena, CA, USA

DOI: https://doi.org/10.3201/eid2610.202694

of sustained transmission by investigation within the facility and were included in this analysis. Residents were included if they were listed on the facility's census sheet on the day the investigation was opened. All types of staff, both clinical and nonclinical, were required to participate.

A case-patient was defined as a person with a nasopharyngeal swab specimen that tested positive for SARS-CoV-2 by real-time reverse transcription PCR (rRT-PCR) at a commercial laboratory or the Los Angeles County Public Health Laboratory (Downey, CA, USA). Laboratory results were combined with case investigation data collected by PPHD public health nurses. Symptom data were extracted from case reports compiled during the case investigation (*10*), patient medical records (hospital and physician notes), and facility clinical staff assessments and records for residents. Residents and staff were classified as symptomatic if they had had ≥1 new or worsened signs or symptoms of COVID-19 in the 14 days before nasal swab specimen collection. Persons with subjective fever or temperature >100.0°F (37.8°C), muscle aches, cough, shortness of breath, fatigue, headache, new loss of taste or smell, sore throat, runny nose, nausea or vomiting, diarrhea, low oxygen saturation, or clinical oxygen requirement (as determined by the patient's physician) were classified as symptomatic (*11*).

A total of 1,093 persons (608 residents and 485 staff members) were eligible for rRT-PCR testing for SARS-CoV-2 based on facilitywide testing strategies at the 9 LTCF sites (Table 1). Test results for 85.9% (938/1,093) of the staff and residents were obtained by PPHD, specifically 95.7% (582/608) of residents and 73.6% (356/485) of staff. The overall population (residents and staff) prevalence of SARS-CoV-2 among these 9 facilities was 67.3% (631/938). The overall prevalence of asymptomatic infection among those who tested positive was 40.7% (257/631). The prevalence of SARS-CoV-2 infection among staff involved with direct patient care, such as certified nursing assistants (CNAs), licensed vocational nurses (LVNs), registered nurses (RNs), and other caregivers (68.5%, 150/219) was higher than among those not providing direct patient care, such as activity, dietary, and maintenance workers (48.1%, 25/52). A larger percentage of female staff (62.5%) than male staff (46.5%) functioned in clinical roles. The prevalence of SARS-CoV-2 infection among all residents was 70.1% (408/582); among female residents, the prevalence was 71.4% (237/332), and among male residents, it was 68.4% (171/250). Female residents had a higher rate of asymptomatic infection (51.0%, 121/237) than male residents (47.4%, 81/171).

Varying levels of SARS-CoV-2 prevalence were identified across facilities. The lowest levels were among residents and staff in facility E (30.6% of

Table 1. Demographics and COVID-19 characteristics by staff and residents among long-term care facilities, Pasadena, California, USA, April 2020*

Characteristic	Total eligible	Persons tested	Confirmed COVID-19†	Asymptomatic infection†
Staff	485	356 (73.4)	223 (62.6)	55 (24.7)
Age, y, mean (SD)	443	41.8 (13.3)	42.8 (12.7)	39.8 (14.2)
Sex				
F	328	249 (75.9)	170 (68.3)	39 (22.9)
M	157	107 (68.2)	53 (49.5)	16 (30.2)
Staff role				
Activities	15	9 (60.0)	4 (44.4)	0
Administration	32	26 (81.3)	18 (69.2)	5 (27.8)
Dietary	42	31 (73.8)	16 (51.6)	2 (12.5)
Housekeeping	19	14 (73.7)	8 (57.1)	2 (25.0)
Maintenance	14	12 (85.7)	5 (41.7)	4 (20.0)
CNA	149	115 (77.2)	78 (67.8)	20 (25.6)
LVN	66	46 (70.0)	34 (73.9)	5 (14.7)
RN	34	23 (67.6)	14 (60.9)	3 (21.4)
Other caregiver‡	49	35 (71.4)	24 (68.6)	3 (12.5)
Other/unknown‡	65	45 (69.2)	22 (48.9)	11 (50.0)
Residents	608	582 (95.7)	408 (70.1)	202 (49.5)
Age, y, mean (SD)	603	78.0 (13.3)	78.4 (13.0)	77.1 (13.0)
Sex				
F	347	332 (95.7)	237 (71.4)	121 (51.0)
M	261	250 (95.8)	171 (68.4)	81 (47.4)

*Values are no. (%) except as indicated. CNA, certified nursing assistant; COVID-19, coronavirus disease; LVN, licensed vocational nurse; RN, registered nurse.

†Severe acute respiratory syndrome coronavirus 2 detected on nasopharyngeal swab tested by reverse transcription PCR. Asymptomatic infection includes confirmed COVID-19 cases with no reported typical or atypical symptoms of COVID-19. Percentage with results is equal to the number of persons with laboratory results by the number eligible in the facility. The percentage confirmed includes the number of persons with a positive PCR COVID-19 result by the number of persons with laboratory results.

‡Other caregivers include physical therapists, respiratory therapists, rehabilitation workers, and caseworkers. Others include web developers and marketing personnel.

Table 2. Results from facilitywide testing by facility and association to the facility, Pasadena, California, USA, April 2020*

Category	Total eligible, no.	Persons tested, no. (%)	Confirmed COVID-19, no. (%)	Asymptomatic infection, no. (%)
Total	1,092	938 (85.9)	631 (67.3)	257 (40.7)
Staff	485	356 (73.6)	223 (62.6)	55 (24.7)
Residents	608	582 (95.7)	408 (70.1)	202 (49.5)
Facility A	196	174 (88.8)	123 (70.7)	79 (64.2)
Staff	109	88 (80.7)	46 (52.3)	13 (28.3)
Residents	87	86 (98.9)	77 (89.5)	66 (85.7)
Facility B	87	86 (98.9)	69 (80.2)	27 (39.1)
Staff	35	34 (97.1)	23 (67.6)	4 (17.4)
Residents	52	52 (100)	46 (88.5)	23 (50.0)
Facility C	112	109 (97.3)	90 (82.3)	34 (37.8)
Staff	35	35 (100)	25 (71.4)	6 (24.0)
Residents	77	74 (96.1)	65 (87.8)	28 (43.1)
Facility D	134	122 (91.0)	88 (72.1)	35 (39.8)
Staff	33	26 (78.8)	26 (100)	6 (23.1)
Residents	101	96 (95.0)	62 (64.6)	29 (46.8)
Facility E	98	71 (72.4)	18 (25.4)	9 (50.0)
Staff	62	35 (56.5)	7 (20.0)	2 (28.6)
Residents	36	36 (100)	11 (30.6)	7 (63.6)
Facility F	79	78 (98.7)	67 (85.9)	14 (20.9)
Staff	25	25 (100)	25 (100)	6 (24.0)
Residents	54	53 (98.1)	42 (79.2)	8 (19.0)
Facility G	117	110 (94.0)	76 (69.1)	26 (34.2)
Staff	21	16 (76.2)	16 (100)	3 (18.8)
Residents	96	94 (97.9)	60 (63.8)	23 (38.3)
Facility H	212	148 (69.8)	63 (42.6)	20 (31.7)
Staff	142	87 (61.3)	36 (41.4)	11 (30.6)
Residents	70	61 (87.1)	27 (44.3)	9 (33.3)
Facility I	57	50 (87.7)	37 (74.0)	13 (35.1)
Staff	22	20 (90.9)	19 (95.0)	4 (21.1)
Residents	35	30 (85.7)	18 (60.0)	9 (50.0)

*Results include the percentage of staff and residents who had a severe acute respiratory syndrome coronavirus 2 reverse transcription PCR test result (positive or negative). A positive result was taken as confirmation of COVID-19 infection. Asymptomatic infection was defined as a confirmed COVID-19 infection with no reported typical or atypical symptoms. Percentage of population with test results is equal to the number of persons with test results divided by the number eligible staff/residents in the facility. Percentage of confirmed COVID-19 is equal to the number of persons with a positive test result divided by the number of persons with test results. COVID-19, coronavirus disease.

residents [11/36], 20.0% of staff [7/35]), the highest among residents in facilities A (89.5%, 77/86), B (88.5%, 46/52), and C (87.8%, 65/74) and among staff in facilities D (26/26), F (25/25), and G (16/16) (Table 2). The prevalence of asymptomatic infection among staff members ranged from 17.4% (facility B, 4/23) to 30.6% (facility H, 11/36) (Table 2). The prevalence of asymptomatic infection among residents ranged from 19.0% (facility F, 8/42) to 85.7% (facility A, 66/77) (Table 2).

Conclusions

The ability of SARS-CoV-2 to spread rapidly among residents and staff in congregate settings poses a major infection control challenge. Our findings demonstrate a high proportion of asymptomatic infection, even within moderately affected facilities, and support the use of mass testing-based strategies in concert with symptom screening. Data from the facilitywide screenings indicate that the rate of asymptomatic infection among staff, on average, was 1 in 4, and among residents was 1 in 2.

Early in the COVID-19 pandemic, the supply of both nasopharyngeal swabs and test kits for SARS-CoV-2 rRT-PCR testing in the United States was extremely limited and made available only for symptomatic persons meeting certain criteria determined by the Centers for Disease Control and Prevention (CDC) (*12*). Diagnostic testing remained limited for many weeks, and LTCFs relied on symptom screening to exclude potentially infectious staff from work. On March 30, CDC published a change for the COVID-19 period of exposure risk from onset of symptoms to 48 hours before symptom onset (*13*). This change meant that symptom screening alone could be insufficient in protecting LTCF residents from contracting COVID-19 from asymptomatic, but infectious, staff, and studies have suggested a role for asymptomatic transmission in COVID-19 outbreaks (*14*).

Our findings demonstrate a high prevalence of both symptomatic and asymptomatic COVID-19 infection among residents and staff in 9 LTCFs. Because the potential for asymptomatic transmission of SARS-CoV-2 is concerning, for greater effectiveness, infection control efforts in LTCFs should include both mass testing–based strategies and symptom screening.

About the Authors

Dr. Feaster is the lead epidemiologist for the City of Pasadena Public Health Department, Pasadena, California, USA, and is responsible for communicable disease investigation and chronic disease health assessment for the city of Pasadena. Dr. Goh is the health officer and director for the City of Pasadena Public Health Department.

References

1. Centers for Disease Control and Prevention. Corona virus disease 2019 (COVID-19): cases in the U.S. [cited 2020 Jun 1]. https://www.cdc.gov/coronavirus/2019-ncov/cases-updates/cases-in-us.html
2. Harcourt J, Tamin A, Lu X, Kamili S, Sakthivel SK, Murray J, et al. Severe acute respiratory syndrome coronavirus 2 from patient with coronavirus disease, United States. Emerg Infect Dis. 2020;26:1266–73. https://doi.org/10.3201/eid2606.200516
3. Garg S, Kim L, Whitaker M, O'Halloran A, Cummings C, Holstein R, et al. Hospitalization rates and characteristics of patients hospitalized with laboratory-confirmed coronavirus disease 2019—COVID-NET, 14 states, March 1–30, 2020. MMWR Morb Mortal Wkly Rep. 2020;69:458–64. https://doi.org/10.15585/mmwr.mm6915e3
4. Zhao H, Huang Y, Huang Y. Mortality in older patients with COVID-19. J Am Geriatr Soc. 2020 May 25 [Epub ahead of print]. https://doi.org/10.1111/jgs.16649
5. Centers for Disease Control and Prevention. People who are at higher risk for severe illness [cited 2020 May 27]. https://www.cdc.gov/coronavirus/2019-ncov/need-extra-precautions/people-at-higher-risk.html
6. US Census Bureau. Age and sex: table S0101 [cited 2020 May 27]. https://data.census.gov
7. US Centers for Medicare and Medicaid Services. Nursing home compare; 2020 [cited 2020 May 28]. https://www.medicare.gov/nursinghomecompare/search.html
8. Arons MM, Hatfield KM, Reddy SC, Kimball A, James A, Jacobs JR, et al.; Public Health—Seattle and King County and CDC COVID-19 Investigation Team. Presymptomatic SARS-CoV-2 infections and transmission in a skilled nursing facility. N Engl J Med. 2020;382:2081–90. https://doi.org/10.1056/NEJMoa2008457
9. Centers for Disease Control and Prevention. CDC 2019-novel coronavirus (2019-NCoV) real-time RT-PCR diagnostic panel. 2020 [cited 2020 May 27]. https://www.fda.gov/media/134922/download
10. California Department of Public Health. Communicable disease control forms [cited 2020 May 28]. https://www.cdph.ca.gov/Programs/PSB/Pages/CommunicableDiseaseControl.aspx
11. Centers for Disease Control and Prevention. Symptoms of coronavirus; 2020 [cited 2020 May 27]. https://www.cdc.gov/coronavirus/2019-ncov/symptoms-testing/symptoms.html
12. Centers for Disease Control and Prevention. Updated guidance on evaluating and testing persons for coronavirus disease 2019 (COVID-19) [cited 2020 May 27]. https://emergency.cdc.gov/han/2020/han00429.asp
13. Centers for Disease Control and Prevention. Public health recommendations for community-related exposure; 2020 [cited 2020 May 27]. https://www.cdc.gov/coronavirus/2019-ncov/php/public-health-recommendations.html
14. Furukawa NW, Brooks JT, Sobel J. Evidence supporting transmission of severe acute respiratory syndrome coronavirus 2 while presymptomatic or asymptomatic. Emerg Infect Dis. 2020 Jun 21 [Epub ahead of print]. https://doi.org/10.3201/eid2607.201595

Address for correspondence: Matt Feaster, Pasadena Public Health Department, 1845 N Fair Oaks Ave, Pasadena, CA 91103, USA; email: mfeaster@cityofpasadena.net

Tickborne Relapsing Fever, Jerusalem, Israel, 2004–2018

Saar Hashavya,[1] Itai Gross,[1] Matan Gross, Noa Hurvitz, Giora Weiser, Violeta Temper, Orli Megged

To compare tickborne relapsing fever (TBRF) in children and adults in Jerusalem, Israel, we collected data from the medical records of all 92 patients with TBRF during 2004–2018. The 30 children with TBRF had more episodes of fever and lower inflammatory markers than adult patients.

Tickborne relapsing fever (TBRF), caused by *Borrelia* species bacteria, is transmitted by soft ticks of the genus *Ornithodoros* (*1*,*2*). TBRF is characterized by recurring episodes of fever often accompanied by headache, nausea, vomiting, dyspnea, and joint pain (*3*). Although highly endemic to certain regions of the world, such as West Africa (*4*), Iran (*5*), and Morocco (*6*), TBRF occurs worldwide (*7*,*8*).

In Israel, TBRF is endemic and is caused by *B. persica*, which is transmitted to humans by the *O. tholozani* soft tick (*9*,*10*). TBRF remains challenging to diagnose because of its nonspecific symptoms. To compare TBRF in children and adults, we assessed anamnestic, clinical, and laboratory parameters of persons with TBRF at 3 emergency departments (EDs) in Jerusalem, Israel.

The Study

We reviewed the computerized databases of Hadassah Ein-Kerem Medical Center, Hadassah Mount-Scopus Medical Center, and Shaare Zedek Medical Center for all patients who had a discharge diagnosis of borreliosis (International Classification of Diseases, 10th Revision, code A69.2) during 2004–2018. These hospitals treated most patients in Jerusalem. All patients in the study with thick or thin blood film were positive for spirochetes or had positive results from a *B. persica* homemade Flagellin gene CR (*10*). For thin blood film, 1 µL was used, and for thick blood film, 10 µL. For both films, we used Giemza stain to show *Borrelia*. We completed thin and thick films for all patients with clinically suspected borreliosis. PCR was also routinely performed except for sporadic cases, for which insufficient blood remained the tube after complete blood count and films were conducted.

We defined relapse as recurrence of symptoms and positive laboratory results, after completion of treatment and without new exposures. The information collected comprised demographics (age, ethnicity, and sex); history (visits to caves, exposure to tick bites); duration of fever and number of relapses of fever; incubation period; physical examination findings; laboratory results; and hospitalization data, including length, referral to intensive care unit, and drug treatment. To determine the characteristics of TBRF in children, we compared children <18 years of age with adults.

The Hadassah medical center institutional review board approved this study and provided a consent waiver (approval no. 0345-18-HMO) We used χ^2 tests to compare proportions and Student *t* and Mann-Whitney U tests to compare continuous nonparametric variables, and we considered $p<0.05$ significant. We conducted statistical analysis using SPSS Statistics 21.0 (IBM Inc., https://www.ibm.com).

Illnesses of 92 patients with blood film positive for spirochete or a positive Borrelia persica PCR met the case definition (Table). Forty (43%) patients were admitted to the hospital; the rest were discharged from the ED. The average age (± SD) was 21.3 (±10.9) years; 30 (33%) patients were children <18 years of age. Seventy-five (82%) patients were male (Figure).

Children had an average of 1.71 (95% CI 1.22–2.21) relapses of fever, whereas adults had 0.67 (95% CI 0.5–0.83) relapses ($p<0.01$); 40% of children had >1 relapse. The 2 groups (adults and children) did not differ significantly in terms of need for intensive care unit or hospital admission. Recent cave visits were reported for nearly 83% of patients. Although the difference was not significant, gastrointestinal symptoms (abdominal pain, vomiting, and diarrhea) occurred more often among children than adults (53.3% vs. 35.5; $p = 0.1$).

Author affiliations: Hadassah Medical Center, Jerusalem, Israel (S. Hashavya, I. Gross, M. Gross, V. Temper); Hebrew University, Ein Kerem, Israel (N. Hurvitz); Shaare Zedek Medical Center, Jerusalem (G. Weiser, O. Megged)

DOI: https://doi.org/10.3201/eid2610.181988

[1]These authors contributed equally to this article.

A tick bite mark was the most common finding on physical examination (36.7% of children vs. 27.4% of adults), followed by organomegaly (16.7% vs. 19.4%). Although the difference was not significant, neurologic signs on physical examination were more common among children than adults (13.3% vs. 3.2%).

Platelet counts were higher in children than in adults, and fewer children had thrombocytopenia (Table). C-reactive protein levels were significantly

Table. Characteristics of persons with tickborne relapsing fever, Jerusalem, Israel, 2004–2018*

Variable	Children and adolescents, n = 30	Adults, n = 62	Total, n = 92	p value
Age, y†				
Mean (95% CI)	11.65 (10.3–13.1)	25.97 (23.5–28.5)	21.3 (21.23–21.37)	<0.01
Median (range)	12 (3–18)	22.5 (19–70)	19 (3–70)	
Sex, no. (%)				
M	21 (70.0)	54 (87.1)	75 (81.5)	0.09
F	9 (30)	8 (12.9)	17 (18.5)	
Hospitalization, d				
Mean (95% CI)	2.57 (1.82–3.32)	2.66 (2.31–3.01)	2.63 (2.62–2.64)	0.39
Median (range)	2	2	2	
Mean no. ED visits (95% CI)	1.26 (1.12–1.4)	1.21 (0.99–1.43)	1.231 (1.12–1.34)	0.6
ICU admission, no. (%)	0	2 (3.2)	2 (2.2)	0.45
Treatment with doxycycline, no. (%)	25 (83.3)	61 (98.4)	86 (93.5)	0.09
Jarisch–Herxheimer reaction, no. (%)	4 (13.3)	15 (24.19)	19 (20.7)	0.35
Exposure history				
Cave visits, no. (%)	24 (80.0)	52 (83.9)	76 (82.6)	0.82
Known tick bite, no. (%)	9 (30.0)	21 (33.8)	30 (32.6)	0.88
Mean incubation period, d, (95% CI)	8.41 (6.22–10.6)	9.4 (7.06–11.74)	9.1 (9.05–9.15)	0.61
Fever				
Mean duration before ED visit, d (95% CI)	12.4 (8.53–16.27)	10 (7.31–12.7)	9.76 (9.69–9.85)	0.13
>1 Relapse of fever, no. (%)	12 (40.0)	7 (11.3)	19 (20.6)	<0.01
No. fever episodes at diagnosis				
1	6	31		<0.01
2	10	20		
3	2	4		
4	6	4		
5	4	0		
Missing information	2	3		
Signs and symptoms, no. (%)				
Gastrointestinal	16 (53.3)	22 (35.5)	38 (41.3)	0.1
Respiratory	1 (3.3)	5 (8.1)	6 (6.5)	0.39
Myalgia	8 (26.7)	22 (35.5)	30 (32.6)	0.4
Malaise	11 (36.7)	24 (38.7)	35 (38.0)	0.85
CNS symptoms	19 (63.3)	32 (51.6)	51 (55.4)	0.29
History of shivering	6 (20.0)	19 (30.6)	25 (27.2)	0.29
Organomegaly	5 (16.7)	12 (19.4)	17 (18.5)	0.76
Rash	6 (20.0)	7 (11.3)	13 (14.1)	0.26
CNS signs	4 (13.3)	2 (3.2)	6 (6.5)	0.07
Bite mark, no. (%)	11 (36.7)	17 (27.4)	28 (30.4)	0.36
Laboratory results‡				
Leukocytes, mean 10^9/L (95% CI)	8.65 (7.71–9.59)	9.74 (7.32–12.16)	9.37 (9.35–9.39)	0.13
PMN, mean 10^9/L (95% CI)	5.16 (4.22–6.1)	7.12 (5.34–8.89)	6.45 (9.43–6.47)	<0.01
PMN %, mean (95% CI)	0.58 (0.51–0.64)	0.72 (0.54–0.9)	0.674 (0.67–0.68)	<0.01
Lymphocytes, mean, 10^9/L (± SD)	1.85 (1.39–2.31)	1.23 (0.92–1.54)	1.442 (1.44–1.45)	<0.01
PLT, mean 10^9/L (95% CI)	174.2 (146–203)	136.93 (102.85–171.02)	149.64 (149.13–150.15)	0.04
PLT <150,000, no. (%)	12 (40)	35 (56.5)	47 (51.1)	0.2
Hemoglobin, mean g/dL (95% CI)	11.98 (11.3–12.7)	13.35 (10.03–16.67)	12.88 (12.87–12.89)	<0.01
CRP, median mg/dL (IQR)	7.93 (6.35–9.5)	16.87 (12.67–21.07)	12.2 (5.5–17.8)	<0.01
ESR, median mm/h (IQR)§	53.92 (40.76–67.09)	53.96 (40.53–67.39)	50 (30–75)	0.99
Hyponatremia, no. (%)	9 (30.0)	17 (27.4)	26 (28.2)	0.8
Elevated creatinine level, no. (%)¶	2 (6.7)	13 (21)	15 (16.3)	0.08
Elevated liver enzymes, no. (%)#	0	8 (12.9)	8 (8.7)	0.04

*CNS, central nervous system; CRP, C-reactive protein; ED, emergency department; ESR, erythrocyte sedimentation rate; ICU, intensive care unit; IQR, interquartile range; PLT, platelets; PMN, polymorphonuclear.

†Number of persons in each group were as follows: 2–5 y: 3; 6–9 y: 5; 10–13 y: 10; 14–17 y: 12; 14–17 y: 12; 18–22 y: 31; 23–29 y: 16; 30–45 y: 10; and 46–70 y: 5.

‡Reference ranges: Platelets (10^9/L), 150,000-400,000; C-reactive protein (mg/dL), <0.5; ESR (mm/h) <20.

§Children, n = 13; adults, n = 26.

¶Elevated creatinine levels in comparison to age-adjusted reference (*11*).

#Elevated aspartate transaminase and/or alanine aminotransferase in comparison to age-adjusted reference (*11*).

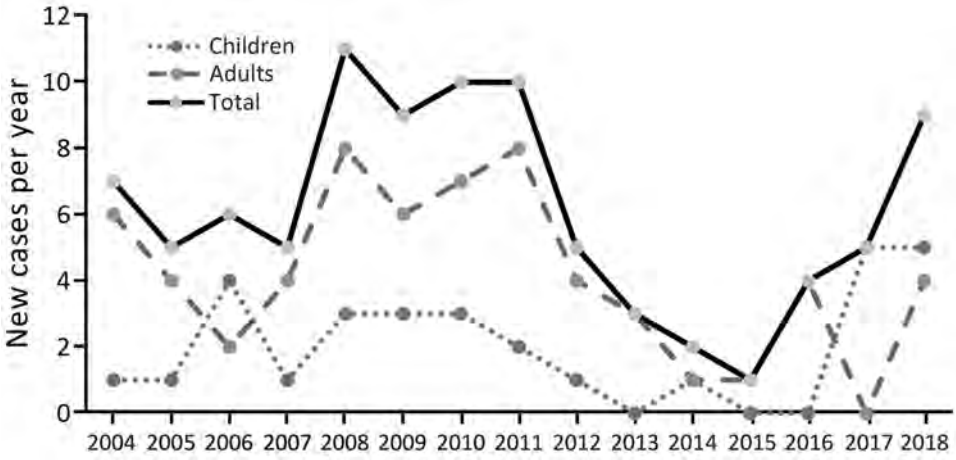

Figure. Annual number of new tickborne relapsing fever cases, Jerusalem, Israel.

lower in children; erythrocyte sedimentation rate and total leukocyte count did not differ significantly between children and adults. The distribution of leukocyte counts differed significantly between the 2 groups: children had a lower neutrophil count and higher lymphocyte count. Children also had a lower percentage of elevated liver enzymes (0% vs. 12.9%; p = 0.04).

Twenty-six children (83%) were treated with doxycycline; 3 received azithromycin (10 mg/kg/d); and 2 received amoxicillin (50 mg/kg/d, divided into 3 daily doses). By contrast, 61 adults (98%) were treated with doxycycline (1 adult treated with ceftriaxone [2 g/day] was discharged with doxycycline). Children treated with doxycycline received 4.4 mg/kg/day, divided into 2 daily doses, and adults received 100 mg 2 times/day. One adult treated with doxycycline had 2 relapses, was re-treated with doxycycline, and recovered fully. All the patients treated with azithromycin recovered. However, illness relapsed in both children treated with amoxicillin; 1 was subsequently treated with azithromycin, and the other was treated with intravenous penicillin and intravenous ceftriaxone and discharged with azithromycin. A Jarisch-Herxheimer reaction occurred in nearly 21% of all patients (Table). All patients fully recovered.

Conclusions

TBRF in children was characterized by more relapsing febrile episodes before medical advice was sought. One possible explanation is that febrile illnesses are more common in children than in adults, which may delay the decision to take a child to the ED or to begin a more thorough investigation in the ED. Gastrointestinal symptoms were reported more commonly in children and were the second most common symptom after fever. Findings of children from Iran who had TBRF were similar (*5*). In our study, no meningeal involvement occurred in the older group of adults; however, 1 child had suspected meningitis (21 cells in his cerebrospinal fluid with negative PCR). The expected rate is 4% in adults but is rare in children (*5*,*7*).

In adults, we found increased levels of C-reactive protein, relatively higher leukocyte counts (in reference to age norms), and higher neutrophil counts than in children. The difference in neutrophil count could be only partially explained by the difference in age-adjusted norms because only 10 children were <10 years. These findings, in addition to longer duration of fever and more relapses that did not require hospitalization, might suggest a milder course of illness in children. A possible explanation is that signs and symptoms tend to appear later in the course of the disease, and TBRF symptoms tend to be milder during relapses (*12*).

The 2 children treated with amoxicillin experienced relapses, whereas only 1 patient treated with doxycycline and none of the patients treated with azithromycin had relapse. Use of doxycycline remains controversial, despite recent reports showing its safety in children (*13*). Consistent with the literature, our findings support the safety and efficaciousness of erythromycin as an alternative treatment for children with TBRF (*5*,*14*).

This study has several limitations. Because of its retrospective design, all parameters were data retrieved from medical charts. The study's small sample size, especially the number of children, hindered identification of other subtle differences between children and adults. Nevertheless, this study provides data on the differences between the manifestations of TBRF in children and adults.

About the Author

Dr. Hashavia is the director of Pediatric Emergency Medicine Hadassah Hospital Ein Kerem. His primary research interests include clinical assessment of infectious disease in pediatric emergency medicine, pediatric trauma, and pediatric emergency medicine. Dr. Gross works in the Department of Pediatric Emergency Medicine, Hadassah Medical Center. His primary research interests include emergency medicine, pediatric trauma, and pediatric infectious diseases.

References

1. Nicholson FD. Tick fever in Palestine. BMJ. 1919;2:811. https://doi.org/10.1136/bmj.2.3077.811
2. Sidi G, Davidovitch N, Balicer RD, Anis E, Grotto I, Schwartz E. Tickborne relapsing fever in Israel. Emerg Infect Dis. 2005;11:1784–6. https://doi.org/10.3201/eid1111.050521
3. Assous MV, Wilamowski A. Relapsing fever borreliosis in Eurasia—forgotten, but certainly not gone! Clin Microbiol Infect. 2009;15:407–14. https://doi.org/10.1111/j.1469-0691.2009.02767.x
4. Trape JF, Diatta G, Arnathau C, Bitam I, Sarih M, Belghyti D, et al. The epidemiology and geographic distribution of relapsing fever borreliosis in West and North Africa, with a review of the *Ornithodoros erraticus complex* (Acari: Ixodida). [Erratum in: PLoS One. 2014;9(1).] PLoS One. 2013;8:e78473. https://doi.org/10.1371/journal.pone.0078473
5. Ayazi P, Mahyar A, Oveisi S, Esmailzadehha N, Nooroozi S. Tick-borne relapsing fever in children in the north-west of Iran, Qazvin. Prague Med Rep. 2015;116:193–202. https://doi.org/10.14712/23362936.2015.58
6. Diatta G, Souidi Y, Granjon L, Arnathau C, Durand P, Chauvancy G, et al. Epidemiology of tick-borne borreliosis in Morocco. PLoS Negl Trop Dis. 2012;6:e1810. https://doi.org/10.1371/journal.pntd.0001810
7. Castilla-Guerra L, Marín-Martín J, Colmenero-Camacho MA. Tick-borne relapsing fever, southern Spain, 2004–2015. Emerg Infect Dis. 2016;22:2217–9.
8. Dworkin MS, Shoemaker PC, Fritz CL, Dowell ME, Anderson DE Jr. The epidemiology of tick-borne relapsing fever in the United States. Am J Trop Med Hyg. 2002;66:753–8. https://doi.org/10.4269/ajtmh.2002.66.753
9. Parola P, Raoult D. Ticks and tickborne bacterial diseases in humans: an emerging infectious threat. Clin Infect Dis. 2001;32:897–928 https://academic.oup.com/cid/article/32/6/897/306927. https://doi.org/10.1086/319347
10. Assous MV, Wilamowski A, Bercovier H, Marva E. Molecular characterization of tickborne relapsing fever Borrelia, Israel. Emerg Infect Dis. 2006;12:1740–3. https://doi.org/10.3201/eid1211.060715
11. Kahl L, Hughes H. The Harriet Lane handbook. Mobile medicine series. 21st ed. Philadelphia: Elsevier; 2017.
12. Brady MT, Jackson MA, Long SS. Redbook 2018 [cited 2008 Dec 26].
13. Gaillard T, Briolant S, Madamet M, Pradines B. The end of a dogma: the safety of doxycycline use in young children for malaria treatment. Malar J. 2017;16:148. https://doi.org/10.1186/s12936-017-1797-9
14. Le CT. Tick-borne relapsing fever in children. Pediatrics. 1980;66:963–6.

Address for correspondence: Itai Gross, Hadassah Medical Center, Ein Karem, 91120, Jerusalem, Israel; email: itaigross@gmail.com

Seawater-Associated Highly Pathogenic *Francisella hispaniensis* Infections Causing Multiple Organ Failure

Hua Zhou,[1] Qing Yang,[1] Lisha Shen, Yake Yao, Jun Xu, Junhui Ye, Xiaomai Wu, Yunsong Yu, Ziqin Li, Jianying Zhou, Shangxin Yang

A rare case of *Francisella hispaniensis* infection associated with seawater exposure occurred in a deep-sea diving fisherman in Zhejiang, China. He had skin and soft tissue infection that progressed to bacteremia and multiple organ failure. Moxifloxacin treatment cleared the infections, but the patient suffered a sequela of heart damage.

Francisella tularensis, the agent of tularemia, is an important human pathogen (*1*). Other *Francisella* species, such as *F. philomiragia*, mainly associated with saltwater exposure, rarely also cause human infections (*2*). *F. hispaniensis*, first isolated from the blood of a patient in Spain (*3*), is an emerging human pathogen, but its epidemiology and pathogenicity remain a mystery because only 2 cases have been reported (*3*,*4*). We report a case of *F. hispaniensis* infection in China.

Case Report

On September 6, 2018, a 64-year-old male fisherman sought care for a prominent cutaneous ulcer on the right lower chest, chest pain, and fever for 16 days and was admitted to The First Affiliated Hospital of Zhejiang University (Hangzhou, China). He was previously healthy without remarkable medical history. He worked as a deep-sea diving fisherman in Sanmen Bay, Taizhou, a coastal city in Zhejiang Province, adjoining the East China Sea. A superficial wound progressed to cellulitis in the right lower chest after a deep-sea dive without protective clothing. Low-grade fever and chest pain then developed. He received amoxicillin/clavulanic acid at a local clinic, and his fever resolved after 2 days. Because he felt better, he stopped taking the amoxicillin/clavulanic acid and resumed deep-sea diving. Two days later, his chest wound had worsened with purulent discharge, and his low-grade fever returned. Twelve days later he sought care at another hospital because of high fever and respiratory distress. He received 2 days of ceftizoxime followed by imipenem for 7 days, but his condition deteriorated, and irritability, chest tightness, nausea, vomiting, abdominal distension, chills, and high fever (39.4°C) developed. At admission to The First Affiliated Hospital of Zhejiang University School of Medicine, he had sepsis, hypotension, and leukocytosis and immediately received norepinephrine intravenous pumping, endotracheal intubation, sedation, mechanical ventilation, and continuous renal replacement therapy. His lower chest showed a large ulcer with bleeding, purulent discharge, and tissue necrosis (Figure 1, panel A). Laboratory test results showed highly elevated inflammatory markers, acidosis, coagulopathy, and elevated liver enzymes, bilirubin, creatinine, and troponin (Table 1). Chest computed tomography scan showed right lower lobe consolidation, pleural effusion in the right thoracic cavity, and multiple calcified lymph nodes in the mediastinum. Abdomen computed tomography

Author affiliations: The First Affiliated Hospital of Zhejiang University School of Medicine, Hangzhou, China (H. Zhou, L. Shen, Y. Yao, J. Xu, J. Zhou); State Key Laboratory for Diagnostic and Treatment of Infectious Diseases, The First Affiliated Hospital of Zhejiang University School of Medicine, Hangzhou (Q. Yang); Sanmen People's Hosptial, Taizhou, China (J. Ye); Taizhou Hospital, Taizhou (X. Wu); Sir Run Run Shaw Hospital of Zhejiang University School of Medicine, Hangzhou (Y. Yu); Zhejiang-California International Nanosystems Institute, Zhejiang University, Hangzhou (Z. Li, S. Yang); UCLA School of Medicine, Los Angeles, California, USA (S. Yang)

DOI: https://doi.org/10.3201/eid2610.190844

[1]These authors contributed equally to this article.

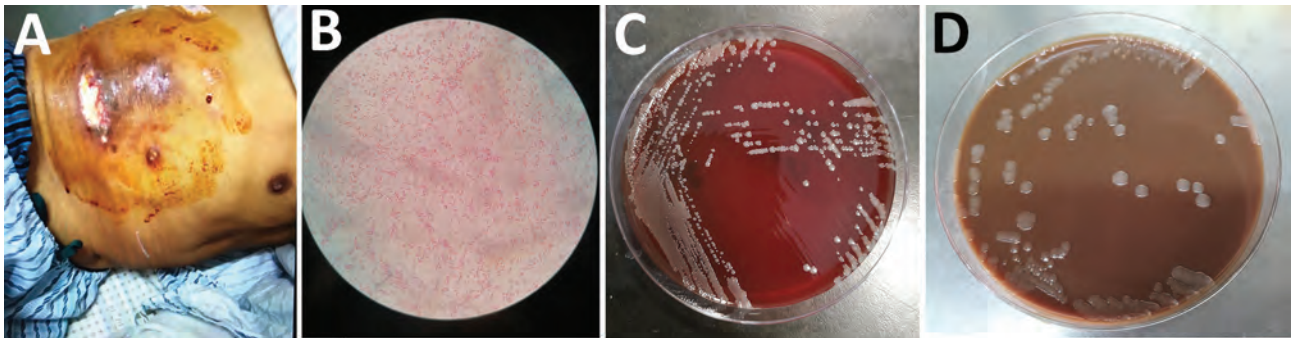

Figure 1. Chest wound of a 64-year-old male fisherman and isolated bacteria morphology, China. A) Ulcer and necrosis in the lower chest. B) Gram-negative cocci isolated from blood and wound. C) Growth on blood agar after 5 days with CO_2. D) Growth on chocolate agar after 5 days with CO_2.

scan showed hepatosplenomegaly and effusion in the abdominal and pelvic cavities. Echocardiography showed decreased left ventricular systolic function and diffuse abnormal movement of left ventricular wall. Electrocardiograph showed cardiac arrhythmia with sinus bradycardia, ventricular premature beats, and paroxysmal ventricular tachycardia. Acute diffuse myocarditis was diagnosed and prompted dobutamine treatment.

Blood, pleural fluid, and wound culture all grew gram-negative cocci (Figure 1, panel B), identified by Vitek2 (bioMérieux, https://www.biomerieux.com) as *Sphingomonas paucimobilis*. The bacteria grew well on the regular sheep blood agar and showed medium-sized, smooth-edged, mucoid and greyish white colonies (Figure 1, panel C). They grew better on chocolate agar (Figure 1, panel D) but did not grow on MacConkey agar. The bacteria were catalase weakly positive, oxidase positive, indole negative, and β-lactamase positive. Because *S. paucimobilis* is usually considered an environmental bacterium and unlikely to cause such severe systemic infections, we sent the patient's blood for shotgun metagenomic sequencing test and the bacterial isolate for whole-genome sequencing (WGS) using Illumina MiniSeq (https://www.illumina.com). Metagenomic sequencing yielded a positive result as *F. tularensis*, but WGS identified *F. hispaniensis*, on the basis of k-mer and single-nucleotide polymorphism phylogenetic tree analyses performed using CLCbio (QIAGEN, https://www.qiagen.com) (Figure 2), which showed the bacteria clustered closely with 2 other *F. hispaniensis* strains (*3*,*4*) and very

Table 1. Blood test results during progression of *Francisella hispaniensis* infection and after treatment of a 64-year-old fisherman with multiple organ failure, China

Blood test (reference range)	Outside hospital, 4 d after fever onset	At admission, 16 d after fever onset	After treatment, 14 d after admission
Leukocytes, cells/mm^3 (4,000–10,000)	16,600	22,800	10,700
Differential count, %			
Neutrophils (50–70)	90.6	81.1	84.2
Lymphocytes (20–40)	5.1	16	8.7
Platelets/mm^3 (83,000–303,000)	174,000	145,000	159,000
Hemoglobin, g/dL (13.1–17.2)	13.4	10.7	6.8
Creatinine, mg/dL (0.7–1.2)	0.6	2.6	1.5
Albumin, g/dL (3.5–5.5)	2.97	2.81	2.72
Alanine aminotransferase, U/L (5–40)	47	394	27
Aspartate aminotransferase, U/L (8–40)	53	1911	22
Total bilirubin, mg/dL (0–1.3)	0.9	6.3	1.2
Direct bilirubin, mg/dL (0–0.3)	0.4	4.8	0.8
Activated partial thromboplastin time, s (14.5–21.5)	40.1	82.5	36.5
Prothrombin time, s (10.0–13.5)	15.1	40.8	12.8
Fibrinogen, g/L (2.0–4.0)	8.83	1.28	3.2
Troponin I, ng/mL (0–0.06)	Not available	1.13	0.1
N-terminal pro-brain natriuretic peptide, pg/mL (0–80)	Not available	>9,000	1,845
Arterial blood pH (7.35–7.45)	7.45	7.21	7.48
Arterial partial pressure of oxygen, mm Hg (80–100)	50	130	138
Arterial partial pressure of carbon dioxide, mm Hg (35–45)	32	36	32
Lactate, mmol/L (0.5–2.2)	Not available	14.2	1.6
C-reactive protein, mg/L (0–8)	Not available	292.6	96.8
Procalcitonin, ng/mL (0–0.5)	Not available	12.84	0.30

distantly with other *Francisella* species. To verify the results, we mapped the raw sequencing reads to the most closely related reference genome *F. hispaniensis* FSC454 (GenBank accession no. CP018093) using Geneious (BioMatters, https://www.geneious.com), which resulted in 96.1% genome coverage with 97.9% pairwise identity. The FSC454 and Zhejiang2018 strains differ by only 1 nt (A1029G) in the 16S rRNA gene (99.94% identity) and 10 nt changes in the *recA* gene (99.07% identity).

Drug susceptibility tests showed resistance to colistin, trimethoprim/sulfamethoxazole, third-generation cephalosporins, and carbapenems but susceptibility to piperacillin/tazobactam, cefepime, fluoroquinolones, aminoglycosides, and tetracyclines (Table 2). Because a Bla-2/FTU-1 class-A β-lactamase is expressed among most *Francisella* species (*6*), the strain reported here also carries a homologue gene of 867 bp with 89.7% identity to the reference gene (GenBank accession no. NG_049110_FTU-1) (*7*). No plasmids were identified. Other resistance genes identified were *aph(3')-Ia*, predicting resistance to kanamycin; *mdf(A)*, predicting resistance to macrolide; and *catA1*, predicting resistance to phenicol. However, broth microdilution tests showed low MIC for kanamycin, erythromycin, azithromycin, and chloramphenicol (Table 2). The reason for the inconsistency between the resistance genes detected and phenotypic susceptibility results is unclear and requires further investigation.

On the basis of the MIC results and the literature (*4*,*8*,*9*), we chose moxifloxacin (400 mg 1×/d injection) to treat the infection. After 14 days of treatment, the patient's symptoms markedly improved, and the chest wound started to heal. Most blood test results had returned to normal ranges (Table 1). However, his heart suffered long-term damage because of the myocarditis, and he required a pacemaker. He was discharged 28 days after admission.

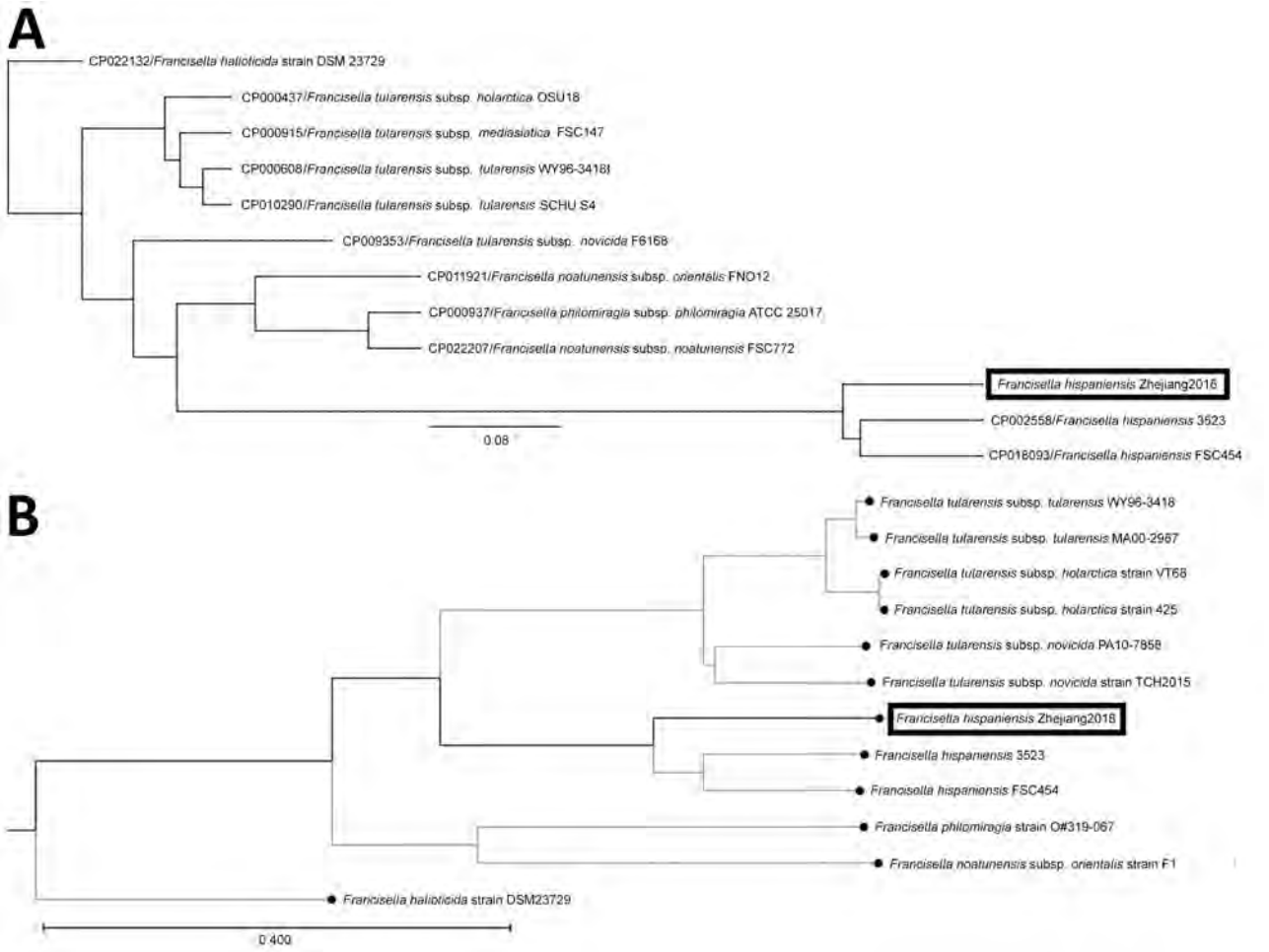

Figure 2. Comparisons of *Francisella hispaniensis* isolate from a 64-year-old male fisherman, China (black boxes), and reference sequences. A) Single-nucleotide polymorphisms. Scale bar for indicates expected substitutions per nucleotide position. B) k-mer phylogenetic tree. Scale bar indicates the branch lengths within the tree.

Table 2. Drug susceptibility testing results of a *Francisella hispaniensis* isolate from a 64-year-old fisherman, China

Antimicrobial drug	Interpretation*	MIC, μg/mL
Amikacin	S	≤2
Colistin	R	≥16
Levofloxacin	S	≤0.12
Trimethoprim/sulfamethoxazole	R	≥320
Tobramycin	S	≤1
Piperacillin/tazobactam	S	≤4
Cefoperazone/sulbactam	R	≥64
Ciprofloxacin	S	≤0.25
Imipenem	R	≥16
Minocycline	S	≤1
Ceftazidime	R	≥64
Cefepime	S	4
Meropenem	R	≥16
Tigecycline	S	≤0.5
Kanamycin	NA	2
Chloramphenicol	NA	2
Erythromycin	NA	1
Azithromycin	NA	0.5
Amoxicillin/clavulanic acid	NA	≥32

*Interpretation was based on the breakpoints for Non-*Enterobacteriaceae* (*5*). NA, breakpoint not available; R, resistant; S, susceptible.

Conclusions

In the 2 previously reported human *F. hispaniensis* infections, the bacteria were isolated from blood (*3*,*4*). The patient we report first suffered a trauma to unprotected skin of his chest that was exposed to seawater from which the bacteria entered the wound and caused the skin and soft tissue infections that progressed to bacteremia and sepsis. Like *F. tularensis*, *F. hispaniensis* appeared to be highly pathogenic and caused respiratory failure, septic shock, and multiple organ dysfunction syndrome. Unlike *F. tularensis*, *F. hispaniensis* grew well under regular culture condition. However, because of its rarity in the clinical setting, conventional biochemical methods misidentified the bacterium as *S. paucimobilis*. WGS is a powerful molecular method to provide the definitive identification.

Most interestingly, the bacteria appeared to have originated from seawater. Sanmen Bay has muddy beaches with shallow seawater and high microbial richness suitable for marine aquaculture (http://www.sanmen.gov.cn/art/2018/6/5/art_1519452_20483713.html). *F. hispaniensis* also probably lives in seawater and under the right conditions could cause human infections. In 1 *F. hispaniensis* case, a woman in Australia had a fishhook injury, which was consistent with the seawater exposure hypothesis (*4*). Other *Fransicella* species, such as *F. noatunensis*, which inhabits the ocean, are major pathogens for fish and shellfish (*10*). The patient in our report acquired infection in August, the hottest month in Zhejiang Province. The high temperature could promote bacteria growth in the seawater and increase the likelihood of human exposure.

The *F. hispaniensis* isolate in our report exhibited a similar antimicrobial susceptibility pattern to *F. tularensis*. This finding is consistent with a study showing susceptibility of all 91 *Francisella* strains tested to aminoglycosides, tetracycline, and fluoroquinolones (*11*). Fluroquinolones, such as ciprofloxacin, are highly effective in treating infections caused by *F. tularensis* (*12*), *F. philomiragia* (*2*,*13*), *F. novicida* (*14*), and *F. hispanensis* (*4*). Third-generation cephalosporins and carbapenems are generally not active against *Francisella* spp. (*9*,*11*), as shown by failed treatment with ceftizoxime and imipenem in the case we describe. Studies based on mouse models showed moxifloxacin is more effective than ciprofloxacin in treating tularemia and is less affected by treatment delay (*9*,*15*). In this patient, moxifloxacin successfully treated *F. hispaniensis* infections without relapse.

In summary, clinicians need to be aware of the emerging and highly pathogenic *F. hispaniensis*, which is resistant to many β-lactams, including the cephalosporins and carbarpenems commonly used for empirical treatment. Our report also demonstrates that seawater exposure can be a risk factor for acquiring *F. hispaniensis* infection.

Acknowledgments

We thank Bin Hu and Jiale Zhou for performing the metagenomic sequencing test and WGS tests.

This work was supported by a research grant from the National Natural Science Foundation of China (81971897). The research funding was provided to H.Z.

About the Author

Dr. Hua Zhou is a clinical physician and researcher at the Department of Respiratory and Critical Care Medicine, First Affiliated Hospital of Zhejiang University School of Medicine. His primary research interest is the diagnosis and treatment of respiratory tract infections and sepsis.

References

1. Maurin M, Gyuranecz M. Tularaemia: clinical aspects in Europe. Lancet Infect Dis. 2016;16:113–24. https://doi.org/10.1016/S1473-3099(15)00355-2
2. Kreitmann L, Terriou L, Launay D, Caspar Y, Courcol R, Maurin M, et al. Disseminated infection caused by *Francisella philomiragia*, France, 2014. Emerg Infect Dis. 2015;21:2260–1. https://doi.org/10.3201/eid2112.150615
3. Huber B, Escudero R, Busse HJ, Seibold E, Scholz HC, Anda P, et al. Description of *Francisella hispaniensis* sp. nov., isolated from human blood, reclassification of *Francisella novicida* (Larson et al. 1955) Olsufiev et al. 1959 as *Francisella*

tularensis subsp. *novicida* comb. nov. and emended description of the genus *Francisella*. Int J Syst Evol Microbiol. 2010;60:1887–96.
4. Aravena-Román M, Merritt A, Inglis TJ. First case of *Francisella bacteraemia* in Western Australia. New Microbes New Infect. 2015;8:75–7. https://doi.org/10.1016/j.nmni.2015.10.004
5. Clinical and Laboratory Standards Institute. Performance standards for antimicrobial susceptibility testing; twenty-ninth informational supplement (M100-S29). Wayne (PA): The Institute; 2019.
6. Bina XR, Wang C, Miller MA, Bina JE. The Bla2 beta-lactamase from the live-vaccine strain of *Francisella tularensis* encodes a functional protein that is only active against penicillin-class beta-lactam antibiotics. Arch Microbiol. 2006;186:219–28. https://doi.org/10.1007/s00203-006-0140-6
7. Antunes NT, Frase H, Toth M, Vakulenko SB. The class A β-lactamase FTU-1 is native to *Francisella tularensis*. Antimicrob Agents Chemother. 2012;56:666–71. https://doi.org/10.1128/AAC.05305-11
8. Ellis J, Oyston PC, Green M, Titball RW. Tularemia. Clin Microbiol Rev. 2002;15:631–46. https://doi.org/10.1128/CMR.15.4.631-646.2002
9. Caspar Y, Maurin M. *Francisella tularensis* susceptibility to antibiotics: a comprehensive review of the data obtained in vitro and in animal models. Front Cell Infect Microbiol. 2017;7:122. https://doi.org/10.3389/fcimb.2017.00122
10. Birkbeck TH, Feist SW, Verner-Jeffreys DW. *Francisella* infections in fish and shellfish. J Fish Dis. 2011;34:173–87. https://doi.org/10.1111/j.1365-2761.2010.01226.x
11. Georgi E, Schacht E, Scholz HC, Splettstoesser WD. Standardized broth microdilution antimicrobial susceptibility testing of *Francisella tularensis* subsp. *holarctica* strains from Europe and rare *Francisella* species. J Antimicrob Chemother. 2012;67:2429–33. https://doi.org/10.1093/jac/dks238
12. Boisset S, Caspar Y, Sutera V, Maurin M. New therapeutic approaches for treatment of tularaemia: a review. Front Cell Infect Microbiol. 2014;4:40. https://doi.org/10.3389/fcimb.2014.00040
13. Mailman TL, Schmidt MH. *Francisella philomiragia* adenitis and pulmonary nodules in a child with chronic granulomatous disease. Can J Infect Dis Med Microbiol. 2005;16:245–8. https://doi.org/10.1155/2005/486417
14. Brett ME, Respicio-Kingry LB, Yendell S, Ratard R, Hand J, Balsamo G, et al. Outbreak of *Francisella novicida* bacteremia among inmates at a louisiana correctional facility. Clin Infect Dis. 2014;59:826–33. https://doi.org/10.1093/cid/ciu430
15. Piercy T, Steward J, Lever MS, Brooks TJ. In vivo efficacy of fluoroquinolones against systemic tularaemia infection in mice. J Antimicrob Chemother. 2005;56:1069–73. https://doi.org/10.1093/jac/dki359

Address for correspondence: Jianying Zhou, Department of Respiratory and Critical Care Medicine, The First Affiliated Hospital of Zhejiang University School of Medicine, 79 Qingchun Rd, Hangzhou, Zhejiang, China; email: zjyhz@zju.edu.cn; Shangxin Yang, UCLA Clinical Microbiology Laboratory, 11633 San Vicente Blvd., Los Angeles, CA 90049, USA; email: shangxinyang@mednet.ucla.edu

Basic Reproduction Number of Chikungunya Virus Transmitted by *Aedes* Mosquitoes

Najmul Haider, Francesco Vairo, Giuseppe Ippolito, Alimuddin Zumla, Richard A. Kock

We estimated the weighted mean basic reproduction number (R_0) of chikungunya virus based on outbreak size. R_0 was 3.4 (95% CI 2.4–4.2) and varied for 2 primary chikungunya mosquito vectors: 4.1 (95% CI 1.5–6.6) for *Aedes aegypti* and 2.8 (95% CI 1.8–3.8) for *Ae. albopictus*.

The basic reproduction number (R_0) of an infection is the mean number of secondary cases a single infectious person causes in a completely susceptible population. The magnitude of R_0 is used to measure the risk and spread of an epidemic or pandemic. To control an outbreak, the R_0 should be reduced to ≤1 through interventions, such as vaccination. Because little information is available at the beginning of an epidemic, the estimated R_0 commonly is used to assess public health preparedness needs, the impact of the possible epidemic, and success of the control measures. Information on R_0 often is lacking for emerging diseases like chikungunya, a mosquito-borne viral disease of humans and nonhuman primates.

Chikungunya virus (CHIKV) is a member of the Alphavirus genus (family Togaviridae) transmitted by *Aedes* mosquitoes, primarily *Ae. aegypti* and *Ae. albopictus*. *Ae. aegypti* mosquitoes are aggressive human biters and the main vectors for CHIKV outbreaks in Asia, where epidemics occur primarily in urban settings (*1*). *Ae. albopictus* mosquitoes, on the other hand, feed from several mammals besides humans and are responsible for CHIKV outbreaks in rural and urban areas in Africa (*1*).

CHIKV outbreaks were reported from >100 countries worldwide during 2014–2019 (*2*). Epidemiologic understanding of CHIKV changed after outbreaks on the island of La Réunion in the Indian Ocean during 2005–2006, when *Ae. albopictus* mosquitoes were identified as the outbreak vector (*1*,*3*). The global expansion of CHIKV partially is attributed to viral adaptation to this new mosquito vector, which facilitated a mutation in the coding for the envelop protein 1 A226V (E1-A226V) gene of CHIKV, increasing the competence of *Ae. albopictus* mosquitoes to transmit the virus from mosquitoes to humans (*1*–*3*).

In humans, CHIV infection is characterized by sudden onset of intense polyarthralgia, high fever, and skin rash. CHIKV causes debilitating joint pain that can limit daily activities and last a few months to several years (*2*); progression to the chronic stage (>3 months) occurs in 4.1%–78.6% of cases (*4*). To estimate R_0 of CHIKV outbreaks, we analyzed empirical data on R_0 available from open sources.

The Study

We used the search terms "Basic reproduction number" or "R_0" AND "chikungunya" to identify published articles from Google Scholar and PubMed. We identified 11 articles describing estimated R_0 of CHIKV from outbreak data during 2000–2019. We found 5 articles on outbreaks in Africa, all on La Réunion (*3*,*5*–*8*); 1 on an outbreak in Cambodia (*1*); 2 on outbreaks in Italy (*9*,*10*); and 3 on outbreaks in the Americas (*11*,*12*; N. Báez-Hernández et al. unpub. data, https://www.biorxiv.org/content/10.1101/122556v1).

The authors estimated R_0 by using mathematical (compartmental) models fitted with respective outbreak data (*1*,*3*,*5*–*12*). We considered the estimated values comparable and extracted the R_0 from each. We then estimated the weighted mean R_0 of CHIKV based on outbreak size, such as number of reported cases included in the estimation of R_0 in the original article, and further estimated the mean R_0 for different mosquito vectors and E1-A226V gene mutations.

The largest CHIKV outbreak occurred on La Réunion and affected 266,000 of the 785,000 inhabitants (*3*). Several models with differing levels of data

Author affiliations: The Royal Veterinary College, University of London, London, UK (N. Haider, R.A. Kock); National Institute for Infectious Diseases Lazzaro Spallanzani, Rome, Italy (F. Vairo, G. Ippolito); University College London, London (A. Zumla)

DOI: https://doi.org/10.3201/eid2610.190957

estimated the R_0 of the La Réunion outbreaks between 0.89 and 4.1 (*3*,*5*–*7*). The R_0 also was estimated from CHIKV outbreaks in Italy in 2007 (*10*) and 2017 (*9*), Cambodia in 2012 (*1*), Venezuela in 2014 (*11*), Colombia in 2015 (*12*), and Mexico in 2015 (N. Báez-Hernández et al. unpub. data, https://www.biorxiv.org/content/10.1101/122556v1) (Table).

We estimated the weighted mean R_0 of CHIKV to be 3.4 (95% CI 2.4–4.2). We analyzed the data and estimated the R_0 for *Ae. aegypti* and *Ae. albopictus* mosquitoes separately for outbreaks in which the R_0 of CHIKV was described for each species. We estimated the R_0 to be 4.1 (95% CI 1.5–6.6) for *Ae. aegypti* mosquitoes and 2.8 (95% CI 1.8–3.8) for *Ae. albopictus* mosquitoes. Although the difference is not statistically significant (p = 0.12), we expected a lower R_0 for outbreaks involving *Ae. albopictus* mosquitoes because this species also feeds on animals, which might have reduced the attack rate on humans and transmission across the population. However, outbreaks associated with *Ae. albopictus* mosquitoes can be prolonged and the outbreak response can have economic consequences. We estimated the R_0 to be 3.5 (95% CI 1.9–4.9) during outbreaks involving the E1-A226V mutation, which is higher than R_0 of 2.1 from the 2017 outbreak in Italy that did not have the gene mutation.

CHIKV infections among humans can have severe health consequences, despite the low case fatality rate. CHIKV infection has 3 stages: acute, postacute, and chronic. The acute phase usually lasts for 1–3 weeks and is characterized by fever, intense myalgia, arthralgia, and symmetric joint pain in both legs that can limit even the simplest daily activities. The postacute stage usually lasts 1–3 months after the acute phase and is characterized by persistent inflammatory arthralgia, arthritis, tenosynovitis, and bursitis. The chronic stage starts after 3 months and can last for months to years after acute infection (*2*).

In a study in Brazil, ≥68% of persons with CHIKV remained chronically infected for up to 1 year (*13*). On Réunion Island, a small group of patients had clinical signs for 6 years. Although the reason for persistence is unclear, it might be strain related and associated with the E1-A226V mutation. Therefore, despite being less severe and causing fewer deaths than other mosquitoborne diseases, CHIKV can have lingering physical and psychological consequences for those affected. Infected persons also can experience economic consequences because they might not be able to work for several weeks or more.

R_0 does not remain constant. For arboviruses, R_0 can vary based on the density of hosts and vectors; mosquito species, survival, and biting rate; and vector competence and capacity, all of which can depend on environmental and microclimatic factors. Further, the vector competence of *Ae. aegypti* mosquitoes for CHIKV might be different from that for *Ae. albopictus* mosquitoes, which could influence outbreak dynamics. For example, 1 study reported the transmission efficiency of *Ae. albopictus* mosquitoes as 97% and of *Ae. aegypti* mosquitoes as 83% (*14*).

The outbreaks included in our study occurred in tropical and subtropical countries and in the more temperate climate of Italy. We did not consider climatic conditions during reported outbreaks, which might play a role in determining the size and R_0 of CHIKV outbreaks. We also did not consider the variation of data quality in published articles, except for the outbreak size, which might affect estimated R_0. However, defining adjustments for data quality would have been difficult and might have introduced unwanted bias.

Conclusions

We found the overall mean R_0 for CHIKV was 3.4 (95% CI 2.4–4.2). Our estimated R_0 of 4.1 (95% CI 1.5–6.6) for *Ae. aegypti* mosquitoes suggests CHIKV could spread rapidly and cause high disease incidence in urban areas, where this species thrives. Our estimated CHIKV R_0 for *Ae. albopictus* mosquitoes of 2.8 (95%

Table. The basic reproduction number (R_0) of chikungunya virus estimated from empirical outbreak data, 2000–2019

Year	Country or region	Continent	R_0 range (95% CI)	Mosquito species	Lineage	E1-A226V mutation*	Reference
2006	La Réunion	Africa	4.1	*Ae. albopictus*	Indian Ocean	Y	(*3*)
2006	La Réunion	Africa	0.9–2.3	*Ae. albopictus*	Indian Ocean	Y	(*7*)
2006	La Réunion	Africa	1.5–1.8	*Ae. albopictus*	Indian Ocean	Y	(*5*)
2006	La Réunion	Africa	3.4	*Ae. albopictus*	Indian Ocean	Y	(*6*)
2006	La Réunion	Africa	3.7 (2–11)	*Ae. albopictus*	Indian Ocean	Y	(*8*)
2007	Italy	Europe	3.3 (1.8–6.0)	*Ae. albopictus*	Indian Ocean	Mixed	(*10*)
2012	Cambodia	Asia	6.5 (6.2–6.8)	*Ae. aegypti*	Asian	Y	(*1*)
2014	Italy	Europe	2.1 (1.5–2.6)	*Ae. albopictus*	Indian Ocean	N	(*9*)
2014	Venezuela	South America	3.7	*Ae. aegypti*	Asian	N	(*11*)
2015	Mexico	North America	3.44	*Ae. aegypti*	Asian	N	†
2014	Colombia	South America	1–9	*Ae. aegypti*	Asian	N	(*12*)

*Envelope 1 A226V gene.
†N. Báez-Hernández et al., unpub data, https://www.biorxiv.org/content/10.1101/122556v1.

CI 1.5–6.6) was lower than for *Ae. aegypti* mosquitoes. In rural areas, where *Ae. albopictus* mosquitoes are more prevalent, sylvatic cycles, maintenance of biodiversity including natural mosquito populations, and presence of hosts other than humans might reduce the effects of an outbreak. Early interventions targeting *Aedes* mosquitoes will be vital to controlling CHIKV outbreaks.

All authors are part of PANDORA-ID-NET Consortium funded by the European and Developing Countries Clinical Trials Partnership (EDCTP2) program (EDCTP grant no. RIA2016E-1609), which is supported under Horizon 2020, the European Union's Framework Programme for Research and Innovation. The members were part of an international outbreak response on chikungunya virus outbreaks in Republic of Congo.

G.I. and F.V. acknowledge support for research on emerging infections from the Italian Ministry of Health, through grants to Ricerca Corrente linea 1 to National Institute for Infectious Diseases, Lazzaro Spallanzani, IRCCS, Rome. G.I., F.V., and A.Z. are members of the International Public Health Crisis Group that performs independent analysis and research activities on epidemic and endemic events naturally occurring or related to the deliberate release of pathogens, and provides strategic, organizational, educational, logistic support, and advice for preparedness and response. F.V. and G.I. are professors at Saint Camillus International University of Health Sciences, Rome, Italy.

About the Author

Dr. Haider is a veterinarian, epidemiologist, and public health researcher based in the Royal Veterinary College, London, UK. His research interests focus on emerging infectious diseases, including chikungunya and Lassa fever virus, and interrupting the chain of transmission.

References

1. Robinson M, Conan A, Duong V, Ly S, Ngan C, Buchy P, et al. A model for a chikungunya outbreak in a rural Cambodian setting: implications for disease control in uninfected areas. PLoS Negl Trop Dis. 2014;8:e3120. https://doi.org/10.1371/journal.pntd.0003120
2. Vairo F, Haider N, Kock R, Ntoumi F, Ippolito G, Zumla A. Chikungunya: epidemiology, pathogenesis, clinical features, management, and prevention. Infect Dis Clin North Am. 2019;33:1003–25. https://doi.org/10.1016/j.idc.2019.08.006
3. Yakob L, Clements ACA. A mathematical model of chikungunya dynamics and control: the major epidemic on Réunion Island. PLoS One. 2013;8:e57448. https://doi.org/10.1371/journal.pone.0057448
4. Rodríguez-Morales AJ, Cardona-Ospina JA, Fernanda Urbano-Garzón S, Sebastian Hurtado-Zapata J. Prevalence of post-chikungunya infection chronic inflammatory arthritis: a systematic review and meta-analysis. Arthritis Care Res (Hoboken). 2016;68:1849–58. https://doi.org/10.1002/acr.22900
5. Dumont Y, Chiroleu F. Vector control for the chikungunya disease. Math Biosci Eng. 2010;7:313–45. https://doi.org/10.3934/mbe.2010.7.313
6. Bacaër N. Approximation of the basic reproduction number R_0 for vector-borne diseases with a periodic vector population. Bull Math Biol. 2007;69:1067–91. https://doi.org/10.1007/s11538-006-9166-9
7. Dumont Y, Chiroleu F, Domerg C. On a temporal model for the chikungunya disease: modeling, theory and numerics. Math Biosci. 2008;213:80–91. https://doi.org/10.1016/j.mbs.2008.02.008
8. Boëlle P-Y, Thomas G, Vergu E, Renault P, Valleron A-J, Flahault A. Investigating transmission in a two-wave epidemic of chikungunya fever, Réunion Island. Vector-Borne Zoonotic Dis. 2008;8:207–17. https://doi.org/10.1089/vbz.2006.0620
9. Manica M, Guzzetta G, Poletti P, Filipponi F, Solimini A, Caputo B, et al. Transmission dynamics of the ongoing chikungunya outbreak in Central Italy: from coastal areas to the metropolitan city of Rome, summer 2017. Euro Surveill. 2017;22:17-00685. https://doi.org/10.2807/1560-7917.ES.2017.22.44.17-00685
10. Poletti P, Messeri G, Ajelli M, Vallorani R, Rizzo C, Merler S. Transmission potential of chikungunya virus and control measures: the case of Italy. PLoS One. 2011;6:e18860. https://doi.org/10.1371/journal.pone.0018860
11. Lizarazo E, Vincenti-Gonzalez M, Grillet ME, Bethencourt S, Diaz O, Ojeda N, et al. Spatial dynamics of chikungunya virus, Venezuela, 2014. Emerg Infect Dis. 2019;25:672–80. https://doi.org/10.3201/eid2504.172121
12. Peña-García VH, Christofferson RC. Correlation of the basic reproduction number (R_0) and eco-environmental variables in Colombian municipalities with chikungunya outbreaks during 2014–2016. PLoS Negl Trop Dis. 2019;13:e0007878. PubMed https://doi.org/10.1371/journal.pntd.0007878
13. Dias JP, Costa MCN, Campos GS, Paixão ES, Natividade MS, Barreto FR, et al. Seroprevalence of chikungunya virus after its emergence in Brazil. Emerg Infect Dis. 2018;24:617–24. PubMed https://doi.org/10.3201/eid2404.171370
14. Vega-Rúa A, Zouache K, Girod R, Failloux A-B, Lourenço-de-Oliveira R. High level of vector competence of *Aedes aegypti* and *Aedes albopictus* from ten American countries as a crucial factor in the spread of chikungunya virus. J Virol. 2014;88:6294–306. https://doi.org/10.1128/JVI.00370-14

Address for correspondence: Najmul Haider, Centre for Emerging, Endemic and Exotic Diseases, Room no. CEE 001, Royal Veterinary College, University of London, Hawkshead Ln, North Mymms, Hertfordshire AL9 7TA, UK; email: nhaider@rvc.ac.uk

Deaths Associated with Pneumonic Plague, 1946–2017

Alex P. Salam,[1] Amanda Rojek,[1] Erhui Cai, Mihaja Raberahona, Peter Horby

The death rate for persons with treated pneumonic plague is often reported as 50%, but firm evidence for this figure is minimal. We conducted a meta-analysis of articles reporting the death rate for persons treated for pneumonic plague. The rate was 17%, substantially lower than the frequently cited 50%.

Yersinia pestis, the causative agent of plague, is a Tier 1 select agent because of the high case-fatality rate associated with pneumonic plague and its potential as a bioterrorism agent in aerosolized form (https://emergency.cdc.gov/agent/agentlistcategory.asp). The death rate for persons with untreated primary pneumonic plague was reported to be almost 100% (*1*); the death rate for persons treated for primary pneumonic plague was 50% (*1*). Overall, the death rate for persons treated for primary pneumonic plague was high despite the sensitivity of *Y. pestis* to aminoglycosides, quinolones, and tetracyclines (*2*,*3*) and the relatively good penetration of some of these antimicrobial drugs into lungs (*4*,*5*). During the 2017 Madagascar pneumonic plague outbreak, the observed death rate for treated persons appeared to be substantially lower than that reported in the literature (*6*). Many articles that quoted a 50% death rate for treated primary pneumonic plague were cited in a 2000 study by Ratsitorahina et al. (*7*), which described a small outbreak in Madagascar in 1997. The article indicated that the data showed an overall death rate of 53% but did not state the number of deaths. However, the death rate for treated persons with confirmed or probable plague was 10%. On reviewing reports that cited Ratsitorahina et al., we identified 9 studies that referenced 50% of persons treated for pneumonic plague who died, 1 study that referenced 40%, and none referencing lower rates. One was a review cited 9 times about persons treated for primary pneumonic plague for whom the death rate was 50%. We identified 6 reports that stated but did not reference a 50% death rate for persons treated for pneumonic plague.

Author affiliations: United Kingdom Public Health Rapid Support Team, London, UK (A.P. Salam); Centre for Tropical Medicine and Global Health, University of Oxford, Oxford, UK (A.P. Salam, E. Cai, M. Raberahona, P. Horby); Centre Hospitalier Befelatanana, Antananarivo, Madagascar (M. Raberahona); Centre for Integrated Critical Care, University of Melbourne, Melbourne, Victoria, Australia (M. Raberahona)

DOI: https://doi.org/10.3201/eid2610.191270

The Study

To address the lack of evidence supporting the frequently cited 50% death rate for persons treated for primary pneumonic plague, we conducted a systematic review and meta-analysis. We followed PRISMA (Preferred Reporting Items for Systematic Reviews and Meta-Analyses, http://www.prisma-statement.org) and MOOSE (Meta-analysis of Observational Studies in Epidemiology [*8*]) guidelines. The study was prospectively registered on PROSPERO (CRD42018086223) (https://www.crd.york.ac.uk/PROSPERO).

We searched PubMed and Embase covering 1946–2017 using the search terms "Yersinia pestis" or "plague" and "pneumon*" and limited our search to human data. We searched references and included articles describing death (within a 28-day period from illness onset) among patients with confirmed, probable, and suspected primary or undifferentiated (i.e., primary or secondary not distinguished pneumonic plague, 1999 World Health Organization case definition, https://www.who.int/csr/resources/publications/plague/WHO_CDS_CSR_EDC_99_2_EN/en/). We did not restrict by study type, language, or minimum patient number.

Two authors reviewed and extracted data; a third author resolved any disagreements. Data fields extracted included year and country of the outbreak, number of patients who survived and died (stratified by antimicrobial drug status), number of patients receiving different antimicrobial

[1]These co–first authors contributed equally to this article.

drug classes, time to antimicrobial drug administration, and receipt of plague vaccination or prophylaxis (these patients were excluded). We calculated the risk from the number of events and participants in each group.

We performed a meta-analysis using a binomial-specific method. We assessed heterogeneity using the χ^2 test and quantified results with the I^2 statistic. In addition, we preplanned 2 sensitivity analyses to examine whether our estimation of death was influenced by the inclusion of specific articles (pneumonic plague was not confirmed as primary disease or patients with suspected and probable disease). We conducted statistical analysis using R version 3.6.0 (R Project, https://www.r-project.org).

We reviewed 362 articles (Appendix Figure 1, https://wwwnc.cdc.gov/EID/article/26/10/19-1270-App1.pdf). We described 1,107 patients in 44 articles (Appendix Table). Twenty-nine articles reported antimicrobial drug use in 108 patients with confirmed or probable pneumonic plague. For pneumonic plague patients receiving antimicrobial drug therapy, the pooled death rate was 17% (95% CI 8%–31%; I^2 = 47%) (Appendix Figure 2). Pneumonic plague patients who did not receive antimicrobial drug therapy had a pooled death rate of 98% (95% CI 73%–100%; I^2 = 47%) (Appendix Figure 3). Pneumonic plague patients for whom antimicrobial drug status was unknown had a pooled death rate of 46% (95% CI 32%–61%) (Appendix Figure 4). Heterogeneity was significant (I^2 = 91%; p<0.01). The pooled death rates were similar when sensitivity analysis was conducted (Table). Antimicrobial drugs in the reports were aminoglycosides (90 courses), quinolones (24 courses), sulfonamides (22 courses), chloramphenicol (16 courses), tetracyclines (14 courses), and cotrimoxazole (3 courses). Six reports described time to from admission to antimicrobial drug administration, but the nonstandardized reporting precluded stratification by this measure.

Table. Sensitivity analysis of antimicrobial drug use and rates of pneumonic plague–related deaths, 1946–2017

Antimicrobial drug use	Confirmed cases, % (95% CI)	Total cases, % (95% CI)
Treated		
Primary plague	27 (14–47)	6 (1–31)
Undifferentiated	28 (6–72)	6 (1–31)
Not treated		
Primary plague	94 (82–98)	99 (22–100)
Undifferentiated	No data	100*
Unknown		
Primary plague	No data	29 (13–51)
Undifferentiated	42 (23–64)	51 (31–71)

*Crude analysis; model fails under this condition.

Conclusions

Our meta-analysis identified a 17% death rate for persons treated for pneumonic plague, in contrast to the 50% often reported in the literature. The death rate for the 2017 Madagascar outbreak was published after we completed our systematic review but is consistent with our findings (25% in confirmed cases) (*9*). These figures compare with 13.6% for patients who died in the hospital of community-acquired pneumonia; 12.3% who died of *Streptococcus pneumoniae* infection; 14.7% who died of *Legionella* species infection; and 32%–61% who died of *Staphylococcus aureus*, *Escherichia coli*, *Klebsiella* species, or *Pseudomonas aeruginosa* infections (*10*). However, persons who died of other etiologic causes were predominantly elderly and had underlying conditions (*10*).

Our review indicated insufficient standardized data to stratify death by time from symptom onset to antimicrobial drug administration. The literature we assessed often stated that pneumonic plague is fatal in almost all patients who start antimicrobial drugs >24 hours after symptom onset. Generally, descriptions cite either 1 article, in which 11 patients treated within 24 hours survived and 2 treated after 24 hours died (*11*), or a handful of isolated case reports. However, case reports and series also exist in which patients survived despite starting antimicrobial drugs >24 hours after symptom onset (*12*–*14*).

An accurate estimate of death is crucial for several reasons. First, it is helpful for public health planning during outbreaks, including the allocation of healthcare resources and the development of social mobilization campaigns. The commonly reported high death rate associated with primary pneumonic plague contributes to fear and panic among healthcare workers and the public. For example, anecdotal reports indicating concerns during the Madagascar outbreak were the following: healthcare workers taking continuous antimicrobial drug prophylaxis, mass public use of over-the-counter antimicrobial drugs, asymptomatic persons visiting the hospital, and sick persons avoiding the hospital. Accurate assessment of death is also essential for clinical trial design. For example, the required sample size would be 134 (power 0.8, α = 0.025) for a binary outcome superiority trial in which the death rate in the control arm was 50% and the intervention was assumed to reduce death by 50% (similar to the assumptions in a clinical trial of gentamicin vs. doxycycline in Tanzania in 2002) (*15*). However, a sample size of 476 would be required in a trial in which the death rate in the control arm was 20%. A sample size renders a superiority trial unfeasible. Even during the Madagascar outbreak, the largest

outbreak of pneumonic plague this century, the final number of confirmed pneumonic plague patients was only 32 (*9*).

The major limitation of our meta-analysis is the sporadic reporting of clinical data and the relatively small number of cases for which antimicrobial drugs treatment status was described. Reporting bias in the literature also is likely, and pneumonic plague patients who survive are more likely than those who do not to be reported. Nonetheless, data indicate that the percentage of persons who die of treated pneumonic plague appears to be substantially lower than is frequently reported in the literature.

Acknowledgments

We thank Freya Shearer for assisting with statistical programming.

The UK Public Health Rapid Support Team is funded by UK aid from the Department of Health and Social Care and is jointly run by Public Health England and the London School of Hygiene & Tropical Medicine. The University of Oxford and King's College London are academic partners. P.H. is supported by funding from the Department for International Development and the Welcome Trust (215091/Z/18/Z) and the Bill & Melinda Gates Foundation (OPP1209135).

About the Author

Dr. Salam is the clinical researcher for the United Kingdom Public Health Rapid Support Team. His primary research interests include clinical research in epidemic prone diseases. Dr. Rojek is senior clinical fellow at the Centre for Integrated Critical Care, University of Melbourne. Her primary research interests include clinical research in epidemic-prone diseases.

References

1. Prentice MB, Rahalison L. Plague. Lancet. 2007;369:1196–207. https://doi.org/10.1016/S0140-6736(07)60566-2
2. Centers for Disease Control and Prevention. Recommended antibiotic treatment for plague [cited 2015 Aug 25]. https://www.cdc.gov/plague/resources/Recommended-antibiotics-for-plague-web-site-rev-Jan2018-P.pdf
3. Wendte JM, Ponnusamy D, Reiber D, Blair JL, Clinkenbeard KD.In vitro efficacy of antibiotics commonly used to treat human plague against intracellular *Yersinia pestis.* Antimicrob Agents Chemother. 2011;55:3752–7. https://doi.org/10.1128/AAC.01481-10
4. Honeybourne D. Antibiotic penetration into lung tissues. Thorax. 1994;49:104–6. https://doi.org/10.1136/thx.49.2.104
5. Valcke Y, Pauwels R, Van der Straeten M. Pharmacokinetics of antibiotics in the lungs. Eur Respir J. 1990;3:715–22.
6. Salam AP, Raberahona M, Andriantsalama P, Read L, Andrianarintsiferantsoa F, Razafinambinintsoa T, et al. Factors influencing atypical clinical case presentations during the 2017 Madagascar pneumonic plague outbreak: a prospective cohort study. Am J Trop Med Hyg. 2020;102:1309–15. https://doi.org/10.4269/ajtmh.19-0576
7. Ratsitorahina M, Chanteau S, Rahalison L, Ratsifasoamanana L, Boisier P. Epidemiological and diagnostic aspects of the outbreak of pneumonic plague in Madagascar. Lancet. 2000;355:111–3. https://doi.org/10.1016/S0140-6736(99)05163-6
8. Stroup DF, Berlin JA, Morton SC, Olkin I, Williamson GD, Rennie D, et al. Meta-analysis of observational studies in epidemiology: a proposal for reporting. Meta-analysis Of Observational Studies in Epidemiology (MOOSE) group. JAMA. 2000;283:2008–12. https://doi.org/10.1001/jama.283.15.2008
9. Randremanana R, Andrianaivoarimanana V, Nikolay B, Ramasindrazana B, Paireau J, Ten Bosch QA, et al. Epidemiological characteristics of an urban plague epidemic in Madagascar, August-November, 2017: an outbreak report. Lancet Infect Dis. 2019;19:537–45. https://doi.org/10.1016/S1473-3099(18)30730-8
10. Fine MJ, Smith MA, Carson CA, Mutha SS, Sankey SS, Weissfeld LA, et al. Prognosis and outcomes of patients with community-acquired pneumonia. A meta-analysis. JAMA. 1996;275:134–41. https://doi.org/10.1001/jama.1996.03530260048030
11. McCrumb FR Jr, Mercier S, Robic J, Bouillat M, Smadel JE, Woodward TE, et al. Chloramphenicol and terramycin in the treatment of pneumonic plague. Am J Med. 1953;14:284–93. https://doi.org/10.1016/0002-9343(53)90040-0
12. Begier EM, Asiki G, Anywaine Z, Yockey B, Schriefer ME, Aleti P, et al. Pneumonic plague cluster, Uganda, 2004. Emerg Infect Dis. 2006;12:460–7. https://doi.org/10.3201/eid1203.051051
13. Donaires LF, Céspedes M, Valencia P, Salas JC, Luna ME, Castañeda A, et al. [Primary pneumonic plague with nosocomial transmission in La Libertad, Peru 2010] [in Spanish]. Rev Peru Med Exp Salud Publica. 2010;27:326–36. https://doi.org/10.1590/S1726-46342010000300004
14. Luo H, Dong X, Li F, Xie X, Song Z, Shao Z, et al. A cluster of primary pneumonic plague transmitted in a truck cab in a new enzootic focus in China. Am J Trop Med Hyg. 2013;88:923–8. https://doi.org/10.4269/ajtmh.12-0163
15. Mwengee W, Butler T, Mgema S, Mhina G, Almasi Y, Bradley C, et al. Treatment of plague with gentamicin or doxycycline in a randomized clinical trial in Tanzania. Clin Infect Dis. 2006;42:614–21. https://doi.org/10.1086/500137

Address for correspondence: Peter Horby, University of Oxford, Center for Tropical Medicine and Global Health, Roosevelt Dr., Oxford, OX3 7FZ, UK; email: peter.horby@ndm.ox.ac.uk

Emerging Sand Fly–Borne Phlebovirus in China

Jing Wang,[1] Shihong Fu,[1] Ziqian Xu,[1] Jingxia Cheng,[1] Mang Shi, Na Fan, Jingdong Song, Xiaodong Tian, Jianshu Cheng, Shuqing Ni, Ying He, Wenwen Lei, Fan Li, Heng Peng, Bin Wang, Huanyu Wang, Xiaoqing Lu, Yajun Ma, Guodong Liang

We isolated 17 viral strains capable of causing cytopathic effects in mammalian cells and death in neonatal mice from sand flies in China. Phylogenetic analysis showed that these strains belonged to the genus *Phlebovirus*. These findings highlight the need to control this potentially emerging virus to help safeguard public health.

The genus *Phlebovirus* belongs to the order *Bunyavirales*, family *Phenuiviridae* (*1*). Many phleboviruses are sand fly–borne, including sandfly fever Sicilian virus (SFSV), sandfly fever Naples virus (SFNV), and sandfly fever Toscana virus (TOSV), all of which can cause a febrile condition commonly known as three-day fever (*2*). At present, sand fly–borne phleboviruses and their associated diseases are found primarily in countries along the Mediterranean coast, including Italy (*3*), Turkey (*4*), and Cyprus (*5*); there have been no reports of sand fly–borne phleboviruses in China or East Asia (*2*). We describe 17 phlebovirus isolates from sand fly specimens collected in the natural environment of Shanxi Province in central China.

The Study

In June 2018, we collected bloodsucking insects during the evening and night (6:00 PM–7:00 AM) in Wuxiang County (112°26′ 113°22′E, 36°39′ 37°8′N), Shanxi Province, China, using Wentaitai MM200 traps (Guangzhou Changsheng Chemical Technology Service Co., https://www.globalsources.com/si/AS/Guangzhou-Changsheng/6008849913119/Homepage.htm#). We classified all specimens according to their morphology under ice bath conditions and stored them in liquid nitrogen until laboratory testing (*6*). We collected a total of 4,069 bloodsucking insects: 3,819 sand flies and 250 mosquitoes. After dividing them into 51 pools (50 mosquitoes or 50–100 sand flies in each pool), we ground insect specimens in minimum essential medium on ice and centrifuged them at 12,000 rpm at 4°C for 30 min. We then processed each homogenate in 2 ways: testing them for the presence of virus with GoTaq Green Master Mix phlebovirus primers (TAKARA, https://www.takarabiomed.com.cn) (*7*) and inoculating them into baby hamster kidney (BHK) 21 cells and *Aedes albopictus* C6/36 cells (*6*).

On the third day after inoculation of BHK-21 cells with sand fly specimens, cytopathic effects began to appear (Figure 1). By culturing BHK-21 cells in the presence of supernatant from the sand fly homogenates (Table 1), we obtained 17 viral isolates: 10 strains collected from a sheep pen and 7 from a chicken pen. Pooled supernatants of ground sand flies and viral isolates all showed positive amplification with the phleboviruses primers, and sequencing and analysis revealed that the virus belonged to the genus *Phlebovirus*. We observed no cytopathic effect or *Phlebovirus* genes in C6/36 cells. We used PCR to amplify the cytochrome c oxidase I gene (*8*) and identified *Phlebotomus chinensis* sand flies as the reservoir for each of the 17 phlebovirus-positive pools.

To further characterize the phleboviruses isolates, we used a plaque assay 3 times to purify virus from Wuxiang County, Shanxi Province (SXWX-1813-2) and then inoculated it into neonatal mice (*9*), resulting in substantial morbidity and death. The viral titer used in these experiments was $10^{8.09}$ PFU/mL (4th passage). We observed a large number of virus particles in ultrathin sections of brain tissue of neonatal mice under electron

Author affiliations: Chinese Center for Disease Control and Prevention, Beijing, China (J. Wang, S. Fu, Z. Xu, N. Fan, J. Song, Y. He, W. Lei, Fan Li, H. Wang, G. Liang); Qingdao University, Qingdao, China (J. Wang, N. Fan, B. Wang, X. Lu); Shanxi Province Center for Disease Control and Prevention, Taiyuan, China (J. Cheng, X. Tian); School of Medicine, Sun Yat-sen University, Guangzhou, China (M. Shi); University of Sydney, Sydney, NSW, Australia (M. Shi); Wuxiang County Center for Disease Control and Prevention, Wuxiang, China (J. Cheng, S. Ni); Second Military Medical University, Shanghai, China (H. Peng, Y. Ma)

DOI: https://doi.org/10.3201/eid2610.191374

[1]These authors contributed equally to this article.

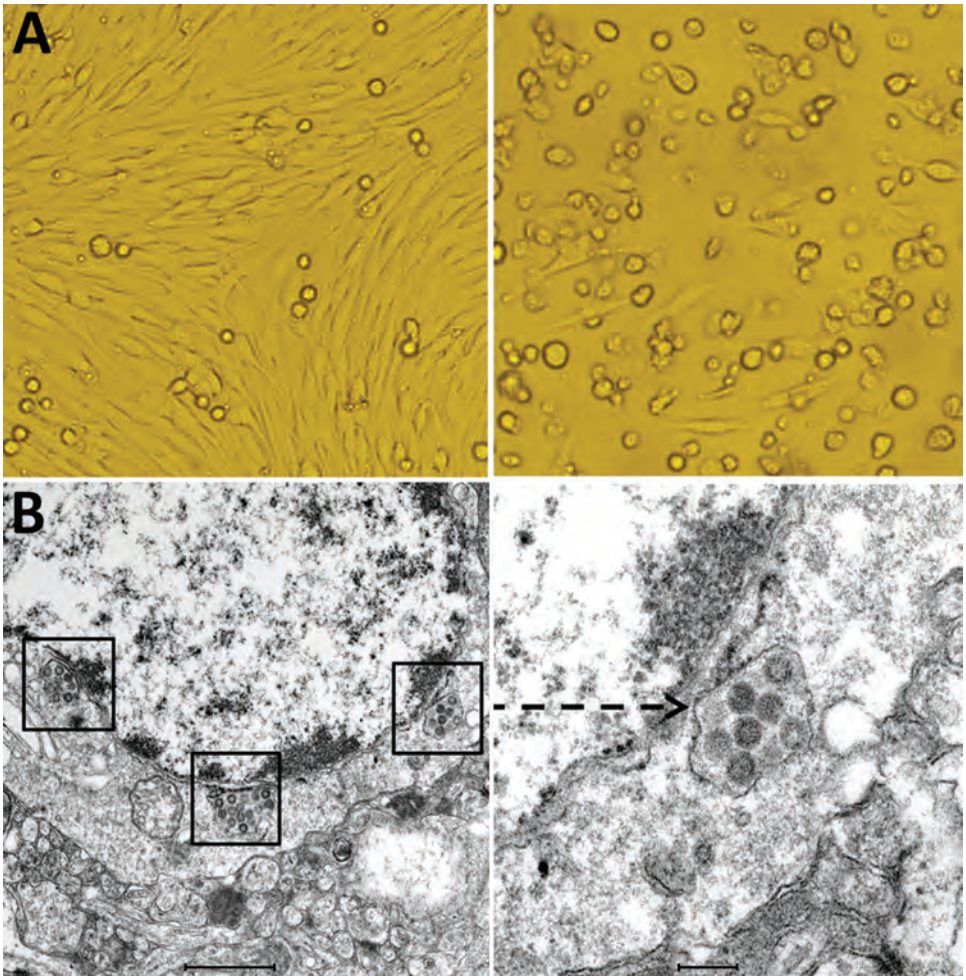

Figure 1. Cytopathogenic effect and electron microscopic morphology of baby hamster kidney 21 (BHK-21) cells infected with phlebovirus, China. A) Left panel shows morphology of BHK-21 cells before inoculation with strain SXWX1813-2; right panel shows morphology 3 days after inoculation (original magnification ×200). BHK-21 cells infected with SXWX1813-2 showed reduced adherence and a large number of rounded and exfoliated cells. B) Left panel shows the viral morphology of SXWX1813–2 on ultrathin slices (scale bar 1 μm; right panel shows the enlarged viral particle (indicated by arrow; scale bar 200 nm).

microscopy; the virus particles were uniform spherical particles with diameters of 80–100 nm (Figure 1) (*9*).

We obtained whole-genome sequences of SXWX1813-2 using a combination of 54 primers covering the viral large (L), medium (M), and small (S) segment genes (Table 2). We used SeqMan (DNAStar, https://www.dnastar.com) for nucleotide sequence splicing, MEGA version 6.0 (https://www.megasoftware.net) for phylogenetic analysis, and Meg alignment (DNAStar) for homology analysis (*6*).

The complete genome of the SXWX1813-2 virus contains 3 segments (Table 2). The L segment (GenBank accession no. MN454526) is 6,456 nt and contains 1 open reading frame (ORF) encoding an RNA-dependent RNA polymerase (RdRp; 2,090 aa). The M segment (accession no. MN454527) is 4,322 nt and contains 1 ORF encoding a glycoprotein precursor (GP; 1362 aa), which is cleaved into mature N and C glycoproteins. The S segment (accession no. MN454528) is 1,693 nt and contains 2 ORFs encoding nonstructural protein (NSP; 260 aa) and nucleocapsid protein (NP; 246 aa). The S and M segment genes of the other 16 viral strains all had the same nucleotide sequence lengths as those of SXWX1813-2.

The nucleotide and amino acid sequences of SXWX1813-2 were compared with those of other

Table 1. Isolation of Wuxiang virus, a new phlebovirus, China

Strain number	No. isolates	Collection place
SXWX1807-1	90	Sheep pen
SXWX1808-2	100	
SXWX1810-1	100	
SXWX1810-2	104	
SXWX1813-1	80	
SXWX1813-2	81	
SXWX1816-1	100	
SXWX1816-4	113	
SXWX1818-1	100	
SXWX1818-2	104	
SXWX1830	13	Chicken pen
SXWX1836-1	100	
SXWX1838-1	90	
SXWX1838-2	81	
SXWX1840-1	100	
SXWX1841-1	100	
SXWX1841-3	100	

phleboviruses. L, M, and S segment genes showed the strongest homology with those of Toros virus (TORV) and Corfou virus (CFUV) (*8*). The homology between L segments was 76.4%–77.1% on the nucleotide level and 88.0%–88.2% on the amino acid level and between M segments was 70.7%–71.9% on the nucleotide level and 75.3%–75.6% on the amino acid level. For the NSP gene, the nucleotide homology was 74.1%–75.2% and the amino acid homology was 83.5%–84.3%; for the NP gene, the nucleotide homology was 81.9%–82.2% and the amino acid homology was 96%–96.4% (Table 2). For the M and S gene segments of the other 16 viral strains compared with those of SXWX1813-2, nucleotide sequences were 96.9%–99.8% and amino acid sequences were 97.3%–100% identical.

Phylogenetic analysis showed that SXWX1813-2 belongs to the mosquito- and sand fly–borne virus group of the *Phlebovirus* genus. Further analysis showed that SXWX1813-2 is closely related to viruses isolated from sandflies in Turkey (TORV) and Greece (CFUV), forming independent branches. (Figure 2, panel A). The remaining 16 strains isolated from sandflies were all located on the same evolutionary branch as SXWX1813-2 (Figure 2, panel B; Appendix Figures 1, 2, https://wwwnc.cdc.gov/EID/article/26/10/19-1374-App1.pdf). These results suggested that the 17 viral strains isolated from sand flies in this study were a new phlebovirus, which we have named Wuxiang virus (WUXV), the SXWX1813-2 isolate designated as the representative member.

Conclusions

Our findings indicate that both sand flies and ticks serve as vectors for phleboviruses, including

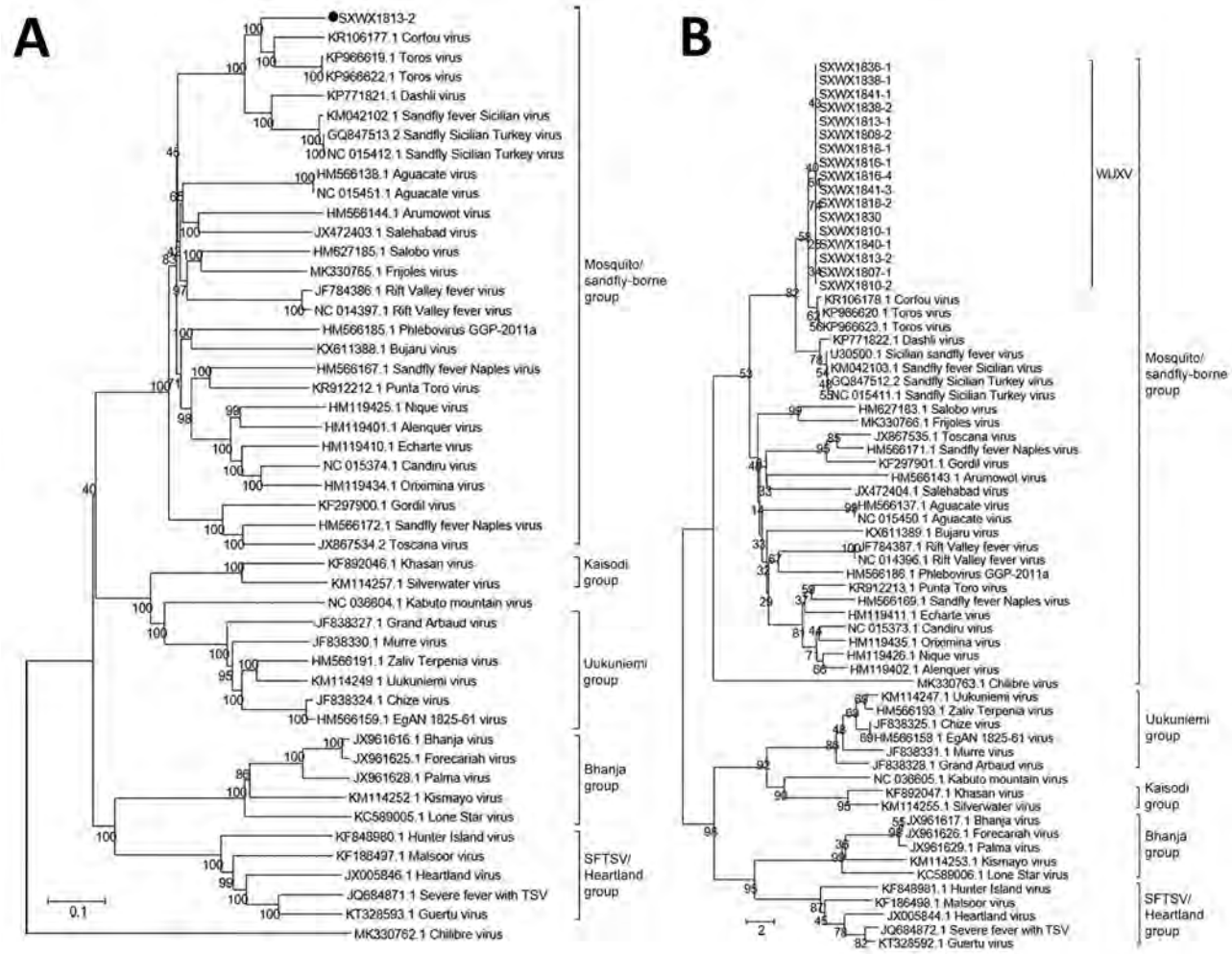

Figure 2. Evolution of nucleotide sequences of the large and medium gene segments of WUXV, a new phlebovirus isolated in China. A) Phylogenetic analysis of nucleotide sequences and molecular genetic evolution analysis of the large gene of WUXV isolate SXWX1813-2 (black dot), and reference isolates. B) Phylogenetic analysis of nucleotide sequences and molecular evolution analyses of the medium genes of 17 WUXV isolates, and reference isolates. MEGA 6.0 (https://www.megasoftware.net) and the neighbor-joining method were used for genetic evolution analysis with 1,000 bootstrap replicates. SFTSV, severe fever with thrombocytopenia syndrome virus; WUXV, Wuxiang virus.

WUXV, in China. In 2011, severe fever with thrombocytopenia syndrome virus, a tickborne virus known to cause fever and hemorrhaging, was reported in China (*10*). In addition, Guertu virus (*11*) was isolated from *Dermacentor nuttalli* ticks collected in Xinjiang, China.

To date, both CFUV (*12*) and TORV have been isolated from sand flies collected along the Mediterranean coast in Greece and Turkey. Sand fly–borne phleboviruses, including SFSV, SFNV, and TOSV, are all endemic to the Mediterranean region (*2*). Recently, Drin virus, closely related to CFUV and evolutionarily similar to CFUV and TORV, was isolated in Albania (*13*). Currently, in the taxonomy of the genus *Phlebovirus* CFUV is listed as a tentative species and TORV as an unclassified virus (*8*). Nucleotide- and amino acid–based homology, combined with phylogenetic analysis of phlebovirus genomes, suggests that WUXV is most closely related to TORV and CFUV, with each forming independent branches, indicating that WUXV may be a member of either the Toros-like or Corfu-like viruses.

Ph. chinensis is the dominant sand fly species in China and serves as the primary vector of *Leishmania* in this country (*14*). In our study, we isolated 17 strains of a sand fly–borne phlebovirus, WUXV, from *Ph. chinensis* sand flies, suggesting that the species can also serve as a vector for phleboviruses in China. This finding also suggests the possibility of co-infection with *Leishmania* and phleboviruses. Our finding of phlebovirus in sand flies in China suggests new challenges for controlling a potentially emerging virus to help safeguard public health.

BHK-21 cells and *Aedes albopictus* C6/36 cells were provided by the National Institute for Viral Disease Control and Prevention, Chinese Center for Disease Control and Prevention.

This work was supported by the Ministry of Science and Technology of the People's Republic of China (2018ZX10711001, 2018ZX10734-404-003); Development Grant of the State Key Laboratory of Infectious Disease Prevention and Control (2014SKLID103, 2015SKLID505); Key Research and Development (R&D) Projects of Shanxi Province, China (201803D31205); National Natural Sciences Foundation of China (no. 81371848, 31970445).

About the Author

Jing Wang is a master's degree student at the Qingdao University (Qingdao) and Chinese Center for Disease Control and Prevention (Beijing), China. Her research interests are arbovirus and its infection.

References

1. International Committee on Taxonomy of Viruses. Virus taxonomy: 2018b release. 2018 [cited 2019 Jun]. https://talk.ictvonline.org/taxonomy
2. Depaquit J, Grandadam M, Fouque F, Andry PE, Peyrefitte C. Arthropod-borne viruses transmitted by phlebotomine sandflies in Europe: a review. Euro Surveill. 2010;15:19507.
3. Sabin AB. Recent advances in our knowledge of dengue and sandfly fever. Am J Trop Med Hyg. 1955;4:198–207. https://doi.org/10.4269/ajtmh.1955.4.198
4. Çarhan A, Uyar Y, Ozkaya E, Ertek M, Dobler G, Dilcher M, et al. Characterization of a sandfly fever Sicilian virus isolated during a sandfly fever epidemic in Turkey. J Clin Virol. 2010;48:264–9. https://doi.org/10.1016/j.jcv.2010.05.011
5. Papa A, Konstantinou G, Pavlidou V, Antoniadis A. Sandfly fever virus outbreak in Cyprus. Clin Microbiol Infect. 2006;12:192–4. https://doi.org/10.1111/j.1469-0691.2005.01330.x
6. Song S, Li Y, Fu S, Liu H, Li X, Gao X, et al. Could Zika virus emerge in mainland China? Virus isolation from nature in *Culex quinquefasciatus*, 2016. Emerg Microbes Infect. 2017;6: 1–3. https://doi.org/10.1038/emi.2017.80
7. Sánchez-Seco M-P, Echevarría J-M, Hernández L, Estévez D, Navarro-Marí J-M, Tenorio A. Detection and identification of Toscana and other phleboviruses by RT-nested-PCR assays with degenerated primers. J Med Virol. 2003;71:140–9. https://doi.org/10.1002/jmv.10465
8. Alkan C, Erisoz Kasap O, Alten B, de Lamballerie X, Charrel RN. Sandfly-borne phlebovirus isolations from Turkey: new insight into the sandfly fever Sicilian and sandfly fever Naples species. PLoS Negl Trop Dis. 2016;10:e0004519. https://doi.org/10.1371/journal.pntd.0004519
9. Ejiri H, Lim CK, Isawa H, Yamaguchi Y, Sawabe K. Isolation and characterization of Kabuto Mountain virus, a new tick-borne phlebovirus from *Haemaphysalis flava* ticks in Japan. Virus Res. 2018;244:252–61. https://doi.org/10.1016/j.virusres.2017.11.030
10. Yu XJ, Liang MF, Zhang SY, Liu Y, Li JD, Sun YL, et al. Fever with thrombocytopenia associated with a novel bunyavirus in China. N Engl J Med. 2011;364:1523–32. https://doi.org/10.1056/NEJMoa1010095
11. Shen S, Duan X, Wang B, Zhu L, Zhang Y, Zhang J, et al. A novel tick-borne phlebovirus, closely related to severe fever with thrombocytopenia syndrome virus and Heartland virus, is a potential pathogen. Emerg Microbes Infect. 2018;7:1–14. https://doi.org/10.1038/s41426-018-0093-2
12. Rodhain F, Madulo-Leblond G, Hannoun C, Tesh RB. Le virus corfou: Un nouveau *Phlebovirus*isolé de phlébotomes en Grèce. Annales De L'institut Pasteur/Virologie. 1985;136:161–6. https://doi.org/10.1016/S0769-2617(85)80042-3
13. Bino S, Velo E, Kadriaj P, Kota M, Moureau G, Lamballerie X, et al. Detection of a novel phlebovirus (Drin virus) from sand flies in Albania. Viruses. 2019;11:469. https://doi.org/10.3390/v11050469
14. Guan LR, Zhou ZB, Jin CF, Fu Q, Chai JJ. *Phlebotomine sand flies* (Diptera: Psychodidae) transmitting visceral leishmaniasis and their geographical distribution in China: a review. Infect Dis Poverty. 2016;5:15. https://doi.org/10.1186/s40249-016-0107-z

Address for correspondence: Yajun Ma: Department of Naval Medicine, Second Military Medical University, Shanghai 200433, China; email: yajun_ma@163.com; Guodong Liang: State Key Laboratory of Infectious Disease Prevention and Control, National Institute for Viral Disease Control and Prevention, Chinese Center for Disease Control and Prevention, Beijing 102206, China; email: gdliang@hotmail.com

Drug Resistance Spread in 6 Metropolitan Regions, Germany, 2001–2018[1]

Melanie Stecher,[2] Antoine Chaillon,[2] Christoph Stephan, Elena Knops, Niko Kohmer, Clara Lehmann, Josef Eberle, Johannes Bogner, Christoph D. Spinner, Anna Maria Eis-Hübinger, Jan-Christian Wasmuth, Guido Schäfer, Georg Behrens, Sanjay R. Mehta, Jörg Janne Vehreschild, Martin Hoenigl

We analyzed 1,397 HIV-1 *pol* sequences of antiretroviral therapy–naive patients in a total of 7 university hospitals in Bonn, Cologne, Frankfurt, Hamburg, Hannover, and Munich, Germany. Phylogenetic and network analysis elucidated numerous cases of shared drug resistance mutations among genetically linked patients; K103N was the most frequently shared mutation.

The use of antiretroviral therapy (ART) has shown markedly decreased sickness and death rates in persons living with HIV (PLWH) (*1*–*3*). Meanwhile, the emergence of antimicrobial drug resistance in HIV-1 is raising public health concerns (*4*,*5*). Nationwide estimates of the prevalence of drug resistance mutations (DRMs) are not available in Germany (*6*); the reported prevalence of transmitted HIV-1 DRMs differ across regions and risk groups from 10.4%–17.2%, as described in 2 cohort studies from the German ClinSurv-HIV cohort and the Cologne-Bonn cohort (*6*,*7*).

Information about the dynamics and patterns of HIV transmission within defined areas and communities remains incomplete. Thus, we combined phylogenetic analysis with clinical and sociodemographic data, to determine the spread and dynamics of HIV-1 DRMs in 6 metropolitan regions in Germany, including the cities with the highest rates of new HIV-1 infections in 2017: Munich (17.3/100,000 population), Cologne (13.3/100,000 population), and Frankfurt (12.3/100,000 population), (*8*). We conducted this retrospective study in a cooperative effort of partner sites of the Translational Platform HIV (TP-HIV) (Cologne, Germany) and the University of California, San Diego (San Diego, CA, USA). The study was approved by the local ethics committees of the university hospitals of Bonn, Cologne, Munich, Hannover, Frankfurt, and Hamburg. All study participants gave written informed consent.

The Study

We analyzed HIV-1 partial *pol* sequences (HXB2 position 2550–3356), obtained as part of clinical routine care, and sociodemographic data of PLWH who received HIV care at the university hospitals of Bonn, Cologne, Frankfurt, Hamburg, and Hannover and at 2 hospitals in Munich during 2001–2018. Patients could participate in the study if they had recently received their diagnosis of HIV-1 and were ART naive; this conservative approach excluded participants for

Author affiliations: University of Cologne Faculty of Medicine, Cologne, Germany (M. Stecher, C. Lehmann, J.J. Vehreschild); University Hospital of Cologne, Cologne (M. Stecher, E. Knops, C. Lehmann, J.J. Vehreschild); German Center for Infection Research (DZIF), partner site Cologne, Cologne (M. Stecher, C. Lehmann, J.J. Vehreschild); University of California San Diego, San Diego, CA, USA (A. Chaillon, S.R. Mehta, M. Hoenigl); University Hospital of Frankfurt, Frankfurt am Main, Germany (C. Stephan, J.J. Vehreschild); LMU München, Munich, Germany (J. Eberle); German Center for Infection Research (DZIF), partner site Munich, Munich (J. Eberle, J. Bogner, C.D. Spinner); Department of the Ludwig-Maximilians-University, Munich (J. Bogner); Technical University of Munich School of Medicine, Munich (C.D. Spinner); University of Bonn Medical Center, Bonn, Germany (A.M. Eis-Hübinger); University Hospital of Bonn, Bonn (J.-C. Wasmuth); University Hospital Hamburg Eppendorf, Hamburg, Germany (G. Schäfer); Hannover Medical School, Hannover, Germany (G. Behrens); German Center for Infection Research (DZIF), partner site Hannover, Hannover, Germany (G. Behrens); San Diego Veterans Administration Medical Center, San Diego (S.R. Mehta); Medical University of Graz, Graz, Austria (M. Hoenigl)

DOI: https://doi.org/10.3201/eid2610.191506

[1]Preliminary results from this study were presented at the Conference for Retroviruses and Opportunistic Infections (CROI) 2019, March 4–7, 2019, Seattle, Washington, USA.

[2]These first authors contributed equally to this article.

whom the exact start date of ART or history of prior ART was not accurately documented.

Blood samples were collected before ART initiation. We sequenced partial HIV-1 *pol* region as previously described (*7*,*9*). We set the mixed mutation calling threshold at ≥10%, consistent with Sanger sequencing sensitivity (*10*). We identified major DRMs by using the Stanford University Genotypic Resistance Interpretation HVdb version 8.9, (https://hivdb.stanford.edu). We inferred the genetic transmission network as previously described (*7*,*9*,*11*); we inferred putative linkage for genetic distances ≤1.5% (*12*) (Appendix, https://wwwnc.cdc.gov/eid/article/26/10/19-1506-App1.pdf).

We performed statistical analyses by using Stata version 14 (StataCorp LP, https://www.stata.com). We applied Fisher exact or χ^2 test and univariable and multivariable logistic regression models, as appropriate, to determine characteristics that are associated with shared DRM and clustering. A shared DRM was defined as any DRM present in ≥2 genetically linked persons.

Overall, 1,397 HIV-1 infected participants were included. Most were male (82.9%; 1,158/1,397), originated from Germany (69.6%; 972/1,397), and infected with HIV-1 subtype B (72.8%; 1,017/1,397). The most commonly reported transmission risk was men who have sex with men (MSM) (56.7%; 792/1,397) (Table 1).

We identified an overall prevalence of any DRM at the time of diagnosis, excluding polymorphic mutations, of 17.8% (95% CI 15.7%–19.8%), 248/1,397 participants. The proportion varied significantly (p<0.001) by region, ranging from 9.1% (95% CI 5%–13%; 21/231) in Munich, up to 31.4% (95% CI 24%–38%; 53/169) in Hannover. Resistance mutations associated with nucleoside reverse transcriptase inhibitors (NRTIs) (172/1,397; 12.3%) were most frequent, followed by nonnucleoside reverse transcriptase inhibitors (NNRTIs) (124/1,397; 8.9%). The most common single mutations related to NNRTIs were K103N (31/124; 25.0%), and G190A (8/124; 6.5%). Of the NRTI resistance mutations, M41L (25/172; 14.5%), and T215S (18/172; 10.5%) were most frequently observed (Table 2).

Table 1. Characteristics of study participants with HIV harboring drug resistance mutations, Germany, 2001–2018*

Characteristic	No. (%) participants	No. (%) with DRMs	No. (%) with shared DRMs†	p value‡
Total	1,397 (100)	248 (17.8)	19 (8.1)	
Age, y				**0.032**
>45	430 (30.8)	82 (19.1)	2 (0.5)	
25–45	856 (61.3)	145 (16.9)	13 (1.5)	
<25	111 (7.9)	21 (18.9)	4 (3.6)	
Sex				0.059
F	239 (17.1)	39 (16.3)	0	
M	1,158 (82.9)	209 (18.0)	19 (1.6)	
HIV subtype				**0.003**
Non-B	380 (27.2)	65 (17.1)	0	
B	1,017 (72.8)	183 (17.9)	19 (1.9)	
Transmission risk§				0.164
HTS	302 (21.6)	48 (15.9)	2 (0.7)	
MSM	792 (56.7)	138 (17.4)	15 (1.9)	
Endemic	133 (9.5)	22 (16.5)	0	
PWID	24 (1.7)	4 (16.7)	1 (4.2)	
Other/Unknown	146 (10.5)	36 (24.7)	1 (0.7)	
Country of origin				0.104
Germany	972 (69.6)	181 (18.6)	17 (1.7)	
Other	373 (26.7)	58 (15.5)	1 (0.3)	
Unknown	52 (3.7)	9 (17.3)	1 (1.9)	
City				0.051
Cologne	582 (41.7)	110 (18.9)	14 (2.4)	
Hamburg	48 (3.4)	9 (18.8)	0	
Bonn	152 (10.9)	22 (14.5)	3 (1.9)	
Frankfurt	215 (15.4)	33 (15.4)	1 (0.5)	
Hannover	169 (12.1)	53 (31.4)	1 (5.9)	
Munich	231 (16.5)	21 (9.1)	0	
Year of HIV-1 diagnosis				0.206
2001–2006	103 (7.4)	14 (13.6)	0	
2007–2012	705 (50.5)	130 (18.4)	13 (1.8)	
2013–2018	589 (42.2)	104 (17.7)	6 (1.0)	

*DRM, drug resistance mutation; endemic, recent immigration from a country with a HIV prevalence >1%; HTS, heterosexuals; MSM, men who have sex with men; PWID, persons who injected drugs.
†Shared DRM were defined as any DRM present in ≥2 genetically linked patients (≤1.5% GD)
‡Fisher exact and χ^2 test were performed as appropriate. Bold text indicates significant results.
§Polymorphic mutations are not included in the prevalence of DRMs.

Transmission network analyses revealed that 20.7% (289/1,397) of participants had a putative linkage forming 102 transmission clusters. The largest cluster included 12 participants, mostly MSM from Bonn, Cologne, Munich, and Frankfurt (Figure 1, panels A, B). Participants <25 years and 25–45 years of age were significantly more likely to cluster compared with participants >45 years (<25 years, adjusted OR [aOR] 4.38, 95% CI 2.55–7.52, p<0.001; 25–45 years, aOR 1.91, 95% CI 1.36–2.678; p<0.001). Participants infected with HIV-1 subtype B were more likely to cluster than those with non-B subtype (aOR 4.05, 95% CI 2.37–6.90; p<0.001). Geospatial distribution differed; participants from Bonn were linked significantly more often than those from Cologne (aOR 1.63; 95% CI 1.06–2.49; p = 0.025), even though the cities are geographically close (Appendix Table).

The prevalence of transmitted DRM was comparable in clustering (47/289, 16.3%) and nonclustering (201/1,108; 18.1%) participants (p = 0.46) (Appendix Table). Of the 47 sequences harboring DRM, 19 (40.4%) were preferentially shared by participants living predominantly in Cologne (14/19, 73.7%) and Bonn (3/19, 15.8%) (Figure 2, panel A) and by participants reporting MSM as main risk factor (15/19; 78.9%) (Figure 2, panel B). Younger age (<25 years) was associated with a higher proportion of shared DRM (3/11; 3.5%) compared with older age (24–45 years, 13/856 [1.5%]; >45 years, 2/430 [0.5%]) (Table 1).

The most frequently observed putatively shared DRM was K103N, detected in 9/19 (47.4%) participants forming 4 distinct clusters, predominantly originating from Cologne (7/9, 77.8%). The second

Table 2. Proportion of identified drug resistance mutations in newly infected antiretroviral-naive patients with HIV-1, Germany, 2001–2018*

Mutation	Bonn, no. (%)	Cologne, no. (%)	Frankfurt, no. (%)	Hamburg, no. (%)	Hannover, no. (%)	Munich, no. (%)
NRTI						
T215FY	3 (1.21)	19 (7.66)	4 (1.61)	1 (0.40)	19 (7.66)	6 (2.42)
M41L	1 (0.40)	13 (5.24)	3 (1.21)	1 (0.40)	6 (2.42)	1 (0.40)
D67GNS	3 (1.21)	13 (5.24)	0	0	3 (1.21)	1 (0.40)
K219ERQ	3 (1.21)	7 (2.82)	1 (0.40)	0	3 (1.21)	2 (0.81)
M184IV	0	9 (3.63)	0	0	3 (1.21)	1 (0.40)
A62V	0	1 (0.40)	1 (0.40)	1 (0.40)	3 (1.21)	1 (0.40)
E44D	0	4 (1.61)	1 (0.40)	0	2 (0.81)	0
K70RT	0	4 (1.61)	0	0	2 (0.81)	0
L210W	1 (0.40)	2 (0.81)	0	0	3 (1.21)	0
T69D	1 (0.40)	4 (1.61)	0	0	1 (0.40)	0
F77L	0	0	0	0	4 (1.61)	0
L74V	0	4 (1.61)	0	0	0	0
K65R	0	2 (0.81)	0	0	1 (0.40)	0
V75AIM	0	3 (1.21)	0	0	0	0
NNRTI						
E138A†	7 (2.82)	21 (8.47)	11 (4.44)	1 (0.40)	6 (2.42)	3 (1.21)
K103ENT	7 (2.82)	16 (5.13)	5 (2.02)	2 (0.81)	4 (1.61)	3 (1.21)
V179DEF	0	11 (4.44)	4 (1.61)	2 (0.81)	8 (3.23)	5 (2.02)
G190AERS	2 (0.81)	9 (3.63)	0	0	2 (0.81)	1 (0.40)
Y188LHC	2 (0.81)	4 (1.61)	0	0	2 (0.81)	1 (0.40)
L100IV	0	2 (0.81)	3 (1.21)	0	3 (1.21)	0
Y181C	1 (0.40)	3 (1.21)	0	0	1 (0.40)	1 (0.40)
V108I	1 (0.40)	3 (1.21)	0	0	1 (0.40)	0
P225H	1 (0.40)	3 (1.21)	0	0	0	0
V106AIM	0	4 (1.61)	0	0	0	0
M230MI	0	2 (0.81)	0	0	0	0
A98AG	0	1 (0.40)	0	0	0	0
F227FL	0	1 (0.40)	0	0	0	0
H221HY	0	1 (0.40)	0	0	0	0
K101E	0	0	0	0	1 (0.40)	0
K238T	0	1 (0.40)	0	0	0	0
PI						
L90M	0	0	0	0	5 (2.02)	1 (0.40)
M46I	0	0	1 (0.40)	1 (0.40)	2 (0.81)	0
I84V	0	0	0	0	2 (0.81)	0
I47V	0	0	0	1 (0.40)	0	0
L90LM	0	0	0	0	1 (0.40)	0
M46L	0	0	1 (0.40)	0	0	0
V82L	0	0	0	0	0	1 (0.40)

*Data are presented by each city's university hospital as absolute numbers and percentages. No resistances to integrase strand transfer inhibitors were identified. NNRTI, nonnucleoside reverse transcriptase inhibitors; NRTI, nucleoside reverse transcriptase inhibitors; PI, protease inhibitors.
†E138A was not included in the drug resistance mutation/transmitted drug resistance mutation rate of our study population.

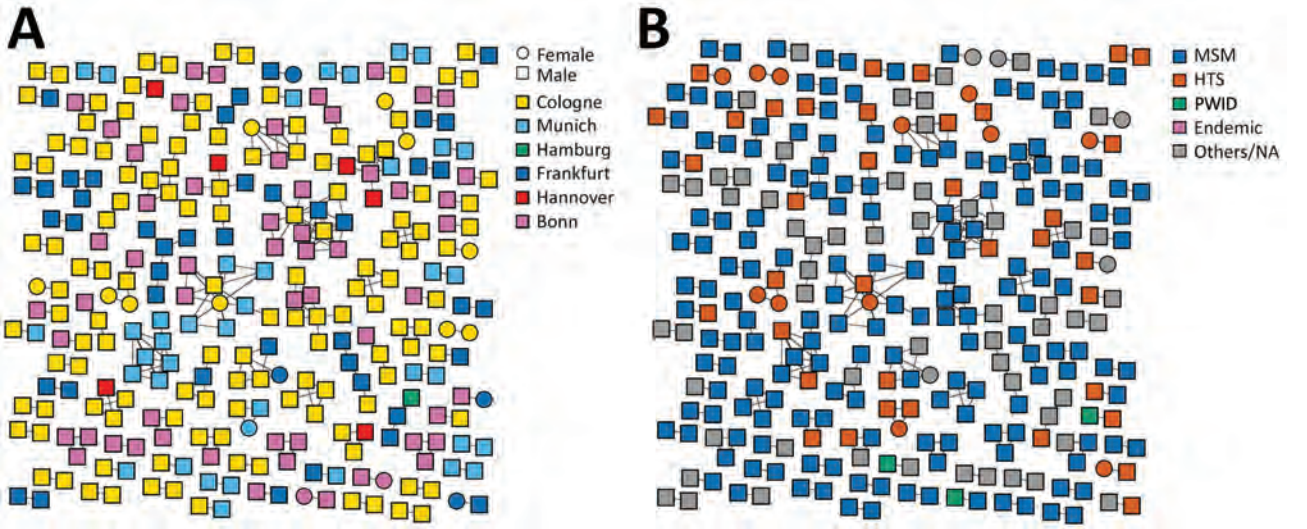

Figure 1. Transmission network analysis by sex and location (A) and by characteristic (B) for 1,397 patients with HIV, Germany, 2001–2018. Endemic, recent immigration from a country with HIV prevalence >1%; HTS, heterosexual patient; MSM, men who have sex with men; NA, not available; PWID, persons who inject drugs.

most common shared DRM was D67N, found in 6/19 (31.6%) participants from Cologne and Bonn.

Conclusions

The increasing prevalence of DRMs in PLWH has become a serious matter of concern for clinicians and public health entities (*4*). In our study, we observed a 17.8% prevalence of DRMs, higher than in previous studies (*6*,*7*). The proportion of NNRTI resistance mutations was 8.9%, which is potentially associated with the common use of NNRTI in first-line ART regimens. K103N represented one quarter of NNRTI resistance mutations, reducing susceptibility to the first-generation drugs nevirapine and efavirenz (*13*). Transmission network analyses revealed that K103N was the most frequently shared DRM.

K65R, K70RT, and M184IV were the most common of the NRTI resistance mutations we observed, particularly among the risk group of MSM living in Cologne and Hannover, indicating potential resistance to preexposure prophylaxis (PrEP) with tenofovir/emtricitabine. Such resistance might be an upcoming challenge as PrEP use increases. Monitoring for HIV infections with these mutations is of utmost importance for preventing an epidemic among high-risk PrEP users; one mitigation is to consider alternative PrEP regimens in regions with high resistance.

Our study had several limitations. First, our sample population could have been biased because participants were not randomly selected; our dataset was limited to ART-naive patients who received an HIV diagnosis at 7 university hospitals during 2001–2018. Although

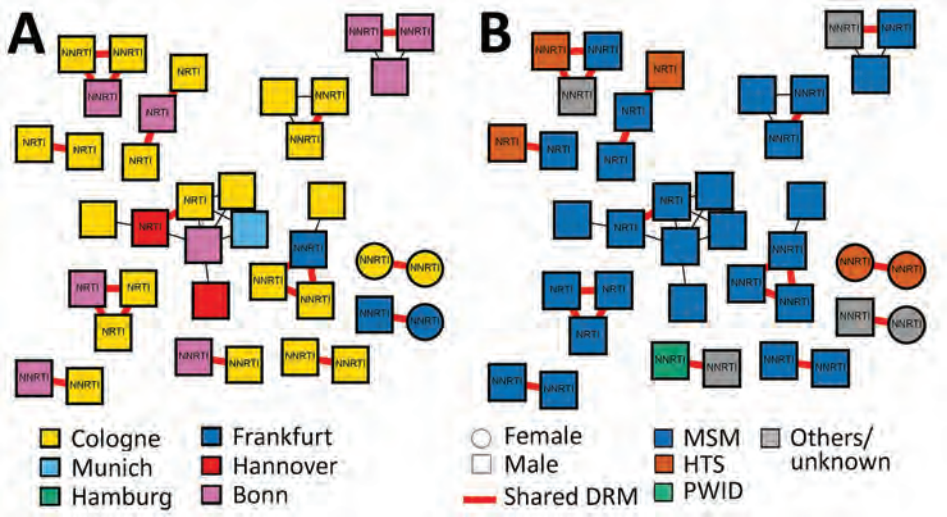

Figure 2. Presence of drug resistance mutations by location (A) and by risk factor (B) for 1,397 patients with HIV, Germany, 2001–2018. DRM, drug resistance mutation; HTS, heterosexual; MSM, men who have sex with men; NNRTI, nonnucleoside reverse transcriptase inhibitor; NRTI, nucleoside reverse transcriptase inhibitor; PWID, persons who inject drugs.

we know no reason why a university hospital setting would not be representative of the region, it is possible that populations treated outside these centers may have different transmission networks and risks; results are not generalizable to the entire regions or nationwide. Second, mixing of heterosexual patients and MSM in clusters may be due to missing single or multiple risk factors. Thus, their role could not be represented in the transmission networks. Third, we have not tested clinical correlates and drug resistance; the clinical relevance was inferred from the Stanford database.

In summary, we found that the overall rate of DRM was high in Germany. Network analysis elucidated cases of shared DRMs among genetically linked persons, mainly in MSM-dominated clusters. Our findings highlight regional differences and illustrate the need to test MSM, especially younger men, for HIV regularly and to evaluate local HIV programs and adapt screening and treatment strategies to local epidemics.

This work was supported by funds from the German Center for Infection Research (DZIF) (grant no. NCT02149004] and supported by the NIH grants (grant nos. AI036214, MH113477, and AI106039). M.H. received grant funding from Gilead.

The study was approved by the local ethics committees of the university hospitals of Bonn (reference no. 279-14), Cologne (reference no. 13-364), Munich (reference no. 438-14), Hannover (reference no. 279-14), Frankfurt (reference no. 279-14), and Hamburg (reference no. 279-14).

The datasets used and analyzed during the current study are available from the corresponding author on reasonable request.

About the Author

Dr. Stecher is an epidemiologist in the Department for Infectious Diseases at the University Hospital of Cologne, Germany. Her primary research interests are infectious diseases, HIV epidemiology, and cohort studies.

References

1. Glass TR, Sterne JA, Schneider MP, De Geest S, Nicca D, Furrer H, et al.; Swiss HIV Cohort Study. Self-reported nonadherence to antiretroviral therapy as a predictor of viral failure and mortality. AIDS. 2015;29:2195–200. https://doi.org/10.1097/QAD.0000000000000782
2. Saag MS, Benson CA, Gandhi RT, Hoy JF, Landovitz RJ, Mugavero MJ, et al. Antiretroviral drugs for treatment and prevention of HIV infection in adults: 2018 recommendations of the international antiviral society-USA panel. JAMA. 2018;320:379–96. https://doi.org/10.1001/jama.2018.8431
3. Robert Koch-Institut. Epidemiologisches bulletin 47 [in German]. 2018 [cited 2020 Jul 31]. https://www.rki.de/DE/Content/Infekt/EpidBull/Archiv/2018/Ausgaben/47_18.pdf
4. Wittkop L, Günthard HF, de Wolf F, Dunn D, Cozzi-Lepri A, de Luca A, et al.; EuroCoord-CHAIN study group. Effect of transmitted drug resistance on virological and immunological response to initial combination antiretroviral therapy for HIV (EuroCoord-CHAIN joint project): a European multicohort study. Lancet Infect Dis. 2011;11:363–71. https://doi.org/10.1016/S1473-3099(11)70032-9
5. Little SJ, Holte S, Routy JP, Daar ES, Markowitz M, Collier AC, et al. Antiretroviral-drug resistance among patients recently infected with HIV. N Engl J Med. 2002;347:385–94. https://doi.org/10.1056/NEJMoa013552
6. Schmidt D, Kollan C, Fätkenheuer G, Schülter E, Stellbrink HJ, Noah C, et al.; ClinSurv-HIV Drug Resistance Study Group in CHAIN. Estimating trends in the proportion of transmitted and acquired HIV drug resistance in a long term observational cohort in Germany. PLoS One. 2014;9:e104474. https://doi.org/10.1371/journal.pone.0104474
7. Stecher M, Chaillon A, Eis-Hubinger AM, Lehmann C, Fatkenheuer G, Wasmuth JC, et al. Pretreatment human immunodeficiency virus type 1 (HIV-1) drug resistance in transmission clusters of the Cologne-Bonn region, Germany. Clin Microbiol Infect. 2019 Feb;25:253.e1–253.e4. https://doi.org/10.1016/j.cmi.2018.09.025
8. Robert Koch-Institut. Epidemiologisches Bulletin 39 [in German]. 2017 [cited 2020 Jul 31]. http://www.rki.de/DE/Content/Infekt/EpidBull/Archiv/2017/Ausgaben/39_17.pdf
9. Stecher M, Chaillon A, Eberle J, Behrens GMN, Eis-Hübinger AM, Lehmann C, et al. Molecular epidemiology of the HIV epidemic in three German metropolitan regions—Cologne/Bonn, Munich, and Hannover, 1999–2016. Sci Rep. 2018;8:6799. https://doi.org/10.1038/s41598-018-25004-8
10. Döring M, Büch J, Friedrich G, Pironti A, Kalaghatgi P, Knops E, et al. geno2pheno[ngs-freq]: a genotypic interpretation system for identifying viral drug resistance using next-generation sequencing data. Nucleic Acids Res. 2018;46(W1):W271–7. https://doi.org/10.1093/nar/gky349
11. Kosakovsky Pond SL, Weaver S, Leigh Brown AJ, Wertheim JO. HIV-TRACE (TRAnsmission Cluster Engine): a tool for large scale molecular epidemiology of HIV-1 and other rapidly evolving pathogens. Mol Biol Evol. 2018;35:1812–9. https://doi.org/10.1093/molbev/msy016
12. Wertheim JO, Leigh Brown AJ, Hepler NL, Mehta SR, Richman DD, Smith DM, et al. The global transmission network of HIV-1. J Infect Dis. 2014;209:304–13. https://doi.org/10.1093/infdis/jit524
13. European AIDS Clinical Society (EACS). European guidelines for treatment of HIV-positive adults in Europe 9.1. 2018 [cited 2020 Jul 31]. http://www.eacsociety.org/files/2018_guidelines-9.1-english.pdf

Address for correspondence: Martin Hoenigl, Division of Infectious Diseases and Global Public Health, Department of Medicine, University of California, San Diego, 200 West Arbor Dr #8208, San Diego, CA 92103, USA; email: mhoenigl@ucsd.edu; Melanie Stecher, Department I for Internal Medicine, University Hospital of Cologne, Herderstraße 52-54, 50931 Köln, Germany; email: melanie.stecher@uk.koeln.de

Human Adenovirus B7d–Associated Urethritis after Suspected Sexual Transmission, Japan

Nozomu Hanaoka, Shin Ito, Naomi Nojiri, Masami Konagaya, Mitsuru Yasuda, Takashi Deguchi, Tsuguto Fujimoto

Outbreaks of acute respiratory disease associated with human adenovirus (HAdV) B7d have been reported, including fatal cases in the United States. In 2018, we detected HAdV-B7d in a patient with urethritis, probably transmitted through sexual contact. Infectious HAdV-B7d was excreted in urine and gargle for ≥10 days after the disappearance of symptoms.

Human adenoviruses (HAdVs) are DNA viruses that can cause respiratory diseases, conjunctivitis, and gastroenteritis (*1*). Seven species (A–G) and ≥100 types have been recognized so far. Among them, HAdV-E4, HAdV-B7, and HAdV-B14 cause severe acute respiratory illness, including severe acute respiratory distress syndrome (*2*). HAdV-B7d, a genome type of HAdV-B7, was originally designated in 1986 using restriction analysis (*3*) and classified as genotype B7d on the basis of complete genome analysis in 2013 (*4*). HAdV-B7d was first reported in China in 1980 (*3*); by the 1990s, HAdV-B7d was the primary circulating genome type in China, but then it was not detected during 1990–2009. In 2011, HAdV-B7d was prevalent throughout Asia, and outbreaks of infant pneumonia related to HAdV-B7d were reported in China (*5*–*7*).

In Japan, routine national surveillance for HAdVs is conducted for epidemic keratoconjunctivitis, pharyngeal conjunctival fever, and infectious gastroenteritis, and reported in the *Infectious Diseases Weekly Report* (*8*). Outbreaks of HAdV-B7d, including 2 fatal cases, were observed in Japan during 1995–1996 (*9*), after which it was rarely detected until the occurrence of the case we describe in 2018 (*10*).

Author affiliations: National Institute of Infectious Diseases, Tokyo, Japan (N. Hanaoka, N. Nojiri, M. Konagaya, T. Fujimoto); iClinic, Sendai City, Japan (S. Ito); Gifu University Hospital, Gifu City, Japan (M. Yasuda); Kizawa Memorial Hospital, Gifu City (T. Deguchi)

DOI: https://doi.org/10.3201/eid2610.191538

In 2014, HAdV-B7d was detected in Oregon and Illinois, USA (*11*,*12*). During 2016–2017, a total of 12 cases were reported, including 3 patients in a residential rehabilitation center, 7 college students, and 2 patients at a tertiary care hospital. Four of those 12 case-patients died; all 4 were in 3 adjacent New Jersey counties and had underlying conditions (*2*,*13*,*14*). In 2018, an HAdV-B7d outbreak at multiple facilities in several US regions resulted in the deaths of 11 infants at rehabilitation center in New Jersey and an 18-year-old freshman at the University of Maryland (*15*). In summary, HAdV-B7d transmission occurred in community and congregate settings throughout the United States, resulting in severe illness and death in some patients with underlying conditions. HAdV-B7d has been more commonly associated with severe respiratory disease and has a higher mortality rate than other HAdV types (*6*,*12*). Therefore, clinicians and public health facilitators should consider HAdV-B7d in patients with severe respiratory infections.

The Study

Since 2013, we have focused on HAdV-associated urethritis and performed pathogen screening from the urine of all-male patients with acute urethritis at iClinic in Sendai City, Miyagi Prefecture, Japan; all patients gave informed consent (reference *16* in Appendix, https://wwwnc.cdc.gov/EID/26/10/19-1538-App1.pdf). Recently, several papers have reported that HAdVs are ranked the third- or fourth-highest causative agents of nonchlamydial, nongonococcal urethritis (reference *17* in Appendix). Furthermore, HAdVs most commonly associated with urethritis are those that cause epidemic keratoconjunctivitis, which are types D37, D56, and D64 (references *16*,*18* in Appendix).

In July 2018, a case of male urethral inflammation associated with HAdV-B7d was detected in a 22-year-old heterosexual man. He was unmarried and did not

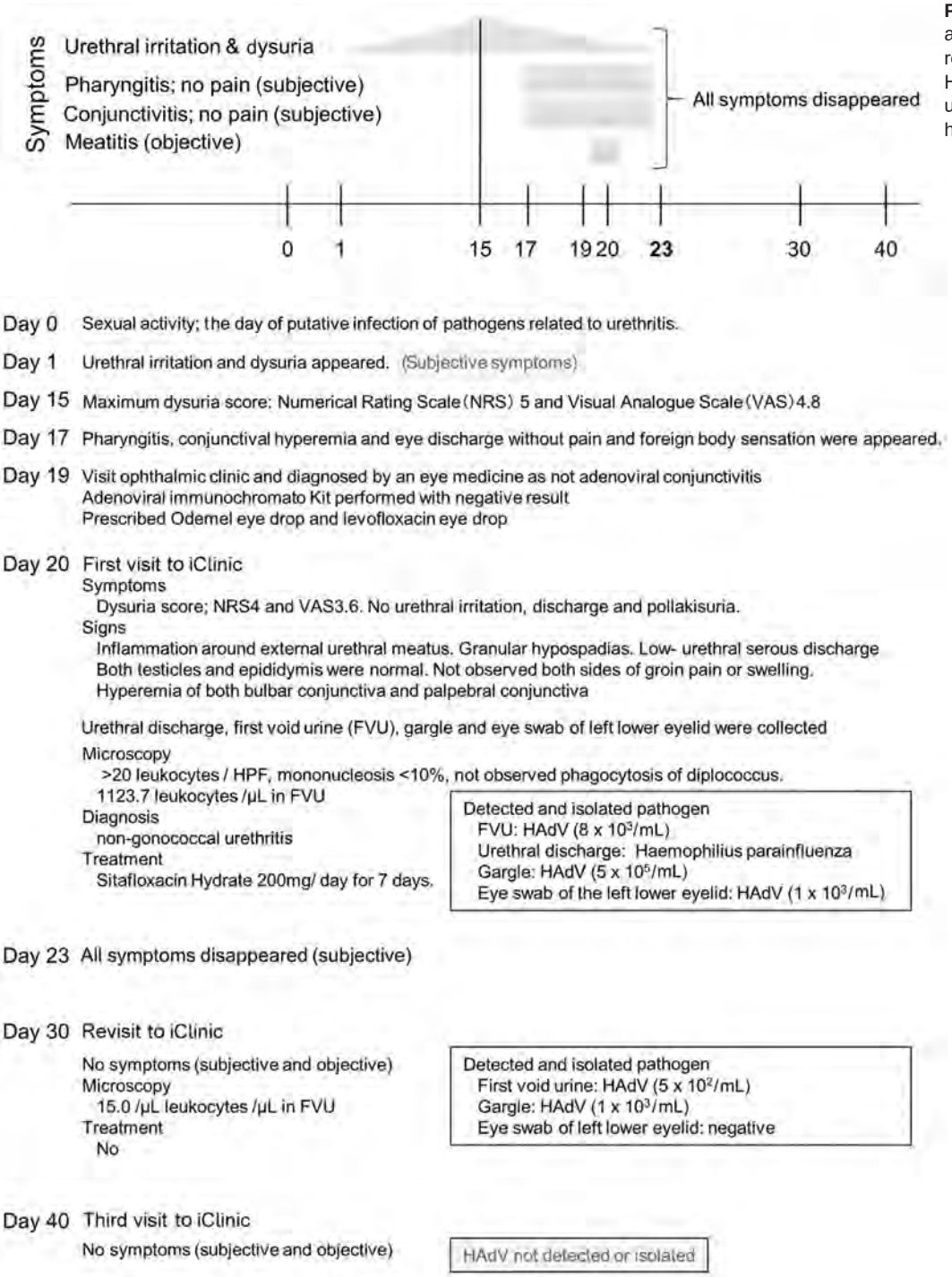

Figure 1. Clinical course and laboratory test results for patient with HAdV B7d–associated urethritis, Japan. HAdV, human adeovirus.

have a specific sexual partner. He had an unremarkable medical history, no history of sexually transmitted infections, and no record of traveling abroad. He claimed to have had 2 sexual encounters during his lifetime; the first was in 2016, but the second, in 2018, we considered to be the putative infection day (day 0) (Figure 1). He described it as a casual sexual encounter with a previously unknown woman and reported the encounter to include protected vaginal intercourse, cunnilingus, and unprotected oral intercourse. The patient denied insertive or receptive anal intercourse as well as mouth-to-mouth kissing. Urethral irritation and dysuria appeared on day 1 and continued to develop gradually (Figure 1); these symptoms might be

caused by mechanical irritation. On day 15, the patient experienced the most pain from his symptoms, reporting a numerical rating scale score of 5/10 and a visual analog scale score of 4.8/10. These scales are subjective scores of pain (reference *19* in Appendix). Pharyngitis and conjunctivitis appeared on day 17. On day 19, he visited an ophthalmic clinic for confirmation of conjunctivitis; however, it was not considered to be adenoviral conjunctivitis because an adenoviral immunochromatographic kit produced a negative result. Fluorometholone and levofloxacin eye drops were prescribed. Because his urethritis symptoms were severe, he visited a sexually transmitted diseases clinic (Sendai city, Miyagi prefecture, Japan) on day 20. The patient reported no fever, chills, or malaise; on the basis of his symptoms and results of a physical examination (Figure 1), we diagnosed nongonococcal urethritis. Because we could not exclude the possibility of bacterial infection, we prescribed sitafloxacin hydrate (200 mg/d for 7 days). Pathogen screening at the first visit to the clinic detected *Haemophilus parainfluenzae* bacteria from urethral discharge, but the clinical significance was unclear.

We isolated HAdV in A549 cells from first-void urine, throat gargle, and eye discharge fluid by a previously described method (reference *16* in Appendix). No other pathogens were identified. Sequences of the HAdV hexon, fiber, and penton open reading frames obtained by Sanger sequencing from all 3 specimen sources were identical. The full genome sequence was obtained from the urine isolate (designated strain 293) (Appendix Tables 1, 2) and deposited in GenBank (accession no. LC530212). We also performed a BLAST analysis (https://blast.ncbi.nlm.nih.gov/Blast.cgi) as previously described (*2*) with reference sequences of HAdV type 7 (Appendix Figure 1, Figure 2). On the basis of the phylogenetic tree analysis of whole-genome sequences, we classified the isolated HAdV-B7 strain into the same cluster as HAdV-B7d. In addition, we performed an in silico analysis of the genome using Restriction Analyzer software (http://www.molbiotools.com/restrictionanalyzer.html) by comparing the patterns of the 293 isolate with a reference HAdV-7d sequence and the following enzymes: *Bam*HI, BclI, BstEII, *Hpa*I, and *Sma*I (Appendix Figure 2). After these analyses, we identified the 293 isolate as HAdV-7d. On

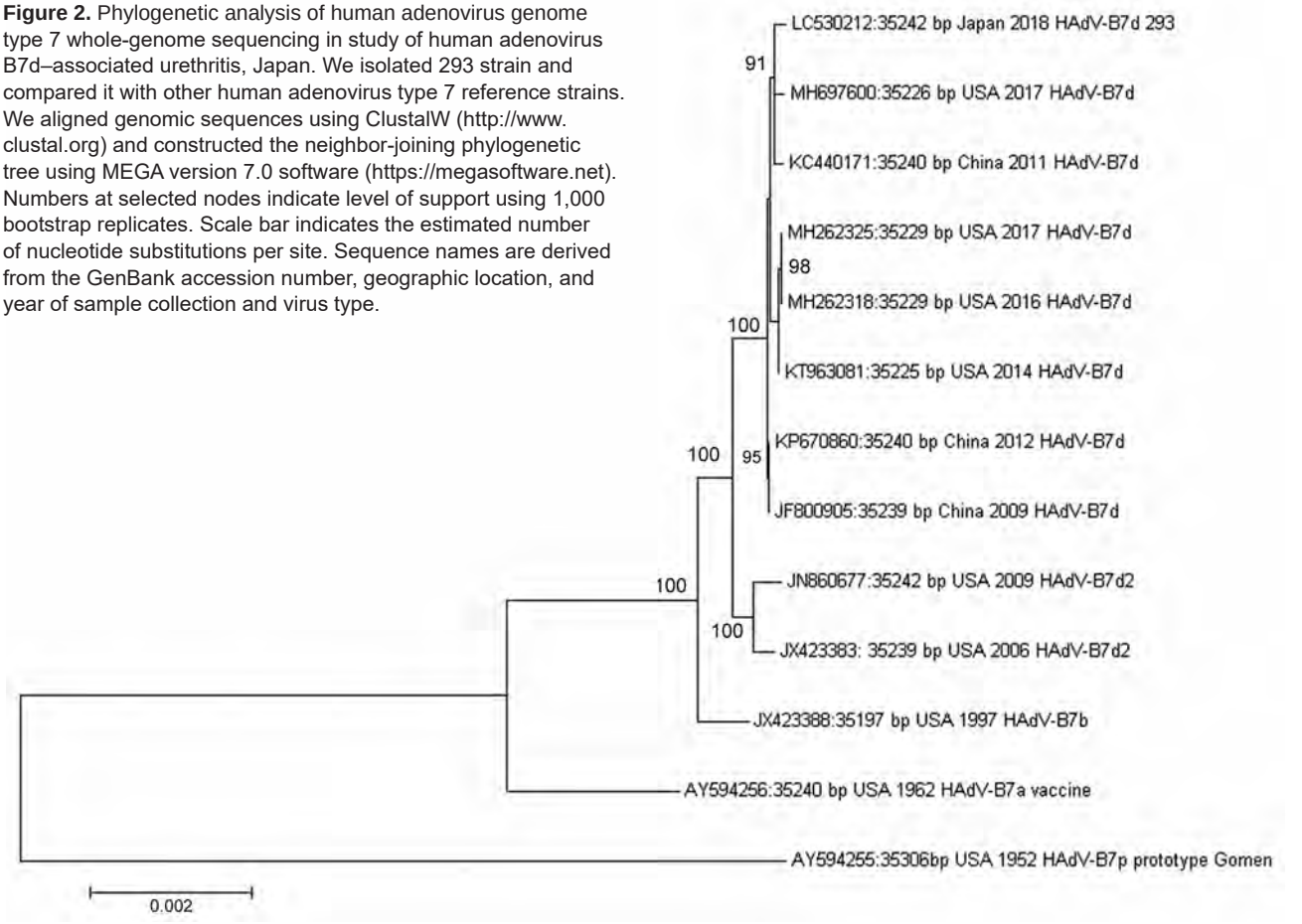

Figure 2. Phylogenetic analysis of human adenovirus genome type 7 whole-genome sequencing in study of human adenovirus B7d–associated urethritis, Japan. We isolated 293 strain and compared it with other human adenovirus type 7 reference strains. We aligned genomic sequences using ClustalW (http://www.clustal.org) and constructed the neighbor-joining phylogenetic tree using MEGA version 7.0 software (https://megasoftware.net). Numbers at selected nodes indicate level of support using 1,000 bootstrap replicates. Scale bar indicates the estimated number of nucleotide substitutions per site. Sequence names are derived from the GenBank accession number, geographic location, and year of sample collection and virus type.

the basis of these results, we concluded that the patient acquired the HAdV-B7d infection, which caused urethritis, conjunctivitis, and pharyngitis, during sexual intercourse. All symptoms disappeared by day 23. When the patient revisited the clinic on day 30, he had no urethral symptoms. We detected HAdV-B7d strains isolated from first-void urine and gargle but not from eye discharge; no other pathogens tested in this study were detected. On day 40, the patient's third visit to the clinic, no pathogens were detected. Approximately 2 months later, no symptoms were observed, and we confirmed a good prognosis.

Conclusions

HAdVs infect mucous membranes and can infect the urethra. Documented cases of HAdV urethritis are most often associated with certain species D HAdVs that cause epidemic keratoconjuctivitis (references *16–18* in Appendix). Our finding of HAdV-B7d, a virus more commonly associated with acute respiratory infections, in this patient was unexpected. Although we identified *H. parainfluenza* from urethral discharge at the first clinic visit, we suspect that it may have contributed to but not caused the patient's primary symptoms. The isolated HAdV-B7d strains in this study were excreted in urine and gargle for ≥1 week after all symptoms had disappeared (Figure 1), which suggests that HAdV-B7d infection may cause urethritis and involve viral shedding into urine.

This work was partly supported by the Japan Society for the Promotion of Science KAKENHI grants (grant nos. JP 25861458 and JP 15K20119) and partly supported by a grant for Research on Emerging and Re-emerging Infectious Diseases and Immunization from the Japanese Ministry of Health, Labour and Welfare (grant no. 10110713).

About the Author

Dr. Hanaoka is a senior scientist at Laboratory Diagnosis Division, Infectious Disease Surveillance Center, National Institute of Infectious Diseases, Japan. His research interests are epidemiology, etiology, and the development of diagnostic methods for human adenovirus.

References

1. Crenshaw BJ, Jones LB, Bell CR, Kumar S, Matthews QL. Perspective on adenoviruses: epidemiology, pathogenicity, and gene therapy. Biomedicines. 2019;7:61. https://doi.org/10.3390/biomedicines7030061
2. Killerby ME, Rozwadowski F, Lu X, Caulcrick-Grimes M, McHugh L, Haldeman AM, et al. Respiratory illness associated with emergent human adenovirus genome type 7d, New Jersey, 2016–2017. Open Forum Infect Dis. 2019;6:2016–17. https://doi.org/10.1093/ofid/ofz017
3. Li Q-G, Wadell G. Analysis of 15 different genome types of adenovirus type 7 isolated on five continents. J Virol. 1986;60:331–5. https://doi.org/10.1128/JVI.60.1.331-335.1986
4. Tang L, An J, Yu P, Xu W. Complete genome sequence of human adenovirus type 7 associated with fatal infant pneumonia. Genome Announc. 2013;1:e00182-12. https://doi.org/10.1128/genomeA.00182-12
5. Zhao S, Wan C, Ke C, Seto J, Dehghan S, Zou L, et al. Re-emergent human adenovirus genome type 7d caused an acute respiratory disease outbreak in Southern China after a twenty-one year absence. Sci Rep. 2015;4:7365. https://doi.org/10.1038/srep07365
6. Yu Z, Zeng Z, Zhang J, Pan Y, Chen M, Guo Y, et al. Fatal community-acquired pneumonia in children caused by re-emergent human adenovirus 7d associated with higher severity of illness and fatality rate. Sci Rep. 2016;6:37216. https://doi.org/10.1038/srep37216
7. Ng O-T, Thoon KC, Chua HY, Tan NWH, Chong CY, Tee NWS, et al. Severe pediatric adenovirus 7 disease in Singapore linked to recent outbreaks across Asia. Emerg Infect Dis. 2015;21:1192–6. https://doi.org/10.3201/eid2107.141443
8. National Institute of Infectious Diseases. Infectious Diseases Weekly Report [cited 2020 Aug 21]. https://www.niid.go.jp/niid/en/idwr-e.html
9. National Institute of Infectious Diseases. Adenovirus type 7, Japan, April 1995–December 1996. Infectious Agents Surveillance Report. 1997;18:79–80 [cited 2020 Aug 21]. http://idsc.nih.go.jp/iasr/18/206/tpc206.html
10. National Institute of Infectious Diseases. Adenovirus infections, 2008 to June 2017, Japan. Infectious Agents Surveillance Report. 2017;38:133–135 [cited 2020 Aug 21]. https://www.niid.go.jp/niid/en/iasr-e/865-iasr/7390-449te.html
11. Kajon AE, Ison MG. Severe infections with human adenovirus 7d in 2 adults in family, Illinois, USA, 2014. Emerg Infect Dis. 2016;22:730–3. https://doi.org/10.3201/eid2204.151403
12. Scott MK, Chommanard C, Lu X, Appelgate D, Grenz L, Schneider E, et al. Human adenovirus associated with severe respiratory infection, Oregon, USA, 2013–2014. Emerg Infect Dis. 2016;22:1044–51. https://doi.org/10.3201/eid2206.151898
13. Rozwadowski F, Caulcrick-Grimes M, McHugh L, Haldeman A, Fulton T, Killerby M, et al. Notes from the field: fatalities associated with human adenovirus type 7 at a substance abuse rehabilitation facility—New Jersey, 2017. MMWR Morb Mortal Wkly Rep. 2018;67:371–372.
14. Biggs HM, Lu X, Dettinger L, Sakthivel S, Watson JT, Boktor SW. Adenovirus-associated influenza-like illness among college students, Pennsylvania, USA. Emerg Infect Dis. 2018;24:2117–9. https://doi.org/10.3201/eid2411.180488
15. Meehan S. 30 adenovirus cases confirmed at University of Maryland; at least eight hospitalized. Baltimore Sun. 2018 [cited 2020 Aug 13]. https://www.baltimoresun.com/education/bs-md-adenovirus-20181207-story.html

Address for correspondence: Nozomu Hanaoka, Laboratory Diagnosis Division, Infectious Disease Surveillance Center, National Institute of Infectious Diseases, 1-23-1 Toyama, Shinjyu-ku, Tokyo 162-8640, Japan; email: nozomu@nih.go.jp

Polyester Vascular Graft Material and Risk for Intracavitary Thoracic Vascular Graft Infection[1]

Tiziano A. Schweizer, Srikanth Mairpady Shambat, Vanina Dengler Haunreiter, Carlos A. Mestres, Alberto Weber, Francesco Maisano, Annelies S. Zinkernagel,[2] Barbara Hasse[2]

Prosthetic vascular graft infections of the thoracic aorta are rare but can be fatal. Our comparison of collagen- and gelatin-coated grafts showed that collagen-coated grafts were associated with increased biofilm formation and bacterial adherence in vitro and with higher rates of perioperative vascular graft infections in vivo.

Prosthetic vascular graft infections (PVGIs) of the thoracic aorta occur in 1%–3% of patients, but lethality rates are >20% (*1*,*2*). Because of an aging population with multiple medical conditions, more vascular grafts are being implanted, resulting in more PVGIs. Infection often occurs during the perioperative period (*3*) as a consequence of inoculation with bacteria mostly originating from the patient's own skin flora. PVGIs are biofilm-associated infections in which the matrix around the bacteria impairs chances of treatment success (*4*). Hence, the primary aim is to prevent perioperative infections by identifying risk factors, such as type of prosthesis.

The few comparative studies reported have focused mostly on use of antibiotic-bonded grafts to reduce the risk for PVGIs in vitro and in vivo (*5*–*7*). However, lack of approval by regulatory authorities, reduced commercial availability, and lack of long-term follow-up data on infection-free survival should be considered (*8*–*10*). Furthermore, selection pressure from the use of topical antibiotics might lead to resistance. *Staphylococcus aureus* has been shown to colonize rifampin-bonded grafts 7 days after implantation (*10*). Hence, implanted grafts are usually coated with proteinaceous solutions only, allowing for quick integration into host tissue. We compared susceptibility of 2 graft materials to biofilm formation in vitro and rates of infections in vivo.

For our in vitro study, we compared the susceptibility of 2 thoracic vascular woven polyester grafts with different coatings—collagen (collagen graft, InterGard Hemabridge, https://www.getinge.com) and gelatin (gelatin graft, Terumo Aortic, Gelweave, https://terumoaortic.com)—to biofilm formation. The collagen graft is coated with a highly purified form of cross-linked bovine type 1 collagen. The gelatin graft is coated with a modified mammalian gelatin. Gelatin is derived mainly from type 1 collagen by heat denaturation, a process during which collagen loses its native triple helical structure. The resorption time for collagen is 4–8 weeks and for gelatin, 14 days. For our in vivo study, we investigated the rate of infections associated with the 2 grafts among prospective patients undergoing open-chest cardiac surgery at the University Hospital Zurich (Zurich, Switzerland).

The Study

For the in vitro experiments, we dissected the grafts into 5 × 5 mm square pieces and inoculated them with bacterial strains representing pathogens implicated in thoracic PVGI in our patient cohort. These were derived from either Vascular Graft Cohort Study (VASGRA) patients or laboratory strains (Appendix Table 1, Figure 1, https://wwwnc.cdc.gov/EID/article/26/10/19-1711-App1.pdf) and maintained on Columbia blood agar plates (bioMérieux SA, https://www.biomerieux.com) and in tryptic

Author affiliations: University Hospital Zurich, Zurich, Switzerland (T.A. Schweizer, S. Mairpady Shambat, V. Dengler Haunreiter, C.A. Mestres, F. Maisano, A.S. Zinkernagel, B. Hasse); HerzZentrum Hirslanden Zurich, Zurich (A. Weber)

DOI: https://doi.org/10.3201/eid2610.191711

[1]This work was presented in part at the Joint Meeting Club de Pathologie Infectieuse and Swiss Society of Microbiology Meeting, Bern, Switzerland, 2019 Feb 6; and at the International Society of Cardiovascular Infectious Diseases Symposium, Lausanne, Switzerland, 2019 Jun 2–4.

[2]These senior authors contributed equally to this article.

soy broth (Becton Dickinson, https://www.bd.com) at 37°C. Graft patches were incubated with bacteria in tryptic soy broth–glucose solution (glucose concentration 8 mmol/L) at 37°C for 72 h, and medium was exchanged every 24 h. The patches were washed with phosphate-buffered saline (PBS), sonicated at 44 khz, and the resulting optical density at a wavelength of 600 was measured in a microplate reader. All bacteria, apart from *Pseudomonas aeruginosa* strain 2, showed increased biofilm formation on the collagen graft compared with the gelatin graft patches (Figure, panel A).

Biofilms of selected strains were stained with SYTO 9 of the LIVE/DEAD *Bac*Light Bacterial Viability Kit (ThermoFisher Scientific, https://www.thermofisher.com) according to the manufacturer's instructions. The graft patches were placed in 8-well microslides (ibidi, https://ibidi.com) and visualized by confocal laser scanning microscopy with a Leica TCS SP8 inverted microscope (https://www.leica-microsystems.com) under a 63×/1.4 oil immersion objective. We selected 2 representative spots per graft patch, providing a stack of horizontally acquired images (512 × 512 pixels representing an area of 244.8 µm × 244.8 µm) with a z-step size of 0.12 µm. We processed the obtained stacks by using Imaris 9.2.0 software (Bitplane; Oxford Instruments, https://imaris.oxinst.com/support/imaris-release-notes/9-2-0). Biofilm height and volume were determined as previously described (*11*). This approach illustrated the increased biofilm formation on collagen graft patches (Appendix Figure 2). Quantitative analysis from the obtained confocal laser scanning microscopy images corroborated the initial findings because biofilm grown on collagen graft patches displayed increased total biofilm mass volume as well as maximal biofilm height (Figure, panel B).

One possible explanation for the increased susceptibility to biofilm formation could be the distinct coatings of the grafts. Hence, we coated well plates overnight at 4°C with either rat tail collagen 1 (10 µg/mL; ThermoFisher Scientific) or type B gelatin solution (10 µg/mL; Sigma-Aldrich, https://www.sigmaaldrich.com). The plates were incubated with bacteria at 37°C for 30 min. Bacteria were washed, stained with 0.1% crystal violet (Fluka; Sigma Aldrich, https://www.sigmaaldrich.com), solubilized in 95% ethanol, and the resulting optical density at 570 nm was measured. The tested strains adhered substantially better to collagen (Figure, panel C). Our findings are supported by studies demonstrating the potential of gram-positive bacteria to adhere to collagen, whereas only minor affinity was observed for gelatin (*12*,*13*).

To assess the effects of these findings in vivo, we analyzed 412 prospective participants with woven polyester grafts: 28 VASGRA participants in whom intracavitary thoracic PVGI developed and 384 contemporaneous open-chest cardiac surgery patients in whom PVGI did not develop (controls) (Table). Data and strains isolated from patients were used in accordance with Cantonal Ethics Committee approval KEK-ZH-Nr. 2012-0583. For statistical analyses with GraphPad Prism 8 (GraphPad

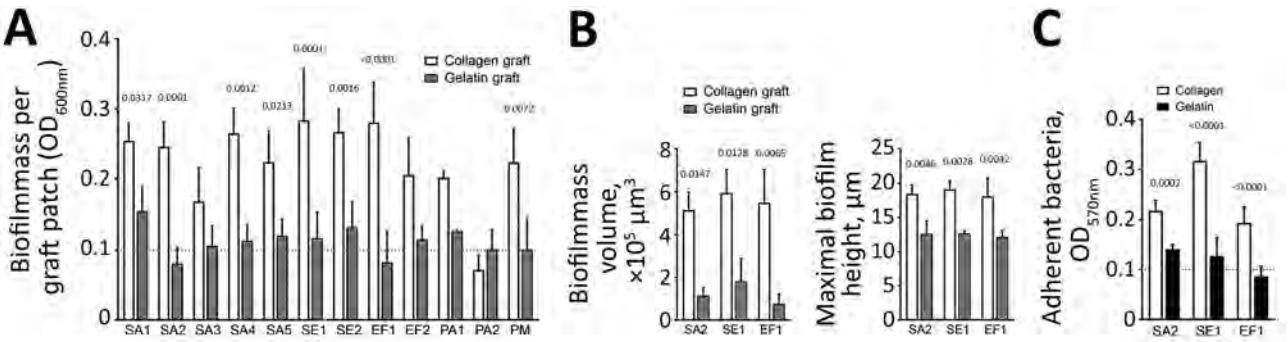

Figure. Increased susceptibility of collagen graft to biofilm formation compared with gelatin graft. Graft patches were inoculated with indicated bacterial strains for 72 h and analyzed quantitatively and qualitatively. A) Biofilm formation on the graft patches determined by optical density measurements. B) Total biofilm mass volume and maximal biofilm height, respectively, formed on the graft patches by the 3 clinical isolates—SA2, SE1, and EF— determined from the confocal laser scanning microscopy images with imaris software (https://imaris.oxinst.com). C) Adherence assay to the 2 different coatings used by the grafts. The limit of reliable detection of the plate reader is indicated by the dashed line (OD_{600nm} = 0.1). All data represent mean ± SD of 3 biological replicates performed in at least 2 technical replicates and were analyzed by using GraphPad Prism 8 (GraphPad Software, https://www.graphpad.com). The values above the graphs represent p values, calculated by using 2-way analysis of variance with the Sidak multiple comparison to determine statistical significance between the 2 graft types or coatings (panels A–C). EF, *Enterococcus faecalis*; OD_{600nm}, optical density at a wavelength of 600; PA, *Pseudomonas aeruginosa*; PM, *Pasteurella multocida*; PVGI, prosthetic vascular graft infection; SA, *Staphylococcus aureus*; SE, S. *epidermidis*.

Software, https://www.graphpad.com), we used nonparametric tests (Fisher exact or Wilcoxon rank-sum, as appropriate). When normalized to the total number of control patients (n = 384 who had undergone the cardiac surgery but had no PVGI), the calculated percentage of intracavitary thoracic PVGI (n = 28 VASGRA patients who had undergone the cardiac surgery and had PVGI) was higher for patients in the collagen-graft (10.8%) versus the gelatin-graft group (3.52%; p<0.005).

Conclusions

We found more biofilm formation on collagen-coated polyester vascular grafts than on gelatin-coated grafts, possibly because the tested strains adhered substantially better to collagen than to

Table. Risk for early and late intracavitary thoracic PVGI among cardiac surgery patients with vascular woven polyester grafts coated with collagen or gelatin, Zurich, Switzerland*

Demographics and risk factors	Early thoracic PVGI, n = 15	Late thoracic PVGI, n = 13	Cardiac surgery, no PVGI, n = 384	p value†
Demographic				
Sex				0.27
M	3 (20)	3 (23)	54 (14)	
F	12 (80)	10 (77)	330 (86)	
Caucasian race	15 (100)	12 (92)	375 (98)	0.51
Age, y, median (IQR)	65 (54–68)	65 (51–68)	58 (49–67)	0.89
Risk factors				
BMI, kg/m^2, median (IQR)	27 (24–33)	26 (23–28)	26 (24–29)	0.97
Smoking				0.69
Never	6 (40)	6 (46)	150 (39)	
Former/current	9 (60)	7 (54)	234 (61)	
Alcohol consumption	4 (27)	3 (23)	131 (34.0)	0.41
Hypertension	12 (80)	8 (62)	273 (72)	1.0
Diabetes mellitus	2 (13)	1 (8)	54 (14)	0.78
Dyslipidemia	7 (47)	6 (46)	196 (51)	0.70
Cardiac events	8 (53)	7 (54)	173 (45)	0.43
Cerebrovascular events	3 (20)	3 (23)	58 (15)	0.41
Coagulopathy	0 (0)	0 (0)	4 (1.0)	1.0
Malignancy,	4 (27)	2 (15)	69 (18)	0.62
Charlson Comorbidity Index score, median (IQR)	2 (1–5)	2 (1–4)	1 (1–3)	0.27
Index surgery				0.55
Dissection	7 (57)	6 (46)	154 (40)	
Aneurysm/pseudoaneurysm	8 (53)	7 (54)	230 (60)	
Symptoms at index operation				0.004
Asymptomatic	4 (27)	5 (23)	223 (58)	
Symptomatic	9 (60)	10 (77)	161 (42)	
Setting of index operation				0.08
Elective	9 (60)	7 (54)	284 (74)	
Urgent/emergency	6 (40)	6 (46)	100 (26)	
ASA class at index operation				<0.001
Grade ≤III	7 (47)	3 (23)	38 (10)	
Grade >III	8 (53)	10 (77)	346 (90)	
Cardiopulmonary bypass time, min, median (IQR)	174 (154–338)	163 (84–363)	206 (154–338)	0.23
Polyester vascular woven grafts				0.005
Collagen graft	11 (74)	9 (69)	165 (39.5)	
Gelatin graft	4 (27)	4 (31)	219 (52.4)	
PVGI				
Assumed route				NA
Perioperative	15 (100)	0	NA	
Hematogenous	0	8 (62)	NA	
Contiguous	0	5 (38)	NA	
Microorganisms				NA
Staphylococcus aureus	4 (27)	3 (23)	NA	
Coagulase-negative staphylococci	2 (13)	1 (7.7)	NA	
Enterococcus faecalis	0	2 (15)		
Streptococcus spp	4 (27)	0	NA	
Cutibacterium acnes	1 (7)	2 (15)	NA	
Pseudomonas aeruginosa	1 (7)	0	NA	
Pasteurella multocida	1 (7)	0	NA	
Culture negative	2 (14)	3 (23)	NA	

*Values are no. (%) unless otherwise indicated. ASA, American Society of Anesthesiology; BMI, body mass index; IQR, interquartile range; NA, not applicable; PVGI, prosthetic vascular graft infection.
†p values from Fisher exact test (categorical variables) and Wilcoxon rank-sum test (continuous variables) comparing patients with PVGI (early and late combined) and patients without PVGI.

gelatin. When we analyzed prospective patients with PVGI and contemporary controls, the percentage of PVGI associated with collagen-coated grafts was also higher.

The strengths of our study include use of patient-derived strains of bacteria and the prospective collection of patients with incident PVGIs and controls. Our study has some limitations. First, it was a single-center study, resulting in low patient numbers, and the role of the graft material as a risk factor for PVGI is difficult to prove because of the rarity of the infection. Furthermore, data for patients with PVGI have to be interpreted with caution because some patients have additional foreign material in the heart. Second, publicly available information on the exact type of coating as well as the application procedures used is lacking. In addition, the experiments were performed in a static experimental setup instead of a flow chamber. However, because we were interested in direct bacterial adherence to the graft material, simulating a scenario in which infection would occur as consequence of unintentional inoculation during the perioperative period, we believe that the setup used is adequate. We did not reproduce a gram-positive and gram-negative mixed biofilm formation experiment because a monomicrobial setup enabled us to determine which material and coating was more susceptible to bacterial adherence in a more controllable fashion.

In conclusion, biofilm formation was increased on collagen-coated vascular grafts compared with gelatin-coated grafts in vitro. As opposed to another risk factor analysis from the VASGRA study (*3*), in our study, the graft material was associated with the PVGI rate. Parameters such as vascularization potential, secure pseudointima growth, and reduced thrombogenicity are perceived as affecting successful integration and functionality of prosthetic vascular grafts (*14*). Further parameters should be considered in the future design and development of vascular prostheses to reduce the emerging trend of PVGI.

Members of the VASGRA Cohort Study (in alphabetical order): A. Anagnostopoulos, B. Hasse, N. Eberhard, M. Hoffmann, L. Husmann, D. Jaeger, R. Kopp, B. Ledergerber, C. A. Mestres, Z. Rancic, R. Zbinden, A. Zimmermann, A. S. Zinkernagel.

Acknowledgments

We are grateful to our patients for their participation in the study. We thank study nurses Caroline Mueller and Simone Bürgin, and we thank Christine Laich and Christine Voegtli for administrative assistance. Confocal imaging was performed with the support of the Center for Microscopy and Image Analysis, University of Zurich. Data included in this publication are part of a master thesis at the Faculty of Science, University of Zurich (T.A.S.).

This study was financed within the framework of VASGRA, supported by the Swiss National Science Foundation grant 320030_184918/1 (to B.H.) and 31003A_176252 (to A.S.Z.). This work was also supported by the Clinical Research Priority Program of the University of Zurich for the Clinical Research Priority Program Precision Medicine for Bacterial Infections. The funders had no role in study design, data collection and analysis, decision to publish, or preparation of the manuscript.

B.H. and A.S.Z. designed the study. T.A.S. and S.M.S. performed the experiments, analyzed the data and wrote the first draft. All authors contributed to data collection and interpretation of the data, reviewed drafts of the manuscript, wrote the final version of the manuscript, and approved the final manuscript.

About the Author

Mr. Schweizer is a PhD student at the Department of Infectious Diseases and Hospital Epidemiology at the University Hospital of Zurich. His primary research interests include bacterial and fungal chronic infections as well as the resulting host–pathogen interactions.

References

1. Hasse B, Husmann L, Zinkernagel A, Weber R, Lachat M, Mayer D. Vascular graft infections. Swiss Med Wkly. 2013;143:w13754.
2. Wilson WR, Bower TC, Creager MA, Amin-Hanjani S, O'Gara PT, Lockhart PB, et al. Vascular graft infections, mycotic aneurysms, and endovascular infections: a scientific statement from the American Heart Association. Circulation. 2016;134:e412–60. https://doi.org/10.1161/CIR.0000000000000457
3. Anagnostopoulos A, Ledergerber B, Kuster SP, Scherrer AU, Naf B, Greiner MA, et al. Inadequate perioperative prophylaxis and postsurgical complications after graft implantation are important risk factors for subsequent vascular graft infections – prospective results from the VASGRA cohort study. Clin Infect Dis. 2018;69:621–30. https://doi.org/10.1093/cid/ciy956
4. Costerton JW, Cheng KJ, Geesey GG, Ladd TI, Nickel JC, Dasgupta M, et al. Bacterial biofilms in nature and disease. Annu Rev Microbiol. 1987;41:435–64. https://doi.org/10.1146/annurev.mi.41.100187.002251
5. Aboshady I, Raad I, Vela D, Hassan M, Aboshady Y, Safi HJ, et al. Prevention of perioperative vascular prosthetic infection with a novel triple antimicrobial-bonded arterial graft. J Vasc Surg. 2016;64:1805–14. https://doi.org/10.1016/j.jvs.2015.09.061
6. Osińska-Jaroszuk M, Ginalska G, Belcarz A, Uryniak A. Vascular prostheses with covalently bound gentamicin and

amikacin reveal superior antibacterial properties than silver-impregnated ones—an in vitro study. Eur J Vasc Endovasc Surg. 2009;38:697–706. https://doi.org/10.1016/j.ejvs.2009.09.003
7. Ricco JB, Assadian A, Schneider F, Assadian O. In vitro evaluation of the antimicrobial efficacy of a new silver-triclosan vs a silver collagen-coated polyester vascular graft against methicillin-resistant *Staphylococcus aureus*. J Vasc Surg. 2012;55:823–9. https://doi.org/10.1016/j.jvs.2011.08.015
8. Berard X, Stecken L, Pinaquy JB, Cazanave C, Puges M, Pereyre S, et al. Comparison of the antimicrobial properties of silver impregnated vascular grafts with and without triclosan. Eur J Vasc Endovasc Surg. 2016;51:285–92. https://doi.org/10.1016/j.ejvs.2015.10.016
9. Goëau-Brissonnière OA, Fabre D, Leflon-Guibout V, Di Centa I, Nicolas-Chanoine M-H, Coggia M. Comparison of the resistance to infection of rifampin-bonded gelatin-sealed and silver/collagen-coated polyester prostheses. J Vasc Surg. 2002;35:1260–3. https://doi.org/10.1016/S0741-5214(02)67047-8
10. Schmacht D, Armstrong P, Johnson B, Pierre K, Back M, Honeyman A, et al. Graft infectivity of rifampin and silver-bonded polyester grafts to MRSA contamination. Vasc Endovascular Surg. 2005;39:411–20. https://doi.org/10.1177/153857440503900505
11. Turonova H, Briandet R, Rodrigues R, Hernould M, Hayek N, Stintzi A, et al. Biofilm spatial organization by the emerging pathogen *Campylobacter jejuni*: comparison between NCTC 11168 and 81-176 strains under microaerobic and oxygen-enriched conditions. Front Microbiol. 2015;6:709. https://doi.org/10.3389/fmicb.2015.00709
12. Carret G, Emonard H, Fardel G, Druguet M, Herbage D, Flandrois JP. Gelatin and collagen binding to *Staphylococcus aureus* strains. Ann Inst Pasteur Microbiol (1985). 1985; 136A:241–5. https://doi.org/10.1016/S0769-2609(85)80063-6
13. Elasri MO, Thomas JR, Skinner RA, Blevins JS, Beenken KE, Nelson CL, et al. *Staphylococcus aureus* collagen adhesin contributes to the pathogenesis of osteomyelitis. Bone. 2002;30:275–80. https://doi.org/10.1016/S8756-3282(01)00632-9
14. Drury JK, Ashton TR, Cunningham JD, Maini R, Pollock JG. Experimental and clinical experience with a gelatin impregnated Dacron prosthesis. Ann Vasc Surg. 1987;1:542–7. https://doi.org/10.1016/S0890-5096(06)61437-4

Address for correspondence: Barbara Hasse, Department of Infectious Diseases and Hospital Epidemiology, University Hospital Zurich, Raemistrasse 100, 8091 Zurich, Switzerland; email: barbara.hasse@usz.ch

Silent Circulation of Rift Valley Fever in Humans, Botswana, 2013–2014

Claire E. Sanderson, Ferran Jori, Naazneen Moolla, Janusz T. Paweska, Nesredin Oumer, Kathleen A. Alexander

We evaluated the prevalence of Rift Valley fever virus IgG and IgM in human serum samples (n = 1,276) collected in 2013–2014 in northern Botswana. Our findings provide evidence of active circulation of this virus in humans in the absence of clinical disease in this region.

The World Health Organization considers Rift Valley fever (RVF) a priority disease because of its substantial public health impact and the lack of available interventions to prevent and halt epidemics (*1*). RVF virus (RVFV) is primarily transmitted to animals through infected *Aedes* and *Culex* mosquitoes, while human transmission has been attributed to direct contact with the blood and tissues of RVFV-infected livestock. RVF outbreaks have been challenging to forecast, with interepidemic or interepizootic years irregularly interspersed with epizootic years (*2*).

In Botswana, RVFV exposure and infection dynamics are incompletely understood. Despite numerous large-scale RVF outbreaks across southern Africa being reported to the World Animal Health Information Database (https://www.oie.int/wahis_2/public/wahid.php/Wahidhome/Home), no outbreaks in people have been detected in Botswana. However, previous surveys have found serologic evidence of virus exposure in humans (1959, 1984–1986), African buffalo (*Syncerus caffer*), and domestic cattle (*3*–*5*). According to the World Animal Health Information Database, RFV disease outbreaks in Botswana have only been reported in livestock (n = 4 outbreaks). It is presently unclear why low-level virus circulation has not been associated with detectable outbreaks in humans or how the virus is maintained during interepizootic years. Here, we evaluate archived human serum samples for evidence of RVFV-specific IgG and IgM and discuss the implications for public health in this region.

Author affiliations: Virginia Tech, Blacksburg, Virginia, USA, and Chobe Research Institute, Center for African Resources: Communities, Animals, and Land Use, Kasane, Botswana (C.E. Sanderson, K.A. Alexander); Animals, Health, Territories, Risks, Ecosystems Unit, Université de Montpellier, Montpellier, France, and Botswana College of Agriculture, Gaborone, Botswana (F. Jori); National Institute of Communicable Diseases, Sandringham-Johannesburg, South Africa (N. Moolla, J.T. Paweska); University of the Witswatersrand, Johannesburg (J.T. Paweska); Botswana Ministry of Health, Gaborone (N. Oumer).

DOI: https://doi.org/10.3201/eid2610.191837

The Study

We determined the historical occurrence of suspected and documented cases of RVF in the human population in Botswana by evaluating inpatient records from Kasane Primary Hospital (Chobe District, 1962–2019) and nationwide monthly outpatient data from all 17 districts (1985–2019). Human serum samples (n = 1,276; mean age 32 [SD ±12], range 1–91; 2013–2014) were collected from government health facilities within the Chobe District and screened using a recombinant nucleocapsid IgG indirect ELISA (*6*), with positive samples confirmed by inhibition ELISA (*7*). We screened IgG-positive samples for IgM using IgM-capture ELISA (*8*). This research was conducted with permission from the Botswana Ministry of Health and the Virginia Tech Institutional Review Board (Permit #11–573).

We found no reports of RVFV infections, confirmed or suspected, from Botswana's passive health surveillance systems. Despite this, 5% (95% CI 4%–6%) of serum samples tested positive for IgG (mean age 46 [SD ±17], range 17–91; Table 1); of these, 11% (95% CI 5%–21%) were positive for IgM (mean age 32 years [SD ±8] range 24–47). Both IgG- and IgM-seropositive samples were found across sampled years, but no significant differences could be detected by year of testing (IgG and IgM $\chi^2 = 0.27$; $p = 0.60$) or season (seasonal data for IgG only available for 2013; $\chi^2 = 0.98$; $p = 0.32$). However, all IgM-positive samples (n = 7) were obtained during the wet season (November 2013–February

Table 1. Prevalence of Rift Valley fever virus IgG-positive human serum samples by sex and age group, Botswana*

		Women		Men		Unknown	
Age group	Age, y	No. patients	No. IgG positive (%, 95% CI)	No. patients	No. IgG positive (%, 95% CI)	No. patients	No. IgG positive (%, 95% CI)
Child	<12	15	0 (0, 0–20)	17	0 (0, 0–18)	2	0 (0, 0–66)
Adolescent	13–19	57	1 (2, 0–9)	9	0 (0, 0–30)	1	0 (0, 0–79)
Young adult	20–24	152	2 (1, 0–5)	26	1 (4, 1–19)	2	0 (0, 0–66)
Adult	25–44	538	24 (4, 3–7)	150	7 (5, 2–9)	25	0 (0, 0–13)
Middle-aged	45–64	78	7 (9, 4–17)	45	4 (9, 4–21)	4	1 (25, 5–70)
Aged	65–79	5	1 (20, 4–62)	10	5 (50, 24–76)	1	0 (0, 0–79)
Elderly	>80	5	2 (40, 12–77)	3	2 (67, 21–94)	0	NA
Unknown	NA	11	1 (9, 2–38)	6	2 (33, 10–70)	114	5 (4, 2–10)
Total		861	38 (4, 3–6)	266	21 (9, 6–14)	149	6 (4, 2–9)

*NA, not applicable

2014). During the ensuing dry season, a RVF outbreak in livestock (n = 2 cows; July 2014) was reported in the Chobe Enclave (World Animal Health Information Database). In northern Botswana, rainfall and flood height affect mosquito dynamics, with models showing *Culex pipiens* mosquitoes to be most abundant in December (*9*), corresponding to human RVFV serological data previously collected in the region (*5*). The detection of IgM-positive patients confirms that RVFV was actively circulating in humans in the Chobe District in 2013 and 2014, with a single outbreak potentially associated with RVFV infection in both humans and livestock.

In South Africa, large RVFV outbreaks in livestock have occurred every 20–30 years, and concomitant infection in humans have occurred during these periods (*10*). In Botswana, no human infections have been recorded, nor have large outbreaks in livestock occurred, suggesting that the dynamics of RVFV transmission and persistence differ between these countries. This difference may be reflective of differing agricultural production intensities and livestock composition; the Chobe District solely supports subsistence farming and has fewer small domestic ruminants.

Overall, findings significantly differed by sex; men (n = 266, 9%, 95% CI 6%–13%) had higher IgG seroprevalence than women (n = 861, 4%, 95% CI 3%–6%) (χ^2 = 4.96, p = 0.03; sex unknown, n = 149; Table 1). In contrast, all IgM-positive patients were female, except for 1, for whom sex was unknown. Sex-specific roles in animal care and food preparation might influence RVFV exposure patterns. In the Chobe District, 54% (95% CI 46%–61%) of interviewed households owned livestock (*11*), and men predominately cared for (97%, 95% CI 91%–99%; K.A. Alexander, unpub. data) and slaughtered large livestock (*12*). It is unclear why IgM was detected only in women; however, women are involved in handling butchered meat in food preparation (12), and exposure differences may influence transmission risk from potentially infected animal tissues and fluids. Women (46%, 95% CI 32%–61%) and men (54%, 95% CI 39%–68%) both care for small livestock (K.A. Alexander, unpub. data).

When we sorted patients into 7 age groups, elderly (≥80 years old) and aged (65–79 years old) patients had significantly higher seroprevalence levels than other age groups (Table 2). A significant difference was also detected between middle-aged patients (45–64 years old) and young adults (20–24 years old) (Table 2), possibly because older patients have been exposed more often to RVF outbreaks as a function of time. However, low sample sizes in the elderly and aged groups may have skewed our results. All IgM-positive patients were 24–47 years of age. We found no evidence of RVFV in patients <17 years old, likely because of a lack of exposure to diseased animals (Figure).

Among seropositive patients, visits to health facilities were primarily for routine health care, HIV treatment and noninfectious disease. This finding suggests that RVF can occur with only mild or subclinical manifestations in affected people, which concurs with reports from other RVF-endemic regions (*13*). However, some IgG-positive patients

Table 2. Comparison of Rift Valley fever virus IgG prevalence across age groups, Botswana*

Age group	Age, y	%, 95% CI	Adolescent	Young adult	Adult	Middle-aged	Aged
Adolescent	13–19	2 (0–8)	NA	NA	NA	NA	NA
Young adult	20–24	2 (0–5)	1.00	NA	NA	NA	NA
Adult	25–44	5 (3–6)	0.404	0.158	NA	NA	NA
Middle-aged	45–64	9 (5–15)	0.0814	**0.008**	0.07	NA	NA
Aged	65–79	40 (20–64)	**<0.001**	**<0.001**	**<0.001**	**0.007**	NA
Elderly	>80	50 (22–78)	**<0.001**	**<0.001**	**<0.001**	**0.01**	0.7

*Bold indicates significance (p value <0.05 by χ^2 test). NA, not applicable.

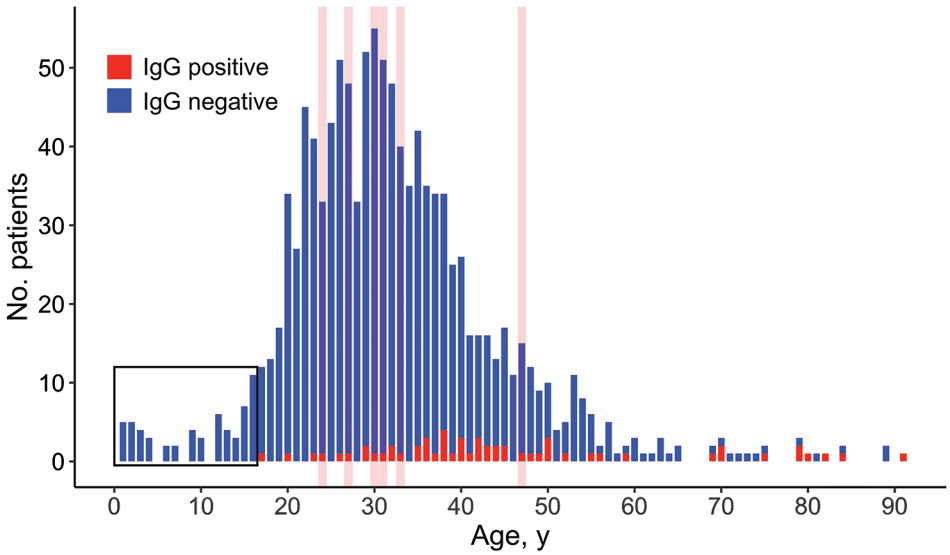

Figure. Number of Rift Valley fever virus IgG-positive and IgG-negative human serum samples by age at time of sampling, Botswana. The overlaid pink lines indicate the age of patients who also tested positive for Rift Valley fever virus IgM. No patients <17 years of age tested IgG positive for Rift Valley fever virus (black box). The figure was created in the open source statistical program R version 3.6.1 (https://www.rproject.org) using ggplot2 (https://ggplot2.tidyverse.org).

in our study did have symptoms possibly attributable to RVF infection, including leg paralysis, swollen legs, and arthritis. Pregnancy was reported in 3 IgM-positive patients (43%, 95% CI 16%–75%); the outcomes of these pregnancies are unknown, but previous studies indicate that women infected with RVFV are 7 times more likely to miscarry than uninfected women (*14*).

Where data were available, we found a significant association between IgG seroprevalence and HIV status ($\chi^2 = 6.4$; $p = 0.01$); 48% (95% CI 36%–61%) of IgG-positive patients were also HIV positive. It is unknown when these patients became infected with RVFV or HIV, but concurrent infection can increase the development of RVF symptoms involving the central nervous system, as well as fatality rates (*15*). Although nearly one third of IgM-positive patients were infected with HIV (29%, 95% CI 8%–64%), we could not detect a significant association with HIV status ($\chi^2 = 0.67$; $p = 0.4$), likely because of the small sample size.

Conclusions

RVFV appears to be endemically circulating in northern Botswana, with people likely exposed to the virus regularly over time. Whereas viral reservoirs are uncertain, both livestock and wildlife present potential opportunities for human exposure to RVFV. In Botswana, government hospitals use syndromic diagnoses to treat patients; however, because no human cases have been reported and the disease can be asymptomatic, many RVF cases are likely misdiagnosed or undiagnosed. Increased diagnostic capacity and public health awareness of RVFV in Botswana is required to further elucidate risk factors associated with human infection, especially in high-risk populations. These findings underscore the urgent need for more intensive investigations into RVFV transmission and persistence at the human-animal-vector interface.

Acknowledgments

We thank the Botswana Ministry of Health and the Chobe District Health Team for their support on this project.

This project was funded by the National Science Foundation Dynamics of Coupled Natural and Human Systems (#1518486) and Ecology and Evolution of Infectious Diseases (#1518663).

About the Author

Claire E. Sanderson is a research associate in the Fish and Wildlife Conservation Department at Virginia Tech and the Research Coordinator at the Center for African Resources: Communities, Animals, and Land Use (CARACAL). Her research interests broadly encompass disease ecology, behavioral ecology, conservation biology, and population genetics.

References

1. Mehand MS, Al-Shorbaji F, Millett P, Murgue B. The WHO R&D Blueprint: 2018 review of emerging infectious diseases requiring urgent research and development efforts. Antiviral Res. 2018;159:63–7. PubMed https://doi.org/10.1016/j.antiviral.2018.09.009
2. Olive M-M, Goodman SM, Reynes J-M. The role of wild mammals in the maintenance of Rift Valley fever virus. J Wildl Dis. 2012;48:241–66. https://doi.org/10.7589/0090-3558-48.2.241

3. Jori F, Alexander KA, Mokopasetso M, Munstermann S, Moagabo K, Paweska JT. Serological evidence of Rift Valley fever virus circulation in domestic cattle and African buffalo in northern Botswana (2010–2011). Front Vet Sci. 2015;2:63. https://doi.org/10.3389/fvets.2015.00063
4. Kokernot RH, Szlamp EL, Levitt J, McIntosh BM. Survey for antibodies against arthropod-borne viruses in the sera of indigenous residents of the Caprivi Strip and Bechuanaland Protectorate. Trans R Soc Trop Med Hyg. 1965;59:553–62. https://doi.org/10.1016/0035-9203(65)90158-6
5. Tessier SF, Rollin PE, Sureau P. Viral haemorrhagic fever survey in Chobe (Botswana). Trans R Soc Trop Med Hyg. 1987;81:699–700. https://doi.org/10.1016/0035-9203(87)90462-7
6. Jansen van Vuren P, Potgieter AC, Paweska JT, van Dijk AA. Preparation and evaluation of a recombinant Rift Valley fever virus N protein for the detection of IgG and IgM antibodies in humans and animals by indirect ELISA. J Virol Methods. 2007;140:106–14. https://doi.org/10.1016/j.jviromet.2006.11.005
7. Paweska JT, Mortimer E, Leman PA, Swanepoel R. An inhibition enzyme-linked immunosorbent assay for the detection of antibody to Rift Valley fever virus in humans, domestic and wild ruminants. J Virol Methods. 2005;127:10–8. https://doi.org/10.1016/j.jviromet.2005.02.008
8. Paweska JT, Burt FJ, Swanepoel R. Validation of IgG-sandwich and IgM-capture ELISA for the detection of antibody to Rift Valley fever virus in humans. J Virol Methods. 2005;124:173–81. https://doi.org/10.1016/j.jviromet.2004.11.020
9. Pachka H, Annelise T, Alan K, Power T, Patrick K, Véronique C, et al. Rift Valley fever vector diversity and impact of meteorological and environmental factors on *Culex pipiens* dynamics in the Okavango Delta, Botswana. Parasit Vectors. 2016;9:434. https://doi.org/10.1186/s13071-016-1712-1
10. Ngoshe YB, Avenant A, Rostal MK, Karesh WB, Paweska JT, Bagge W, et al. Patterns of Rift Valley fever virus seropositivity in domestic ruminants in central South Africa four years after a large outbreak. Sci Rep. 2020;10:5489. https://doi.org/10.1038/s41598-020-62453-6
11. Alexander K, Ramotadima M, Sanderson CE. The power of consensus: developing a community voice in land use planning and tourism development in biodiversity hotspots. Ecosyst Serv. 2018;30:350–61. https://doi.org/10.1016/j.ecoser.2018.02.008
12. Mooketsi C. Butchery styles and the processing of cattle carcasses in Botswana. PULA: Botswana Journal of African Studies. 2001;15:108–24.
13. Al-Hazmi M, Ayoola EA, Abdurahman M, Banzal S, Ashraf J, El-Bushra A, et al. Epidemic Rift Valley fever in Saudi Arabia: a clinical study of severe illness in humans. Clin Infect Dis. 2003;36:245–52. https://doi.org/10.1371/journal.pntd.0002065
14. Baudin M, Jumaa AM, Jomma HJE, Karsany MS, Bucht G, Näslund J, et al. Association of Rift Valley fever virus infection with miscarriage in Sudanese women: a cross-sectional study. Lancet Glob Health. 2016;4:e864–71. https://doi.org/ 10.1016/S2214-109X(16)30176-0
15. Mohamed M, Mosha F, Mghamba J, Zaki SR, Shieh W-J, Paweska J, et al. Epidemiologic and clinical aspects of a Rift Valley fever outbreak in humans in Tanzania, 2007. Am J Trop Med Hyg. 2010;83(2_Suppl):22–7. https://doi.org/10.4269/ajtmh.2010.09-0318

Address for correspondence: Kathleen Alexander, Virginia Tech, Integrated Life Sciences Building, 1981 Kraft Dr, Blacksburg, VA 24060, USA; email: kathyalx@vt.edu

Limitations of Ribotyping as Genotyping Method for *Corynebacterium ulcerans*

Tsuyoshi Sekizuka, Chihiro Katsukawa,[1] Makoto Kuroda, Keigo Shibayama, Ken Otsuji, Mitsumasa Saito, Akihiko Yamamoto, Masaaki Iwaki

We conducted molecular typing of a *Corynebacterium ulcerans* isolate from a woman who died in Japan in 2016. Genomic DNA modification might have affected the isolate's ribotyping profile. Multilocus sequence typing results (sequence type 337) were more accurate. Whole-genome sequencing had greater ability to discriminate lineages at high resolution.

Corynebacterium ulcerans is a zoonotic pathogen that causes an illness categorized in World Health Organization documents as diphtheria (*1*). Genotyping methods such as ribotyping, multilocus sequence typing (MLST), and whole-genome sequencing are used to classify isolates. During the 1990s and early 2000s, the standard molecular typing method of *Corynebacterium diphtheriae* was conventional ribotyping (*2*,*3*). Ribotyping is also used to classify *C. ulcerans* (*4*) and compare isolates (*5*–*9*). Today, the standard method is MLST because of its objectivity and reproducibility (*8*,*10*). We sequenced 3 isolates of *C. ulcerans* from patients in Japan to analyze the accuracy of conventional ribotyping, MLST, and whole-genome sequencing.

The Study

In 2016, a 66-year-old woman in Fukuoka, Japan, died of a diphtheria-like disease. Otsuji et al. isolated toxigenic *C. ulcerans* from the patient's tracheal pseudomembrane and blood (*6*). We analyzed the isolate (FH2016-1) from the pseudomembrane alongside the first (*11*) and second (*5*) *C. ulcerans* isolates taken from patients in Japan; the first isolate (0102) was taken in 2001 and the second isolate (0211) in 2002.

Author affiliations: National Institute of Infectious Diseases, Tokyo, Japan (T. Sekizuka, M. Kuroda, K. Shibyama, A. Yamamoto, M. Iwaki); Osaka Prefectural Institute of Public Health, Osaka, Japan (C. Katsukawa); University of Occupational and Environmental Health, Kitakyushu, Japan (K. Otsuji, M. Saito)

DOI: https://doi.org/10.3201/eid2610.200086

Strains 0102 and 0211 (named for the initial isolates taken in 2001 and 2002) are the 2 major ribotypes of *C. ulcerans* in Japan. Our conventional ribotyping of the isolates found the pattern obtained from FH2016-1 was indistinguishable from that of 0102, indicating that FH2016-1 belongs to strain 0102 (Figure 1, panel A).

We also whole-genome sequenced strains FH2016-1 and 0211 using the NextSeq500 Illumina (for strain FH2016-1 [Illumina, https://www.illumina.com]), Illumina GAII (for strain 0211 [Illumina]), ABI 3730xl (Thermo Fisher, https://www.thermofisher.com), and PacBio Sequel (Pacific Biosciences of California, Inc., https://www.pacb.com) sequencers, followed by de novo assembly. We deposited complete sequences and assembly methods in GenBank under accession nos. AP019663 (strain FH2016-1) and AP019662 (strain 0211). Using these sequences and the previously published genome sequence (*12*) of strain 0102 (GenBank accession no. AP012284), we conducted in silico ribotyping of *Bst*EII-digested fragments that hybridized with OligoMix5 probes, producing a predicted pattern for each sequence (*13*). The predicted patterns of all 3 strains matched the conventional ribotype pattern of strain 0211. However, the conventional ribotyping patterns of strains FH2016-1 and 0102 did not match the in silico–predicted ribotype pattern (Figure 1, panel A).

The discrepancy between the conventional and in silico–predicted patterns is caused by impaired restriction digestion at specific *Bst*EII sites. In these strains, the conventional (modified) ribotype pattern differed from the in silico–predicted (unmodified) ribotype pattern by a shift of 4 fragments (Appendix Figure 1, panel A, https://wwwnc.cdc.gov/EID/article/26/10/20-0086-App1.pdf). For example, in silico typing predicted that 3 *Bst*EII sites would be digested at nt 770,000 of strain FH2016-1. PacBio modification analysis revealed that 1 of these sites might have been modified

[1]Current affiliation: Osaka Prefecture University, Osaka, Japan.

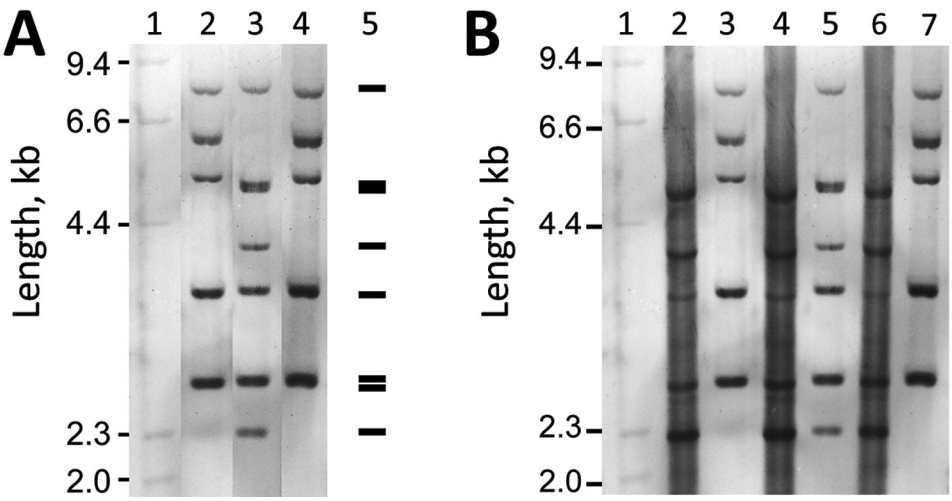

Figure 1. Alteration of ribotyping patterns by genomic DNA modification of *Corynebacterium ulcerans* strains 0102, 0211, and FH2016–1, Japan, 2001–2016. Ribotyping was performed as described previously (*4*,*11*). *Hin*dIII-digested, digoxigenin-labeled λ phage DNA segments were used as length markers. A) Conventional ribotyping patterns of strains 0102, 0211, and FH2016-1. 1, λ*Hin*dIII; 2, 0102; 3, 0211; 4, FH2016-1; 5, Pattern predicted by in silico typing. B) Ribotyping patterns of genomic DNA and whole-genome amplified DNA as substrates. 1, λ*Hin*dIII; 2, 0102 WGA; 3, 0102 native; 4, 0211 WGA; 5, 0211 native; 6, FH2016-1 WGA; 7, FH2016-1 native. The label "WGA" indicates whole-genome amplified DNA as a substrate; "native" indicates genomic DNA. WGA (unmodified) DNA of the 3 strains show identical patterns. The pattern matches that of native 0211 (unmodified genomic DNA). In contrast, native FH2016-1 and 0102 are modified and show different patterns from their WGA counterparts.

(Appendix Figure 1, panel B). *Bst*EII is sensitive to methylation and other types of DNA modification (*14*). Thus, the difference in restriction fragment patterns was closely related to the nucleotide modifications within *Bst*EII recognition sites (Appendix Figure 1, panel B). Other *Bst*EII sites also might have been modified, resulting in the 4-fragment shift. Accordingly, we did not observe this shift in ribotypes of unmodified DNA substrate prepared by whole-genome amplification of the 3 strains (*15*) (Figure 1, panel B). The patterns of unmodified DNA matched the pattern of strain 0211 (Figure 1, panel B) and the in silico–predicted pattern (Figure 1, panel A). The ≥6.1-kb bands seen in "native" lanes were not visible in whole-genome amplification lanes, potentially because of the failure of whole-genome amplification to generate large fragments. These results indicate that ribotyping patterns might be substantially affected by DNA modification.

The sequences of strains FH2016-1, 0102, and 0211 were highly homologous. For example, they shared complete sequence identity (data not shown) for a structural gene (locus tag CULCFH20161_03390) encoding a DNA methylase. However, we observed small differences in their genomes (Table, https://wwwnc.cdc.gov/eid/article/26/10/20-0086-t1; Figure 2; Appendix Table 1). We expected factors contributing to genomic DNA modification to be common between strains FH2016-1 and 0102, but not 0211. Scanning the genomes of the 3 strains for such factors resulted in 15 candidate open reading frames (ORFs) (Table). None of these ORFs contained motifs related to DNA methylation; however, these ORFs might still contribute to DNA modification of other gene products. The nature of the modification(s) remains unknown.

Conventional ribotyping (Figure 1, panel A) showed that strains FH2016-1 and 0102 were closely related. However, comparison of 30 genome sequences of strains from around the world (Appendix Table 2, Figure 2) revealed that all 3 strains from Japan belong to a single phylogenetic cluster and sequence type (ST) 337. Whether the 3 isolates represent the entire population of *C. ulcerans* in Japan is unclear. However, more than half the isolates we have analyzed (≈20) are ST337 (M. Iwaki and A. Yamamoto, unpub. data), suggesting a small amount of genetic diversity among the *C. ulcerans* population in Japan.

Close-up view of the phylogenetic tree showed that these strains from Japan divided into 2 different lineages. At most, 117 single nucleotide variations and 59 insertions/deletions existed between any 2 strains (Figure 2). Although this result indicated low variability

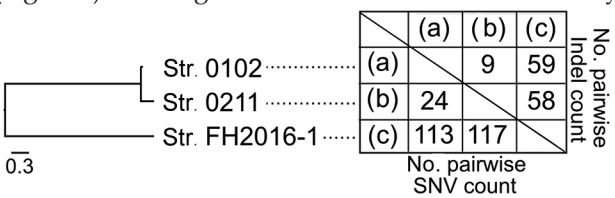

Figure 2. Genetic similarity among 3 selected strains of *Corynebacterium ulcerans*, Japan, 2001–2016. Strain 0102 is represented by (a), strain 0211 by (b), and strain FH2016–1 by (c). Numbers of SNVs and indels between strains are shown. A phylogenetic tree generated by SNV data are shown on the left. Indel, insertion/deletion; SNV, single-nucleotide variation.

among the 3 strains, it also showed that strain FH2016-1 was genetically distinct from 0102 and 0211 (Figure 2). Thus, the genome sequence analysis indicated that conventional ribotyping did not reflect lineage accurately and resulted in a misleading classification of these specimens. In contrast, MLST, which is now the preferred method of molecular typing (*8*,*10*), provided more accurate results. We queried the genomic sequences of the 3 strains on the PubMLST website (https://pubmlst.org) and analyzed them at 7 alleles (*atpA*, *dnaE*, *dnaK*, *fusA*, *leuA*, *odhA*, and *rpoB*). The same sequence type (ST337) was assigned to all 3 strains, reflecting the low genetic variability among these strains.

Conclusions

Our study of 3 strains of *C. ulcerans* showed that conventional ribotyping is less accurate than other methods of phylogenetic analysis. In comparison, MLST is less erroneous, and whole-genome sequencing produces results with greater resolution than those of conventional ribotyping. MLST produced results with lower resolution than whole-genome sequencing while maintaining a high level of accuracy. MLST and whole-genome sequencing improve the accuracy and efficiency of phylogenetic analysis of *C. ulcerans*.

Acknowledgments

We are grateful to Kaoru Umeda for her comments on the manuscript.

This research was supported by the Japan Agency for Medical Research and Development under grant nos. JP18fk0108017, JP19fk0108097, and JP19fk0108103.

About the Author

Dr. Sekizuka is chief at Laboratory of Bacterial Genomics, Pathogen Genomics Center, National Institute of Infectious Diseases (Shinjuku-ku, Tokyo). His primary research interests include genomic molecular epidemiology with genomics and bioinformatics, and pathogen identification with metagenomics.

References

1. World Health Organization. Diphtheria. In: Vaccine preventable diseases surveillance standards. Geneva: The Organization; 2018.
2. De Zoysa A, Hawkey P, Charlett A, Efstratiou A. Comparison of four molecular typing methods for characterization of *Corynebacterium diphtheriae* and determination of transcontinental spread of *C. diphtheriae* based on *Bst*EII rRNA gene profiles. J Clin Microbiol. 2008;46:3626–35. https://doi.org/10.1128/JCM.00300-08
3. Grimont PAD, Grimont F, Efstratiou A, De Zoysa A, Mazurova I, Ruckly C, et al.; European Laboratory Working Group on Diphtheria. International nomenclature for *Corynebacterium diphtheriae* ribotypes. Res Microbiol. 2004;155:162–6. https://doi.org/10.1016/j.resmic.2003.12.005
4. De Zoysa A, Hawkey PM, Engler K, George R, Mann G, Reilly W, et al. Characterization of toxigenic *Corynebacterium ulcerans* strains isolated from humans and domestic cats in the United Kingdom. J Clin Microbiol. 2005;43:4377–81. https://doi.org/10.1128/JCM.43.9.4377-4381.2005
5. Komiya T, Seto Y, De Zoysa A, Iwaki M, Hatanaka A, Tsunoda A, et al. Two Japanese *Corynebacterium ulcerans* isolates from the same hospital: ribotype, toxigenicity and serum antitoxin titre. J Med Microbiol. 2010;59:1497–504. https://doi.org/10.1099/jmm.0.022491-0
6. Otsuji K, Fukuda K, Endo T, Shimizu S, Harayama N, Ogawa M, et al. The first fatal case of *Corynebacterium ulcerans* infection in Japan. JMM Case Rep. 2017;4:e005106. https://doi.org/10.1099/jmmcr.0.005106
7. Yasuda I, Matsuyama H, Ishifuji T, Yamashita Y, Takaki M, Morimoto K, et al. Severe pneumonia caused by toxigenic *Corynebacterium ulcerans* infection, Japan. Emerg Infect Dis. 2018;24:588–91. https://doi.org/10.3201/eid2403.171837
8. Katsukawa C, Komiya T, Umeda K, Goto M, Yanai T, Takahashi M, et al. Toxigenic *Corynebacterium ulcerans* isolated from a hunting dog and its diphtheria toxin antibody titer. Microbiol Immunol. 2016;60:177–86. https://doi.org/10.1111/1348-0421.12364
9. Katsukawa C, Umeda K, Inamori I, Kosono Y, Tanigawa T, Komiya T, et al. Toxigenic *Corynebacterium ulcerans* isolated from a wild bird (ural owl) and its feed (shrew-moles): comparison of molecular types with human isolates. BMC Res Notes. 2016;9:181. https://doi.org/10.1186/s13104-016-1979-5
10. König C, Meinel DM, Margos G, Konrad R, Sing A. Multilocus sequence typing of *Corynebacterium ulcerans* provides evidence for zoonotic transmission and for increased prevalence of certain sequence types among toxigenic strains. J Clin Microbiol. 2014;52:4318–24. https://doi.org/10.1128/JCM.02291-14
11. Hatanaka A, Tsunoda A, Okamoto M, Ooe K, Nakamura A, Miyakoshi M, et al. *Corynebacterium ulcerans* diphtheria in Japan. Emerg Infect Dis. 2003;9:752–3. https://doi.org/10.3201/eid0906.020645
12. Sekizuka T, Yamamoto A, Komiya T, Kenri T, Takeuchi F, Shibayama K, et al. *Corynebacterium ulcerans* 0102 carries the gene encoding diphtheria toxin on a prophage different from the *C. diphtheriae* NCTC 13129 prophage. BMC Microbiol. 2012;12:72. https://doi.org/10.1186/1471-2180-12-72
13. Regnault B, Grimont F, Grimont PAD. Universal ribotyping method using a chemically labelled oligonucleotide probe mixture. Res Microbiol. 1997;148:649–59. https://doi.org/10.1016/S0923-2508(99)80064-3
14. Roberts RJ, Vincze T, Posfai J, Macelis D. REBASE—a database for DNA restriction and modification: enzymes, genes and genomes. Nucleic Acids Res. 2015;43(D1):D298–9. https://doi.org/10.1093/nar/gku1046
15. Nelson JR. Random-primed, Phi29 DNA polymerase-based whole genome amplification. Curr Protoc Mol Biol. 2014;105:15.13.1.

Address for correspondence: Masaaki Iwaki, Department of Bacteriology II and Management Department of Biosafety and Laboratory Animal, National Institute of Infectious Diseases, 4-7-1 Gakuen, Musashimurayama-shi, Tokyo 208-0011, Japan; email: miwaki@nih.go.jp

Seoul Orthohantavirus in Wild Black Rats, Senegal, 2012–2013

Moussa M. Diagne, Idrissa Dieng, Laurent Granjon, Héloïse Lucaccioni, Abdourahmane Sow, Oumar Ndiaye, Martin Faye, Khalilou Bâ, Yamar Bâ, Mamoudou Diallo, Oumar Faye, Jean-Marc Duplantier, Mawlouth Diallo, Pascal Handschumacher, Ousmane Faye, Amadou A. Sall

Hantaviruses cause hemorrhagic fever in humans worldwide. However, few hantavirus surveillance campaigns occur in Africa. We detected Seoul orthohantavirus in black rats in Senegal, although we did not find serologic evidence of this disease in humans. These findings highlight the need for increased surveillance of hantaviruses in this region.

Hantaviruses (family *Hantaviridae*, genus *Orthohantavirus*) are RNA viruses transmitted by aerosolized excreta from infected rodents and shrews. In humans, they cause hemorrhagic fever with renal syndrome (more often observed in Asia and Europe) and cardiopulmonary syndrome (more common in the Americas) (*1*). Only 1 case has been confirmed in Africa, in the Central African Republic in 1987 (*2*). However, studies from 2006 through 2013 have discovered new hantaviruses in autochthonous African rodents, moles, and bats (*3*,*4*). In addition, serologic evidence in humans and rodents in Africa suggest local circulation (*5*). For example, a study in rural areas of Senegal found 11.5% of rodents and 16.6% of humans had antibodies against hantaviruses (*3*). More recently, serologic evidence of hantaviruses was reported in domestic and peridomestic rodents from some regions in Senegal (*6*).

Author affiliations: Institut Pasteur, Dakar, Senegal (M.M. Diagne, I. Dieng, A. Sow, O. Ndiaye, M. Faye, Y. Bâ, Oum. Faye, Maw. Diallo, Ous. Faye, A.A. Sall); Centre de Gestion des Populations, Institut de Recherche pour le Développement, Montpellier, France (L. Granjon, J.-M. Duplantier); Université Paris Nanterre, Nanterre, France (H. Lucaccioni); Institut de recherche pour le développement Senegal, Dakar (K. Bâ, Mam. Diallo); Sciences Economiques & Sociales de la Santé & Traitement de l'Information Médicale, Marseille, France (P. Handschumacher); Aix Marseille University, Marseille (P. Handschumacher); Institut National de la Santé et de la Recherche Médicale, Marseille (P. Handschumacher)

DOI: https://doi.org/10.3201/eid2610.201306

Southeastern Senegal has become a major trade area because of urbanization and substantial improvement of its road and rail networks in the late 1990s (*7*). Within a few years, these changes led to the rapid spread of a major invasive rodent species, the black rat (*Rattus rattus* [family *Murinae*]), which is a reservoir for Seoul orthohantavirus (SEOV) (*4*,*5*,*7*). To assess the prevalence of hantaviruses in rodents, we screened for hantaviruses in *R. rattus* rats and commensal or peridomestic co-existing rodents in 2012–2013, approximately 15 years after the 1998 opening of a tarred road in eastern Senegal.

The Study

The national ethics committee for research of Senegal approved the study (authorization no. 0360-MSAS/DPRS/DR, on October 24, 2011). During May 2012–December 2013, we trapped small mammals as previously described (*8*) inside dwelling places and their surroundings (immediate and local) over periods of 1–6 consecutive days.

We caught 1,414 small mammals, including 403 black rats, from 10 different species (Appendix Table, https://wwwnc.cdc.gov/EID/article/26/10/20-1306-App1.pdf). We sampled whole blood, brain, and visceral organ tissues, which we then transferred to the Institut Pasteur (Dakar, Senegal). We triturated each solid sample in Leibovitz-15 medium (GIBCO-BRL, https://www.thermofisher.com) and centrifuged them to collect the suspension. To collect serum, we centrifuged whole blood samples. We extracted RNA from these different suspensions using the QIAamp RNA Viral Kit (QIAGEN, https://www.qiagen.com) according to the manufacturer's recommendations. To make cDNA, we used avian myeloblastosis virus reverse transcriptase (Promega, https://www.promega.com) followed by a nested conventional PCR with GoTaq Polymerase (Promega, https://www.promega.com) and a highly conserved hantavirus primers

system selective for the partial large segment protein gene (*9*). We sequenced amplicons using GENEWIZ (https://www.genewiz.com), assembled them using EMBOSS Merger software (http://www.bioinformatics.nl/cgi-bin/emboss/merger), and analyzed them with BLAST (http://blast.ncbi.nlm.nih.gov/Blast.cgi). We performed sequence alignment with Mafft (*10*) and built a maximum-likelihood phylogenetic tree with iQ-TREE (*11*), using 1,000 replicates for bootstrapping.

Of the 1,414 mammals, 13 black rats tested positive for hantavirus RNA. We detected RNA in 14 samples: 9 brain homogenates, 4 multiorgan homogenates, and 1 serum sample. We confirmed the positive samples using PCR with highly conserved hantavirus small segment primers (*12*). Sequence analysis of partial large (deposited under GenBank accession nos. MT276868–81) and small (deposited under GenBank accession nos. MT276854–67) segments revealed 99.42% identity with SEOV strain Rn-HD27 from China

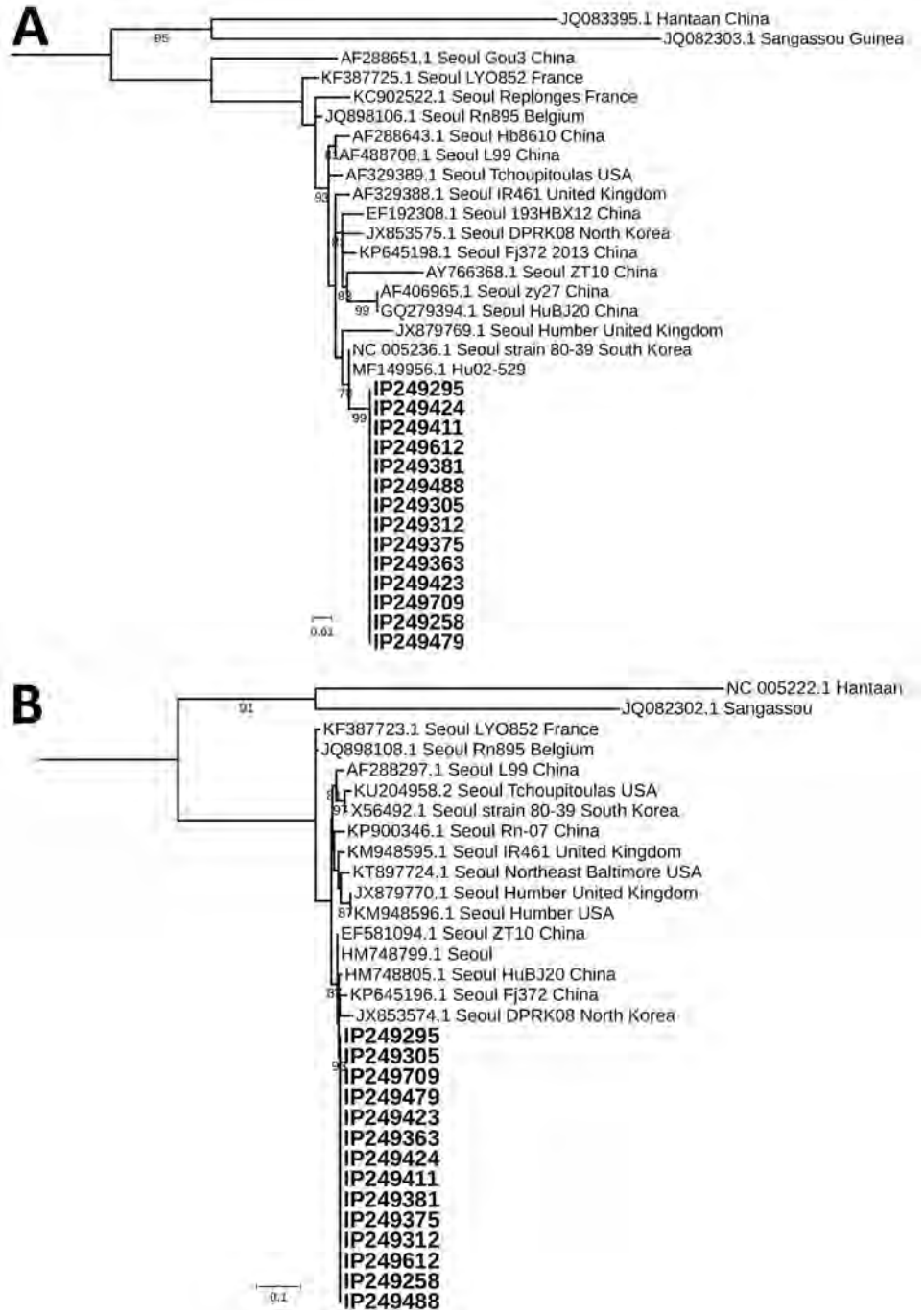

Figure 1. Phylogenetic analysis of Seoul orthohantavirus strains from black rats (*Rattus rattus* [family *Murinae*]; boldface) and reference sequences, Senegal, 2012–2013. Phylogenetic trees were generated by the maximum-likelihood method using the transition plus invariate sites plus gamma 4 model of the small segment (266 nt) (A) and the large segment (347 nt) (B). The numbers at each node are bootstrap probabilities (>90%) as determined for 1,000 iterations. GenBank numbers are indicated for reference sequences. Scale bars indicate 0.01 substitutions per nucleotide (A) and 0.1 substitutions per nucleotide (B).

(GenBank accession no. HM748799) and 99.64% identity with SEOV strain Hu02-529 from South Korea (GenBank accession no. MF149956) (Figure 1).

We detected SEOV RNA in 13 black rats caught in 3 villages: Goumbayel (7 rodents), Soutouta (4 rodents), and Dianke Makha (2 rodents). These villages were located ≈1 hour's drive from the main road between Tambacounda and Kidira (Figure 2). Frequent movement of goods and humans between these 3 villages might explain the low genetic diversity among the new SEOV strains from black rats. We did not observe signs of disease in the infected animals at the time of capture. Of the 4 villages that yielded the highest numbers of black rats in this study, 3 harbored rats infected with SEOV (Figure 2) (*7*). High densities of black rats might contribute to the occurrence of hantavirus in these villages, especially because host demography might affect hantavirus circulation (*13*).

Seasonal patterns might complicate these findings. We surveyed the villages harboring SEOV-infected rats in February 2013, which might be a

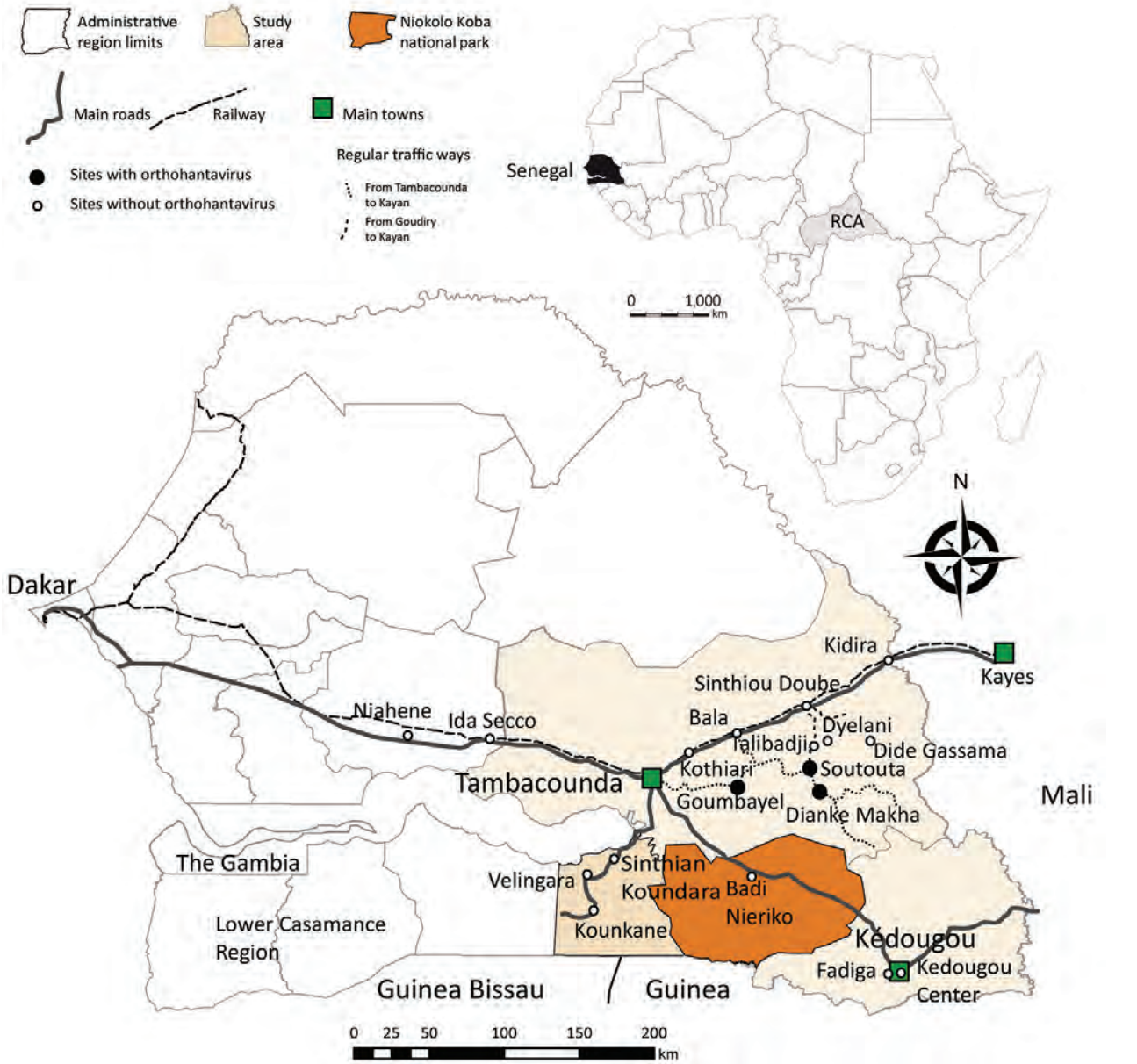

Figure 2. Locations of trapping sites (circles) used in study of rodentborne Seoul orthohantavirus in Senegal, 2012–2013. Black circles indicate trapping locations of Seoul orthohantavirus–infected black rats (*Rattus rattus* [family *Murinae*]). Inset shows location of Senegal in Africa. Map created using the package maptools installed in R studio version 1.2.1335 (https://rstudio.com/products/rstudio/) and shapefiles downloaded from the free domain of the Geographic Information System (http://www.diva-gis.org).

Table. Human exposures to rodents in selected villages, Senegal, 2012–2013

Village/town	No. participants	No. (%) participants in contact with rodents	No. distinct species encountered	Black rats	Time period
Tambacounda					
Youpe Hamady	87	70 (80.5)	4	No	2012 Oct 19–20
Talibadji	33	11 (33.3)	3	Yes	2012 Oct 21
Sinthiou Doube	39	37 (94.9)	4	Yes	2012 Oct 22
Ndiobene	45	20 (44.4)	2	No	2012 Oct 22
Dianke Makha	101	40 (39.6)	5	Yes	2012 Sep 10
Soutouta	89	83 (93.3)	4	Yes	2012 Sep 11
Kedougou					
Kedougou	147	111 (75.5)	6	Yes	2013 Mar 9–10
Total	541	372 (68.8)			

favorable period for rodent reproduction, population increase, and thus hantavirus circulation (*13*). Despite the presence of juveniles, *R. rattus* populations had relatively high proportions of sexually active animals (75% in Goumbayel, 48% in Soutouta, and 71% in Dianke Makha) (Appendix Figure). These data suggest that high level of interactions (male–female, adult–juvenile) occurred in these populations during that period, possibly promoting viral circulation. Conversely, we investigated nearby villages (Dieylani, Dide Gassama, Koussan, and Talibadji, in which we did not find evidence of hantavirus-infected black rats) in October 2012, at the end of the rainy season. Our investigations in May 2012 and November 2013 of the Kedougou area did not detect evidence of SEOV.

To assess potential human transmission, we performed parallel studies of human populations in some villages. Participants consented to an interview about rodent exposure and gave blood samples. During October 2012–March 2013, we recruited 541 participants with a mean age of 24 years (range 2–91 years) (Table). Of the 541 participants, 372 (68.8%) reported close contact with rodents. The highest rates of rodent exposure were in Soutouta and Sinthiou Doube (Table). We performed an in-house ELISA specific to IgG against SEOV on the human serum samples using reagents from the US Centers for Disease Control and Prevention (Atlanta, GA, USA). No IgG against SEOV was detected in the tested human samples, regardless of whether the participant's village had evidence of SEOV-infected black rats; this finding suggests a lack of human exposure. The role of species diversity in virus transmission is extremely complex (*14*). The relatively low SEOV prevalence in black rats (Appendix Table) might explain the negative results of the human serologic survey.

Conclusions

We found SEOV, a hantavirus pathogenic to humans, in black rats in southeastern Senegal. Phylogenic analyses grouped the newly detected SEOV with strains from Asia. Exchanges between Africa and Asia can potentially increase the opportunities for pathogens to expand their geographic range as previously described (*15*).

In-depth phylogenetic analysis of complete genomes would help elucidate the molecular evolution of this virus in Africa. This study highlights the need to improve hantavirus surveillance in Senegal and other countries in Africa for public health prevention strategies.

Acknowledgments

We thank Coly Bâ, Ambroise Dalecky, Christophe Amidi Diagne, Philippe Gauthier, Laëtitia Husse, Mamadou Kane, Youssou Niang, and Aliou Sow for their outstanding work during trapping sessions. We thank Oumar Ndiaye and Magueye Ndiaye for their technical laboratory support. We also thank Pierre Rollin for helping to obtain ELISA reagents.

This work was supported by grant nos. ANR-11-CE-PL-0010 and ANR-11-JSV7-0006 (A.A.S., O.F., M.M.D., A.G., Y.B., M.D.) from the Agence Nationale de la Recherche.

About the Author

Dr. Diagne is a postdoctoral researcher at the Virology Department of Institut Pasteur de Dakar. His research interests include arboviruses and hemorrhagic fever viruses, such as hantaviruses in animal reservoirs and humans.

References

1. Bi Z, Formenty PB, Roth CE. Hantavirus infection: a review and global update. J Infect Dev Ctries. 2008;2:3–23. https://doi.org/10.3855/jidc.317
2. Coulaud X, Chouaib E, Georges AJ, Rollin P, Gonzalez JP. First human case of haemorrhagic fever with renal syndrome in the Central African Republic. Trans R Soc Trop Med Hyg. 1987;81:686. https://doi.org/10.1016/0035-9203(87)90455-X
3. Witkowski PT, Klempa B, Ithete NL, Auste B, Mfune JKE, Hoveka J, et al. Hantaviruses in Africa. Virus Res. 2014; 187:34–42. https://doi.org/10.1016/j.virusres.2013.12.039

4. Milholland MT, Castro-Arellano I, Suzán G, Garcia-Peña GE, Lee TE Jr, Rohde RE, et al. Global diversity and distribution of hantaviruses and their hosts. EcoHealth. 2018;15:163–208. https://doi.org/10.1007/s10393-017-1305-2
5. Saluzzo JF, Digoutte JP, Adam F, Bauer SP, McCormick JB. Serological evidence for Hantaan-related virus infection in rodents and in Senegal. Trans R Soc Trop Med Hyg. 1985;79:874–5. https://doi.org/10.1016/0035-9203(85)90145-2
6. Diagne CA, Charbonnel N, Henttonen H, Sironen T, Brouat C. Serological survey of zoonotic viruses in invasive and native commensal rodents in Senegal, West Africa. Vector Borne Zoonotic Dis. 2017;17:730–3. https://doi.org/10.1089/vbz.2017.2135
7. Lucaccioni H, Granjon L, Dalecky A, Fossati O, Le Fur J, Duplantier J-M, et al. From human geography to biological invasions: the black rat distribution in the changing southeastern of Senegal. PLoS One. 2016;11:e0163547. https://doi.org/10.1371/journal.pone.0163547
8. Dalecky A, Ba K, Piry S, Lippens C, Diagne CA, Kane M, et al. Range expansion of the invasive house mouse *Mus musculus domesticus* in Senegal, West Africa: a synthesis of trapping data over three decades, 1983–2014. Mammal Rev. 2015;45:176–90. https://doi.org/10.1111/mam.12043
9. Klempa B, Fichet-Calvet E, Lecompte E, Auste B, Aniskin V, Meisel H, et al. Hantavirus in African wood mouse, Guinea. Emerg Infect Dis. 2006;12:838–40. https://doi.org/10.3201/eid1205.051487
10. Katoh K, Misawa K, Kuma K, Miyata T. MAFFT: a novel method for rapid multiple sequence alignment based on fast Fourier transform. Nucleic Acids Res. 2002;30:3059–66. https://doi.org/10.1093/nar/gkf436
11. Nguyen L-T, Schmidt HA, von Haeseler A, Minh BQ. IQ-TREE: a fast and effective stochastic algorithm for estimating maximum-likelihood phylogenies. Mol Biol Evol. 2015;32:268–74. https://doi.org/10.1093/molbev/msu300
12. Arthur RR, Lofts RS, Gomez J, Glass GE, Leduc JW, Childs JE. Grouping of hantaviruses by small (S) genome segment polymerase chain reaction and amplification of viral RNA from wild-caught rats. Am J Trop Med Hyg. 1992;47:210–4.
13. Tian H, Stenseth NC. The ecological dynamics of hantavirus diseases: from environmental variability to disease prevention largely based on data from China. PLoS Negl Trop Dis. 2019;13:e0006901. https://doi.org/10.1371/journal.pntd.0006901
14. Luis AD, Kuenzi AJ, Mills JN. Species diversity concurrently dilutes and amplifies transmission in a zoonotic host-pathogen system through competing mechanisms. Proc Natl Acad Sci U S A. 2018;115:7979–84. https://doi.org/10.1073/pnas.1807106115
15. Simon-Loriere E, Faye O, Prot M, Casademont I, Fall G, Fernandez-Garcia MD, et al. Autochthonous Japanese encephalitis with yellow fever coinfection in Africa. N Engl J Med. 2017;376:1483–5. https://doi.org/10.1056/NEJMc1701600

Address for correspondence: Moussa Moïse Diagne, Virology Department, Institut Pasteur de Dakar, 36 Avenue Pasteur, BP.220, Dakar, Senegal; email: MoussaMoise.DIAGNE@pasteur.sn

Contact Tracing during Coronavirus Disease Outbreak, South Korea, 2020

Young Joon Park,[1] Young June Choe,[1] Ok Park, Shin Young Park, Young-Man Kim, Jieun Kim, Sanghui Kweon, Yeonhee Woo, Jin Gwack, Seong Sun Kim, Jin Lee, Junghee Hyun, Boyeong Ryu, Yoon Suk Jang, Hwami Kim, Seung Hwan Shin, Seonju Yi, Sangeun Lee, Hee Kyoung Kim, Hyeyoung Lee, Yeowon Jin, Eunmi Park, Seung Woo Choi, Miyoung Kim, Jeongsuk Song, Si Won Choi, Dongwook Kim, Byoung-Hak Jeon, Hyosoon Yoo, Eun Kyeong Jeong, on behalf of the COVID-19 National Emergency Response Center, Epidemiology and Case Management Team

We analyzed reports for 59,073 contacts of 5,706 coronavirus disease (COVID-19) index patients reported in South Korea during January 20–March 27, 2020. Of 10,592 household contacts, 11.8% had COVID-19. Of 48,481 nonhousehold contacts, 1.9% had COVID-19. Use of personal protective measures and social distancing reduces the likelihood of transmission.

Effective contact tracing is critical to controlling the spread of coronavirus disease (COVID-19) (*1*). South Korea adopted a rigorous contact-tracing program comprising traditional shoe-leather epidemiology and new methods to track contacts by linking large databases (global positioning system, credit card transactions, and closed-circuit television). We describe a nationwide COVID-19 contact tracing program in South Korea to guide evidence-based policy to mitigate the pandemic (*2*).

The Study

South Korea's public health system comprises a national-level governance (Korea Centers for Disease Control and Prevention), 17 regional governments, and 254 local public health centers. The first case of COVID-19 was identified on January 20, 2020; by May 13, a total of 10,962 cases had been reported. All reported COVID-19 patients were tested using reverse transcription PCR, and case information was sent to Korea Centers for Disease Control and Prevention.

We defined an index case as the first identified laboratory-confirmed case or the first documented case in an epidemiologic investigation within a cluster. Contacts in high-risk groups (household contacts of COVID-19 patients, healthcare personnel) were routinely tested; in non–high-risk groups, only symptomatic persons were tested. Non–high-risk asymptomatic contacts had to self-quarantine for 14 days and were placed under twice-daily active surveillance by public health workers. We defined a household contact as a person who lived in the household of a COVID-19 patient and a nonhousehold contact as a person who did not reside in the same household as a confirmed COVID-19 patient. All index patients were eligible for inclusion in this analysis if we identified $\geq$1 contact. We defined a detected case as a contact with symptom onset after that of a confirmed COVID-19 index patient.

We grouped index patients by age: 0–9, 10–19, 20–29, 30–39, 40–49, 50–59, 60–69, 70–79, and $\geq$80 years. Because we could not determine direction of transmission, we calculated the proportion of detected cases by the equation [number of detected cases/number of contacts traced] × 100, excluding the index patient; we also calculated 95% CIs. We compared the difference in detected cases between household and nonhousehold contacts across the stratified age groups.

We conducted statistical analyses using RStudio (https://rstudio.com). We conducted this study as a

Author affiliations: Korea Centers for Disease Control and Prevention, Cheongju, South Korea (Y.J. Park, O. Park, S.Y. Park, Y.-M. Kim, J. Kim, S. Kweon, Y. Woo, J. Gwack, S.S. Kim, J. Lee, J. Hyun, B. Ryu, Y.S. Jang, H. Kim, S.H. Shin, S. Yi, S. Lee, H.K. Kim, H. Lee, Y. Jin, E. Park, S.W. Choi, M. Kim, J. Song, S.W. Choi, D. Kim, B.-H. Jeon, H. Yoo, E.K. Jeong); Hallym University College of Medicine, Chuncheon, South Korea (Y.J. Choe)

DOI: https://doi.org/10.3201/eid2610.201315

[1]These authors contributed equally to this article.

legally mandated public health investigation under the authority of the Korean Infectious Diseases Control and Prevention Act (nos. 12444 and 13392).

We monitored 59,073 contacts of 5,706 COVID-19 index patients for an average of 9.9 (range 8.2–12.5) days after severe acute respiratory syndrome coronavirus 2 (SARS-CoV-2) infection was detected (Table 1). Of 10,592 household contacts, index patients of 3,417 (32.3%) were 20–29 years of age, followed by those 50–59 (19.3%) and 40–49 (16.5%) years of age (Table 2). A total of 11.8% (95% CI 11.2%–12.4%) of household contacts of index patients had COVID-19; in households with an index patient 10–19 years of age, 18.6% (95% CI 14.0%–24.0%) of contacts had COVID-19. For 48,481 nonhousehold contacts, the detection rate was 1.9% (95% CI 1.8%–2.0%) (Table 2). With index patients 30–39 years of age as reference, detection of COVID-19 contacts was significantly higher for index patients >40 years of age in nonhousehold settings. For most age groups, COVID-19 was detected in significantly more household than nonhousehold contacts (Table 2).

Conclusions

We detected COVID-19 in 11.8% of household contacts; rates were higher for contacts of children than adults. These risks largely reflected transmission in the middle of mitigation and therefore might characterize transmission dynamics during school closure (*3*). Higher household than nonhousehold detection might partly reflect transmission during social distancing, when family members largely stayed home except to perform essential tasks, possibly creating spread within the household. Clarifying the dynamics of SARS-CoV-2 transmission will help in determining control strategies at the individual and population levels. Studies have increasingly examined transmission within households. Earlier studies on the infection rate for symptomatic household contacts in the United States reported 10.5% (95% CI 2.9%–31.4%), significantly higher than for nonhousehold contacts (*4*). Recent reports on COVID-19 transmission have estimated higher secondary attack rates among household than nonhousehold contacts. Compiled reports from China, France, and Hong Kong estimated the secondary attack rates for close contacts to be 35% (95% CI 27%–44%) (*5*). The difference in attack rates for household contacts in different parts of the world may reflect variation in households and country-specific strategies on COVID-19 containment and mitigation. Given the high infection rate within families, personal protective measures should be used at home to reduce the risk for transmission (*6*). If feasible, cohort isolation outside of hospitals, such as in a Community Treatment Center, might be a viable option for managing household transmission (*7*).

We also found the highest COVID-19 rate (18.6% [95% CI 14.0%–24.0%]) for household contacts of school-aged children and the lowest (5.3% [95% CI 1.3%–13.7%]) for household contacts of children 0–9 years in the middle of school closure. Despite closure of their schools, these children might have interacted with each other, although we do not have data to support that hypothesis. A contact survey in Wuhan and Shanghai, China, showed that school closure and social distancing significantly reduced the rate of COVID-19 among contacts of school-aged children (*8*). In the case of seasonal influenza epidemics, the highest secondary attack rate occurs among young children (*9*). Children who attend day care or school also are at high risk for transmitting respiratory viruses to household members (*10*). The low detection rate for household contacts of preschool-aged children in South Korea might be attributable to social distancing during these periods. Yet, a recent report from Shenzhen, China, showed that the proportion of infected children increased during the outbreak from 2% to 13%, suggesting the importance of school closure (*11*). Further evidence, including serologic studies, is needed to evaluate the public health benefit of school closure as part of mitigation strategies.

Our observation has several limitations. First, the number of cases might have been underestimated because all asymptomatic patients might

Table 1. Contacts traced by age group of index coronavirus disease patients, South Korea, January 20–March 27, 2020

Index patient age, y	No. (%) index patients	No. (%) contacts traced	No. contacts traced/index patient	Average time contacts monitored, d
0–9	29 (0.5)	237 (0.4)	8.2	12.5
10–19	124 (2.2)	457 (0.8)	3.7	9.0
20–29	1,695 (29.7)	15,810 (26.8)	9.3	9.8
30–39	668 (11.7)	8,636 (14.6)	12.9	11.1
40–49	807 (14.1)	9,709 (16.4)	12.0	11.0
50–59	1,107 (19.4)	11,353 (19.2)	10.3	9.6
60–69	736 (12.9)	8,490 (14.4)	11.5	8.2
70–79	338 (5.9)	2,389 (4.0)	7.1	8.5
≥80	202 (3.5)	1,992 (3.4)	9.9	9.4
Total	5,706	59,073	10.4	9.9

Table 2. Rates of coronavirus disease among household and nonhousehold contacts, South Korea, January 20–March 27, 2020

	Household		Nonhousehold	
Index patient age, y	No. contacts positive/ no. contacts traced	% Positive (95% CI)	No. contact positive/ no. contacts traced	% Positive (95% CI)
0–9	3/57	5.3 (1.3–13.7)	2/180	1.1 (0.2–3.6)
10–19	43/231	18.6 (14.0–24.0)	2/226	0.9 (0.1–2.9)
20–29	240/3,417	7.0 (6.2–7.9)	138/12,393	1.1 (0.9–1.3)
30–39	143/1,229	11.6 (9.9–13.5)	70/7,407	0.9 (0.7–1.2)
40–49	206/1,749	11.8 (10.3–13.4)	161/7,960	2.0 (1.7–2.3)
50–59	300/2,045	14.7 (13.2–16.3)	166/9,308	1.8 (1.5–2.1)
60–69	177/1,039	17.0 (14.8–19.4)	215/7,451	2.9 (2.5–3.3)
70–79	86/477	18.0 (14.8–21.7)	92/1,912	4.8 (3.9–5.8)
≥80	50/348	14.4 (11.0–18.4)	75/1,644	4.6 (3.6–5.7)
Total	1,248/10,592	11.8 (11.2–12.4)	921/48,481	1.9 (1.8–2.0)

not have been identified. In addition, detected cases could have resulted from exposure outside the household. Second, given the different thresholds for testing policy between households and nonhousehold contacts, we cannot assess the true difference in transmissibility between households and nonhouseholds. Comparing symptomatic COVID-19 patients of both groups would be more accurate. Despite these limitations, the sample size was large and representative of most COVID-19 patients early during the outbreak in South Korea. Our large-scale investigation showed that pattern of transmission was similar to those of other respiratory viruses (*12*). Although the detection rate for contacts of preschool-aged children was lower, young children may show higher attack rates when the school closure ends, contributing to community transmission of COVID-19.

The role of household transmission of SARS-CoV-2 amid reopening of schools and loosening of social distancing underscores the need for a time-sensitive epidemiologic study to guide public health policy. Contact tracing is especially important in light of upcoming future SARS-CoV-2 waves, for which social distancing and personal hygiene will remain the most viable options for prevention. Understanding the role of hygiene and infection control measures is critical to reducing household spread, and the role of masking within the home, especially if any family members are at high risk, needs to be studied.

We showed that household transmission of SARS-CoV-2 was high if the index patient was 10–19 years of age. In the current mitigation strategy that includes physical distancing, optimizing the likelihood of reducing individual, family, and community disease is important. Implementation of public health recommendations, including hand and respiratory hygiene, should be encouraged to reduce transmission of SARS-CoV-2 within affected households.

Acknowledgments

We thank the Ministry of Interior and Safety, Si/Do and Si/Gun/Gu, medical staff in health centers, and medical facilities for their efforts in responding to COVID-19 outbreak.

About the Author

Dr. Young Joon Park is the preventive medicine physician leading the Epidemiology and Case Management Team for the COVID-19 National Emergency Response Center, Korea Centers for Disease Control and Prevention. His primary research interests include epidemiologic investigation of infectious disease outbreaks. Dr. Choe is an assistant professor at Hallym University College of Medicine. Her research focuses on infectious diseases epidemiology.

References

1. World Health Organization. Contact tracing in the context of COVID-19 [cited 2020 May 15]. https://www.who.int/publications/i/item/contact-tracing-in-the-context-of-covid-19
2. COVID-19 National Emergency Response Center. Epidemiology & Case Management Team, Korea Centers for Disease Control & Prevention. Contact transmission of COVID-19 in South Korea: novel investigation techniques for tracing contacts. Osong Public Health Res Perspect. 2020;11:60–3. https://doi.org/10.24171/j.phrp.2020.11.1.09
3. Choe YJ, Choi EH. Are we ready for coronavirus disease 2019 arriving at schools? J Korean Med Sci. 2020;35:e127. https://doi.org/10.3346/jkms.2020.35.e127
4. Burke RM, Midgley CM, Dratch A, Fenstersheib M, Haupt T, Holshue M, et al. Active monitoring of persons exposed to patients with confirmed COVID-19—United States, January–February 2020. MMWR Morb Mortal Wkly Rep. 2020;69:245–6. https://doi.org/10.15585/mmwr.mm6909e1
5. Liu Y, Eggo RM, Kucharski AJ. Secondary attack rate and superspreading events for SARS-CoV-2. Lancet. 2020;395:e47. https://doi.org/10.1016/S0140-6736(20)30462-1
6. Jefferson T, Del Mar C, Dooley L, Ferroni E, Al-Ansary LA, Bawazeer GA, et al. Physical interventions to interrupt or reduce the spread of respiratory viruses: systematic review. BMJ. 2009;339(sep21 1):b3675. https://doi.org/10.1136/bmj.b3675
7. Park PG, Kim CH, Heo Y, Kim TS, Park CW, Kim CH. Out-of-hospital cohort treatment of coronavirus disease 2019

patients with mild symptoms in Korea: an experience from a single community treatment center. J Korean Med Sci. 2020;35:e140. https://doi.org/10.3346/jkms.2020.35.e140
8. Zhang J, Litvinova M, Liang Y, Wang Y, Wang W, Zhao S, et al. Changes in contact patterns shape the dynamics of the COVID-19 outbreak in China. Science. 2020;368:1481–6. https://doi.org/10.1126/science.abb8001
9. Principi N, Esposito S, Marchisio P, Gasparini R, Crovari P. Socioeconomic impact of influenza on healthy children and their families. Pediatr Infect Dis J. 2003;22(Suppl):S207–10. https://doi.org/10.1097/01.inf.0000092188.48726.e4
10. Ferguson NM, Cummings DA, Fraser C, Cajka JC, Cooley PC, Burke DS. Strategies for mitigating an influenza pandemic. Nature. 2006;442:448–52. https://doi.org/10.1038/nature04795
11. Liu J, Liao X, Qian S, Yuan J, Wang F, Liu Y, et al. Community transmission of severe acute respiratory syndrome coronavirus 2, Shenzhen, China, 2020. Emerg Infect Dis. 2020;26:1320–3. https://doi.org/10.3201/eid2606.200239
12. Choe YJ, Smit MA, Mermel LA. Comparison of common respiratory virus peak incidence among varying age groups in Rhode Island, 2012–2016. JAMA Netw Open. 2020;3:e207041. https://doi.org/10.1001/jamanetworkopen.2020.7041

Address for correspondence: Eun Kyeong Jeong, Korea Centers for Disease Control and Prevention, Osong Health Technology Administration Complex, 187, Osongsaengmyeong 2-ro, Osong-eup, Heungdeok-gu, Cheongju, Chungcheongbuk-do, South Korea, email: jeongek@korea.kr

Pooling Upper Respiratory Specimens for Rapid Mass Screening of COVID-19 by Real-Time RT-PCR

So Yeon Kim,[1] Jaehyeon Lee,[1] Heungsup Sung, Hyukmin Lee, Myung Guk Han, Cheon Kwon Yoo, Sang Won Lee,[2] Ki Ho Hong[2]

To validate the specimen-pooling strategy for real-time reverse transcription PCR detection of severe acute respiratory syndrome coronavirus 2, we generated different pools including positive specimens, reflecting the distribution of cycle threshold values at initial diagnosis. Cumulative sensitivities of tested pool sizes suggest pooling of ≤6 specimens for surveillance by this method.

After the first report of the coronavirus disease (COVID-19) outbreak in Wuhan, China (*1*), the World Health Organization announced pandemic status on March 11, 2020 (*2*). Real-time reverse transcription PCR (rRT-PCR) detection of the causative agent, severe acute respiratory syndrome coronavirus 2 (SARS-CoV-2), is a confirmatory diagnostic tool for COVID-19 (*3*).

A mass screening test for COVID-19 is urgently needed in South Korea because of the increasing number of confirmed cases in long-term care hospitals and public facilities, as well as imported cases. Testing specimens pooled before RNA extraction and subsequently retesting single specimens from positive pools is an efficient strategy for rapid mass screening as well as for increasing testing capacity and conserving resources.

Testing pooled specimens is a well-known method and has been used in blood banks worldwide to screen for infectious disease; however, only a few studies have evaluated specimen pooling for SARS-CoV-2 (*4*,*5*; R. Hanel et al., unpub. data. https://arxiv.org/abs/2003.09944v1; M.J. Farfan et al., unpub. data, https://doi.org/10.1101/2020.04.15.20067199). Therefore, we evaluated the pooling strategy for SARS-CoV-2 testing using clinical specimens from 3 hospitals in South Korea: Seoul Medical Center and National Medical Center, both in Seoul, and Jeonbuk National University Hospital in Jeonju. The Institutional Review Boards of the hospitals approved this study. Written consent from participants was waived.

The Study

Pooled upper respiratory specimens were prepared from 50 individual SARS-CoV-2–positive specimens and 300 individual SARS-CoV-2–negative specimens. Either a single nasopharyngeal swab (NPS) or a nasopharyngeal and an oropharyngeal swab (NPS/OPS) were collected in an eNAT tube (Copan Italy, https://www.copangroup.com). Laboratory diagnosis of SARS-CoV-2 infection was performed with all specimens using the following rRT-PCR kits targeting the *E* and *RdRp* genes: STANDARD M nCoV Real-time Detection (SD Biosensor, https://sdbiosensor.com) or PowerCheck 2019-nCoV Real-Time Detection (Kogene Biotech, https://kogene.co.kr).

For the SARS-CoV-2–positive pooled specimens, we selected 50 individual SARS-CoV-2–positive specimens on the basis of the observed population distribution of cycle threshold (C_t) values of rRT-PCR for patients confirmed positive during January 20–March 2, 2020 (Figure 1). We grouped the C_t values into 8 strata, decided the sampling number adequate for each stratum, and selected a total of 50 specimens

Author affiliations: National Medical Center, Seoul, South Korea (S.Y. Kim); Jeonbuk National University Medical School and Hospital, Jeonju, South Korea (J. Lee); Asan Medical Center and University of Ulsan College of Medicine, Seoul (H. Sung); Yonsei University College of Medicine, Seoul (H. Lee); Korea Centers for Disease Control and Prevention, Cheongju (M.G. Han, S.W. Lee, C.K. Yoo); Seoul Medical Center, Seoul (K.H. Hong)

DOI: https://doi.org/10.3201/eid2610.201955

[1]These first authors contributed equally to this article.

[2]These authors contributed equally to this article.

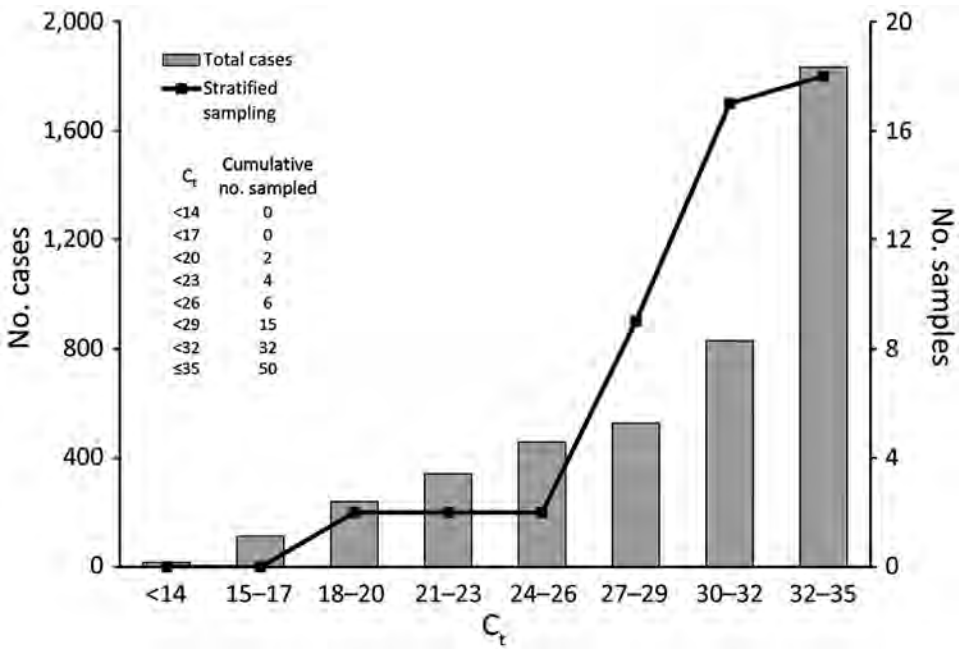

Figure 1. Distribution of *RdRp* gene C_t values for specimens from 4,364 confirmed patients in South Korea at their initial diagnosis of coronavirus disease (COVID-19) and the specimens selected by stratified sampling. This figure shows the first *RdRp* gene C_t values of patients receiving a COVID-19 diagnosis (bars). We selected positive samples with the stratified sampling method based on that distribution (line).Cumulative numbers of selected specimens per stratum are shown. C_t, cycle threshold.

for 8 strata (Figure 1). We pooled the selected individual SARS-CoV-2–positive specimens with different numbers of SARS-CoV-2–negative specimens to generate 50 sets of pooled specimens in duplicate; the pool sizes of each set were 2, 4, 6, 8, 10, and 16. We prepared a total of 600 pooled specimens. To evaluate clinical specificity in SARS-CoV-2–negative pooled specimens, we randomly combined 16 specimens from 300 negative specimens and generated 60 negative pooled specimens (Appendix, https://wwwnc.cdc.gov/EID/article/26/10/20-1955-App1.pdf).

The following 3 automated RNA extraction systems were used: MagNa Pure 96 (Roche Diagnostics, https://www.roche.com), Real-prep (BioSewoom, www.biosewoom.com), and eMAG (bioMérieux, https://www.biomerieux.com). We followed the extraction protocol provided by each manufacturer with an input volume of 200 µL and elution volume of 50 µL

We performed rRT-PCR using PowerCheck 2019-nCoV for all pooled specimens. The interpretation guideline by the manufacturer for SARS-CoV-2 positivity was a C_t cutoff of ≤35 for a single specimen; however, we assessed every amplified curve throughout 40 total PCR cycles. For either the *E* or *RdRp* gene, when we observed any amplified curve before the end of the 40 amplification cycles, we interpreted the result as positive for the pooled specimens. When we observed no amplification curves for both genes, we interpreted the result as negative.

We performed all statistical analyses with MedCalc version 19.2.1 (MedCalc Software Ltd, https://www.medcalc.org). The distribution of C_t values in individual specimens (Figure 1) showed negative skewness. In total, 61% of confirmed cases had C_t ≥30, which was near the cutoff value. We selected positive samples for pooling according to this distribution pattern.

The pooled positive specimens had 100% sensitivity in pool sizes 2, 4, and 6 and 97%–99% sensitivity in pool sizes 8, 10, and 16 (Table). To ensure a conservative estimation of sensitivity, we calculated the cumulative sensitivities on the assumption that the false-negative results that occurred in smaller pool sizes could also occur in larger pool sizes.

Table. Test performance of pooled specimens compared with individual specimens for severe acute respiratory syndrome coronavirus 2

No. specimens in pool	Amplification in *E* or *RdRp* gene, %	No amplifications	Sensitivity of pools, % (95% CI)	Cumulative sensitivity, %*
2	100	0	100 (96–100)	100
4	100	0	100 (96–100)	100
6	100	0	100 (96–100)	100
8	97	3	97 (92–99)	97
10	99	1	99 (95–100)	96
16	96	4	96 (90–98)	92

*Calculated sensitivity based on the accumulated discrepancy numbers under the dilution fold

Therefore, every negative result that occurred in smaller pool sizes was included in the calculation of cumulative sensitivities in larger pool sizes. The cumulative sensitivities of pool size 6 was 100%, of 8, 97%, of 10, 96%, and of 16, 92%. The clinical specificity of pool size 16 was 97% (58/60, 95% CI 87%-99%). The mean C_t values increased for both the *E* and *RdRp* genes as the pool size increased (Figure 2; Appendix Figure).

Conclusions

We evaluated the clinical sensitivity and specificity of SARS-CoV-2 rRT-PCR using pooled upper respiratory specimens from confirmed cases. Because pooled specimens are expected to be used as a screening tool, the clinical sensitivity of pooled specimens at a given pool size is especially important.

A limitation of previous studies is that the C_t values of positive specimens from patients at the time of diagnosis were not considered in the study design. The C_t values of specimens in previous studies were relatively low (*6*). Because specimens with high C_t values, meaning low virus titers, are expected to be vulnerable to pooling, the distribution of C_t values in the actual population should be reflected when determining the pool size. We analyzed the actual distribution of C_t values from 4,364 initially confirmed cases, and the distribution showed skewness with regard to the PCR cutoff value.

Yelin et al. (*4*) suggested that the pool size using RNA extracts could be ≤64; however, we do not recommend increasing the pool size to 64, corresponding to a theoretical increase in C_t values of 6, given the associated loss in sensitivity; doing so may cause false negative results.

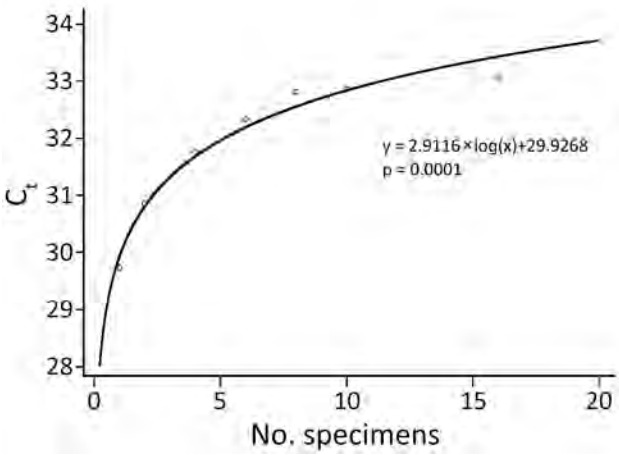

Figure 2. Mean C_t values of *RdRp* genes of 50 specimens from coronavirus disease patients in South Korea by pool size. The trend line shows logarithmic regression. C_t, cycle threshold.

The pooling strategy showed efficiency when the positive rates in the population were low (*7*). We showed clinical sensitivities and cumulative sensitivities of the pooled specimens that were sampled after stratification by data, including low viral titers. On the basis of our results, we recommend pooling ≤6 specimens in clinical practice. Pooling >6 specimens might cause false-negative results, considering the observed abundance of specimens with high C_t values in the population.

This study has some limitations. First, the analytical performance of the PCR kit used has not been evaluated fully because it is one of the earliest available commercial PCR kits that received the Emergency Use Authorization in Korea. Second, the positive cutoff in the kit was a C_t value ≤35 within 40 amplification cycles. Therefore, this study did not include individual specimens with a C_t value >35, which is interpreted as an inconclusive result by this kit. Third, we did not evaluate cost-effectiveness on the basis of the hypothesized prevalence. Last, we did not evaluate the effect of specimen volume in the pools; increasing the input volume from each specimen may improve the sensitivity of the pooling test.

Our protocol will be helpful for screening persons in groups at high risk for COVID-19 infection quickly and quarantining those confirmed positive, even in situations with limited time and test resources. Epidemiologic factors should be considered when choosing an adequate pooling number. Symptomatic case-patients should be tested individually without pooling to enable effective and timely action. We have included practical guidelines for specimen-pooling procedures in the Appendix.

Acknowledgments

We thank Mallikarjun Handigund for his contribution in generating the data for this study, and Joongyub Lee for his contribution to the statistical analysis. We thank all laboratory technologists in the Department of Molecular Diagnostics at National Medical Center, Jeonbuk National University Hospital, and Seoul Medical Center for their contributions in generating the data for this study.

Author contributions: S.W.L. and K.H.H. take responsibility for the integrity of the data and the accuracy of the data analysis. S.Y.K. and J.L. contributed equally to this study.

About the Author

Dr. Kim is a medical doctor and director of the Department of Laboratory Medicine, National Medical Center, Seoul, South Korea. Her research interests include

molecular diagnostics and infectious diseases. Dr. Lee is a medical doctor and assistant professor in the Department of Laboratory Medicine, Jeonbuk National University Medical School and Hospital, Jeonju, South Korea. His research interests include clinical microbiology and infectious disease.

References

1. Zhu N, Zhang D, Wang W, Li X, Yang B, Song J, et al.; China Novel Coronavirus Investigating and Research Team. A novel coronavirus from patients with pneumonia in China, 2019. N Engl J Med. 2020;382:727–33. https://doi.org/10.1056/NEJMoa2001017
2. World Health Organization. WHO Director-General's opening remarks at the media briefing on COVID-19—11 March 2020. Geneva: The Organization; 2020 [cited 2020 Aug 19]. https://www.who.int/dg/speeches/detail/who-director-general-s-opening-remarks-at-the-media-briefing-on-covid-19---11-march-2020
3. Hong KH, Lee SW, Kim TS, Huh HJ, Lee J, Kim SY, et al. Guidelines for laboratory diagnosis of coronavirus disease 2019 (COVID-19) in Korea. Ann Lab Med. 2020;40:351–60. https://doi.org/10.3343/alm.2020.40.5.351
4. Yelin I, Aharony N, Shaer Tamar E, Argoetti A, Messer E, Berenbaum D, et al. Evaluation of COVID-19 RT-qPCR test in multi-sample pools. Clin Infect Dis. 2020 May 2 [Epub ahead of print]. https://doi.org/10.1093/cid/ciaa531
5. Hogan CA, Sahoo MK, Pinsky BA. Sample pooling as a strategy to detect community transmission of SARS-CoV-2. JAMA. 2020;323:1967–9. https://doi.org/10.1001/jama.2020.5445
6. Lohse S, Pfuhl T, Berkó-Göttel B, Rissland J, Geißler T, Gärtner B, et al. Pooling of samples for testing for SARS-CoV-2 in asymptomatic people. Lancet Infect Dis. 2020 Apr 28 [Epub ahead of print]. https://doi.org/10.1016/S1473-3099(20)30362-5
7. European Centre for Disease Prevention and Control. Methodology for estimating point prevalence of SARSCoV-2 infection by pooled RT-PCR testing. Stockholm: The Centre; 2020 [cited 2020 Aug 19]. https://www.ecdc.europa.eu/en/publications-data/methodology-estimating-point-prevalence-sars-cov-2-infection-pooled-rt-pcr

Address for correspondence: Ki Ho Hong, Department of Laboratory Medicine, Seoul Medical Center, 156 Sinnae-ro, Jungnang-gu, Seoul, 02053, South Korea; email: kihohongmd@gmail.com

Coronavirus Disease among Persons with Sickle Cell Disease, United States, March 20–May 21, 2020

Julie A. Panepinto, Amanda Brandow, Lana Mucalo, Fouza Yusuf, Ashima Singh, Bradley Taylor, Katherine Woods, Amanda B. Payne, Georgina Peacock, Laura A. Schieve

Sickle cell disease (SCD) disproportionately affects Black or African American persons in the United States and can cause multisystem organ damage and reduced lifespan. Among 178 persons with SCD in the United States who were reported to an SCD–coronavirus disease case registry, 122 (69%) were hospitalized and 13 (7%) died.

Sickle cell disease (SCD), an inherited hemoglobinopathy that most commonly affects persons of African ancestry, is estimated to affect 1 in 365 Black persons in the United States (*1*). Persons with SCD produce abnormal hemoglobin that causes erythrocytes to become rigid and deform under low oxygen conditions, leading to ischemia–reperfusion injury in the microvasculature with subsequent organ damage and pain. SCD affects nearly every organ system; average life expectancy estimates of affected persons are 43–54 years (*2*,*3*). Persons with SCD are at increased risk for pulmonary disease and pneumonia.

Previous studies have shown that influenza severity and hospitalization rates are higher among persons with SCD than those without SCD (*4*,*5*). Thus, persons with SCD could be at higher risk for development of severe disease if infected with severe acute respiratory syndrome coronavirus 2 (SARS-CoV-2), the causative agent of coronavirus disease (COVID-19). Although empirical data are limited, cases of COVID-19 have been reported in persons with SCD (*6*–*8*), and a study of COVID-19 intensive care unit (ICU) admissions reported 2 (4%) of 48 children had SCD (*9*). We describe a large series of COVID-19 cases and associated deaths among persons with SCD in the United States.

Author affiliations: Medical College of Wisconsin, Milwaukee, Wisconsin, USA (J.A. Panepinto, A. Brandow, L. Mucalo, F. Yusuf, A. Singh, B. Taylor, K. Woods); Centers for Disease Control and Prevention, Atlanta, USA (A.B. Payne, G. Peacock, L. Schieve)

DOI: https://doi.org/10.3201/eid2610.201792

The Study

The Medical College of Wisconsin established the SECURE-SCD Registry to collect data on COVID-19 cases occurring globally in persons living with SCD. A link to the registry (https://covidsicklecell.org) was distributed to healthcare providers caring for patients with SCD by medical professional and patient advocacy networks and was made available on the Centers for Disease Control and Prevention website. Providers were asked to report all confirmed COVID-19 cases among patients with SCD to this registry; they were specifically asked to report only confirmed COVID-19 cases and to report cases after resolution of acute illness or death. Persons who had the sickle cell trait were not included in this registry, nor were persons with SCD who had suspected but not confirmed COVID-19. Providers were asked to report if the patient died of COVID-19 or complications of COVID-19. All data were deidentified without protected health information.

For each case, providers were asked to complete a short form with questions on demographics; SCD genotype; SCD-related health history; and COVID-19 clinical course, severity, and interventions. In addition to data on COVID-19 clinical severity indicators, such as hospitalization, ICU admission, and death, COVID-19 severity level based on patient manifestations were collected by using established criteria for asymptomatic, mild, moderate, severe, and critical (*10*) (Table).

This analysis was limited to cases among persons with SCD living in the United States reported during March 20–May 21, 2020. We describe the reported cases and deaths caused by COVID-19 and provide

case-fatality rates. Given uncertainty in the sample representativeness and ongoing data reporting to the SECURE-SCD Registry, we view these data as a hypothesis-generating case series. Thus, we did not use statistical tests to assess the significance of differences in mortality rates by subgroup.

As of May 21, 2020, a total of 178 COVID-19 cases were reported to the SECURE-SCD Registry among persons living in 22 states. The mean age of these case-patients was 28.6 years; 57% were female, and 80% were Black (Table). A total of 76% of case-patients had sickle cell types HbSS or HbSβ^0-thalassemia, which is consistent with estimates of SCD genotype distribution in the United States (*11*). Recent (within the past 3 years) adverse events indicative of vasoocclusive crises were common among case-patients; 54% reported ≥3 pain episodes requiring hospitalization and 32% reported ≥1 acute chest syndrome episodes.

Table. Characteristics of COVID-19 cases and cases resulting in death that were reported to the Secure-SCD Registry, United States, March 20–May 21, 2020*

Characteristic	No. (%) case-patients†	No. (%) deaths†	Case-fatality rate, %
Total	178	13	7.3
Sickle cell disease genotype‡			
HbSS/HbSβ^0	135 (75.8)	7 (53.9)	5.2
HbSC/HbSβ^+	42 (23.6)	5 (38.5)	11.9
Mean (SD) age, y	28.6 (14.5)	28.5 (14.6)	NA
Median age, y	26	38	NA
Age range, y	<1–69	12–69	NA
Age group, y			
<19	44 (24.7)	1 (7.7)	2.3
≥19	134 (75.3)	12 (92.3)	9.0
Sex			
F	101 (56.7)	6 (46.2)	5.9
M	75 (42.1)	6 (46.2)	8.0
Race/ethnicity			
Black or African American (and not Hispanic or Latino)	142 (79.8)	13 (100.0)	9.2
Hispanic or Latino (and not Black of African American)	21 (11.8)	0	0
SCD health history			
Hospitalized for pain ≥3 times in past 3 y	96 (53.9)	11 (84.6)	11.5
≥1 episodes of acute chest syndrome in past 3 y§	57 (32.0)	3 (23.1)	5.3
Chronic transfusion	23 (12.9)	0	0
Pulmonary hypertension	23 (12.9)	5 (38.5)	21.7
Renal disease			
Albuminuria	27 (15.2)	1 (7.7)	3.7
Decreased renal function	22 (12.4)	3 (23.1)	13.6
SCD nephropathy	17 (9.6)	2 (15.4)	11.8
Stroke			
Overt	22 (12.4)	4 (30.8)	18.2
Silent	10 (5.6)	0	0
COVID-19 case indices			
COVID-19 severity¶			
Asymptomatic	11 (6.2)	0	0
Mild	96 (53.9)	3 (23.1)	3.1
Moderate	32 (18.0)	2 (15.4)	6.3
Severe	30 (16.8)	1 (7.7)	3.3
Critical	9 (5.1)	7 (53.8)	77.8
Accessed care through emergency department	153 (86.0)	13 (100.0)	8.5
Hospitalized	122 (68.5)	11 (84.6)	9.0
Admitted to intensive care unit	19 (10.7)	6 (46.2)	31.6
Ventilator use	10 (5.6)	7 (53.9)	70.0
Received transfusion	68 (38.2)	8 (61.5)	11.8
Received exchange transfusion	16 (9.0)	3 (23.1)	18.6
Received dialysis	4 (2.2)	3 (23.1)	75.0

*Values are no. (%) unless otherwise indicated. COVID-19, coronavirus disease; Hb, hemoglobin; NA, not applicable; SCD, sickle cell disease.
†Numbers do not always add up to total no. case-patients because of missing data.
‡SCD genotypes are HbSS (homozygous for hemoglobin S, a severe phenotype associated with shortest survival); HbSβ^0-thalassemia (compound heterozygous for hemoglobin S and β^0-thalassemia, clinically indistinguishable from HbSS); HbSC (heterozygous for hemoglobin S and hemoglobin C, usually moderate clinical severity); HbSβ+-thalassemia (heterozygous for hemoglobin S and reduced amounts of β-globin, usually milder severity).
§Acute chest syndrome is a multicausal pneumonia-like illness.
¶COVID-19 severity level classified as asymptomatic, no clinical signs or symptoms during the positive COVID-19 period; mild, symptoms of acute upper respiratory tract infection, including fever, fatigue, myalgia, cough, sore throat, runny nose, and sneezing or gastrointestinal symptoms or digestive symptoms, such as nausea, vomiting, abdominal pain and diarrhea; moderate, pneumonia, with or without clinical symptoms, no hypoxia; severe, early respiratory symptoms or gastrointestinal symptoms followed by dyspnea and hypoxia (O_2 saturations <92%); critical, acute respiratory distress syndrome, respiratory failure, encephalopathy, shock, coagulopathy, and multiorgan impairment (lung, heart, kidney, brain) that might be life threatening.

Prevalence of pulmonary hypertension, previous stroke, renal disease, and use of chronic transfusion therapy were all >10%.

A total of 6% of COVID-19 case-patients were asymptomatic, 54% had mild disease severity, 18% had moderate disease severity, 17% had severe disease severity, and 5% had critical disease severity. Nearly 90% of case-patients accessed care through an emergency department, 69% were hospitalized, 11% were admitted to an ICU, 6% required a ventilator, 38% required a transfusion, and 2% required dialysis.

A total of 13 (7%) patients died (Table). Their mean age was 38.5 years, and >90% were adults. Nearly 40% of deaths were among persons who had genotypes generally associated with milder SCD (types HbSC or HbSβ+-thalassemia). Patients who died had high proportions of frequent pain episodes in the previous 3 years (85%), pulmonary hypertension (39%), decreased renal function (23%), SCD nephropathy (15%), and overt stroke (31%). Of the 13 deaths, 8 were among persons who had severe or critical COVID-19; 5 deaths were observed in persons who had mild or moderate COVID-19.

Conclusions

Our findings suggest that persons who have SCD and become infected with SARS-CoV-2 have a high risk for a severe disease course and a high case-fatality rate. Among confirmed COVID-19 case-patients reported to the registry, the 69% hospitalization rate, 11% ICU admission rate, and 7% mortality rate are alarming, given that the mean patient age was <40 years. Comparison to a previous report of COVID-19 in the general US population indicates that hospitalization, ICU admission, and case-fatality rates for persons with SCD could be much higher than persons of similar ages in the US population-at-large (*12*). For example, COVID-19 case-fatality rates were reported as <1% for persons 20–44 years of age and for persons 45–54 years of age in the population-at-large (*12*).

These data should be considered in the context that these cases may not be representative of all COVID-19 cases among persons with SCD. There may be bias toward more severe cases in this registry; however, providers were asked to report all COVID-19 cases among their SCD patients. Also, whereas providers were specifically instructed to report only confirmed COVID-19 cases, further guidance was not provided on case confirmation, nor were laboratory testing results included in the registry; thus, we cannot rule out the possibility that a small number of suspected cases were erroneously reported.

Our findings are consistent with expectations based on SCD pathophysiology. SCD can cause multisystem organ damage, life-long disability, and reduced lifespan. Nonetheless, in this case series, COVID-19 deaths occurred in persons who had severe and mild-to-moderate SCD genotypes. Also, deaths occurred in COVID-19 case-patients classified as having mild-to-moderate disease severity. We did not have data to assess whether this finding was caused in part by an impact of SARS-CoV-2 exacerbating preexisting cardiac or SCD concurrent conditions; further study is needed.

Persons with SCD face socioeconomic and healthcare access disparities that might compound their already high risk for severe COVID-19 because of their underlying disease and concurrent conditions. SCD complications might negatively impact educational achievement and employment (*13,14*). Accessing appropriate healthcare is difficult given the lack of providers with SCD expertise. SCD patients might delay seeking care, and emergency department visits are high among this population that is placed at increased risk for poor health (*14*).

Our findings underscore the need to consider the unique circumstances faced by high-risk subgroups. SCD is one of many possible explanations for higher rates of illness and mortality from COVID-19 among Black populations in the United States. As with all high-risk groups, staying home, social distancing, and hand hygiene are necessary for persons with SCD (*15*), along with prompt care-seeking if COVID-19 is suspected or SCD complications arise. In addition, specific socioeconomic and healthcare access challenges that many persons with SCD face (i.e., social determinants of health) need to be considered in implementing prevention measures.

Acknowledgments

We thank the patients reported, the healthcare personnel who cared for them, and the providers and institutions who contributed to the SECURE-SCD Registry for participating in this study. Details for contributing providers and institutions are available at https://covidsicklecell.org.

This study was supported in part by the National Center for Advancing Translational Sciences, National Institutes of Health (grant no. UL1TR001436).

About the Author

Dr. Panepinto is a professor of pediatrics at the Medical College of Wisconsin/Children's of Wisconsin, Milwaukee, WI. Her primary research interests are patient-centered outcomes and health services research.

References

1. Hassell KL. Population estimates of sickle cell disease in the U.S. Am J Prev Med. 2010;38(Suppl):S512–21. https://doi.org/10.1016/j.amepre.2009.12.022
2. Lubeck D, Agodoa I, Bhakta N, Danese M, Pappu K, Howard R, et al. Estimated life expectancy and income of patients with sickle cell disease compared with those without sickle cell disease. JAMA Netw Open. 2019;2:e1915374. https://doi.org/10.1001/jamanetworkopen.2019.15374
3. Paulukonis ST, Eckman JR, Snyder AB, Hagar W, Feuchtbaum LB, Zhou M, et al. Defining sickle cell disease mortality using a population-based surveillance system, 2004 through 2008. Public Health Rep. 2016;131:367–75. https://doi.org/10.1177/003335491613100221
4. Bundy DG, Strouse JJ, Casella JF, Miller MR. Burden of influenza-related hospitalizations among children with sickle cell disease. Pediatrics. 2010;125:234–43. https://doi.org/10.1542/peds.2009-1465
5. Inusa B, Zuckerman M, Gadong N, Afif M, Arnott S, Heath P, et al. Pandemic influenza A (H1N1) virus infections in children with sickle cell disease. Blood. 2010;115:2329–30. https://doi.org/10.1182/blood-2009-12-260836
6. Beerkens F, John M, Puliafito B, Corbett V, Edwards C, Tremblay D. COVID-19 pneumonia as a cause of acute chest syndrome in an adult sickle cell patient. Am J Hematol. 2020;95:E154–6. https://doi.org/10.1002/ajh.25809
7. Nur E, Gaartman AE, van Tuijn CF, Tang MW, Biemond BJ. Vaso-occlusive crisis and acute chest syndrome in sickle cell disease due to 2019 novel coronavirus disease (COVID-19). Am J Hematol. 2020;95:725–6. https://doi.org/10.1002/ajh.25821
8. Odièvre MH, de Marcellus C, Ducou Le Pointe H, Allali S, Romain AS, Youn J, et al. Dramatic improvement after tocilizumab of severe COVID-19 in a child with sickle cell disease and acute chest syndrome. Am J Hematol. 2020;May 1:ajh.25855. https://doi.org/10.1002/ajh.25855
9. Shekerdemian LS, Mahmood NR, Wolfe KK, Riggs BJ, Ross CE, McKiernan CA, et al.; International COVID-19 PICU Collaborative. Characteristics and outcomes of children with coronavirus disease 2019 (COVID-19) infection admitted to US and Canadian pediatric intensive care units. JAMA Pediatr. 2020. https://doi.org/10.1001/jamapediatrics.2020.1948
10. Dong Y, Mo X, Hu Y, Qi X, Jiang F, Jiang Z, et al. Epidemiology of COVID-19 among children in China. Pediatrics. 2020;145:e20200702. https://doi.org/10.1542/peds.2020-0702
11. Saraf SL, Molokie RE, Nouraie M, Sable CA, Luchtman-Jones L, Ensing GJ, et al. Differences in the clinical and genotypic presentation of sickle cell disease around the world. Paediatr Respir Rev. 2014;15:4–12.
12. Bialek S, Boundy E, Bowen V, Chow N, Cohn A, Dowling N, et al.; CDC COVID-19 Response Team. Severe outcomes among patients with coronavirus disease 2019 (COVID-19)—United States, February 12–March 16, 2020. MMWR Morb Mortal Wkly Rep. 2020;69:343–6. https://doi.org/10.15585/mmwr.mm6912e2
13. King AA, DeBaun MR, White DA. Need for cognitive rehabilitation for children with sickle cell disease and strokes. Expert Rev Neurother. 2008;8:291–6. https://doi.org/10.1586/14737175.8.2.291
14. Williams H, Silva RN, Cline D, Freiermuth C, Tanabe P. Social and behavioral factors in sickle cell disease: employment predicts decreased health care utilization. J Health Care Poor Underserved. 2018;29:814–29. https://doi.org/10.1353/hpu.2018.0060
15. Centers for Disease Control and Prevention. CDC guidance for persons at higher risk of severe COVID-19 [cited 2020 Jul 6]. https://www.cdc.gov/coronavirus/2019-ncov/need-extra-precautions/people-with-medical-conditions.html?CDC_AA_refVal=https%3A%2F%2Fwww.cdc.gov%2Fcoronavirus%2F2019-ncov%2Fneed-extra-precautions%2Fgroups-at-higher-risk.html

Address for correspondence: Julie A. Panepinto, Department of Pediatrics, Medical College of Wisconsin, Midwest Athletes Against Cancer and Blood Disorders Fund Research Center, Ste 3050, 8701 Watertown Plank Rd, Milwaukee, WI 53226-0509, USA; email: jpanepin@mcw.edu

The Last Plague or Before the Graying

Ronald O. Valdiserri

When the last plague struck adulthood was new.
Youth *finis* – but not so far behind that one couldn't feel its humming.
AIDS stained everything with sorrow, yes, but it also fired action.
Those years the only verbs I breathed were *demand, confront, claim*!

Christened by a blood test that found no antibodies,
We lucky ones were labeled "negative."
An ironic nomenclature: deemed HIV-free despite being seized by the disease.
Scorched by anger ignited through society's indifference.

Blazing to fight against the epidemic, each in his own way.
Quietly, as "buddies," tendering service in shaded sick rooms,
Or loudly, through defiant pageants of outrage hurled in public.
Never doubting our capacity to beat-back the epidemic.

But that was before the graying, when possibilities measured time.
Now, on maturity's leeward slope, comes a new plague, a different virus.
SARS-CoV-2, the unrelenting agent of COVID-19:
Inescapable television image, societal stopwatch, economic paralytic.

Unlike HIV in biography and in its command of instant global attention.
Different, too, my reaction: scrappy resolve replaced now by enervation.
And I wonder, do mounting years explain this change or could it be the times?
Whence the source: the inevitable stiffening of age or pessimism's bloodless clinch?

About the Author

Dr. Valdiserri is a professor in the Department of Epidemiology, Rollins School of Public Health, Emory University, Atlanta, GA. He previously held senior leadership positions at the Centers for Disease Control and Prevention, the US Department of Veterans Affairs, and the Office of the Assistant Secretary for Health, Department of Health and Human Services. He has written extensively on the public health aspects of HIV/AIDS, sexually transmitted infections, and viral hepatitis.

Address for correspondence: Ronald O. Valdiserri, Emory University, 201 Dowman Dr, Atlanta GA 30322, USA; email: rvaldis@emory.edu

Author affiliations: Emory University Rollins School of Public Health, Atlanta, Georgia, GA

DOI: https://doi.org/10.3201/eid2610.202788

Eliminating Spiked Bovine Spongiform Encephalopathy Agent Activity from Heparin

Cyrus Bett, Omozusi Andrews, David M. Asher, Teresa Pilant, David Keire, Luisa Gregori

Author affiliations: US Food and Drug Administration, Silver Spring, Maryland, USA (C. Bett, O. Andrews, D.M. Asher, T. Pilant, L. Gregori); US Food and Drug Administration, St. Louis, Missouri, USA (D. Keire)

DOI: https://doi.org/10.3201/eid2610.200142

US manufacturers, concerned about bovine spongiform encephalopathy (BSE), ceased marketing bovine heparin in the 1990s. Recent short supplies of safe porcine heparin suggest that reintroducing bovine heparin might benefit public health. We purified heparin from crude bovine extract spiked with BSE agent, removing substantial infectivity and abnormal prion proteins (PrP^{TSE}).

Heparin is a widely used injectable anticoagulant. In the 1990s, bovine-derived heparin was withdrawn from the US market because of concerns about possible contamination of bovine tissues with the agent of bovine spongiform encephalopathy (BSE), the causative agent of variant Creutzfeldt-Jakob disease (vCJD) in humans (*1*). Currently, only porcine heparin, mostly from China, is marketed in the United States. The US Food and Drug Administration has encouraged reintroduction of bovine-sourced heparin into the US market to improve the reliability of the heparin supply chain by diversifying sources (*2*,*3*). The risk that BSE agent might contaminate bovine tissues is now very small because of safeguards implemented during the BSE crisis (*4*).

We previously showed that a model 4-step bench-scale heparin manufacturing process cleared substantial amounts of spiked scrapie agent, a surrogate for BSE agent (*5*). Our protocol yielded heparin with physicochemical identity, purity, and potency similar to those of United States Pharmacopeia (USP) standard heparin. In this study, we spiked commercial crude bovine heparin with BSE agent itself and processed samples using the same manufacturing process we applied to scrapie agent. We tested each intermediate product for residual abnormal prion protein (PrP^{TSE}, a biochemical marker of BSE) and infectivity. We assayed BSE infectivity using intracerebral inoculations of 30-µL volumes into BSE-susceptible transgenic mice (TgBo110) overexpressing the bovine prion-protein–encoding (*PRNP*) gene (*6*). To overcome heparin's acute toxicity when administered intracerebrally into mice, we diluted the samples; 10^{-4} was the lowest dilution tolerated.

We ended the study 2 years after inoculations, testing brains of all mice for PrP^{TSE} using the Herd-Check BSE-Scrapie Ag Test (IDEXX Laboratories, https://www.idexx.com) (*7*), which was previously found to be more sensitive than Western blots (*8*), to assign final disease status (Table). We detected infectivity in samples up to the diatomaceous-earth (DE) filtration step. We estimated removals by DE filtration conservatively, assuming that a 10-fold lower dilution, not tested, would have infected all mice. Sodium hydroxide (NaOH) treatment removed 1.7 log_{10} of BSE infectivity and DE filtration removed ≥1.1

Table. Reduction of BSE agent measured by animal infectivity bioassay and PrP^{TSE} amplification with RT-QuIC*

	Samples with heparin					Samples after heparin removed				
Brain dilutions	BSE spike	NaOH treatment	DE filtration	H_2O_2 bleaching	Final product	BSE spike	NaOH treatment	DE filtration	H_2O_2 bleaching	Final product
10^{-1}	NT	NT	NT	NT	NT	NT	NT	NT	NT	3/5
10^{-2}	NT	NT	NT	NT	NT	5/5	5/5	2/4	2/5	0/5
10^{-3}	NT	NT	NT	NT	NT	5/5	3/4	2/4	0/5	0/5
10^{-4}	19/19	16/16	3/19	0/19	0/20	4/4	3/5	0/5	0/5	0/5
10^{-5}	8/8	3/10	0/10	0/10	0/10	2/4	0/5	0/5	0/5	0/5
10^{-6}	9/9	0/10	0/10	0/10	0/10	2/5	0/5	0/5	0/5	NT
10^{-7}	0/5	NT	NT	NT	NT	0/5	NT	NT	NT	NT

	Animal bioassay						RT-QuIC		
	Samples with heparin			Samples after heparin removed			Samples after heparin removed		
	log_{10} ID_{50}/g	log_{10} removal		log_{10} ID_{50}/g	log_{10} removal		log_{10} SD_{50}/g	log_{10} removal	
Sample	brain	Step	Total	brain	Step	Total	brain	Step	Total
BSE spike	8.0	NA	NA	6.9	NA	NA	9.0 ± 0.2	NA	NA
NaOH treatment	6.3	1.7	1.7	5.4	1.5	1.5	6.6 ± 0.3	2.4	2.4
DE filtration	≤5.2	≥1.1	≥2.8	≤4.0	≥1.4	≥2.9	5.3 ± 0.1	1.3	3.7
H_2O_2 bleaching	ND	NA	NA	≤3.4	≥0.6	≥3.5	5.0 ± 0.4	0.3	4.0
Final product	ND	NA	NA	≤2.6	≥0.8	≥4.3	5.0 ± 0.6	0.0	4.0

*Values are the number of animals with confirmed BSE divided by the number of animals inoculated. BSE, bovine spongiform encephalopathy; DE diatomaceous earth; H_2O_2, hydrogen peroxide; ID_{50}, 50% infectious dose; NA, not applicable; NaOH, sodium hydroxide; ND, not detectable; NT, not tested; RT-QuIC, real-time quaking-induced conversion; SD_{50}, 50% seeding dose; TSE, transmissible spongiform encephalopathies.

$\log_{10}$ of BSE infectivity. To increase sensitivity of the mouse bioassay, we removed heparin by centrifuging samples (20,000 × *g*, 1 hr, 4°C), washed the pellets, resuspended them in inoculation buffer, and inoculated mice as described. We tested brains of all mice for PrP^{TSE} as reported previously (*5*). We detected residual infectivity in all aliquots, including the final product. NaOH treatment removed 1.5 $\log_{10}$ of BSE infectivity. We estimated removals by other steps. DE filtration removed ≥1.4 $\log_{10}$ of BSE infectivity. The hydrogen peroxide bleaching and methanol precipitation (final product) steps each removed <1 $\log_{10}$ of infectivity, considered negligible. Thus, cumulatively, scaled-down heparin purification removed a total of ≥2.9 $\log_{10}$ of BSE infectivity; NaOH treatment and DE filtration were the only effective steps.

We also quantified residual PrP^{TSE} in each sample using the real-time quaking-induced conversion (RT-QuIC) assay with hamster–sheep chimeric prion protein (*9*) as substrate, expressing results as $\log_{10}$ 50% seeding doses (SD_{50}), as reported previously (*5*). We detected PrP^{TSE} in unspun BSE spike and NaOH-treated samples but only inconsistent signals in aliquots from successive steps (data not shown). To increase sensitivity and remove heparin interfering with RT-QuIC at low concentrations of PrP^{TSE}, we centrifuged all samples as we did previously. To quantify PrP^{TSE}, we resuspended pellets and serially diluted each sample in phosphate-buffered saline 0.05% sodium dodecyl sulfate, adding 2 µL of each dilution to seed RT-QuIC, each dilution into quadruplicate wells (see $\log_{10}$ SD_{50} values in Table). NaOH treatment removed 2.4 $\log_{10}$ of PrP^{TSE} and DE filtration steps removed 1.3 $\log_{10}$ of PrP^{TSE}. Hydrogen peroxide bleaching and methanol precipitation reduced PrP^{TSE} by only negligible amounts. Thus, processing from crude heparin to final pharmaceutical heparin cumulatively removed 3.7 $\log_{10}$ of spiked PrP^{TSE}.

We showed previously, using a rodent-adapted scrapie agent, that heparin processing removed 3.6 $\log_{10}$ of scrapie infectivity and 3.4 $\log_{10}$ of PrP^{TSE} (*5*). Here, we report studies with the more relevant BSE agent itself, showing similar reduction by 3.7 $\log_{10}$ of PrP^{TSE}. We could demonstrate only ≥2.9 $\log_{10}$ reduction in infectivity, because the starting titer of the BSE-infected brain homogenate was low. However, we detected both residual BSE infectivity and PrP^{TSE} seeding activity after final steps of processing, so our model process did not yield sterile heparin. We found NaOH treatment and DE filtration to be the most effective steps for removing both BSE infectivity and PrP^{TSE} seeding activity, consistent with previous results using scrapie agent.

Overall, our data suggest that typical heparin manufacturing is likely to remove substantial amounts of BSE agent. Furthermore, a probabilistic model assessing the vCJD risk for bovine heparin sourced from cattle in the United States and Canada estimated the risk to be very low (*10*). The demonstrated ability of a typical heparin purification process to remove substantial amounts of contaminating BSE agent, taken together with careful selection of low-risk bovine material to manufacture heparin, provides additional assurance of safety, supporting eventual reintroduction of bovine heparin to the US market.

Acknowledgments

We thank the staff in the Food and Drug Administration (FDA) Division of Veterinary Services for the outstanding care of animals. We owe special thanks to the staff in the laboratory of Byron Caughey at Rocky Mountain Laboratory, National Institute of Allergy and Infectious Diseases, National Institutes of Health, Hamilton, Montana, for giving us the recombinant constructs.

The FDA Animal Care and Use Committee approved all animal studies (ASP #2015-07). Intramural grants from the FDA supported the work.

About the Author

Dr. Bett is a chemist at the US Food and Drug Administration, Silver Spring, Maryland, USA. His research focuses on protecting biological products from contamination with TSE agents to advance public health.

References

1. Will RG, Ironside JW, Zeidler M, Estibeiro K, Cousens SN, Smith PG, et al. A new variant of Creutzfeldt-Jakob disease in the UK. Lancet. 1996;347:921–5. https://doi.org/10.1016/s0140-6736(96)91412-9
2. US Food and Drug Administration. FDA encourages reintroduction of bovine-sourced heparin [cited 2019 Dec 15]. https://www.fda.gov/Drugs/DevelopmentApprovalProcess/Manufacturing/ucm600976.htm
3. Keire D, Mulloy B, Chase C, Al-Hakim A, Cairatti D, Gray E, et al. Diversifying the global heparin supply chain: reintroduction of bovine heparin in the United States? Biopharm Int. 2015;28:36–42 [cited 2019 Dec 13]. http://www.pharmtech.com/diversifying-global-heparin-supply-chain-reintroduction-bovine-heparin-united-states
4. World Organization for Animal Health. BSE situation in the world and annual incidence rate (1989–31/12/2016) [cited 2019 Dec 18]. https://www.oie.int/en/animal-health-in-the-world/bse-situation-in-the-world-and-annual-incidence-rate
5. Bett C, Grgac K, Long D, Karfunkle M, Keire DA, Asher DM, et al. A heparin purification process removes spiked transmissible spongiform encephalopathy agent. AAPS J. 2017;19:765–71. https://doi.org/10.1208/s12248-017-0047-y
6. Castilla J, Gutiérrez Adán A, Brun A, Pintado B, Ramírez MA, Parra B, et al. Early detection of PrPres in BSE-infected

bovine PrP transgenic mice. Arch Virol. 2003;148:677–91. https://doi.org/10.1007/s00705-002-0958-4
7. Bett C, Piccardo P, Cervenak J, Torres J-M, Asher DM, Gregori L. Both murine host and inoculum modulate expression of experimental variant Creutzfeldt-Jakob disease. J Gen Virol. 2018;99:422–33. https://doi.org/10.1099/jgv.0.001017
8. Gray JG, Dudas S, Czub S. A study on the analytical sensitivity of 6 BSE tests used by the Canadian BSE reference laboratory. PloS One. 2011;6:e17633. https://doi.org/10.1371/journal.pone.0017633
9. Orrú CD, Groveman BR, Raymond LD, Hughson AG, Nonno R,Zou W, et al. Bank vole prion protein as an apparently universal substrate for RT-QuIC-based detection and discrimination of prion strains. PLoS Pathog. 2015;11:e1004983. https://doi.org/10.1371/journal.ppat.1004983
10. Huang Y, Forshee RA, Keire D, Lee S, Gregori L, Asher DM, et al. Assessment of risk of variant Creutzfeldt-Jakob disease (vCJD) from use of bovine heparin. Pharmacoepidemiol Drug Saf. 2020;29:575–81. https://doi.org/10.1002/pds.4982

Address for correspondence: Cyrus Bett, US Food and Drug Administration, 10903 New Hampshire Ave, Silver Spring, MD 20993, USA; email: cyrus.bett@fda.hhs.gov

Undetected Circulation of African Swine Fever in Wild Boar, Asia

Timothée Vergne, Claire Guinat, Dirk U. Pfeiffer

Author affiliations: National Veterinary School of Toulouse, Toulouse, France (T. Vergne, C. Guinat); Institut National de Recherche pour l'Agriculture, l'Alimentation et l'Environnement, Toulouse (T. Vergne, C. Guinat); City University of Hong Kong, Hong Kong, China (D.U. Pfeiffer)

DOI: https://doi.org/10.3201/eid2610.200608

African swine fever is a growing threat to the livestock industry. We examined data indicating that in most countries in Asia, most notified events were related to farm outbreaks; meanwhile, only a few wild boar cases were reported. We hypothesize the virus circulates unnoticed in wild boar populations in Asia.

African swine fever (ASF) is one of the greatest threats to the livestock industry worldwide. Since 2007, ASF virus (ASFV) has been reported in 34 countries in Europe and Asia (*1*). Some strains of ASF can be associated with case-fatality ratios of almost 100% and with economic damage caused by trade disruptions (*2*). The absence of a safe and effective vaccine and the evolving understanding of the epidemiologic role of wild boar have complicated efforts to control this disease (*3*).

Observations from the Russian Federation, Ukraine, and Romania have suggested that ASFV primarily circulates among small pig farms and spills over into commercial farms occasionally and into wild boar populations regularly (*4*). However, more recent reports from several countries in Europe, including the Baltic states and Belgium, suggest the virus might maintain itself within wild boar populations and occasionally spill over into domestic pig farms. This newly described epidemiologic cycle proposes direct transmission among wild boar and indirect intraspecific transmission through contaminated wild boar carcasses (*4*). This cycle also suggests the persistence of ASFV in wild boar populations even in the context of low wild boar density and despite high death rates caused by the disease (*5*).

In August 2018, ASFV was detected in China, the leading pig producer worldwide. Since then, the virus has also been reported in Mongolia, Vietnam, Cambodia, Hong Kong, North Korea, South Korea, Laos, Myanmar, the Philippines, Timor-Leste, Papua New Guinea, Indonesia, and India (*1*). The large-scale spread of ASFV demonstrates the challenges of controlling the disease in this region, which has a high density of domestic pigs, a high proportion of low biosecurity farms, a widespread practice of feeding pigs with food waste (*6*), and a complex pork trade network involving wet markets and slaughterhouses with poor hygiene (*2*).

Maps of predicted habitat suitability suggest that most areas of East and Southeast Asia are highly suitable for wild boar (*7*). Although information is limited about the spatial distribution of wild boar in Asia, studies suggest that in some regions of China, wild boar density could be similar (*8*) to that of eastern Poland, where ASFV has circulated in wild boar for ≥5 years (*9*). Reports of crop losses caused by wild boar in China (*10*) indicate that close interactions between wild boar and human activities occur in the region.

The widespread presence of ASFV in pigs in Asia implies regular environmental spillover from the pig supply chain. Therefore, it is highly likely that ASFV is already widely circulating within some wild boar populations in Asia, causing substantial wild boar death. Because life expectancy of ASFV-infected

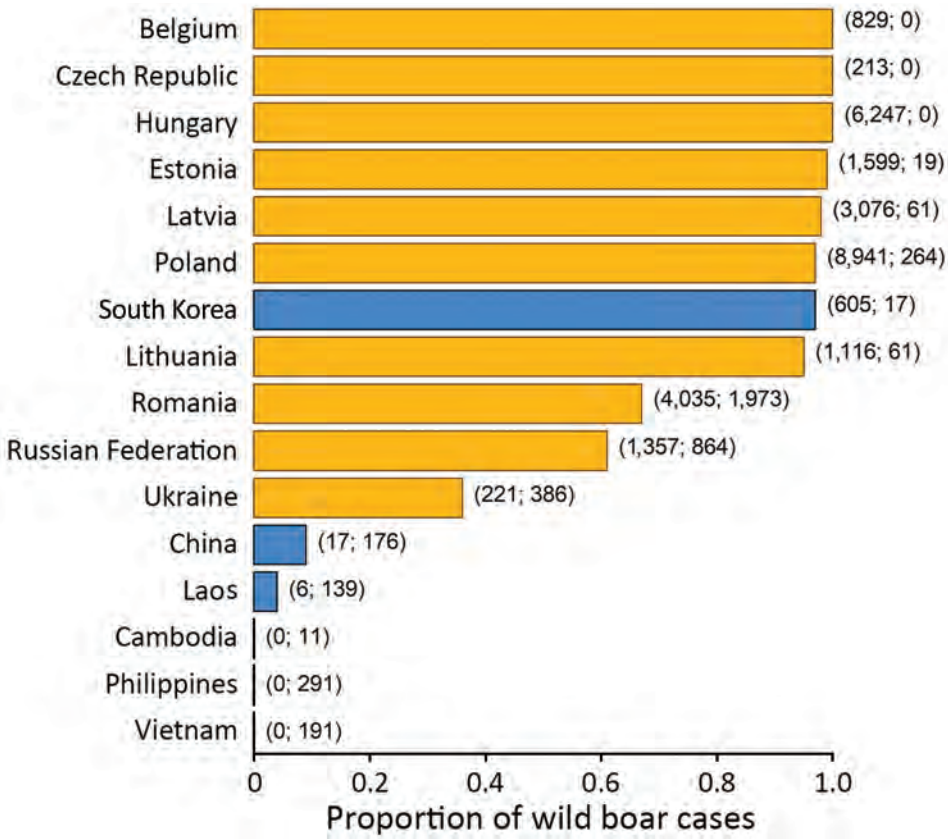

Figure. Proportion of wild boar cases out of the total number of reported African swine fever events in the most affected countries in Europe (orange) and Asia (blue). Numbers in parentheses at right side of bars indicate the reported number of wild boar cases and the reported number of outbreaks in farms, from the date of the first reported ASF event in these countries through May 8, 2020 (*1*).

animals is very short, the most effective way to conduct surveillance in boar populations is to monitor reports of infected boar carcasses. Numbers of reported ASFV wild boar cases and farm outbreaks vary by nation. Except for South Korea, which reported 605 infected wild boar carcasses and 17 outbreaks in domestic pig farms from the time of the emergence of the virus in Asia until May 8, 2020, countries in Asia reported a much lower ratio of wild boar cases to farm outbreaks than their counterparts in Europe (Figure) (*1*). In these countries (excluding South Korea), there were only 23 reports of infected wild boar carcasses (in China and Laos only) despite 843 official ASF notifications of farm outbreaks after the virus emerged in Asia in August 2018 (Figure) (*1*).

The near absence of notifications of ASFV-infected wild boar cases in Asia highlights shortcomings in surveillance for ASF in wildlife, jeopardizing the success of ASF control policies in the region. We believe this lack of surveillance partly results from government division of responsibilities; in most countries, responsibility for ASF surveillance in livestock belongs to a different government department than that for monitoring wildlife populations (*6*). We argue that long-term success of ASF control in Asia is possible only with risk-based ASF surveillance in wild boar populations by a multisectoral effort of wildlife and agricultural departments. Although surveillance of wild boar is a necessary component of an ASF control strategy, it must be complemented by effective ASF control measures in domestic pigs, such as improved regional coordination, increased resources for surveillance, incentives for farmers to report outbreaks, and enforcement of interventions (*2*). Without these measures, the region might become a major hub of ASFV infection.

About the Author

Dr. Vergne is an associate professor of veterinary public health at the National Veterinary School of Toulouse, Toulouse, France. His primary research interests include disease transmission and improving surveillance and intervention strategies for animal infectious diseases.

References

1. Food and Agriculture Organization of the United Nations. EMPRES Global Animal Disease Information System [cited 2020 May 8]. http://empres-i.fao.org/eipws3g
2. Dixon LK, Stahl K, Jori F, Vial L, Pfeiffer DU. African swine fever epidemiology and control. Annu Rev Anim Biosci. 2020;8:221–6. PubMed https://doi.org/10.1146/annurev-animal-021419-083741

3. Gavier-Widén D, Ståhl K, Dixon L. No hasty solutions for African swine fever. Science. 2020;367:622–4. https://doi.org/10.1126/science.aaz8590
4. Chenais E, Ståhl K, Guberti V, Depner K. Identification of wild boar–habitat epidemiologic cycle in African swine fever epizootic. Emerg Infect Dis. 2018;24:810–2. https://doi.org/10.3201/eid2404.172127
5. Abrahantes JC, Gogin A, Richardson J, Gervelmeyer A, et al.; European Food Safety Authority. Epidemiological analyses on African swine fever in the Baltic countries and Poland. EFSA Journal. 2017;15:e04732. https://doi.org/10.2903/j.efsa.2017.4732
6. Vergne T, Chen-Fu C, Li S, Cappelle J, Edwards J, Martin V, et al. Pig empire under infectious threat: risk of African swine fever introduction into the People's Republic of China. Vet Rec. 2017;181:117. https://doi.org/10.1136/vr.103950
7. Bosch J, Iglesias I, Muñoz MJ, de la Torre A. A cartographic tool for managing African swine fever in Eurasia: mapping wild boar distribution based on the quality of available habitats. Transbound Emerg Dis. 2017;64:1720–33. https://doi.org/10.1111/tbed.12559
8. Wu S, Chen H, Cai X. Preliminary study on the population structures and reproductive habit in wild boar (*Sus scrofa*) in Dawaling Natural Reserve. Acta Theriologica Sinica. 2000;20:151–6.
9. Śmietanka K, Woźniakowski G, Kozak E, Niemczuk K, Frączyk M, Bocian Ł, et al. African swine fever epidemic, Poland, 2014–2015. Emerg Infect Dis. 2016;22:1201–7. https://doi.org/10.3201/eid2207.151708
10. Liu Q, Yan K, Lu Y, Li M, Yan Y. Conflict between wild boars (*Sus scrofa*) and farmers: distribution, impacts, and suggestions for management of wild boars in the Three Gorges Reservoir Area. Journal of Mountain Science. 2019;16:2404–16. https://doi.org/10.1007/s11629-019-5453-4

Address for correspondence: Timothée Vergne, UMR ENVT-INRAE 1225, National Veterinary School of Toulouse, 23 chemin des Capelles, 31300 Toulouse, France; email: timothee.vergne@envt.fr

Review of Mental Health Response to COVID-19, China

Adriana Miu, Hui Cao, Bohan Zhang,[1] Huaiyu Zhang

Author affiliations: University of Texas Southwestern Medical Center, Dallas, Texas, USA (A. Miu); Beijing Institute of Education, Beijing, China (H. Cao); Lesley University, Cambridge, Massachusetts, USA (B. Zhang); University of California San Francisco, San Francisco, California, USA (H. Zhang)

DOI: https://doi.org/10.3201/eid2610.201113

[1]Current affiliation: Private practice, Nanjing, China.

Public mental health response to coronavirus disease is essential. After reviewing systemic and local efforts in China, we found efficient coordination and human resources. We recommend better symptom assessment, monitoring of organizations, and basic needs protection. This recommendation can inform how other countries can overcome mental health challenges during this pandemic.

The coronavirus disease (COVID-19) outbreak and quarantines have caused major distress in China (*1*,*2*). Therefore, effective public mental health response to COVID-19 is needed (*3*). We review systemic and local mental health efforts in China based on psychiatric emergency guidelines from the Inter-Agency Standing Committee (*4*). These guidelines are coordination between multiple sectors; human resources; assessment, monitoring, and evaluation; and protection and human rights standards. Our discussion will inform mental health response for the COVID-19 pandemic.

Mental health efforts in China have been coordinated and facilitated through multiple systems, including government, academic societies, universities, hospitals, and nonprofit organizations (*5*). Services include a countrywide 24/7 hotline, text support through apps, psychoeducation materials, and webinars (*5*). The government prioritized psychosocial support for COVID-19, as shown by the National Health Commission mandate requiring all mental health associations to provide psychosocial support, establish professional focus groups, and aid the provincial and city health departments (*6*).

Academic organizations in psychology (Chinese Psychological Society [CPS]) (Table) and psychiatry (Chinese Society of Psychiatry) provide evidence-based guidelines on psychosocial support and training (*5*,*7*). The Ministry of Education (MoE) has mandated all college counselors across the nation to volunteer for the primary Huazhong University hotline at the epicenter in Wuhan (*8*). At the systemic level, there is good coordination and resource allocation. The government agencies coordinate human resources, and academic associations provide professional knowledge and guidelines for frontline effort.

Coordination and resource allocation were compiled from local efforts at the Wuhan epicenter (Appendix, https://wwwnc.cdc.gov/EID/article/26/10/20-1113-App1.pdf). On January 23, 2020, immediately after the quarantine, Zhongnan Hospital and the Hubei Psychological Consultant Association began offering hotline services. As of April 30, more than 2,000 persons had been served. Beyond the hotline, Wuhan University and Huazhong

Table. Case-patients with coronavirus disease in China and respective response from the Chinese Psychological Society

Date	Coronavirus disease	Chinese Psychological Society response
2019 Dec 9	First suspected case	None
2019 Dec 31	Cluster of pneumonia cases in Wuhan	None
2020 Jan 20	Cases in China, Thailand, Japan, and South Korea	None
2020 Jan 21	Cases reported in other provinces	None
2020 Jan 23	Lockdown of Wuhan	None
2020 Jan 25	Cases in all of China except Tibet	None
2020 Jan 26	No event	Published self-help article on emotional support
2020 Jan 27	Lockdown of all cities in Hubei	None
2020 Jan 28	No event	Conducted first round of training for supervisors
2020 Jan 29	No event	Published list of psychologist consultants
2020 Jan 30	World Health Organization declared public health emergency of international concern	None
2020 Jan 31	No event	Published handbook for hotline organizations and volunteers
2020 Feb 2	No event	Published list of organizations for hotline and counseling
2020 Feb 3	No event	Updated guidelines for hotline organization
2020 Feb 5	Foreign airlines cancelled flights to China	None
2020 Feb 6	No event	Published ethics guidelines
2020 Feb 7	Death of whistleblower doctor	None
2020 Feb 7	No event	Published webinars for general public
2020 Feb 9	No event	Published handbook on self-care for volunteers
2020 Feb 10	No event	Conducted second round of training for supervisors
2020 Feb 13	No event	Published hotline support questions and answers
2020 Mar 3	No event	Updated handbook for hotline organizations and volunteers
2020 Mar 3	No event	Published list of 52 recommended hotline organizations
2020 Mar 8	No event	Conducted 7-day self-help psychosocial support for healthcare workers

University provide online text support through apps staffed by >3,000 professionals across China. This support demonstrates how hospitals, professional associations, and universities have collectively provided immediate resources. Furthermore, resources have been mobilized from other regions to support the epicenter. The hotline of Huazhong University became the primary hotline for Hubei residents and was staffed by college counselors throughout China under the mandate of the MoE (*8*). Psychologists and nurses from other provinces were dispatched to Wuhan Third Hospital on January 28. Psychosocial efforts might be sourced by different organizations, but they illustrate pooling of resources and coordination from other regions to ensure access to psychosocial support at the epicenter.

The MoE and CPS recruited professionals and volunteers across China, which suggests adequate resource allocation (*5*,*7*,*8*). CPS trained 1,448 registered psychologists in train-the-trainer workshops (*8*); these psychologists in turn supervised and provided live consultations to frontline volunteers (*7*). China has also implemented Artificial Intelligence Tree Holes Rescue to reduce suicidal risk. These programs demonstrate efficient task-sharing, by pooling professionals together, supervising less-trained staff, and using technology to overcome resource shortages.

The Inter-Agency Standing Committee calls for assessment of mental well-being and program evaluation of psychsocial support effectiveness (*4*). Guidelines of the National Health Commission document the need for assessment and program evaluation, but enforcement was unclear beyond the guidelines (*6*). Although there were nationwide surveys of psychological well-being (*9*,*10*), they did not describe use of surveys in psychological services. Clinical assessment, such as previous mental illness history or stressors (e.g., grief, financial stress), should be routinely integrated into services.

CPS published a list of approved hotline organizations based on survey evaluation of organizations (*8*). However, this survey was not conducted until 3 weeks after the outbreak. At the outset of a psychiatric emergency, a team of professionals should evaluate and monitor whether individual organizations meet national guidelines. A negative experience from an unregulated organization can deter persons from seeking help.

Although COVID-19 does not cause intentional harm, there are human rights issues on access to basic needs (*4*). During the sudden lockdown of Wuhan, access to food and medical needs was threatened because of food hoarding, price gouging, and transportation freeze. In response, the government coordinated supply with tons of vegetables and meat. These threats were documented by nationwide surveys of well-being of persons. Professionals can further use these documentations to advocate for victims. For example, professionals can educate policymakers about the need for transparency, such

as informing the public about food shortage while reassuring the public that supply will arrive in a few days. China has provided free, country-wide psychosocial support, funded by the government and institutions (*5*–*7*). The accessibility is remarkable compared with that in other countries that depend on health insurance benefits.

Our review suggests that China has overcome resource shortages with coordination and resource allocation in its mental health response. The government, universities, and academic societies provide coordination, and independent organizations provide local support. We recommend integration of assessment in direct support, monitoring of organizations, and advocating for affected persons. These recommendations can inform how other countries can overcome shortage of mental health resources when facing this pandemic.

About the Author

Dr. Miu is an assistant professor and a licensed clinical psychologist in the Department of Psychiatry at the University of Texas, Southwestern Medical Center, Dallas, TX. Her research interests include social–cognitive factors, such as growth mindset and hostile attribution bias.

References

1. Brooks SK, Webster RK, Smith LE, Woodland L, Wessely S, Greenberg N, et al. The psychological impact of quarantine and how to reduce it: rapid review of the evidence. Lancet. 2020;395:912–20. https://doi.org/10.1016/S0140-6736(20)30460-8
2. Gao J, Zheng P, Jia Y, Chen H, Mao Y, Chen S, et al. Mental health problems and social media exposure during COVID-19 outbreak. PLoS One. 2020;15:e0231924. https://doi.org/10.1371/journal.pone.0231924
3. Dong L, Bouey J. Public mental health crisis during COVID-19 pandemic, China. Emerg Infect Dis. 2020;26:1616–8. https://doi.org/10.3201/eid2607.202407
4. Inter-Agency Standing Committee. IASC guidelines on mental health and psychosocial support in emergency settings. Geneva: The Committee; 2007.
5. Li W, Yang Y, Liu ZH, Zhao YJ, Zhang Q, Zhang L, et al. Progression of mental health services during the COVID-19 outbreak in China. Int J Biol Sci. 2020;16:1732–8. https://doi.org/10.7150/ijbs.45120
6. National Health Commission of China. Principles of the emergency psychological crisis interventions for the new coronavirus pneumonia, January 26, 2020 [in Chinese] [cited 2020 Mar 7]. http://www.nhc.gov.cn/jkj/s3577/202001/6adc08b966594253b2b791be5c3b9467
7. Chinese Psychological Society. Preventing disease fighting disease, 2020 [in Chinese] [cited 2020 Apr 28]. http://www.cpsbeijing.org/cms/show.action?code= publish_ff8080817000ff3001706647285d02f0&siteid=100000&channelid=0000000188
8. Ministry of Education. MoE requests psychological support be provided to relieve novel coronavirus-related stress, January 28, 2020 [in Chinese] [cited 2020 Apr 28]. http://www.moe.gov.cn/jyb_xwfb/gzdt_gzdt/s5987/202001/t20200128_416721.html
9. Qiu J, Shen B, Zhao M, Wang Z, Xie B, Xu Y. A nationwide survey of psychological distress among Chinese people in the COVID-19 epidemic: implications and policy recommendations. Gen Psychiatr. 2020;33:e100213. https://doi.org/10.1136/gpsych-2020-100213
10. Gao J, Zheng P, Jia Y, Chen H, Mao Y, Chen S, et al. Mental health problems and social media exposure during COVID-19 outbreak. PLoS One. 2020;15:e0231924. https://doi.org/10.1371/journal.pone.0231924

Address for correspondence: Adriana Miu, Department of Psychiatry, University of Texas Southwestern Medical Center, 6363 Forest Park Rd, Dallas, TX 75235, USA; email: adriana.miu@utsouthwestern.edu

Antibody Responses to SARS-CoV-2 at 8 Weeks Postinfection in Asymptomatic Patients

Pyoeng Gyun Choe,[1] Chang Kyung Kang,[1] Hyeon Jeong Suh, Jongtak Jung, EunKyo Kang, Sun Young Lee, Kyoung-Ho Song, Hong Bin Kim, Nam Joong Kim, Wan Beom Park, Eu Suk Kim, and Myoung-don Oh

Author affiliations: Seoul National University Hospital, Seoul, South Korea (P.G. Choe, C.K. Kang, H.J. Suh, E.K. Kang, S.Y. Lee, N.J. Kim, W.B. Park, M.-D. Oh); Seoul National University Bundang Hospital, Seongnam, South Korea (J. Jung, K.-H. Song, H.B. Kim, E.S. Kim)

DOI: https://doi.org/10.3201/eid2610.202211

We compared levels of severe acute respiratory syndrome coronavirus 2 neutralizing antibodies in recovery plasma from 7 completely asymptomatic coronavirus disease patients with those in symptomatic patients in South Korea. We found that serologic diagnostic testing was positive for 71% (5/7) of completely asymptomatic patients, but neutralizing antibody response occurred in all 7 patients.

[1]These first authors equally contributed to this article.

Severe acute respiratory syndrome coronavirus 2 (SARS-CoV-2), a new strain of betacoronavirus that causes coronavirus disease (COVID-19), quickly spread worldwide; the World Health Organization declared COVID-19 a pandemic on March 11, 2020 (*1*). Recent studies showed that a substantial number of asymptomatic COVID-19 patients contributed to the rapid dissemination of SARS-CoV-2 (*2*). In hospitalized COVID-19 patients, neutralizing antibody production was shown to increase after the first week of symptom onset, which correlated with disease severity (*3*,*4*). However, the neutralizing antibody response in asymptomatic patients is unclear.

In this study, we analyzed the completely asymptomatic COVID-19 patients who were isolated in a community treatment center (CTC) operated by Seoul National University (SNU) Hospital in response to a huge COVID-19 outbreak in Deagu, South Korea. During the CTC stay, physicians and nurses comprehensively evaluated the patients using a video consultation system twice daily (*5*–*7*). The completely asymptomatic patients were defined as those with body temperature <37.5°C and no symptoms (e.g., subjective fever, myalgia, rhinorrhea, sore throat, cough, sputum, chest discomfort) during the entire CTC stay. A total of 15 completely asymptomatic patients were confirmed among 113 patients with SARS-CoV-2 infection in the CTC (*8*). We also evaluated COVID-19 patients with pneumonia who were admitted to the Biocontainment Unit in SNU Hospital and SNU Bundang Hospital (Seongnam, South Korea). We classified pneumonia cases as subtle pneumonia (infiltrations were observed only in the computed tomography images) or apparent pneumonia (infiltrations were observed in chest radiograph) with mild or severe manifestation; case-patients with severe pneumonia required oxygen therapy.

We semiquantitatively measured SARS-CoV-2 IgG using a commercial ELISA kit (Euroimmun, https://www.euroimmun.com) according to the manufacturer's instructions. Optical density ratio (sample/calibrator) was interpreted as positive (≥1.1), borderline (≥0.8 to <1.1), or negative (<0.8) according to the manufacturer's recommendation. We performed neutralization assays as previously described (*9*), using the BetaCoV/Korea/SNU01/2020 virus (*10*) and 2-fold serially diluted plasma samples (2-fold to 4,096-fold). We recorded the highest dilution of plasma that showed inhibition activity of SARS-CoV-2 as the neutralizing antibody titer. We performed the assay in duplicate with negative control samples from healthy volunteers and patients 7–12 months after recovery from laboratory-confirmed Middle East respiratory syndrome coronavirus infection. The Institutional Review Boards of Seoul National University Hospital approved the study (IRB no. H-2004-158-1118).

Seven completely asymptomatic COVID-19 patients from the CTC and 17 patients with COVID-19 pneumonia from SNU-affiliated hospitals participated in this study (Appendix Table, https://wwwnc.cdc.gov/EID/article/26/10/20-2211-App1.pdf). Of the completely asymptomatic patients, ELISA showed positive results in 5 (71%) patients, borderline result in 1 (14%) patient, and negative result in 1 (14%) patient. ELISA showed higher optical density value in patients with pneumonia; titers correlated with disease severity (Figure). All patients showed neutralizing antibody response. We calculated the geometric mean titer of neutralizing antibody in all asymptomatic patients and in 4 of each type of pneumonia patient (subtle, mild, or severe); geometric mean titer was 78 in asymptomatic patients (n = 7), 256 in patients with subtle pneumonia (n = 4), and 3,158 in patients with apparent pneumonia (n = 8; 4 mild and 4 severe cases).

Neutralizing antibodies play an essential role in virus clearance and have been considered a critical immune player for protection against viral diseases. Knowledge of the neutralizing antibody response in asymptomatic patients is critical for diagnosing the disease, understanding pathogenesis, and interpreting seroepidemiologic data to define prevalence and risk factors for infection. Production of neutralizing antibodies in asymptomatic COVID-19 patients was reported recently. Wu et al. reported that ≈30% of recovered mild COVID-19 patients generated a deficient level of neutralizing antibody titers; in 10 of the 175 patients, the level was below the limit of detection (F. Wu et al., unpub. data, https://doi.org/10.1101/2020.03.30.20047365). The difference in results from our study compared with the previous study might be caused by differences in the timing of the test. In the previous study, antibody tests were performed 2–3 weeks after symptom onset, whereas we tested 2 months after symptom onset or laboratory diagnosis. Seroconversion in asymptomatic patients might take longer.

In our study, the neutralizing antibody titer correlated with the severity of the disease. This result suggests that patients with more severe disease might be more protected against reinfection and those with asymptomatic or mild disease could be more vulnerable to waning immunity over time because the initial immune response was not as strong as in patients with more severe disease.

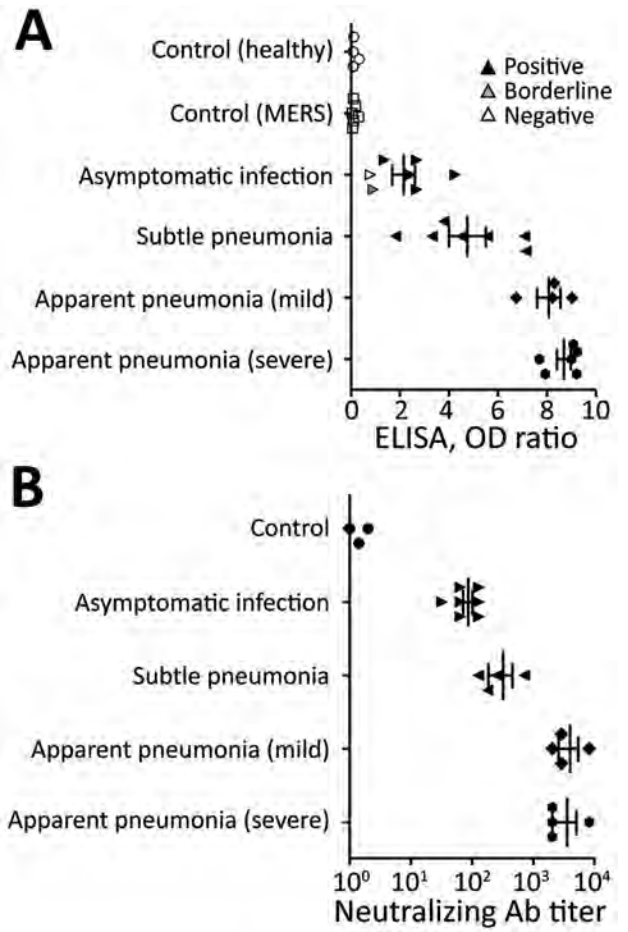

Figure. Antibody response against severe acute respiratory syndrome coronavirus 2 at 8 weeks postinfection among patients and controls in South Korea. A) Serologic diagnostic test (ELISA) results. OD ratio indicates the ratio of the extinction of the patient sample over the extinction of the calibrator. B) Neutralization assay results. For each patient type, an outlined symbol indicates a negative test result, gray symbol a borderline result, and black symbol a positive result, as tested according to manufacturer recommendation. Bars represent mean values and SE. From each patient group other than the completely asymptomatic group, 3–4 patients were randomly selected for neutralization assay. The controls included 1 healthy volunteer and 2 patients with MERS. Ab, antibody; MERS, Middle East respiratory syndrome; OD, optical density.

The ELISA results showed good agreement with the neutralizing antibody results. Negative ELISA results in some asymptomatic patients may be a limitation of the ELISA or may be attributed to patients with cross-neutralizing antibodies in their serum. Despite the limitation of our small sample size, our findings suggest that seroepidemiologic studies may detect mild COVID-19 infection in completely asymptomatic patients by the presence of neutralizing antibodies at 8 weeks postinfection.

Acknowledgments

We thank Kyung Sook Ahn for the administrative support, and Areum Jo and Su Jin Choi for the technical support.

This study was supported by the research fund of Seoul National University Hospital (grant no. 04-2020-0030).

About the Author

Dr. Choe is a clinical scientist at Seoul National University Hospital. His research interests focus on preventing healthcare-associated infection and responding to emerging infectious diseases.

References

1. World Health Organization. WHO Director-General's opening remarks at the media briefing on COVID-19, 11 March 2020. 2020 [cited 2020 Mar 12]. https://www.who.int/dg/speeches/detail/who-director-general-s-opening-remarks-at-the-media-briefing-on-covid-19---11-march-2020
2. Kimball A, Hatfield KM, Arons M, James A, Taylor J, Spicer K, et al.; Public Health – Seattle & King County; CDC COVID-19 Investigation Team. Asymptomatic and presymptomatic SARS-CoV-2 infections in residents of a long-term care skilled nursing facility—King County, Washington, March 2020. MMWR Morb Mortal Wkly Rep. 2020;69:377–81. https://doi.org/10.15585/mmwr.mm6913e1
3. Perera RA, Mok CK, Tsang OT, Lv H, Ko RL, Wu NC, et al. Serological assays for severe acute respiratory syndrome coronavirus 2 (SARS-CoV-2), March 2020. Euro Surveill. 2020; 25. https://doi.org/10.2807/1560-7917.ES.2020.25.16.2000421
4. Long QX, Liu BZ, Deng HJ, Wu GC, Deng K, Chen YK, et al. Antibody responses to SARS-CoV-2 in patients with COVID-19. Nat Med. 2020. https://doi.org/10.1038/s41591-020-0897-1
5. Kang E, Lee SY, Jung H, Kim MS, Cho B, Kim YS. Operating protocols of a community treatment center for isolation of patients with coronavirus disease, South Korea. Emerg Infect Dis. 2020 Jun 22 [Epub ahead of print]. https://doi.org/10.3201/eid2610.201460
6. Choi WS, Kim HS, Kim B, Nam S, Sohn JW. Community treatment centers for isolation of asymptomatic and mildly symptomatic patients with coronavirus disease, South Korea. Emerg Infect Dis. 2020 Jun 22 [Epub ahead of print]. https://doi.org/10.3201/eid2610.201539
7. Lee Y-H, Hong CM, Kim DH, Lee TH, Lee J. Clinical course of asymptomatic and mildly symptomatic patients with coronavirus disease admitted to community treatment centers, South Korea. Emerg Infect Dis. 2020 Jun 22 [Epub ahead of print]. https://doi.org/10.3201/eid2610.201620
8. Choe PG, Kang E, Lee SY, Oh B, Im D, Lee HY, et al. Selecting coronavirus disease 19 patients with negligible risk of progression; early experience from non-hospital isolation facility in Korea. Korean J Intern Med. 2020 [Epub ahead of print]. https://doi.org/10.3904/kjim.2020.159
9. Shen C, Wang Z, Zhao F, Yang Y, Li J, Yuan J, et al. Treatment of 5 critically ill patients with COVID-19 with convalescent plasma. JAMA. 2020;323:1582–9. https://doi.org/10.1001/jama.2020.4783
10. Park WB, Kwon NJ, Choi SJ, Kang CK, Choe PG, Kim JY, et al. Virus isolation from the first patient with SARS-CoV-2 in Korea. J Korean Med Sci. 2020;35:e84. https://doi.org/10.3346/jkms.2020.35.e84

Address for correspondence: Wan Beom Park, Department of Internal Medicine, Seoul National University Hospital, 101 Daehak-ro, Jongno-gu, Seoul, 03080, South Korea; email: wbpark1@snu.ac.kr; Eu Suk Kim, Department of Internal Medicine, Seoul National University Bundang Hospital, 82, Gumi-ro 173 Beom-gil, Bundang-gu, Seongnam-si, Gyeonggi-do, 13620, South Korea; email: eskim@snubh.org

Retrospective Screening for SARS-CoV-2 RNA in California, USA, Late 2019

Catherine A. Hogan, Natasha Garamani, Malaya K. Sahoo, ChunHong Huang, James Zehnder, Benjamin A. Pinsky

Author affiliations: Stanford University School of Medicine, Stanford, California, USA (C.A. Hogan, N. Garamani, M.K. Sahoo, C. Huang, J. Zehnder, B.A. Pinsky); Stanford Health Care, Palo Alto, California, USA (C.A. Hogan, B.A. Pinsky)

DOI: https://doi.org/10.3201/eid2610.202296

To investigate the possibility of earlier cases of severe acute respiratory syndrome coronavirus 2 infection than previously recognized, we retrospectively tested pooled samples from 1,700 persons with respiratory signs/symptoms seen at Stanford Health Care, Palo Alto, California, USA, during the last 2 months of 2019. We found no evidence of earlier infection.

Phylogenetic analyses of severe acute respiratory syndrome coronavirus 2 (SARS-CoV-2) suggest virus emergence weeks, if not months, before the World Health Organization was notified of the original cluster of cases in Wuhan, China (*1*). These analyses have estimated that SARS-CoV-2 emerged from October 6, 2019, through December 11, 2019 (*2*). Given this timeline, interest in retrospectively identifying patient zero in different geographic areas has been growing, to better determine the spread of SARS-CoV-2 and to inform current and future surveillance strategies for emerging infectious diseases.

Given the high volume of international travel before implementation of travel restrictions, travel-associated coronavirus disease (COVID-19) cases may have occurred in the United States earlier than previously recognized (*3*). However, monitoring for early community transmission of SARS-CoV-2 in the United States was challenging because the clinical manifestations of COVID-19 are similar to those of other respiratory virus infections, and emergence of COVID-19 overlapped with the annual respiratory virus season. In addition, local COVID-19 case finding and contact tracing efforts were limited by strict indications for testing based on specific risk factors, coupled with limited testing capacity (*4*,*5*).

A case of COVID-19 in the San Francisco Bay area, California, was confirmed by autopsy on February 6, 2020. To determine whether the virus had been spreading earlier than previously recognized in northern California, we extended our recently reported pooled screening strategy (*4*) to a retrospective study that included the last 2 months of 2019.

Our study evaluated all nasopharyngeal swab samples collected October 31, 2019–December 31, 2019, at Stanford Health Care (Palo Alto, California, USA) for which sufficient residual sample volume was available. These samples were collected from inpatients and outpatients who had had negative routine respiratory virus test results (Respiratory Pathogen Panel; GenMark Diagnostics, https://www.genmarkdx.com, or Xpert Xpress Flu RSV; Cepheid, https://www.cepheid.com) and had not been tested for SARS-CoV-2. Pool size was determined after literature review, accounting for an expected prevalence of <1% (*6*,*7*). Pools were created by combining 10 nasopharyngeal samples, and screening was performed by real-time reverse transcription PCR targeting the nucleocapsid gene (region N2) (*8*). We extracted demographic characteristics for a randomly selected subset of 100 persons. Trends of routine respiratory virus positivity were examined for the same period covered by the retrospective SARS-CoV-2 testing. This study was approved by the Stanford institutional review board, and individual patient consent was waived.

We tested 1,700 individual nasopharyngeal specimens (170 pools) for SARS-CoV-2. Of these, 841 samples had previously tested negative by the Respiratory Pathogen Panel and 859 by the Xpert Xpress Flu RSV. From the subset of persons for whom demographic data had been analyzed, most (67%) were adults. Most (64%) persons had consulted the emergency department for testing, followed by an outpatient clinic (23%) or an inpatient ward (13%). No SARS-CoV-2–positive pools were identified. The study period corresponded to the onset of the 2019–2020 respiratory virus season, during which the number of cases of influenza A, influenza B, and respiratory syncytial virus increased and the frequency

of other seasonal viruses varied (Appendix Figure, https://wwwnc.cdc.gov/EID/article/26/10/20-2296-App1.pdf) according to testing of separate samples collected during the same period as the study.

Pooled testing of 1,700 nasopharyngeal samples collected from persons in Palo Alto, California, who had respiratory signs/symptoms during the last 2 months of 2019 detected no case of COVID-19. This study and previous studies indicate that in the San Francisco Bay area, symptomatic persons without risk factors and with SARS-CoV-2 infection began seeking medical attention at the end of February 2020 (*9*,*10*).

Our study is limited by sampling from a single institution, corresponding to a population that may not be representative of the underlying area as a whole. Further retrospective SARS-CoV-2 reverse transcription PCR screening using specimens collected at other institutions throughout the United States will be needed to fully determine early community transmission. Our research will complement phylogenetic viral sequence analysis and large-scale seroprevalence studies to characterize the regional and national emergence of SARS-CoV-2. It is possible that use of pooled testing led to lower sensitivity; however, pool sizes of 10 samples maintain high performance compared with individual samples. Given that we included only samples negative for conventional respiratory viruses, we cannot exclude the possibility that we missed cases of SARS-CoV-2 co-infection with another respiratory virus.

Our pooled screening strategy for investigating local community transmission of SARS-CoV-2 in the San Francisco Bay area of California during late 2019 during the onset of the respiratory virus season identified no COVID-19 cases. This finding is consistent with limited transmission in this population at this time.

About the Author

Dr. Hogan is an infectious diseases physician, medical microbiologist, and currently a visiting instructor and global health diagnostics fellow at the Stanford Department of Pathology. Her research interests include novel and point-of-care diagnostic methods, clinical impact of diagnostic methods, and tropical medicine.

References

1. Zhu N, Zhang D, Wang W, Li X, Yang B, Song J, et al.; China Novel Coronavirus Investigating and Research Team. A novel coronavirus from patients with pneumonia in China, 2019. N Engl J Med. 2020;382:727–33. https://doi.org/10.1056/NEJMoa2001017
2. van Dorp L, Acman M, Richard D, Shaw LP, Ford CE, Ormond L, et al. Emergence of genomic diversity and recurrent mutations in SARS-CoV-2. Infect Genet Evol. 2020 May 5 [Epub ahead of print]. https://doi.org/10.1016/j.meegid.2020.104351
3. Kelly J, Thomas P. Disaster in motion: where flights from coronavirus-ravaged countries landed in US [cited 2020 May 13]. https://abcnews.go.com/Health/disaster-motion-flights-coronavirus-ravaged-countries-landed-us/story?id=70025470
4. Centers for Disease Control and Prevention (CDC). Overview of testing for SARS-CoV-2 [cited 2020 May 13]. https://www.cdc.gov/coronavirus/2019-ncov/hcp/clinical-criteria.html
5. Sharfstein JM, Becker SJ, Mello MM. Diagnostic testing for the novel coronavirus. JAMA. 2020 Mar 9 [Epub ahead of print]. https://doi.org/10.1001/jama.2020.3864
6. Aragón-Caqueo D, Fernández-Salinas J, Laroze D. Optimization of group size in pool testing strategy for SARS-CoV-2: a simple mathematical model. J Med Virol. 2020 Apr 24 [Epub ahead of print]. https://doi.org/10.1002/jmv.25929
7. Lohse S, Pfuhl T, Berkó-Göttel B, Rissland J, Geißler T, Gärtner B, et al. Pooling of samples for testing for SARS-CoV-2 in asymptomatic people. Lancet Infect Dis. 2020 Apr 28 [Epub ahead of print]. https://doi.org/10.1016/S1473-3099(20)30362-5
8. Bulterys PL, Garamani N, Stevens B, Sahoo MK, Huang C, Hogan CA, et al. Comparison of a laboratory-developed test targeting the envelope gene with three nucleic acid amplification tests for detection of SARS-CoV-2. J Clin Virol. 2020 May 8 [Epub ahead of print]. https://doi.org/10.1016/j.jcv.2020.104427
9. Hogan CA, Sahoo MK, Pinsky BA. Sample pooling as a strategy to detect community transmission of SARS-CoV-2. JAMA. 2020;323:1967. https://doi.org/10.1001/jama.2020.5445
10. Zwald ML, Lin W, Sondermeyer Cooksey GL, Weiss C, Suarez A, Fischer M, et al. Rapid sentinel surveillance for COVID-19–Santa Clara County, California, March 2020. MMWR Morb Mortal Wkly Rep. 2020;69:419–21. https://doi.org/10.15585/mmwr.mm6914e3

Address for correspondence: Benjamin A. Pinsky, Stanford Health Care Clinical Virology Laboratory, 3375 Hillview Ave, Rm 2913, Palo Alto, CA 94304, USA; email: bpinsky@stanford.edu

Using Virus Sequencing to Determine Source of SARS-CoV-2 Transmission for Healthcare Worker

Nasia Safdar, Gage K. Moreno, Katarina M. Braun, Thomas C. Friedrich, David H. O'Connor

Author affiliations: University of Wisconsin School of Medicine and Public Health, Madison, Wisconsin, USA (N. Safdar); William S. Middleton Memorial Veterans Hospital, Madison (N. Safdar); University of Wisconsin–Madison, Madison (G.K. Moreno, K.M. Braun, T.C. Friedrich, D.H. O'Connor)

DOI: https://doi.org/10.3201/eid2610.202322

Whether a healthcare worker's severe acute respiratory syndrome coronavirus 2 (SARS-CoV-2) infection is community or hospital acquired affects prevention practices. We used virus sequencing to determine that infection of a healthcare worker who cared for 2 SARS-CoV-2–infected patients was probably community acquired. Appropriate personal protective equipment may have protected against hospital-acquired infection.

Healthcare workers (HCWs) are at the front lines of the coronavirus disease (COVID-19) pandemic; their interactions with patients and in the community put them at risk for infection with severe acute respiratory syndrome coronavirus 2 (SARS-CoV-2) (*1*,*2*). Concern about whether HCWs are adequately protected from exposure while caring for patients has been fueled by limited availability of recommended personal protective equipment (PPE), in particular N95 respirators. Determining an HCW's source of SARS-CoV-2 infection—community versus healthcare system—is crucial for evaluating the effectiveness of hospital infection control and PPE practices. Although SARS-CoV-2 infections in HCWs are often presumed to be acquired during the course of patient care, few reports unambiguously identify the source of acquisition. Forensic genomics, using viral sequencing, may be a promising approach.

We report a case of SARS-CoV-2 infection of an HCW at the University of Wisconsin–Madison (Madison, WI, USA) who performed direct care for 2 non–critically ill patients with confirmed SARS-CoV-2 infections (patients 1 and 2). The University of Wisconsin–Madison Institutional Board deemed this study to be quality improvement rather than research and therefore exempt from review.

At the time of this investigation, community prevalence of SARS-CoV-2 in Dane County, Wisconsin, was relatively low (cumulative prevalence ≈0.06% as of April 17, 2020). During this time, precautions in place included universal masking for HCWs, universal face covering for hospital visitors, and masking of symptomatic patients when entering the healthcare system. Hospitalwide hand hygiene compliance rates were 93%–96%.

While caring for patients 1 and 2, the HCW in this study wore a barrier facemask made to ASTM International (https://www.astm.org) standards, a face shield, reusable gowns, and nonsterile gloves. Four days after providing care for these patients, the HCW began experiencing headache, fever, and sore throat. A nasopharyngeal swab sample was positive for SARS-CoV-2 viral RNA. To establish the possible source of infection, we interviewed the HCW's family member, who had experienced a febrile illness 8 days before the HCW's onset of symptoms but was not tested initially because of limited testing availability. A nasopharyngeal swab sample from the family member was also positive for SARS-CoV-2 (Figure 1).

We sequenced viral RNA isolated from nasopharyngeal swab samples from patients 1 and 2, the HCW, and the family member. To determine whether the HCW most likely acquired infection in the healthcare setting or in the community, we compared consensus SARS-CoV-2 sequences from these 4 persons.

All 4 samples were prepared for sequencing by using the ARTIC protocol (https://artic.network/ncov-2019/ncov2019-bioinformatics-sop.html) and were sequenced on an Oxford Nanopore GridION device (Nanopore Technologies, https://nanoporetech.com/products/gridion). Consensus sequences were derived by using a modified version of the ARTIC bioinformatics protocol (https://www.protocols.io/view/ncov-2019-sequencing-protocol-bbmuik6w), which analyzes data after 100,000 reads have been obtained from each sample (analysis pipelines are available at GitHub, https://github.com/katarinabraun/SARS-CoV-2_sequencing/tree/master/Pipelines_to_process_data/Nanopore_pipeline_ARTIC).

The sequence from the HCW was identical to that of the HCW's family member but distinct from that of patients 1 and 2 (Figure 2). Although we cannot with absolute certainty exclude the possibility that the HCW was infected by another asymptomatic, untested hospitalized patient, the identical virus sequences from the HCW and the HCW's family member provide strong circumstantial evidence for a chain of virus transmission outside of the hospital.

Within 2 days of the positive SARS-CoV-2 test result for the HCW, sequencing of the virus identified the probable source of infection as community transmission. This finding offers reassurance to HCWs

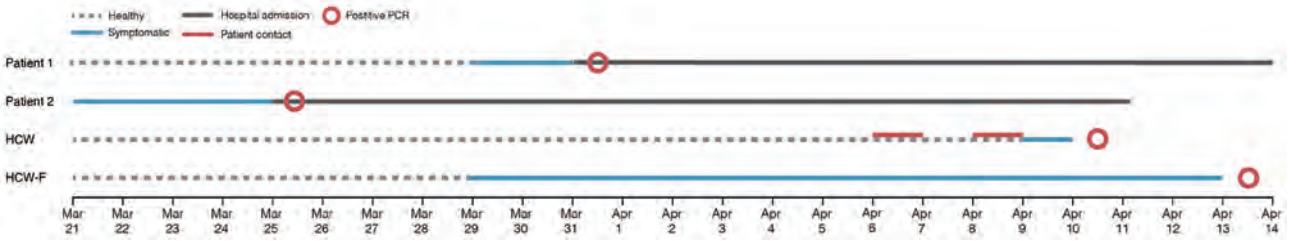

Figure 1. Timeline of infection, contact, and testing of HCW, HCW's family member, and coronavirus disease patients 1 and 2, Madison, Wisconsin, USA, 2020. HCW, healthcare worker; HCW-F, HCW's family member.

caring for patients with COVID-19 that appropriate PPE may protect against hospital-acquired SARS-CoV-2 infection. Conversely, had sequencing demonstrated nosocomial transmission, that would have provided an impetus for revisiting infection control strategies. On the basis of these results, sequencing of SARS-CoV-2 from HCWs and known contacts, within and outside of patient care settings, should be an essential component of a comprehensive strategy to protect the health of HCWs and other frontline workers.

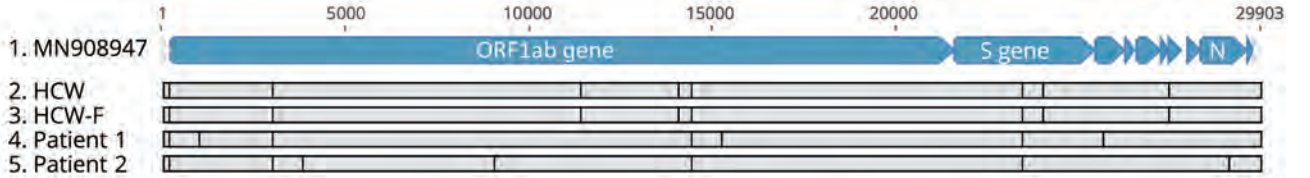

Position	Location	Reference	HCW	HCW-F	Patient 1	Patient 2	Annotation
241	3′ UTR	C	T	T	T	T	
1059	ORF1ab	C	·	·	T	·	T265I
3307	ORF1ab	C	T	T	T	T	Synonymous
3871	ORF1ab	G	·	·	·	T	K1202N
9053	ORF1ab	G	·	·	·	T	V2930L
11417	ORF1ab	G	T	T	·	·	V3718F
14073	ORF1ab	T	C	C	·	·	Synonymous
14408	ORF1ab	C	T	T	T	T	P4715L
23403	S	A	G	G	G	G	D614G
23947	S	A	G	G	·	·	Synonymous
25563	ORF3a	G	·	·	T	·	Q57H
27348	ORF6a	T	G	G	·	·	Y49*
29008	N	T	·	·	·	C	Synonymous

Figure 2. Severe acute respiratory syndrome coronavirus (SARS-CoV-2) consensus-level single-nucleotide variants (SNVs) from investigation of SARS-CoV-2 infection in HCW, Madison, Wisconsin, USA, 2020. The top alignment image depicts the SARS-CoV-2 genome for all persons evaluated in this investigation and highlights SNVs identified relative to the original SARS-CoV-2 reference isolate from Wuhan, China (GenBank accession no. MN908947.3). The table contains additional information about each of these SNVs. Light blue shading indicates A2a clade-defining mutations. Dots indicate identity with reference sequence. Asterisk indicates a tyrosine-to–stop codon change. HCW, healthcare worker; HCW-F, HCW's family member; ORF, open reading frame; UTR, untranslated region.

Acknowledgment

We thank Fauzia Osman for creating Figure 1.

N.S. is supported by National Institutes of Health award 1DP2AI144244-01, G.K.M. is supported by National Science Foundation award HRD-1612530, and K.M.B. is supported by National Institutes of Health award F30 AI145182-01A1.

About the Author

Dr. Safdar is an infectious diseases physician, scientist, and hospital epidemiologist. Her research focuses on patient and healthcare worker safety in healthcare settings.

References

1. Burrer SL, de Perio MA, Hughes MM, Kuhar DT, Luckhaupt SE, McDaniel CJ, et al.; CDC COVID-19 Response Team. Characteristics of health care personnel with COVID-19—United States, February 12–April 9, 2020. MMWR Morb Mortal Wkly Rep. 2020;69:477–81. https://doi.org/10.15585/mmwr.mm6915e6
2. Zhan M, Qin Y, Xue X, Zhu S. Death from Covid-19 of 23 health care workers in China. N Engl J Med. 2020;382:2267–8. https://doi.org/10.1056/NEJMc2005696

Address for correspondence: Nasia Safdar, University of Wisconsin School of Medicine and Public Health, Department of Population Health Sciences, 1685 Highland Ave, Madison, WI 53705, USA; email: ns2@medicine.wisc.edu

Disappearance of SARS-CoV-2 Antibodies in Infants Born to Women with COVID-19, Wuhan, China

Jinzhi Gao,[1] Wei Li,[1] Xiaolin Hu, Ying Wei, Jianli Wu, Xiaoping Luo, Suhua Chen, Ling Chen

Author affiliation: Tongji Hospital, Tongji Medical College, Huazhong University of Science and Technology, Wuhan, China

DOI: https://doi.org/10.3201/eid2610.202328

[1]These first authors contributed equally to this article.

We report the detection and decline over time of severe acute respiratory syndrome coronavirus 2 antibodies in infants born to women with coronavirus disease. Among 11 infants tested at birth, all had detectable IgG and 5 had detectable IgM. IgG titers with positive IgM declined more slowly than those without.

Although the diagnosis of coronavirus disease (COVID-19) by reverse transcription PCR (RT-PCR) is efficient and specific, IgM and IgG production and decay are useful to assess past or recent infection, especially for patients with negative nucleic acid tests (*1*). Evidence of IgM and IgG in adults with COVID-19 appeared around 13 days after illness onset (*2*). Plateau IgM levels lasted for 4 weeks and gradually declined (*3*). Although IgG lasted for a longer time, only 19.5% patients had a ≥4-fold increase in titers during convalescence, a finding that was helpful for diagnosis of existing or acute infection (*2*,*3*).

However, to our knowledge, antibody persistence in infants born to women with COVID-19 has not yet been reported. IgM is the antibody isotype produced initially in the immune response and the first immunoglobulin class to be synthesized by a fetus or infant. Maternal IgM does not cross the placental barrier intact; therefore, positive IgM in early infants is potential evidence of intrauterine vertical transmission (*1*). Although IgG is transferred passively from mother to fetus through the placenta, the duration of passive immunity from maternal IgG is still unclear.

We implemented assays for severe acute respiratory syndrome coronavirus 2 (SARS-CoV-2)–specific antibodies and SARS-CoV-2 nucleic acid tests in 64 infants admitted to the neonatal section of Tongji Hospital (Wuhan, China) during January 19–April 12, 2020. Among these, 24 infants (ranging in gestational age from 31 weeks to 41 weeks, 2 days) were born to women with PCR-confirmed COVID-19 (Table) and 40 infants (ranging in gestational age from 35 weeks, 3 days, to 41 weeks, 3 days) were born to women without COVID-19. Because antibody testing was implemented in early March, the timing of antibody testing in infants was inconsistent. We conducted SARS-CoV-2 nucleic acid tests by using a qualitative SARS-CoV-2 RT-PCR (DAAn GENE Biotech, http://www.daangene.com). We performed quantitative assessment of IgG and IgM by using the IFlash3000 Chemiluminescence Immunoassay Analyzer (YHLO Biotech, http://en.szyhlo.com), which has been proven to be a highly accurate method to detect SARS-CoV-2 antibodies (*4*). We considered IgM or IgG titers >10 AU/mL to be positive.

Among the 40 infants born to women without COVID-19, results of nucleic acid tests from throat and anal swab specimens and results of antibody assays were negative. Among the 24 infants born to women with COVID-19, 15 (62.5%) had detectable IgG and 6 (25.0%) had detectable IgM; nucleic acid test results were all negative. None of the 24 infants had complications related to pneumonia, a finding that is consistent with a previous report (*5*). Among 11 infants with antibody titers detected at birth, all had detectable IgG (100%) and 5 (45.5%) had detectable IgM, 1 of whom had high IgM levels (infant described in case 19 in the Table). Although the IgG titers in all 15 infants with positive IgG decreased gradually, the IgG levels declined more slowly in infants with positive IgM compared with those without (Figure). The infant described in case 19 was born 33 days after the mother had COVID-19

Table. Sequential severe acute respiratory syndrome coronavirus 2–specific antibodies assay in 24 infants born to mothers with PCR-confirmed coronavirus disease, Wuhan, China, January 19–April 12, 2020*

		IgM/IgG titers, AU/mL, by age of infant							GA, wk+d	
Case no.		0 d	7 d	14 d	28 d	45 d	60 d	75 d	At symptom onset	At birth
1	Mother							7.5/**116.9***	33+4	36+3
	Infant							0.8/0.3		
2	Mother							4.4/**118.3**	38+5	38+5
	Infant							0.5/2.5		
3	Mother						5.0/**83.3**		37+5	38+2
	Infant						0.4/0.2			
4	Mother					**14.5/100.8**			39+1	39+5
	Infant					0.3/0.3				
5	Mother								34	35+2
	Infant		0.7/2.8	0.4/3.5	0.3/0.9					
6	Mother					7.0/**93.0**			39+3	40
	Infant					0.4/0.3				
7	Mother					**51.1/94.6**			39+4	41+2
	Infant					0.3/0.9				
8	Mother						**67.0/92.6**		37+4	38+4
	Infant						0.3/0.1			
9	Mother					**17.8/104.3**			38+2	39+5
	Infant					0.4/8.2				
10	Mother				**15.3/95.4**			9.9/**108.7**	38+1	39+5
	Infant				2.2/**32.7**			0.7/**19.5**		
11	Mother				**11.3/112.5**			5.3/**105.6**	35+5	38+2
	Infant		3.6/**166.0**	5.3/**120.8**	1.0/**36.2**			0.4/**16.2**		
12	Mother					**+/+†**		**37.9/94.6**	29+4	31
	Infant		5.7/**142.0**	2.6/**113.9**	1.8/**75.3**	0.3/**22.0**		0.4/**11.3**		
13	Mother				**+/+**				34+3	38
	Infant	3.5/**134.1**	2.4/**125.0**	2.8/**119.0**	0.7/**24.6**					
14	Mother				7.0/**61.1**		1.9/**59.5**		34+6	39
	Infant	2.2/**78.4**	1.5/**76.9**	3.0/**80.9**	0.8/**28.6**		0.5/**13.0**			
15	Mother	0.7/**58.9**							NA	37+2
	Infant	8.5/**174.5**			7.8/**122.7**					
16	Mother	**+/+**							NA	38+3
	Infant	0.7/**101.0**								
17	Mother	**+/+**				1.5/**104.2**			NA	38+3
	Infant	1.2/**110.4**	**10.4/108.9**		2.1/**68.2**					
18	Mother	**–/+**			4.8/**54.5**				NA	39+5
	Infant	6.6/**96.2**	**11.3/86.0**	**11.9/88.3**	2.5/**60.9**					
19	Mother	**2,581.6/281**			**40.2/89.8**	**13.9/99.6**		6.9/**94.2**	32+1	38
	Infant	**184.3/147.2**	**42.6/161.6**	**21.2/83.8**	5.5/**79.2**	1.6/**57.0**		0.3/**25.9**		
20	Mother			6.9/**82.8**			6.0/**81.3**		31+1	39+5
	Infant			**25.7/68.8**		3.0/**58.4**	0.4/**47.4**			
21	Mother	**+/+**					5.1/**139.0**		30+3	38
	Infant	**26.0/145.8**	**41.8/120.1**	**42.9/110.1**	**38.0/89.5**		**14.2/105.3**			
22	Mother	**+/+**							30	30
	Infant	**22.8/116.5**	**11.8/104.4**	8.7/**99.8**	1.9/**75.2**					
23	Mother	**+/+**			**10.5/101.6**			4.3/**115.6**	32+1	32+1
	Infant	**15.8/222.1**	**33.8/182.5**	9.0/**88.2**	6.1/**82.5**			0.5/**31.1**		
24	Mother	**+/+**	**–/+**		8.0/**83.9**				NA	NA
	Infant	**30.1/106.0**	**29.5/84.6**	**31.5/94.9**	9.7/**73.1**					

*Bold text indicates titer >10 AU/mL (i.e., above cutoff). GA, gestational age; NA, not available; –, negative; +, positive.
†Some mothers delivered in other hospitals, and antibody testing was conducted using other qualitative antibody-detection kits.

diagnosed (41 days since symptom onset) and by elective cesarean section at 38 weeks' gestation because of the mother's previous cesarean section. The infant had high IgM and IgG titers in the umbilical cord blood and peripheral blood on the first day of life, which gradually decreased at repeated tests thereafter (Table). The infant also had negative nucleic acid tests results in a series of specimens, including cord blood, placenta, amniotic fluid, stool, urine, peripheral blood, and gastric juice at different timepoints. The placenta sample described in case 19 was collected during surgery and sent for pathologic examination, which revealed slight inflammation with slight fibrin deposition and lymphocyte infiltrates (Appendix Figure, https://wwwnc.cdc.gov/EID/article/26/10/20-2328-App1.pdf).

Although positive results in SARS-CoV-2 nucleic acid or virus-specific IgM in infants have been reported previously, evidence of vertical transmission of SARS-CoV-2 is not complete (*6*–*8*). We report the dynamic changes of SARS-CoV-2–specific antibodies in infants born to mothers with COVID-19. Five of 11 infants were seropositive for IgM at birth; however, these findings was not sufficient to confirm

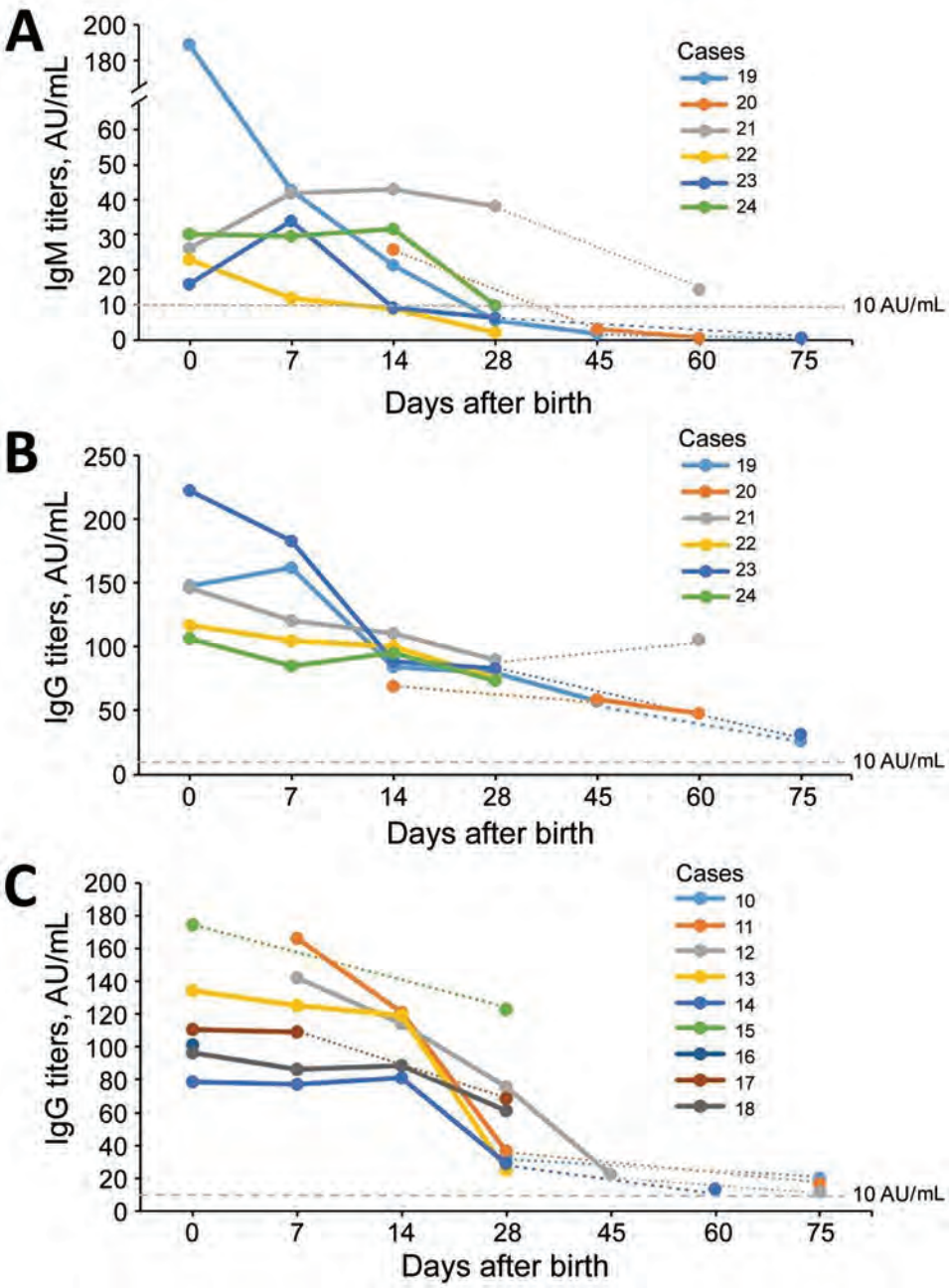

Figure. Temporal changes in severe acute respiratory syndrome coronavirus 2–specific antibodies in infants born to women with coronavirus disease, Wuhan, China. A, B) Dynamic changes of IgM (A) and IgG (B) titers in infants with positive IgM. C) Dynamic changes of IgG titers in infants with negative IgM. The IgM and IgG titers gradually decreased with time. IgG titers with positive IgM declined more slowly than those without, and the duration was as long as 75 days.

SARS-CoV-2 vertical transmission without positive nucleic acid testing. The study was also limited by a small sample size. However, these findings show a rapid rate of decline in antibody titers, suggesting lack of protective passive immunity in infants, and IgM detection in infants, supporting a growing body of evidence of possible vertical transmission. We still do not have a correlate of immunity (e.g., we do not know exactly what level of antibody titers are considered protective against infection), and whether infants testing positive by PCR at birth have higher levels of IgM or IgG remains to be seen. More work is needed to understand SARS-CoV-2 immunity in infants; such findings might have implications for potential vaccination efforts.

Acknowledgments

The authors are grateful for the insightful editorial advice provided by Shujie Liao and Dongrui Deng.

This work was funded by Tongji Hospital, Tongji Medical College, Huazhong University of Science and Technology, Wuhan, China (grant no. XXGZBDYJ005).

About the Author

Dr. Gao is a physician in the Department of Pediatrics, Tongji Hospital, Tongji Medical College, Huazhong University of Science and Technology, Wuhan, China. Her primary research interests include neonatology and infectious diseases.

References

1. Kimberlin DW, Stagno S. Can SARS-CoV-2 infection be acquired in utero? More definitive evidence is needed. JAMA. 2020 Mar 26 [Epub ahead of print]. https://doi.org/10.1001/jama.2020.4868
2. Long QX, Liu BZ, Deng HJ, Wu GC, Deng K, Chen YK, et al. Antibody responses to SARS-CoV-2 in patients with COVID-19. Nat Med. 2020;26:845–8. https://doi.org/10.1038/s41591-020-0897-1
3. Xiao AT, Gao C, Zhang S. Profile of specific antibodies to SARS-CoV-2: the first report. J Infect. 2020;81:147–78. https://doi.org/10.1016/j.jinf.2020.03.012
4. Infantino M, Grossi V, Lari B, Bambi R, Perri A, Manneschi M, et al. Diagnostic accuracy of an automated chemiluminescent immunoassay for anti-SARS-CoV-2 IgM and IgG antibodies: an Italian experience. J Med Virol. 2020 Apr 24 [Epub ahead of print]. https://doi.org/10.1002/jmv.25932
5. Liu W, Wang J, Li W, Zhou Z, Liu S, Rong Z. Clinical characteristics of 19 neonates born to mothers with COVID-19. Front Med. 2020;14:193–8. https://doi.org/10.1007/s11684-020-0772-y
6. Alzamora MC, Paredes T, Caceres D, Webb CM, Valdez LM, La Rosa M. Severe COVID-19 during pregnancy and possible vertical transmission. Am J Perinatol. 2020 Apr 18 [Epub ahead of print].
7. Zeng H, Xu C, Fan J, Tang Y, Deng Q, Zhang W, et al. Antibodies in infants born to mothers with COVID-19 pneumonia. JAMA. 2020;323:1848. https://doi.org/10.1001/jama.2020.4861
8. Dong L, Tian J, He S, Zhu C, Wang J, Liu C, et al. Possible vertical transmission of SARS-CoV-2 from an infected mother to her newborn. JAMA. 2020;323:1846–8. https://doi.org/10.1001/jama.2020.4621

Address for correspondence: Ling Chen, Department of Pediatrics, Tongji Hospital, Tongji Medical College, Huazhong University of Science and Technology, 1095 Jiefang Ave, Wuhan 430030, China; email: chenling@tjh.tjmu.edu.cn; Suhua Chen, Department of Obstetrics and Gynecology, Tongji Hospital, Tongji Medical College, Huazhong University of Science and Technology, 1095 Jiefang Ave, Wuhan 430030, China; email: tj_csh@163.com

Culture-Competent SARS-CoV-2 in Nasopharynx of Symptomatic Neonates, Children, and Adolescents

Arnaud G. L'Huillier,[1] Giulia Torriani,[1] Fiona Pigny, Laurent Kaiser, Isabella Eckerle

Author affiliation: Geneva University Hospitals and Faculty of Medicine, University of Geneva, Geneva, Switzerland

DOI: https://doi.org/10.3201/eid2610.202403

Children do not seem to drive transmission of severe acute respiratory syndrome coronavirus 2 (SARS-CoV-2). We isolated culture-competent virus in vitro from 12 (52%) of 23 SARS-CoV-2–infected children; the youngest was 7 days old. Our findings show that symptomatic neonates, children, and teenagers shed infectious SARS-CoV-2, suggesting that transmission from them is plausible.

Children are underrepresented in coronavirus disease (COVID-19) case numbers (*1*,*2*). Severity in most children is limited, and children do not seem to be major drivers of transmission (*3*,*4*). However, severe acute respiratory syndrome

[1]These authors contributed equally to this article.

coronavirus 2 (SARS-CoV-2) infects children of all ages (*1*,*3*). Despite the high proportion of mild or asymptomatic infections (*5*), they should be considered as transmitters unless proven otherwise. To address this point, the laboratory of the Geneva University Hospitals and Faculty of Medicine, University of Geneva (Geneva, Switzerland), used cell culture to systematically assess cultivable SARS-CoV-2 in the upper respiratory tract (URT) of 23 children with COVID-19.

All nasopharyngeal specimens (NPS) were collected with a flocked swab in universal transport medium (Floqswab; Copan, https://www.copan-group.com) and tested for SARS-CoV-2 by reverse transcription PCR during January 25–March 31, 2020 (Appendix, https://wwwnc.cdc.gov/EID/article/26/10/20-2403-App1.pdf). We seeded Vero E6 cells at 8×10^4 cells/well in a 24-well plate and inoculated them with 200 µL of viral transport medium the following day. Cells were inoculated for 1 h at 37°C; inoculum was removed; cells were washed once with phosphate buffered saline; and regular cell growth medium containing 10% fetal calf serum was added. We observed cells on days 2, 4, and 6 for cytopathic effect (CPE) by light microscopy. We harvested supernatant at first observation of CPE or, if no CPE occurred, on day 6. For a second passage, we transferred 20 µL supernatant of CPE-positive specimens onto new Vero E6 cells. We collected supernatant after inoculation and on observation of CPE and confirmed isolation of replication competent SARS-CoV-2 by an increase in viral RNA (Appendix).

Of 638 patients <16 years of age, 23 (3.6%) tested positive for SARS-CoV-2. Median age was 12.0 years (interquartile range [IQR] 3.8–14.5 years, range 7 days–15.9 years). Thirteen patients had an URT infection; 2 each had fever without source and pneumonia (Table). Samples were collected a median of 2 (IQR 1–3) days after symptom onset. Median viral RNA load at diagnosis was 3.0×10^6 copies/mL (mean 4.4×10^8 [IQR 6.9×10^3–4.4×10^8] copies/mL; peak 5.3×10^9 copies/mL).

We isolated SARS-CoV-2 from 12 (52%) children. We determined SARS-CoV-2 isolation by presence of CPE and increased viral RNA in the supernatant (Table; Appendix Figure). SARS-CoV-2 replication in all 12 positive isolates was confirmed by a second passage.

We isolated virus from children of all ages; the youngest was 7 days of age. Median viral load was higher for patients with isolation (1.7×10^8 [mean 7.9×10^8, IQR 4.7×10^6–1.0×10^9] copies/mL) than for those without isolation (6.9×10^3 [mean 5.4×10^7, IQR 4.2×10^3–1.8×10^6] copies/mL; p = 0.002) (Figure). Sex, age, duration of symptoms, clinical diagnosis, symptoms, and likelihood of admission did not differ between patients with and without isolation (Appendix Table).

Table. Characteristics and results of children <16 years of age with coronavirus disease, Geneva University Hospitals and Faculty of Medicine, University of Geneva, Switzerland, January 25–March 31, 2020*

Patient	Age	Days from symptom onset to diagnosis	Clinical diagnosis	Hospital admission	Viral RNA copies/mL	Isolate
1	12.6 y	1	URTI	No	2.8×10^7	Negative
2	5.7 y	1	URTI	No	1.8×10^6	Negative
3	14.8 y	1	URTI	No	9.9×10^6	Positive
4	12.0 y	2	Obstructive bronchitis	No	6.9×10^3	Negative
5	3.9 y	4	URTI	No	4.5×10^3	Negative
6	13.9 y	2	Pneumonia	Yes	8.6×10^7	Positive
7	9.0 y	2	Croup	No	6.2×10^3	Negative
8	10.1 y	3	URTI	No	3.3×10^5	Negative
9	3 mo	Not reported	Not reported	Yes	2.8×10^2	Negative
10	2.2 y	Not reported	Not reported	Yes	5.9×10^2	Negative
11	8.4 y	1	URTI	No	5.6×10^8	Negative
12	7 d	1	URTI	No	1.3×10^8	Positive
13	12.9 y	4	Pneumonia	Yes	4.2×10^3	Negative
14	15.7 y	Not reported	Not reported	No	2.5×10^4	Negative
15	12.3 y	2	Influenza-like illness	No	1.1×10^9	Positive
16	15.9 y	1	Fever without source	Yes	2.2×10^8	Positive
17	1 mo	0	Fever without source	Yes	5.3×10^9	Positive
18	2 mo	1	URTI	No	4.4×10^8	Positive
19	5.9 y	1	URTI	No	1.6×10^9	Positive
20	15.9 y	2	URTI	No	6.8×10^8	Positive
21	14.4 y	5	URTI	Yes	1.4×10^5	Positive
22	14.6 y	3	URTI	No	1.2×10^4	Positive
23	14.4 y	2	URTI	No	3.0×10^6	Positive

*URTI, upper respiratory tract infection.

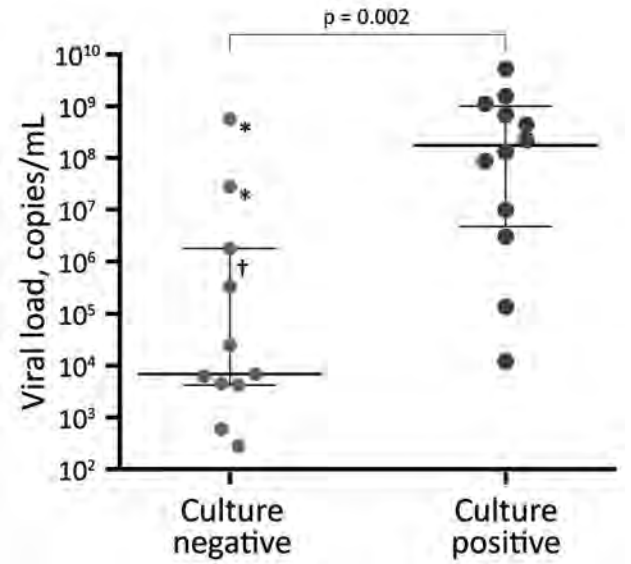

Figure. Severe acute respiratory syndrome coronavirus 2 initial RNA copy numbers from nasopharyngeal swabs of culture-negative and culture-positive specimens from children <16 years of age, Geneva University Hospitals Geneva, Switzerland, January 25–March 31, 2020. Thick horizontal bars indicate median RNA; thin horizontal bars indicate interquartile range. Asterisk (*) indicates specimen collected outside the institution, suggesting a longer time to freezing at –80°C; dagger (†) indicates specimen with ≈48 hours from specimen collection to freezing at –80°C.

Our data show that viral load at diagnosis is comparable to that of adults (*6*,*7*) and that symptomatic children of all ages shed infectious virus in early acute illness, a prerequisite for further transmission. Isolation of infectious virus was largely comparable with that of adults, although 2 specimens yielded an isolate at lower viral load (1.2×10^4 and 1.4×10^5 copies/mL) (*6*).

A limitation of our study was the small number of children assessed. However, although the Canton of Geneva was a region severely affected by SARS-CoV-2 (*8*), only 23 cases were diagnosed in children at our hospital during the study period. These findings confirm that children are not a major risk group for COVID-19. Another limitation is our reliance solely on leftover material initially received for routine diagnostic purposes that we retrospectively analyzed. Using such specimens has several disadvantages: preanalytic quality of specimens could be affected by suboptimal times between sample collection and storage at -80°C because of transport and diagnostic processing time, resulting in loss in infectivity and failure of virus isolation even in the presence of high viral load. Therefore, our findings probably underestimate the true rate of infectious virus presence in symptomatic children, and we cannot comment whether our data reflect the rates of infectious virus shedding in the community. Because of the limited leftover volume of the specimens, we were unable to further investigate the quantity of infectious viral particles. Most patients were managed as outpatients and self-isolated at home, so no consecutive sampling was possible to assess infectious virus in multiple samples over the course of disease.

SARS-CoV-2 viral load and shedding patterns of culture-competent virus in 12 symptomatic children resemble those in adults. Therefore, transmission of SARS-CoV-2 from children is plausible. Considering the relatively low frequency of infected children, even in severely affected areas, biological or other unknown factors could lead to the lower transmission in this population. Large serologic investigations and systematic surveillance for acute respiratory diseases and asymptomatic presentations are needed to assess the role of children in this pandemic.

Acknowledgments

We thank Manel Essaidi-Laziosi for her help with the laboratory work and Erik Boehm for help with editing the manuscript.

About the Author

Dr. L'Huillier is a junior staff physician at Geneva University Hospitals and Faculty of Medicine, University of Geneva. His primary research interests include emerging viruses and transplant virology.

References

1. Livingston E, Bucher K. Coronavirus disease 2019 (COVID-19) in Italy. JAMA. 2020;323:1335. https://doi.org/10.1001/jama.2020.4344
2. Qiu H, Wu J, Hong L, Luo Y, Song Q, Chen D. Clinical and epidemiological features of 36 children with coronavirus disease 2019 (COVID-19) in Zhejiang, China: an observational cohort study. Lancet Infect Dis. 2020;20:689–96. https://doi.org/10.1016/S1473-3099(20)30198-5
3. Lu X, Zhang L, Du H, Zhang J, Li YY, Qu J, et al.; Chinese Pediatric Novel Coronavirus Study Team. SARS-CoV-2 infection in children. N Engl J Med. 2020;382:1663–5. https://doi.org/10.1056/NEJMc2005073
4. World Health Organization. Report of the WHO–China Joint Mission on Coronavirus Disease 2019 (COVID-19). 28 February 2020 [cited 2020 Jun 29]. https://www.who.int/publications/i/item/report-of-the-who-china-joint-mission-on-coronavirus-disease-2019-(covid-19)
5. Parri N, Lenge M, Buonsenso D; Coronavirus Infection in Pediatric Emergency Departments (CONFIDENCE) Research Group. Children with Covid-19 in pediatric emergency departments in Italy. N Engl J Med. 2020 May 1 [Epub ahead of print]. https://doi.org/10.1056/NEJMc2007617

6. Wölfel R, Corman VM, Guggemos W, Seilmaier M, Zange S, Müller MA, et al. Virological assessment of hospitalized patients with COVID-2019. Nature. 2020;581:465–9. https://doi.org/10.1038/s41586-020-2196-x
7. Jones TC, Mühlemann B, Veith T, Zuchowski M, Hofmann J, Stein A, et al. An analysis of SARS-CoV-2 viral load by patient age [cited 2020 May 3]. https://zoonosen.charite.de/fileadmin/user_upload/microsites/m_cc05/virologie-ccm/dateien_upload/Weitere_Dateien/analysis-of-SARS-CoV-2-viral-load-by-patient-age.pdf
8. Stringhini S, Wisniak A, Piumatti G, Azman AS, Lauer SA, Baysson H, et al. Seroprevalence of anti-SARS-CoV-2 IgG antibodies in Geneva, Switzerland (SEROCoV-POP): a population-based study. Lancet. 2020 Jun 11 [Epub ahead of print]. https://doi.org/10.1016/S0140-6736(20)31304-0

Address for correspondence: Isabella Eckerle, Laboratory of Virology and Geneva Centre for Emerging Viral Diseases, Geneva University Hospitals and Faculty of Medicine, University of Geneva, 4 Rue Gabrielle-Perret-Gentil, 1211 Geneva 14, Switzerland; email: isabella.eckerle@hcuge.ch

Viral RNA Load in Mildly Symptomatic and Asymptomatic Children with COVID-19, Seoul, South Korea

Mi Seon Han,[1] Moon-Woo Seong,[1] Namhee Kim, Sue Shin, Sung Im Cho, Hyunwoong Park, Taek Soo Kim, Sung Sup Park, Eun Hwa Choi

Author affiliations: Seoul Metropolitan Government–Seoul National University Boramae Medical Center, Seoul, South Korea (M.S. Han, N. Kim, S. Shin, H. Park); Seoul National University College of Medicine, Seoul (M.-W. Seong, S. Shin, H. Park, T.S. Kim, S.S. Park, E.H. Choi); Seoul National University Hospital, Seoul (M.-W. Seong, S.I. Cho, T.S. Kim, S.S. Park); Seoul National University Children's Hospital, Seoul (E.H. Choi)

DOI: https://doi.org/10.3201/eid2610.202449

Along with positive SARS-CoV-2 RNA in nasopharyngeal swabs, viral RNA was detectable at high concentration for >3 weeks in fecal samples from 12 mildly symptomatic and asymptomatic children with COVID-19 in Seoul, South Korea. Saliva also tested positive during the early phase of infection. If proven infectious, feces and saliva could serve as transmission sources.

In the current pandemic of coronavirus disease (COVID-19), detecting severe acute respiratory syndrome coronavirus 2 (SARS-CoV-2) in children suspected of having the disease is essential for both infection control and establishing a definite causal relationship in unprecedented cases (*1*,*2*). However, efforts are hindered by negative SARS-CoV-2 test results for respiratory specimens and possible cross-reactivity with other coronaviruses among seropositive cases (*2*,*3*). Little is known about the value of various samples other than nasopharyngeal or oropharyngeal swab specimens in diagnosing COVID-19 and understanding the viral dynamics of SARS-CoV-2 in children. Virus RNA was persistently detected in rectal swab specimens in a previous study, although the infectiousness of the virus is unknown (*4*). We analyzed the viral RNA load kinetics of SARS-CoV-2 in various clinical specimens in children with COVID-19.

In South Korea, all confirmed case-patients, regardless of disease severity, must be isolated in hospitals or isolation facilities. For this study, we included all children <18 years of age who were confirmed to have COVID-19 by positive results for SARS-CoV-2 in combined nasopharyngeal and oropharyngeal swab specimens and who were hospitalized in Seoul Metropolitan Government–Seoul National University Boramae Medical Center during March 8–April 28, 2020. We extracted RNA from clinical specimens and detected SARS-CoV-2 by using the Allplex 2019-nCoV Assay kit (Seegene, http://www.seegene.com). We performed quantitation of the viral RNA with a standard curve constructed using in vitro transcribed RNA. This study was approved by the institutional review board at SMG-SNU Boramae Medical Center; written consent was waived.

We included 12 children in the study; 9 were mildly symptomatic and 3 were asymptomatic (Appendix Table 1, https://wwwnc.cdc.gov/EID/article/26/10/20-2449-App1.pdf). Median age was 6.5 years (range 27 days–16 years). Nasopharyngeal swab specimens tested positive for SARS-CoV-2 RNA in all 12 children, and 11 (92%) had positive RNA in their fecal specimens (Appendix Table 2). We collected saliva samples from 11 children; 8 (73%) tested positive.

Viral RNA load in the nasopharyngeal swabs peaked early at median 7.56 (range 6.19–10.56) $\log_{10}$ copies/mL and decreased over time ($p<0.001$ for trend) (Figure, panel A). The positivity of the specimens was 75% during week 2 and 55% during week 3 (Appendix Table 2). In comparison, the median initial fecal RNA load was 7.68 (range <4.10–10.27) $\log_{10}$ copies/mL and

[1]These authors contributed equally to this article.

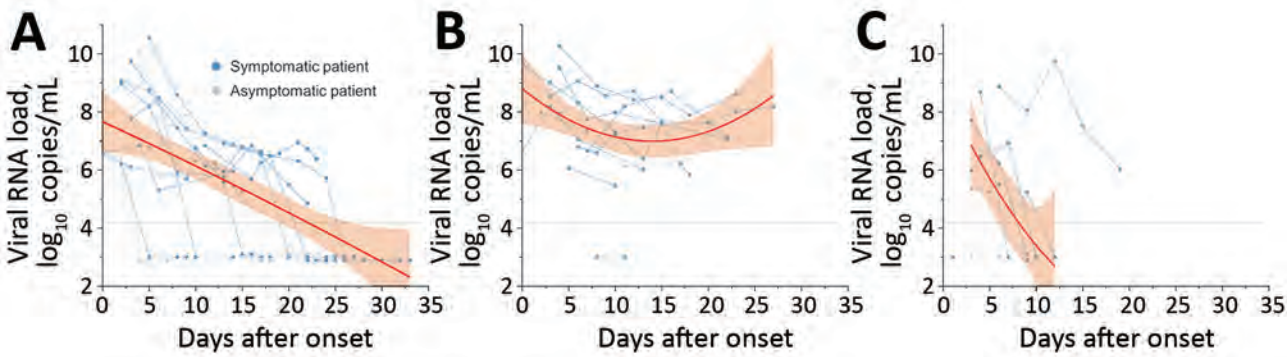

Figure. Changes in severe acute respiratory syndrome coronavirus 2 viral RNA load in A) nasopharyngeal swabs, B) feces, and C) saliva of mildly symptomatic and asymptomatic children with coronavirus disease over time, South Korea. The thick red line indicates trend in viral RNA load over time, and the shaded areas represent 95% CIs. The dashed line indicates the detection limit (1.25×10^4 copies/mL). Specimens with undetectable viral RNA loads are shown under the dashed line. Days after onset indicates days after symptom onset for symptomatic patients, days after diagnosis for asymptomatic patients.

remained steadily high (p = 0.148 for trend) for >3 weeks (Figure, panel B). Fecal positivity remained ≥80%. The median RNA load in fecal samples was significantly higher than that for nasopharyngeal swab specimens during week 2 (7.26 vs. 6.19 $\log_{10}$ copies/mL; p = 0.006) and week 3 (7.61 versus 5.49 $\log_{10}$ copies/mL; p = 0.006). Except for 1 case, the RNA load in saliva declined rapidly with time (p = 0.003 for trend) (Figure, panel C). Positivity in saliva samples was 80% in week 1 but dropped sharply to 33% in week 2 and 11% in week 3.

We collected urine specimens from the 12 patients after a median of 3 (range 0–8) days and plasma specimens at 2 (range 0–8) days from onset. Of these, urine samples of 2 (17%) patients tested positive (median load 5.69 [range 3.82–7.55] $\log_{10}$ copies/mL). Only 1 (8%) patient, 27 days of age, had RNA detected in plasma.

Symptomatic children had higher initial RNA load in nasopharyngeal swab specimens than asymptomatic children (9.01 vs. 6.32 $\log_{10}$ copies/mL; p = 0.048). We observed no significant differences in feces and in saliva and no correlation between RNA load and age.

In this study, we detected SARS-CoV-2 RNA in feces of 92% of mildly ill or asymptomatic children with COVID-19. In addition, the RNA load in feces remained steadily high, whereas that in nasopharyngeal swab specimens and saliva declined with time in both symptomatic and asymptomatic children. The detection of SARS-CoV-2 RNA in feces does not necessarily mean that infectious virus is present; thus, lack of virus isolation in our study limits interpretation in the context of infectivity. However, viable virus was isolated in feces in previous studies, and infectivity was dependent on viral RNA load (*3*,*5*,*6*). Considering these findings, proper handwashing when changing diapers in infants and adequate hygiene measures in restrooms are recommended to prevent the potential spread of the virus among household contacts.

Our findings also suggest that feces is a promising and reliable source for detecting both current and recent SARS-CoV-2 infection because the viral RNA is present in high loads for a prolonged time. Fecal specimens could aid in seeking the etiologic relationship between COVID-19 and unexpected manifestations in children.

We also detected SARS-CoV-2 RNA in saliva during the early phase of the infection for a short period of time. Live virus was isolated in saliva in a previous study, and the possibility of airborne transmission of the virus through normal speaking has been raised (*7*,*8*). Although the viral load in saliva drops rapidly, our findings suggest the necessity for children to wear masks, especially in schools, where children would talk in close proximity.

About the Author

Dr. Han is a clinical assistant professor in the Division of Pediatric Infectious Diseases, Department of Pediatrics at Seoul Metropolitan Government–Seoul National University Boramae Medical Center, Seoul, South Korea. Her research interests include respiratory virus infections and infectious diseases in immunocompromised hosts.

References

1. Riphagen S, Gomez X, Gonzalez-Martinez C, Wilkinson N, Theocharis P. Hyperinflammatory shock in children during COVID-19 pandemic. Lancet. 2020;395:1607–8. https://doi.org/10.1016/S0140-6736(20)31094-1
2. Verdoni L, Mazza A, Gervasoni A, Martelli L, Ruggeri M, Ciuffreda M, et al. An outbreak of severe Kawasaki-like

disease at the Italian epicentre of the SARS-CoV-2 epidemic: an observational cohort study. Lancet. 2020 May 13 [Epub ahead of print]. https://doi.org/10.1016/S0140-6736(20)31103-X
3. Wölfel R, Corman VM, Guggemos W, Seilmaier M, Zange S, Müller MA, et al. Virological assessment of hospitalized patients with COVID-2019. Nature. 2020;581:465–9. https://doi.org/10.1038/s41586-020-2196-x
4. Xu Y, Li X, Zhu B, Liang H, Fang C, Gong Y, et al. Characteristics of pediatric SARS-CoV-2 infection and potential evidence for persistent fecal viral shedding. Nat Med. 2020;26:502–5. https://doi.org/10.1038/s41591-020-0817-4
5. Xiao F, Sun J, Xu Y, Li F, Huang X, Li H, et al. Infectious SARS-CoV-2 in feces of patient with severe COVID-19. Emerg Infect Dis. 2020 May 18 [Epub ahead of print]. https://doi.org/10.3201/eid2608.200681
6. Xiao F, Tang M, Zheng X, Liu Y, Li X, Shan H. Evidence for gastrointestinal infection of SARS-CoV-2. Gastroenterology. 2020;158:1831–1833.e3. https://doi.org/10.1053/j.gastro.2020.02.055
7. To KK-W, Tsang OT-Y, Yip CC-Y, Chan K-H, Wu T-C, Chan JM-C, et al. Consistent detection of 2019 novel coronavirus in saliva. Clin Infect Dis. 2020 Feb 12 [Epub ahead of print]. https://doi.org/10.1093/cid/ciaa149
8. Stadnytskyi V, Bax CE, Bax A, Anfinrud P. The airborne lifetime of small speech droplets and their potential importance in SARS-CoV-2 transmission. Proc Natl Acad Sci U S A. 2020 May 13 [Epub ahead of print]. https://doi.org/10.1073/pnas.2006874117

Address for Correspondence: Eun Hwa Choi, Department of Pediatrics, Seoul National University Children's Hospital, 101 Daehak-ro, Jongno-gu, Seoul, 03080, South Korea; email: eunchoi@snu.ac.kr

Coronavirus Disease Exposure and Spread from Nightclubs, South Korea

Cho Ryok Kang, Jin Yong Lee, Yoojin Park, In Sil Huh, Hyon Jeen Ham, Jin Kyeong Han, Jung Il Kim, Baeg Ju Na, Seoul Metropolitan Government COVID-19 Rapid Response Team (SCoRR Team)

Author affiliations: Seoul Metropolitan Government, Seoul, South Korea (C.R. Kang, H.J. Ham, J.K. Han, J.I. Kim, B.J. Na); Seoul National University Boramae Medical Centre, Seoul (J.Y. Lee); Seoul Centre for Infectious Disease Control and Prevention, Seoul (Y. Park, I.S. Huh)

DOI: https://doi.org/10.3201/eid2610.202573

At least 246 cases of coronavirus disease (COVID-19) have been linked to nightclubs in Seoul, South Korea. During the April 30–May 5 holiday, young adults from across the country who visited nightclubs in Seoul contracted COVID-19 and spread it nationally. Nightclubs were temporarily closed to limit COVID-19 spread.

South Korea had 10,801 confirmed cases of coronavirus disease (COVID-19) by May 4, 2020 (*1*). The epidemic curve of the cumulative number of cases had plateaued in April (Appendix Figure 1, https://wwwnc.cdc.gov/EID/article/26/10/20-2573-App1.pdf). Nightclubs that had been closed as part of the social distancing policy reopened on April 30, ahead of the April 30–May 5 Golden Week holiday. People from around the country visited the Itaewon area (Itaewon-dong) in downtown Seoul during the holiday period. Itaewon is known for its diversity and contains a US Army base, multiple embassies, and several well-known nightclubs.

Starting on May 6, several COVID-19 cases were confirmed among persons who had visited nightclubs in Itaewon during the holiday. Secondary transmission by case-patients linked to the Itaewon nightclubs led to local transmission of COVID-19 in other parts of the country (Figure). On May 9, the Seoul Metropolitan Government announced indefinite closure of all nightclubs in Seoul to control the source of the outbreak. Subsequently, several regions prohibited mass gatherings.

The Seoul Metropolitan Government and Yongsan-gu Office, in cooperation with the Seoul Metropolitan Police Agency, conducted contact tracing of persons who had visited any of the 5 major nightclubs in Itaewon during April 30–May 6. The use of cell phone location data, credit card records, and lists of nightclub visitors led to the identification of 5,517 persons for screening; of those, 1,257 were actively monitored. An additional 57,536 persons who had spent >30 minutes in the vicinity of the nightclubs, as determined by their cell phone location data, were sent a series of text messages encouraging them to undergo testing.

After media outlets reported that venues at the epicenter of the outbreak were gay nightclubs, a rumor spread that this COVID-19 outbreak originated among gay men. Authorities became concerned that this rumor could adversely affect nightclub visitors' willingness to be tested. Because of prejudice against homosexuality, gay men in South Korea usually experience discrimination and stigmatization and so are often unwilling to reveal their sexual identity (*2*). Thus, the Seoul Metropolitan Government consulted sexual-minority groups to discuss ways to encourage

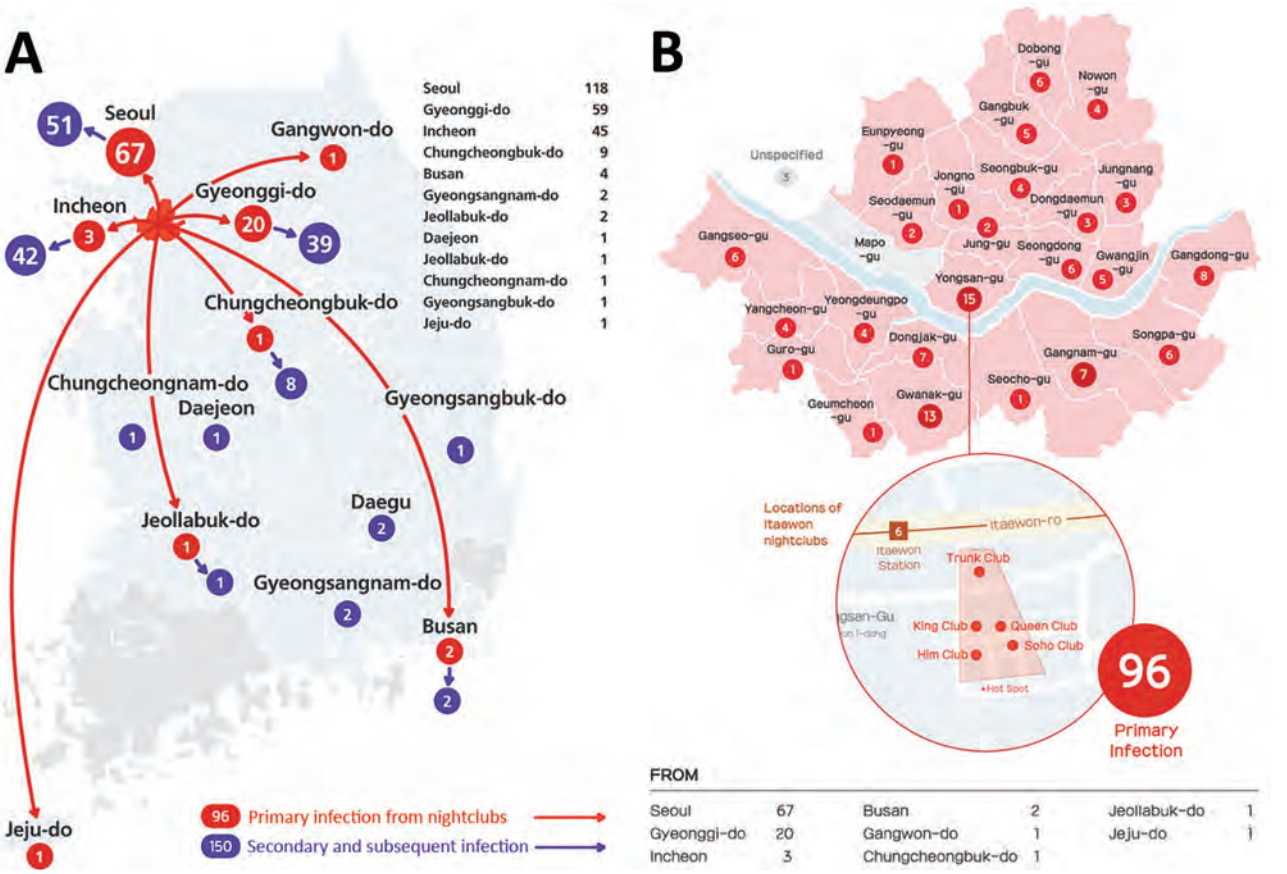

Figure. Cases related to the COVID-19 outbreak in nightclubs in Itaewon, Seoul, South Korea, that were diagnosed in major cities and provinces of South Korea as of May 25, 2020. A) Distribution of cases by city (n = 246). B) Distribution of primary and secondary cases contracted in nightclubs within the Seoul metropolitan area, by neighborhood in which the nightclubs are located (n = 118, of which 96 contracted the disease in Seoul nightclubs).

testing among gay men. The sexual-minority groups recommended anonymous testing. Therefore, the Seoul Metropolitan Government introduced anonymous testing and stated that the only information that patients were required to provide was their cell phone number for contact purposes. Through the lesbian, gay, bisexual, and transgender community, we advertised that screening clinics of public health centers were conducting anonymous testing for COVID-19; we also advertised anonymous testing through mass media.

We conducted large-scale testing for active case-finding among persons who had visited the Itaewon nightclubs. Patients' cell phone numbers were checked on site before testing. Demographic data were obtained by contacting those who tested positive. Of the 41,612 total tests conducted by May 25, a total of 35,827 (86.1%) were conducted on Itaewon nightclub visitors, 5,785 (13.9%) on contacts of case-patients linked to the Itaewon nightclubs, and 1,627 (3.9%) tests conducted on anonymous persons. The prevalence of positive results for COVID-19 in nightclub visitors was 0.19% (67/35,827); in their contacts, 0.88% (51/5,785); and in anonymously tested persons, 0.06% (1/1,627).

As of May 25, a total of 246 confirmed nightclub-associated cases had been reported; 96 (39%) of those were primary cases and 150 (61%) were secondary cases (Figure). The estimated attack rate among nightclub visitors was 1.74% (96/5,517). Of the total number of confirmed cases, 118 positive case-patients (47.9%) live in Seoul; among those, 67 (56.8%) were primary cases, 32 (27.1%) secondary cases, 7 (5.9%) tertiary cases, 4 (3.4%) quaternary cases, 4 (3.4%) fifth-order cases, and 4 (3.4%) sixth-order cases. Infections related to the nightclub outbreak continued to spread further in the community; in Seoul, COVID-19 cases related to the outbreak were identified in 9 different workplaces (several companies, the Army base, and a hospital) and 6 multiuse facilities (pubs, coin karaoke facilities, and a fitness center). In addition, we

identified 7 cases of household transmission (Appendix Figure 2).

In summary, we identified 246 COVID-19 cases associated with the reopening of nightclubs in Seoul. To conduct contact tracing for this outbreak, we used multiple forms of advanced information technology, including location data from mobile devices, credit card payment history, geographic positioning service data, drug utilization review, public transportation transit pass records, and closed-circuit television footage (*3*). Despite the low incidence of COVID-19 in the postpeak period of the pandemic, superspreading related to visiting nightclubs in Seoul has the potential to spark a resurgence of cases in South Korea.

Acknowledgments

We thank 25 public health centers in Seoul for their efforts in responding to the COVID-19 outbreak.

About the Author

Ms. Kang is a public health officer with the Seoul Metropolitan Government. Her main research interest is the epidemiology of infectious diseases.

References

1. Korea Centers for Disease Control and Prevention. Update on COVID-19 in Korea as of 4 May [in Korean]. 2020 May 04 [cited 2020 May 20]. http://ncov.mohw.go.kr/tcmBoardView.do?brdId=&brdGubun=&dataGubun=&ncvContSeq=354347&contSeq=354347&board_id=&gubun=ALL
2. Youn G. Attitudinal changes toward homosexuality during the past two decades (1994–2014) in Korea. J Homosex. 2018;65:100–16. https://doi.org/10.1080/00918369.2017.1310512
3. Park S, Choi GJ, Ko H. Information technology–based tracing strategy in response to COVID-19 in South Korea—privacy controversies. JAMA. 2020;323:2129–30. https://doi.org/10.1001/jama.2020.6602

Address for correspondence: Jin Yong Lee, Department of Public Health and Community Medicine, Seoul Metropolitan Government–Seoul National University Boramae Medical Center, Seoul, 07061, South Korea; email: jylee2000@gmail.com

Rapid Screening Evaluation of SARS-CoV-2 IgG Assays Using Z-Scores to Standardize Results

Marie K. Das, Anu Chaudhary, Andrew Bryan, Mark H. Wener, Susan L. Fink, Chihiro Morishima

Author affiliation: University of Washington, Seattle, Washington, USA

DOI: https://doi.org/10.3201/eid2610.202632

Many serologic tests are now available for measuring severe acute respiratory syndrome coronavirus 2 antibodies to evaluate potential protective immunity and for seroprevalence studies. We describe an approach to standardizing positivity thresholds and quantitative values for different assays that uses z-scores to enable rapid and efficient comparison of serologic test performance.

Measurement of severe acute respiratory syndrome coronavirus 2 (SARS-CoV-2) antibodies has become increasingly important for assessing potential immunity as the coronavirus disease (COVID-19) pandemic evolves. Most immunoassays for SARS-CoV-2 antibodies yield quantitative converted to qualitative results, requiring a positivity threshold whose basis might be unclear when provided by the manufacturer. Using specimens from hospitalized patients with acute COVID-19 and archived pre–COVID-19 serum samples, we established standardized positivity thresholds and quantitative values for multiple commercially available immunoassays, which enabled efficient screening comparison of serologic reagents.

Remnant blood specimens were selected from a convenience sample of patients given diagnoses of COVID-19 by using a laboratory-developed reverse transcription PCR (*1*). Serologic testing was performed at the University of Washington Clinical Immunology Laboratory after institutional review board approval (study #9954).

We used 4 commercial SARS-CoV-2 IgG ELISA kits: Euroimmun IgG Kit (lot no. E200225BV; https://www.euroimmun.com) with recombinant structural protein (spike [S] 1 domain) as target (*2*); Epitope Diagnostics (EPI) EDI Novel Coronavirus COVID19 IgG Kit (lot no. P529, http://www.epitopediagnostics.com) with nucleocapsid protein (NP) as target; ImmunoDiagnostics anti-SARS-CoV-2-NP IgG Kit (lot no. N0313; https://www.immunodiagnostics.com.hk) with NP as target; and ImmunoDiagnostics anti-SARS-CoV-2-S1RBD IgG Kit (lot no. S0313) with receptor-binding

Table. Results from 4 immunoassays for severe acute respiratory syndrome coronavirus 2 IgG using a standardized z-score threshold of 3*

Days from symptom onset	EU IgG	EPI IgG	ID NP IgG	ID S1RBD IgG
0–6	0/4 (0)	0/4 (0)	2/4 (50)	2/4 (50)
7–13	1/11 (9)	7/11 (64)	7/11 (64)	1/11 (9)
14–20	7/8 (88)	8/8 (100)	8/8 (100)	0/8 (0)

*Values are no. positive/no. tested (%). EU, Euroimmun (https://www.euroimmun.com); EPI, Epitope Diagnostics (http://www.epitopediagnostics.com); ID, ImmunoDiagnostics (https://www.immunodiagnostics.com.hk); NP, nucleocapsid protein; RBD, receptor-binding domain; S1, spike protein.

domain (RBD) of the S1 protein as target. All testing was performed according to manufacturer's protocols.

To standardize results, optical density (OD) scores for each sample were converted to z-scores by using the equation z-score = (test OD – mean negative control OD)/mean negative control SD. For Euroimmun, the OD ratio was calculated by using a kit calibrator. Negative control serum samples had been collected during April 2015–November 2019 from 25 healthy community blood donors. A conservative z-score ≥3 (number of SDs above the negative control mean) was considered positive to minimize false-positive results.

A total of 23 samples were tested from a cohort of 11 patients with reverse transcription PCR–confirmed COVID-19. The standardized results illustrate the differing sensitivities of the 4 assays (Table). As expected, positive results were strongly associated with time after symptom onset, consistent with results of previous studies (*2*–*5*). In contrast to the other assays, the ImmunoDiagnostics S1RBD Kit did not show typical seroconversion, although an assay that used RBD from a local academic laboratory demonstrated seroconversion (data not shown).

We provide serial results for 3 patients over the first 3 weeks after symptom onset (Figure). Using the z-score threshold ≥3, we found that patient 1, who recovered, had positive IgG responses by 3 assays. Patient 10 had IgG responses detected by 2 assays,

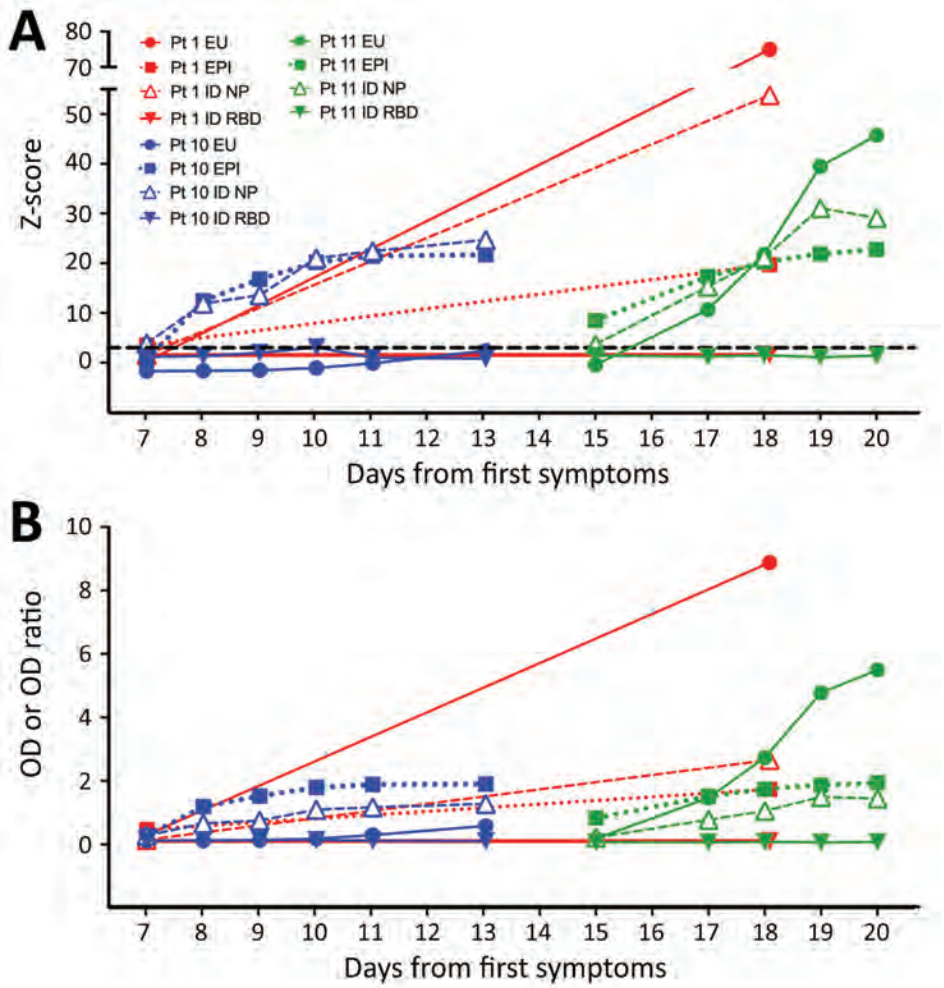

Figure. Results from 4 severe acute respiratory syndrome coronavirus 2 IgG assays, by days from first symptoms, for 3 patients with serial results demonstrating seroconversion. Immunoassay results are shown as z-scores (A), calculated from OD or OD ratio (EU) results (B) as described, and respective negative control population means and SDs for each assay (n = 25). Control samples were collected from healthy persons during 2015–2019 and tested with all 4 assays. For all patients, results from different assays are indicated as EU IgG (solid circles); EPI IgG (solid squares); ID NP IgG (open triangles); and ID S1RBD IgG (solid triangles). Red indicates results for patient 1, blue indicates results for patient 10, and green indicates results for patient 11. Dashed line in panel A indicates the z-score positivity threshold of 3. EPI, Epitope Diagnostics (http://www.epitopediagnostics.com); EU, Euroimmun (https://www.euroimmun.com); ID, ImmunoDiagnostics (https://www.immunodiagnostics.com.hk); NP, nucleocapsid protein; OD, optical density; RBD, receptor-binding domain; S, spike protein.

and patient 11 had IgG responses detected by 3 assays (Figure, panel A); both of these patients died. Antibody responses measured by different kits standardized as z-scores showed relative differences from raw OD results (Figure, panel B). A definitive comparison between quantitative values would require further characterization and optimization of quantitative performance. However, we show the benefit of comparing results from different assays in a standardized way (Figure). Although our small sample size precludes any conclusions regarding seroconversion and relationship to disease course, variability in antibody response kinetics between persons was demonstrated.

Among 25 negative control samples, 6 were positive by EPI-provided thresholds, but negative by the other tests, suggesting that the recommended EPI cutoff was inappropriately low. All 25 control results were included in EPI z-score calculations, and led to a positivity threshold higher than recommended by EPI. In contrast, our local population-based z-score cutoff was lower than the threshold recommended by EU. Despite these differences, qualitative results obtained by using manufacturer-supplied cutoffs and z-scores were identical for EU and EPI results for our limited sample set. The ID kits did not include a recommended positivity threshold, but use of a z-score of 3, and results generated by using the same local negative control samples as the other kits facilitated an unbiased comparison.

Three patients had discordant qualitative results for Euroimmun, EPI, and ImmunoDiagnostics NP assays. Patient 10 had nucleocapsid responses (EPI and ImmunoDiagnostics NP) but no S1 response (Euroimmun) detected, and patients 4 and 5 had nucleocapsid antibody responses just above positivity thresholds detected by 1 but not the other assays. Different studies have reported serologic results using in-house (*2*) or manufacturer-recommended thresholds (*6*,*7*). The choice of thresholds could affect identification of immune versus nonimmune persons and of seroprevalence in a population, particularly if asymptomatic or mildly affected persons have low levels of antibodies.

Clinical assay validation is always required, but is particularly needed for COVID-19 antibody assays given the current emergency use climate with limited regulatory oversight. Use of pre–COVID-19–era reference specimens to calculate standardized z-score results for immunoassays with different or no manufacturer-recommended cutoffs, and a small sample of locally collected specimens from SARS-CoV-2–infected persons enabled rapid comparison. As attention turns to calculated measurement of vaccine-induced responses, comparison of quantitative assays is likely to become important, and z-scores (with ≥20 control samples tested once) should also find utility in that setting. Finally, careful evaluation of manufacturer-recommended positivity thresholds for SARS-CoV-2 qualitative antibody tests is warranted.

Acknowledgments

We thank members of the University of Washington Clinical Immunology Laboratory for retrieving specimens (led by Carol Home), and organizing specimens (led by Minjun Apodaca), and for performing the assays.

This study was supported by the Department of Laboratory Medicine, University of Washington.

About the Author

Dr. Das is a laboratory medicine and pathology resident at the University of Washington, Seattle, WA. Her research interests include molecular genetic pathology, hematopathology, and serology.

References

1. Bhatraju PK, Ghassemieh BJ, Nichols M, Kim R, Jerome KR, Nalla AK, et al. COVID-19 in critically ill patients in the Seattle region: case series. N Engl J Med. 2020;382:2012–22. https://doi.org/10.1056/NEJMoa2004500
2. Okba NM, Müller MA, Li W, Wang C, GeurtsvanKessel CH, Corman VM, et al. Severe acute respiratory syndrome coronavirus 2–specific antibody responses in coronavirus disease 2019 patients. Emerg Infect Dis. 2020;26:1478–88. https://doi.org/10.3201/eid2607.200841
3. Zhao J, Yuan Q, Wang H, Liu W, Liao X, Su Y, et al. Antibody responses to SARS-CoV-2 in patients of novel coronavirus disease 2019. Clin Infect Dis. 2020;Mar 28:ciaa3444.
4. Wölfel R, Corman VM, Guggemos W, Seilmaier M, Zange S, Müller MA, et al. Virological assessment of hospitalized patients with COVID-2019. Nature. 2020;581:465–9. https://doi.org/10.1038/s41586-020-2196-x
5. Long QX, Liu BZ, Deng HJ, Wu GC, Deng K, Chen YK, et al. Antibody responses to SARS-CoV-2 in patients with COVID-19. Nat Med. 2020;26:845–8. https://doi.org/10.1038/s41591-020-0897-1
6. Montesinos I, Gruson D, Kabamba B, Dahma H, Van den Wijngaert S, Reza S, et al. Evaluation of two automated and three rapid lateral flow immunoassays for the detection of anti–SARS-CoV-2 antibodies. J Clin Virol. 2020;128:104413. https://doi.org/10.1016/j.jcv.2020.104413
7. Jääskeläinen AJ, Kekäläinen E, Kallio-Kokko H, Mannonen L, Kortela E, Vapalahti O, et al. Evaluation of commercial and automated SARS-CoV-2 IgG and IgA ELISAs using coronavirus disease (COVID-19) patient samples. Euro Surveill. 2020;25:2000603. https://doi.org/10.2807/1560-7917.ES.2020.25.18.2000603

Address for correspondence: Chihiro Morishima, Department of Laboratory Medicine, University of Washington, Box 357110, 1959 NE Pacific St, Seattle, WA 98195, USA; email: chihiro@uw.edu

Relative Bradycardia in Patients with Mild-to-Moderate Coronavirus Disease, Japan

Kazuhiko Ikeuchi, Makoto Saito, Shinya Yamamoto, Hiroyuki Nagai, Eisuke Adachi

Author affilation: The University of Tokyo, Tokyo, Japan

DOI: https://doi.org/10.3201/eid2610.202648

Coronavirus disease is reported to affect the cardiovascular system. We showed that relative bradycardia was a common characteristic for 54 patients with PCR-confirmed mild-to-moderate coronavirus disease in Japan. This clinical sign could help clinicians to diagnose this disease.

Pulse rate usually increases 18 beats/min for each 1°C increase in body temperature (*1*). However, in some specific infectious diseases, pulse rate does not increase as expected, a condition called relative bradycardia. High fever (temperature >39°C) for patients with coronavirus disease (COVID-19) has been reported (*2*,*3*), but the association between fever and pulse rate has not been investigated. We investigated relative bradycardia as a characteristic clinical feature in patients with mild-to-moderate COVID-19.

Retrospective analyses of routinely collected clinical records of COVID-19 patients were approved by the ethics committee of the Institute of Medical Science, The University of Tokyo (approval no. 2020–5-0420). During March 1–May 14, we identified all adult hospitalized patients with COVID-19 at a university hospital in Tokyo, Japan. We confirmed diagnoses of COVID-19 by using reverse transcription PCR. Patients who had known factors that could affect pulse rate (e.g., concurrent conditions or medications) were excluded.

We obtained the highest body temperature in each day during hospitalization and the pulse rate at the time. To account for within-person correlation, we used 2-level mixed-effects linear regression (with random intercept) for analysis of factors associated with pulse rate: age, sex, time from first symptoms, systolic blood pressure, diastolic blood pressure, respiratory rate, and percutaneous oxygen saturation.

We performed variable selection by backward elimination using a p value of 0.05 by likelihood ratio test as the cutoff value. We performed statistical analysis by using Stata MP 15.1 (StataCorp, https://www.stata.com). Relative bradycardia was defined as an increase in pulse rate <18 beats/min for each 1°C increase in body temperature (*1*).

During the study period, 57 patients with COVID-19 were admitted to our hospital (Table); 3 patients were excluded (2 were receiving beta-blockers and 1 had a pulmonary embolism). The median age was 45.5 years (range 20–81 years), and 72.2% (39/54) of patients were male. Median time from the appearance of first symptoms to admission was 9 days (range 2–25 days). At admission, median body temperature was 37.2°C (range 36.1°C–39.2°C), pulse rate 84 beats/min (range 62–134 beats/min), and systolic blood pressure, 116 mm Hg (range 80–170 mm Hg). During admission, 13.0% (7/54) of patients had high fever (temperature >38.9°C), and all had a pulse rate <120 beats/min (range 72–114 beats/min).

We performed computed tomography and electrocardiography for all patients: no patients were given a diagnosis of cardiac disease. Computed tomography showed pneumonia for 49 (90.7%) patients, and 11 (20.4%) patients required oxygen therapy without intubation. A total of 24 patients received COVID-19–specific treatment (favipiravir, n = 15; hydroxychloroquine, n = 10; both drugs, n = 1); no patients received vasopressors, or corticosteroids for COVID-19. All patients improved and were discharged.

Body temperature, respiratory rate, systolic blood pressure, and time after the first symptoms (in days) were associated with pulse rate by univariable analysis (Appendix Table, https://wwwnc.cdc.gov/EID/article/26/10/20-2648-App1.pdf). However, only body temperature was independently associated with pulse rate by multivariable analysis. The predicted change in pulse rate was 7.37 (95% CI 5.92–8.82) beats/min for each 1°C increase in body temperature (Figure).

Relative bradycardia is a characteristic physical finding in some intracellular bacterial infections, viral infections, and noninfectious diseases (*4*). Our data showed that a predicted change in pulse rate was <18 beats/min for each 1°C increase in patients with COVID-19. Furthermore, all patients with high fever also met another criterion of relative bradycardia (i.e., body temperature >38.9°C with pulse rate <120 beats/min) (*1*).

Although the mechanism of relative bradycardia is not known, a hypothesis is that increased levels of inflammatory cytokines, such as interleukin-6, which was reported for patients with COVID-19, can increase vagal tone and decrease heart rate variability (*4*–*6*).

Table. Characteristics of patients with relative bradycardia and mild-to-moderate coronavirus disease, Japan

Characteristic	No. assessed	Value*
Age, y	54	45.5 (20–81)
Sex		
M	39	39 (72.2)
F	15	15 (27.8)
Body mass index, kg/m^2	54	23.7 (15.9–51.1)
Current smoker	48	16 (33.3)
Days from symptom onset to admission	54	9 (2–25)
Vital signs at admission		
Body temperature, °C	54	37.2 (36.1–39.2)
Pulse rate, beats/min	54	84 (62–134)
Systolic blood pressure, mm Hg	54	116 (80–170)
Diastolic blood pressure, mm Hg	54	70.5 (51–124)
Respiratory rate, breaths/min	53	18 (16–26)
Percutaneous oxygen saturation, %†	54	97 (92–100)
Highest temperature during admission,°C	54	
<37.5	54	27 (50.0)
37.5–38.9	54	20 (37.0)
>38.9°C	54	7 (13.0)
Laboratory findings at admission		
Leukocyte count, cells/mm^3	54	5,530 (2,690–16,700)
Lymphocyte count, cells/mm^3	54	1,251 (381–2,852)
Hemoglobin, g/dL	54	14.7 (11.1–17.3)
Platelet count, × 1,000/mm^3	54	231 (106–444)
Blood urea nitrogen, mmol/L	54	4.3 (2.1–7.9)
Creatinine, μmol/L	54	69.0 (34.5–120.2)
Sodium, mmol/L	53	139 (132–148)
Potassium, mmol/L	53	4.0 (3.1–4.8)
Creatine kinase, U/L	52	74 (22–674)
C-reactive protein, mg/L	54	17.9 (0.1–215.6)
Brain natriuretic peptide, pg/mL	52	5.8 (5.8–43.2)
D-dimer, mg/L	50	0.5 (0.5–6.5)
Concurrent conditions		
Hypertension	54	8 (14.8)
Diabetes	54	5 (9.3)
Chronic obstructive pulmonary disease	54	1 (1.9)
Coronary heart disease	54	0 (0)
HIV Infection	54	4 (7.4)

*Values are median (range) or no. (%).
†Nine patients required oxygen therapy at admission.

Another hypothesis is that the toxic effect on the nervous system caused by SARS-CoV-2 (*7*) disturbs autonomic control of heart rate. Angiotensin-converting enzyme 2, which is the receptor for SARS-CoV-2, is known to be expressed on cardiac cells (*8*). Therefore, relative bradycardia might reflect a characteristic inflammatory response to COVID-19, directly or indirectly affecting cardiovascular system.

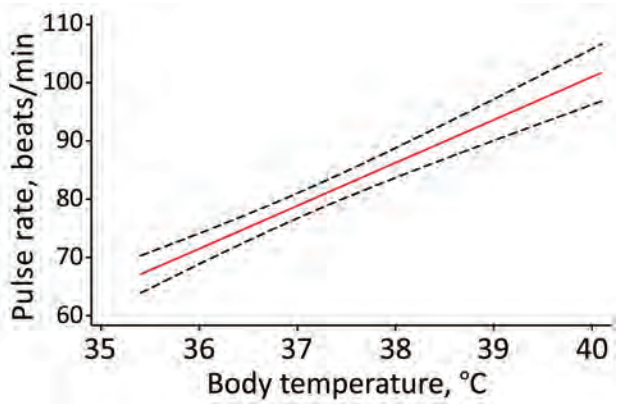

Figure. Predicted pulse rate over body temperature (red line) based on final random intercept model for relative bradycardia in patients with mild-to-moderate coronavirus disease, Japan. Black dashed lines indicate 95% CIs.

There are several limitations in our study. First, 34 patients received antipyretic medicines during their hospitalization (acetaminophen, n = 33; loxoprofen, n = 1), and 1 patient received prednisolone (5 mg/day) for myasthenia gravis. Because fever was underestimated for patients who received these medications, relative bradycardia might be a more common clinical sign. In our cohort, body temperature decreased over time. Although there was a relationship between pulse rate and time after first symptom in a univariable model, this finding was probably confounded by body temperature and thus not significant when adjusted. Second, our data did not include patients who were intubated. Additional research on patients with severe respiratory dysfunction is needed.

In summary, relative bradycardia was a characteristic clinical finding in patients who had mild-to-moderate COVID-19 in Japan. This clinical sign could help clinicians diagnose COVID-19.

About the Author

Dr. Ikeuchi is a graduate student at the Institute of Medical Science, University of Tokyo, Tokyo, Japan. His primary research interest is HIV.

References

1. Cunha BA. The diagnostic significance of relative bradycardia in infectious disease. Clin Microbiol Infect. 2000; 6:633–4. https://doi.org/10.1046/j.1469-0691.2000.0194f.x
2. Guan WJ, Ni ZY, Hu Y, Liang WH, Ou CQ, He JX, et al.; China Medical Treatment Expert Group for Covid-19. Clinical characteristics of coronavirus disease 2019 in China. N Engl J Med. 2020;382:1708–20. https://doi.org/10.1056/NEJMoa2002032
3. Lian J, Jin X, Hao S, Cai H, Zhang S, Zheng L, et al. Analysis of epidemiological and clinical features in older patients with corona virus disease 2019 (COVID-19) out of Wuhan. Clin Infect Dis. 2020;Mar 25:ciaa242. https://doi.org/10.1093/cid/ciaa242
4. Ye F, Hatahet M, Youniss MA, Toklu HZ, Mazza JJ, Yale S. The clinical significance of relative bradycardia. WMJ. 2018;117:73–8.
5. Ye F, Winchester D, Stalvey C, Jansen M, Lee A, Khuddus M, et al. Proposed mechanisms of relative bradycardia. Med Hypotheses. 2018;119:63–7. https://doi.org/10.1016/j.mehy.2018.07.014
6. Hajiasgharzadeh K, Mirnajafi-Zadeh J, Mani AR. Interleukin-6 impairs chronotropic responsiveness to cholinergic stimulation and decreases heart rate variability in mice. Eur J Pharmacol. 2011;673:70–7. https://doi.org/10.1016/j.ejphar.2011.10.013
7. Mao L, Jin H, Wang M, Hu Y, Chen S, He Q, et al. Neurologic manifestations of hospitalized patients with coronavirus disease 2019 in Wuhan, China. JAMA Neurol. 2020;77:683–90. https://doi.org/10.1001/jamaneurol.2020.1127
8. Li W, Moore MJ, Vasilieva N, Sui J, Wong SK, Berne MA, et al. Angiotensin-converting enzyme 2 is a functional receptor for the SARS coronavirus. Nature. 2003;426:450–4. https://doi.org/10.1038/nature02145

Address for correspondence: Eisuke Adachi, Department of Infectious Diseases and Applied Immunology, Institute of Medical Science, The University of Tokyo, 4-6-1 Shirokanedai, Minato-ku, Tokyo, Japan; email: eadachi-ims@umin.ac.jp

Effect of COVID-19 on Tuberculosis Notification, South Korea

Nakwon Kwak, Seung-Sik Hwang, Jae-Joon Yim

Author affiliations: Seoul National University College of Medicine, Seoul, South Korea (N. Kwak, J.-J. Yim); Seoul National University Graduate School of Public Health, Seoul (S.-S. Hwang)

DOI: https://doi.org/10.3201/eid2610.20-2782

After South Korea raised its infectious disease alert to the highest level in response to coronavirus disease emergence, tuberculosis notification during the first 18 weeks of 2020 decreased significantly from the same period for each year during 2015–2019. Adequate measures to diagnose, control, and prevent tuberculosis need to be maintained.

The first case of coronavirus disease (COVID-19) in South Korea was identified on January 20, 2020, and an outbreak from a church hastened widespread transmission throughout the country (*1*). On February 23, the government of South Korea raised the country's infectious disease alert to the highest level and initiated vigorous infection control measures: establishing widespread diagnostic capacity, initiating local contact tracing, mandating physical distancing, and redesigning triage and treatment systems (*2*). While this alert level remains in effect, such measures could negatively affect other communicable diseases, such as tuberculosis (TB) (*3*). To investigate the effect of COVID-19 on TB diagnoses, we traced the number of notified TB cases in South Korea before and after the COVID-19 outbreak started and compared them with previous years, during which the burden of TB has been at an intermediate level.

We gathered the weekly number of newly notified TB cases for 2015–2020 from the Public Health Weekly Report released by the Korea Centers for Disease Control and Prevention. In South Korea, physicians and healthcare workers are required to report confirmed or clinically diagnosed TB to health authorities within 24 hours, irrespective of any previous history of TB treatment (*4*). The Public Health Weekly Report publishes the number of notified TB cases by province every week (*1*). In addition, the number of confirmed COVID-19 cases is posted daily on the Korea Centers for Disease Control and Prevention website (*1*).

We calculated the mean number of weekly TB notifications from the 1st through the 18th week of each year from 2015 through 2019. We also collected the

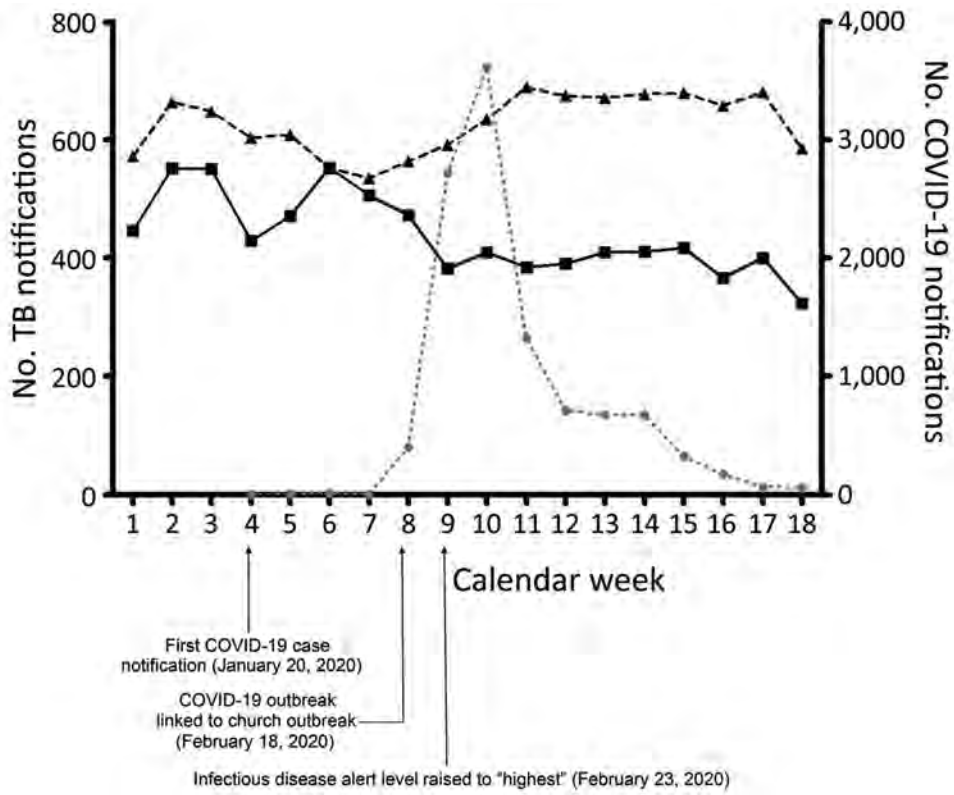

Figure. Mean weekly number of TB and COVID-19 case notifications in 2020 compared with the previous 5-year period, South Korea. Triangles indicate TB cases during 2015–2019; squares indicate TB cases during 2020; circles indicate COVID-19 cases during 2020. COVID-19, coronavirus disease; TB, tuberculosis.

weekly number of notified TB cases during the same period in 2020. We compared the number of cases before and after the highest alert level was declared (weeks 1–8 [before the COVID-19 outbreak began] and weeks 9–18 [after the COVID-19 outbreak began]). We estimated the change in the number of notified TB cases in 2020 after the COVID-19 outbreak started by comparing the latest numbers with those from previous years using a Bayesian structural time-series model (*5*). We used R statistical software version 4.0.2 (https://www.r-project.org) for all statistical analyses.

During 2015–2019, a mean number of 594 TB cases were notified weekly during weeks 1–8 and a mean number of 655 TB cases were notified weekly during weeks 9–18. In 2020, a mean of 498 TB cases were notified each week during weeks 1–8; the mean number of notifications during weeks 9–18 decreased to 390 cases/week. After COVID-19 began, TB notification decreased by 24% (121 cases/week; $p<0.01$ from the predicted number in 2020 based on a Bayesian structural time-series model) (Figure). In Daegu and Gyeongbuk Provinces, the epicenter of COVID-19 in South Korea, TB notification decreased by 23% (14 cases/week; $p = 0.003$). In other provinces, patterns were similar; TB notification decreased by 25% (112 cases/week; $p = 0.001$) after COVID-19 began (Table).

Our analysis demonstrated that the COVID-19 pandemic led to a decrease in TB notification in South Korea and that this reduction was not confined to the Daegu and Gyeongbuk Province areas. Although the

Table. Weekly mean number of TB case notifications in 2020 compared with the previous 5-year period, South Korea

Location, calendar week†	Mean no. TB cases 2015–2019	Mean no. TB cases 2020	Difference between actual and predicted cases after COVID-19 in 2020 (95% CI)
All provinces			−121 (−165 to −86)
1–8	594	498	
9–18	655	390	
Daegu and Gyeongbuk Provinces			−14 (−24 to −3)
1–8	70	57	
9–18	77	46	
Other provinces			−112 (−153 to −79)
1–8	524	441	
9–18	576	344	

*COVID-19, coronavirus disease; TB, tuberculosis.
†Weeks 1–8, before COVID-19 outbreak; weeks 9–18, after start of COVID-19 outbreak.

number of TB cases in South Korea has decreased steadily since 2010 (*6*), the 24% decrease in TB notification after COVID-19 began is larger than that predicted by our time-series model.

The reduced number of TB notifications could reflect decreased transmission associated with physical distancing and the increased use of face masks. Recent analysis proposed that physical distancing could decrease transmission of TB by 10% in high TB burden countries (*7*). However, the 24% reduction in South Korea, which has an intermediate burden of TB, suggests the additional contribution of other factors. First, during the COVID-19 outbreak, interventions such as TB contact investigation and preventive therapy may have been deprioritized and delayed (*3*). Second, patients with newly developed respiratory symptoms could not visit chest clinics easily because those patients were redirected to COVID-19 screening clinics to prevent in-hospital transmission (*8*).

The negative effect of the COVID-19 outbreak on TB has not been confined to diagnosis. In South Korea, outpatient clinics and emergency departments have been temporarily closed after patients visiting the facility have been identified as having COVID-19 (*9*). Negative-pressure units also have been prioritized for COVID-19 patients (*2*). Overall healthcare use worsens during outbreaks of communicable diseases, as demonstrated by the 10%–23% decrease in emergency department visits, even for life-threatening conditions, after COVID-19 began, as reported in the United States (*10*).

In summary, we found that TB notifications decreased significantly with the surge of COVID-19 in South Korea. Adequate measures to diagnose, control, and prevent TB, a much older and more burdensome infectious killer than COVID-19, need to be maintained during this pandemic.

About the Author

Dr. Kwak is an assistant professor and a chest physician at Seoul National University Hospital. His research interests focus on nontuberculous mycobacterial pulmonary disease and pulmonary tuberculosis.

References

1. Korea Centers for Disease Control and Prevention. Public Health Weekly Report [in Korean] [cited 2020 Jul 1]. https://www.cdc.go.kr/board/board.es?mid=a30501000000&bid=0031&cg_code=C04
2. Oh J, Lee J-K, Schwarz D, Ratcliffe HL, Markuns JF, Hirschhorn LR. National response to covid-19 in the Republic of Korea and lessons learned for other countries. Health Syst Reform. 2020;6:e1753464. https://doi.org/10.1080/23288604.2020.1753464
3. Pai M. COVID-19 coronavirus and tuberculosis: we need a damage control plan. Forbes. 2020 Mar 17 [cited 2020 Jul 1]. https://www.forbes.com/sites/madhukarpai/2020/03/17/covid-19-and-tuberculosis-we-need-a-damage-control-plan/#f72dd45295ca
4. Kim JH, Yim J-J. Achievements in and challenges of tuberculosis control in South Korea. Emerg Infect Dis. 2015;21:1913–20. https://doi.org/10.3201/eid2111.141894
5. Brodersen KH, Gallusser F, Koehler J, Remy N, Scott SL. Inferring causal impact using Bayesian structural time-series models. Ann Appl Stat. 2015;9:247–74. https://doi.org/10.1214/14-AOAS788
6. Korea Centers for Disease Control and Prevention. Annual report on the notified tuberculosis in Korea. 2019 [in Korean] [cited 2020 Jul 14]. http://tbzero.cdc.go.kr/tbzero/main.do?pageEvent=N
7. Stop TB Partnership. The potential impact of the covid-19 response on tuberculosis in high-burden countries: modelling analysis [cited 2020 Jul 1]. http://www.stoptb.org/assets/documents/news/Modeling%20Report_1%20May%202020_FINAL.pdf
8. Ministry of Health and Welfare. Republic of Korea. Guidelines for the operation of screening center for COVID-19. 8th version [in Korean] [cited 2020 Jul 1]. http://ncov.mohw.go.kr/duBoardList.do?brdId=2&brdGubun=24
9. Lee H, Heo JW, Kim SW, Lee J, Choi JH. A lesson from temporary closing of a single university-affiliated hospital owing to in-hospital transmission of coronavirus disease 2019. J Korean Med Sci. 2020;35:e145.
10. Lange SJ, Ritchey MD, Goodman AB, Dias T, Twentyman E, Fuld J, et al. Potential indirect effects of the COVID-19 pandemic on use of emergency departments for acute life-threatening conditions—United States, January–May 2020. MMWR Morb Mortal Wkly Rep. 2020;69:795–800. https://doi.org/10.15585/mmwr.mm6925e2

Address for correspondence: Jae-Joon Yim, Division of Pulmonary and Critical Care Medicine, Department of Internal Medicine, Seoul National University College of Medicine, 101 Daehak-Ro, Jongno-Gu, Seoul 110-744, South Korea; email: yimjj@snu.ac.kr

Effects of COVID-19 Prevention Measures on Other Common Infections, Taiwan

Hong-Hsi Lee, Sheng-Hsuan Lin

Author affiliations: New York University School of Medicine, New York, New York, USA (H.H. Lee); National Chiao Tung University, Hsinchu, Taiwan (S.H. Lin)

DOI: https://doi.org/10.3201/eid2610.203193

To determine whether policies to limit transmission of severe acute respiratory syndrome coronavirus 2 (SARS-CoV-2) hinder spread of other infectious diseases, we analyzed the National Health Insurance database in Taiwan. Rates of other infections were significantly lower after SARS-CoV-2 prevention measures were announced. This finding can be applied to cost-effectiveness of SARS-CoV-2 prevention.

Drawing from experience with the severe acute respiratory syndrome epidemic in 2003, the Taiwan government has established a central command system for a quick response to epidemics arising from China (*1*). Since the first confirmed case of coronavirus disease (COVID-19) in Taiwan was reported, Taiwan officials acted immediately with regard to border control, public health education (mask wearing and handwashing), ensuring adequate medical equipment, and early suspension of classes. These policies may not only reduce the spread of severe acute respiratory syndrome coronavirus 2 (SARS-CoV-2) but may also have similar effects on spread of other infectious diseases (*2*,*3*). Using nationwide weekly surveillance data (*4*), we compared the activity of common infections during 2015–2020 with the timeline of actions and policies implemented to protect against spread of SARS-CoV-2 in Taiwan.

The Taiwan National infectious Disease Statistics System (*4*) from the Taiwan Centers for Disease Control monitors emergency and outpatient visits for patients with acute infections, diagnosed according to clinical manifestations and laboratory results in 181 hospitals (covering 97.5% of emergency visits), through the National Health Insurance database and reports weekly statistical data. Using these data, we compared the number of outpatient visits for influenza, pneumonia, enterovirus infection, and scarlet fever and the number of confirmed cases of severe complicated influenza in the 2019–20 influenza season (week 40 in 2019 through week 18 in 2020; 1,931,471 cases) versus the same data for the 5 previous influenza seasons (10,688,851 total cases).

To estimate the change in outpatient visits or confirmed case numbers (hereafter called activity) after the COVID-19 outbreak (weeks 1–18 in 2020), we used a difference-in-difference regression model. The model included a categorical variable for each week, a categorical variable for each year, and the interaction variables for each week after the outbreak and for the 2019–20 season. Because of concerns about the COVID-19 pandemic, during the first quarter of 2020, the overall number of hospital visits in Taiwan dropped by 14%. We conducted a sensitivity analysis by multiplying 1/(1 – 0.14) times the number of cases for the 5 selected diseases during these periods. Institutional board review was not required because we used only deidentified, secondary statistical data for this study.

Overall infection activity was lower during the 2019–20 season than during the 5 previous seasons. For the 2019–20 season, activities of all 5 diseases notably decreased after weeks 6–7 (Figure). According to the difference-in-difference analysis, activities of influenza and severe complicated influenza were significantly lower after week 7 during the 2019–20 season than during the 5 previous seasons. Comparing the 2019–20 season with the 5 previous seasons, outpatient pneumonia activity was lower after week 8, enterovirus activity after week 16, and scarlet fever activity after week 10 (Table; Figure).

In Taiwan, infection rates for 5 selected diseases were lower in 2020 than in previous seasons. This observation correlates with implementation of actions and policies against COVID-19, such as early vigilance and taking proactive measures to prevent droplet and contact transmission in public and at schools. The effect of social distancing in Taiwan was unclear because related measures were not officially announced until the COVID-19 pandemic started subsiding in early April (*4*). These policies potentially have indirect effects on noninfectious diseases associated with acute viral infections, such as myocardial infarction and ischemic stroke (*5*,*6*). By comparing the cost of SARS-CoV-2 prevention and the effect on the economy and health during the pandemic in Taiwan and other areas, we could evaluate the cost-effectiveness of these measures and use this information to develop policies for future disease control.

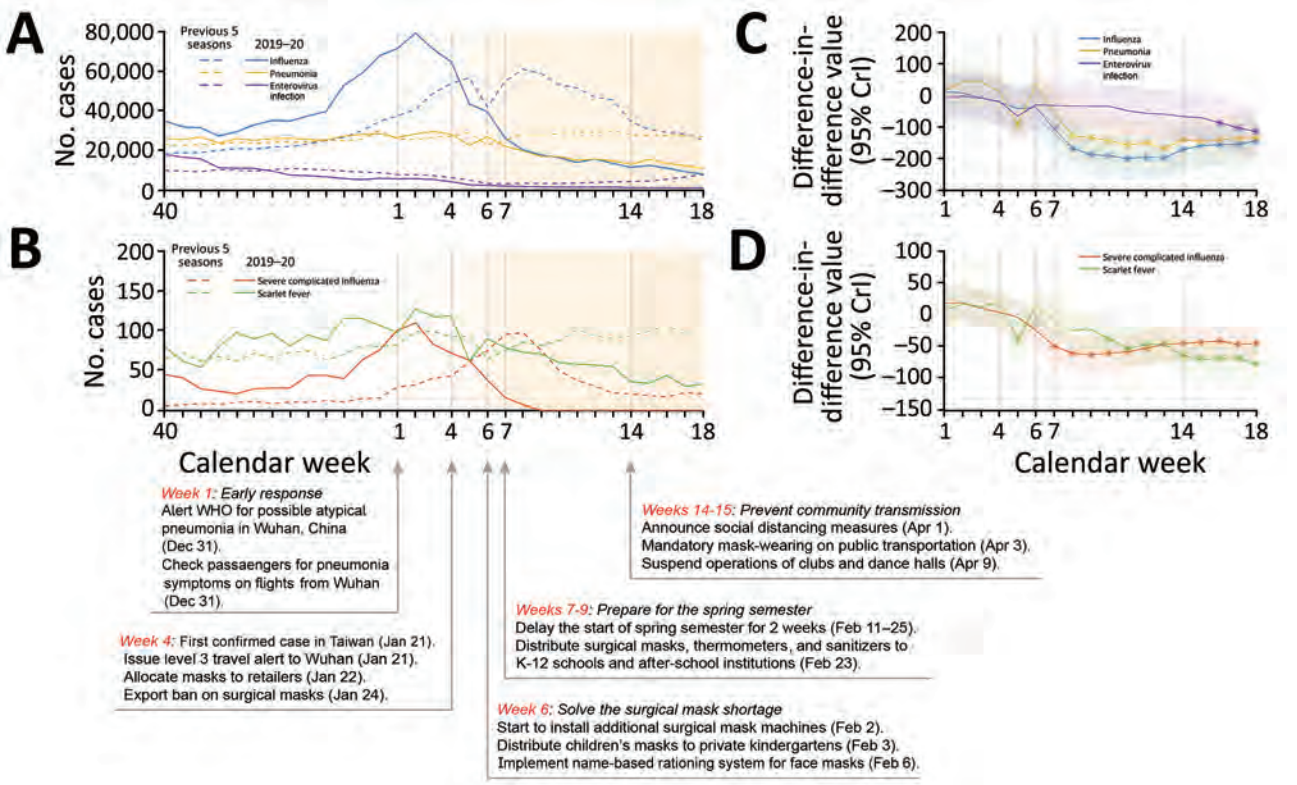

Figure. Infection activities and measures against coronavirus disease (COVID-19) in Taiwan, 2015–2020, comparing activities of influenza, severe complicated influenza, pneumonia, enterovirus infection, and scarlet fever during the 2019–20 influenza season versus the same data for the 5 previous influenza seasons by using difference-in-difference analysis. A) Number of cases of influenza, pneumonia, and enterovirus infection; B) number of cases of severe complicated influenza and scarlet fever; C) difference-in-difference value in 2020 vs. 2015–2019 (95% credible interval [CrI]) for influenza, pneumonia, and enterovirus infection; D) difference-in-difference value in 2020 vs. 2015–2019 (95% CrI) for severe complicated influenza and scarlet fever. Negative 95% CrI indicates fewer cases in the 2019–20 season than in the 5 previous seasons (p<0.05). Vertical dotted lines indicate timeline of actions and policies against COVID-19 (weeks 4, 6, 7, and 14; see panel B). WHO, World Health Organization; K-12, kindergarten through 12th grade.

Table. Statistical significance according to difference-in-difference analysis of activities of influenza, severe complicated influenza, pneumonia, enterovirus infection, and scarlet fever during the 2019–20 season versus 5 previous seasons, Taiwan, 2015–2020*

	p value				
Calendar week	Influenza	Severe complicated influenza	Pneumonia	Enterovirus	Scarlet fever
1	0.76	0.22	0.71	0.83	0.64
2	0.83	0.21	0.26	0.94	0.27
3	0.80	0.53	0.27	0.81	0.41
4	0.52	0.82	0.76	0.62	0.19
5	0.22	0.75	**0.02**	0.10	**0.005**
6	0.25	0.08	0.33	0.44	0.38
7	**0.002**	**<0.001**	0.13	0.46	0.56
8	**<0.001**	**<0.001**	**0.001**	0.38	0.09
9	**<0.001**	**<0.001**	**<0.001**	0.37	0.11
10	**<0.001**	**<0.001**	**<0.001**	0.37	**0.008**
11	**<0.001**	**<0.001**	**<0.001**	0.21	**<0.001**
12	**<0.001**	**<0.001**	**<0.001**	0.15	**0.001**
13	**<0.001**	**0.001**	**<0.001**	0.13	**0.002**
14	**<0.001**	**0.002**	**<0.001**	0.09	**<0.001**
15	**<0.001**	**0.003**	**<0.001**	0.07	**<0.001**
16	**<0.001**	**0.004**	**<0.001**	**0.03**	**<0.001**
17	**<0.001**	**0.001**	**<0.001**	**0.009**	**<0.001**
18	**<0.001**	**0.002**	**<0.001**	**0.004**	**<0.001**

*Boldface indicates significance at p<0.05.

About the Author

Dr. Lee is a postdoctoral fellow in the Department of Radiology, New York University School of Medicine. His research focuses on retrieving microstructural information of the human brain via diffusion magnetic resonance imaging techniques, segmentation and analysis of microscopy data in the brain white matter, Monte Carlo simulation of diffusion in realistic tissue microgeometry, and the medical imaging processing pipeline.

References

1. Wang CJ, Ng CY, Brook RH. Response to COVID-19 in Taiwan: big data analytics, new technology, and proactive testing. JAMA. 2020;323:1341. https://doi.org/10.1001/jama.2020.3151
2. Sakamoto H, Ishikane M, Ueda P. Seasonal influenza activity during the SARS-CoV-2 outbreak in Japan. JAMA. 2020;323:1969. https://doi.org/10.1001/jama.2020.6173
3. Kuo SC, Shih SM, Chien LH, Hsiung CA. Collateral benefit of COVID-19 control measures on influenza activity, Taiwan. Emerg Infect Dis. 2020;26:1928–30. https://dx.doi.org/10.3201/eid2608.201192
4. Taiwan Centers for Disease Control. Taiwan National Infectious Disease Statistics System [cited 2020 Jul 5]. https://nidss.cdc.gov.tw
5. Vardeny O, Madjid M, Solomon SD. Applying the lessons of influenza to coronavirus during a time of uncertainty. Circulation. 2020;141:1667–9. https://doi.org/10.1161/CIRCULATIONAHA.120.046837
6. Lindsberg PJ, Grau AJ. Inflammation and infections as risk factors for ischemic stroke. Stroke. 2003;34:2518–32. https://doi.org/10.1161/01.STR.0000089015.51603.CC

Address for correspondence: Sheng-Hsuan Lin, Assembly Building I, 1001 University Rd, Institute of Statistics, National Chiao Tung University, Hsinchu 30010, Taiwan; email: shenglin@stat.nctu.edu.tw

Macrolide-Resistant *Bordetella pertussis*, Vietnam, 2016-2017

Kazunari Kamachi,[1] Hong T. Duong, Anh D. Dang, Hai T. Do, Kentaro Koide, Nao Otsuka, Keigo Shibayama, Ha Thi Thu Hoang[1]

Author affiliations: National Institute of Infectious Diseases, Tokyo, Japan (K. Kamachi, K. Koide, N. Otsuka, K. Shibayama); National Institute of Hygiene and Epidemiology, Hanoi, Vietnam (H.T. Duong, A.D. Dang, H.T.T. Hoang); Center for Pediatric Tropical Diseases, National Hospital of Pediatrics, Hanoi (H.T. Do)

DOI: https://doi.org/10.3201/eid2610.201035

Macrolide-resistant *Bordetella pertussis* emerged in Vietnam during 2016-2017. Direct analyses of swab samples from 10 patients with pertussis revealed a macrolide-resistant mutation, A2047G, in the 23S rRNA. We identified the MT104 genotype of macrolide-resistant *B. pertussis* (which is prevalent in mainland China) and its variants in these patients.

Pertussis (whooping cough) is a highly contagious disease caused by the gram-negative bacterium *Bordetella pertussis*. Vaccination is an effective method to prevent and control pertussis, but in many countries, pertussis incidence remains despite high vaccination coverage. Macrolides are commonly used to treat pertussis, but macrolide-resistant *B. pertussis* (MRBP) strains have been observed in mainland China and Iran (*1*–*4*). In China, MRBP is isolated with increasing frequency (57.5%–91.9%) and has been since the early 2010s (*4*,*5*). Most MRBP isolates from China have a homogeneous A2047G mutation in each of the 3 copies of the 23S rRNA gene, which is associated with macrolide resistance (*1*,*3*,*4*). In contrast, MRBP is rare in Iran; the A2047G mutation is not identified in the Iran MRBP isolate (*6*). China has several reports of MRBP, but our knowledge about these bacteria in other countries in Asia is limited.

To survey MRBP in Vietnam, which neighbors China, we performed a retrospective analysis of stored DNA samples from nasopharyngeal swabs collected during 2016–2018 from 53 patients with pertussis in northern Vietnam (median age 3 months [range 31 days–32 years]; 14 patients in 2016, 38 in 2017, and 1 in 2018) (Appendix Table, https://wwwnc.cdc.gov/EID/article/26/10/20-2035-App1.pdf). Nucleic acid amplification testing was used to diagnose

[1]These authors contributed equally to this article

B. pertussis in patients who were infected with this condition. We used the cycleave real-time PCR targeting the A2047 mutation in the *B. pertussis* 23S rRNA to examine the 53 DNA samples (Appendix). Of these DNA samples, 10 (19%) were positive for the A2047G mutation. PCR-based sequencing validated the presence of the mutation (*3*). Nine of these samples were from infants 32 days–4 months of age, and 1 was from a woman 29 years of age (Table). Geographically, 7 DNA samples were found in Hanoi and 3 in other provinces (Ha Nam and Thai Binh) (Appendix Figure 1). Five patients were treated with β-lactam antimicrobial drugs; the treatments for other patients and their epidemiologic links are unknown.

We used multilocus variable-number tandem-repeat analysis (MLVA) to determine the genotypes of the MRBP by direct genotyping (*7*). We classified the MLVA profiles into the following 3 genotypes: MT104 (n = 8) and new genotypes A and B (n = 1 each) (Table). Genotypes A and B were minor single-locus variants of MT104, differing in 1 of the 6 variable-number tandem-repeat (VNTR) loci. Phylogenetic analysis revealed that the MRBP belonging to genotypes A and B were closely related to MT104 (Appendix Figure 2). We also characterized *B. pertussis* virulence–associated allelic genes (*ptxP*, *ptxA*, *prn*, and *fim3*) by DNA sequence-based typing (*7*). Of the 10 MRBP DNA samples, 9 yielded a complete profile of virulence-associated allelic genes, 8 were *ptxP1/ptxA1/prn1/fim3A*, and 1 was *ptxP1/ptxA1/prn1/fim3B* (Table). The allelic profile *ptxP1/ptxA1/prn1* is common in MRBP strains prevalent in China (*8*). In addition, 9 of the MRBP DNA samples exhibited the C5330T mutation in *fhaB3*, which is frequently observed in MRBP in China (*9*) (Appendix Table).

Genotyping assays revealed that MRBP strains in Vietnam were closely related to an MRBP strain identified in China. The major MLVA types reported recently in China are MT55, MT104, and MT195 (*8*,*9*). These types are closely related; they have only 1 difference at 1 VNTR locus. All isolates of these genotypes contained the macrolide resistance A2047G mutation in the 23S rRNA. A clinical strain of MT104-MRBP was first identified in 2012 in Shannxi, China. Subsequently, this clinical strain of MT104-MRBP was found throughout the country (*9*).

In Vietnam, the *B. pertussis* population comprises 2 major strains, MT27 and MT104 (Appendix Figure 2). The MT27 strain is common in industrialized countries but not in China (*8*,*9*). In contrast, the MT104 strain is not common in industrialized countries but frequent in China. We define a clonal complex as genotypes differing in only 1 of the 6 VNTRs. We have 2 clonal complexes in the *B. pertussis* population in Vietnam, 1 containing MT104 and genotypes A and B and another containing MT18, MT27, and MT28. MRBP genotypes A and B differ from MT104 by a single repeat at 1 VNTR locus. MRBP genotypes A and B are grouped within the clonal complex of MRBP. This finding suggests that the MRBP-MT104 strain was imported from China to Vietnam before 2016 and subsequently mutated to genotypes A and B over time. Macrolides are the third most common antimicrobial drugs used in Vietnam (*10*), and they are commonly available at private pharmacies without prescriptions, suggesting that the uncontrolled use of macrolides might have selected MRBP in the country.

In conclusion, we reported the emergence of MRBP in Vietnam during 2016-2017. We detected MRBP strains that have the same or a similar phylogenetic lineage as 1 of the MRBP strains prevalent in China. Because MRBP is a serious threat to public health, global surveillance of MRBP is needed, especially in countries in Asia.

Table. Direct genotyping of *Bordetella pertussis* with the detected macrolide-resistant A2047G mutation in the 23S rRNA gene, Vietnam, 2016–2017*

Patient no.	Age/sex	Year/province	MLVA type	Repeat no. VNTRs†	Allele type of virulence-associated genes‡				C5330 in *fhaB*§
					ptxP	*ptxA*	*prn*	*fim3*	
1	2.5 mo/M	2016/Hanoi	MT104	8/6/0/7/6/10	1	1	1	A	NA
2	2 mo/F	2016/Ha Nam	New type A	8/6/0/6/6/10	1	1	1	A	C5330T
3	32 d/F	2016/Hanoi	New type B	9/6/0/7/6/10	1	1	1	A	C5330T
4	3 mo/F	2016/Hanoi	MT104	8/6/0/7/6/10	1	1	1	A	C5330T
5	2 mo/M	2016/Hanoi	MT104	8/6/0/7/6/10	1	1	1	A	C5330T
6	29 y/F	2016/Hanoi	MT104	8/6/0/7/6/10	1	1	1	B	C5330T
7	4 mo/F	2017/Thai Binh	MT104	8/6/0/7/6/10	NA	1	1	B	C5330T
8	52 d/F	2017/Ha Nam	MT104	8/6/0/7/6/10	1	1	1	A	C5330T
9	3 mo/M	2017/Hanoi	MT104	8/6/0/7/6/10	1	1	1	A	C5330T
10	3 mo/M	2017/Hanoi	MT104	8/6/0/7/6/10	1	1	1	A	C5330T

*MLVA, multilocus variable-number tandem-repeat analysis; NA, not analyzed; VNTR, variable-number tandem-repeat.
†The order is VNTR1/VNTR3a/VNTR3b/VNTR4/VNTR5/VNTR6.
‡*B. pertussis* virulence–associated allelic genes (*ptxP*, *ptxA*, *prn*, and *fim3*).
§*fhaB3* allele carries the single-nucleotide polymorphism mutation C5330T.

This study was supported by grants for Research Program on Emerging and Re-emerging Infectious Diseases from the Japan Agency for Medical Research and Development, AMED (no. JP18fk0108049), Research on Emerging and Re-emerging Infectious Diseases from the Ministry of Health, Labor, and Welfare of Japan (19HA1001), and the Expanded Program on Immunization, Vietnam.

About the Authors

Dr. Kamachi is the chief of the Pertussis Control Laboratory at the National Institute of Infectious Diseases, Tokyo, Japan. His research interests include molecular epidemiology and virulence of *Bordetella* spp. Dr. Hoang is the head of the Bacteriology Department at the National Institute of Hygiene and Epidemiology, Hanoi, Vietnam. Her research interests include the epidemiology and molecular evolution of bacterial infectious diseases.

References

1. Wang Z, Li Y, Hou T, Liu X, Liu Y, Yu T, et al. Appearance of macrolide-resistant *Bordetella pertussis* strains in China. Antimicrob Agents Chemother. 2013;57:5193–4. https://doi.org/10.1128/AAC.01081-13
2. Shahcheraghi F, Nakhost Lotfi M, Nikbin VS, Shooraj F, Azizian R, Parzadeh M, et al. The first macrolide-resistant *Bordetella pertussis* strains isolated from Iranian patients. Jundishapur J Microbiol. 2014;7:e10880. https://doi.org/10.5812/jjm.10880
3. Wang Z, Cui Z, Li Y, Hou T, Liu X, Xi Y, et al. High prevalence of erythromycin-resistant *Bordetella pertussis* in Xi'an, China. Clin Microbiol Infect. 2014;20:O825–30. https://doi.org/10.1111/1469-0691.12671
4. Yang Y, Yao K, Ma X, Shi W, Yuan L, Yang Y. Variation in *Bordetella pertussis* susceptibility to erythromycin and virulence-related genotype changes in China (1970–2014). PLoS One. 2015;10:e0138941. https://doi.org/10.1371/journal.pone.0138941
5. Fu P, Wang C, Tian H, Kang Z, Zeng M. *Bordetella pertussis* infection in infants and young children in Shanghai, China, 2016–2017: clinical features, genotype variations of antigenic genes and macrolides resistance. Pediatr Infect Dis J. 2019;38:370–6. https://doi.org/10.1097/INF.0000000000002160
6. Mirzaei B, Bameri Z, Babaei R, Shahcheraghi F. Isolation of high level macrolide resistant *Bordetella pertussis* without transition mutation at domain V in Iran. Jundishapur J Microbiol. 2015;8:e18190. https://doi.org/10.5812/jjm.8(5)2015.18190
7. Moriuchi T, Vichit O, Vutthikol Y, Hossain MS, Samnang C, Toda K, et al. Molecular epidemiology of *Bordetella pertussis* in Cambodia determined by direct genotyping of clinical specimens. Int J Infect Dis. 2017;62:56–8. https://doi.org/10.1016/j.ijid.2017.07.015
8. Li L, Deng J, Ma X, Zhou K, Meng Q, Yuan L, et al. High prevalence of macrolide-resistant *Bordetella pertussis* and *ptxP1* genotype, mainland China, 2014–2016. Emerg Infect Dis. 2019;25:2205–14. https://doi.org/10.3201/eid2512.181836
9. Xu Z, Wang Z, Luan Y, Li Y, Liu X, Peng X, et al. Genomic epidemiology of erythromycin-resistant *Bordetella pertussis* in China. Emerg Microbes Infect. 2019;8:461–70. https://doi.org/10.1080/22221751.2019.1587315
10. Global Antibiotic Resistance Partnership. The GARP-Vietnam National Working Group. Situation analysis: antibiotic use and resistance in Vietnam [cited 2020 July 7th]. https://cddep.org/wp-content/uploads/2017/06/vn_report_web_1_8.pdf

Address for correspondence: Kazunari Kamachi, Department of Bacteriology II, National Institute of Infectious Diseases, 4-7-1 Gakuen, Musashimurayama, Tokyo 208-0011, Japan; email: kamachi@nih.go.jp

COVID-19 in Patient with Sarcoidosis Receiving Long-Term Hydroxychloroquine Treatment, France, 2020

François Bénézit, Audrey Le Bot, Stéphane Jouneau, Florian Lemaître, Charlotte Pronier, Pierre-Axel Lentz, Solène Patrat-Delon, Matthieu Revest, Vincent Thibault, Pierre Tattevin

Author affiliation: Pontchaillou University Hospital, Rennes, France

DOI: https://doi.org/10.3201/eid2610.201816

Because of in vitro studies, hydroxychloroquine has been evaluated as a preexposure or postexposure prophylaxis for coronavirus disease (COVID-19) and as a possible COVID-19 curative treatment. We report a patient with sarcoidosis who was receiving long-term hydroxychloroquine treatment and contracted COVID-19, despite adequate plasma concentrations.

Because of in vitro studies suggesting potential activity on severe acute respiratory syndrome coronavirus 2 (SARS-CoV-2) (*1*,*2*), hydroxychloroquine has been one of the main candidate drugs evaluated for coronavirus disease (COVID-19), both as a curative treatment and as preexposure or postexposure prophylaxis. We report a case of COVID-19 in a patient receiving long-term hydroxychloroquine treatment despite plasma concentrations within the therapeutic range for autoimmune diseases, such as systemic lupus erythematosus.

A 40-year-old man was admitted to Pontchaillou University Hospital, Rennes, France, for treatment of COVID-19. His medical history was remarkable only for pulmonary sarcoidosis, diagnosed in 2015; it was well controlled with hydroxychloroquine (200 mg 2×/d) with no other immunomodulatory drugs and no adherence issues. Twelve days before admission, he had received a diagnosis of COVID-19 in the outpatient department after a 4-day course of cough, myalgia, and low-grade fever. He had positive results by PCR for SARS-CoV-2 on a nasopharyngeal sample (RdRp gene; Pasteur COV_IP2/4, Paris, France; https://www.who.int/docs/default-source/coronaviruse/real-time-rt-pcr-assays-for-the-detection-of-sars-cov-2-institut-pasteur-paris.pdf?sfvrsn=3662fcb6_2). Physical examination was unremarkable except for a body temperature of 37.8°C. He was not admitted to the hospital at that time and was advised to continue his long-term treatment with hydroxychloroquine. His symptoms initially improved, but he developed shortness of breath with minimal exertion starting on day 14 of symptoms, gradually worsening over the next 2 days. He was admitted on day 16 because of constant shortness of breath and thoracic pain.

At admission, the patient's body temperature was 36.6°C, heart rate was 82 beats/min, respiratory rate 20 breaths/min, blood pressure 115/72 mm Hg, and arterial oxygen saturation 96% while breathing room air. Lung auscultation revealed diffuse, fine crackles. Trough hydroxycholoroquine plasma concentration was 0.9 μg/mL (therapeutic range for autoimmune diseases 0.3–1.0 μg/mL). Thoracic computed tomography (CT) scan with pulmonary angiography ruled out pulmonary embolism but revealed diffuse ground-glass opacities, superimposed on the baseline sarcoidosis lesions (Figure). Electrocardiogram and serum troponin level were unremarkable. He was treated with prophylactic enoxaparin (60 mg 1×/d) and was discharged on day 18. Because he was afebrile and his condition improved shortly after admission, no additional workup for secondary pneumonia was performed, and he received no antibacterial treatment. All symptoms finally resolved, except for minor asthenia and cough (last follow-up at 40 days after discharge).

This observation of COVID-19 with diffuse interstitial pneumonia requiring hospital admission in a patient on long-term hydroxychloroquine treatment suggests that hydroxychloroquine may not be as effective as suggested by in vitro data. This patient had always been considered highly adherent to his medications, which was confirmed by therapeutic drug monitoring. Because plasma concentration was within therapeutic range by the time the patient was admitted, the failure of hydroxychloroquine to prevent COVID-19 cannot be attributed to underdosage or suboptimal adherence. Two recent studies suggested that hydroxychloroquine provides no protection against COVID-19 in patients with a broad range of autoimmune diseases from New York, USA (*3*), and in patients with systemic lupus erythematosus from France (*4*). The case we present is unique in that the patient was not receiving any immunomodulatory agent other than hydroxychloroquine.

Our observations have limitations. First, no CT scan was performed during the first visit, and no nasopharyngeal PCR was performed at the second visit. However, this patient was managed in line with the recommendations in France and most other countries

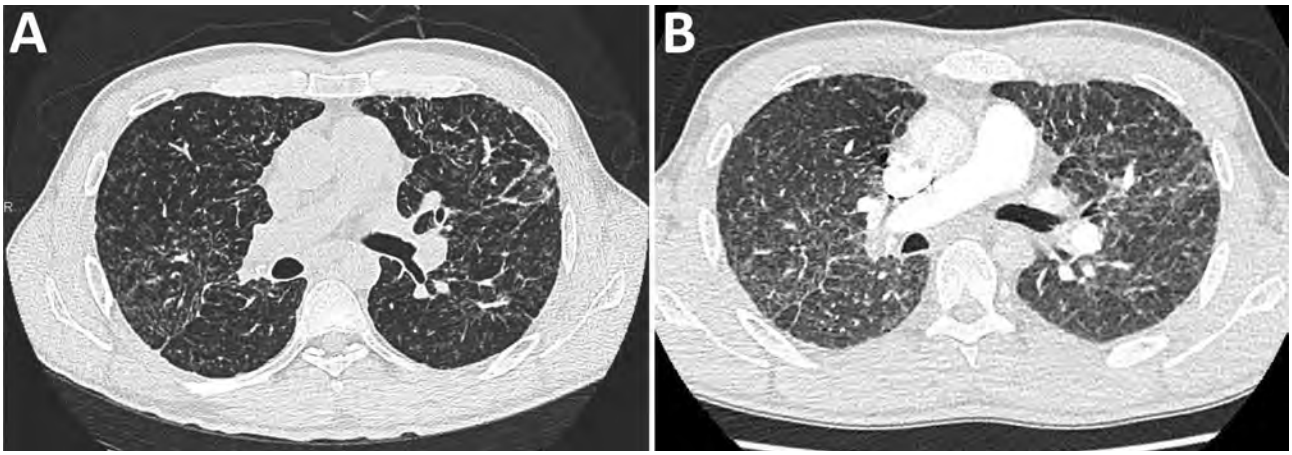

Figure. Computed tomography (CT) scans of a coronavirus disease (COVID-19) patient with sarcoidosis who had been receiving long-term hydroxychloroquine treatment, France. A) Thoracic CT scan from November 2019, showing baseline pulmonary sarcoidosis lesions. B) Thoracic CT scan performed April 4, 2020, showing diffuse ground-glass opacities characteristic of COVID-19.

by that time. For the first visit, CT scan was not indicated because the diagnosis was obtained otherwise (positive PCR), and the patient had no criteria for admission; at the second visit, there was no indication to repeat PCR because it would have had no effect on the diagnosis or the management of the patient, and access to these tests was restricted. Second, the optimal dosing of hydroxychloroquine has not been defined for COVID-19; recent reports have suggested that target plasma concentrations should be 1–2 μg/mL in this population, based on chloroquine or hydroxychloroquine concentrations required to observe the virustatic effect in vitro and in silico (0.3–2.1 μg/mL) and toxic concentrations in humans (starting from 2 μg/mL) (*1*,*5*). Thus, the hydroxychloroquine plasma therapeutic range for autoimmune diseases may not be appropriate for the treatment of COVID-19: a dosage of 400 mg twice daily for 1 day, followed by 200 mg twice daily for another 4 days, has been recommended based on pharmacokinetic/pharmacodynamic data (*1*). Third, plasma concentration within the therapeutic range does not ensure that therapeutic concentrations are obtained in the lungs, the primary target for SARS-CoV-2.

Previous studies on hydroxychloroquine use during COVID-19 have found contradictory results, but they were all limited by small sample size, heterogenous hydroxychloroquine dosages, no or limited therapeutic drug monitoring, or methodological flaws (*6*). Ongoing randomized trials should resolve the ongoing controversy.

About the Author

Dr. Bénézit is an infectious diseases physician at the Pontchaillou University Hospital in Rennes, France. His primary interests include respiratory viruses and emerging infectious diseases.

References

1. Yao X, Ye F, Zhang M, Cui C, Huang B, Niu P, et al. In vitro antiviral activity and projection of optimized dosing design of hydroxychloroquine for the treatment of severe acute respiratory syndrome coronavirus 2 (SARS-CoV-2). Clin Infect Dis. 2020 Mar 9 [Epub ahead of print]. https://doi.org/10.1093/cid/ciaa237
2. Liu J, Cao R, Xu M, Wang X, Zhang H, Hu H, et al. Hydroxychloroquine, a less toxic derivative of chloroquine, is effective in inhibiting SARS-CoV-2 infection in vitro. Cell Discov. 2020;6:16. http://dx.doi.org/10.1038/s41421-020-0156-0
3. Haberman R, Axelrad J, Chen A, Castillo R, Yan D, Izmirly P, et al. Covid-19 in Immune-Mediated Inflammatory Diseases—Case Series from New York. N Engl J Med. 2020 Apr 29 [Epub ahead of print]. https://doi.org/10.1056/NEJMc2009567
4. Mathian A, Mahevas M, Rohmer J, Roumier M, Cohen-Aubart F, Amador-Borrero B, et al. Clinical course of coronavirus disease 2019 (COVID-19) in a series of 17 patients with systemic lupus erythematosus under long-term treatment with hydroxychloroquine. Ann Rheum Dis. 2020 Apr 24 [Epub ahead of print]. https://doi.org/10.1136/annrheumdis-2020-217566
5. Perinel S, Launay M, Botelho-Nevers É, Diconne É, Louf-Durier A, Lachand R, et al. Towards optimization of hydroxychloroquine dosing in intensive care unit COVID-19 patients. Clin Infect Dis. 2020 Apr 7 [Epub ahead of print]. https://doi.org/10.1093/cid/ciaa394
6. Yazdany J, Kim AHJ. Use of hydroxychloroquine and chloroquine during the COVID-19 pandemic: what every clinician should know. Ann Intern Med. 2020 Mar 31 [Epub ahead of print]. https://doi.org/10.7326/M20-1334

Address for correspondence: Pierre Tattevin, Infectious Diseases and Intensive Care Unit, Pontchaillou University Hospital, 2 rue Henri Le Guilloux, 35033 Rennes CEDEX 9, France; email: pierre.tattevin@chu-rennes.fr

Inappropriate Administration of Rabies Postexposure Prophylaxis, Cook County, Illinois, USA

Hannah D. Steinberg, Kelley Bemis, Mabel M. Frias, Demian Christiansen

Author affiliations: Cook County Department of Public Health, Forest Park, Illinois, USA (H.D. Steinberg, K. Bemis, M.M. Frias, D. Christiansen); Council of State and Territorial Epidemiologists, Atlanta, Georgia, USA (H.D. Steinberg)

DOI: https://doi.org/10.3201/eid2610.200232

Administration of rabies postexposure prophylaxis (PEP) is expensive and time-consuming. In suburban Cook County, Illinois, USA, administration of 55.5% of PEP treatments did not follow Advisory Committee on Immunization Practices guidelines. Health department consultation lowered the odds of inappropriate PEP administration by 87%. Providers should consult their health department before prescribing PEP.

Rabies is typically fatal to unvaccinated patients; however, the prompt administration of postexposure prophylaxis (PEP) can prevent disease onset (*1*).

When a patient is exposed to a potentially rabid animal, that patient's physician must determine whether administration of PEP is prudent. The Advisory Committee on Immunization Practices (ACIP) publishes guidelines indicating when physicians should administer PEP (*1,2*). Lack of adherence to these guidelines might result in unnecessary costs and medical risks (e.g., injection site reactions, systemic hypersensitivity reactions) (*1,3*). In the United States, a full course of PEP (usually 4 vaccine doses and 1 immunoglobulin dose [*2*]) costs $3,800 on average (*4*). In Illinois, the patient, their insurance provider, or both pay for PEP. Illinois physicians must report PEP initiation to local public health departments (*5*).

We retrospectively evaluated patients who received PEP in suburban Cook County, Illinois, during 2015–2018 and were reported to the Cook County Department of Public Health (CCDPH). Although Chicago is in Cook County, it has its own health department and was therefore not included in this study. We used a multivariable logit link generalized estimating equation model (*6*) to evaluate predictors of inappropriate PEP administration according to ACIP guidelines. We analyzed factors such as patient age, patient sex, area of residence, exposing animal species, and whether a state or local health department was consulted before PEP initiation. We controlled for clustering by exposure incident (i.e., multiple persons exposed to the same animal) by using robust variance estimators and assuming an independent correlation structure. We conducted statistical analyses in R version 3.5.3 (*7*) and ran models using geepack version 1.2–1 (*6*). Because the purpose of this study was to evaluate and inform public health practices, it was not considered human subjects research by the Cook County Health Office of Research and Regulatory Affairs and was exempt from institutional board review.

During 2015–2018, a total of 656 residents initiated PEP. We excluded 45 cases because of missing data; these cases were proportionally distributed in time and geographic area. Of the 611 patients, 339 (55.5%) did not meet ACIP guidelines for potential rabies exposures (Table), a proportion that aligns with previously reported ranges in other US jurisdictions (*8*). The 5 most common reasons for inappropriate PEP administration: 1) the patient had a bat in their home but no known contact with the bat and the patient did not wake to the bat in their room (187 persons); 2) PEP was given after a provoked bite from a dog or cat with no signs of rabies (85 persons); 3) the animal involved was available for confinement or testing (18 persons); 4) the patient had no known animal contact (17 persons); and 5) the animal involved tested negative for rabies (16 persons).

Table. PEP recipients and factors associated with inappropriate administration of PEP, suburban Cook County, IL, 2015–2018*

Variable	Total, no. (%), n = 611	Exposure met ACIP guidelines for PEP administration, no. (%)		Unadjusted GEE model† OR (95% CI)	Adjusted GEE model‡ aOR (95% CI)
		Yes, n = 272	No, n = 339		
District§					
North	309 (50.6)	125 (45.9)	184 (54.3)	Referent	Referent
West	131 (21.4)	54 (19.9)	77 (22.7)	0.97 (0.52–1.80)	0.76 (0.39–1.47)
Southwest	82 (13.4)	47 (17.3)	35 (10.3)	0.51 (0.27–0.94)	0.41 (0.20–0.83)
South	89 (14.6)	46 (16.9)	43 (12.7)	0.64 (0.35–1.15)	0.52 (0.27–0.98)
Age, y					
0–5	47 (7.7)	24 (8.8)	23 (6.8)	0.84 (0.44–1.62)	0.74 (0.36–1.50)
6–17	170 (27.8)	64 (23.5)	106 (31.3)	1.46 (0.92–2.32)	1.49 (0.90–2.45)
18–25	50 (8.2)	23 (8.5)	27 (8.0)	1.03 (0.55–1.94)	1.20 (0.53–2.72)
≥26	344 (56.3)	161 (59.2)	183 (54.0)	Referent	Referent
Sex					
F	317 (51.9)	131 (48.2)	186 (54.9)	Referent	Referent
M	294 (48.1)	141 (51.8)	153 (45.1)	0.76 (0.53–1.10)	0.77 (0.51–1.15)
Exposing animal					
Bat	393 (64.3)	181 (66.5)	212 (62.5)	Referent	Referent
Cat	35 (5.7)	6 (2.2)	29 (8.6)	4.13 (1.62–10.50)	4.15 (1.49–11.60)
Dog	111 (18.2)	39 (14.3)	72 (21.2)	1.58 (0.91–2.72)	2.05 (1.07–3.96)
Raccoon	31 (5.1)	26 (9.6)	5 (1.5)	0.16 (0.06–0.45)	0.19 (0.06–0.57)
Other	41 (6.7)	20 (7.4)	21 (6.2)	0.90 (0.45–1.79)	0.93 (0.43–2.01)
HD consult¶					
Yes	183 (30.0)	138 (50.7)	45 (13.3)	0.15 (0.09–0.23)	0.13 (0.08–0.22)
No	428 (70.0)	134 (49.3)	294 (86.7)	Referent	Referent

*ACIP, Advisory Committee on Immunization Practices; aOR, adjusted odds ratio; GEE, generalized estimating equation; HD, health department; PEP, rabies postexposure prophylaxis; OR, odds ratio.
†Bivariate GEE model for PEP inappropriateness as a function of the given categorical variable.
‡Multivariable GEE model for PEP inappropriateness as a function of all the predictors included in the table.
§Suburban Cook County residential district of patient's home address.
¶Whether healthcare provider contacted a state or local health department to discuss appropriateness of PEP.

The results of the generalized estimating equation model showed that provider consultation with the health department, species of the exposing animal, and patient area of residence were factors associated with appropriate administration of PEP (Table). The most protective factor against inappropriate PEP administration was a health department consultation, a service CCDPH offers free of charge 24 hours a day, 7 days a week. After adjusting for patient age, sex, area of residence, and exposing animal, we found patients who received PEP were 87% less likely to have received inappropriate treatment if their healthcare provider consulted a health department (adjusted odds ratio [aOR] 0.13, 95% CI 0.08–0.22). Because 428 patients (70.0%) received PEP without health department consultation, this service could be used to reduce the unnecessary administration of PEP.

Certain animal species were also associated with inappropriate PEP administration. We found greater odds of inappropriate PEP administration associated with exposure to dogs (aOR 2.05, 95% CI 1.07–3.96) and cats (aOR 4.15, 95% CI 1.49–11.60) than bats. Exposure to raccoons was associated with reduced odds of inappropriate PEP administration (aOR 0.19, 95% CI 0.06–0.57) (Table). The reason for this pattern might be that ACIP guidelines are more complicated for domestic than wild animal exposures (e.g., determining whether a bite was provoked). Health departments can assist providers with these determinations before initiating PEP.

Patient residential district was associated with inappropriate PEP administration, whereas patient age and sex were not (Table). This finding suggests additional local factors might exist, such as differences in wealth, cost-aversion, or rabies awareness, for which we did not control in our estimates.

PEP is an expensive and time-consuming treatment. Although clinicians should encourage PEP for patients with potential exposures to rabies, they should avoid it when risk for rabies does not exist (*1*). Health departments around the United States follow the ACIP guidelines for recommending PEP (*1*,*2*) and have unique knowledge of their local rabies epidemiology. Providers should consider the benefits and risks of PEP and consult their health department before prescribing PEP.

This study was supported in part by an appointment to the Applied Epidemiology Fellowship Program administered by the Council of State and Territorial Epidemiologists and funded by the Centers for Disease Control and Prevention (cooperative agreement no. 1 NU38OT000297-01-00).

About the Author

Ms. Steinberg is a participant in the Council of State and Territorial Epidemiologists Applied Epidemiology Fellowship Program. Her research interests include infectious disease dynamics and social determinants of health.

References

1. Manning SE, Rupprecht CE, Fishbein D, Hanlon CA, Lumlertdacha B, Guerra M, et al.; Advisory Committee on Immunization Practices Centers for Disease Control and Prevention. Human rabies prevention—United States, 2008: recommendations of the Advisory Committee on Immunization Practices. MMWR Recomm Rep. 2008;57:1–28.
2. Rupprecht CE, Briggs D, Brown CM, Franka R, Katz SL, Kerr HD, et al.; Centers for Disease Control and Prevention. Use of a reduced (4-dose) vaccine schedule for postexposure prophylaxis to prevent human rabies: recommendations of the Advisory Committee on Immunization Practices. MMWR Recomm Rep. 2010;59:1–9.
3. Christian KA, Blanton JD, Auslander M, Rupprecht CE. Epidemiology of rabies post-exposure prophylaxis—United States of America, 2006–2008. Vaccine. 2009;27:7156–61. https://doi.org/10.1016/j.vaccine.2009.09.028
4. Centers for Disease Control and Prevention. Cost of rabies prevention. 2019 [cited 2019 Jul 16]. https://www.cdc.gov/rabies/location/usa/cost.html
5. Illinois General Assembly-Joint Committee on Administrative Rules. Illinois administrative code, title 77, part 690, section 690.601: rabies, potential human exposure and animal rabies. 2014 [cited 2019 Jul 16]. http://www.ilga.gov/commission/jcar/admincode/077/077006900D06010R.html
6. Halekoh U, Højsgaard S, Yan J. The R package geepack for generalized estimating equations. J Stat Softw. 2006;15. https://doi.org/10.18637/jss.v015.i02
7. R Core Team. R: a language and environment for statistical computing. Vienna (Austria): R Foundation for Statistical Computing; 2019.
8. Moran GJ, Talan DA, Mower W, Newdow M, Ong S, Nakase JY, et al.; Emergency ID Net Study Group. Appropriateness of rabies postexposure prophylaxis treatment for animal exposures. JAMA. 2000;284:1001–7. https://doi.org/10.1001/jama.284.8.1001

Address for correspondence: Demian Christiansen, Cook County Department of Public Health, 7556 W Jackson Blvd, Forest Park, IL 60130, USA; email: dchristiansen@cookcountyhhs.org

Mycobacterium leprae on Palatine Tonsils and Adenoids of Asymptomatic Patients, Brazil

Marilda Aparecida Milanez Morgado de Abreu,[1] Gisele Alborghetti Nai, Juliana D'Andrea Molina, Rafael Tomaz Gomes, Natalia de Paula, Ana Maria Roselino[1]

Author affiliations: Regional Hospital, Presidente Prudente, Brazil (M.A.M. Morgado de Abreu, R.T. Gomes); University of Oeste Paulista, Presidente Prudente (M.A.M. Morgado de Abreu, G.A. Nai, J.A. Molina); and University of São Paulo, Ribeirão Preto, Brazil (N. de Paula, A.M. Roselino).

DOI: https://doi.org/10.3201/eid2610.191267

We investigated palatine tonsil and adenoid specimens excised from otorhinolaryngological patients in a leprosy-endemic region of Brazil. Fite-Faraco staining identified *Mycobacterium* spp. in 9 of 397 specimen blocks. Immunohistochemistry and molecular analysis confirmed the presence of *Mycobacterium leprae*, indicating that these organs can house *M. leprae* in persons inhabiting a leprosy-endemic region.

Leprosy is a chronic infectious disease caused by *Mycobacterium leprae* that especially affects skin and peripheral nerves (*1*). In 2018, the registered global prevalence in the 6 World Health Organization regions was 184,238 cases (0.24/10,000 population), showing a decrease of 8,475 cases over the previous year (*2*). Although its incidence in Brazil has declined during 2009–2018, leprosy continues to be a major public health problem at the national level (*1*). Reports of *M. leprae* resistance against antimicrobial drugs used in multidrug therapy raise concern about the future of leprosy treatment (*2*). Therefore, not only does leprosy persist, but the emergence of multidrug-resistant *M. leprae* is a potential threat to global public health (*3*,*4*).

Although the exact mode of leprosy transmission is not known, it is thought that the upper respiratory tract, in particular the nasal mucosa, is the usual site of primary infection (*3*). Because we have previously identified *M. leprae* in oral mucosa of leprosy patients (*5*), we aimed to investigate other anatomic sites that could host this microorganism to clarify the epidemiology and transmission mechanisms of leprosy.

In this study, we hypothesized that *M. leprae*, after penetration through the airway mucosa, could infect the palatine tonsils and adenoids, because these organs represent the first immune defense line against inhaled or ingested antigens (*6*). We also theorized that if leprosy is a highly contagious disease (*1*), a considerable part of the population in endemic regions might be infected with *M. leprae*.

We conducted a cross-sectional study of 397 paraffin-embedded blocks of palatine tonsils and adenoids extracted from 144 patients due to otorhinolaryngological indication during 2011–2016 at the Regional Hospital, Presidente Prudente, Brazil. The local Research Ethics Committee approved the study (protocol #1.920.994).

Microscopic analysis using hematoxylin-eosin staining did not reveal granulomas. We analyzed 50 fields in the 100× objective (1,000× magnification) per slide stained with Fite-Faraco; of the positive cases (9 [2.3%] slides from 8 [5.6%] patients, 6 men and 2 women [mean age 11 ± 5.5 years]), we observed only 1 acid-fast rod per slide. We studied all the blocks of these 8 patients, a total of 20 blocks (Table).

Immunohistochemistry with 1:20,000 anti–phenolic glycolipid-I (anti-PGL-I) antibody (Bei Resources, https://www.beiresources.org), specific for *M. leprae*, was conducted with the Mach 1 polymer-based biotin-free detection kit (Biocare Medical, https://biocare.net) (*5*). We used deparaffinized skin sections from multibacillary leprosy as positive control. For the negative control, we omitted the antibody. To confirm specificity, we used deparaffinized skin sections from paucibacillary leprosy and atopic dermatitis (excluding inflammatory cell recognition by the antibody), normal human scalp, and tuberculous lung section.

We extracted DNA from paraffin sections with isopropanol-ammonium acetate (*1*). The resulting DNA was used in conventional PCR with sense 5′-ATTTCTGCCGCTGGTATCGGT-3′ and antisense 5′-TGCGCTAGAAGGTTGCCGTAT-3′ primers (ThermoFisher Scientific, https://www.thermofisher.com) to amplify *M. leprae* microsatellite sequences, according to a previous report (*7*). We assessed amplicons of 148 bp on 2% agarose gel. The assays included negative (DNA omission) and positive (DNA from multibacillary leprosy skin sample) controls. We confirmed specificity with DNA extracted from *M. tuberculosis* culture. In addition, we conducted PCR with TB1/TB2 primers to detect *Mycobacterium* spp. and with T4/T5 primers to detect *M. tuberculosis* (*5*).

Immunohistochemistry was positive in 18/20 (90%) blocks. By PCR, 19 (95%) were positive with RLEP and 5 were simultaneously positive with TB1/TB2; all 19 positive by PCR were negative by T4/T5

[1]These authors contributed equally to this article.

Table. Patient data and results of Fite-Faraco staining, immunohistochemistry with anti–PGL-I antibody, and PCR assays in study of *Mycobacterium leprae* on palatine tonsils and adenoids, Brazil, 2019*

Patient no.	Age, y/sex	Lymphoid organ	Fite-Faraco stain	IHC anti–PGL-I	PCR RLEP	*M. leprae* identification by DNA sequencing, %
1	20/F	AD	+	+	+	ND
2	19/M	RPT	+	+	+	ND
		LPT	–	+	+	ND
3	10/M	RPT	+	+	+	100
		LPT	–	+	+	ND
4	9/M	RPT	–	+	+	ND
		LPT	+	+	+	99
		AD	+	+	+	ND
5	7/M	RPT	–	+	+	ND
		LPT	+	+	+	ND
		AD	–	+	+	ND
6	4/M	RPT	–	+	+	ND
		LPT	+	+	+	99
		AD	–	–	+	ND
7	13/F	RPT	+	+	+	98
		LPT	–	+	+	ND
		AD	–	+	+	ND
8	6/M	RPT	–	–	–	ND
		LPT	+	+	+	ND
		AD	–	+	+	98
Total positive results			9	18	19	

*AD, adenoid; PGL-I, phenolic glycolipid I; IHC, immunohistochemistry; LPT, left palatine tonsil; ND, not determined; RLEP, *M. leprae* repetitive DNA sequence; RPT, right palatine tonsil; –, negative; +, positive.

primers. Samples that tested negative in IHC or PCR were also negative in Fite-Faraco staining (Table).

Little attention has been paid to the role that mucosa-associated lymphoid tissue (MALT) plays in the mechanisms used by mycobacteria during host invasion. In tuberculosis infection, bacilli cross mucous membranes and penetrate into palatine tonsils and adenoids, where they initiate an immune response. However, bacilli may develop immune-evasion strategies and disseminate into the organism or return to the mucosa surface and be eliminated to the environment (*8*). This process might also occur in leprosy, but to our knowledge there are no reports on this subject.

Our results corroborate the hypothesis that *M. leprae* bacilli infect palatine tonsils and adenoids. Prospective studies with a larger population group are necessary to clarify these findings. We could not infer from this retrospective study with paraffinized samples whether patients who had positive results for *M. leprae* identification had leprosy or were asymptomatic carriers. In both clinical scenarios, however, our findings indicate that palatine tonsils and adenoids may represent reservoirs for *M. leprae* bacilli in persons inhabiting a leprosy-endemic region.

Acknowledgments

We thank Sandra Rodrigues and Aline Turatti for their technical laboratory assistance.

The Paulista Foundation against Leprosy provided partial research support.

About the Author

Dr. Morgado de Abreu is a professor and coordinator at the program of specialization in dermatology, Regional Hospital and University of Oeste Paulista, Presidente Prudente. Her research interests include infectious diseases, with emphasis on the epidemiology and mechanisms of leprosy transmission.

References

1. Lastória JC, Abreu MA. Leprosy: review of the epidemiological, clinical, and etiopathogenic aspects—part 1. An Bras Dermatol. 2014;89:205–18. https://doi.org/10.1590/abd1806-4841.20142450
2. World Health Organization. Global leprosy update, 2018: moving towards a leprosy-free world. WER No. 35/36. Wkly Epidemiol Rec. 2019;94:389–412.
3. Levis W, Rendini T, Martiniuk F. Increasing virulence in leprosy indicated by global *Mycobacterium* spp. Emerg Infect Dis. 2018;24:183a–184. https://doi.org/10.3201/eid2401.171785
4. Cambau E, Saunderson P, Matsuoka M, Cole ST, Kai M, Suffys P, et al.; WHO surveillance network of antimicrobial resistance in leprosy. Antimicrobial resistance in leprosy: results of the first prospective open survey conducted by a WHO surveillance network for the period 2009–15. Clin Microbiol Infect. 2018;24:1305–10. https://doi.org/10.1016/j.cmi.2018.02.022
5. Morgado de Abreu MAM, Roselino AM, Enokihara M, Nonogaki S, Prestes-Carneiro LE, Weckx LLM, et al. *Mycobacterium leprae* is identified in the oral mucosa from paucibacillary and multibacillary leprosy patients. Clin Microbiol Infect. 2014;20:59–64. https://doi.org/10.1111/1469-0691.12190
6. Brandtzaeg P. Immunology of tonsils and adenoids: everything the ENT surgeon needs to know. Int J Pediatr Otorhinolaryngol. 2003;67(Suppl 1):S69–76. https://doi.org/10.1016/j.ijporl.2003.08.018

7. Azevedo MC, Ramuno NM, Fachin LR, Tassa M, Rosa PS, Belone AF, et al. qPCR detection of *Mycobacterium leprae* in biopsies and slit skin smear of different leprosy clinical forms. Braz J Infect Dis. 2017;21:71–8. https://doi.org/10.1016/j.bjid.2016.09.017
8. Lugton I. Mucosa-associated lymphoid tissues as sites for uptake, carriage and excretion of tubercle bacilli and other pathogenic mycobacteria. Immunol Cell Biol. 1999;77:364–72. https://doi.org/10.1046/j.1440-1711.1999.00836.x

Address for correspondence: Marilda A.M. Morgado de Abreu, rua São Paulo, 1949, centro, CEP 17900-000, Dracena, SP, Brazil; email: marilda@morgadoeabreu.com.br

Fatal *Chlamydia avium* Infection in Captive Picazuro Pigeons, the Netherlands

Marja Kik, Marloes Heijne, Jooske IJzer, Guy Grinwis, Yvonne Pannekoek, Andrea Gröne

Author affiliations: Utrecht University, Utrecht, the Netherlands (M. Kik, J. IJzer, G. Grinwis, A. Gröne); Wageningen Bioveterinary Research, Lelystad, the Netherlands (M. Heijne); University of Amsterdam, Amsterdam, the Netherlands (Y. Pannekoek)

DOI: https://doi.org/10.3201/eid2610.191412

In 2016, an outbreak of *Chlamydia avium* infection occurred among Picazuro pigeons (*Patagioenas picazuro*) living in an aviary in the Netherlands. Molecular typing revealed a unique strain of *C. avium*. Our findings show that *C. avium* infection, which usually causes subclinical infection, can cause fatal disease in pigeons.

Until approximately 2014, *Chlamydia psittaci* was the only *Chlamydia* species detected in birds. Researchers have catalogued ≈465 bird species affected by this pathogen, which mainly causes subclinical infections but sometimes results in acute disease and death (*1*). In humans, *C. psittaci* is highly infectious and can cause severe pneumonia. *Chlamydia* bacteria, which are present in (dried) excreta or feather dust, are transmitted through direct contact or inhalation. In 2014, researchers proposed 2 new members of *Chlamydiaceae*: *C. avium* and *C. gallinacea* (*2*). *C. avium* affects pigeons and psittacine birds, whereas *C. gallinacea* affects poultry. Most *C. avium* and *C. gallinacea* infections in birds are subclinical, and the zoonotic potential of these species is unknown (*3*).

In 2016, an outbreak of *C. avium* infection occurred among 11 Picazuro pigeons (*Patagioenas picazuro*) housed in an aviary with other bird species in the Netherlands. The birds lost weight, had ruffled feathers, and were anorexic. Despite treatment with fluids, force-feeding, and in 1 bird, doxycycline treatment (50 mg/kg 1×/d), all 11 animals died or were euthanized. Necropsy revealed that 9 of these birds were in poor physical condition, lacking fat and pectoral muscle mass. The livers and spleens were enlarged; the livers extended an average of 0.5 cm beyond the rear edge of the sternum, whereas the mean diameter of the spleens was 1.0 cm, approximately twice as large as the normal size. We suspected *Chlamydia* infection because of intracellular inclusions in Stamp (modified Ziehl Neelsen)–stained cytology of liver and spleen. We found multifocal heterophilic and lymphoplasmacytic infiltrates with necrosis in the liver and lymphoid depletion with necrosis and heterophilic infiltrates in the spleen. We stained slides with polyclonal antibodies against *Chlamydia* (bioMérieux, https://www.biomerieux.com) after a standard Avidin Biotin Complex protocol (*4*); liver and kidney tissues from 7 birds tested positive for *Chlamydia*. We did not observe any histologic changes consistent with viral inclusions or bacterial infection.

Because psittacosis in birds is a notifiable disease in the Netherlands, we informed public health authorities of our results. We forwarded frozen tissue samples to the Wageningen Bioveterinary Research institute to confirm *C. psittaci* infection. We also collected and forwarded 2 Picazuro pigeon carcasses and 3 pooled fecal samples from contact birds (i.e., Roseate spoonbill [*Platalea ajaja*], Puna ibis [*Plegadis ridgwayi*], and Scarlet ibis [*Eudocimus ruber*]), from the aviary. Two liver samples, 2 conjunctival and cloacal swabs, and 3 pooled fecal samples initially tested negative for *C. psittaci*, *C. abortus*, *C. felis*, and *C. caviae* in a PCR selective for the *omp*A gene. Because the liver and kidney samples of 7 pigeons tested positive for antibodies against *Chlamydia*, we submitted samples from all 11 pigeons and the 3 pooled fecal samples for further testing with real-time PCR selective for the 23S gene of *Chlamydiaceae* (*5*) and a duplex real-time PCR selective for *C. gallinacea* and *C. avium* (*3*,*6*). All 11 pigeons tested positive for *C. avium* in ≥1 samples of conjunctiva, cloaca, liver or intestines. The pooled fecal samples of contact birds tested negative in a PCR for *Chlamydiaceae* (Appendix, https://wwwnc.cdc.gov/EID/article/26/10/20-0086-App1.pdf).

We used Buffalo green monkey cells to isolate *Chlamydia* from the spleen of 1 of the pigeons that tested positive. Multilocus sequence typing using the concatenated sequences of 7 housekeeping genes revealed that this isolate is a unique sequence type, 254, that is closely related to the other 3 *C. avium* strains previously described (2) (Figure).

The clinical signs, histopathologic results, and positive intralesional immunohistochemistry findings (Appendix) showed that the birds had generalized disease consistent with a *Chlamydia* infection. Real-time PCR revealed an infection with *C. avium*. Further analysis with multilocus sequence typing showed the isolated strain is unique, but most closely related to other reported *C. avium* strains. *C. avium* has been detected mainly in urban or feral pigeons without clinical signs and in co-infections of feral pigeons with *C. psittaci* (2).

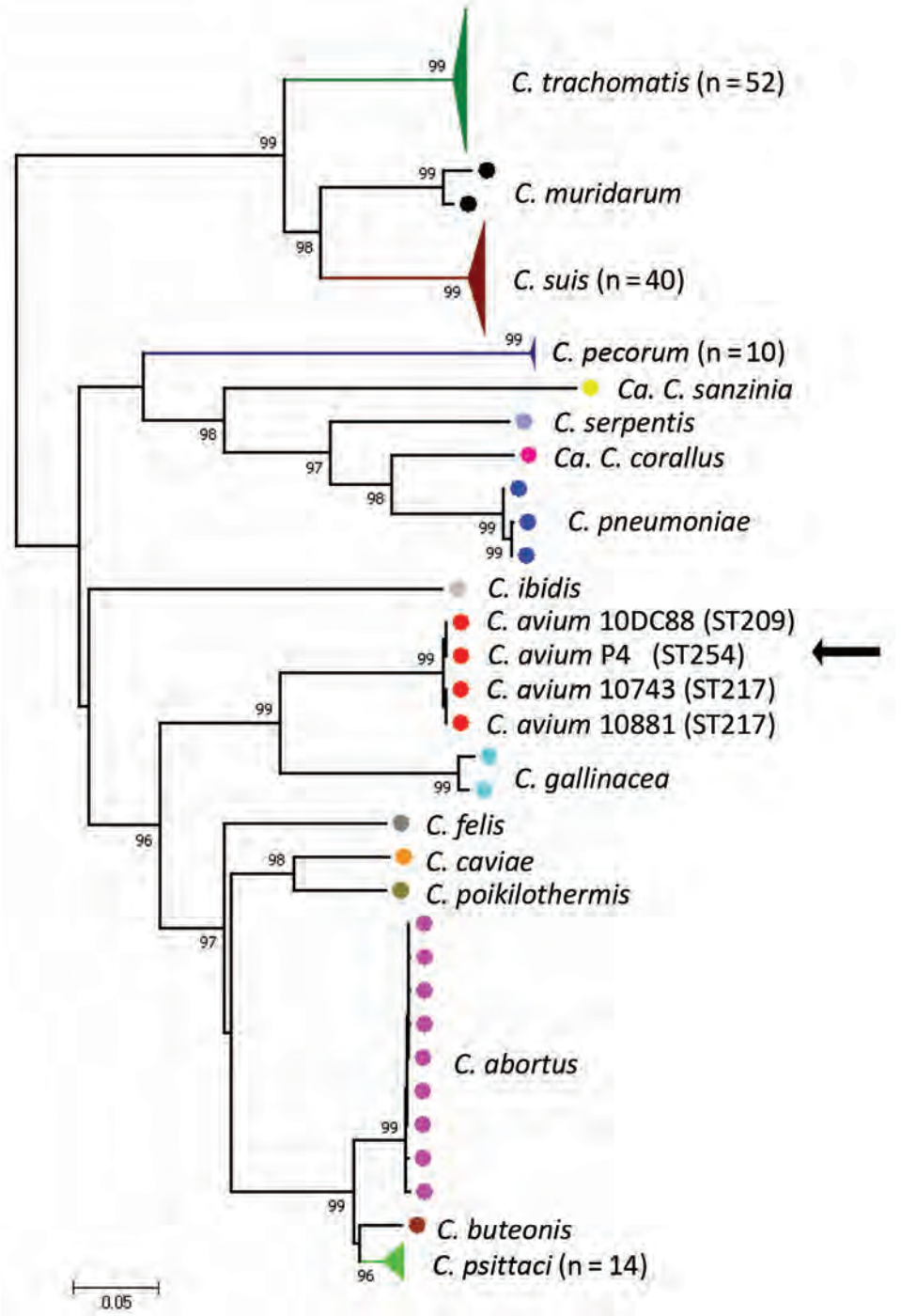

Figure. Phylogenetic analyses of concatenated sequences of 7 housekeeping gene fragments of *Chlamydiaceae*, the Netherlands, 2016. Numbers indicate bootstrap values >90%. Filled circles represent isolates, colored by species. Filled colored triangles represent >9 isolates of the same species; total number of isolates used for the analyses is indicated. The sequence types of the *C. avium* isolates are labeled. *C. avium* isolate P4 is indicated by the arrow. Scale bar indicates sequence divergence. ST, sequence type.

Our results show that *C. avium* strains might also cause severe, potentially fatal infections in birds. Data on *C. avium* are limited, but several factors might explain the severity of the clinical signs. Unlike previously reported cases, these pigeons were held in captivity. Furthermore, we cannot exclude possible differences in virulence between sequence types of *C. avium*. No human cases were reported during this outbreak, so the zoonotic potential of *C. avium* remains unknown.

Acknowledgments

We thank Rachel Thomas for proofreading. We also thank Frank Harders and Annemieke Dinkla for their technical assistance in DNA isolation and sequencing.

This work was partly funded by the Dutch Ministry of Agriculture, Nature and Food Quality (grant no. WOT-01-002-005.02).

About the Author

Dr. Kik is a veterinary pathologist at Utrecht University. Her research interests include the pathology of exotic animals and wildlife.

References

1. Kaleta EF, Taday EM. Avian host range of *Chlamydophila* spp. based on isolation, antigen detection and serology. Avian Pathol. 2003;32:435–62. https://doi.org/10.1080/0307945031 0001593613
2. Sachse K, Laroucau K, Riege K, Wehner S, Dilcher M, Creasy HH, et al. Evidence for the existence of two new members of the family *Chlamydiaceae* and proposal of *Chlamydia avium* sp. nov. and *Chlamydia gallinacea* sp. nov. Syst Appl Microbiol. 2014;37:79–88. https://doi.org/10.1016/j.syapm.2013.12.004
3. Sachse K, Laroucau K. Two more species of *Chlamydia*-does it make a difference? Pathog Dis. 2015;73:1–3. https://doi.org/10.1093/femspd/ftu008
4. Key M. Immunohistochemical staining methods. In: Kumar GL, Rudbeck L, editors. Immunohistochemical staining methods. 5th ed. Carpinteria (CA): Dako Corporation; 2009. p. 57–60.
5. Zocevic A, Vorimore F, Vicari N, Gasparini J, Jacquin L, Sachse K, et al. A real-time PCR assay for the detection of atypical strains of *Chlamydiaceae* from pigeons. PLoS One. 2013;8:e58741. https://doi.org/10.1371/journal.pone.0058741
6. Pannekoek Y, Morelli G, Kusecek B, Morré SA, Ossewaarde JM, Langerak AA, et al. Multi locus sequence typing of Chlamydiales: clonal groupings within the obligate intracellular bacteria *Chlamydia trachomatis*. BMC Microbiol. 2008;8:42. https://doi.org/10.1186/1471-2180-8-42

Address for correspondence: Marja Kik, Faculty of Veterinary Medicine, Pathobiology, Utrecht University, Yalelaan 1, 3584 CL Utrecht, the Netherlands; email: info@kikdierenarts.nl

Streptococcus equi Subspecies *zooepidemicus* and Sudden Deaths in Swine, Canada

Matheus de O. Costa, Brad Lage

Author affiliations: University of Minnesota, St. Paul, Minnesota, USA (M.O. Costa); University of Saskatchewan, Saskatoon, Saskatchewan, Canada (M.O. Costa); Utrecht University, Utrecht, the Netherlands (M.O. Costa); Maple Leaf Agri-Farms, Landmark, Manitoba, Canada (B. Lage)

DOI: https://doi.org/10.3201/eid2610.191485

Historically described as a commensal of the swine upper respiratory tract, *Streptococcus equi* subspecies *zooepidemicus* was previously reported as an important swine pathogen only in Asia. Here we report the isolation and whole genome characterization of *S. equi* subsp. *zooepidemicus* associated with a sudden death outbreak in pigs in Canada.

Streptococcus equi subspecies *zooepidemicus* is considered a commensal and opportunistic pathogen of several warm-blooded hosts, including humans, horses, canines, and swine. It is a gram-positive, β-hemolytic coccus belonging to the Lancefield group C and can cause severe disease characterized by pneumonia, septicemia, and meningitis (*1*,*2*). *S. equi* subsp. *zooepidemicus* has been suggested as a normal inhabitant of the palatine tonsils of pigs, being detected by both culture and high-throughput sequencing in samples collected from healthy animals (*3*). However, strains virulent to pigs have also been reported, particularly associated with high-mortality outbreaks of sudden death and respiratory disease in China (*4*). No vaccines are available for this pathogen, and control and prevention methods are rarely applied because of its normally harmless commensal nature in swine. Here, we report an outbreak of sudden death associated with *S. equi* subsp. *zooepidemicus* in pigs housed in intensive commercial rearing facilities in Canada.

In April 2019, an outbreak of sudden deaths and abortions occurred in 4 loose-housed, commercial sow farms (≈9,000 sows) in a large vertically integrated swine system in Manitoba, Canada. This outbreak increased the cumulative death in the 3 affected sow herds by >1,000 animals over a 12-week period. The abortion rate during this time was ≈11× normal.

The sows were often described as apparently healthy during morning checks. However, over the course of hours, infected sows would become

unwilling to stand, develop fever and lethargy, then die with no other apparent clinical signs. Other sows would abort and then go on to develop similar symptoms. Stress factors, such as mixing groups of sows and the presence of other sick animals, appeared to exacerbate outbreaks within pens.

Animals were electronically fed a commercial grade, nutritionally balanced diet and had ad libitum access to water. Gross postmortem examination of multiple animals, either euthanized or recently deceased, revealed rhinitis (mild, diffuse mucopurulent discharge); pulmonary edema; gall bladder edema; and hemorrhagic lymphadenopathy (tan-colored to hemorrhagic), consisting of submandibular, cervical neck, and bronchial lymph nodes. These signs, taken together, suggest sepsis. We used real-time PCR to test all of the dead sows for porcine reproductive and respiratory syndrome virus, *Mycoplasma hyopneumoniae*, simian immunodeficiency virus A, and porcine circovirus types 2 and 3; results were negative for each.

In parallel, we observed gram-positive cocci in imprints from heart and submandibular lymph nodes. After aerobic bacterial culture followed by matrix-assisted laser desorption/ionization-time of flight (MALDI-TOF) mass spectrometry for identification of isolates revealed varying levels of *S. equi* subsp. *zooepidemicus* in liver, kidney, heart, brain, lung, spleen, and submandibular lymph nodes. Isolate identification was confirmed by 2 different veterinary diagnostic laboratories. We found isolates SAMN13058951, SAMN13058952, SAMN13058953, SAMN13058954, SAMN13058955, SAMN13058956, and SAMN13058957 resistant to lincomycin, neomycin, and tetracycline and susceptible to ampicillin, ceftiofur, penicillin, and tilmicosin in a Kirby-Bauer disk diffusion assay.

We extracted DNA from isolates using DNeasy Powersoil Pro kit (QIAGEN, https://www.qiagen.com), quantified by Nanodrop (3300) and PicoGreen (Quant-iT dsDNA; Invitrogen, https://www.thermofisher.com), then processed it for sequencing using a Illumina Nextera XT library prep kit (Illumina, https://www.illumina.com). We performed sequencing using MiSeq Nano V2, 2×250 paired-end (Illumina). Samples yielded an average of 149,017 high quality reads, suggesting 50× coverage. We conducted genome assembly, annotation, and downstream analyses using the PATRIC package (*5*). Genomes averaged 2.1 million bp in size and 41.34% in guanine-cytosine content.

All isolates were similar to previously published *S. equi* subsp. *zooepidemicus* genomes (Figure), demonstrating a whole-genome average nucleotide identity score of 99.7% to strain ATCC35246. This particular strain was isolated from a septicemic pig during an outbreak that killed >300,000 pigs in Sichuan Province, China, in 1976 (*6*). All isolates had an average nucleotide identity score of 97.3% compared with *S. equi* subsp. *equi* strain 4047, an isolate considered virulent and obtained from a horse diagnosed with strangles in the United Kingdom (*7*). In addition, all isolates obtained from pigs, regardless of from which outbreak, were profiled as multilocus sequence type

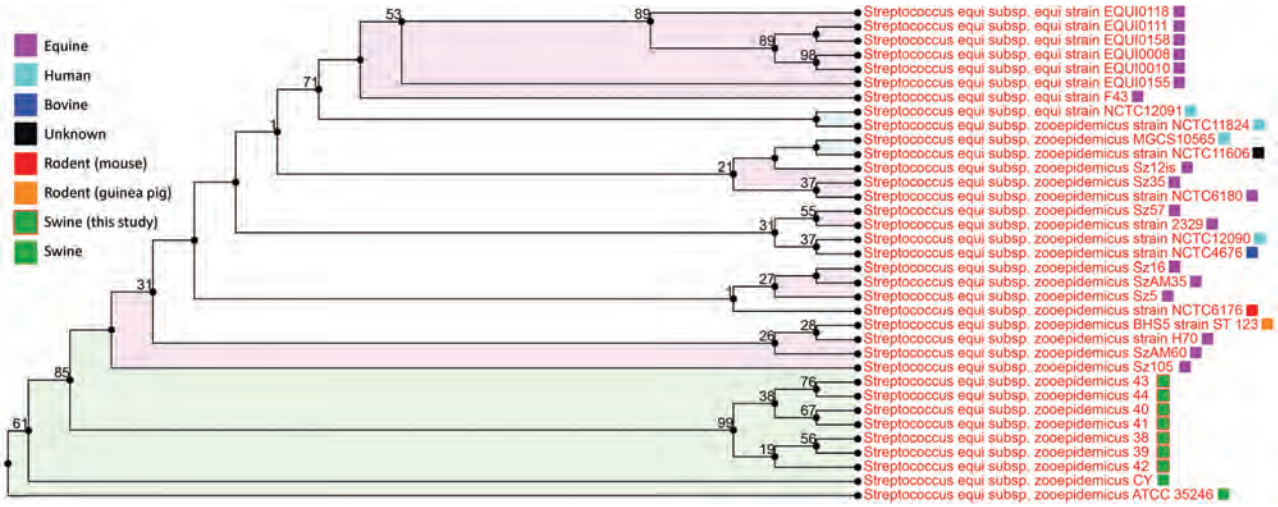

Figure. Phylogenetic tree (all-shared proteins) of *Streptococcus equi* subspecies *zooepidemicus* whole-genome sequences obtained from outbreak in pigs from Canada (blue blocks, PRJNA578379), compared with previously characterized genome sequences from GenBank (n = 28). Tree inferred using BLAST (https://blast.ncbi.nlm.nih.gov), followed by FastTree within the PATRIC package (*5*). Support values shown indicate the number of times a particular branch was observed in the support trees using gene-wise jackknifing. Shaded colors reflect similar host taxonomy associated with a branch (>3 isolates).

194, including strains ATCC35246 and CY (also recovered from a diseased pig in China) (*8*). Antimicrobial resistance genes identified in isolates from this outbreak included *gidB*, *S12p* (streptomycin-resistant), *rpoB* (rifampin-resistant), *S10p* (tetracycline-resistant), *kasA* (triclosan-resistant), *PgsA*, *LiaR*, *LiaS* (daptomycin-resistant), *folA*, *Dft* (trimethoprim-resistant), *folP* (sulfadiazine-resistant), and *FabK* (triclosan-resistant). Virulence factors found, including the previously described *szm*, *szp*, *lmb*, *fbpZ*, *skc*, and *has* operons and *mga* regulon (*9*), help explain the high virulence of these isolates.

Taken together, these findings suggest the emergence of *S. equi* subsp. *zooepidemicus* sequence type 194 as a cause of death in pigs in Canada and possibly other regions of North America. This specific sequence type seems to be particularly virulent to pigs, for reasons that remain unexplained. Given the clinical presentation described here, this pathogen requires special attention and should no longer be overlooked when conducting diagnostic investigations, despite its historically accepted status as a commensal organism.

Acknowledgments

We acknowledge the Manitoba Veterinary Diagnostic Services for its assistance.

About the Author

Dr. Costa is an assistant professor at the University of Minnesota, USA, and Adjunct Professor at the University of Saskatchewan, Canada, and Utrecht University, the Netherlands. His research interests include swine bacterial pathogens for which no preventive or control methods are available besides antibiotics. Dr. Lage is the head veterinarian at Maple Leaf Agri-Farms, the swine division for Maple Leaf Foods, in Landmark, Manitoba.

References

1. Pelkonen S, Lindahl SB, Suomala P, Karhukorpi J, Vuorinen S, Koivula I, et al. Transmission of *Streptococcus equi* subspecies *zooepidemicus* infection from horses to humans. Emerg Infect Dis. 2013;19:1041–8.
2. FitzGerald W, Crowe B, Brennan P, Cassidy JP, Leahy M, McElroy MC, et al. Acute fatal haemorrhagic pneumonia caused by *Streptococcus equi zooepidemicus* in greyhounds in Ireland with subsequent typing of the isolates. Vet Rec. 2017;181:119. https://doi.org/10.1136/vr.104275
3. Kernaghan S, Bujold AR, MacInnes JI. The microbiome of the soft palate of swine. Anim Health Res Rev. 2012;13:110–20. https://doi.org/10.1017/S1466252312000102
4. Feng Z, Hu J. Outbreak of swine streptococcosis in Sichan province and identification of pathogen. Anim Husbandry Vet Med Lett. 1977;2:7–12.
5. Wattam AR, Davis JJ, Assaf R, Boisvert S, Brettin T, Bun C, et al. Improvements to PATRIC, the all-bacterial Bioinformatics Database and Analysis Resource Center. Nucleic Acids Res. 2017;45:D535–42. https://doi.org/10.1093/nar/gkw1017
6. Waller AS, Robinson C. *Streptococcus zooepidemicus* and *Streptococcus equi* evolution: the role of CRISPRs. Biochem Soc Trans. 2013;41:1437–43. https://doi.org/10.1042/BST20130165
7. Kelly C, Bugg M, Robinson C, Mitchell Z, Davis-Poynter N, Newton JR, et al. Sequence variation of the SeM gene of *Streptococcus equi* allows discrimination of the source of strangles outbreaks. J Clin Microbiol. 2006;44:480–6. https://jcm.asm.org/content/44/2/480
8. Mao Y, Fan H-J, Zhou Y-H, Lu C-P. Immunoproteomic assay of antigenic surface proteins in *Streptococcus equi* ssp. *zooepidemicus*. Agric Sci China. 2011;10:1096–105. https://doi.org/10.1016/S1671-2927(11)60099-0
9. Xu, B., Zhang, P., Zhou, H., Sun, Y., Tang, J., & Fan, H. (2019). Identification of novel genes associated with anti-phagocytic functions in *Streptococcus equi* subsp. *zooepidemicus*. Vet Microbiol, 233, 28–38. https://doi.org/10.1016/j.vetmic.2019.04.023

Address for correspondence: Matheus de Oliveira Costa, University of Minnesota, 1988 Fitch Ave, St. Paul, MN 55346, USA; email: matheus.costa@usask.ca

Pulmonary Infection Related to Mimivirus in Patient with Primary Ciliary Dyskinesia

Fatemeh Sakhaee, Farzam Vaziri, Golnaz Bahramali, Seyed Davar Siadat, Abolfazl Fateh

Author affiliation: Pasteur Institute of Iran, Tehran, Iran

DOI: https://doi.org/10.3201/eid2610.191613

Primary ciliary dyskinesia is a rare autosomal recessive disorder that causes oto-sino-pulmonary disease. We report a case of pulmonary infection related to mimivirus in a 10-year-old boy with primary ciliary dyskinesia that was identified using molecular techniques. Our findings indicate that the lineage C of mimivirus may cause pneumonia in humans.

In patients with primary ciliary dyskinesia (PCD), several bacterial pathogens are associated with the occurrence of pulmonary disease. However, in these

patients, the many possible causative agents of pneumonia, especially viruses, have not been investigated (*1*). Since the detection of antibodies against mimivirus in patients with pneumonia, the potential role of mimivirus as a respiratory pathogen has been suggested (*2*).

In February 2017, a 10-year-old boy had severe pulmonary infection, caused by *Pseudomonas aeruginosa*. He had been mechanically ventilated for ≈10 days in the intensive care unit (ICU). One year later, he reported cough, fever, and night perspiration with excessive sputum. His physician speculated the recurrence of *P. aeruginosa* infection and treated him with colistin and ciprofloxacin for 3 weeks. However, symptoms of atypical pneumonia continued after 1 month.

In May 2018, care was sought agin for the child, who had excessive sputum production, weakness, chills, cough, fever, and night perspiration. He was referred to the Pasteur Institute of Iran for evaluation for nontuberculous mycobacteria. His sputum production, cough, and fever had persisted for 4 months.

The patient's biological parameters showed elevated leukocyte count (11.9 × 1,000 cells/mL^3), erythrocyte sedimentation rate (79 mm/h), and C-reactive protein (42.8 mg/L). Computed tomography scan indicated consolidation in the right lower lobe and bilateral basilar infiltrates.

Three sputum and 3 bronchoalveolar lavage (BAL) samples were sent to the laboratory for evaluation for nontuberculous mycobacteria. The results of smear, culture, and PCR for acid-fast bacilli were negative in all samples. We also evaluated what Wijers et al. found to be the most common infectious agents in PCD patients (*3*) but did not detect them in culture or PCR.

We used real-time PCR to identify mimivirus DNA, as previously described (*4*). Five (3 BAL and 2 sputum) of 6 samples were positive for mimivirus. All control samples were negative. We also sequenced the mimivirus genome using an Illumina Hiseq 2000 system (Illumina, https://www.illumina.com). Analysis of a partial genome sequence (≈730 kbp) showed 99% homology to megavirus LBA111 (mimivirus lineage C) and the species *Megavirus chilensis*. We named the virus mimivirus PCD-1 (Appendix Figure, https://wwwnc.cdc.gov/EID/article/26/10/19-1613-App1.pdf).

To elucidate the evolutionary correlation between the mimivirus PCD-1 and other mimiviruses, we conducted phylogenetic analyses of 4 genes: the major capsid protein, the VV A18 helicase, the family B-DNA polymerase, and the D5 helicase (Figure). The phylogenetic trees indicated the close correlation of mimivirus PCD-1 with megavirus LBA111.

The role of giant viruses in human infections remains controversial. Nevertheless, small-scale reports have supported their role (*2*,*4*). We detected mimivirus DNA in sputum and BAL specimens from a 10-year-old boy with PCD in whom pneumonia developed. The negative results of culture and PCR for other pathogens strongly suggest that he had mimivirus pneumonia.

Isolation of mimivirus DNA in respiratory specimens of patients with nosocomial pneumonia who are

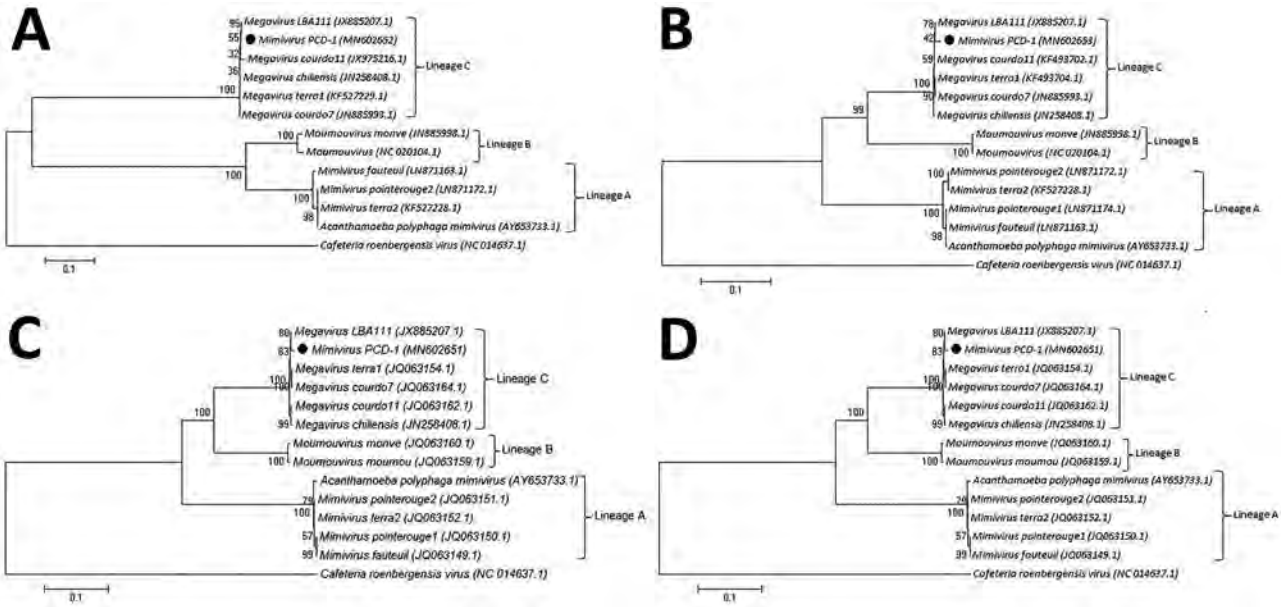

Figure. Neighbor-joining tree based on nucleotide acid sequences of mimivirus from a patient in Tehran, Iran (black circles), and reference sequences. A) The major capsid protein. B) The VV A18 helicase. C) The family B DNA polymerase. D) The D5-ATPase-helicase genes. Numbers indicate bootstrap values. Scale bar indicates substitutions per nucleotide position.

admitted to ICUs verifies that this virus has reached the respiratory tract in these patients (*5*,*6*). The patient in this report was hospitalized in an ICU for 15 days and was mechanically ventilated for ≈10 days. Several studies supported the hypothesis that mimivirus occurs in pneumonia patients with ICU ventilation and is probably responsible for pneumonia and should be treated as a class 2 pathogen (*2*,*7*–*9*).

Although 2 previous studies have shown mimivirus infection in lower respiratory BAL specimens (*2*,*4*), we detected the virus in both upper and lower respiratory tracts, including in sputum specimens. The presence of this virus in the upper respiratory tract needs to be considered.

The first mimivirus isolated from respiratory samples belonged to lineage C (*4*). Consistent with this finding, the mimivirus PCD-1 from this patient was also from lineage C. In addition, another lineage C mimivirus (Shan virus) was found from the feces of a patient with pneumonia in Tunisia (*10*). This lineage of mimivirus may be responsible for pulmonary infection in patients; however, future research needs to confirm this result.

In summary, we detected mimivirus in a patient with primary ciliary dyskinesia who had pneumonia develop. Whether mimivirus is a causative agent of pneumonia or only extremely immunogenic is unclear, but clinicians should be aware of the potential role of this virus in human infections.

Acknowledgments

We thank all the personnel of the Department of Mycobacteriology and Pulmonary Research, Pasteur Institute of Iran, for their assistance in this project.

About the Author

Ms. Sakhaee is a clinical microbiologist at the Pasteur Institute of Iran, Tehran, Iran. Her primary research interests focus on epidemiologic and clinical aspects of pulmonary infections.

References

1. Alanin MC, Nielsen KG, von Buchwald C, Skov M, Aanaes K, Høiby N, et al. A longitudinal study of lung bacterial pathogens in patients with primary ciliary dyskinesia. Clin Microbiol Infect. 2015;21:1093.e1–7. https://doi.org/10.1016/j.cmi.2015.08.020
2. La Scola B, Marrie TJ, Auffray J-P, Raoult D. Mimivirus in pneumonia patients. Emerg Infect Dis. 2005;11:449–52. https://doi.org/10.3201/eid1103.040538
3. Wijers CD, Chmiel JF, Gaston BM. Bacterial infections in patients with primary ciliary dyskinesia: comparison with cystic fibrosis. Chron Respir Dis. 2017;14:392–406. https://doi.org/10.1177/1479972317694621
4. Saadi H, Pagnier I, Colson P, Cherif JK, Beji M, Boughalmi M, et al. First isolation of mimivirus in a patient with pneumonia. Clin Infect Dis. 2013;57:e127–34. https://doi.org/10.1093/cid/cit354
5. Berger P, Papazian L, Drancourt M, La Scola B, Auffray J-P, Raoult D. Ameba-associated microorganisms and diagnosis of nosocomial pneumonia. Emerg Infect Dis. 2006;12:248–55. https://doi.org/10.3201/eid1202.050434
6. Bousbia S, Papazian L, Saux P, Forel J-M, Auffray J-P, Martin C, et al. Serologic prevalence of amoeba-associated microorganisms in intensive care unit pneumonia patients. PLoS One. 2013;8:e58111. https://doi.org/10.1371/journal.pone.0058111
7. Vincent A, La Scola B, Forel J-M, Pauly V, Raoult D, Papazian L. Clinical significance of a positive serology for mimivirus in patients presenting a suspicion of ventilator-associated pneumonia. Crit Care Med. 2009;37:111–8. https://doi.org/10.1097/CCM.0b013e318192fa8b
8. Raoult D, Renesto P, Brouqui P. Laboratory infection of a technician by mimivirus. Ann Intern Med. 2006;144:702–3. https://doi.org/10.7326/0003-4819-144-9-200605020-00025
9. Vanspauwen MJ, Franssen FM, Raoult D, Wouters EF, Bruggeman CA, Linssen CF. Infections with mimivirus in patients with chronic obstructive pulmonary disease. Respir Med. 2012;106:1690–4. https://doi.org/10.1016/j.rmed.2012.08.019
10. Saadi H, Reteno D-GI, Colson P, Aherfi S, Minodier P, Pagnier I, et al. Shan virus: a new mimivirus isolated from the stool of a Tunisian patient with pneumonia. Intervirology. 2013;56:424–9. https://oi.org/10.1159/000354564

Address for correspondence: Abolfazl Fateh, Department of Mycobacteriology and Pulmonary Research and Microbiology Research Center; Pasteur Institute of Iran, No. 69, 12th Farwardin Ave, Tehran, Iran; email: afateh2@gmail.com

Q Fever Endocarditis and a New Genotype of *Coxiella burnetii*, Greece

Ioulia Karageorgou, Nektarios Kogerakis, Stavroula Labropoulou, Sophia Hatzianastasiou, Andreas Mentis, George Stavridis, Emmanouil Angelakis

Author affiliations: Hellenic Pasteur Institute, Athens, Greece (I. Karageorgou, S. Labropoulou, A. Mentis, E. Angelakis); Onassis Cardiac Surgery Center, Athens (N. Kogerakis, S. Hatzianastasiou, G. Stavridis); Aix Marseille Université, Marseille, France (E. Angelakis)

DOI: https://doi.org/10.3201/eid2610.191616

Underdiagnosis of *Coxiella burnetii* infections in Greece is possible because of lack of awareness by physicians, and most suspected cases are in patients with no bovine contact. We found serologic evidence of *C. burnetii* infection throughout Greece and identified a new *C. burnetii* genotype in the aortic valve of a patient with Q fever endocarditis.

Q fever is a worldwide zoonosis caused by an obligate intracellular bacterium, *Coxiella burnetii* (*1*,*2*). Although the classification of *C. burnetii* by the Centers for Disease Control and Prevention (Atlanta, GA, USA) as a potential bioterrorism agent resulted in the disease becoming reportable in many countries (*3*), Q fever is not considered a public health problem in Greece, and few cases have been recorded (*3*).

etymologia

Mimivirus [mĭm′ĭ-vī′rəs]

Clyde Partin

If virus (Latin: slimy) challenges the definition of what constitutes life, the DNA mimivirus tests how we define virus. This unidentifiable "bacterium" infecting *Acanthamoeba polyphaga*, was isolated in 1992 from a hospital cooling tower in Bradford, England. Thus, the original name was *Bradfordcoccus*, and it was considered a culprit for a pneumonia outbreak at this hospital.

Researchers brought samples to Didier Raoult and colleagues at Aix-Marseille University, who eventually identified this "bacterium" as a novel virus in 2003. The physical size, genomic content, and ability of the outer protein coat to stain gram positive, thus mimicking (Latin: imitate) prokaryotic bacteria, indicated that this pathogen might be a bacterium.

Raoult initially claimed that the moniker meant "mimicking microbe" but later sheepishly recounted a childhood memory about his father, a physician–scientist, who created stories to explain evolution. Featured prominently in these whimsical narratives was an anthropomorphic character named "Mimi the amoeba."

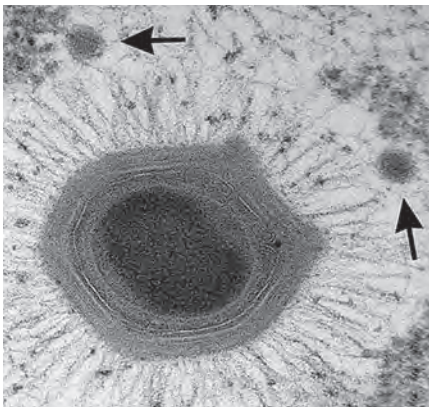

Acanthamoeba polyphaga mimivirus, with two satellite Sputnik virophages (arrows). Thin-section electron microscopy courtesy of J.Y. Bou Khalil and B. La Scola, IHU Mediterranée Infection, France.

Sources

1. Redefining life [cited 2020 Jul 2]. https://www.rsb.org.uk/biologist-features/158-biologist/features/1490-larger-than-life
2. Viruses reconsidered [cited 2020 Jul 20]. https://www.the-scientist.com/features/viruses-reconsidered-37867

Author affiliation: Emory University School of Medicine, Atlanta, Georgia, USA

Address for correspondence: Clyde Partin, Emory University School of Medicine, 1365 Clifton Rd NE, Clinic A, 1st Fl, Atlanta, GA 30322, USA; email: wpart01@emory.edu

DOI: https://doi.org/10.3201/eid2610.ET2610

Our referent laboratory for the diagnosis of Q fever was deployed in the Hellenic Pasteur Institute in February 2019. We tested serum samples from all patients by using an immunofluorescence assay (IFA) for *C. burnetii* phase I and II antigens as described (*4*,*5*). Patients are classified as having acute Q fever; persistent, focalized *C. burnetii* infection; or evidence of past infection (*6*). Moreover, anticardiolipin IgG is routinely measured for patients given a diagnosis of acute Q fever (*6*).

During the first 7 months of testing, we received 209 serum samples from patients suspected of having Q fever. We provided diagnoses of acute Q fever for 1 (0.5%) patient and persistent *C. burnetii* focalized endocarditis for 2 (1.0%) patients; 12 (6.0%) patients showed evidence of *C. burnetii* infection. The patient given a diagnosis of acute Q fever also had high levels of anticardiolipin IgG (>140 GPLU). Further investigation also showed large, transient, aortic vegetation. Thus, this patient was considered as possibly having acute Q fever endocarditis (*4*,*7*), but contact with the patient was lost.

Epidemiologic information was obtained for 102 patients, including all patients with a positive IFA result for *C. burnettii*. This information showed that only 22% of these patients reported previous contact with bovids. Most patients reported a previous tick bite (35%); contact with cats (16%), dogs (7%), rats (4%), or other animals (7%). In addition, 9% of these patients reported no animal contact.

We provide a detailed history for 1 patient given a diagnosis of persistent *C. burnetii* focalized endocarditis. A 45-year-old sheepherder, a resident of a rural area in southern Greece, came to the local district hospital with a 2-week history of spiking fevers, peripheral edema, and night sweats. He reported nonspecific symptoms gradually leading to anorexia and debilitating weakness for the previous year.

Cardiac ultrasound showed a severely regurgitant bicuspid aortic valve, a paravalvular abscess (2.6 cm × 1.6 cm), aortic root dilatation (5.3 cm), and vegetations. Cardiac computed tomography confirmed the ultrasound findings. IFA results were positive for

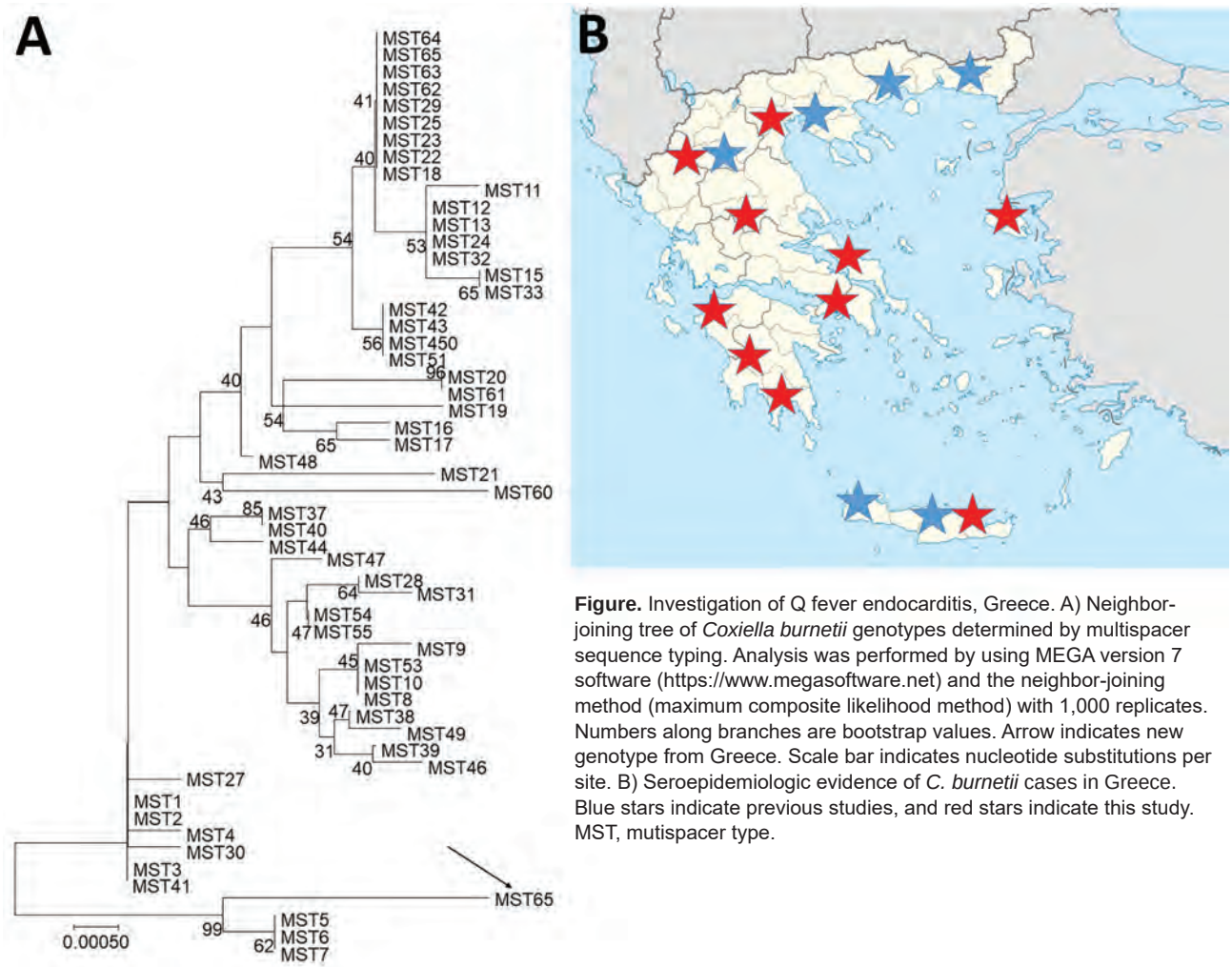

Figure. Investigation of Q fever endocarditis, Greece. A) Neighbor-joining tree of *Coxiella burnetii* genotypes determined by multispacer sequence typing. Analysis was performed by using MEGA version 7 software (https://www.megasoftware.net) and the neighbor-joining method (maximum composite likelihood method) with 1,000 replicates. Numbers along branches are bootstrap values. Arrow indicates new genotype from Greece. Scale bar indicates nucleotide substitutions per site. B) Seroepidemiologic evidence of *C. burnetii* cases in Greece. Blue stars indicate previous studies, and red stars indicate this study. MST, mutispacer type.

C. burnetii: phase I IgG titer 1:3,200, phase I IgM titer 0; and phase II IgG titer 1:3,200, phase II IgM titer 0. This serum sample was negative for *C. burnetii* by real-time PCR for insertion sequence (IS) 1111 and the IS30A spacers (*8*). Thus, we provided a diagnosis of *C. burnetii* endocarditis, and the patient was transferred to a tertiary care center for surgical management.

The patient underwent an aortic root replacement (Bentall procedure) with pericardial composite graft after extensive debridement and reconstruction of the root with the use of autologous pericardium. His aortic valve was positive for *C. burnetii* for IS1111 and IS30A spacers by real-time PCR. Multispacer sequence typing (MST) was performed as described and consisted of 10 different spacers of the *C. burnetii* genome: Cox2, 5, 6, 18, 20, 22, 37, 51, 56, and 57 (*5*). We identified a new MST genotype (MST65) by using web-based MST database (http://ifr48.timone.univ-mrs.fr/MST_Coxiella/mst) (Figure, panel A).

The patient was given oral doxycycline (100 mg 2×/d) and hydroxychloroquine (200 mg 3×/d) for ≥24 months (*9*). A convalescence-phase serum sample obtained after 6 months of treatment was positive for *C. burnetii*: phase I IgG titer 1:800, phase I IgM titer 0, and phase II IgG titer 1:800, phase II IgM 0.

Our preliminary data show that physicians in Greece are not familiar with Q fever because most of the suspected cases were in patients without bovine contact. A limitation of our study was that culture was not performed because of the absence of a Biosafety Level 3 laboratory. The fact that we did not provide diagnoses of classic, acute Q fever showed that *C. burnetii* infection is suspected mostly in culture-negative serious endocarditis case-patients. Moreover, we identified a new *C. burnetii* genotype in the aortic valve of a patient who had Q fever endocarditis. Recently, it was found that *C. burnetii* genotype 32 is circulating in sheep and goat in 8 different areas of Greece (*10*). The clinical manifestations of Q fever depend, at least in part, on the *C. burnetii* genotype (*5*). However, although acute clinical manifestations are strain-specific, all genotypes have been associated with endocarditis (*5*).

We raise the question of underdiagnosis of C. *burnetii* infections in Greece. Our data have affected local clinical practice because we found serologic evidence of C. *burnetii* infection throughout most of Greece (Figure, panel B).

About the Author

Dr. Karageorgou is a biologist and researcher at the Hellenic Pasteur Institute in Athens, Greece. Her primary research interest is zoonotic pathogens.

References

1. Angelakis E, Raoult D. Q fever. Vet Microbiol. 2010;140:297–309. https://doi.org/10.1016/j.vetmic.2009.07.016
2. Eldin C, Mélenotte C, Mediannikov O, Ghigo E, Million M, Edouard S, et al. From Q fever to *Coxiella burnetii* infection: a paradigm change. Clin Microbiol Rev. 2017;30:115–90. https://doi.org/10.1128/CMR.00045-16
3. Kokkini S, Chochlakis D, Vranakis I, Angelakis E, Tselentis Y, Gikas A, et al. Antibody kinetics in serological indication of chronic Q fever: the Greek experience. Int J Infect Dis. 2013;17:e977–80. https://doi.org/10.1016/j.ijid.2013.04.010
4. Million M, Thuny F, Bardin N, Angelakis E, Edouard S, Bessis S, et al. Antiphospholipid antibody syndrome with alvular vegetations in acute Q fever. Clin Infect Dis. 2016;62:537–44. https://doi.org/10.1093/cid/civ956
5. Angelakis E, Million M, D'Amato F, Rouli L, Richet H, Stein A, et al. Q fever and pregnancy: disease, prevention, and strain specificity. Eur J Clin Microbiol Infect Dis. 2013;32:361–8. https://doi.org/10.1007/s10096-012-1750-3
6. Melenotte C, Protopopescu C, Million M, Edouard S, Carrieri MP, Eldin C, et al. Clinical features and complications of *Coxiella burnetii* infections from the French National Reference Center for Q Fever. JAMA Netw Open. 2018;1:e181580. https://doi.org/10.1001/jamanetworkopen.2018.1580
7. Melenotte C, Epelboin L, Million M, Hubert S, Monsec T, Djossou F, et al. Acute Q fever endocarditis: a paradigm shift following the systematic use of transthoracic echocardiography during acute Q fever. Clin Infect Dis. 2019;69:1987–95. https://doi.org/10.1093/cid/ciz120
8. Angelakis E, Mediannikov O, Socolovschi C, Mouffok N, Bassene H, Tall A, et al. *Coxiella burnetii*-positive PCR in febrile patients in rural and urban Africa. Int J Infect Dis. 2014;28:107–10. https://doi.org/10.1016/j.ijid.2014.05.029
9. Melenotte C, Million M, Raoult D. New insights in *Coxiella burnetii* infection: diagnosis and therapeutic update. Expert Rev Anti Infect Ther. 2020;18:75–86. https://doi.org/10.1080/14787210.2020.1699055
10. Chochlakis D, Santos AS, Giadinis ND, Papadopoulos D, Boubaris L, Kalaitzakis E, et al. Genotyping of *Coxiella burnetii* in sheep and goat abortion samples. BMC Microbiol. 2018;18:204. https://doi.org/10.1186/s12866-018-1353-y

Address for correspondence: Emmanouil Angelakis, Aix Marseille Université, Institut de Recherche pour le Développement, Assistance Publique Hôpitaux de Marseille, Vecteurs Infections Tropicales et Méditerranéennes, Institut Méditerranée Infection, 19–21 Blvd Jean Moulin, Marseille 13005, France; email: e.angelakis@hotmail.com

High Prevalence of *Rickettsia raoultii* and Associated Pathogens in Canine Ticks, South Korea

Min-Goo Seo, Oh-Deog Kwon, Dongmi Kwak

Author affiliations: Animal and Plant Quarantine Agency, Gimcheon, South Korea (M.-G. Seo); Kyungpook National University, Daegu, South Korea (O.-D. Kwon, D. Kwak)

DOI: https://doi.org/10.3201/eid2610.191649

We studied the prevalence of tickborne pathogens in canine ticks, South Korea, during 2010–2015. Results revealed a high prevalence of the emerging pathogen *Rickettsia raoultii*. Dog ticks may be maintenance hosts for tickborne pathogens, suggesting the need to continually evaluate the potential public health threat posed by *R. raoultii*–infected ticks.

Ticks are responsible for mechanical damage to animal blood vessels and skin and are known to transmit a wide range of bacteria, viruses, and protozoa, causing severe infections in animals and humans (*1*). Most defined Rickettsiales are considered zoonotic emerging or reemerging pathogens; some can cause severe human illnesses, including anaplasmosis, rickettsioses, scrub typhus, and ehrlichiosis (*2*). Determining the ecology of local tick species and recognizing the tickborne pathogens they carry are of paramount public health importance. Our study assessed risk factors for and the prevalence and coinfectivity of several tickborne pathogens in ticks collected from dogs in South Korea.

Rickettsia spp. are emerging or reemerging pathogens with public health relevance; 1 species, *R. raoultii*, causes human tickborne lymphadenitis in many countries in Europe (*3*). Of note, *R. raoultii* had not been detected in humans, animals, or vectors in South Korea until recently, but it now appears to be endemic in ticks infesting dogs. We collected a total of 980 ticks in central (n = 442) and southern (n = 538) South Korea from 102 dogs during 2010–2015. We used both morphological and molecular methods (Appendix, https://wwwnc.cdc.gov/EID/article/26/10/19-1649-App1.pdf) to identify the tick species, which included *Haemaphysalis longicornis*, *H. flava*, and *Ixodes nipponensis*, then sorted them into 364 pools (1–7 ticks per pool) by dog, identified tick species, and developmental stage (larva, nymph, and adult).

Our findings are consistent with the results of a previous study from South Korea, in which *H. longicornis* ticks were found in 201 (48.9%), *Haemaphysalis* spp. ticks in 130 (31.6%), *H. flava* ticks in 71 (17.3%), and *I. nipponensis* ticks in 7 (1.7%) of 411 dogs (*4*). A previous study of *H. longicornis* tick prevalence proposed that, rather than rodents as previously thought, larger mammals, including dogs, might be the hosts for this tick species (*5*). Additional surveys are needed to assess the natural hosts of *H. longicornis* ticks.

Several tickborne pathogens were then screened by using primer sets specific to each pathogen (Appendix). The 16S rRNA genes of *R. raoultii* were found in 149 (40.9%), *R. monacensis* in 1 (0.3%), and *Candidatus* Rickettsia principis in 2 (0.6%) of 364 tick pools (Figure; Appendix Table 1). *R. raoultii* was detected in 100 nymph and 49 adult *H. longicornis* ticks in South Korea. *R. raoultii*–positive ticks were collected from 25 (24.5%) of 102 dogs, a relatively high proportion of those observed in this study.

R. monacensis causes spotted fever–like disease and has been found in multiple hard tick species in several European countries (*2*). It was detected in 16 (55.2%) of 29 pools of *I. nipponensis* ticks from small mammals in South Korea (*6*). In this study, however, *R. monacensis* was found in only 1 (0.3%) of 364 tick pools, in an adult *I. nipponensis* tick. One spotted fever group rickettsiae with *Candidatus* status was also identified in ticks in this study; *Candidatus* R. principis was identified in 2 (3.0%) of 67 *H. japonica douglasii* ticks in Russia in 2006 (*7*). In this study, *Candidatus* R. principis (0.6%) was detected in 1 *H. longicornis* nymph and 1 *H. flava* nymph. Additional tickborne pathogens were detected (Appendix Table 1, Figures 1, 2): the *E. canis* 16S rRNA gene was identified in 1 *H. longicornis* nymph (0.3%), and the *T. luwenshuni* 18S rRNA gene was identified in 20 *H. longicornis* nymphs (10.9%) and 24 *H. longicornis* adults (26.1%). No other tickborne pathogens were detected in this study.

Increased seasonal tick populations and activity in the summer and autumn impact the transmission of tickborne pathogens (*8*). In this study, we collected ticks from May to September, and found that tick abundance and distribution patterns were similar to those in a previous study in South Korea (*8*), which showed that both ticks and tickborne pathogens were more prevalent in southern regions and during the summer. South Korea is also steadily shifting to a subtropical climate due to global warming (*9*), which may influence this seasonal effect, as well. In another previous study in South Korea (*4*), ticks were collected from stray or pet dogs, but no ticks were found on military working dogs. These military dogs received routine veterinary care for preventive ectoparasite treatments. Therefore, tick prevention measures

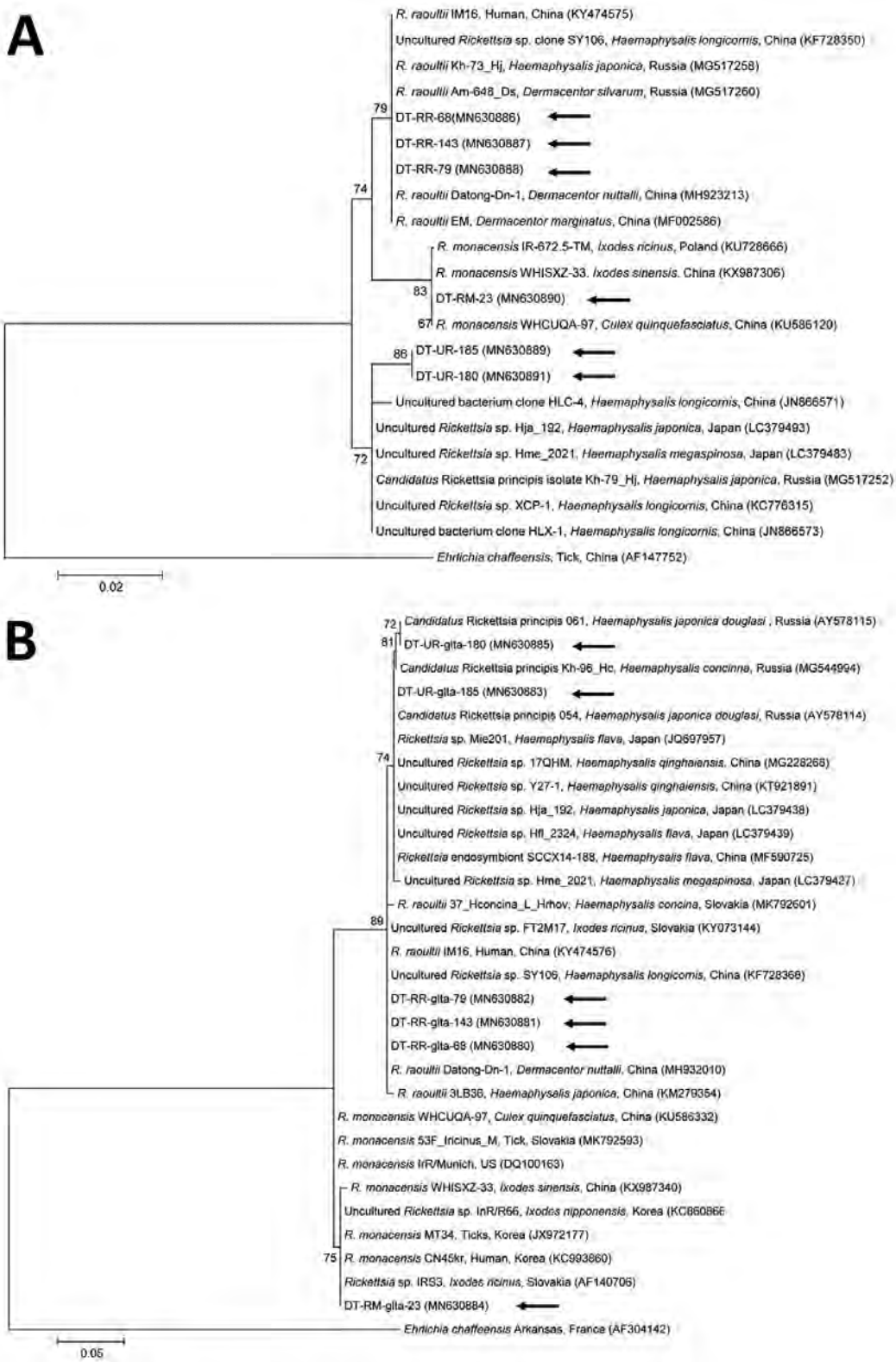

Figure. Phylogenetic trees constructed using the maximum-likelihood method based on nucleotide sequences of *Rickettsia* spp. from canine ticks, South Korea (black arrows), and reference sequences. A) 16S rRNA; (B) *glt*A. *Ehrlichia chaffeensis* sequences were used as outgroups. GenBank accession numbers for reference sequences are shown with the sequence name. Branch numbers indicate bootstrap support (1,000 replicates). Scale bar indicates phylogenetic distance.

should be effective in endemic areas with known tick seasons, when infestations are higher.

Our findings indicate the zoonotic potential of dog ticks in South Korea. Physicians and public health officers therefore need to be aware of the high potential and clinical complexity of infection with *R. raoultii* and other tickborne pathogens in order to confirm suitable testing and treatment needs in endemic areas (*10*). Therefore, we strongly recommend continuous evaluation of the potential public health threat posed by infected ticks to humans in South Korea. A better understanding of local tick species, including *H. longicornis*, and a more thorough characterization of TBP agents, such as *R. raoultii*, are critical.

This work was supported by a grant from the Basic Science Research Program through the National Research Foundation (NRF) of Korea funded by the Ministry of Education (grant number: NRF-2016R1D1A1B02015366).

The authors declare no conflict of interest.

About the Author

Dr. Seo received a PhD degree at Kyungpook National University, South Korea, and is currently working as a research scientist at the Animal and Plant Quarantine Agency, Gimcheon, South Korea. His primary research interests are vectors and vectorborne diseases.

References

1. Dantas-Torres F, Chomel BB, Otranto D. Ticks and tick-borne diseases: a One Health perspective. Trends Parasitol. 2012;28:437–46. [Erratum in: Trends Parasitol. 2013;29:516] https://doi.org/10.1016/j.pt.2012.07.003
2. Raoult D, Parola P, editors. Rickettsial diseases. New York: Informa Healthcare; 2007.
3. Oteo JA, Portillo A. Tick-borne rickettsioses in Europe. Ticks Tick Borne Dis. 2012;3:271–8. https://doi.org/10.1016/j.ttbdis.2012.10.035
4. Choe HC, Fudge M, Sames WJ, Robbins RG, InYong L, Chevalier NA, et al. Tick surveillance of dogs in the Republic of Korea. Systematic and Applied Acarology. 2011;16:215–22. https://doi.org/10.11158/saa.16.3.5
5. Zheng H, Yu Z, Zhou L, Yang X, Liu J. Seasonal abundance and activity of the hard tick *Haemaphysalis longicornis* (Acari: Ixodidae) in North China. Exp Appl Acarol. 2012;56:133–41. https://doi.org/10.1007/s10493-011-9505-x
6. Lee KM, Choi YJ, Shin SH, Choi MK, Song HJ, Kim HC, et al. Spotted fever group rickettsia closely related to *Rickettsia monacensis* isolated from ticks in South Jeolla province, Korea. Microbiol Immunol. 2013;57:487–95. https://doi.org/10.1111/1348-0421.12062
7. Mediannikov O, Sidelnikov Y, Ivanov L, Fournier PE, Tarasevich I, Raoult D. Far eastern tick-borne rickettsiosis: identification of two new cases and tick vector. Ann N Y Acad Sci. 2006;1078:80–8. https://doi.org/10.1196/annals.1374.010
8. Im JH, Baek J, Durey A, Kwon HY, Chung MH, Lee JS. Current status of tick-borne diseases in South Korea. Vector Borne Zoonotic Dis. 2019;19:225–33. https://doi.org/10.1089/vbz.2018.2298
9. Seo MG, Lee SH, VanBik D, Ouh IO, Yun SH, Choi E, et al. Detection and genotyping of *Coxiella burnetii* and *Coxiella*-like bacteria in horses in South Korea. PLoS One. 2016;11:e0156710. https://doi.org/10.1371/journal.pone.0156710
10. Li H, Zhang PH, Huang Y, Du J, Cui N, Yang ZD, et al. Isolation and identification of *Rickettsia raoultii* in human cases: a surveillance study in 3 medical centers in China. Clin Infect Dis. 2018;66:1109–15. https://doi.org/10.1093/cid/cix917

Address for correspondence: Dongmi Kwak, College of Veterinary Medicine, Kyungpook National University, 80 Daehakro, Bukgu, Daegu 41566, South Korea; email: dmkwak@knu.ac.kr

COMMENT LETTERS

Pulmonary Embolism and Increased Levels of D-Dimer in Patients with Coronavirus Disease

Kok Hoe Chan, Jihad Slim, Hamid S. Shaaban

Author affiliation: St. Michael's Medical Center, Newark, New Jersey, USA

DOI: https://doi.org/10.3201/eid2610.202127

To the Editor: We read with great interest the recent report by Griffin et. al. (*1*). Griffin et al. reported on 3 patients in whom pulmonary embolism developed after the cytokine storm phase of coronavirus disease (COVID-19); the patients were treated with steroids and tocilizumab. We have observed a transient elevation of D-dimer in patients after tocilizumab treatment, which leads to an interesting discussion about whether the pulmonary embolism observed in these COVID-19 patients was due to a persistent hypercoagulable state in the late phase of the disease or a transient one related to tocilizumab.

Tocilizumab is a humanized antihuman interleukin-6 (IL-6) receptor monoclonal antibody that inhibits IL-6 signaling. Use of tocilizumab in the COVID-19 pandemic has been growing. It

presumptively targets the cytokine storm phase of the disease by inhibiting the IL-6 pathway (*2*). However, IL-6 has a multifaceted role in venous thromboembolism, and Zhang et al. has reported that upregulation of IL-6 as the result of aberrant downregulation of miR-338-5p may lead to venous thromboembolism (*3*).

Conversely, using a rat model, Nosaka et al. demonstrated the importance of iIL-6 in resolving thrombi through macrophage recruitment and proteolytic enzymes induction (*4*). The absence of IL-6, in fact, leads to the thrombus growing (*4*). Moreover, tocilizumab has been reported to decrease factor XIII, chemerin, and plasminogen activator inhibitor levels (*5*). Factor XIII is involved in fibrin stabilization; blocking this factor may lead to fibrin clot instability, causing microthrombi to dislodge, increasing the likelihood of thrombophilia.

The association of tocilizumab with thrombosis is not clearly understood. However, the potential for adverse effects that we describe may warrant a short period of therapeutic anticoagulation before and after administering tocilizumab. The hypercoagulable state reported in the findings by Griffin et. al. may represent a side effect of tocilizumab rather than being a condition secondary to COVID-19, or it could result from a combination of both.

References

1. Griffin DO, Jensen A, Khan M, Chin J, Chin K, Saad J, et al. Pulmonary embolism and increased levels of D-dimer in patients with coronavirus disease. Emerg Infect Dis. 2020 Apr 29 [Epub ahead of print]. https://doi.org/10.3201/eid2608.201477
2. Zhang C, Wu Z, Li JW, Zhao H, Wang GQ. The cytokine release syndrome (CRS) of severe COVID-19 and Interleukin-6 receptor (IL-6R) antagonist tocilizumab may be the key to reduce the mortality. Int J Antimicrob Agents. 2020 Mar 29 [Epub ahead of print]. https://doi.org/10.1016/j.ijantimicag.2020.105954
3. Zhang Y, Zhang Z, Wei R, Miao X, Sun S, Liang G, et al. IL (interleukin)-6 contributes to deep vein thrombosis and is negatively regulated by miR-338-5p. Arterioscler Thromb Vasc Biol. 2020;40:323–34. PubMed https://doi.org/10.1161/ATVBAHA.119.313137
4. Nosaka M, Ishida Y, Kimura A, Kuninaka Y, Taruya A, Ozaki M, et al. Crucial involvement of IL-6 in thrombus resolution in mice via macrophage recruitment and the induction of proteolytic enzymes. Front Immunol. 2020;10:3150. https://doi.org/10.3389/fimmu.2019.03150
5. Jewell P, Ansorge O, Kuker W, Irani SR, Zamboni G. Tocilizumab-associated multifocal cerebral thrombotic microangiopathy. Neurol Clin Pract. 2016;6:e24–6. https://doi.org/10.1212/CPJ.0000000000000220

Address for correspondence: Kok Hoe Chan, Saint Michael's Medical Center, 111 Central Ave, Newark, NJ 07101, USA; email: kchan2@primehealthcare.com

Work Environment Surrounding COVID-19 Outbreak in Call Center, South Korea

Taeshik Kim

Author affiliation: Seoul Metropolitan Government–Seoul National University Boramae Medical Center, Seoul, South Korea

DOI: https://doi.org/10.3201/eid2610.202647

To the Editor: I read with interest the recent synopsis by Park et al. (*1*) about a coronavirus disease outbreak in a call center, in which I was involved as a field epidemiologist. I would like to share my perspective as an occupational physician.

The work environment of the call center was an important reason for the high attack rate on the 11th floor. The width of the desks was 1.2 m, and most employees had worked without face masks despite the high risk for severe acute respiratory syndrome coronavirus 2 transmission associated with having persons continuously engaged in phone calls through headsets in an enclosed space. Call centers are known for their poor working conditions, the lack of power among employees, and high demands of the job (https://www.diva-portal.org/smash/get/diva2:20713/fulltext01.pdf).

In addition, presenteeism (i.e., attending work while ill) also affected the high attack rate (*2*,*3*). At least 10 employees continued to work despite having symptoms. In South Korea, sick leave and other benefits are not available for most workers (*4*). Given the lack of sick leave and concerns about disincentives for absences, employees could not have left the workplace easily. Without sick leave, workers are reluctant to apply for workers' compensation, the only alternative, and employers avoid registering workplace accidents for fear of penalties. These factors explain why the occupational accident rate does not reflect reality. A paradoxical discrepancy has been observed between South Korea and the average European Union country in both lower occupational accident rates (484 vs. 1,558/100,000 workers) and higher fatal accident rates (10.54 vs. 1.65/100,000 workers) (*5*).

The outbreak in the call center reflects the work environment and compensation system in South Korea. To prevent transmission of severe acute respiratory syndrome coronavirus 2 in the workplace, South Korea needs not only improvements in physical working conditions (e.g., use of physical distancing and telework) but also introduction of sick leave and a more accessible workers' compensation system.

About the Author

Dr. Kim is a specialist in occupational and environment medicine in the Department of Public Health and Community Medicine, Seoul Metropolitan Government–Seoul National University Boramae Medical Center. He is currently investigating the coronavirus disease outbreak.

References

1. Park SY, Kim YM, Yi S, Lee S, Na BJ, Kim CB, et al. Coronavirus disease outbreak in call center, South Korea. Emerg Infect Dis. 2020;26:1666–70. https://doi.org/10.3201/eid2608.201274
2. Yi J-S, Kim H. Factors related to presenteeism among South Korean workers exposed to workplace psychological adverse social behavior. Int J Environ Res Public Health. 2020;17:3472. https://doi.org/10.3390/ijerph17103472
3. Widera E, Chang A, Chen HL. Presenteeism: a public health hazard. J Gen Intern Med. 2010;25:1244–7. https://doi.org/10.1007/s11606-010-1422-x
4. Jung HW, Sohn M, Chung H. Designing the sickness benefit scheme in South Korea: using the implication from schemes of advanced nations. Health Policy Manag. 2019;29:112–29.
5. South Korea Ministry of Employment and Labor. Statistics of occupational injuries and diseases 2017. Seoul, South Korea: Ministry of Employment and Labor; 2018.

Address for correspondence: Taeshik Kim, Department of Public Health and Community Medicine, Seoul Metropolitan Government–Seoul National University Boramae Medical Center, 20, Boramae-ro 5Gil, Dongjak-gu, Seoul 07061, South Korea; email: taeshik.kim@gmail.com

Stemming the Rising Tide of Human-Biting Ticks and Tickborne Diseases, United States

Andrea Egizi, Robert A. Jordan

Author affiliation: Tick-borne Disease Program, Monmouth County Mosquito Control Division, Tinton Falls, New Jersey, USA

DOI: https://doi.org/10.3201/eid2610.201271

To the Editor: We agree with Eisen (*1*) that local/county vector control agencies (VCAs) are well-positioned to address tickborne disease prevention. However, addressing tickborne diseases using VCAs requires substantial long-term support from local administrators and taxpayers and would necessitate changing the way vector control programs are currently funded to a more proactive approach.

Sustainable funding is critical because ticks rebound quickly when management efforts cease (*2*). Many VCA budgets are eroded in the years between mosquitoborne disease outbreaks, leaving them ill-prepared for the next outbreak (*3*). Consequently, tickborne disease programs could experience major setbacks if their resources are redirected during a mosquitoborne disease outbreak.

Eisen acknowledges (*1*) that known barriers to implementation of community-based tick control include a lack of optimized best practices for tick suppression that link reductions in tick populations to measurable reductions in human disease, as well as the lack of real-world cost estimates for their implementation. Tickborne disease programs without proper budgets and realistic expectations that purport to reduce incidence but fail to do so (or fail to do so quickly) run the risk of undermining public trust and willingness to sustain funding.

Last, we caution that managing ticks in residential situations (as opposed to high-risk public open spaces and trails) is fraught with technical and public relations challenges, legal issues, and likely insurmountable funding demands (*4*,*5*). The complex array of environmental and social factors contributing to the increase in tickborne disease cases (e.g., forest management practices, climate change, land use, and an aging population) is frankly beyond the scope of any individual VCA to address without higher-level (state and federal) coordination.

A proactive approach with higher-level coordination will help manage tickborne disease. To give VCAs the best chance to combat tickborne disease, they must be adequately and sustainably funded to manage mosquitoes and ticks, even during years of fiscal challenge.

Acknowledgment

We thank Victoria Thompson for comments on this manuscript.

References

1. Eisen L. Stemming the rising tide of human-biting ticks and tickborne diseases, United States. Emerg Infect Dis. 2020;26:641–7. https://doi.org/10.3201/eid2604.191629
2. Schulze TL, Jordan RA, Hung RW, Schulze CJ. Effectiveness of the 4-Poster passive topical treatment device in the control of *Ixodes scapularis* and *Amblyomma americanum* (Acari: Ixodidae) in New Jersey. Vector Borne Zoonotic Dis.

2009;9:389–400. https://doi.org/10.1089/vbz.2008.0160
3. Vazquez-Prokopec GM, Chaves LF, Ritchie SA, Davis J, Kitron U. Unforeseen costs of cutting mosquito surveillance budgets. PLoS Negl Trop Dis. 2010;4:e858. https://doi.org/10.1371/journal.pntd.0000858
4. Jordan RA, Schulze TL, Jahn MB. Effects of reduced deer density on the abundance of *Ixodes scapularis* (Acari: Ixodidae) and Lyme disease incidence in a northern New Jersey endemic area. J Med Entomol. 2007;44:752–7. https://doi.org/10.1093/jmedent/44.5.752
5. Schulze TL, Jordan RA, Schulze CJ, Healy SP, Jahn MB, Piesman J. Integrated use of 4-Poster passive topical treatment devices for deer, targeted acaricide applications, and Maxforce TMS bait boxes to rapidly suppress populations of *Ixodes scapularis* (Acari: Ixodidae) in a residential landscape. J Med Entomol. 2007;44:830–9. https://doi.org/10.1093/jmedent/44.5.830

Address for correspondence: Robert A. Jordan, Tick-borne Disease Program, Monmouth County Mosquito Control Division, 1901 Wayside Rd, Tinton Falls, New Jersey, USA; email: Robert.Jordan@co.monmouth.nj.us

Rhabdomyolysis as Potential Late Complication Associated with COVID-19

Kok Hoe Chan, Jihad Slim

Author affiliation: Saint Michael's Medical Center, New York Medical College, Newark, New Jersey, USA

DOI: https://doi.org/10.3201/eid2610.202225

To the Editor: Jin and Tong described a patient with severe coronavirus disease (COVID-19) in whom rhabdomyolysis developed on day 9 of hospitalization (*1*). The interplay between severe acute respiratory syndrome coronavirus 2 and rhabdomyolysis is not yet understood; we consider possible etiologies for this case of rhabdomyolysis.

We reported 2 case-patients with COVID-19 who also had weakness and elevated creatinine kinase levels (but no respiratory symptoms) (*2*). As part of his COVID-19 treatment regimen, the patient reported by Jin and Tong received lopinavir and meropenem, which can cause rhabdomyolysis (*3*,*4*). Meropenem is associated with rhabdomyolysis by inducing severe hypomagnesemia and hypokalemia; it would be helpful to know the trends in the patient's electrolytes before rhabdomyolysis developed (*3*). A cytokine storm might also have caused this complication because rhabdomyolysis developed on day 15 of COVID-19 symptoms and coincided with the peak of inflammatory markers (C-reactive protein). On the other hand, the combination of hypoxia and hypercoagulability might have induced an ischemic event that inhibited blood flow to the involved muscles, triggering rhabdomyolysis.

Clinicians treating rhabdomyolysis concurrent with COVID-19 must assess the many differential diagnoses, including severe acute respiratory syndrome coronavirus 2–induced myositis, reactions to medication, cytokine storm, hypoxia, or a thromboembolic event. This differential diagnosis is crucial because each condition has a distinct therapeutic approach.

References

1. Jin M, Tong Q. Rhabdomyolysis as potential late complication associated with COVID-19. Emerg Infect Dis. 2020;26:1618–20. https://doi.org/10.3201/eid2607.200445
2. Chan KH, Farouji I, Abu Hanoud A, Slim J. Weakness and elevated creatinine kinase as the initial presentation of coronavirus disease 2019 (COVID-19). Am J Emerg Med. 2020 May 11 [Epub ahead of print].
3. de Kanter CT, Keuter M, van der Lee MJ, Koopmans PP, Burger DM. Rhabdomyolysis in an HIV-infected patient with impaired renal function concomitantly treated with rosuvastatin and lopinavir/ritonavir. Antivir Ther. 2011;16:435–7. https://doi.org/10.3851/IMP1747
4. Margolin L. Impaired rehabilitation secondary to muscle weakness induced by meropenem. Clin Drug Investig. 2004;24:61–2. https://doi.org/10.2165/00044011-200424010-00008

Address for correspondence: Kok Hoe Chan, Saint Michael's Medical Center, Newark, NJ 07101, USA; email: kchan2@primehealthcare.com

The Mosquito: A Human History of Our Deadliest Predator

Timothy C. Winegard; Dutton, Penguin Random House, New York, NY, USA, 2019; ISBN (hardcover): 9781524743413; ISBN (ebook): 9781524743437; ISBN (export): 9781524745608; Pages: 496; Price: $28.00 (Hardcover)

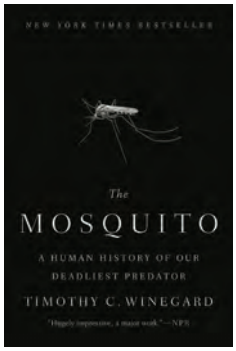

The Mosquito: A Human History of Our Deadliest Predator details the interrelation between mosquitoborne diseases and the progression of pivotal historical events. Winegard incorporates his expertise in military history with a comprehensive review of the evolution of various mosquitoborne diseases, and delivers a captivating account of humans' incessant battle with the mosquito. Each chapter of this nonfiction account details the dynamic ways in which mosquitoes influence human survival in each major period throughout history.

This book describes how mosquitoes and their diseases have shaped the outcomes of war, the spread of religion, and the development of modern culture. Attacks from "General *Anopheles*," which delivered malaria to the Persians as they navigated swampy terrain, ultimately led to a victory by the Greeks during the Greco-Persian Wars. Mosquitoes aided the rise and the fall of the Roman Empire because the Pontine Marshes served as a barrier to enemies and a direct source of disease. Christianity spread across Europe and had a reputation as a healing religion that valued treating persons affected by the mosquitoborne diseases. Christians failed to capture the Holy Land during the Crusades partially because *Plasmodium*-infected mosquitoes attacked inexperienced Crusaders.

Winegard emphasizes the effect of mosquitoborne diseases on the development of the United States. European explorers delivered a lethal dose of mosquitoborne disease to the New World, contributing to the destruction of indigenous populations and the subsequent colonization of the Americas. Partial acquired and genetic immunity to vectorborne diseases drove the demand for enslaved persons from Africa, ensuring the productivity of plantation economies. Widespread malaria delayed the Union victory during the American Civil War, contributing to Abraham Lincoln's decision to focus on the elimination of slavery. Without malaria, a rapid Confederate defeat might not have led to the Emancipation Proclamation of 1863. Although mosquitoes probably were not the sole reason for these historical outcomes, they most likely contributed substantially to the progression of events.

Winegard emphasizes that, despite modern scientific advancements, the mosquito's legacy to shape human history is not finished. The development of DDT and antimalarial drugs, such as atabrine and chloroquine during World War II, followed by the subsequent emergence of resistance to these treatments, provide evidence for the need to continue research of mosquitoborne diseases. This book also touches on the controversial topic of clustered regularly interspaced short palindromic repeats, an innovative technology that could genetically alter mosquitoes to prevent human diseases. Although Winegard describes the potential usefulness of this powerful tool, organisms and the environment may suffer unintended devastating consequences.

This book is a fascinating account of the value of mosquitoes in shaping human culture and existence across time. Persons interested in the interplay between history and disease and future implications will learn much and enjoy the accumulation of knowledge and the exciting narrative presentation.

Teah Snyder

Author affiliation: University of Massachusetts, Amherst, Massachusetts, USA

DOI: https://doi.org/10.3201/eid2610.202806

Address for correspondence: Teah Snyder, 42 River Rd, Aprt 34, Sunderland, MA 01375, USA; email: tsnyder@umass.edu

Yi Taek-gyun (c. 1808–1883), *Books and Scholars' Accouterments* (late 1800s). Ten-panel folding screen; ink and color on silk. Overall size: 77 3/4 in × 155 1/2 in/197.5 cm × 395 cm; painting size: 54 13/16 in × 130 1/4 in/139.3 cm × 330.8 cm. Open access image from The Cleveland Museum of Art, Cleveland, Ohio, USA; Leonard C. Hanna, Jr. Fund.

"All Bookshelves Are Magical"

Byron Breedlove

During these times when social distancing and quarantining are widely practiced, people around the world are watching news or entertainment being broadcast from makeshift home studios and teleconferencing to stay connected with staff, team members, collaborators, family, and friends. Frequently sharing screen time with the speakers are all manner of bookshelves in the background, and the collections of books and ephemera on the shelves have provided grist for stories and commentaries by many journalists and bloggers throughout the year.

For instance, Vogue.com editor Stuart Emmrich admits to becoming obsessed with what is in the background—especially the books: "Ah, yes, bookshelves. Rows of carefully arranged books seem to be the go-to choice of most of the reporters and commentators who provide the bulk of the cable-news programming. Thus, my curiosity about their reading habits." For those of us without our own curated collections of books to share, photographs of shelves brimming with books are available as virtual stand-ins. Penguin Random House even has images of "credibility bookshelf" backgrounds available to download.

Featuring bookcases in the background is not, however, a novel idea by any means. King Jeongjo, the 22nd ruler of the Korean Chosŏn (also called Yi) Dynasty during 1776–1800, was an early proponent of this practice. He positioned a painted screen displaying books and other objects behind his throne. Art historian Sunglim Kim explains that the king used the screen "as a vicarious substitute for reading and studying, as he did not have as much time to spend with his books as he wanted."

Known as *Chaekgeori,* this style of still life painting flourished during the latter part of the Chosŏn Dynasty, the last and longest-lived imperial dynasty (1392–1910) of Korea. Sooa McCormick, Assistant Curator of Korean Art, Cleveland Museum of Art, notes that *Chaekgeori* is translated into English as "books and things." Works in this genre reflect an admiration for learning and scholarship, and effects akin to those found in Western *trompe l'oeil* (French: deceive the eye) painting were commonly used to create the

Author affiliation: Centers for Disease Control and Prevention, Atlanta, Georgia, USA

DOI: https://doi.org/10.3201/eid2610.AC2610

three-dimensional spatial illusion characteristic of these compositions.

Most *Chaekgeori* are not signed or dated; consequently, the identities of many of their creators remain unknown. *Books and Scholars' Accouterments*, this month's cover image, is a rare exception. The Cleveland Museum of Art explains that the third panel from the right features a hidden seal that reveals the artist as Yi Taek-gyun. To date, only about a dozen such hidden seal impressions have been found, including three for this artist. Despite his standing as an established court artist, details about the life and work of Yi Taek-gyun are scarce. The Asian Art Museum, San Francisco, notes that he came from a family of court painters and that he changed his name several times. He used Yi Hyeongrok until 1864 and Yi Eungrok from 1864 to 1871 before switching to Yi Taek-gyun.

Extending across 10 folding panels, *Books and Scholars' Accouterments* depicts unusual and luxurious accessories that a 19th-century Korean scholar may have collected and displayed in a private study. Viewed as a montage, this tableau is dominated by a uniformly dark blue background, neatly stacked books with honey-colored pages, and objects carefully arranged on the shelves. The orthogonal lines that define the shelves and the contrasting dark shading for the background and light shading for the tops and bottoms of the shelves create a perception of recessed space and consistent depth.

Books, the primary motif within this still life genre, appear on 27 shelves. Some alcoves hold only books; others also feature writing implements, ceramics, pottery, flowers, and exotic luxuries and delicacies. Specifically among the myriad items showcased are peacock feathers, a bamboo brush holder, a three-tier lunch container, a red cup and lid, a thin crackle-patterned vase, narcissus flowers, scrolls jutting from a translucent glass bowl, a red incense burner on a tripod, and a plate of pomegranates and finger citrons on a wooden stand.

Yi Taek-gyun's mastery of colors, textures, and details is apparent. Kim explains that the challenge of creating diverse collections of items was appealing for *Chaekgeori* painters who "explored every visual possibility of the object—shape, color, and texture—to create a feast of sensuality."

Contemporary English author Neil Gaiman once said, "All bookshelves are magical." Indeed, *Chaekgeori* paintings reveal something of the wonder and joy of books, their historical association with knowledge and scholarship, and even the dynamic struggle between order and chaos often playing out on our bookshelves.

Since the French *Journal des Sçavans* and the English *Philosophical Transactions of the Royal Society* debuted in 1665, book reviews have been staples of scientific and scholarly periodicals. *Emerging Infectious Diseases* published its first book review in September 1997. Including that review for *Virus Hunter* from 1997 and the one for *The Mosquito: Human History of Our Deadliest Predator* appearing in this issue, the journal has published 236 book reviews that cover an assortment of subjects apropos to understanding factors involved in disease emergence, prevention, and elimination.[1] Readers of this journal no doubt have many of those books in their own collections and perhaps can enjoy envisioning what a *Chaekgeori* painting featuring their own books and scholarly accouterments would include.

Bibliography

1. Asian Art Museum. Books and scholars' possessions (Chaekgeori) [cited 2020 Aug 19]. http://asianart.emuseum.com/view/objects/asitem/items$0040:13843
2. Black K, Wagner E. Ch'aekkŏri paintings: a Korean jigsaw puzzle [cited 2020 Aug 11]. www.jstor.org/stable/20111228
3. The Cleveland Museum of Art. Books and scholars' accouterments [cited 2020 Jul 20]. https://www.clevelandart.org/art/2011.37
4. The Cleveland Museum of Art. Chaekgeori: pleasure of possessions in Korean painted screens [cited 2020 Jul 20]. https://www.clevelandart.org/about/press/media-kit/cleveland-museum-art-presents-chaekgeori-pleasure-possessions-korean-painted-screens
5. Emmrich S. If you can't stop staring at TV anchors' home backgrounds, you're not alone [cited 2020 Aug 20]. https://www.vogue.com/article/news-anchors-broadcasting-from-home-bookshelves-flowers-coronavirus
6. Kim S. Chaekgeori: multi-dimensional messages in late Joseon Korea [cited 2020 Aug 20]. www.jstor.org/stable/43676731
7. McCormick S. Books and other things in Korean painted screens [cited 2020 Jul 20]. https://www.clevelandart.org/magazine/cleveland-art-julyaugust-2017/chaekgeori
8. Penguin Random House. Download these 'credibility bookshelf' backgrounds for zoom [cited 2020 Aug 20]. https://www.penguinrandomhouse.ca/blog/1768/download-these-credibility-bookshelf-backgrounds-zoom
9. Swoger B. The (mostly true) origins of the scientific journal [cited 2020 Sep 3]. https://blogs.scientificamerican.com/information-culture/the-mostly-true-origins-of-the-scientific-journal

Address for correspondence: Byron Breedlove, EID Journal, Centers for Disease Control and Prevention, 1600 Clifton Rd NE, Mailstop H16-2, Atlanta, GA 30329-4027, USA; email: wbb1@cdc.gov

[1]Readers searching for specific books reviewed in *Emerging Infectious Diseases* have a pair of options available: examine the list of books and media reviews by year or use the article index by types search feature.

EMERGING INFECTIOUS DISEASES®

Upcoming Issue

- The Problem of Dark Matter in Neonatal Sepsis
- Measuring Timeliness of Outbreak Detection, Notification, and Control in the WHO African Region, 2017–2019
- Three Patients with COVID-19 and Pulmonary Tuberculosis, Wuhan, China, January–February 2020
- Validated Methods for Removing Select Agent Samples from Biosafety Level 3 Laboratories
- Epidemiology of COVID-19 Outbreak on Cruise Ship Quarantined at Yokohama, Japan, February 2020
- High Dengue Burden and Circulation of 4 Virus Serotypes among Children with Undifferentiated Fever, Kenya, 2014–2017
- Systematic Review and Meta-Analyses of Incidence for Group B *Streptococcus* Disease in Infants and Antimicrobial Resistance, China
- Analysis of SARS-CoV-2 Transmission in Different Settings, Brunei
- Modeling Treatment Strategies to Inform Yaws Eradication
- *Streptococcus pneumoniae* Serotype 12F-CC4846 and Invasive Pneumococcal Disease after Introduction of 13-Valent Pneumococcal Conjugate Vaccine, Japan, 2017
- Azithromycin to Prevent Pertussis in Household Contacts, Catalonia and Navarre, Spain, 2012–2013
- Two New Cases of Pulmonary Infection by Mycobacterium shigaense
- Multiple Introductions of *Salmonella* Typhi H58 with Reduced Fluoroquinolone Susceptibility, Chile
- Asymptomatic Transmission of SARS-CoV-2 on Evacuation Flight
- SARS-CoV-2 Virus Culture and Subgenomic RNA for Respiratory Specimens from Patients with Mild Coronavirus Disease
- Chikungunya Virus Infection in Blood Donors and Patients with Acute Febrile Illness, Mandalay, Myanmar, 2019
- Potential Role of Social Distancing in Mitigating Spread of Coronavirus Disease, South Korea
- Identification of a Novel α-herpesvirus Associated with Ulcerative Stomatitis in Donkeys
- Multidrug-Resistant Hypervirulent Group B *Streptococcus* in Neonatal Invasive Infections, France, 2007–2019
- Multidrug-Resistant *Candida auris* Infections in Critically Ill Coronavirus Disease Patients, India, April–July 2020
- Worldwide Effects of Coronavirus Disease Pandemic on Tuberculosis Services, January–April 2020
- Surveillance of Pneumonia and Influenza Mortality to Distinguish Thresholds versus Anomaly Detection
- Four Patients with COVID-19 and Tuberculosis, Singapore, April–May 2020
- Seroprevalence of SARS-CoV-2–Specific Antibodies, Faroe Islands
- Detection of SARS-CoV-2 in Hemodialysis Effluent of Patient with COVID-19 Pneumonia, Japan
- Seroprevalence of SARS-CoV-2 and Infection Fatality Ratio, Orleans and Jefferson Parishes, Louisiana, USA, May 2020
- Detection of SARS-CoV-2 in Hemodialysis Effluent of Patient with COVID-19 Pneumonia, Japan

Complete list of articles in the November issue at http://www.cdc.gov/eid/upcoming.htm

Earning CME Credit

To obtain credit, you should first read the journal article. After reading the article, you should be able to answer the following, related, multiple-choice questions. To complete the questions (with a minimum 75% passing score) and earn continuing medical education (CME) credit, please go to http://www.medscape.org/journal/eid. Credit cannot be obtained for tests completed on paper, although you may use the worksheet below to keep a record of your answers.

You must be a registered user on http://www.medscape.org. If you are not registered on http://www.medscape.org, please click on the "Register" link on the right hand side of the website.

Only one answer is correct for each question. Once you successfully answer all post-test questions, you will be able to view and/or print your certificate. For questions regarding this activity, contact the accredited provider, CME@medscape.net. For technical assistance, contact CME@medscape.net. American Medical Association's Physician's Recognition Award (AMA PRA) credits are accepted in the US as evidence of participation in CME activities. For further information on this award, please go to https://www.ama-assn.org. The AMA has determined that physicians not licensed in the US who participate in this CME activity are eligible for AMA PRA Category 1 Credits™. Through agreements that the AMA has made with agencies in some countries, AMA PRA credit may be acceptable as evidence of participation in CME activities. If you are not licensed in the US, please complete the questions online, print the AMA PRA CME credit certificate, and present it to your national medical association for review.

Article Title

Healthcare-Associated Legionnaires' Disease, Europe, 2008–2017

CME Questions

1. Which of the following settings is associated with the highest proportion of Legionnaires' disease (LD) cases in the European Union?

A. Animal-human transmission; farm-related
B. Healthcare-associated (HCA)
C. Travel-associated
D. Community-acquired

2. Which of the following statements regarding temporal trends in the prevalence of LD in the current study is most accurate?

A. Community-acquired cases increased over time whereas HCA cases declined
B. HCA cases increased over time whereas community-acquired cases declined
C. Community-acquired and HCA cases both increased over time
D. Community-acquired and HCA cases were both stable over time

3. Which of the following statements regarding the characteristics of LD infection in the current study is most accurate?

A. HCA LD was more common as a proportion of LD among individuals age <20 years vs 50 to 59 years
B. HCA LD was more common as a proportion of LD among individuals age 50 to 59 years vs ≥60 years
C. In adjusted analyses, men were more likely to have HCA LD than women
D. HCA LD prevalence was highest in December and January

4. Which of the following statements regarding the laboratory tests for LD and clinical outcomes in the current study is most accurate?

A. Rates of culture-confirmed LD were lower in hospital-associated LD vs other healthcare settings
B. Most cases of HCA LD were linked to *Legionella pneumophila* serogroup 3
C. Nearly 30% of cases of HCA LD died
D. The highest risk for death was associated with *L. pneumophila* serogroup 1

Earning CME Credit

To obtain credit, you should first read the journal article. After reading the article, you should be able to answer the following, related, multiple-choice questions. To complete the questions (with a minimum 75% passing score) and earn continuing medical education (CME) credit, please go to http://www.medscape.org/journal/eid. Credit cannot be obtained for tests completed on paper, although you may use the worksheet below to keep a record of your answers.

You must be a registered user on http://www.medscape.org. If you are not registered on http://www.medscape.org, please click on the "Register" link on the right hand side of the website.

Only one answer is correct for each question. Once you successfully answer all post-test questions, you will be able to view and/or print your certificate. For questions regarding this activity, contact the accredited provider, CME@medscape.net. For technical assistance, contact CME@medscape.net. American Medical Association's Physician's Recognition Award (AMA PRA) credits are accepted in the US as evidence of participation in CME activities. For further information on this award, please go to https://www.ama-assn.org. The AMA has determined that physicians not licensed in the US who participate in this CME activity are eligible for AMA PRA Category 1 Credits™. Through agreements that the AMA has made with agencies in some countries, AMA PRA credit may be acceptable as evidence of participation in CME activities. If you are not licensed in the US, please complete the questions online, print the AMA PRA CME credit certificate, and present it to your national medical association for review.

Article Title

Lessons Learned from a Decade of Investigations of Shiga Toxin–Producing *Escherichia coli* Outbreaks Linked to Leafy Greens, United States and Canada

CME Questions

1. You are advising a local public health department regarding prevention of Shiga toxin–producing *Escherichia coli* (STEC) outbreaks linked to leafy greens. According to the study of epidemiologic, laboratory and traceback data from US and Canadian STEC O157 and non-STEC O157 outbreaks linked to leafy greens during 2009 to 2018 by Marshall and colleagues, which of the following statements about epidemiologic findings of STEC outbreaks linked to leafy greens is correct?

A. During 2009 to 2018 in the United States and Canada, there were 40 outbreaks (1–9/y), 1212 illnesses, 77 cases of hemolytic uremic syndrome, and 8 deaths identified from STEC outbreaks linked to leafy greens
B. More outbreaks were linked to cabbage than to any other type of leafy green
C. Most outbreaks occurred in the spring and summer
D. Most STEC outbreaks linked to leafy greens were caused by non-STEC O157 STEC

2. According to the study of epidemiologic, laboratory, and traceback data from US and Canadian STEC O157 and non-STEC O157 outbreaks linked to leafy greens during 2009 to 2018 by Marshall and colleagues, which of the following statements about barriers to solving outbreaks linked to leafy greens is correct?

A. Links between outbreak timing and harvest location were easily identified
B. Barriers in epidemiologic and traceback investigations complicated identification of the ultimate outbreak source, hindering timely communication of actionable advice for consumers.
C. Investigations of leafy green outbreaks typically included environmental assessments
D. One-quarter of STEC outbreak investigations identified leafy greens as a suspected rather than confirmed source

3. According to the study of epidemiologic, laboratory, and traceback data from US and Canadian STEC O157 and non-STEC O157 outbreaks linked to leafy greens during 2009 to 2018 by Marshall and colleagues, which of the following statements about research and public policy needs to prevent future STEC outbreaks linked to leafy greens is correct?

A. Studies comparing the risk for STEC contamination and bacterial survival dynamics by leafy green type are unlikely to offer useful information
B. Traceability of leafy greens is relatively straightforward
C. The 2 large 2018 outbreaks did not result in any major policy changes
D. Federal and state health partners, researchers, the leafy green industry, and retailers should collaborate to fill knowledge gaps and implement and assess interventions to reduce STEC contamination

DEPARTMENT OF
HEALTH & HUMAN SERVICES
Public Health Service
Centers for Disease Control and Prevention (CDC)
Mailstop D61, Atlanta, GA 30329-4027

ISSN 1080-6040